MODULATION OF NMDA RECEPTORS: FROM BENCH SIDE TO CLINICAL APPLICATIONS IN PSYCHIATRY

EDITED BY: Natasa Petronijevic, Nevena V. Radonjic and Hsien-Yuan Lane

PUBLISHED IN: Frontiers in Psychiatry

frontiers Research Topics

frontiers

ISSN 1664-8714
ISBN 978-2-88976-095-4
DOI 10.3389/978-2-88976-095-4

About Frontiers

Frontiers is more than just an open-access publisher of scholarly articles: it is a pioneering approach to the world of academia, radically improving the way scholarly research is managed. The grand vision of Frontiers is a world where all people have an equal opportunity to seek, share and generate knowledge. Frontiers provides immediate and permanent online open access to all its publications, but this alone is not enough to realize our grand goals.

Frontiers Journal Series

The Frontiers Journal Series is a multi-tier and interdisciplinary set of open-access, online journals, promising a paradigm shift from the current review, selection and dissemination processes in academic publishing. All Frontiers journals are driven by researchers for researchers; therefore, they constitute a service to the scholarly community. At the same time, the Frontiers Journal Series operates on a revolutionary invention, the tiered publishing system, initially addressing specific communities of scholars, and gradually climbing up to broader public understanding, thus serving the interests of the lay society, too.

Dedication to Quality

Each Frontiers article is a landmark of the highest quality, thanks to genuinely collaborative interactions between authors and review editors, who include some of the world's best academicians. Research must be certified by peers before entering a stream of knowledge that may eventually reach the public - and shape society; therefore, Frontiers only applies the most rigorous and unbiased reviews.
Frontiers revolutionizes research publishing by freely delivering the most outstanding research, evaluated with no bias from both the academic and social point of view. By applying the most advanced information technologies, Frontiers is catapulting scholarly publishing into a new generation.

What are Frontiers Research Topics?

Frontiers Research Topics are very popular trademarks of the Frontiers Journals Series: they are collections of at least ten articles, all centered on a particular subject. With their unique mix of varied contributions from Original Research to Review Articles, Frontiers Research Topics unify the most influential researchers, the latest key findings and historical advances in a hot research area! Find out more on how to host your own Frontiers Research Topic or contribute to one as an author by contacting the Frontiers Editorial Office: frontiersin.org/about/contact

MODULATION OF NMDA RECEPTORS: FROM BENCH SIDE TO CLINICAL APPLICATIONS IN PSYCHIATRY

Topic Editors:
Natasa Petronijevic, University of Belgrade, Serbia
Nevena V. Radonjic, Upstate Medical University, United States
Hsien-Yuan Lane, China Medical University, Taiwan

Citation: Petronijevic, N., Radonjic, N. V., Lane, H.-Y., eds. (2022). Modulation of NMDA Receptors: From Bench Side to Clinical Applications in Psychiatry. Lausanne: Frontiers Media SA. doi: 10.3389/978-2-88976-095-4

Table of Contents

frontiers | Frontiers in Psychiatry

EDITORIAL
published: 13 April 2022
doi: 10.3389/fpsyt.2022.896327

Editorial: Modulation of NMDA Receptors: From Bench Side to Clinical Applications in Psychiatry

Nataša Petronijević [1], Hsien-Yuan Lane [2,3,4] and Nevena V. Radonjić [5]*

[1] Faculty of Medicine, Institute of Medical and Clinical Biochemistry, University of Belgrade, Belgrade, Serbia, [2] Graduate Institute of Biomedical Sciences, China Medical University, Taichung, Taiwan, [3] Department of Psychiatry & Brain Disease Research Center, China Medical University Hospital, Taichung, Taiwan, [4] Department of Psychology, College of Medical and Health Sciences, Asia University, Taichung, Taiwan, [5] Department of Psychiatry and Behavioral Sciences, SUNY Upstate Medical University, Syracuse, New York, NY, United States

Keywords: NMDA receptors, ketamine, D-serine, kynurenic acid, depression, schizophrenia, Alzheimer's disease, alcohol use disorder

Editorial on the Research Topic

Modulation of NMDA Receptors: From Bench Side to Clinical Applications in Psychiatry

N-methyl -D- aspartate receptors (NMDARs) have a complex role in the developing and mature brain. Disruptions in NMDAR signaling have been observed in different psychiatric disorders such as schizophrenia, depressive disorder, and Alzheimer's disease (AD) (1). The articles in this Research Topic further advance our knowledge on the complex role of NMDARs in normal and pathological conditions and explore the possibility of novel therapeutic uses of NMDAR modulators.

The NMDAR hypofunction hypothesis of schizophrenia (2) is the basis for the current use of NMDAR modulators in modeling of this disease in animals and as potential therapeutics.

In the review article, Pei et al. address the use of direct and indirect NMDAR glycine-site modulators, such as glycine, D-cycloserine, D-serine, glycine transporter 1 (GlyT1) inhibitors, and D-amino acid oxidase (DAAO) inhibitors in the treatment of clinical symptoms and cognitive impairments seen in schizophrenia. Reviewed preclinical and clinical studies suggest that indirect NMDAR glycine-site enhancers such as GlyT1 inhibitors (sarcosine) and DAAO inhibitors (sodium benzoate, TAK-831) seem to be more potent in clinical efficacy and with fewer side effects than direct NMDAR glycine-site agonists, including glycine, D-cycloserine, and D-serine.

Due to the fact that D-serine is one of the most frequently used NMDAR modulators and findings of its nephrotoxicity in rats, important is the review of Meftah et al. that summarizes current findings of the safety of D-serine treatment in different mammals, including humans. The toxicity of D-serine to endocrine, cardiovascular, gastrointestinal and extrapyramidal systems, with a special focus on the kidneys, is comprehensively discussed. The authors conclude that in humans D-serine appears to be safe at currently studied maximal doses and suggest that in future work even higher doses combined with DAAO inhibitors should be investigated.

The kynurenic acid (KYNA), an endogenous NMDA receptor antagonist, is elevated in the brain of patients with schizophrenia (3). Wright et al. utilized pre-natal exposure to kynurenine to model prenatal insult in rats and have found gender and circadian changes in the extracellular levels of glutamate, GABA and KYNA in rat hippocampi. The authors suggested that sex and time-dependent changes in hippocampal neuromodulation, elicited by prenatal KYNA elevation, may influence behavioral phenotypes, and have translational relevance to psychotic disorders.

OPEN ACCESS

Edited and reviewed by:
Marijn Lijffijt,
Baylor College of Medicine,
United States

****Correspondence:***
Nataša Petronijević
natasapetronijevic@yahoo.com

Specialty section:
This article was submitted to Psychopharmacology, a section of the journal Frontiers in Psychiatry

Received: *14 March 2022*
Accepted: *22 March 2022*
Published: *13 April 2022*

Citation:
Petronijević N, Lane H-Y and Radonjić NV (2022) Editorial: Modulation of NMDA Receptors: From Bench Side to Clinical Applications in Psychiatry. Front. Psychiatry 13:896327. doi: 10.3389/fpsyt.2022.896327

Mallien et al. focused to identify the cellular substrates of psychosis induced by NMDAR hypofunction at post-adolescent stages. For these purposes, they have analyzed the effect of the inducible ablation of NMDARs in ErbB4 expressing cells, as neuregulin 1 and its receptor ErbB4 have been identified as schizophrenia-associated susceptibility factors that closely interact with NMDARs. They concluded that post-adolescent NMDAR deletion, even in a wider cell population than parvalbumin-positive interneurons, is not sufficient to generate behavioral changes that mimic psychiatric disorders.

With ketamine's demonstrated efficacy in the treatment of unipolar depression (4), there are emerging questions on the mechanism of actions underlying its observed fast clinical improvement and the potential role of NMDA transmission in bipolar depression. Yang et al. in their article highlight the importance of NMDAR transmission in the generation of mental representation during working memory. They further postulate that the very rapid, antidepressant effect of intranasal ketamine may involve the disruption of NMDAR-generated aversive mood states by the anterior and subgenual cingulate cortices, providing the opportunity for the return of top-down regulation by higher prefrontal cortex areas.

The effects of a single intravenous infusion of ketamine hydrochloride on magnetoencephalographic recordings in drug-free individuals with major depressive disorder performing an attentional task during scanning, have been investigated by Gilbert et al. Dynamic causal modeling was used to model effective connectivity of excitatory and inhibitory pathways. The authors provide additional support for the GABA disinhibition hypotheses of depression and the role of AMPA receptors in ketamine's antidepressant effects.

Dong et al. in their article address the impact of another oral NMDAR antagonist, D-cycloserine, combined with lurasidone on glutamate and glutamine in bipolar depression. This preliminary pilot study demonstrated that a lower mean glutamate level post-treatment after administration of NMDAR antagonist in combination with lurasidone predicts a better antidepressant response in bipolar depression. Authors propose that in the future, attenuation of the glutamate response to NMDAR antagonists could potentially be used as a biomarker for screening of NMDAR antagonists for their antidepressant potential.

Recent studies suggested that ketamine's rapid-acting antidepressant effect is potentially mediated by the opioid system (5). Bowman et al. have investigated the resting state electroencephalography profiles induced by co-administration of ketamine with either antipsychotic clozapine, or opioid receptor antagonist naltrexone, in freely moving rats to clarify this issue further. They demonstrated that the effect of clozapine, ketamine and naltrexone on local field potentials (LFP) depends of the locomotor state and that both clozapine and naltrexone modulated the effect of ketamine LFPs.

Balanced NMDAR activity is required for optimal brain and neurocognitive function (6). In an overview, Orzylowski et al. summarize the potential role of D-serine in normal and pathological aging such as AD. They review both preclinical and human studies of D-serine's modulation of cognition. Albeit controversial, it has been suggested that, in normal aging, decreased serine racemase expression, lower D-serine concentration, and NMDARs downregulation may lead to impaired synaptic plasticity and declined cognitive function. On the other hand, in AD, increased serine racemase expression, higher D-serine levels, and NMDAR overactivation tend to generate neurotoxicity and dementia. D-Serine and DAAO have been proposed as possible biomarkers and D-serine and DAAO inhibitors as potential therapeutics in early-phase AD.

Besides its role in schizophrenia and depression, the glutamatergic system and NMDARs have also been implicated in the pathophysiology of alcohol use disorder (7). Alcohol exposure upregulates Fyn, a protein tyrosine kinase that indirectly modulates NMDAR signaling by phosphorylating the NR2B subunit. Thompson et al. showed that saracatinib, the Src/Fyn kinase inhibitor, at the doses and regimen used in the study did not affect alcohol-seeking/craving or consumption in habitual mice or heavy drinking human participants.

AUTHOR CONTRIBUTIONS

All authors listed have made a substantial, direct, and intellectual contribution to the work and approved it for publication.

FUNDING

This work was partially supported by National Health Research Institutes, Taiwan (NHRI- EX 111-11133NI), Ministry of Science and Technology, Taiwan (109-2314-B-039-039-MY3 and MOST 110-2622-B039-001), and China Medical University Hospital, Taiwan (DMR-111-243).

REFERENCES

1. Lin CH, Hashimoto K, Lane HY. Editorial: glutamate-related biomarkers for neuropsychiatric disorders. *Front Psychiatry*. (2019) 10:904. doi: 10.3389/fpsyt.2019.00904
2. Lee G, Zhou Y. NMDAR Hypofunction Animal Models of Schizophrenia. *Front Mol Neurosci*. (2019) 12:185. doi: 10.3389/fnmol.2019.00185
3. Linderholm KR, Skogh E, Olsson SK, Dahl ML, Holtze M, Engberg et al. Increased levels of kynurenine and kynurenic acid in the CSF of patients with schizophrenia. *Schizophr Bull*. (2012) 38:426–32. doi: 10.1093/schbul/sbq086
4. Krystal JH, Abdallah CG, Sanacora G, Charney DS, Duman RS. Ketamine: a paradigm shift for depression research and treatment. *Neuron*. (2019) 101:774–8. doi: 10.1016/j.neuron.2019.02.005
5. Sleigh J, Harvey M, Voss L, Denny B. 3. Ketamine - more mechanisms of action than just NMDA blockade. *Trends Anaesthesia Critical Care*. (2014) 4:76–81. doi: 10.1016/j.tacc.2014.03.002

6. Wang R, Reddy PH. Role of glutamate and NMDA receptors in Alzheimer's disease. *J Alzheimers Dis*. (2017) 57:1041–8. doi: 10.3233/JAD-160763
7. Ron D, Wang J. The NMDA receptor and alcohol addiction. In: Van Dongen AM, editor. *Biology of the NMDA Receptor*. Boca Raton, FL: CRC Press/Taylor & Francis (2009). Ch. 4.

Conflict of Interest: The authors declare that the research was conducted in the absence of any commercial or financial relationships that could be construed as a potential conflict of interest.

Publisher's Note: All claims expressed in this article are solely those of the authors and do not necessarily represent those of their affiliated organizations, or those of the publisher, the editors and the reviewers. Any product that may be evaluated in this article, or claim that may be made by its manufacturer, is not guaranteed or endorsed by the publisher.

frontiers in Psychiatry

REVIEW
published: 09 April 2021
doi: 10.3389/fpsyt.2021.654322

NMDAR Neurotransmission Needed for Persistent Neuronal Firing: Potential Roles in Mental Disorders

Shengtao Yang[1], *Hyojung Seo*[1,2], *Min Wang*[1] *and Amy F. T. Arnsten*[1]*

[1] *Department of Neuroscience, Yale University School of Medicine, New Haven, CT, United States,* [2] *Department of Psychiatry, Yale University School of Medicine, New Haven, CT, United States*

OPEN ACCESS

Edited by:
Nevena V. Radonjic, Upstate Medical University, United States

Reviewed by:
Mira Jakovcevski, Max Planck Institute of Psychiatry (MPI), Germany
Wen-Jun Gao, Drexel University, United States

***Correspondence:**
Amy F. T. Arnsten
amy.arnsten@yale.edu

Specialty section:
This article was submitted to Molecular Psychiatry, a section of the journal Frontiers in Psychiatry

Received: *15 January 2021*
Accepted: *25 February 2021*
Published: *09 April 2021*

Citation:
Yang S, Seo H, Wang M and Arnsten AFT (2021) NMDAR Neurotransmission Needed for Persistent Neuronal Firing: Potential Roles in Mental Disorders. Front. Psychiatry 12:654322. doi: 10.3389/fpsyt.2021.654322

The dorsolateral prefrontal cortex (dlPFC) generates the mental representations that are the foundation of abstract thought, and provides top-down regulation of emotion through projections to the medial PFC and cingulate cortices. Physiological recordings from dlPFC Delay cells have shown that the generation of mental representations during working memory relies on NMDAR neurotransmission, with surprisingly little contribution from AMPAR. Systemic administration of low "antidepressant" doses of the NMDAR antagonist, ketamine, erodes these representations and reduces dlPFC Delay cell firing. In contrast to the dlPFC, V1 neuronal firing to visual stimuli depends on AMPAR, with much less contribution from NMDAR. Similarly, neurons in the dlPFC that respond to sensory events (cue cells, response feedback cells) rely on AMPAR, and systemic ketamine increases their firing. Insults to NMDAR transmission, and the impaired ability for dlPFC to generate mental representations, may contribute to cognitive deficits in schizophrenia, e.g., from genetic insults that weaken NMDAR transmission, or from blockade of NMDAR by kynurenic acid. Elevated levels of kynurenic acid in dlPFC may also contribute to cognitive deficits in other disorders with pronounced neuroinflammation (e.g., Alzheimer's disease), or peripheral infections where kynurenine can enter brain (e.g., delirium from sepsis, "brain fog" in COVID19). Much less is known about NMDAR actions in the primate cingulate cortices. However, NMDAR neurotransmission appears to process the affective and visceral responses to pain and other aversive experiences mediated by the cingulate cortices, which may contribute to sustained alterations in mood state. We hypothesize that the very rapid, antidepressant effects of intranasal ketamine may involve the disruption of NMDAR-generated aversive mood states by the anterior and subgenual cingulate cortices, providing a "foot in the door" to allow the subsequent return of top-down regulation by higher PFC areas. Thus, the detrimental vs. therapeutic effects of NMDAR blockade may be circuit dependent.

Keywords: NMDAR (NMDA receptor), prefrontal cortex, cingulate cortex, working memory, depression

INTRODUCTION

The recent discovery that the NMDA receptor (NMDAR) antagonist, ketamine, can produce rapid, antidepressant actions has stirred interest in the possible mechanisms underlying these therapeutic effects, and why blockade of NMDAR can produce such a swift change in mood. The current review discusses how NMDAR-calcium mechanisms are needed for sustained neural representations, e.g., such as the persistent representation of visual space in working memory by circuits in the dorsolateral prefrontal cortex (dlPFC), and suggests that parallel mechanisms in the cingulate circuits mediating mood and emotion may be overactivated in depression, and aided by NMDAR blockade (1, 2).

NMDAR are heterotetramers composed of GluN1 and GluN2 (A-D) or GluN3 (A-B) subunits- usually with two GluN1 and two GluN2 subunits (3). The GluN2B subunit, also known as the NR2B subunit, has been of particular interest, as it closes more slowly than the common, GluN2A subunit, and fluxes high levels of calcium into the neuron (4). Although previous research in rodent classic circuits had found that NMDA-GluN2B were mostly at extra-synaptic locations (5), or played a role only in immature neurons (6), more recent research has shown that GluN2B play a critical, synaptic role in the primate cortical circuits mediating higher cognition, providing the synaptic events that generate sustained representations of visual space in working memory in the dlPFC (7, 8). The high levels of calcium influx into spines may be especially important for maintaining a depolarized post-synaptic membrane, permitting continued neural firing needed to sustain representations over long time periods (9). Recent research has also shown that expression of NMDAR with GluN2B subunits encoded by the *GRIN2B* gene expands across primate cortical evolution (10), and across the cortical hierarchy in humans, with especially high levels in association and limbic cortices such as the anterior cingulate cortex (11). The following paper explores the hypothesis that the critical role of GluN2B in generating sustained representations in dlPFC may extend to the generation of aversive mood state by the anterior and subgenual cingulate cortices, and that NMDAR blockade by ketamine may be helpful by relieving this self-perpetuating, aversive network activity.

Abbreviations: ACC, anterior cingulate cortex; AMPAR, α-amino-3-hydroxy-5-methyl-4-isoxazolepropionic acid receptor, an ionotropic glutamate receptor; BA24, Brodmann's area 24, part of the anterior cingulate cortex; BA25, Brodmann's area 25, also known as the subgenual cingulate cortex; BA32, Brodmann's area 32, part of the ventromedial cortex; BA46, Brodmann's area 46, part of the dorsolateral prefrontal cortex; dlPFC, dorsolateral prefrontal cortex; GABA, Gamma-AminoButyric Acid, an inhibitory neurotransmitter; GluN2B, a subunit of the NMDAR, which closes slowly and fluxes high levels of calcium; HPA axis, Hypothalamus Pituitary Adrenal gland axis for control of cortisol release from the adrenal cortex (corticosterone in rodents); immunoEM, Immunoelectron microscopy; PFC, prefrontal cortex; LIP, lateral intraparietal cortex specialized for analyzing visual space; M1R, cholinergic muscarinic M1 receptor; mPFC, medial prefrontal cortex; MT, middle temporal visual cortical area specialized for analyzing visual motion; Nic, α7R, cholinergic nicotinic α7 receptor; NMDAR, N-methyl-D-aspartate receptor, an ionotropic glutamate receptor; PFC, prefrontal cortex; PSD, postsynaptic density; V1, primary visual cortex.

The paper will briefly review PFC circuits in primates and their regulation of the cingulate cortices, and then discuss the critical role of NMDAR for generating mental representations in dlPFC, the expansion in NMDAR-GluN2B transmission across the cortical hierarchy and across cortical evolution, and the role of NMDAR-GluN2B in the cingulate cortices mediating affective pain responses and depression. It will briefly discuss how stress exposure impairs higher PFC regulation, and will close with an exploration of the idea that ketamine's rapid antidepressant actions may involve blocking mental representations of aversive mood state in the cingulate cortices.

PRIMATE PREFRONTAL CORTICAL CIRCUITS

The PFC greatly expands and differentiates over brain evolution, allowing representations of information in the absence of sensory stimulation. The primate PFC is topographically organized across multiple dimensions, e.g., with "simpler" representative functions found more caudally and more complex (e.g., metacognition) more rostrally in the frontal pole (12, 13). There are also topographic differences across the dorsolateral to ventromedial dimensions (14), where the dlPFC represents the outer world (e.g., with inputs from parietal areas that process visual space, **Figure 1A**), while the ventral and medial PFC regions represent the inner world, including taste and olfaction combining to represent flavor in orbital (ventral) PFC, and projections from the medial thalamus to the medial anterior cingulate cortex (ACC, BA24) mediating the emotional aspects of pain (**Figure 1A**). Neurons in the dorsomedial PFC also can represent persistent signatures of loss during a competitive game (15), and anterior cingulate neurons respond to errors (16), suggesting these regions are also activated by aversive psychological events. This information is relayed to the subgenual cingulate (BA25) that has extensive visceromotor connections to induce the physical aspects of the emotional response to pain [**Figure 1A**; (14)]. For example, BA25 projects to the amygdala, and the hypothalamus and brainstem to effect the autonomic nervous system and facial expression, and to the periaqueductal gray and medial subthalamic nucleus to alter behavioral response (14, 17–19), e.g., "freezing" behavior in response to a threat.

The more newly evolved, rostral and lateral areas of PFC provide top-down regulation of the more primitive medial and caudal areas. For example, the dlPFC can regulates emotion via direct projections to BA24 (20, 21), and indirect projections to BA25 via BA10m or BA32 to BA25 (22, 23) (**Figure 1A**). The pathways from dlPFC to BA32 and then to BA25 are now known in great detail at the ultrastructural level (23–25), showing how dlPFC and BA32 are positioned to either inhibit or activate emotional responses by BA25.

An important note about species differences: rodents do not have rostral PFC areas (e.g., frontal pole) or a dlPFC, and even the medial and orbital PFC areas they do have are much less developed and differentiated than those in primates (26). Indeed, the dorsal to ventral topography of medial PFC

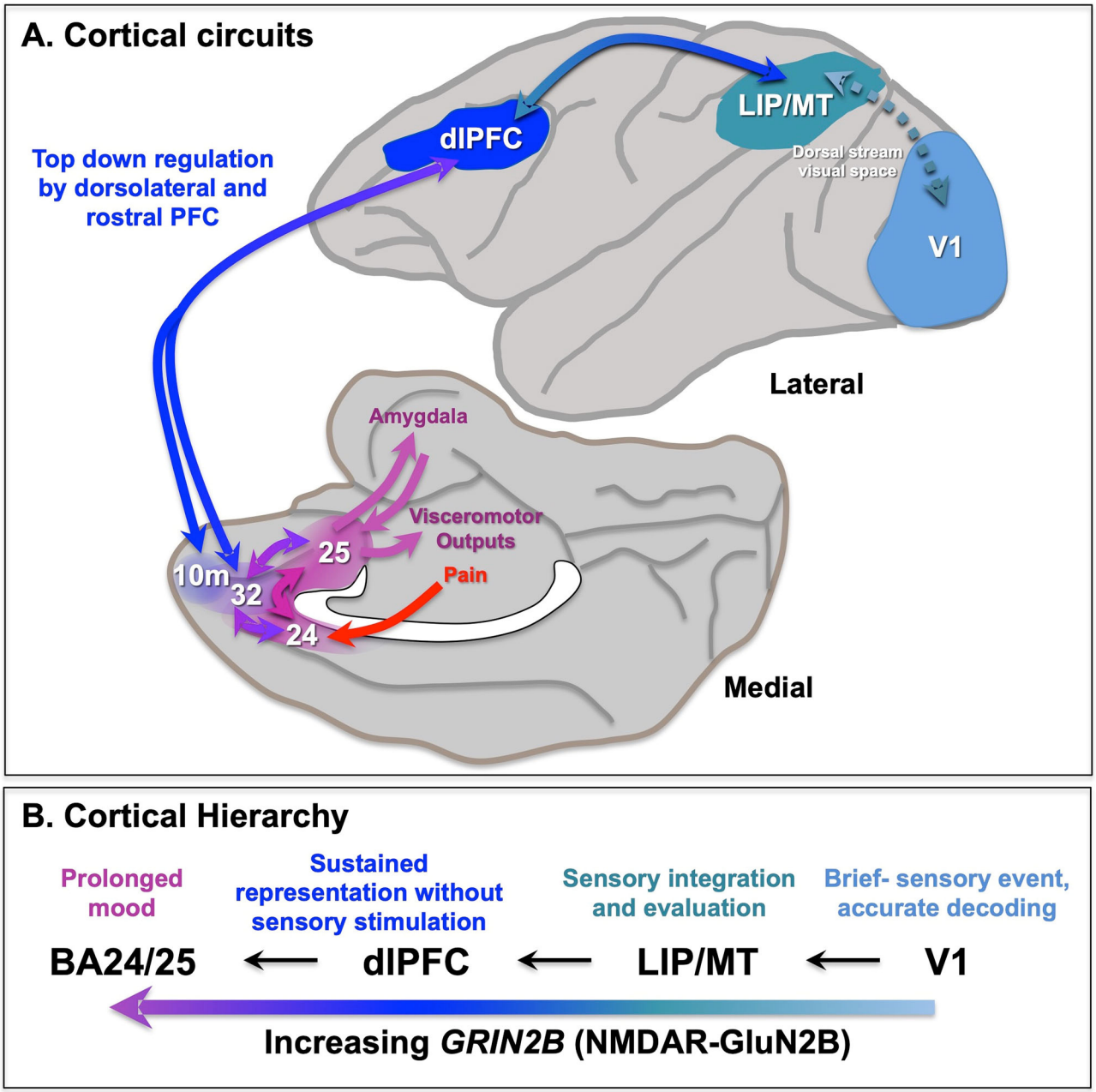

FIGURE 1 | Primate cortical circuits. **(A)** Schematic diagram of circuits in the rhesus monkey cortex, where the lateral surface represents the outer world, and the medial and orbital surface represents inner state. The dorsal stream is shown on the lateral surface, where dlPFC represents visual space in working memory, and generates the goals for top-down regulation of emotion. The medial surface shows the pathways mediating the emotional response to pain, arising from medial thalamic projections to the insular cortex (not shown) and the anterior cingulate cortex BA24, which both project to BA25 (subgenual cingulate). BA25 is a major center for visceromotor outputs, e.g., to the amygdala, brainstem, and hypothalamus to alter heart rate. These cingulate cortices are often overactive in depression, and a target of DBS treatments. The dlPFC provides top-down regulation of emotion through indirect projections to BA25 via areas BA10m and BA32, and direct projections to BA24 (not shown). **(B)** The increasing timescales across the primate cortical hierarchy, and their relationship to GRIN2B expression. Based on (11) and (9). LIP, lateral intraparietal cortex; MT, middle temporal visual cortex.

subregions appears to be reversed from rodent to monkey, with the most ventral BA25 activating the stress response in monkeys, but inhibiting it in rodents (27). This may be due to the medial PFC being less differentiated in rodents, with a dorsal-ventral gradient in many medial PFC connections (28). Thus, the actual circuit connections, e.g., with excitatory vs. inhibitory neurons in amygdala, need to be identified for proper interpretation.

THE CRITICAL ROLE OF NMDAR-Glun2B IN THE GENERATION OF MENTAL REPRESENTATIONS BY THE dlPFC

The primate dlPFC has the remarkable ability to generate and sustain mental representations without sensory stimulation, the foundation of abstract thought (29). dlPFC "Delay cells" are able to maintain persistent firing across the delay period in a working memory task, sustaining representations over many seconds e.g., remembering a position in visual space (30). "Delay cells" appear to reside in pyramidal cell microcircuits in deep layer III of the dlPFC that have extensive recurrent excitatory connections [**Figure 2A**; (29, 31)], as well as lateral inhibition from parvalbumin-containing interneurons to refine spatial tuning (29, 32). The persistent firing of Delay cells across the delay period depends on NMDAR stimulation (7), a finding predicted by computational models (33). Thus, iontophoresis (local electrical application) of low doses of NMDAR antagonists, including antagonists that selectively block those with GluN2A or GluN2B subunits, markedly reduces Delay cell firing (7). An example is shown in **Figure 2B**, where under control conditions a Delay cell can sustain the representation of the cue that had been flashed at 270° over many seconds in working memory. However, the Delay cell is no longer able to represent spatial information in working memory following the local iontophoretic blockade of NMDAR GluN2B with the antagonist, TCN237.

Immunoelectron microscopy (immunoEM) showed that NMDAR-GluN2B are expressed exclusively within the post-synaptic density (PSD) in layer III dlPFC spines, and are *not* extra-synaptic, consistent with their direct mediation of

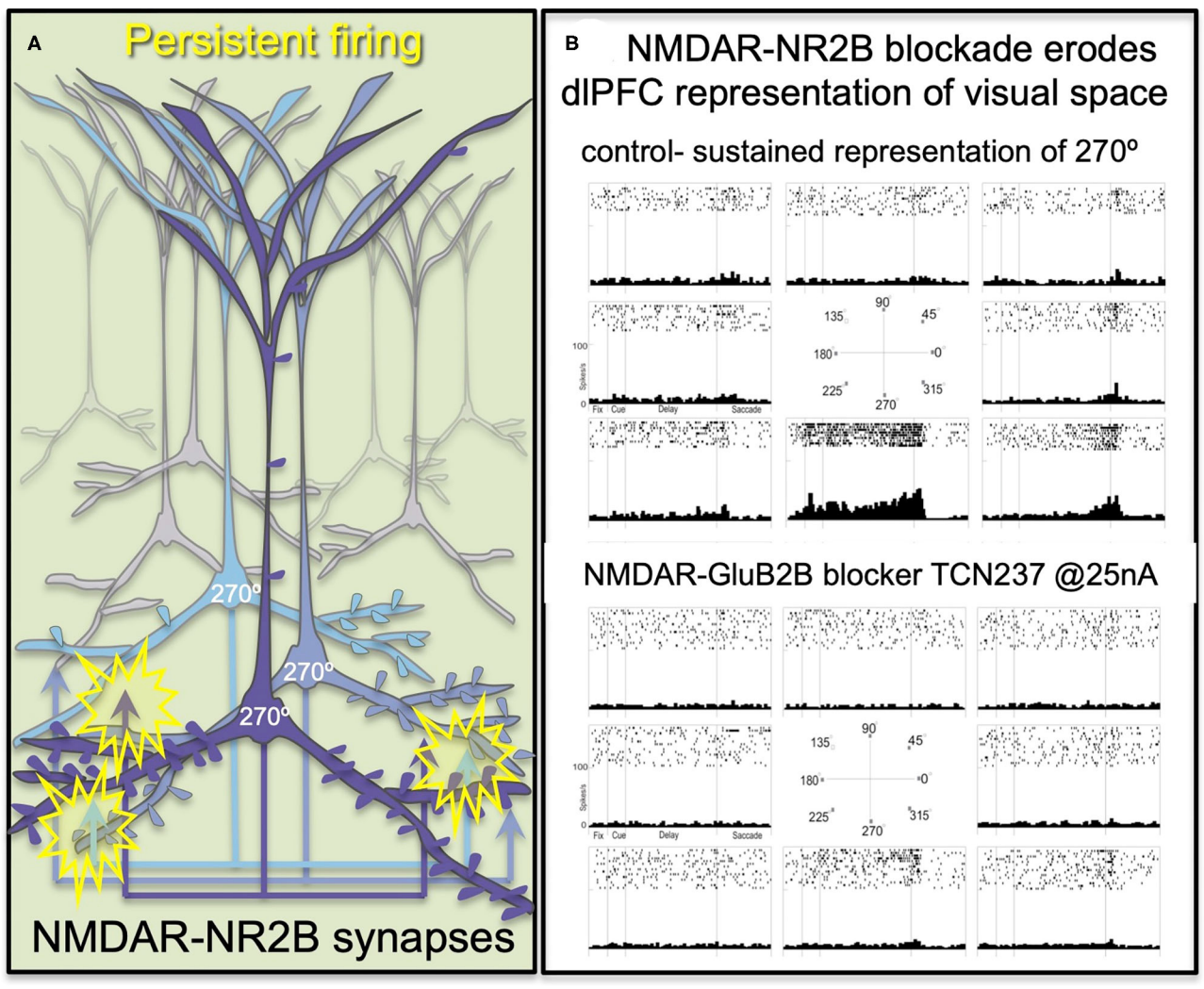

FIGURE 2 | The persistent firing of dlPFC Delay cells depends on NMDAR with GluN2B subunits. **(A)** Schematic illustration of the recurrent excitatory microcircuits in deep layer III of dlPFC that generate persistent firing. **(B)** A dlPFC Delay cell that represents the spatial position of 270° during a spatial working memory task, maintaining firing across the delay period for only that preferred location. Iontophoresis of the selective NMDAR- GluN2B antagonist, TCN237, completely blocks the ability of the neuron to generate representations of visual space.

neurotransmission (7). The ability of GluN2B subunits to flux large amounts of calcium may be a key aspect of why they support persistent firing in computational models (33) and in Delay cells (7).

In contrast to NMDAR, blockade of AMPAR has remarkably subtle effects on Delay cell firing (7) (**Figures 3A,B**). This finding was initially confusing, as it is generally thought that AMPAR are essential to depolarize the PSD membrane and relieve the magnesium (Mg^{2+}) block within the NMDAR pore, permitting NMDAR actions (**Figure 3C**). However, in dlPFC, this key permissive role appears to be played by acetylcholine acting at Nic-α7R and muscarinic M1R within the glutamate synapse (34, 35) which may depolarize the PSD to support persistent firing (**Figures 3A,B**). M1R may depolarize the PSD via closing of KCNQ channels localized in the PSD, and/or by enhancing levels of internal calcium release. These physiological data are consistent with behavioral data showing that Ach depletion from dlPFC is as deleterious as removing the cortex itself (36). As acetylcholine is released during wakefulness but not deep sleep, these mechanisms also help to coordinate cognitive state with arousal state, permitting conscious experience during wakefulness, but may render us unconscious during deep sleep when there is no acetylcholine release. Thus, as summarized in **Figures 3A,B**, Delay cell firing in dlPFC depends on NMDAR stimulation, including those with GluN2B subunits, with permissive actions by acetylcholine and more limited contributions from AMPAR.

AMPAR neurotransmission does play an important role in some dlPFC neurons that respond to sensory events, i.e., dlPFC Cue cells, and dlPFC response feedback cells that are thought to convey the corollary discharge back to dlPFC that the intended motor response has occurred (7). As these events require accurate timing, it is logical that they would have more of a reliance on rapid AMPAR neurotransmission.

Systemic ketamine treatment has differential effects on dlPFC neuronal firing depending upon their reliance on AMPAR vs. NMDAR neurotransmission. Consistent with their reliance on NMDAR neurotransmission, dlPFC Delay cells show *decreased* firing following systemic administration of the NMDAR antagonist, ketamine, at low doses used to treat intractable depression (7). This is only seen during cognitive performance and is not evident at rest. In contrast, systemic ketamine administration *increases* the spontaneous firing of response feedback neurons that rely on AMPAR (7), which resembles the increased firing seen with deep layer neurons in rat mPFC following NMDAR blockade, the basis for the "glutamate surge" (37). Some of this heterogeneity may arise from the balance of NMDAR on pyramidal cells vs. GABAergic interneurons, where pyramidal cell circuits with extensive recurrent NMDAR excitation may show loss of firing, while those circuits with extensive NMDAR on interneurons (e.g., in the primary sensory cortices) may have an overall increase in glutamate signaling. These data caution that ketamine's actions are heterogeneous, and that methods that average the response of large populations of neurons under resting conditions (e.g., resting fMRI, multi-electrode recording) may miss critical ketamine actions such as the loss of representations during working memory. The fact that ketamine's effects are circuit-specific creates a complicated picture, confounding our ability to identify the specific actions relevant to its antidepressant effects, distinguished from its actions that lead to cognitive disorder.

The importance of NMDAR transmission to the generation of mental representations needed for working memory and abstract thought may have relevance to a number of conditions where NMDAR are blocked or genetically weakened. The data from monkeys help to explain the profound cognitive alterations that can occur in the encephalitis arising from anti-NMDAR antibodies (38). The loss of mental representations with NMDAR blockade also helps to explain the profound cognitive impairments in schizophrenia where there can be genetic mutations that weaken NMDAR signaling (39), and/or blockade of NMDAR by kynurenic acid, especially under conditions of inflammation (40). Blockade of NMDAR by kynurenic acid may also contribute to cognitive deficits in Alzheimer's disease (41), given the importance of inflammatory signaling in early stages of disease. It is also possible that systemic infection may impair higher brain functions through the uptake of kyrurenine across the blood brain barrier (42). For example, the pervasive cognitive deficits in delirium might arise from high levels of kyrurenine crossing into the brain during systemic infection (43), and that the residual "brain fog" from infections such as COVID19 (44–46), which also leads to systemic kynurenine production, may also involve sustained blockade of NMDAR in higher cortical circuits by kynurenic acid. As there are pharmacological tools to reduce kynurenine production that may relieve NMDAR blockade, these are important areas for future research.

NMDAR-Glun2B EXPRESSION INCREASES ACROSS THE PRIMATE CORTICAL HIERARCHY AND ACROSS PRIMATE EVOLUTION

There are multiple differences in function and physiology across the cortical hierarchy from primary sensory cortices, to association cortices to limbic cortices (**Figure 1B**). For example, there are increasing time scales in neuronal firing across the cortical hierarchy in rhesus monkeys (47) and in gray/white matter ratios in humans that correspond to transcriptional expression patterns (11). In particular, there is increasing expressing of the NMDAR GluN2B gene, *GRIN2B,* across the cortical hierarchy in humans, with low levels in primary visual cortex, high levels in dlPFC, and higher levels still in anterior cingulate cortices (11). As *GRIN2B* expression in dlPFC also increases across primate evolution, it suggests that this receptor plays an increasing role in primate mental experience.

Physiological studies in rodents (48) and monkeys are consistent with this hypothesis, as NMDAR-GluN2B has a much larger role in neurotransmission in the PFC than in the primary visual cortex, area V1. In rat medial PFC, the recurrent excitatory connections in layer V depend on NMDAR-GluN2B neurotransmission, while neurons in V1 showed much less reliance on these receptors (48). Similar results were seen in rhesus monkey dlPFC vs. V1. Neurons in V1 respond to

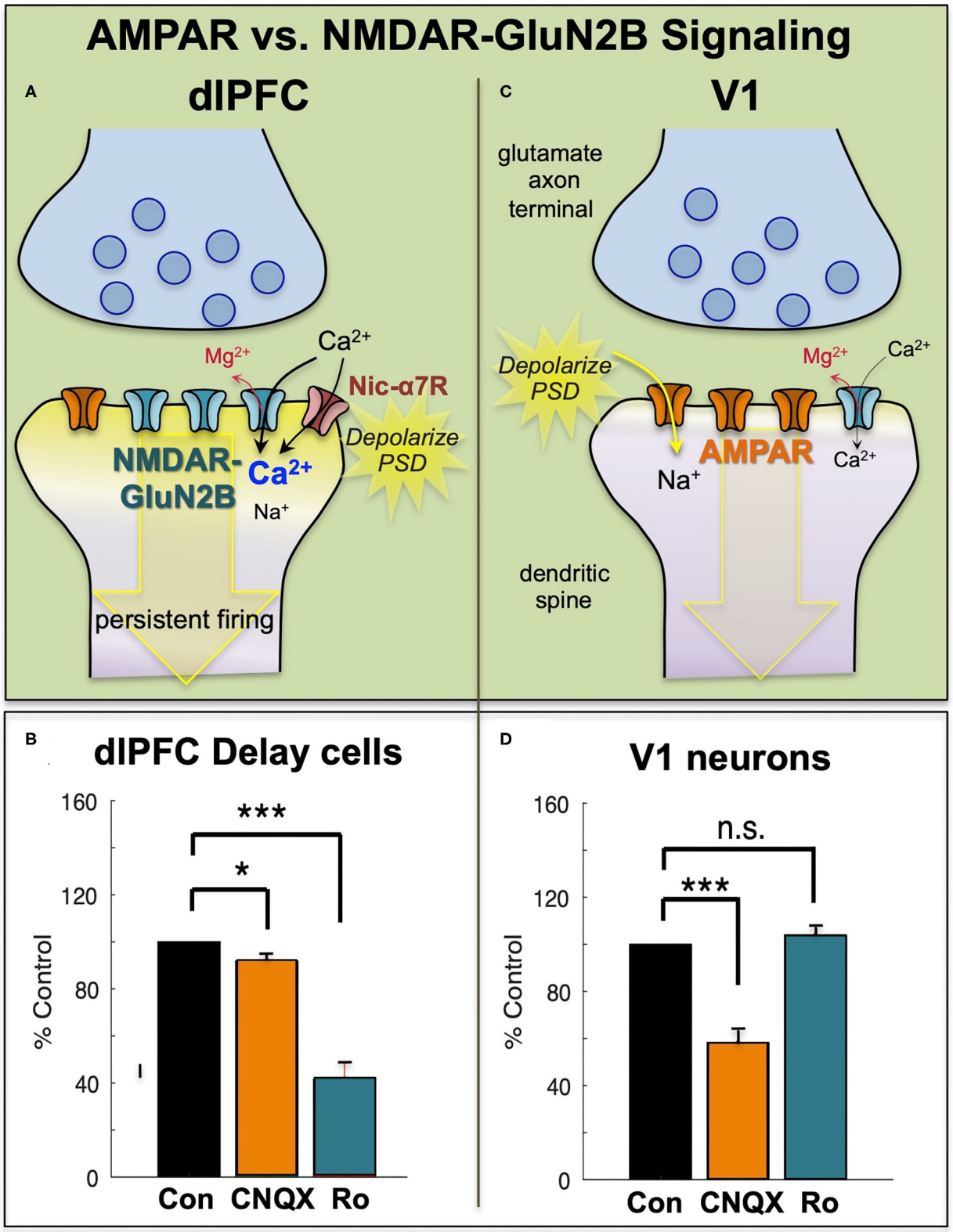

FIGURE 3 | The primate dlPFC and primary visual cortex (V1) have very different neurotransmission. **(A)** The dlPFC depends on NMDAR neurotransmission, including those with slowly closing GluN2B subunits, that are exclusively within the PSD. The permissive excitatory effects to relieve the magnesium (Mg^{2+}) block of the NMDAR

(Continued)

FIGURE 3 | ion channel are provided by acetylcholine (including Nic-a7R), with a surprisingly small influence from AMPAR. **(B)** Iontophoresis of the AMPAR antagonist, CNQX, has only subtle effects on dlPFC Delay cell firing, while blockade of NMDAR- GluN2B with Ro25-6981 (Ro) markedly reduces Delay cell firing. **(C)** Neurons in primate V1 show a more classic profile, relying heavily on AMPAR neurotransmission, with less influence by NMDAR. **(D)** Iontophoresis of low doses of the AMPAR antagonist, CNQX, markedly reduces V1 neuronal firing, while blockade of NMDAR- GluN2B with Ro has little effect. Adapted from (9) and (8). $^{*}p < 0.05$, $^{***}p < 0.001$.

the presentation of visual stimuli of a preferred orientation in their receptive field. These neurons have a great reliance on AMPAR transmission, where even low doses of AMPAR blockers such as CNQX markedly reduce stimulus-related firing (8) (**Figures 3C,D**). In contrast, high doses of NMDAR blockers are needed to reduce V1 neuronal firing [(8), **Figures 3C,D**]. A reliance on AMPAR stimulation is consistent with the function of V1 neurons, as the rapid kinetics of these receptors, in addition to their membrane properties (49), would allow accurate timing to encode the onset and offset of a sensory event. Thus, NMDAR transmission is not uniform across the primate cortex, and may be a feature of neurons requiring sustained neuronal firing for cognitive and possibly affective functions.

The very high levels of *GRIN2B* expression in the human anterior cingulate cortex (11) suggests that these receptor subtypes may be particularly important for the functioning of the cingulate cortices, e.g., in error detection, affective pain processing, and visceral affective responding. These limbic cortices and their corresponding connections are part of the neural networks that create "mood," a sustained brain state. Given the role of NMDAR-GluN2B in mediating sustained firing in dlPFC, it is possible that these receptors have a parallel role in anterior and subgenual cingulate cortex. Although there are currently no direct iontophoretic recordings from primate anterior or subgenual cingulate cortex examining the role of GluN2B in cingulate physiology, this will be an important arena for future research. The following section outlines the importance of these receptors to cingulate processing of pain and visceral responding.

THE ROLE OF NMDAR-GluN2B IN THE CINGULATE CORTICES MEDIATING AFFECTIVE PAIN RESPONSES AND DEPRESSION

The anterior cingulate (BA24) and subgenual cingulate (BA25) cortices mediate the emotional responses to pain [(14), reviewed in (2)], and are overactive in depression (50, 51). For example, the ACC is overactive in chronic pain and is a common ablation site for neurosurgical alleviation of intractable pain (52). In particular, BA25 in particular overactive in depression and a focus of deep brain stimulation (DBS) to relieve intractable depression (51). As described below, there is accumulating evidence that the emotional responses of the anterior and subgenual cingulate cortices rely on NMDAR-GluN2B neurotransmission, and that these aversive responses are reduced by ketamine administration in the treatment of chronic pain and depression.

Increasing evidence indicates that the response to pain in the rodent ACC (BA24) is mediated by NMDAR, including those with GluR2B subunits (53). GluR2B upregulate in response to chronic pain (54, 55), and long-term potentiation in the anterior cingulate cortex in response to painful stimuli is mediated by NMDAR-calcium-cAMP signaling, including NMDAR with GluR2B subunits, consistent with the sensitized response to chronic pain [reviewed in (56, 57)]. Systemic administration of ketamine, or of its active enatiomer, esketamine, reduces the response to pain as well as accompanying depressive symptoms in both rodents (58) and humans (59–62).

The subgenual cingulate (BA25) has extensive subcortical projections to mediate the emotional and visceral response to pain or other affective experiences (14), including to the lateral habenula (63), a nucleus activated by aversive events (64). Recent studies in marmosets have illuminated its functional role and relationship to ketamine treatment. These studies showed that pharmacological inactivation of BA25 decreased the autonomic and behavioral correlates of negative emotion expectation, while inactivation of BA32 increased them via generalization (27), consistent with BA32 providing top-down regulation of BA25. Conversely, activation of BA25 in marmosets induced an anhedonic state and reduced willingness to work for reward that was reversed by systemic administration of ketamine (65). 18F-FDG PET imaging of the marmosets showed that activation of BA25 was accompanied by activation of BA24 and insular cortex, while systemic ketamine treatment reduced the activation of these cortical areas (65). Over-activation of BA25 in marmosets also reduced vagal tone and heart rate variability, reduced the extinction of an aversive response and potentiated cortisol release during threat (66). Activation of BA25 in this study was associated with increased activity in the amygdala, the hypothalamus, and the temporal association area TH (66), but decreased the activity of the frontopolar cortex area 9, the dlPFC area 46, the central orbitofrontal cortex area13, and the lateral caudate (66). However, in this study, systemic ketamine did not reverse the effects of threat, suggesting that primitive responses to threat (e.g., in amygdala) may still control network activity. These data suggest that ketamine treatment may be most effective under conditions of safety. Research is still needed to determine how local infusion of ketamine into BA24 and/or BA25 alters emotional responding.

UNCONTROLLABLE STRESS IMPAIRS HIGHER PFC FUNCTIONS

The findings from the Roberts lab that activation of BA25 in marmoset reduces the activity of the rostral PFC and the dlPFC are consistent with a long line of research showing that these more newly evolved PFC areas are weakened by exposure to uncontrollable stress. As described above, under control conditions the dlPFC and rostral PFC can regulate emotion via projections to BA25 (**Figures 1A**, **4A**), which in

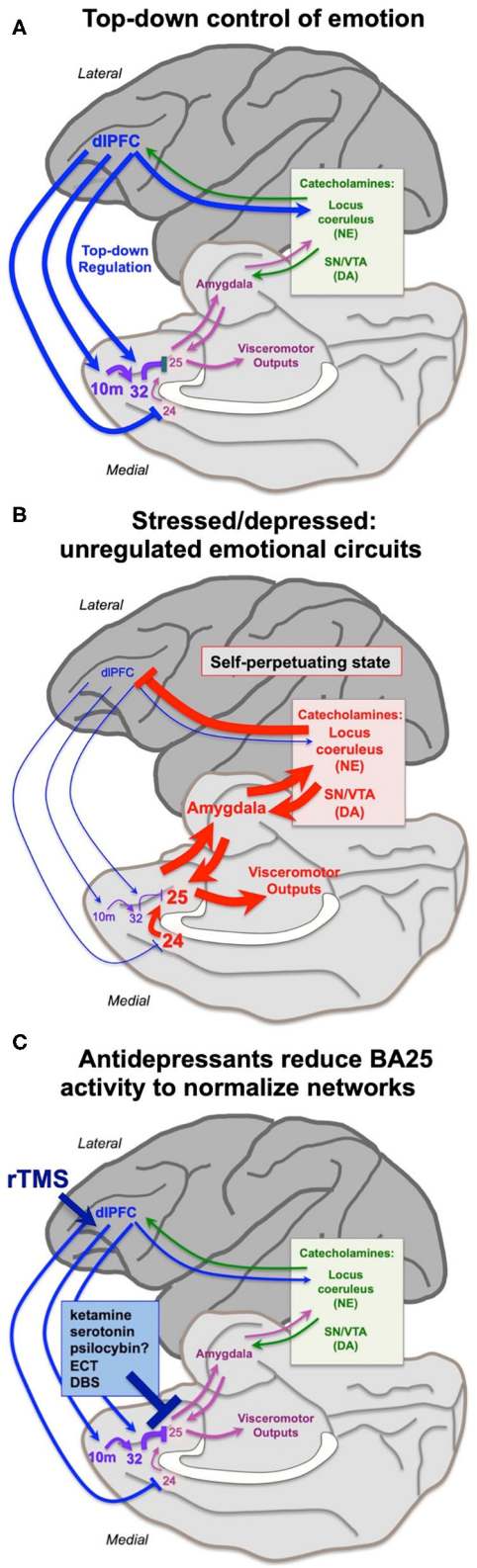

FIGURE 4 | Hypothesis regarding the state of cortical circuits under conditions of health vs. depression, and their normalization by antidepressant treatments. *(Continued)*

FIGURE 4 | (A) Under healthy conditions, the dlPFC and rostral medial PFC areas provide top-down regulation of the cingulate cortices via medial PFC connections, reducing BA25 activation of the stress response. The dlPFC also projects directly to the monoamine nuclei in the brainstem to regulate catecholamine release. **(B)** Under conditions of stress or depression, elevated activity in the cingulate cortices can activate the amygdala, and very high levels of catecholamine release in cortex takes higher PFC areas such as dlPFC "offline." Thus, there is a self-perpetuating, unregulated state, where primitive circuits prevail. **(C)** Many antidepressant treatments reduce the activity of BA25. This may give the cortex a "foot in the door" to restore top-down regulation, especially when treatments promote dendritic spine restoration in higher PFC circuits. Other treatments may directly enhance the top-down regulation by the left dlPFC, e.g., rTMS and insight therapies.

turn can control the activity of the brain's emotional circuits, including the amygdala, hypothalamus and brainstem (23, 25). A recent imaging study observed these rapid dynamics in human brain, where uncontrollable stress exposure initially reduced the activity of BA32, which then normalized in correspondence with reducing the stress response, and BA32 increased its functional connectivity with the dlPFC (67).

The more primitive cingulate and amygdala circuits may remove the top-down regulation by higher PFC circuits through activation of catecholamine neurons in the brainstem, which can weaken PFC connectivity. The PFC and cingulate cortices receive catecholamine innervation (68) and can also regulate the activity of the monoamine nuclei in the brainstem (18, 63, 69). The dlPFC requires moderate levels of catecholamines to function, but high levels of catecholamines released during even mild uncontrollable stress rapidly take the dlPFC "offline" [reviewed in (9, 70)]. Studies in rodents have shown that psychological stressors or threatening stimuli activate projections from the amygdala, e.g., to the locus coeruleus, increasing catecholamine release in the medial PFC (71–76). High levels of catecholamines in dlPFC drive feedforward calcium-cAMP signaling, opening nearby potassium (K^+) channels on spines to rapidly weaken synaptic efficacy. This reduces the recurrent excitation underlying the persistent neuronal firing needed for mental representations [reviewed in (77, 78)]. High levels of glucocorticoids, released due to hypothalamic-pituitary-adrenal (HPA) actions, can also impair PFC working memory function (79), and may do so in part by blocking the extraneuronal catecholamine transporters on glia, which normally serve to reduce catecholamine levels in the extracellular space (80). In contrast to the dlPFC, high levels of catecholamines and glucocorticoids enhance the affective functioning of the amygdala (81–83), thus flipping the brain from a reflective to reflexive state. The rapid loss of dlPFC executive and working memory functions from a hypercatecholaminergic state has now been documented in humans (84–86) in addition to the original studies in rodents and monkeys (9, 77, 78). Thus, BA25 and amygdala can rapidly remove their regulation from higher order PFC circuits through activation of excessive catecholamine release in these higher PFC regions (**Figure 4B**). The cingulate cortices may also inhibit dlPFC by activating inhibitory GABAergic interneurons in the dlPFC (87).

This state of weakened higher PFC circuits and stronger BA24/BA25/amygdala control of brain responding is codified by chronic stress, which induces spine loss and dendritic retraction in PFC neurons which correlate with impaired working memory and attention regulation (88–90). Much of this research has been done in rats, where it is important to identify the projections of the neurons under study. Shansky's (91) elegant studies have shown that chronic stress exposure causes atrophy of cortico-cortical projecting mPFC neurons, but expands the dendrites of PFC neurons that activate the amygdala (i.e. those that are similar to primate BA25). Weaker connectivity and reduced gray matter in higher PFC circuits following chronic stress exposure has also been documented in humans (92, 93). Thus, chronic stress can create a self-perpetuating state where high levels of BA25/amygdala activity maintain a high catecholamine state, which simultaneously strengthens the amygdala but weakens higher PFC areas, removing inhibitory regulation of emotional response (**Figure 4B**). It is not known how catecholamines alter the activity of BA24 or BA25 in primates; this would be an important area for future research. Studies in rats have shown that the spine loss and dendritic retraction caused by chronic stress exposure can reverse with substantial time spent in a non-stressed state, at least in young animals, indicating a plastic dendritic response (94).

HYPOTHESIS: THE RAPID ANTIDEPRESSANT ACTIONS OF KETAMINE MAY ARISE FROM BLOCKADE OF MENTAL REPRESENTATIONS GENERATING AVERSIVE MOOD STATE IN CINGULATE CORTICES

The loss of rostral PFC and dlPFC activity in concert with increased cingulate and amygdala activation would shift mental state from an outward, cognitively-engaged frame of mind to one focused inwardly on aversive experience. This is common in depression, where there is often loss of perspective, reduced empathy for others, anhedonia, and an urgent need for relief of mental anguish (95). Symptoms such as loss of motivation and psychomotor paralysis might also arise from BA25 activation of the peri-aqueductal gray and subthalamic nucleus that are positioned to reduce motor, cognitive and affective actions. Thus, the overactive subgenual cingulate must be inhibited to give more rostral PFC and dlPFC areas a "foot in the door" to regain regulation of the brain, including the regrowth of spines in higher PFC areas (96, 97), to restore top-down higher network connections.

We have hypothesized that ketamine interrupts the self-perpetuating cycle of primitive circuit activity that is sustained by BA25 overactivity, allowing higher PFC circuits the opportunity to restore more normal functioning [**Figures 4B,C**; (2)]. As noted by Mayberg (51), all effective antidepressant treatments, whether pharmacological (selective serotonin reuptake inhibitors (SSRIs), possibly psilocybin?), electrical (ECT, DBS) or cognitive (talk therapy, CBT), reduce BA25 hyperactivity in depressed patients (**Figure 4C**). rTMS (repetitive transcranial magnetic stimulation) to strengthen the functioning of the left dlPFC may also help to restore regulation of the cingulate cortices (**Figure 4C**), as the efficacy of this treatment correlates with reduced activity of the anterior cingulate cortex (98), and weaker connectivity of the subgenual cingulate cortex (99). The antidepressant effects of SSRIs may be related to the very high levels of serotonin transporters in BA25 (100), although research is still needed to determine the receptor mechanisms by which serotonin can inhibit BA25 neuronal firing. We have proposed that ketamine's therapeutic effects may arise from ultra-rapid inhibition of BA25 neurons (2). As described above, systemic ketamine administration can overcome the deleterious effects of BA25 over-activation in marmosets (65), and can also normalize BA25 hyperactivity in depressed subjects (101), which may involve blockade of NMDAR transmission in the cingulate circuits representing a sustained, aversive state. Ketamine also reduces burst firing in the habenula, which may also contribute to its ultrarapid therapeutic effects (64).

Intranasal ketamine or esketamine administration may produce ultra-rapid antidepressant effects by delivering the drug directly to the anterior and subgenual cingulate cortices, which reside directly caudal to the nasal epithelium (2). Ultra-rapid effects have been documented following this route of administration, with significant improvement at 40 min (102), maximal improvement at 24 h, with therapeutic effects waning, but still evident at 48 h post-administration (102). We have proposed that the initial improvement at 40 min would arise from NMDAR blockade of excessive neuronal firing in the anterior and subgenual cingulate cortices, allowing a restoration of regulation by higher PFC areas, where spine growth would provide more sustained antidepressant actions (2).

Support for this hypothesis comes from a remarkable recent rodent study, where dendritic spine changes in medial PFC could be monitored *in vivo* (103). Prolonged exposure to chronic unpredictable stress increased "depressive-like behaviors" in the mice, and caused a retraction of dendritic spines in the mPFC, while systemic administration of ketamine normalized behavior and restored spine density (103). However, this study found that ketamine improved behavior *prior* to spine re-emergence (103), suggesting that the initial beneficial effects may arise from alterations in neuronal firing, while the longer-term, sustained antidepressant response requires regrowth of spines in PFC circuits that provide top-down regulation. Finally, our data from the dlPFC in monkeys would suggest that ketamine levels would need to dissipate before full dlPFC function could be restored, given the reliance of layer III dlPFC circuits on NMDAR-GluN2B neurotransmission. This hypothesis would be consistent with the maximal therapeutic effects observed 24 h after ketamine administration.

In closing, we are learning that NMDAR transmission is especially important for persistent neuronal firing. It is possible that the sustained neuronal activity underlying mood state, and particularly an aversive mental state, similarly relies on NMDAR transmission, and thus is relieved by NMDAR blockade from ketamine.

AUTHOR CONTRIBUTIONS

All authors listed have made a substantial, direct and intellectual contribution to the work, and approved it for publication.

FUNDING

This work was1 funded by R01 MH108643-01 to AA and R01 MH093354-05 to MW.

REFERENCES

1. Arnsten AF, Murray JD, Seo H, Lee D. Ketamine's antidepressant actions: potential mechanisms in the primate medial prefrontal circuits that represent aversive experience. *Biol Psychiatry.* (2016) 79:713–5. doi: 10.1016/j.biopsych.2016.02.014
2. Opler LA, Opler MG, Arnsten AFT. Ameliorating treatment-refractory depression with intranasal ketamine: potential NMDA receptor actions in the pain circuitry representing mental anguish. *CNS Spectrums.* (2016) 21:12–22. doi: 10.1017/S1092852914000686
3. Qiu S, Li XY, Zhuo M. Post-translational modification of NMDA receptor GluN2B subunit and its roles in chronic pain and memory. *Semin Cell Dev Biol.* (2011) 22:521–9. doi: 10.1016/j.semcdb.2011.06.003
4. Erreger K, Dravid SM, Banke TG, Wyllie DJ, Traynelis SF. Subunit-specific gating controls rat NR1/NR2A and NR1/NR2B NMDA channel kinetics and synaptic signalling profiles. *J Physiol.* (2005) 563:345–58. doi: 10.1113/jphysiol.2004.080028
5. Goebel-Goody SM, Davies KD, Alvestad Linger RM, Freund RK, Browning MD. Phospho-regulation of synaptic and extrasynaptic N-methyl-d-aspartate receptors in adult hippocampal slices. *Neuroscience.* (2009) 158:1446–59. doi: 10.1016/j.neuroscience.2008.11.006
6. Liu XB, Murray KD, Jones EG. Switching of NMDA receptor 2A and 2B subunits at thalamic and cortical synapses during early postnatal development. *J Neurosci.* (2004) 24:8885–95. doi: 10.1523/JNEUROSCI.2476-04.2004
7. Wang M, Yang Y, Wang CJ, Gamo NJ, Jin LE, Mazer JA, et al. NMDA receptors subserve working memory persistent neuronal firing In dorsolateral prefrontal cortex. *Neuron.* (2013) 77:736–49. doi: 10.1016/j.neuron.2012.12.032
8. Yang ST, Wang M, Paspalas CP, Crimins JL, Altman MT, Mazer JA, et al. Core differences in synaptic signaling between primary visual and dorsolateral prefrontal cortex. *Cereb Cortex.* (2018) 28:1458–71. doi: 10.1093/cercor/bhx357
9. Arnsten AFT, Datta D, Wang M. The genie in the bottle-magnified calcium signaling in dorsolateral prefrontal cortex. *Mol Psychiatry.* (2020). doi: 10.1038/s41380-020-00973-3. [Epub ahead of print].
10. Muntan,é G, Horvath JE, Hof PR, Ely JJ, Hopkins WD, Raghanti MA, et al. Analysis of synaptic gene expression in the neocortex of primates reveals evolutionary changes in glutamatergic neurotransmission. *Cereb Cortex.* (2015) 25:1596–607. doi: 10.1093/cercor/bht354
11. Burt JB, Demirta,s M, Eckner WJ, Navejar NM, Ji JL, Martin WJ, et al. Hierarchy of transcriptomic specialization across human cortex captured by structural neuroimaging topography. *Nature Neurosci.* (2018) 21:1251–9. doi: 10.1038/s41593-018-0195-0
12. Badre D, D'esposito M. Functional magnetic resonance imaging evidence for a hierarchical organization of the prefrontal cortex. *J Cogn Neurosci.* (2007) 19:2082–99. doi: 10.1162/jocn.2007.19.12.2082
13. Tsujimoto S, Genovesio A, Wise SP. Frontal pole cortex: encoding ends at the end of the endbrain. *Trends Cogn Sci.* (2011) 15:169–76. doi: 10.1016/j.tics.2011.02.001
14. Price DD. Psychological and neural mechanisms of the affective dimension of pain. *Science.* (2000) 288:1769–72. doi: 10.1126/science.288.5472.1769
15. Seo H, Lee D. Behavioral and neural changes after gains and losses of conditioned reinforcers. *J Neurosci.* (2009) 29:3627–41. doi: 10.1523/JNEUROSCI.4726-08.2009
16. Ito S, Stuphorn V, Brown JW, Schall JD. Performance monitoring by the anterior cingulate cortex during saccade countermanding. *Science.* (2003) 302:120–2. doi: 10.1126/science.1087847
17. An X, Bandler R, Ongür D, Price JL. Prefrontal cortical projections to longitudinal columns in the midbrain periaqueductal gray in macaque monkeys. *J Comp Neurol.* (1998) 401:455–79. doi: 10.1002/(SICI)1096-9861(19981130)401:4<455::AID-CNE3>3.0.CO;2-6
18. Freedman LJ, Insel TR, Smith Y. Subcortical projections of area 25 (subgenual cortex) of the macaque monkey. *J Comp Neurol.* (2000) 421:172–88. doi: 10.1002/(SICI)1096-9861(20000529)421:2<172::AID-CNE4>3.0.CO;2-8
19. Haynes WI, Haber SN. The organization of prefrontal-subthalamic inputs in primates provides an anatomical substrate for both functional specificity and integration: implications for Basal Ganglia models and deep brain stimulation. *J Neurosci.* (2013) 4804–14. doi: 10.1523/JNEUROSCI.4674-12.2013
20. Pandya DN, Dye P, Butters N. Efferent cortico-cortical projections of the prefrontal cortex in the rhesus monkey. *Brain Res.* (1971) 31:35–46. doi: 10.1016/0006-8993(71)90632-9
21. Pandya DN, Van Hoesen GW, Mesulam MM. Efferent connections of the cingulate gyrus in the rhesus monkey. *Exp Brain Res.* (1981) 42:319–30. doi: 10.1007/BF00237497
22. Barbas H, Pandya DN. Architecture and intrinsic connections of the prefrontal cortex in the rhesus monkey. *J Comp Neurol.* (1989) 286:353–75. doi: 10.1002/cne.902860306
23. Barbas H, Joyce MK, Garcia-Cabezas MA, John Y. Serial prefrontal pathways are positioned to balance cognition emotion in primates. *J Neurosci.* (2020). 40:8306–28. doi: 10.1523/JNEUROSCI.0860-20.2020
24. Barbas H, Wang J, Joyce MKP, García-Cabezas MÁ. Pathway mechanism for excitatory and inhibitory control in working memory. *J Neurophysiol.* (2018) 120:2659–78. doi: 10.1152/jn.00936.2017
25. Joyce MKP, Barbas H. Cortical connections position primate area 25 as a keystone for interoception, emotion, and memory. *J Neurosci.* (2018) 38:1677–98. doi: 10.1523/JNEUROSCI.2363-17.2017
26. Wise SP. Forward frontal fields: phylogeny and fundamental function. *Trends Neurosci.* (2008) 31:599–608. doi: 10.1016/j.tins.2008.08.008
27. Wallis CU, Cardinal RN, Alexander L, Roberts AC, Clarke HF. Opposing roles of primate areas 25 and 32 and their putative rodent homologs in the regulation of negative emotion. *Proc Natl Acad Sci USA.* (2017) 114:E4075–84. doi: 10.1073/pnas.1620115114
28. Heidbreder CA, Groenewegen HJ. The medial prefrontal cortex in the rat: evidence for a dorso-ventral distinction based upon functional and anatomical characteristics. *Neurosci Biobehav Rev.* (2003) 7:555–79. doi: 10.1016/j.neubiorev.2003.09.003
29. Goldman-Rakic PS. Cellular basis of working memory. *Neuron.* (1995) 14:477–85. doi: 10.1016/0896-6273(95)90304-6
30. Funahashi S, Bruce CJ, Goldman-Rakic PS. Mnemonic coding of visual space in the monkey's dorsolateral prefrontal cortex. *J Neurophysiol.* (1989) 61:331–49. doi: 10.1152/jn.1989.61.2.331
31. González-Burgos G, Barrionuevo G, Lewis DA. Horizontal synaptic connections in monkey prefrontal cortex: an *in vitro* electrophysiological study. *Cereb Cortex.* (2000) 10:82–92. doi: 10.1093/cercor/10.1.82
32. González-Burgos G, Krimer LS, Povysheva NV, Barrionuevo G, Lewis DA. Functional properties of fast spiking interneurons and their synaptic connections with pyramidal cells in primate dorsolateral prefrontal cortex. *J Neurophysiol.* (2005) 93:942–53. doi: 10.1152/jn.00787.2004
33. Wang XJ. Synaptic basis of cortical persistent activity: the importance of NMDA receptors to working memory. *J Neurosci.* (1999) 19:9587–603. doi: 10.1523/JNEUROSCI.19-21-09587.1999
34. Yang Y, Paspalas CD, Jin LE, Picciotto MR, Arnsten AFT, Wang M. Nicotinic α7 receptors enhance NMDA cognitive circuits in

dorsolateral prefrontal cortex. *Proc Nat Acad Sci USA.* (2013) 110:12078–83. doi: 10.1073/pnas.1307849110
35. Galvin VC, Yang S-T, Paspalas CD, Yang Y, Jin LE, Datta D, et al. Muscarinic M1 receptors modulate working memory performance and activity via KCNQ potassium channels in primate prefrontal cortex. *Neuron.* (2020) 106:649–61. doi: 10.1016/j.neuron.2020.02.030
36. Croxson PL, Kyriazis DA, Baxter MG. Cholinergic modulation of a specific memory function of prefrontal cortex. *Nat Neurosci.* (2011) 14:1510–2. doi: 10.1038/nn.2971
37. Homayoun H, Moghaddam B. NMDA receptor hypofunction produces opposite effects on prefrontal cortex interneurons and pyramidal neurons. *J Neurosci.* (2007) 27:11496–500. doi: 10.1523/JNEUROSCI.2213-07.2007
38. Lynch DR, Rattelle A, Dong YN, Roslin K, Gleichman AJ, Panzer JA. Anti-NMDA receptor encephalitis: clinical features and basic mechanisms. *Adv Pharmacol.* (2018) 82:235–60. doi: 10.1016/bs.apha.2017.08.005
39. Weickert CS, Fung SJ, Catts VS, Schofield PR, Allen KM, Moore LT, et al. Molecular evidence of *N*-methyl-D-aspartate receptor hypofunction in schizophrenia. *Mol Psychiatry*. (2012). 18:1185–92. doi: 10.1038/mp.2012.137
40. Kindler J, Lim CK, Weickert CS, Boerrigter D, Galletly C, Liu D, et al. Dysregulation of kynurenine metabolism is related to proinflammatory cytokines, attention, and prefrontal cortex volume in schizophrenia. *Mol Psychiatry.* (2019) 25:2860–72. doi: 10.1038/s41380-019-0401-9
41. Jacobs KR, Lim CK, Blennow K, Zetterberg H, Chatterjee P, Martins RN, et al. Correlation between plasma and CSF concentrations of kynurenine pathway metabolites in Alzheimer's disease and relationship to amyloid-β and tau. *Neurobiol Aging.* (2019) 80:11–20. doi: 10.1016/j.neurobiolaging.2019.03.015
42. Fukui S, Schwarcz R, Rapoport SI, Takada Y, Smith QR. Blood-brain barrier transport of kynurenines: implications for brain synthesis and metabolism. *J Neurochem.* (1991) 56:2007–17. doi: 10.1111/j.1471-4159.1991.tb03460.x
43. Voils SA, Shoulders BR, Singh S, Solberg LM, Garrett TJ, Frye RF. Intensive care unit delirium in surgical patients is associated with upregulation in tryptophan metabolism. *Pharmacotherapy.* (2020) 40:500–6. doi: 10.1002/phar.2392
44. Cai Y, Kim DJ, Takahashi T, David I Broadhurst DI, Ma S, Rattray NJW, et al. Kynurenic acid underlies sex-specific immune responses to COVID-19. *medRxiv [Preprint].* (2020). doi: 10.1101/2020.09.06.20189159
45. Singh R, Salunke DB. Diverse chemical space of indoleamine-2,3-dioxygenase 1 (Ido1) inhibitors. *Eur J Med Chem.* (2020) 211:113071. doi: 10.1016/j.ejmech.2020.113071
46. Thomas T, Stefanoni D, Reisz JA, Nemkov T, Bertolone L, Francis RO, et al. COVID-19 infection alters kynurenine and fatty acid metabolism, correlating with IL-6 levels and renal status. *JCI Insight.* (2020) 5:e140327. doi: 10.1172/jci.insight.140327
47. Murray JD, Bernacchia A, Freedman DJ, Romo R, Wallis JD, Cai X, et al. A hierarchy of intrinsic timescales across primate cortex. *Nat Neurosci.* (2014) 17:1661–3. doi: 10.1038/nn.3862
48. Wang H, Stradtman GGR, Wang XJ, Gao WJ. A specialized NMDA receptor function in layer 5 recurrent microcircuitry of the adult rat prefrontal cortex. *Proc Natl Acad Sci USA*. (2008) 105:16791–6. doi: 10.1073/pnas.0804318105
49. Gilman JP, Medalla M, Luebke JI. Area-specific features of pyramidal neurons-a comparative study in mouse and rhesus monkey. *Cereb Cortex.* (2017) 27:2078–94. doi: 10.1093/cercor/bhw062
50. Drevets WC, Price JL, Simpson JRJ, Todd RD, Reich T, Vannier M, et al. Subgenual prefrontal cortex abnormalities in mood disorders. *Nature.* (1997) 386:824–7. doi: 10.1038/386824a0
51. Mayberg HS, Lozano AM, Voon V, Mcneely HE, Seminowicz D, Hamani C, et al. Deep brain stimulation for treatment-resistant depression. *Neuron.* (2005) 45:651–60. doi: 10.1016/j.neuron.2005.02.014
52. Dougherty DD, Weiss AP, Cosgrove GR, Alpert NM, Cassem EH, Nierenberg AA, et al. Cerebral metabolic correlates as potential predictors of response to anterior cingulotomy for treatment of major depression. *J Neurosurg.* (2003) 99:1010–7. doi: 10.3171/jns.2003.99.6.1010
53. Yang LK, Lu L, Feng B, Wang XS, Yue J, Li XB, et al. FMRP acts as a key messenger for visceral pain modulation. *Mol Pain.* (2020) 16:1744806920972241. doi: 10.1177/1744806920972241
54. Fan J, Wu X, Cao Z, Chen S, Owyang C, Li Y. Up-regulation of anterior cingulate cortex NR2B receptors contributes to visceral pain responses in rats. *Gastroenterology.* (2009) 136:1732–40. doi: 10.1053/j.gastro.2009.01.069
55. Zhou L, Huang J, Gao J, Zhang G, Jiang J. NMDA and AMPA receptors in the anterior cingulate cortex mediates visceral pain in visceral hypersensitivity rats. *Cell Immunol.* (2014) 287:86–90. doi: 10.1016/j.cellimm.2013.12.001
56. Li Y. Synaptic plasticity and synchrony in the anterior cingulate cortex circuitry: a neural network approach to causality of chronic visceral pain and associated cognitive deficits. *Adv Neurobiol.* (2018) 21:219–45. doi: 10.1007/978-3-319-94593-4_8
57. Li XH, Miao HH, Zhuo M. NMDA Receptor Dependent Long-term Potentiation in Chronic Pain. *Neurochem Res.* (2019) 44:531–8. doi: 10.1007/s11064-018-2614-8
58. Humo M, Ayazgök B, Becker LJ, Waltisperger E, Rantamäki T, Yalcin I. Ketamine induces rapid and sustained antidepressant-like effects in chronic pain induced depression: Role of MAPK signaling pathway. *Prog Neuropsychopharmacol Biol Psychiatry.* (2020) 100:109898. doi: 10.1016/j.pnpbp.2020.109898
59. Krystal JH, Sanacora G, Duman RS. Rapid-acting glutamatergic antidepressants: the path to ketamine and beyond. *Biol Psychiatry.* (2013) 73:1133–41. doi: 10.1016/j.biopsych.2013.03.026
60. Persson J. Ketamine in pain management. *CNS Neurosci Ther.* (2013) 19:396–402. doi: 10.1111/cns.12111
61. Yeaman F, Meek R, Egerton-Warburton D, Rosengarten P, Graudins A. Sub-dissociative-dose intranasal ketamine for moderate to severe pain in adult emergency department patients. *Emerg Med Australas.* (2014) 26:237–42. doi: 10.1111/1742-6723.12173
62. Popova V, Daly EJ, Trivedi M, Cooper K, Lane R, Lim P, et al. Efficacy and safety of flexibly dosed esketamine nasal spray combined with a newly initiated oral antidepressant in treatment-resistant depression: a randomized double-blind active-controlled study. *Am J Psychiatry.* (2019) 176:428–38. doi: 10.1176/appi.ajp.2019.19020172
63. Chiba T, Kayahara K, Nakano K. Efferent projections of infralimbic and prelimbic areas of the medial prefrontal cortex in the Japanese monkey, Macaca fuscata. *Brain Research.* (2001) 888:83–101. doi: 10.1016/S0006-8993(00)03013-4
64. Cui Y, Hu S, Hu H. Lateral habenular burst firing as a target of the rapid antidepressant effects of ketamine. *Trends Neurosci.* (2019) 42:179–91. doi: 10.1016/j.tins.2018.12.002
65. Alexander L, Gaskin PLR, Sawiak SJ, Fryer TD, Hong YT, Cockcroft GJ, et al. Fractionating blunted reward processing characteristic of anhedonia by over-activating primate subgenual anterior cingulate cortex. *Neuron.* (2019) 101:307–20. doi: 10.1016/j.neuron.2018.11.021
66. Alexander L, Wood CM, Gaskin PLR, Sawiak SJ, Fryer TD, Hong YT, et al. Over-activation of primate subgenual cingulate cortex enhances the cardiovascular, behavioral and neural responses to threat. *Nat Commun.* (2020) 11:5386. doi: 10.1038/s41467-020-19167-0
67. Sinha R, Lacadie CM, Constable RT, Seo D. Dynamic neural activity during stress signals resilient coping. *Proc Natl Acad Sci USA.* (2016) 113:8837–42. doi: 10.1073/pnas.1600965113
68. Porrino LJ, Goldman-Rakic PS. Brainstem innervation of prefrontal and anterior cingulate cortex in the rhesus monkey revealed by retrograde transport of HRP. *J Comp Neurol.* (1982) 205:63–76. doi: 10.1002/cne.902050107
69. Arnsten AFT, Goldman-Rakic PS. Selective prefrontal cortical projections to the region of the locus coeruleus and raphe nuclei in the rhesus monkey. *Brain Res.* (1984) 306:9–18. doi: 10.1016/0006-8993(84)90351-2
70. Arnsten AFT. Stress signaling pathways that impair prefrontal cortex structure and function. *Nat Rev Neurosci.* (2009) 10:410–22. doi: 10.1038/nrn2648
71. Deutch AY, Roth RH. The determinants of stress-induced activation of the prefrontal cortical dopamine system. *Prog in Brain Res.* (1990) 85:367–403. doi: 10.1016/S0079-6123(08)62691-6
72. Finlay JM, Zigmond MJ, Abercrombie ED. Increased dopamine and norepinephrine release in medial prefrontal cortex induced by acute and chronic stress: effects of diazepam. *Neuroscience.* (1995) 64:619–28. doi: 10.1016/0306-4522(94)00331-X

73. Goldstein LE, Rasmusson AM, Bunney SB, Roth RH. Role of the amygdala in the coordination of behavioral, neuroendocrine and prefrontal cortical monoamine responses to psychological stress in the rat. *J Neurosci.* (1996) 16:4787–98. doi: 10.1523/JNEUROSCI.16-15-04787.1996
74. Murphy BL, Arnsten AFT, Goldman-Rakic PS, Roth RH. Increased dopamine turnover in the prefrontal cortex impairs spatial working memory performance in rats and monkeys. *Proc Nat Acad Sci USA*. (1996) 93:1325–9. doi: 10.1073/pnas.93.3.1325
75. Valentino RJ, Curtis AL, Page ME, Pavcovich LA, Florin-Lechner SM. Activation of the locus coeruleus brain noradrenergic system during stress: circuitry, consequences, and regulation. *Adv Pharmacol.* (1998) 42:781–4. doi: 10.1016/S1054-3589(08)60863-7
76. Van Bockstaele EJ, Colago EE, Valentino RJ. Amygdaloid corticotropin-releasing factor targets locus coeruleus dendrites: substrate for the co-ordination of emotional and cognitive limbs of the stress response. *J Neuroendocrinol.* (1998) 10:743–57. doi: 10.1046/j.1365-2826.1998.00254.x
77. Arnsten AFT. The biology of feeling frazzled. *Science.* (1998) 280:1711–2. doi: 10.1126/science.280.5370.1711
78. Arnsten AF. Stress weakens prefrontal networks: molecular insults to higher cognition. *Nat Neurosci.* (2015) 18:1376–85. doi: 10.1038/nn.4087
79. Barsegyan A, Mackenzie SM, Kurose BD, Mcgaugh JL, Roozendaal B. Glucocorticoids in the prefrontal cortex enhance memory consolidation and impair working memory by a common neural mechanism. *Proc Natl Acad Sci USA*. (2010) 107:16655–60. doi: 10.1073/pnas.1011975107
80. Grundemann D, Schechinger B, Rappold GA, Schomig E. Molecular identification of the cortisone-sensitive extraneuronal catecholamine transporter. *Nature Neuroscience.* (1998) 1:349–51. doi: 10.1038/1557
81. Cahill L, Mcgaugh JL. Modulation of memory storage. *Curr Opin Neurobiol.* (1996) 6:237–42. doi: 10.1016/S0959-4388(96)80078-X
82. Ferry B, Roozendaal B, Mcgaugh JL. Involvement of alpha-1-adrenoceptors in the basolateral amygdala in modulation of memory storage. *Eur J Pharmacol.* (1999) 372:9–16. doi: 10.1016/S0014-2999(99)00169-7
83. Rodrigues SM, Ledoux JE, Sapolsky RM. The influence of stress hormones on fear circuitry. *Annu Rev Neurosci.* (2009) 32:289–313. doi: 10.1146/annurev.neuro.051508.135620
84. Qin S, Hermans EJ, Van Marle HJF, Lou J, Fernandez G. Acute psychological stress reduces working memory-related activity in the dorsolateral prefrontal cortex. *Biological Psychiatry.* (2009) 66:25–32. doi: 10.1016/j.biopsych.2009.03.006
85. Qin S, Cousijn H, Rijpkema M, Luo J, Franke B, Hermans EJ, et al. The effect of moderate acute psychological stress on working memory-related neural activity is modulated by a genetic variation in catecholaminergic function in humans. *Front Integr Neurosci.* (2012) 6:16. doi: 10.3389/fnint.2012.00016
86. Zareyan S, Zhang H, Wang J, Song W, Hampson E, Abbott D, et al. First demonstration of double dissociation between COMT-Met158 and COMT-Val158 cognitive performance when stressed and when calmer. *Cereb Cortex.* (2020) 31:1411–26. doi: 10.1093/cercor/bhaa276
87. Medalla M, Barbas H. Anterior cingulate synapses in prefrontal areas 10 and 46 suggest differential influence in cognitive control. *J Neurosci.* (2010) 30:16068–81. doi: 10.1523/JNEUROSCI.1773-10.2010
88. Liston C, Miller MM, Goldwater DS, Radley JJ, Rocher AB, Hof PR, et al. Stress-induced alterations in prefrontal cortical dendritic morphology predict selective impairments in perceptual attentional set-shifting. *J Neurosci.* (2006) 26:7870–4. doi: 10.1523/JNEUROSCI.1184-06.2006
89. Radley JJ, Rocher AB, Miller M, Janssen WG, Liston C, Hof PR, et al. Repeated stress induces dendritic spine loss in the rat medial prefrontal cortex. *Cereb Cortex.* (2006) 16:313–20. doi: 10.1093/cercor/bhi104
90. Hains AB, Vu MA, Maciejewski PK, Van Dyck CH, Gottron M, Arnsten AF. Inhibition of protein kinase C signaling protects prefrontal cortex dendritic spines and cognition from the effects of chronic stress. *Proc Natl Acad Sci USA*. (2009) 106:17957–62. doi: 10.1073/pnas.0908563106
91. Shansky RM, Hamo C, Hof PR, Mcewen BS, Morrison JH. Stress-induced dendritic remodeling in the prefrontal cortex is circuit specific. *Cereb Cortex.* (2009) 106:17957–62. doi: 10.1093/cercor/bhp003
92. Liston C, Mcewen BS, Casey BJ. Psychosocial stress reversibly disrupts prefrontal processing and attentional control. *Proc Nat Acad Sci USA*. (2009) 106:912–7. doi: 10.1073/pnas.0807041106
93. Ansell EB, Rando K, Tuit K, Guarnaccia J, Sinha R. Cumulative adversity and smaller gray matter volume in medial prefrontal, anterior cingulate, and insula regions. *Biol Psychiatry.* (2012) 72:57–64. doi: 10.1016/j.biopsych.2011.11.022
94. Bloss EB, Janssen WG, Ohm DT, Yuk FJ, Wadsworth S, Saardi KM, et al. Evidence for reduced experience-dependent dendritic spine plasticity in the aging prefrontal cortex. *J Neurosci.* (2011) 31:7831–9. doi: 10.1523/JNEUROSCI.0839-11.2011
95. Association AP. *Diagnostic and Statistical Manual of Mental Disorders (DSM-5)*. Washington, D.C: American Psychiatric Association (2013). doi: 10.1176/appi.books.9780890425596
96. Li N, Lee BT, Liu RJ, Banasr M, Dwyer JM, Iwata M, et al. mTOR-dependent synapse formation underlies the rapid antidepressant effects of NMDA antagonists. *Science.* (2010) 329:959–64. doi: 10.1126/science.1190287
97. Duman RS, Aghajanian GK. Synaptic dysfunction in depression: potential therapeutic targets. *Science.* (2012) 338:68–72. doi: 10.1126/science.1222939
98. Mottaghy FM, Keller CE, Gangitano M, Ly J, Thall M, Parker JA, et al. Correlation of cerebral blood flow and treatment effects of repetitive transcranial magnetic stimulation in depressed patients. *Psychiatry Res.* (2002) 115:1–14. doi: 10.1016/S0925-4927(02)00032-X
99. Fox MD, Buckner RL, White MP, Greicius MD, Pascual-Leone A. Efficacy of transcranial magnetic stimulation targets for depression is related to intrinsic functional connectivity with the subgenual cingulate. *Biol Psychiatry.* (2012) 72:595–603. doi: 10.1016/j.biopsych.2012.04.028
100. Baldinger P, Kranz GS, Haeusler D, Savli M, Spies M, Philippe C, et al. Regional differences in SERT occupancy after acute and prolonged SSRI intake investigated by brain PET. *Neuroimage.* (2014) 88:252–62. doi: 10.1016/j.neuroimage.2013.10.002
101. Morris LS, Costi S, Tan A, Stern ER, Charney DS, Murrough JW. Ketamine normalizes subgenual cingulate cortex hyper-activity in depression. *Neuropsychopharmacology.* (2020) 45:975–81. doi: 10.1038/s41386-019-0591-5
102. Lapidus KA, Levitch CF, Perez AM, Brallier JW, Parides MK, Soleimani L, et al. A randomized controlled trial of intranasal ketamine in Major Depressive Disorder. *Biol Psychiatry.* (2014) 76:970–6. doi: 10.1016/j.biopsych.2014.03.026
103. Moda-Sava RN, Murdock MH, Parekh PK, Fetcho RN, Huang BS, Huynh TN, et al. Sustained rescue of prefrontal circuit dysfunction by antidepressant-induced spine formation. *Science.* (2019) 364:eaat8078. doi: 10.1126/science.aat8078

Conflict of Interest: AA and Yale University receive royalties from Shire/Takeda from the USA sales of Intuniv. They do not receive royalties from generic or nonUSA sales.

The remaining authors declare that the research was conducted in the absence of any commercial or financial relationships that could be construed as a potential conflict of interest.

frontiers in Psychiatry

CLINICAL TRIAL
published: 02 June 2021
doi: 10.3389/fpsyt.2021.653026

Relationship of Brain Glutamate Response to D-Cycloserine and Lurasidone to Antidepressant Response in Bipolar Depression: A Pilot Study

Zhengchao Dong[1,2], *Michael F. Grunebaum*[1,2], *Martin J. Lan*[1,2], *Vashti Wagner*[2], *Tse-Hwei Choo*[1,3], *Matthew S. Milak*[1,2], *Tarek Sobeih*[4], *J. John Mann*[1,2,5] *and Joshua T. Kantrowitz*[1,6,7]*

[1] Department of Psychiatry, College of Physicians and Surgeons, Columbia University, New York, NY, United States, [2] Molecular Imaging and Neuropathology, New York State Psychiatric Institute, New York, NY, United States, [3] Mental Health Data Science, New York State Psychiatric Institute, New York, NY, United States, [4] Information Sciences, Nathan Kline Institute, Orangeburg, NY, United States, [5] Department of Radiology, College of Physicians and Surgeons, Columbia University, New York, NY, United States, [6] Psychotic Disorders, New York State Psychiatric Institute, New York, NY, United States, [7] Information Sciences, Nathan Kline Institute, Orangeburg, NY, United States

OPEN ACCESS

Edited by:
Nevena V. Radonjic,
Upstate Medical University,
United States

Reviewed by:
Bashkim Kadriu,
National Institute of Mental Health,
National Institutes of Health (NIH),
United States
Estêvão Scotti-Muzzi,
University of São Paulo, Brazil

***Correspondence:**
Joshua T. Kantrowitz
jk3380@cumc.columbia.edu

Specialty section:
This article was submitted to Psychopharmacology, a section of the journal Frontiers in Psychiatry

Received: 13 January 2021
Accepted: 10 May 2021
Published: 02 June 2021

Citation:
Dong Z, Grunebaum MF, Lan MJ, Wagner V, Choo T-H, Milak MS, Sobeih T, Mann JJ and Kantrowitz JT (2021) Relationship of Brain Glutamate Response to D-Cycloserine and Lurasidone to Antidepressant Response in Bipolar Depression: A Pilot Study. Front. Psychiatry 12:653026. doi: 10.3389/fpsyt.2021.653026

N-methyl-D-aspartate glutamate-receptor (NMDAR) antagonists such as ketamine have demonstrated efficacy in both major depressive disorder (MDD) and bipolar disorder depression (BP-D). We have previously reported that reduction in Glx (glutamate + glutamine) in the ventromedial prefrontal cortex/anterior cingulate cortex (vmPFC/ACC), measured by proton magnetic resonance spectroscopy (^{1}H MRS) at 3T during a ketamine infusion, mediates the relationship of ketamine dose and blood level to improvement in depression. In the present study, we assessed the impact of D-cycloserine (DCS), an oral NMDAR antagonist combined with lurasidone in BP-D on both glutamate and Glx. Subjects with DSM-V BP-D-I/II and a Montgomery-Asberg Depression Rating Scale (MADRS) score>17, underwent up to three ^{1}H MRS scans. During Scan 1, subjects were randomized to receive double-blind lurasidone 66 mg or placebo. During Scan 2, all subjects received single-blind DCS 950 mg + lurasidone 66 mg, followed by 4 weeks of open label phase of DCS+lurasidone and an optional Scan 3. Five subjects received lurasidone alone and three subjects received placebo for Scan 1. Six subjects received DCS+lurasidone during Scan 2. There was no significant baseline or between treatment-group differences in acute depression improvement or glutamate response. In Scan 2, after a dose of DCS+lurasidone, peak change in glutamate correlated negatively with improvement from baseline MADRS ($r = -0.83$, $p = 0.04$). There were no unexpected adverse events. These preliminary pilot results require replication but provide further support for a link between antidepressant effect and a decrease in glutamate by the NMDAR antagonist class of antidepressants.

Keywords: N-methyl-D-aspartate, glutamate, MRS—^{1}H nuclear magnetic resonance spectra, biomarker, bipolar depression, D-Cycloserine, lurasidone

INTRODUCTION

Bipolar disorder affects 2% of the population in the United States (1). Despite overall effectiveness of FDA approved compounds, many individuals with bipolar depression (BP-D) experience persistent depression despite antidepressant medication treatment, either alone or combined with mood stabilizers. For example, across several recent registration studies, ∼40-50% of subjects were non-responders based upon Montgomery-Asberg Depression Rating Scale (MADRS) (2) scores ≥50% of baseline (3–5).

Recently, the N-methyl-D-asparate glutamate-receptor (NMDAR) antagonist, ketamine, has emerged as a potential treatment option for both major depressive disorder (MDD) (6, 7) and (BP-D) (8). Although the antidepressant mechanism of action of ketamine remains unclear, convergent evidence suggests that dysfunction of glutamatergic systems plays a role in the pathophysiology of BP-D (9, 10).

However, intravenous ketamine use is limited by loss of benefit after about 5–7 days and transient psychotomimetic side effects during administration. Intranasal ketamine is easier to administer but may have more side effects (11, 12). D-cycloserine (DCS), an FDA-approved anti-tuberculosis drug, is an NMDAR antagonist at higher doses. It is primarily an antagonist at >500 mg (13–15), via the glycine co-receptor of the NMDAR and may have a more favorable safety profile than ketamine. Potential antidepressant effects of DCS were first reported in 1959 (16) but not formally studied until recently. Efficacy of DCS in a dose of >500 mg in MDD, including an anti-suicidal effect, is supported by two double-blind studies (15, 17). Recently, we reported an open label study of treatment resistant BP-D—a single infusion of ketamine followed by 8 weeks of a combination of DCS + FDA approved medications for BP-D (including lurasidone). This combination was employed seeking a treatment where an atypical antipsychotic prevented any potential psychomimetic effect of DCS and perhaps had an additional antidepressant action. Indeed, a sustained benefit for the duration of treatment was seen (46% symptom reduction, $p = 0.019$ vs. baseline) without significant safety concerns (18). Of note, there was a decline in benefit over the first 2 weeks post ketamine, that reversed with the ongoing combination of DCS and lurasidone or other FDA-approved treatments for BP-D.

In previous studies, we used proton magnetic resonance spectroscopy (^{1}H MRS) to quantify ketamine effects on Glx (a combination of glutamate (Glu) and glutamine resonance signals: Glu+glutamine) in the ventromedial prefrontal cortex, along with the adjacent anterior cingulate cortex (vmPFC/ACC) in both healthy (19) and depressed (20, 21) individuals. Our focus on the vmPFC and the ACC stems from extensive research implicating these regions in the pathogenesis of mood disorders (22–24) and microdialysis rodent (25, 26) studies suggesting that the glutamatergic surge in response to NMDAR antagonists is maximal in the vmPFC.

In our recently published, placebo-controlled, dose-finding, randomized clinical trial of ketamine (21), we found that improvement in MDD had a positive linear relationship with ketamine dose and blood level, and a negative correlation with Glx response. Reduction of Glx mediated the relationship of ketamine dose and level with antidepressant response. In the present report, we sought to determine whether the same relationship is found within BP-D for DCS combined with lurasidone. This combination of medications seeks to preserve the antidepressant effect of DCS and block its potential psychotomimetic effect with lurasidone. Lurasidone may also augment the antidepressant effect of DCS since it an FDA approved medication for BP-D (3, 4).

To determine the independent biological effect of lurasidone, prior to the DCS/lurasidone scan, all subjects underwent an ^{1}H MRS scan while receiving double-blind lurasidone 66 mg or placebo. We have previously shown that this ^{1}H MRS method is sensitive to DCS-induced changes in Glx in healthy controls (27). Due to upgrades in both scanner quality and ^{1}H MRS methodology (28–30), we now report the more specific ^{1}H MRS outcome of Glu, in place of Glx. We hypothesized that we would find a similar relationship between Glu and DCS+lurasidone mediated antidepressant response, thus adding to our understanding of NMDAR antagonist mechanism of action in depression.

PATIENTS AND METHODS

The study was conducted under a biomarker letter of support (IND 129194) from the US Food and Drug Administration and posted on www.clinicaltrials.gov (NCT03402152).

Enrollment criteria included DSM-V current BP-D-I/II, confirmed by a SCID (31). Subjects had at least moderate depression symptoms, as defined by a MADRS score>17, with no current or chronic psychosis or substance use disorder. To minimize further acute clinical deterioration, subjects were permitted to remain on all current pre-study psychotropics, with the exception that prior antipsychotics and fluoxetine were discontinued at least 24 h before the first MRI to mitigate the effect of such medications on the Glu response to acute administration of DCS or lurasidone.

After screening, each eligible subject underwent up to three ^{1}H MRS scans, on three different days (referred to as Scan 1, Scan 2, and Scan 3, respectively). During Scan 1, all subjects were randomized to receive double-blind lurasidone 66 mg or placebo, and during Scan 2 all subjects received single-blind one dose of NRX-101 (DCS 950 mg + lurasidone 66 mg). All subjects received a dose of pyridoxine (200 mg) along with the study medication to prevent DCS related reductions in Vitamin B6 (32). After Scan 2, subjects were started on a combination of open-label flexibly dosed DCS/lurasidone and daily pyridoxine 200 mg for 4 weeks, culminating in an optional final ^{1}H MRS scan (Scan 3).

Scans 1 and 2 were at least 1 day apart, and subjects and data analysts, including ^{1}H MRS data processing, were blind to treatment order (e.g., unaware that DCS+lurasidone was always administered immediately prior to Scan 2). The mean time between Scans 1 and 2 was 3.3 days (range 1–7 days). After structural MRI and baseline ^{1}H MRS scans (∼30 min), subjects were briefly removed from the scanner for study drug

administration, followed by serial ^{1}H MRS frame acquisitions for up to 70 min following drug administration. Subjects were assessed using a side effects checklist, the C-SSRS and MADRS at baseline, ∼30 min before and after the imaging on the ^{1}H MRS days and weekly during the 4-week follow-up.

The study was terminated by the sponsor after eight randomized subjects due to a corporate decision to pursue a different approach. Thus, we only report pilot results due to the limited sample size.

^{1}H MRS Methodology

Six subjects were scanned on a Siemen Prisma 3.0T MR scanner equipped with a 32-channel surface coil array and two subjects were scanned on a General Electric SIGNA Premier 3T MR scanner equipped with a 21-channel surface coil array. MR data were acquired with the same protocols on both scanners. The protocols for voxel placement and ^{1}H MRS data acquisition for both sessions of before and after medication were the same. First, three-plane scout images were acquired, followed by a high-resolution structural MRI scan in the sagittal planes; Then, high resolution structural MRI images in the oblique axial planes parallel to the AC-PC line were acquired. We placed the ^{1}H MRS voxel ($3.0 \times 2.5 \times 2.5$ cm^3) based on the sagittal and axial MR images in the vmPFC and ACC, with the center of the posterior side of the voxel close to the frontal tip of the cingulate gyrus (**Figure 1**). The ^{1}H MRS data were acquired from the voxel using a commercial version of the PRESS sequence (33) implemented on both scanners with following parameters: TR/TE = 1,500/120 ms (28, 29), spectral width = 2,000 Hz, free induction decay (FID) datapoints = 1,024, number of excitations (NEX) for water unsuppressed ^{1}H MRS scan = 16, and NEX for water suppressed ^{1}H MRS = 240. Total scan time for each ^{1}H MRS frame, including pre-scan, was ∼8 min.

^{1}H MRS Data Processing

We combined the multichannel ^{1}H MRS data, using the unsuppressed water signal as a reference for correcting phase errors and for calculating weighting factors of *S/N*, where *S* is the amplitude of water signal and *N* is the standard deviation of noise of each channel (34). We then corrected frequency and phase shifts among the FIDs in each ^{1}H MRS data file and combined them into a single FID for each baseline and dynamic ^{1}H MRS scan. We removed the residual water signal using a singular value decomposition-based matrix-pencil method (35).

We quantified the ^{1}H MRS data in the time domain using the software packages AMARES (36) imbedded in jMRUI (37). To improve accuracy of the quantification of the metabolites of interest via spectral fitting, we fit all peaks with major contributions, including metabolic peaks of N-acetylaspartate at 2.01 ppm, total creatine (Cr) at 3.02 ppm, total choline at 3.24 ppm and Glu around 2.26 ppm were included in the spectral fitting. In the present paper, we focus on the role of Glu/Cr and Glx/Cr, and did not analyze NAA and Ch. For accurate spectral fitting of Glu, we incorporated prior knowledge in the model of relative frequencies, phases, and amplitudes of the major peaks Glu obtained by fitting the simulated spectra of Glu using AMARES, similar to the approach in the reference (38), where the prior knowledge was obtained from phantom ^{1}H MRS data of Glu. The simulations of Glu spectra for both Siemens and GE data were performed using the MARSS software package (30).

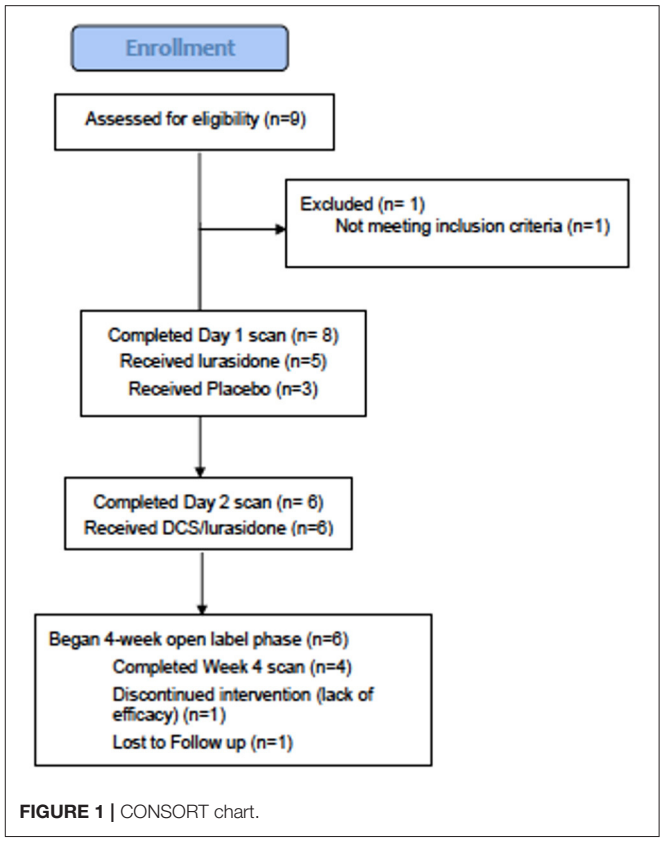

FIGURE 1 | CONSORT chart.

Due to higher quality measurements on our upgraded scanner, we modified the initial analysis plan posted on clinicaltrials.gov, and utilized Glu peak, as opposed to Glx AUC, as the primary metabolite outcome. Glx was analyzed as a secondary measure. Based on pharmacokinetics (39–41) of DCS, our prior finding of the ^{1}H MRS peak at ∼35 min DCS post-dose (27) and our prior ketamine study using peak level (21), Glu ^{1}H MRS peak level was used, defined as a mean from 30 to 46 min post drug. We used Cr as a reference for the relative quantification of Glu and expressed the outcome measure from ^{1}H MRS as Glu/Cr. The rationale for using Cr as a standard is as follows: (1). The Cr level is assumed to be stable over the course of drug administration; and (2). The tissue volumes for Glu and Cr are the same in the voxel and a partial volume effect of using water as a reference is avoided. We used the ratio of standard deviation to estimated amplitude given in the fitting by the jMRUI software, as a metric for quality control and set the threshold to be 20%. No data were excluded (42).

Data Analysis

Prior to analysis, all variables were examined for distribution and outliers. Due to the small sample sizes, parametric tests were utilized only for repeated-measures modeling of change in MADRS, for which residuals were sufficiently normal.

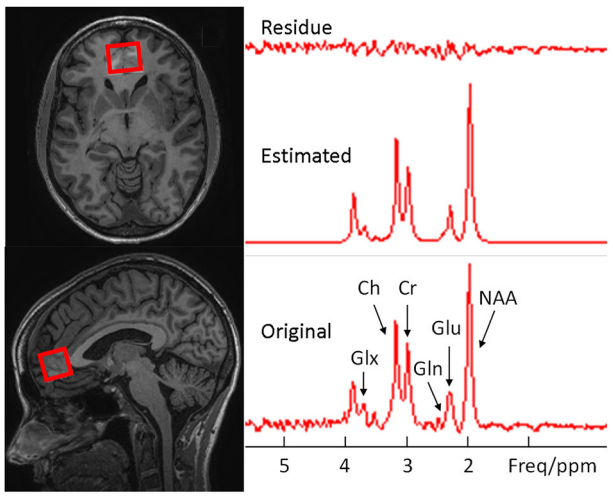

FIGURE 2 | Examples of voxel placement (red outline) on the axial and sagittal localizer images showing the size and location in the medial ventral prefrontal cortex (Left) and the original, estimated, and their difference spectra from the voxel (Right).

TABLE 1 | Baseline demographics, psychopathology and subject disposition.

Age (years)	32.4 ± 13
Sex	7 women
Diagnosis	Bipolar I ($n = 5$) Bipolar II ($n = 3$)
Medications	Mood stabilizer alone ($n = 3$), SSRI + Mood stabilizer ($n = 2$), Unmedicated ($n = 3$)
Illness duration (months)	19.7 ± 34.8
Hospitalizations (n)	1.5 ± 1.4
Manic/hypomanic episodes (n)	5 ± 6.1
MDD episodes (n)	5.9 ± 8.8
Baseline MADRS (screening)	31.5 ± 9.3
Baseline C-SSRS	2 ± 2
Received lurasidone (Scan 1)	$N = 5$
Received placebo (Scan 1)	$N = 3$
Received D-Cycloserine/lurasidone (Scan 2)	$N = 6$
Pre-scan MADRS (Scan 1)	25.3 ± 7.2
Post-scan MADRS (Scan 1)	11.3 ± 8.0
Pre-scan MADRS (Scan 2)	20.0 ± 11.2
Post-scan MADRS (Scan 2)	11.3 ± 10.0

Wilcoxon sign rank tests were used to test for significant Scan 1 percent change in MADRS and Glu within treatment group, and Scan 2 percent change in MADRS and Glu in the overall sample. Additionally, Wilcoxon sign rank tests were also used to assess both baseline and change in MADRS and Glu response from Scan 1 to Scan 2, within subject.

Mixed effects linear regression models were fit to model MADRS change from baseline over the four follow-up weeks. First, an intercept-only model was fit to assess mean change across the 4 weeks. Next, week was added to the model as a categorical predictor to estimate change from baseline at each week. Both models featured a random intercept for subject. Spearman's correlations were used to assess the association between MADRS and Glu responses, on Scan 1 and on Scan 2, separately. Due to the small sample sizes, descriptive statistics are provided in the text.

Significance level was set at $\alpha = 0.05$, with results reported as mean ± standard deviation (SD) and median with interquartile ranges (IQR, 25th percentile, 75th percentile). All analyses were performed using SAS version 9.4 (Cary, NC: SAS Institute Inc.; 2014). The data that support the findings of this study are available on request from the corresponding author if accompanied by a reasonable plan for their use. The data are not publicly available due to privacy or ethical restrictions.

RESULTS

Subjects: 9 subjects consented to participate (**Figure 2**), eight met study criteria and were randomized (**Table 1**). On entering the study, three randomized subjects were unmedicated, and the remaining five randomized subjects were on stable doses of mood stabilizers and antidepressants for at least 1 month, including one subject on oxcarbazepine 600 mg and escitalopram 20 mg, one subject on lithium 450 mg and fluoxetine 60 mg (discontinued prior to scan), one subject on lamotrigine 50 mg and diphenhydramine 50 mg, one subject on sertraline 200 mg, zolpidem 10 mg, gabapentin 1,000 mg and diazepam 10 mg and one subject on valproic acid 1,000 mg, paroxetine 20 mg and dextroamphetamine and amphetamine 20 mg. Six out of eight randomized subjects completed the first two scans, and both non-completers received lurasidone during Scan 1. Four subjects completed the four-week open-label phase, with ^{1}H MRS available for three subjects.

Clinical

Five subjects were randomized to lurasidone and three to placebo on Scan 1. Overall, subjects exhibited a comparable degree of acute improvement from the baseline MADRS after one dose of lurasidone alone (57.0% ± 31.7, $p = 0.06$, $n = 5$) or placebo (72.7% ± 32.6, $p = 0.25$, $n = 3$) at Scan 1; and sustained this improvement after a mean of 3.3 days of one dose of DCS+lurasidone at Scan 2 (67.2% ± 22.6, $p = 0.03$, $n = 6$). Only the DCS+lurasidone improvement at Scan 2 relative to baseline reached statistical significance. Among subjects that completed both scans, there was no significant difference between baseline MADRS on scan days, suggesting a lack of carryover effect from Scan 1 (Signed-Rank Test $p = 0.31$).

Using mixed-effects linear modeling, a significant overall MADRS improvement over time was seen ($t_4 = -6.38$, $p = 0.0031$) over the 4-week treatment, with the final MADRS total decreasing to 17.5 ± 12.0. Weekly contrasts demonstrated significant improvement from baseline at all rating points except at 2 weeks ($p = 0.0038$, **Figure 3** Right). No subjects achieved euthymia, defined by MADRS <8.

No patients exhibited active suicidal ideation, intent or behavior during the study on the C-SSRS (all C-SSRS scores

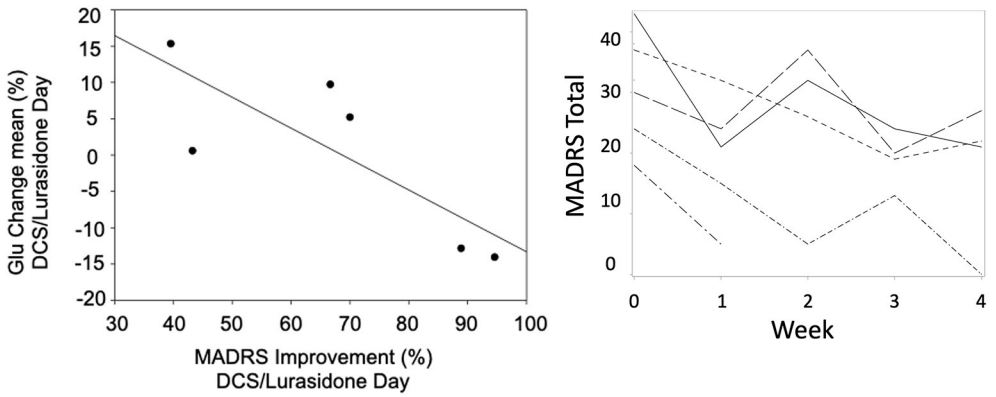

FIGURE 3 | A scatter plot of mean change in Glu vs. improvement from baseline MADRS ($r_s = -0.83$, $p = 0.04$) on the DCS/Lurasidone days (Left). Spaghetti plot of MADRS over time by subject (Right).

<3). There were no unexpected side effects. There was one serious adverse event involving a patient who was observed overnight in hospital for moderate dystonia thought to be related to lurasidone. This subject remained in the study with a reduction in dose.

^{1}H MRS: As previously (27), the Glu peak was ∼35 min post oral drug administration. Consistent with our previous work with ketamine in MDD (21), Glu increase was seen after placebo only. Both lurasidone alone and the DCS+lurasidone combination attenuated the Glu response. However, neither the within nor the between group changes in Glu levels were significant statistically. The changes observed were small: a decrease after lurasidone [Median (IQR) = −6.6% (−16.9%,−1.9%), $n = 5$, $p = 0.31$]; and increase after placebo [Median (IQR)= +12.9% (−9.0%,34.8%), $n = 3$, $p = 1.0$]; and a decrease after DCS+lurasidone treatment [Median (IQR)= −2.7% (−7.6%,−2.2%), $n = 6$, $p = 0.31$] on the ^{1}H MRS scan days (Wilcoxon sign rank test). Within the same subjects, Glu response decreased after DCS+lurasidone and lurasidone alone (median: −3.9% vs. −7.4%, $n = 4$) and increased after placebo (median: 20.3% vs. −6.7%, $n = 2$) but none of these effects were statistically significant.

On the DCS+lurasidone treatment day (Scan 2), change of Glu from baseline on that day correlated negatively with improvement from baseline MADRS ($r_s = -0.83$, $p = 0.04$, **Figure 3**, Left), using Spearman's correlation coefficient. By contrast, on the placebo/lurasidone day (Scan 1), Glu change did not correlate with MADRS change ($r_s = 0.29$, $p = 0.53$). Controlling for Scan 1 treatment-type did not change results for Scan 1 or 2 correlations. There were no significant differences in baseline Glu levels on Scan 1 and Scan 2 [Day 1 Med (IQR) = 0.31 (0.20–0.35); Day 2 Med (IQR) = 0.29 (0.22–0.37); Signed-Rank Test $p = 0.69$], supporting the assumption that this relationship was not due to carryover effects from Scan 1. Only 3 subjects completed Scan 3 (Week 4) ^{1}H MRS, without significant results.

Glx did not show any statistically significant results in Day 1 or Day 2 analysis. Change in Glx on Day 2 did not correlate with either change in Glu on Day 2 ($r_s = 0.54$, $p = 0.27$), nor with MADRS change ($r_s = -0.37$, $p = 0.47$).

DISCUSSION

Due to the small sample size, particularly for the placebo and lurasidone alone groups, the present findings are presented as a preliminary pilot study. Nevertheless, we did observe that lower mean Glu level post treatment with an NMDAR antagonist combined with lurasidone predicts better antidepressant response in BP-D, consistent with prior findings (21) in MDD when ketamine was employed. This relationship was seen despite a lack of significant between-treatment group differences for symptoms or ^{1}H MRS outcomes, and was not seen after treatment with lurasidone alone or placebo. Of course, the small sample size precluded an adequately powered statistical analysis.

In a secondary finding, we demonstrate tolerability and potential efficacy of acute, high-dose DCS in BP-D when combined with lurasidone and no reports of psychotomimetic symptoms when receiving this medication combination. While the analysis was limited by the small sample, statistically significant improvement in depression was seen after an acute dose of DCS+lurasidone, but not with lurasidone alone or placebo. Similarly, the degree of clinical response was comparable to our previous open label findings of efficacy over 8 weeks of DCS combined with atypical antipsychotics (27).

We previously proposed that an increase in Glu may be a stress response because it is most robust in the placebo and healthy control groups (19, 21). While meta-analysis of medicated MDD patients indicate lower levels of Glx, when medication status is considered, the data indicate that medicated MDD has lower Glx or glutamate and untreated MDD may have elevated levels (43). Studies of BP-D have reported higher Glu levels (44–46), as have studies in other relatively treatment resistant populations such as postpartum depression (47). Similarly, a large mega-analysis found that while medial frontal cortex Glu and Glx are generally lower in schizophrenia compared to healthy controls, higher Glu and Glx levels were associated with more severe symptoms and lower levels were associated with antipsychotic treatment (48).

While our small sample size limited the ability to assess between group differences in the Glu response between

scan days, we replicate our previous findings with ketamine (21), finding that DCS combined with lurasidone, appears to diminish the Glx or glutamate response and this effect correlates with degree of antidepressant effect. A reduced stress response is consistent with preclinical studies, indicating that NMDAR antagonist related antidepressant response may produce a resilience effect (49). Similarly, putative glutamatergic treatments in schizophrenia also appear to reduce NMDAR antagonist induced glutamate increases (50). Thus, we have previous proposed that elevated Glu or Glx may be a marker of depressive illness severity (51), and a reduction is an indicator of antidepressant response to NMDAR antagonists.

In our previous study of DCS alone in healthy controls (27), we found a positive peak at ∼35 min post-dose (23 ± 5% increase). In the present report of BP-D patients, we found a small decrease in Glu after DCS+lurasidone treatment, consistent with a blunting of the elevation seen in other studies including those employing the NMDAR antagonist ketamine. Similar to our ketamine study (21), this blunting was correlated with degree of antidepressant effect.

The use of target engagement biomarkers early in drug development can facilitate dose selection and initial proof-of-mechanism assessments (50, 52–54). While the present report was not designed to assess dose response, our results do further support that target engagement at the NMDAR and the NMDAR glycine site, as measured by ^{1}H MRS, is necessary for antidepressant response. Exemplary of this, a recent study of treatment resistant depression (55), found neither antidepressant nor ^{1}H MRS Glu changes in response to AV-101, a competitive antagonist at the NMDAR glycine site. A subsequent study of AV-101 in healthy controls found evidence for a dose response for AV-101 using the auditory steady state response (56), and suggested that higher doses may be needed.

Our study has several limitations, and we emphasize its presentation as a pilot study. The small sample is the principal study limitation. A second concern is the potential carry-over effects from Scan 1 treatment with lurasidone or pre-study medications, especially concomitant mood stabilizers or those with a long half-life such as fluoxetine. Although the discontinuation of other antipsychotics and fluoxetine lowered the blood and brain levels of these medications, this was not for long enough to allow them to wash out of the brain completely. Consequently, although this step reduced the potential impact of such medications, it did not eliminate the possibility of an effect. These limitations are minimized by the lack of baseline Glu and MADRS differences between Scan 1 and 2, and only one subject was taking fluoxetine pre-study. Furthermore, potential variability in Glu from the use of two scanners or pre-study medication differences was minimized because we focused on the acute percentage change in Glu post study drug administration within each day for each subject, not absolute Glu values.

Finally, we focused on Glu in the present report instead of the composite measure of Glx by taking advantages of data acquisition parameter TE = 120 ms, which is optimized for Glu separation (28, 29) and spectral fitting prior knowledge obtained from simulated model spectra (30, 38). While this optimized our ^{1}H MRS sequence for Glu measurements, the spectral overlapping between Glu and Gln might result in a "competition" or a "compensation" between them in the fitting, limiting the accuracy of Gln. Therefore, the variation of Glx may be smaller than that of Gln itself but may still larger than Glu. For this reason, we did not focus on Glx, nor report Gln. This limits the direct comparison to our Glx results in prior studies (21, 27). Better spectral fitting methods need to be developed to improve the fitting of Glu, Gln, and Glx.

In conclusion, our preliminary pilot results are consistent with our previous work. Attenuation of the Glu response being correlated with antidepressant response to NMDAR antagonists requires replication in a larger, multi-dose, controlled study. If replicated, this biomarker may prove to be a method for screening NMDAR antagonists for antidepressant potential.

DATA AVAILABILITY STATEMENT

The raw data supporting the conclusions of this article will be made available by the authors, without undue reservation.

ETHICS STATEMENT

The studies involving human participants were reviewed and approved by NYSPI IRB. The patients/participants provided their written informed consent to participate in this study.

AUTHOR CONTRIBUTIONS

ZD, JM, and JK had full access to all of the data in the study and take responsibility for the integrity of the data and the accuracy of the data analysis. JK, ZD, MM, and JM: substantial contributions to conception and design. JK, ZD, MG, ML, VW, T-HC, TS, and JM: acquisition, analysis, or interpretation of data. JK, T-HC, JM, and ZD: drafting of the manuscript. JK, T-HC, JM, ML, and ZD: critical revision of the manuscript for important intellectual content. All authors reviewed the final submission and gave final approval of the submitted version.

FUNDING

This work was supported by a grant from NeuroRx to JK. The funding agency had no role in manuscript preparation or decision to submit for publication.

ACKNOWLEDGMENTS

We are grateful to Ms. Anina Klein at the Nathan Kline Institute for her invaluable help providing study monitoring.

REFERENCES

1. Merikangas KR, Akiskal HS, Angst J, Greenberg PE, Hirschfeld RM, Petukhova M, et al. Lifetime and 12-month prevalence of bipolar spectrum disorder in the national comorbidity survey replication. *Arch Gen Psychiatry.* (2007) 64:543–52. doi: 10.1001/archpsyc.64.5.543
2. Montgomery SA, Asberg M. A new depression scale designed to be sensitive to change. *Br J Psychiatry.* (1979) 134:382–9. doi: 10.1192/bjp.134.4.382
3. Loebel A, Cucchiaro J, Silva R, Kroger H, Hsu J, Sarma K, et al. Lurasidone monotherapy in the treatment of bipolar i Depression: a Randomized, double-Blind, placebo-Controlled study. *Am J Psychiatry.* (2014) 171:160–8. doi: 10.1176/appi.ajp.2013.13070984
4. Loebel A, Cucchiaro J, Silva R, Kroger H, Sarma K, Xu J, et al. Lurasidone as adjunctive therapy with lithium or valproate for the treatment of bipolar i Depression: a Randomized, double-Blind, placebo-Controlled study. *Am J Psychiatry.* (2014) 171:169–77. doi: 10.1176/appi.ajp.2013.13070985
5. Earley W, Burgess MV, Rekeda L, Dickinson R, Szatmari B, Nemeth G, et al. Cariprazine treatment of bipolar depression: a Randomized double-Blind placebo-Controlled phase 3 study. *Am J Psychiatry.* (2019) 176:439–48. doi: 10.1176/appi.ajp.2018.18070824
6. Diazgranados N, Ibrahim LA, Brutsche NE, Ameli R, Henter ID, Luckenbaugh DA, et al. Rapid resolution of suicidal ideation after a single infusion of an n-methyl-D-aspartate antagonist in patients with treatment-resistant major depressive disorder. *J Clin Psychiatry.* (2010) 71:1605–11. doi: 10.4088/JCP.09m05327blu
7. Grunebaum MF, Galfalvy HC, Choo TH, Keilp JG, Moitra VK, Parris MS, et al. Ketamine for rapid reduction of suicidal thoughts in major depression: a Midazolam-Controlled randomized clinical trial. *Am J Psychiatry.* (2018) 175:327–35. doi: 10.1176/appi.ajp.2017.17060647
8. Grunebaum MF, Ellis SP, Keilp JG, Moitra VK, Cooper TB, Marver JE, et al. Ketamine versus midazolam in bipolar depression with suicidal thoughts: a pilot midazolam-controlled randomized clinical trial. *Bipolar Disord.* (2017) 19:176–83. doi: 10.1111/bdi.12487
9. Lener MS, Niciu MJ, Ballard ED, Park M, Park LT, Nugent AC, et al. Glutamate and gamma-Aminobutyric acid systems in the pathophysiology of major depression and antidepressant response to ketamine. *Biol Psychiatry.* (2017) 81:886–97. doi: 10.1016/j.biopsych.2016.05.005
10. Duman RS, Sanacora G, Krystal JH. Altered connectivity in depression: gABA and glutamate neurotransmitter deficits and reversal by novel treatments. *Neuron.* (2019) 102:75–90. doi: 10.1016/j.neuron.2019.03.013
11. Daly EJ, Trivedi MH, Janik A, Li H, Zhang Y, Li X, et al. Efficacy of esketamine nasal spray plus oral antidepressant treatment for relapse prevention in patients with treatment-Resistant depression: a Randomized clinical trial. *JAMA Psychiatry.* (2019) 76:893–903. doi: 10.1001/jamapsychiatry.2019.1189
12. Gastaldon C, Raschi E, Kane JM, Barbui C, Schoretsanitis G. Post-Marketing safety concerns with esketamine: a Disproportionality analysis of spontaneous reports submitted to the fDA adverse event reporting system. *Psychother Psychosom.* (2021) 90:41–8. doi: 10.1159/000510703
13. Van Berckel BN, Lipsch C, Gispen-De Wied C, Wynne HJ, Blankenstein MA, Van Ree JM, et al. The partial nMDA agonist D-Cycloserine stimulates lH secretion in healthy volunteers. *Psychopharmacology (Berl).* (1998) 138:190–7. doi: 10.1007/s002130050662
14. Heresco-Levy U, Javitt DC, Gelfin Y, Gorelik E, Bar M, Blanaru M, et al. Controlled trial of D-Cycloserine adjuvant therapy for treatment-resistant major depressive disorder. *J Affect Disord.* (2006) 93:239–43. doi: 10.1016/j.jad.2006.03.004
15. Heresco-Levy U, Gelfin G, Bloch B, Levin R, Edelman S, Javitt DC, et al. A randomized add-on trial of high-dose D-Cycloserine for treatment-resistant depression. *Int J Neuropsychopharmacol.* (2013) 16:501–6. doi: 10.1017/S1461145712000910
16. Crane GE. Cyloserine as an antidepressant agent. *Am J Psychiatry.* (1959) 115:1025–6. doi: 10.1176/ajp.115.11.1025
17. Chen MH, Cheng CM, Gueorguieva R, Lin WC, Li CT, Hong CJ, et al. Maintenance of antidepressant and antisuicidal effects by d-cycloserine among patients with treatment-resistant depression who responded to low-dose ketamine infusion: a double-blind randomized placebo-control study. *Neuropsychopharmacology.* (2019) 44:2112–8. doi: 10.1038/s41386-019-0480-y
18. Kantrowitz JT, Halberstam B, Gangwisch J. Single dose ketamine followed by daily D-Cycloserine in treatment resistant bipolar depression. *J Clin Psychiatry.* (2015) 76:737–8. doi: 10.4088/JCP.14l09527
19. Javitt DC, Carter CS, Krystal JH, Kantrowitz JT, Girgis RR, Kegeles LS, et al. Utility of imaging-Based biomarkers for glutamate-Targeted drug development in psychotic disorders: a Randomized clinical trial. *JAMA Psychiatry.* (2018) 75:11–9. doi: 10.1001/jamapsychiatry.2017.3572
20. Milak MS, Proper CJ, Mulhern ST, Parter AL, Kegeles LS, Ogden RT, et al. A pilot in vivo proton magnetic resonance spectroscopy study of amino acid neurotransmitter response to ketamine treatment of major depressive disorder. *Mol Psychiatry.* (2016) 21:320–7. doi: 10.1038/mp.2015.83
21. Milak MS, Rashid R, Dong Z, Kegeles LS, Grunebaum MF, Ogden RT, et al. Assessment of relationship of ketamine dose with magnetic resonance spectroscopy of glx and gABA responses in adults with major depression: a Randomized clinical trial. *JAMA Netw Open.* (2020) 3:e2013211. doi: 10.1001/jamanetworkopen.2020.13211
22. Hanford LC, Nazarov A, Hall GB, Sassi RB. Cortical thickness in bipolar disorder: a systematic review. *Bipolar Disord.* (2016) 18:4–18. doi: 10.1111/bdi.12362
23. Hibar DP, Westlye LT, Doan NT, Jahanshad N, Cheung JW, Ching CRK, et al. Cortical abnormalities in bipolar disorder: an mRI analysis of 6503 individuals from the eNIGMA bipolar disorder working group. *Mol Psychiatry.* (2018) 23:932–42. doi: 10.1038/mp.2017.73
24. Hiser J, Koenigs M. The multifaceted role of the ventromedial prefrontal cortex in emotion, decision making, social cognition, and psychopathology. *Biol Psychiatry.* (2018) 83:638–47. doi: 10.1016/j.biopsych.2017.10.030
25. Moghaddam B, Adams B, Verma A, Daly D. Activation of glutamatergic neurotransmission by ketamine: a novel step in the pathway from nMDA receptor blockade to dopaminergic and cognitive disruptions associated with the prefrontal cortex. *J Neurosci.* (1997) 17:2921–7. doi: 10.1523/JNEUROSCI.17-08-02921.1997
26. Chowdhury GM, Behar KL, Cho W, Thomas MA, Rothman DL, Sanacora G. (1)H-[(1)(3)C]-nuclear magnetic resonance spectroscopy measures of ketamine's effect on amino acid neurotransmitter metabolism. *Biol Psychiatry.* (2012) 71:1022–5. doi: 10.1016/j.biopsych.2011.11.006
27. Kantrowitz JT, Milak MS, Mao X, Shungu DC, Mann JJ. D-Cycloserine, an nMDA glutamate receptor glycine site partial agonist, induces acute increases in brain glutamate plus glutamine and gABA comparable to ketamine. *Am J Psychiatry.* (2016) 173:1241–2. doi: 10.1176/appi.ajp.2016.16060735
28. Snyder J, Wilman A. Field strength dependence of pRESS timings for simultaneous detection of glutamate and glutamine from 1.5 to 7T. *J Magn Reson.* (2010) 203:66–72. doi: 10.1016/j.jmr.2009.12.002
29. Choi C, Ganji SK, Deberardinis RJ, Hatanpaa KJ, Rakheja D, Kovacs Z, et al. 2-hydroxyglutarate detection by magnetic resonance spectroscopy in IDH-mutated patients with gliomas. *Nat Med.* (2012) 18:624–9. doi: 10.1038/nm.2682
30. Landheer K, Swanberg KM, Juchem C. Magnetic resonance spectrum simulator (MARSS), a novel software package for fast and computationally efficient basis set simulation. *NMR Biomed.* (2019) 34:e4129. doi: 10.1002/nbm.4129
31. American Psychiatric Association. *Diagnostic and Statistical Manual of Mental Disorders: DSM-5.* Fifth edition. Arlington, VA: American Psychiatric Association (2013). doi: 10.1176/appi.books.9780890425596
32. Cohen AC. Pyridoxine in the prevention and treatment of convulsions and neurotoxicity due to cycloserine. *Ann N Y Acad Sci.* (1969) 166:346–9. doi: 10.1111/j.1749-6632.1969.tb54286.x
33. Bottomley PA. Spatial localization in nMR spectroscopy in vivo. *Ann N Y Acad Sci.* (1987) 508:333–48. doi: 10.1111/j.1749-6632.1987.tb32915.x
34. Dong Z, Peterson B. The rapid and automatic combination of proton mRSI data using multi-channel coils without water suppression. *Magn Reson Imaging.* (2007) 25:1148–54. doi: 10.1016/j.mri.2007.01.005
35. Dong Z, Dreher W, Leibfritz D. Toward quantitative short-echo-time in vivo proton mR spectroscopy without water suppression. *Magn Reson Med.* (2006) 55:1441–6. doi: 10.1002/mrm.20887
36. Vanhamme L, Van Den Boogaart A, Van Huffel S. Improved method for accurate and efficient quantification of mRS data with use of prior knowledge. *J Magn Reson.* (1997) 129:35–43. doi: 10.1006/jmre.1997.1244

37. Naressi A, Couturier C, Devos JM, Janssen M, Mangeat C, De Beer R, et al. Java-based graphical user interface for the mRUI quantitation package. *MAGMA*. (2001) 12:141–52. doi: 10.1007/BF02668096
38. Kraguljac NV, Reid MA, White DM, Den Hollander J, Lahti AC. Regional decoupling of n-acetyl-aspartate and glutamate in schizophrenia. *Neuropsychopharmacology*. (2012) 37:2635–42. doi: 10.1038/npp.2012.126
39. Zitkova L, Tousek J. Pharmacokinetics of cycloserine and terizidone. *A comparative study*. *Chemotherapy*. (1974) 20:18–28. doi: 10.1159/000221787
40. Zhu M, Nix DE, Adam RD, Childs JM, Peloquin CA. Pharmacokinetics of cycloserine under fasting conditions and with high-fat meal, orange juice, and antacids. *Pharmacotherapy*. (2001) 21:891–7. doi: 10.1592/phco.21.11.891.34524
41. Patel DS, Sharma N, Patel MC, Patel BN, Shrivastav PS, Sanyal M. Development and validation of a selective and sensitive lC-MS/MS method for determination of cycloserine in human plasma: application to bioequivalence study. *J Chromatogr B Analyt Technol Biomed Life Sci*. (2011) 879:2265–73. doi: 10.1016/j.jchromb.2011.06.011
42. Kreis R. The trouble with quality filtering based on relative cramer-Rao lower bounds. *Magn Reson Med*. (2016) 75:15–8. doi: 10.1002/mrm.25568
43. Moriguchi S, Takamiya A, Noda Y, Horita N, Wada M, Tsugawa S, et al. Glutamatergic neurometabolite levels in major depressive disorder: a systematic review and meta-analysis of proton magnetic resonance spectroscopy studies. *Mol Psychiatry*. (2019) 24:952–64. doi: 10.1038/s41380-018-0252-9
44. Chitty KM, Lagopoulos J, Lee RS, Hickie IB, Hermens DF. A systematic review and meta-analysis of proton magnetic resonance spectroscopy and mismatch negativity in bipolar disorder. *Eur Neuropsychopharmacol*. (2013) 23:1348–136. doi: 10.1016/j.euroneuro.2013.07.007
45. Taylor MJ. Could glutamate spectroscopy differentiate bipolar depression from unipolar? *J Affect Disord*. (2014) 167:80–4. doi: 10.1016/j.jad.2014.05.019
46. Scotti-Muzzi E, Umla-Runge K, Soeiro-De-Souza MG. Anterior cingulate cortex neurometabolites in bipolar disorder are influenced by mood state and medication: a meta-analysis of (1)H-MRS studies. *Eur Neuropsychopharmacol*. (2021). doi: 10.1016/j.euroneuro.2021.01.096
47. Mcewen AM, Burgess DT, Hanstock CC, Seres P, Khalili P, Newman SC, et al. Increased glutamate levels in the medial prefrontal cortex in patients with postpartum depression. *Neuropsychopharmacology*. (2012) 37:2428–35. doi: 10.1038/npp.2012.101
48. Merritt K, Mcguire PK, Egerton A, Investigators HMIS, Aleman A. Association of age, antipsychotic medication, and symptom severity in schizophrenia with proton magnetic resonance spectroscopy brain glutamate level: a Mega-analysis of individual participant-Level data. *JAMA Psychiatry*. (2021). doi: 10.1001/jamapsychiatry.2021.0380
49. Brachman RA, Mcgowan JC, Perusini JN, Lim SC, Pham TH, Faye C, et al. Ketamine as a prophylactic against stress-Induced depressive-like behavior. *Biol Psychiatry*. (2016) 79:776–86. doi: 10.1016/j.biopsych.2015.04.022
50. Kantrowitz JT, Grinband J, Goff DC, Lahti AC, Marder SR, Kegeles LS, et al. Proof of mechanism and target engagement of glutamatergic drugs for the treatment of schizophrenia: rCTs of pomaglumetad and tS-134 on ketamine-induced psychotic symptoms and pharmacoBOLD in healthy volunteers. *Neuropsychopharmacology*. (2020) 45:1842–1850. doi: 10.1038/s41386-020-0706-z
51. Kantrowitz JT, Dong Z, Milak MS, Rashid R, Kegeles LS, Javitt DC, et al. *Higher Ventromedial Prefrontal Glx and Glutamate Levels in Unmedicated Major Depressive Disorder* (under review).
52. Grabb MC, Cross AJ, Potter WZ, Mccracken JT. Derisking psychiatric drug development: the nIMH's fast fail program, a Novel precompetitive model. *J Clin Psychopharmacol*. (2016) 36:419–21. doi: 10.1097/JCP.0000000000000536
53. Krystal AD, Pizzagalli DA, Mathew SJ, Sanacora G, Keefe R, Song A, et al. The first implementation of the nIMH fAST-FAIL approach to psychiatric drug development. *Nat Rev Drug Discov*. (2018) 18:82–4. doi: 10.1038/nrd.2018.222
54. Krystal AD, Pizzagalli DA, Smoski M, Mathew SJ, Nurnberger J Jr, Lisanby SH, et al. A randomized proof-of-mechanism trial applying the 'fast-fail' approach to evaluating kappa-opioid antagonism as a treatment for anhedonia. *Nat Med*. (2020) 26:760–8. doi: 10.1038/s41591-020-0806-7
55. Park LT, Kadriu B, Gould TD, Zanos P, Greenstein D, Evans JW, et al. A randomized trial of the n-Methyl-d-Aspartate receptor glycine site antagonist prodrug 4-Chlorokynurenine in treatment-Resistant depression. *Int J Neuropsychopharmacol*. (2020) 23:417–25. doi: 10.1093/ijnp/pyaa025
56. Murphy N, Ramakrishnan N, Vo-Le B, Vo-Le B, Smith MA, Iqbal T, et al. A randomized cross-over trial to define neurophysiological correlates of aV-101 n-methyl-D-aspartate receptor blockade in healthy veterans. *Neuropsychopharmacology*. (2021) 46:820–7. doi: 10.1038/s41386-020-00917-z

Conflict of Interest: JK reports having received consulting payments within the last 24 months from Alphasights, Charles River Associates, Medscape, Putnam, techspert.io, Third Bridge, MEDACorp, Parexel, GroupH, Simon Kucher, ECRI Institute, ExpertConnect, Parexel, Schlesinger Group, CelloHealth, Acsel Health, Strafluence, Guidepoint, L.E.K. and System Analytic. He serves on the MedinCell Psychiatry and Karuna Mechanism of Action (MOA) Advisory Boards. He has conducted clinical research supported by the NIMH, Sunovion, Roche, Alkermes, Cerevance, Corcept, Takeda, Taisho, Lundbeck, Boehringer Ingelheim, NeuroRX and Teva within the last 24 months. JK was a co-investigator on a study that receives lumeteperone and reimbursement for safety testing for an investigator-initiated research from Intra-Cellular Therapies Inc. He owns a small number of shares of common stock from GSK. JM receives royalties for commercial use of the C-SSRS from the Research Foundation for Mental Hygiene.

The remaining authors declare that the research was conducted in the absence of any commercial or financial relationships that could be construed as a potential conflict of interest.

frontiers in Psychiatry

ORIGINAL RESEARCH
published: 18 June 2021
doi: 10.3389/fpsyt.2021.673159

Ketamine and Attentional Bias Toward Emotional Faces: Dynamic Causal Modeling of Magnetoencephalographic Connectivity in Treatment-Resistant Depression

Jessica R. Gilbert, Christina S. Galiano, Allison C. Nugent and Carlos A. Zarate*

Experimental Therapeutics and Pathophysiology Branch, National Institute of Mental Health, National Institutes of Health, Bethesda, MD, United States

OPEN ACCESS

Edited by:
Natasa Petronijevic, University of Belgrade, Serbia

Reviewed by:
Lucas Quarantini, Universidade Federal da Bahia, Brazil
Sophie E. Holmes, Yale University, United States

***Correspondence:**
Jessica R. Gilbert
jessica.gilbert@nih.gov

Specialty section:
This article was submitted to Molecular Psychiatry, a section of the journal Frontiers in Psychiatry

Received: *26 February 2021*
Accepted: *25 May 2021*
Published: *18 June 2021*

Citation:
Gilbert JR, Galiano CS, Nugent AC and Zarate CA (2021) Ketamine and Attentional Bias Toward Emotional Faces: Dynamic Causal Modeling of Magnetoencephalographic Connectivity in Treatment-Resistant Depression. Front. Psychiatry 12:673159. doi: 10.3389/fpsyt.2021.673159

The glutamatergic modulator ketamine rapidly reduces depressive symptoms in individuals with treatment-resistant major depressive disorder (TRD) and bipolar disorder. While its underlying mechanism of antidepressant action is not fully understood, modulating glutamatergically-mediated connectivity appears to be a critical component moderating antidepressant response. This double-blind, crossover, placebo-controlled study analyzed data from 19 drug-free individuals with TRD and 15 healthy volunteers who received a single intravenous infusion of ketamine hydrochloride (0.5 mg/kg) as well as an intravenous infusion of saline placebo. Magnetoencephalographic recordings were collected prior to the first infusion and 6–9 h after both drug and placebo infusions. During scanning, participants completed an attentional dot probe task that included emotional faces. Antidepressant response was measured across time points using the Montgomery-Asberg Depression Rating Scale (MADRS). Dynamic causal modeling (DCM) was used to measure changes in parameter estimates of connectivity *via* a biophysical model that included realistic local neuronal architecture and receptor channel signaling, modeling connectivity between the early visual cortex, fusiform cortex, amygdala, and inferior frontal gyrus. Clinically, ketamine administration significantly reduced depressive symptoms in TRD participants. Within the model, ketamine administration led to faster gamma aminobutyric acid (GABA) and N-methyl-D-aspartate (NMDA) transmission in the early visual cortex, faster NMDA transmission in the fusiform cortex, and slower NMDA transmission in the amygdala. Ketamine administration also led to direct and indirect changes in local inhibition in the early visual cortex and inferior frontal gyrus and to indirect increases in cortical excitability within the amygdala. Finally, reductions in depressive symptoms in TRD participants post-ketamine were associated with faster α-amino-3-hydroxy-5-methyl-4-isoxazolepropionic acid (AMPA) transmission and increases in gain control of spiny stellate cells in the early visual cortex. These findings provide additional support for the GABA and NMDA

inhibition and disinhibition hypotheses of depression and support the role of AMPA throughput in ketamine's antidepressant effects.

Clinical Trial Registration: https://clinicaltrials.gov/ct2/show/NCT00088699?term=NCT00088699&draw=2&rank=1, identifier NCT00088699.

Keywords: ketamine, major depressive disorder, magnetoencephalography, dynamic causal modeling, amygdala

INTRODUCTION

Ketamine's rapid antidepressant effects have galvanized research into the neurobiological underpinnings of mood disorders and have increased focus on the potential role that the glutamatergic and GABAergic systems play in the etiology and pathophysiology of both major depressive disorder (MDD) (1–3) and bipolar depression (4). As a result of promising clinical and preclinical data, interest in investigating the glutamate system has grown exponentially (5), with many studies focusing on ketamine and its glutamatergically-modulating metabolites as viable clinical treatment options (6–8). A wealth of studies have now demonstrated that a single infusion of sub-anesthetic-dose ketamine can rapidly (within hours) relieve depressive symptoms in individuals with both MDD (6, 9) and bipolar depression (7, 10), including those who are treatment-resistant (TRD). Repeat-dose studies have also pointed to continued improvements over longer time periods compared with a single administration (11). Understanding the mechanism of action underlying ketamine's rapid antidepressant effects could help identify novel biomarkers of antidepressant response and expedite the development of novel, rapid-acting therapeutics capable of more effectively treating depressive symptoms without the psychotomimetic side effects and risk for misuse associated with ketamine.

Ketamine is a non-competitive N-methyl-D-aspartate (NMDA) receptor antagonist. Nevertheless, a host of studies suggest the possibility that NMDA receptor antagonism may not be the direct mechanism underlying ketamine's antidepressant effects, and several other mechanisms are being investigated. For instance, recent studies found that the ketamine metabolite (2*R*,6*R*)-hydroxynorketamine (HNK) exerts antidepressant effects in animal models even though it is not an NMDA receptor antagonist at therapeutically relevant concentrations (12); rather, (2*R*,6*R)*-HNK appears to exert antidepressant effects by enhancing α-amino-3-hydroxy-5-methyl-4-isoxazolepropionic acid (AMPA) throughput (13).

In addition, subanesthetic-dose ketamine administration leads to immediate disinhibition of glutamatergic neurons, producing a glutamate surge (14). This surge is thought to result from NMDA receptor blockade by ketamine of fast-spiking gamma-aminobutyric acid (GABA)-ergic interneurons, leading to local inhibition of interneuron tonic firing and the subsequent disinhibition of pyramidal neurons (15, 16). Due to NMDA receptor blockade on post-synaptic excitatory neurons, excess synaptic glutamate is primarily taken up by AMPA receptors, thereby activating neuroplasticity-related signaling pathways, including mammalian target of rapamycin complex 1 (mTORC1) (17, 18) and brain-derived neurotrophic factor (BDNF) (19), both of which result in increased synaptic potentiation and synaptogenesis. Furthermore, a host of cascading intracellular changes following ketamine administration involve eukaryotic elongation factor 2, which promotes BDNF release (20, 21) and homeostatic synaptic scaling mechanisms (22); cellular changes resulting from direct inhibition of extrasynaptic NMDA receptors (23) activate plasticity mechanisms and also promote synaptic potentiation.

Within the field of psychiatry, a growing body of evidence suggests that altering the ratio of cortical excitation/inhibition balance could underlie a host of disorders, including depression (24, 25). Preclinical work has also demonstrated that therapeutic-dose ketamine reduces inhibitory input onto pyramidal cells, thereby increasing synaptically-driven pyramidal cell excitation in single cell and population-level electrophysiological recordings (26). Modeling work has robustly demonstrated that gamma rhythms reflect a balance between network-level excitation and inhibition (27–29). In addition, work from our laboratory and that of others found that therapeutic-dose ketamine administration leads to robust increases in gamma power (30–33) in TRD participants, potentially reflecting alterations in excitation-inhibition balance associated with antidepressant response (32, 34, 35).

Emotional processing deficits have been extensively reported in MDD. For example, compared to healthy volunteers, individuals with MDD showed a bias toward negative emotional information (36, 37), including a bias toward faces demonstrating negative emotions compared to positive emotions (38, 39). In addition, antidepressants are thought to normalize neural activity by potentially increasing activity to positive stimuli and decreasing activity to negative stimuli within brain regions important for emotion processing, including regions of the frontal cortex and the amygdala (40). One task of particular interest is the dot probe attentional task, which has been used to study emotional biases in depression (41). Several neuroimaging studies have identified activation differences between healthy volunteers and participants with MDD using a dot probe task (42–44); anxiolytic effects following stimulation of frontal cortex (45) and pharmacological treatment effects following ketamine (43) on task performance in TRD have also been observed. In addition, ketamine has been shown to normalize brain activation in TRD patients in regions of frontal cortex, while its antidepressant effects are associated with reduced activity to negative stimuli and increased activity to positive stimuli in the amygdala (43). Here we sought to examine the influence of ketamine on effective connectivity using an attentional dot probe task with emotional faces, focusing on modeling connectivity along the ventral face-processing stream,

with particular interest in ketamine effects on activity within the frontal cortex and amygdala.

This study sought to model ketamine-mediated differences in brain network connectivity in a group of participants with TRD and healthy volunteers who underwent both ketamine and placebo saline infusions. This double-blind, crossover, placebo-controlled study used magnetoencephalography (MEG) in tandem with dynamic causal modeling (DCM) to model effective connectivity at three timepoints: (a) baseline, (b) 6–9 h following subanesthetic (0.5 mg/kg) ketamine infusion, and (c) 6–9 h following placebo saline infusion. DCM uses a biophysical model that includes realistic local neuronal architecture to model effective connectivity between regions of interest (ROIs). Model inversion—the fitting of parameterized mean-field neuronal models to electrophysiological data features—results in *in silico* parameter estimates that govern unobservable neuronal states including receptor-mediated connectivity between cell populations (here, a lumped estimate of AMPA/NMDA and GABA for excitatory and inhibitory intrinsic connections, respectively, in addition to AMPA and NMDA drive estimates for all region-to-region connections) and decay times of specific receptor types (here, AMPA, GABA, and NMDA) (46). DCM was used to estimate connectivity in a fully reciprocally connected network of regions activated by the task, including the early visual cortex, fusiform cortex, amygdala, and inferior frontal gyrus. Because the study focused on measuring parameters that were significantly altered following ketamine administration, the post-ketamine scan was directly compared with both the baseline and placebo saline scans. It was predicted that ketamine would increase gamma power in our defined network—particularly in the amygdala—in line with previous findings of gamma power as a putative marker of ketamine-mediated synaptic potentiation (47) and a normalizer of activation in the amygdala post-ketamine administration in TRD participants (43). The study also sought to examine group (TRD participants vs. healthy volunteers) by session (ketamine vs. baseline/placebo) interaction effects on modeled parameter estimates governing receptor time constants and connectivity within the amygdala, a key region involved in the emotional processing of face stimuli.

MATERIALS AND METHODS

Participants

All participants were studied at the National Institute of Mental Health (NIMH) in Bethesda, Maryland between September 2011 and August 2016. The present study used data drawn from a larger clinical trial (NCT00088699) that assessed ketamine's antidepressant effects. The present study comprised 19 individuals with a DSM-IV-TR diagnosis of TRD (48) without psychotic features (11 F, mean age = 36.7 ± 10.9 years) and 15 healthy volunteers (11F, mean age = 34.7 ± 11.8 years). Full demographic and clinical characteristics of the entire sample have been previously described (34). This subset of participants was selected because they had usable MEG scans for all three sessions of interest. Individuals with TRD were 18–65 years old, were experiencing a major depressive episode lasting at least 4 weeks, had not responded to at least one adequate antidepressant trial during the current major depressive episode, and had a Montgomery-Asberg Depression Rating Scale (MADRS) (49) score of $\geq$ 20 at screening and before each infusion. The TRD sample had failed on average 3.8 antidepressant trials across their lifetime. Diagnosis was determined by Structured Clinical Interviews for Axis I DSM-IV-TR Disorders (SCID)–Patient Edition (50). Healthy volunteers were also 18–65 years old, had no Axis I disorder as determined by the Structured Clinical Interviews for Axis I DSM-IV-TR Disorders – Non-Patient Edition, and had no family history of Axis I disorders in first-degree relatives. All TRD participants were hospitalized for the duration of the study and were drug-free from psychotropic medications for at least 2 weeks prior to MEG testing (5 weeks for fluoxetine, 3 weeks for aripiprazole). Healthy volunteers completed study procedures as inpatients but were otherwise outpatients. All participants were also in good health as evaluated by a medical history and physical examination, toxicology screens and urinalysis, blood laboratory results, clinical MRI, and electrocardiogram. The Combined Neuroscience Institutional Review Board at the National Institutes of Health approved the study. All participants provided informed written consent and were matched with an NIMH advocate from the Human Subjects Protection Unit to monitor consent and participation.

Clinical Measurements

The primary clinical outcome measure for TRD patients—the MADRS (49)—was administered 60 min prior to infusions (both ketamine and placebo) and at multiple time points (230 min and Days 1, 2, and 3) following infusions. Clinical outcome for TRD participants was modeled using all available data, controlling for both the period-specific baseline (−60 min rating of that infusion) as well as a participant-average baseline (averaging both −60 min ratings) and infusion. Repeated observations were accounted for by freely estimating the residual variance and covariance for each participant/infusion by drug (i.e., unstructured covariance matrix estimated by drug). The difference between ketamine and placebo was then estimated at 230 min, the time point closest to the MEG scan.

MEG Acquisition and Preprocessing

MEG recordings were collected at baseline and 6–9 h following both ketamine and placebo saline experimenter-blinded infusions. The timing of data collection for the ketamine infusion occurred past the half-life of the drug. Ketamine and placebo infusions occurred 14 days apart, with infusion order randomized across participants.

During each scanning session, participants completed a dot probe task with emotional face stimuli presented using E-Prime presentation software (Psychology Software Tools, Pittsburgh, PA). The task has been described previously (43). Briefly, the task used a mixed block/event-related design. During each trial, a fixation cross was presented centrally for 500 ms, where the participant was instructed to maintain focus. This was followed by the presentation of two simultaneous, side-by-side faces for 500 ms. One face displayed a happy, angry, or neutral expression, while the other was always neutral. After each pair of faces, a single dot was presented for 200 ms behind one of the two

faces, and participants were instructed to press a button to indicate the presentation side (left or right). Trials where the dot replaced the emotional face were considered congruent trials, as the expectation was that attention would be biased toward the emotional face. Trials where the dot replaced the neutral face were considered incongruent. Trials were randomized and counterbalanced for emotion, gender of face, side of emotional face, and side of probe. Each trial was followed by a 1,300 ms blank interstimulus interval. Jitter was also randomly added to reduce expectancy effects, during which a central fixation cross was presented. Trials were additionally blocked into two "angry blocks" and two "happy blocks," with block order randomized across participants. Angry blocks comprised trials with angry and neutral faces or two neutral faces. Happy blocks comprised trials with happy and neutral faces or two neutral faces. This resulted in four emotional face trial types: angry congruent, angry incongruent, happy congruent, and happy incongruent, each having 48 trials over the experimental run. In addition, because neutral pairs were included in both happy and angry blocks, there were a total of 96 neutral paired trials.

Neuromagnetic data were collected using a 275-channel CTF system with SQUID-based axial gradiometers (VSM MedTech Ltd., Couquitlam, BC, Canada) housed in a magnetically-shielded room (Vacuumschmelze, Germany). Data were collected at 600 Hz with a bandwidth of 0–300 Hz. Synthetic third order balancing was used for active noise cancellation. Offline, MEG data were first visually inspected, and trials were removed where visible artifacts (e.g., head movements, jaw clenches, eye blinks, and muscle movements) were present. Second, individual channels showing excessive sensor noise were marked as bad and removed from the analysis. Data were then bandpass filtered from 1 to 58 Hz and epoched from −100 to 1,000 ms peristimulus time. The analysis routines available in the academic freeware SPM12 (Wellcome Trust Centre for Neuroimaging, London, UK, http://www.fil.ion.ucl.ac.uk/spm/) were used for data processing. This work used the computational resources of the NIH HPC Biowulf cluster (http://hpc.nih.gov).

Source Localization and Source Activity Extraction

The multiple sparse priors routine implemented in SPM12 was used to identify gamma frequency (30–58 Hz) sources of activity from each participant's sensor-level data over a peristimulus event time window from −100 to 1,000 ms. Gamma frequency was targeted, as recent findings in both animals and humans have demonstrated robust, ketamine-mediated cortical responses in that band (30–32, 51, 52), in keeping with ketamine's ability to alter excitation-inhibition balance (47). Induced responses to face pairs were localized to 512 potential mesh points using a variational Bayesian approach following co-registration of sensor positions to a canonical template brain. Participant-level activation maps were constructed following inversion of each session (i.e., baseline, placebo, ketamine) separately for all participants. No prior constraints on source location were used. Following the inversion, statistical maps of group activity were computed and a mixed-effects ANOVA was used to define source-localized cortical regions showing a main effect of task across all trial types, thresholded at $p < 0.05$ family-wise error correction. Secondarily, the main effect of infusion (here, ketamine compared with placebo) was tested using a more liberal criterion of $p < 0.05$, uncorrected.

Group-level statistical activation maps demonstrated stimulus-induced gamma-band activity in a network of brain regions including the bilateral early visual cortices, and extending into the parietal and frontal regions (**Figure 1A**). Because the study sought to characterize connectivity in a network of regions activated during visual processing of emotional faces, four regions were investigated in order to model forward and backward connections in a left-lateralized network: early visual cortex, fusiform cortex, amygdala, and inferior frontal gyrus (see **Figure 1** and below for source locations). Early visual cortex, fusiform cortex, and inferior frontal gyrus were defined using their corresponding peak voxels from the average effect contrast in **Figure 1A**. Amygdala was defined using the peak voxel from the infusion contrast in **Figure 1A**. Subsequent DCM analyses focused on characterizing connectivity in these regions in a wide, 1–50 Hz frequency band to model stimulus-induced event-related potentials.

Dynamic Causal Modeling

DCM uses a biophysical model of neural responses based on neural mass models to predict recorded electrophysiological data features (53). Dynamics are modeled using parameterized mean-field models that include coupled differential equations modeling unobservable neuronal states, such as decay times of specific receptors and receptor-mediated connectivity between cell populations. The present study specifically used the "CMM_NMDA" model, a conductance-based neural mass model for electrophysiology, as implemented in SPM12 (http://www.fil.ion.ucl.ac.uk/spm/), to model responses between ROIs. The CMM_NMDA model includes connection parameters for AMPA- and NMDA-mediated glutamatergic signaling as well as GABA signaling. Within the model, superficial pyramidal cells encode and carry feed-forward signaling to stellate cells, while deep pyramidal cells carry feedback signaling to superficial pyramidal cells and inhibitory interneurons (**Figure 1B**). Additional parameters include AMPA, GABA, and NMDA time constants, the inverse of which model the rate of receptor channel opening and closing within each ROI. The model has been extensively described in the literature, and detailed equations can be found elsewhere (30, 54, 55). The model has been used extensively to estimate NMDA and AMPA connectivity changes following ketamine administration in animal (55) and human studies (30, 56, 57).

Thalamic (stimulus-bound) input was modeled with a Gaussian bump function that drove activity in early visual cortex (MNI coordinates: −8, −94, −8) in the model. Two models of message-passing were constructed between the early visual cortex, fusiform cortex (MNI coordinates: −52, −52, −22), amygdala (MNI coordinates: −25, −3, −16), and inferior frontal gyrus (MNI coordinates: −48, −28, −2) (see **Figure 2A**). The first model was a traditional bottom-up processing model that included forward connections from early visual cortex to

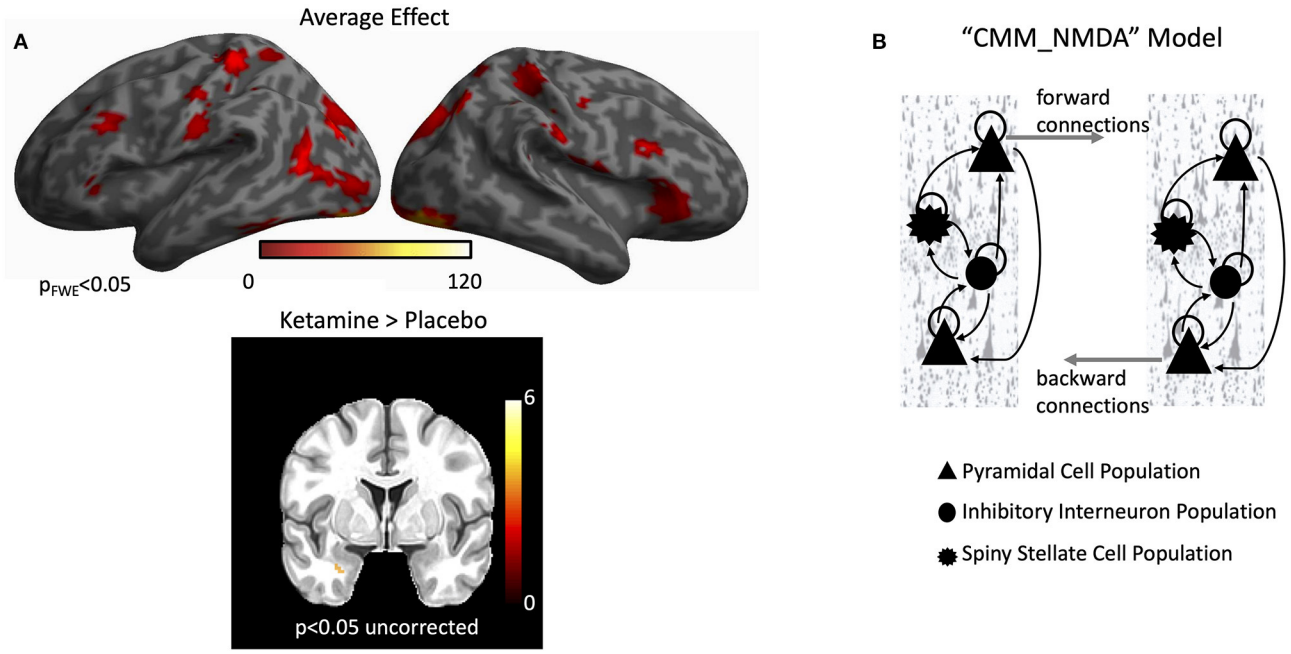

FIGURE 1 | Gamma power and dynamic causal modeling (DCM). **(A)** A network of regions showed robust increases in induced gamma power during the task. These included the bilateral early visual cortex, bilateral fusiform cortex, and bilateral inferior frontal gyrus. When directly testing the effect of infusion, higher induced gamma power was found in the left amygdala for the ketamine infusion. **(B)** The default CMM_NMDA model includes four distinct intrinsic (within region) cell layers: superficial pyramidal cells, spiny stellate cells, inhibitory interneurons, and deep pyramidal cells [adapted from Gilbert et al. (57)]. Intrinsic excitatory connections were mediated by α-amino-3-hydroxy-5-methyl-4-isoxazolepropionic acid (AMPA) and N-methyl-D-aspartate (NMDA) receptors while intrinsic inhibitory connections were mediated by gamma aminobutyric acid (GABA) receptors. Each cell population included a self-gain parameter that reflected precision for each cell type. Each receptor also included distinct time constants and dynamics in the model. Between regions, superficial pyramidal cells carry forward extrinsic signals to excitatory spiny stellate cells. Deep pyramidal cells carry backward extrinsic signals to both superficial pyramidal cells and inhibitory interneurons.

fusiform cortex, fusiform cortex to amygdala, and amygdala to inferior frontal gyrus. Backward connections ensured reciprocal message-passing in a top-down hierarchy. Model 2 included two additional connections: direct forward and reciprocal backward connections between early visual cortex and inferior frontal gyrus. These connections were included to model presumed magnocellular projections to frontal cortex, which have been shown to exert early top-down effects on bottom-up visual signaling (58–60). Face emotion modulated all region-to-region connections in both models (i.e., comparing trials in which happy vs. angry faces appeared).

For the DCM analyses, MEG activity for the extracted time series was fitted over 1–500 ms peristimulus time in a wide frequency band from 1 to 50 Hz using an event-related potential (ERP) model to capture ERPs of evoked activity. For computational efficiency, DCM optimizes a posterior density over free parameters (parameterized by its mean and covariance) *via* a standard variational Bayesian inversion procedure (61). In the present analysis, initial DCMs were computed for each participant and session, and model fits were assessed. The posterior estimates were then used to initialize a second set of DCMs for each participant and session, and model fits were again assessed. This iterative procedure occurred for both Model 1 and Model 2. In both cases, the initialized model resulted in a better fit of the model to the data. The negative free energy bound on the log-model evidence was then used to adjudicate between Model 1 and Model 2 across participants, selecting the model with the greatest log-model evidence for subsequent analyses. Parameter estimates were extracted from optimized DCMs for the winning model for each participant and session to compare ketamine-mediated effects across parameter estimates.

To determine the mixture of parameters that mediated ketamine's effects, a second-level modeling extension of DCM called parametric empirical Bayesian analysis (62) was applied. This analysis refits a full model (where all parameters can covary according to grouping) and provides reduced models where smaller combinations of parameters are considered and informed by differences between sessions. Group, session, and group by session effects on all parameters were specifically tested in the second-level design matrix, where the first column represented the average effect over all participants and sessions, the second column tested for the effect of group, the third column tested for the effect of drug, and the fourth column tested for group by drug interactions. Group by drug interactions were of particular interest, though group and drug effects are also reported here.

Finally, as additional exploratory analyses, *post-hoc* classical statistical tests were conducted to determine whether any parameters identified using parametric empirical Bayesian analysis as significantly contributing to group effect, drug effect, or group by drug interactions were associated with

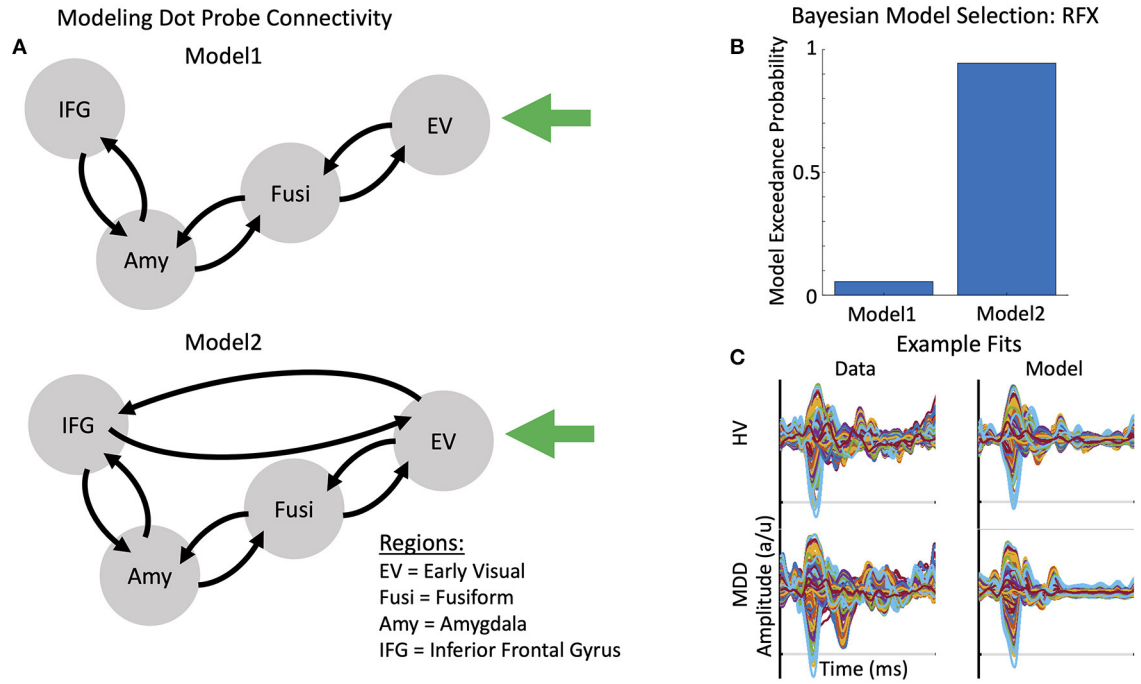

FIGURE 2 | Models of connectivity, winning model, and example model fits. **(A)** Two plausible models were constructed to account for message passing between the early visual cortex (EV), fusiform cortex (Fusi), amygdala (Amy), and inferior frontal gyrus (IFG). Model 1 included reciprocal forward and backward connections from the EV to the Fusi, from the Fusi to the Amy, and from the Amy to the IFG. Model 2 included a direct, reciprocal, forward and backward connection from the EV to the IFG. **(B)** Bayesian Model Selection (BMS) was used to adjudicate between models, demonstrating that Model 2, with fully interconnected feedforward and feedback connections between each region, had the greatest exceedance probability. RFX, random effects. **(C)** Example evoked responses (left) and model fits (right) for a healthy volunteer (HV, top) and participant with treatment-resistant major depressive disorder (MDD) (bottom).

antidepressant response in the TRD participants only. Here, changes in parameter values from baseline to ketamine were specifically examined and correlated with changes in MADRS score from baseline to post-ketamine using pairwise linear correlation as implemented in MATLAB software. Because this analysis was exploratory, a liberal criterion of $p < 0.05$, uncorrected, was used.

RESULTS

Clinical and Behavioral

Clinically, the effect of drug at 230 min post-ketamine infusion compared to 230 min post-placebo infusion was significant [$t_{18} = 2.07$, $p < 0.05$], for an estimated reduction of 5.37 (SE = 2.28) points on total MADRS score (95% CI: −0.05, +9.48) following ketamine administration (ketamine −60 min = 33.37 ± 4.39, ketamine 230 min = 26.95 ± 11.06; placebo −60 min = 32.26 ± 4.79, placebo 230 min = 31.21 ± 5.03). Behaviorally, both reaction time bias (calculated as the difference between congruent and incongruent trials for happy and angry faces, respectively) and accuracy rates on the emotional dot probe task were examined using multi-way ANOVAs to look for main effects of group, session (baseline, placebo, ketamine), emotion (happy vs. angry), and congruency (congruent vs. incongruent; calculated for accuracy scores only). In addition, all two-, three-, and four-way interactions were considered. Although no significant behavioral effects were observed on reaction time bias scores, main effects were found for group ($F = 14.43$, $p < 0.01$) and session ($F = 3.58$, $p < 0.05$) on accuracy scores for participants; in particular, TRD participants were more accurate (mean = 94.2%) than healthy volunteers (mean = 88.8%). In addition, both TRD participants and healthy volunteers were most accurate during the baseline session (mean = 94.2%) followed by the ketamine session (mean = 91.6%) and the placebo session (mean = 89.8%). *Post-hoc* tests using Bonferroni correction found significant accuracy differences between the baseline and placebo sessions across participants ($t = 3.45$, $p < 0.05$).

Source-Level

MEG data were subsequently source-localized to infer the primary generators of the signal using the multiple sparse priors routine. Significant group-level induced gamma-band activation was identified in response to the dot probe task (**Figure 1A**). The network of regions activated included the bilateral early visual cortex extending into higher-order visual areas in the occipital lobe, regions of the temporal lobe including the fusiform gyrus, and regions in both the parietal and frontal lobes, including the inferior frontal gyrus. When testing for the effect of infusion (ketamine vs. placebo), left-lateralized amygdala response was found at the more liberal criterion of $p < 0.05$, uncorrected. We therefore focused on characterizing parameter estimates of

effective connectivity using DCM for electrophysiology using a model that included left-lateralized early visual cortex, fusiform cortex, amygdala, and inferior frontal gyrus (**Figure 2A**).

Dynamic Causal Modeling

Two plausible models were constructed to account for connectivity between ROIs. Using Bayesian model selection to adjudicate between these models, Model 2—which included the addition of forward and backward connections between the early visual cortex and inferior frontal gyrus—was found to have the strongest model evidence (**Figure 2B**). Example model fits for a TRD participant and a healthy volunteer are shown in **Figure 2C**.

Parametric empirical Bayes—an analysis approach that allows testing of random effects of model parameters at the group level—was used to test for parameters contributing to the group effect, drug effect, and group by drug interactions. All fitted parameters in the model were considered, focusing on parameters that exhibited meaningful effects (specifically, parameters having a probability of 95% or greater). All identified parameters are reported in **Tables 1–3**, and parameters showing meaningful group by drug interactions are reported here. Four receptor time constants showed meaningful group by drug interactions, including the GABA time constant in the early visual cortex and the NMDA time constants in the early visual cortex, fusiform cortex, and amygdala (**Figure 3A**). As the inverse of time constants are rate constants, faster rates of GABA and NMDA signal transmission were found in the early visual cortex for TRD participants post-ketamine, while healthy volunteers showed slower GABA signal transmission coupled with faster NMDA signal transmission following ketamine. In the fusiform cortex, faster NMDA signal transmission was observed for TRD participants post-ketamine, while healthy volunteers showed slower signal transmission. Finally, slower NMDA signal transmission in amygdala was observed for both groups post-ketamine.

Our second-level modeling extension also identified five intrinsic, within-region connections that showed meaningful group by drug interaction effects; three were in the early visual cortex, with one each in the amygdala and inferior frontal gyrus (**Figure 3B**). In the early visual cortex, decreased self-inhibitory drive was observed on both spiny stellate cells and inhibitory interneurons for TRD participants post-ketamine; in contrast, healthy volunteers showed increased self-inhibitory drive on both cell types post-ketamine. Ketamine was also found to reduce inhibitory drive from inhibitory interneurons to spiny stellate cells in the early visual cortex for both groups. In the amygdala, increased excitatory drive from deep pyramidal cells to inhibitory interneurons was noted for TRD participants post-ketamine, while healthy volunteers showed decreased excitatory drive between these connections. Finally, reduced self-inhibitory drive on superficial pyramidal cells in the inferior frontal gyrus was noted in healthy volunteers post-ketamine, but no changes were observed in TRD participants.

Parameters Associated With Antidepressant Response

Finally, we explored whether any meaningful parameters identified as contributing to the group effect, drug effect, or group by drug interactions were associated with clinical change at 230 min post-ketamine compared to baseline. Two parameters were found to be associated with antidepressant response (**Figure 4**). First, change in AMPA time constants from baseline to ketamine were associated with antidepressant response in the TRD participants ($r = 0.4917$, $p < 0.05$), with faster AMPA signal transmission post-ketamine associated with better antidepressant response. Second, change in self-inhibitory drive of spiny stellate cells in early visual cortex from baseline to ketamine was associated with antidepressant response ($r = -0.6545$, $p < 0.01$), with larger self-inhibition on spiny stellate cells post-ketamine associated with better antidepressant response.

DISCUSSION

This study used MEG recordings collected while participants completed a dot probe task with emotional faces in tandem with DCM to probe ketamine's effects in individuals with TRD and healthy volunteers. The goal was to measure changes in effective (causal) connectivity within and between the early visual cortex, fusiform cortex, amygdala, and inferior frontal gyrus, in addition to changes in AMPA, GABA, and NMDA receptor time constants, following ketamine administration. We were particularly interested in ketamine's effects in the amygdala, a key region implicated in the pathophysiology of depression (63) demonstrating upregulation to positive faces and downregulation to negative faces during an attentional dot probe task following ketamine administration (43).

Clinically, we found significantly reduced depressive symptoms in our TRD sample post-ketamine, consistent with previous findings (6, 9). Controlling for the period-specific baseline and the participant-average baseline, ketamine was found to result in a 5.37-point reduction in MADRS score in the TRD sample. Behaviorally, no differences in reaction time bias scores were observed on the task. However, accuracy differences were observed between the two groups, with TRD participants significantly more accurate than healthy volunteers during the task. In addition, session effects were noted with regard to accuracy rates, with the best performance occurring during the baseline session, followed by the ketamine and then placebo sessions. Importantly, *post-hoc* tests found significant differences in accuracy between the baseline and placebo sessions only. These findings suggest that healthy volunteers were less engaged in the task and therefore did not perform as well as the TRD participants. In addition, task repetition led to poorer performance, especially following placebo saline infusion, where participants were perhaps least motivated to perform well-during the scan procedures.

We modeled induced gamma-band activity during the dot probe task, identifying a network of brain regions involved in the task. We also modeled regions showing an effect of infusion (ketamine vs. placebo) and found increased gamma

TABLE 1 | Group effects over parameters.

	Parameter	Parameter Estimate (Ep)	Posterior Probability (Pp)
	Time constants		
1	AMPA–Amy*	−0.0978	1
2	GABA–Fusi*	0.1501	1
3	GABA–IFG*	0.1534	1
4	NMDA–EV*	0.1763	1
5	NMDA–IFG*	−0.3113	1
	Intrinsic connectivity		
6	EV: inhibitory self-connection–ss*	0.1285	1
7	EV: inhibitory self-connection–ii	0.0604	0.531
8	Fusi: inhibitory self-connection–ss*	0.2202	1
9	Fusi: inhibitory self-connection–sp*	0.1363	1
10	Amy: excitatory connection–sp to dp*	−0.1424	1
11	IFG: inhibitory self-connection–ss*	0.1437	1

*Parametric empirical Bayes was used to identify the mixing of parameters that contributed to the effect of group. Note that the timing of data collection (6–9 h post-ketamine administration) occurred past the half-life of ketamine. Meaningful parameters were defined as those with a posterior probability (Pp) >95%. Ten parameters were found to significantly contribute to group effects. These included the α-amino-3-hydroxy-5-methyl-4-isoxazolepropionic acid (AMPA) time constant within the amygdala (Amy), gamma aminobutyric acid (GABA) time constants within the fusiform gyrus (Fusi) and inferior frontal gyrus (IFG), and N-methyl-D-aspartate (NMDA) time constants within the early visual cortex (EV) and IFG. In addition, the inhibitory self-connections on spiny stellate cells (ss) within the EV, Fusi, and IFG differed between groups, as did the inhibitory self-connection on superficial pyramidal cells (sp) within the Fusi, and the excitatory connections between sp and deep pyramidal cells (dp) in the Amy. Finally, the inhibitory self-connection on inhibitory interneurons (ii) in the EV showed a group effect, though not at our threshold. *Pp > 0.95.*

TABLE 2 | Drug effects over parameters.

	Parameter	Parameter estimate (Ep)	Posterior probability (Pp)
	Time constants		
1	AMPA–EV*	0.132	1
2	GABA–Amy*	0.1363	1
3	GABA–IFG*	0.1349	1
4	NMDA–EV*	−0.2028	1
5	NMDA–Amy*	0.5303	1
6	NMDA–IFG*	−0.2419	1
	Intrinsic connectivity		
7	EV: excitatory connection–sp to dp*	0.1988	1
8	EV: inhibitory connection–ii to sp*	−0.2011	1
9	IFG: inhibitory self-connection–ss	0.0773	0.502
10	IFG: excitatory connection–ss to ii*	0.1805	1

*Parametric empirical Bayes was used to identify the mixing of parameters that contributed to the effect of drug. Meaningful parameters were defined as those with a probability (Pp) >95%. Nine parameters were found to significantly contribute to drug effects. These included the α-amino-3-hydroxy-5-methyl-4-isoxazolepropionic acid (AMPA) time constant within the early visual cortex (EV), gamma aminobutyric acid (GABA) time constants within the amygdala (Amy) and inferior frontal gyrus (IFG), and N-methyl-D-aspartate (NMDA) time constants within the EV, Amy, and IFG. In addition, the excitatory connections between superficial pyramidal cells (sp) and deep pyramidal cells (dp), and the inhibitory connections between inhibitory interneurons (ii) and sp differed following ketamine in the EV, as did excitatory connections between spiny stellate cells (ss) and ii in the IFG. Finally, the inhibitory self-connection on ss in the IFG showed a drug effect, though not at our threshold. *Pp > 0.95.*

power in the amygdala post-ketamine vs. placebo for both TRD participants and healthy volunteers. These findings are in keeping with preclinical studies suggesting increased cortical excitation following ketamine administration, due to NMDA inhibition reducing the activity of putative GABA interneurons (15). At a delayed rate, this increases the firing rate of pyramidal neurons due to enhanced AMPA throughput (15) that, in turn, leads to increased cortical excitation. Given that gamma power in the amygdala showed a drug-specific effect, with increased cortical excitation post-ketamine, this suggests that increased cortical excitation in this key emotional face processing region may be related to previous reports of normalization of emotional processing following drug administration (43). Notably, normalization of amygdalar activity post-ketamine was previously described in an fMRI study that included an attentional dot probe task with emotional faces in TRD participants (43), though this was not specifically examined in the present study.

Two plausible models of message passing between the early visual cortex and the inferior frontal gyrus were subsequently

TABLE 3 | Group by drug interactions over parameters.

	Parameter	Parameter Estimate (Ep)	Posterior Probability (Pp)
	Time constants		
1	GABA-EV*	−0.1274	1
2	NMDA-EV*	0.1994	1
3	NMDA-Fusi*	−0.1723	1
4	NMDA-Amy*	0.1502	1
	Intrinsic connectivity		
5	EV: inhibitory self-connection–ss*	−0.2778	1
6	EV: inhibitory connection–ii to ss*	−0.1837	1
7	EV: inhibitory self-connection–ii*	−0.4241	1
9	Amy: excitatory connection–dp to ii*	0.1998	1
10	IFG: inhibitory self-connection–sp*	0.1943	1

*Parametric empirical Bayes was used to identify the mixing of parameters that contributed to group by drug interactions. Meaningful parameters were defined as those with a probability (Pp) >95%. Nine parameters were found to significantly contribute to group by drug effects. These included gamma aminobutyric acid (GABA) time constants within the early visual cortex (EV) and N-methyl-D-aspartate (NMDA) time constants within the EV, fusiform cortex (Fusi), and amygdala (Amy). In addition, the inhibitory self-connections on spiny stellate cells (ss) and inhibitory interneurons (ii), as well as inhibitory connections between ii and ss in the EV showed group by drug interactions. Excitatory connections between deep pyramidal cells (dp) and ii in the Amy, in addition to inhibitory self-connections on superficial pyramidal cells (sp) in the inferior frontal gyrus (IFG) also showed group by drug interactions. *Pp > 0.95.*

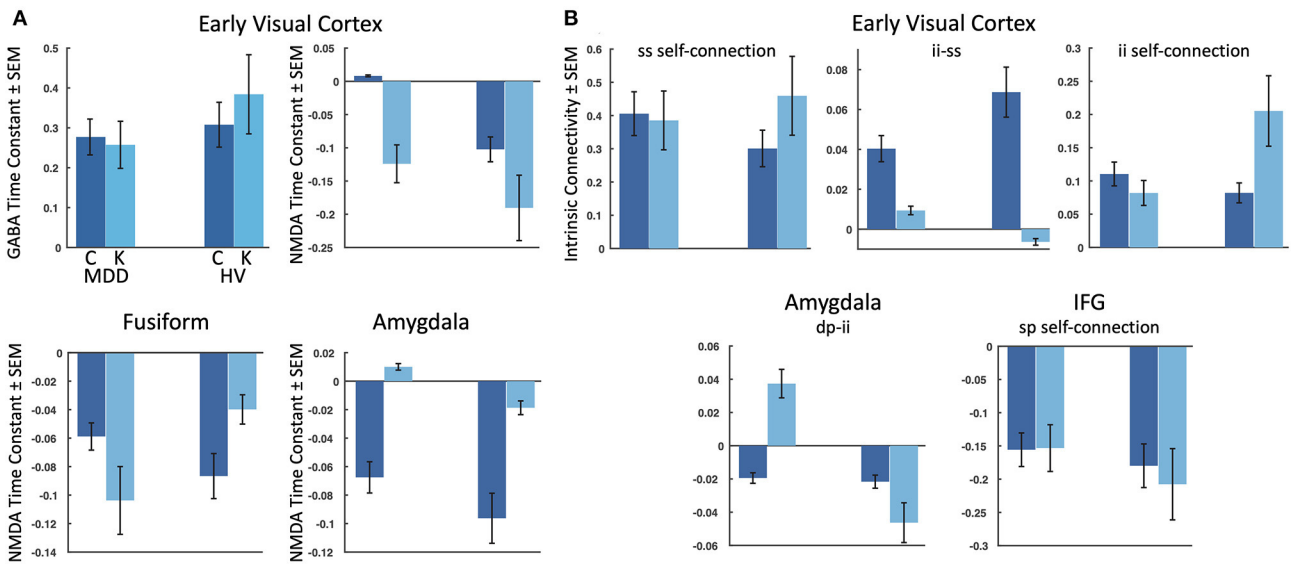

FIGURE 3 | Meaningful parameters showing group by drug interactions. The estimated log mean and variance of each meaningful (95% probability or greater) parameter are plotted for participants with treatment-resistant major depressive disorder (MDD) (left) and healthy volunteers (HV) (right) for: **(A)** the four receptor time constants showing group by drug interactions, and **(B)** the five intrinsic connectivity parameters showing group by drug interactions. IFG, inferior frontal gyrus, C, baseline/placebo sessions, K, ketamine session, ss, spiny stellate cells; ii, inhibitory interneurons; sp, superficial pyramidal cells; dp, deep pyramidal cells.

fit. A model that included traditional feedforward processing along the ventral stream to the amygdala in tandem with feedforward connections from the early visual cortex to the inferior frontal gyrus provided the best model fits, in line with ideas that top-down predictions serve to constrain bottom-up signal propagation (60). All fitted parameters were subsequently extracted, and a Bayesian modeling extension of DCM was used to test for meaningful parameters contributing to the group effect, drug effect, and group by drug interactions. Here, we focus on discussing group by drug interactions, as these are identified parameters where ketamine had differential effects between TRD participants and healthy volunteers. Four modeled receptor time constants showed group by drug interactions, including the GABA and NMDA time constants in the early visual cortex and the NMDA time constants in the fusiform cortex and amygdala. In the early visual cortex, ketamine administration led to faster GABA and NMDA transmission estimates for TRD participants, while GABA transmission slowed for healthy volunteers post-ketamine. In the fusiform cortex, faster NMDA transmission followed ketamine administration for TRD participants, though the rate of transmission slowed for healthy volunteers post-ketamine. Interestingly, a slowing of NMDA transmission was

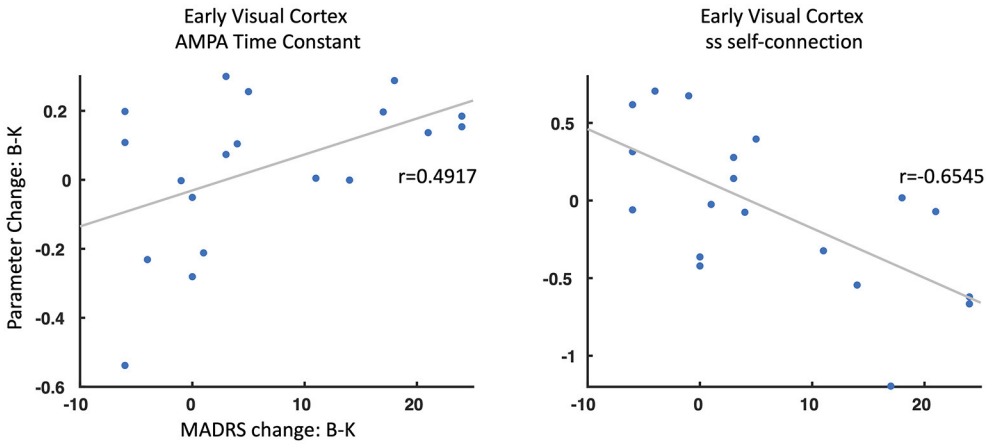

FIGURE 4 | Parameter change and antidepressant response. Two parameters showed a significant association between change from baseline (B) to ketamine (K) sessions and associated changes in Montgomery-Asberg Depression Rating Scale (MADRS) scores (B–K). ss, spiny stellate cells; AMPA, α-amino-3-hydroxy-5-methyl-4-isoxazolepropionic acid.

observed in the amygdala post-ketamine for both TRD and healthy volunteers, though healthy volunteers had significantly faster NMDA transmission at baseline/placebo than TRD participants. As the amygdala ROI was identified based on the effect of infusion (ketamine vs. placebo), slowing of NMDA transmission within this region is clearly related to drug effects. Although no association was noted between NMDA transmission in the amygdala and antidepressant response within our sample, future studies should examine whether these changes in NMDA time constants are related to other clinical measures of mood changes following drug administration.

In addition to changes in receptor time constants, group by drug interactions were found for modeled intrinsic connectivity within the early visual cortex, amygdala, and inferior frontal gyrus. In the early visual cortex, three intrinsic connection parameters showed group by drug changes in inhibitory drive. First, decreased GABAergic inhibitory drive on self-connections were found for both inhibitory interneurons and spiny stellate cells following ketamine in the TRD participants, while healthy volunteers demonstrated increased GABAergic inhibitory drive post-ketamine. These self-connections reflect gain or precision of different cell types, suggesting reductions in self-gain on inhibitory interneurons and spiny stellate cells following ketamine administration in the TRD group. Second, reduced inhibitory drive was observed on the intrinsic connection from inhibitory interneurons to spiny stellate cells in the early visual cortex in our TRD and healthy volunteers. Third, ketamine increased the excitatory drive from deep pyramidal cells to inhibitory interneurons in the amygdala in TRD participants, while healthy volunteers showed reduced excitatory drive for this connection post-ketamine. Finally, ketamine also reduced the inhibitory self-gain on superficial pyramidal cells in the inferior frontal gyrus in our healthy volunteers only. Interestingly, these findings all reflect changes in intrinsic connectivity that regulate or modulate inhibition locally. Within the amygdala in particular, increased excitatory drive onto inhibitory interneurons for TRD participants seems at odds with an increased state of excitability within this region; however, similar accounts of increased pyramidal-to-inhibitory interneuron drive have previously been reported (64) and are thought to reflect a link between increased pyramidal cell excitability locally and downstream effects of increased gamma power.

Separately, we tested whether any meaningful parameters identified in our analysis of group effects, drug effects, or group by drug interactions were associated with antidepressant response in our TRD participants. We specifically examined changes in parameter estimates from the baseline to ketamine sessions (baseline minus ketamine) and correlated them with change in MADRS score from baseline to 230 min post-ketamine (the time point closest to the MEG recording session). Two parameters were found to be associated with antidepressant response, both in the early visual cortex. The first was the AMPA time constant in the early visual cortex, where faster AMPA transmission post-ketamine was associated with better antidepressant response. The second was inhibitory self-gain on spiny stellate cells in the early visual cortex, where larger self-inhibition on spiny stellate cells post-ketamine was associated with better antidepressant response. The findings of an association between AMPA transmission and antidepressant response are particularly striking because AMPA receptor throughput following NMDA receptor blockade (14, 16) is thought to result in delayed increases in synaptic potentiation and synaptogenesis, key mechanisms associated with ketamine's antidepressant effects. Similar associations between AMPA receptor connectivity and antidepressant response were also previously reported in a time window overlapping with our MEG recordings (56, 57).

One important limitation of this study is that MEG recordings were not collected during or immediately following infusions, but rather 6–9 h following ketamine administration in order to avoid side effects while measuring therapeutic drug effects. Thus, we cannot comment on acute changes in modeled

parameter estimates. However, studies of ketamine's acute effects in healthy volunteers suggest robust changes in both gamma power (30, 31) and AMPA and NMDA receptor drive (30) during ketamine infusion. Future studies should explore ketamine's acute effects in TRD participants to better understand the mechanisms *via* which ketamine reduces depressive symptoms. Another limitation is that we set a liberal criteria of $p < 0.05$ uncorrected for determining whether modeled parameters were associated with antidepressant response. Though this increases the likelihood of false positives, previous findings have demonstrated associations between AMPA parameters and antidepressant response in TRD (56, 57). In addition, our study included secondary analyses of data collected during a clinical trial of ketamine's mechanisms of actions, and we limited our sample to participants having baseline, post-ketamine, and post-placebo scan data. Additional work should include a larger sample of study participants to model effective connectivity during a task probing attentional bias toward emotional faces, in order to better characterize effective connectivity changes in regons of the emotion processing network following ketamine administration.

CONCLUSIONS

These findings demonstrate that ketamine administration leads to key changes in estimates of GABA and NMDA time constants measured using MEG in tandem with DCM. In addition to mirroring findings from animal studies measuring the acute effects of ketamine (15), these changes also indicate that ketamine alters estimates of excitatory and inhibitory intrinsic connectivity within key regions important for visual processing of emotional faces. Finally, the findings also underscore the usefulness of DCM for modeling connectivity changes associated with ketamine administration.

DATA AVAILABILITY STATEMENT

The raw data supporting the conclusions of this article will be made available by the authors, without undue reservation.

ETHICS STATEMENT

The studies involving human participants were reviewed and approved by Combined Neuroscience Institutional Review Board at the National Institutes of Health. The patients/participants provided their written informed consent to participate in this study.

AUTHOR CONTRIBUTIONS

JG: designed the study, conducted and interpreted the statistical analysis, and drafted the manuscript. CG: conducted the literature search, assisted in the statistical analysis, and revised the manuscript. AN: conceptualized the study and edited the manuscript for critical intellectual content. CZ: edited the manuscript for critical intellectual content and provided research supervision. All authors contributed to the article and approved the submitted version.

FUNDING

This work was supported by the Intramural Research Program at the National Institute of Mental Health, National Institutes of Health (IRP-NIMH-NIH; ZIA MH002857), by a NARSAD Independent Investigator Award to CZ, and by a Brain and Behavior Mood Disorders Research Award to CZ. The funders had no further role in study design and in the collection, analysis, or interpretation of data; in the writing of the report; or in the decision to submit the paper for publication.

ACKNOWLEDGMENTS

The authors thank the 7SE research unit and staff for their support. Ioline Henter (NIMH) provided invaluable editorial assistance. This work used the computational resources of the NIH HPC Biowulf cluster (http://hpc.nih.gov). The authors are entirely responsible for the scientific content of the paper.

REFERENCES

1. Bernard R, Kerman IA, Thompson RC, Jones EG, Bunney WE, Barchas JD, et al. Altered expression of glutamate signaling, growth factor, and glia genes in the locus coeruleus of patients with major depression. *Mol Psychiatry*. (2011) 16:634–46. doi: 10.1038/mp.2010.44
2. Choudary PV, Molnar M, Evans SJ, Tomita H, Li JZ, Vawter MP, et al. Altered cortical glutamatergic and GABAergic signal transmission with glial involvement in depression. *Proc Natl Acad Sci USA*. (2005) 102:15653–8. doi: 10.1073/pnas.0507901102
3. Luscher B, Shen Q, Sahir N. The GABAergic deficit hypothesis of major depressive disorder. *Mol Psychiatry*. (2011) 16:383–406. doi: 10.1038/mp.2010.120
4. Eastwood SL, Harrison PJ. Markers of glutamate synaptic transmission and plasticity are increased in the anterior cingulate cortex in bipolar disorder. *Biol Psychiatry*. (2010) 67:1010–6. doi: 10.1016/j.biopsych.2009.12.004
5. Ohgi Y, Futamura T, Hashimoto K. Glutamate signaling in synaptogenesis and NMDA receptors as potential therapeutic targets for psychiatric disorders. *Curr Mol Med*. (2015) 15:206–21. doi: 10.2174/1566524015666150330143008
6. Zarate CA Jr, Singh JB, Carlson PJ, Brutsche NE, Ameli R, Luckenbaugh DA, et al. A randomized trial of an N-methyl-D-aspartate antagonist in treatment-resistant major depression. *Arch Gen Psychiatry*. (2006) 63:856–64. doi: 10.1001/archpsyc.63.8.856
7. Diazgranados N, Ibrahim L, Brutsche NE, Newberg A, Kronstein P, Khalife S, et al. A randomized add-on trial of an N-methyl-D-aspartate antagonist in treatment-resistant bipolar depression. *Arch Gen Psychiatry*. (2010) 67:793–802. doi: 10.1001/archgenpsychiatry.2010.90
8. Zanos P, Highland JN, Stewart BW, Georgiou P, Jenne CE, Lovett J, et al. (2R,6R)-hydroxynorketamine exerts mGlu2 receptor-dependent antidepressant actions. *Proc Natl Acad Sci USA*. (2019) 116:6441–50. doi: 10.1073/pnas.1819540116
9. Murrough JW, Iosifescu DV, Chang LC, Al Jurdi RK, Green CE, Perez AM, et al. Antidepressant efficacy of ketamine in treatment-resistant major depression: a two-site randomized controlled trial. *Am J Psychiatry*. (2013) 170:1134–42. doi: 10.1176/appi.ajp.2013.13030392
10. Zarate CA Jr, Brutsche NE, Ibrahim L, Franco-Chaves J, Diazgranados N, Cravchik A, et al. Replication of ketamine's antidepressant efficacy in bipolar

depression: a randomized controlled add-on trial. *Biol Psychiatry*. (2012) 71:939–46. doi: 10.1016/j.biopsych.2011.12.010
11. Phillips JL, Norris S, Talbot J, Birmingham M, Hatchard T, Ortiz A, et al. Single, repeated, and maintenance ketamine infusions for treatment-resistant depression: a randomized controlled trial. *Am J Psychiatry*. (2019) 176:401–9. doi: 10.1176/appi.ajp.2018.18070834
12. Lumsden EW, Troppoli TA, Myers SJ, Zanos P, Aracava Y, Kehr J, et al. Antidepressant-relevant concentrations of the ketamine metabolite (2R,6R)-hydroxynorketamine do not block NMDA receptor function. *Proc Natl Acad Sci USA*. (2019) 116:5160–9. doi: 10.1073/pnas.1816071116
13. Zanos P, Moaddel R, Morris PJ, Georgiou P, Fischell J, Elmer GI, et al. NMDAR inhibition-independent antidepressant actions of ketamine metabolites. *Nature*. (2016) 533:481–6. doi: 10.1038/nature17998
14. Moghaddam B, Adams B, Verma A, Daly D. Activation of glutamatergic neurotransmission by ketamine: a novel step in the pathway from NMDA receptor blockade to dopaminergic and cognitive disruptions associated with the prefrontal cortex. *J Neurosci*. (1997) 17:2921–7. doi: 10.1523/JNEUROSCI.17-08-02921.1997
15. Homayoun H, Moghaddam B. NMDA receptor hypofunction produces opposite effects on prefrontal cortex interneurons and pyramidal neurons. *J Neurosci*. (2007) 27:11496–500. doi: 10.1523/JNEUROSCI.2213-07.2007
16. Duman RS, Sanacora G, Krystal JH. Altered connectivity in depression: GABA and glutamate neurotransmitter deficits and reversal by novel treatments. *Neuron*. (2019) 102:75–90. doi: 10.1016/j.neuron.2019.03.013
17. Li N, Lee B, Liu RJ, Banasr M, Dwyer JM, Iwata M, et al. mTOR-dependent synapse formation underlies the rapid antidepressant effects of NMDA antagonists. *Science*. (2010) 329:959–64. doi: 10.1126/science.1190287
18. Li N, Liu RJ, Dwyer JM, Banasr M, Lee B, Son H, et al. Glutamate N-methyl-D-aspartate receptor antagonists rapidly reverse behavioral and synaptic deficits caused by chronic stress exposure. *Biol Psychiatry*. (2011) 69:754–61. doi: 10.1016/j.biopsych.2010.12.015
19. Liu RJ, Lee FS, Li XY, Bambico F, Duman RS, Aghajanian GK. Brain-derived neurotrophic factor Val66Met allele impairs basal and ketamine-stimulated synaptogenesis in prefrontal cortex. *Biol Psychiatry*. (2012) 71:996–1005. doi: 10.1016/j.biopsych.2011.09.030
20. Autry AE, Adachi M, Nosyreva E, Na ES, Los MF, Cheng P-f, et al. NMDA receptor blockade at rest triggers rapid behavioural antidepressant responses. *Nature*. (2011) 475:91–5. doi: 10.1038/nature10130
21. Monteggia LM, Gideons E, Kavalali ET. The role of eukaryotic elongation factor 2 kinase in rapid antidepressant action of ketamine. *Biol Psychiatry*. (2013) 73:1199–203. doi: 10.1016/j.biopsych.2012.09.006
22. Kavalali ET, Monteggia LM. Targeting homeostatic synaptic plasticity for treatment of mood disorders. *Neuron*. (2020) 106:715–26. doi: 10.1016/j.neuron.2020.05.015
23. Miller OH, Yang L, Wang C-C, Hargroder EA, Zhang Y, Delpire E, et al. GluN2B-containing NMDA receptors regulate depression-like behavior and are critical for the rapid antidepressant actions of ketamine. *eLife*. (2014) 3:e03581. doi: 10.7554/eLife.03581
24. Fogaça MV, Duman RS. Cortical GABAergic dysfunction in stress and depression: new insights for therapeutic interventions. *Front Cell Neurosci*. (2019) 13:87. doi: 10.3389/fncel.2019.00087
25. Godfrey KEM, Gardner AC, Kwon S, Chea W, Muthukumaraswamy SD. Differences in excitatory and inhibitory neurotransmitter levels between depressed patients and healthy controls: a systematic review and meta-analysis. *J Psychiatr Res*. (2018) 105:33–44. doi: 10.1016/j.jpsychires.2018.08.015
26. Widman AJ, McMahon LL. Disinhibition of CA1 pyramidal cells by low-dose ketamine and other antagonists with rapid antidepressant efficacy. *Proc Natl Acad Sci USA*. (2018) 115:E3007–16. doi: 10.1073/pnas.1718883115
27. Economo MN, White JA. Membrane properties and the balance between excitation and inhibition control gamma-frequency oscillations arising from feedback inhibition. *PLoS Comput Biol*. (2012) 8:e1002354. doi: 10.1371/journal.pcbi.1002354
28. Ray S, Maunsell JHR. Do gamma oscillations play a role in cerebral cortex? *Trends Cogn Sci*. (2015) 19:78–85. doi: 10.1016/j.tics.2014.12.002
29. Buzsáki G, Wang X-J. Mechanisms of gamma oscillations. *Ann Rev Neurosci*. (2012) 35:203–25. doi: 10.1146/annurev-neuro-062111-150444
30. Muthukumaraswamy SD, Shaw AD, Jackson LE, Hall J, Moran R, Saxena N. Evidence that subanesthetic doses of ketamine cause sustained disruptions of NMDA and AMPA-mediated frontoparietal connectivity in humans. *J Neurosci*. (2015) 35:11694–706. doi: 10.1523/JNEUROSCI.0903-15.2015
31. Shaw AD, Saxena N, Hall JE, Singh KD, Muthukumaraswamy SD. Ketamine amplifies induced gamma frequency oscillations in the human cerebral cortex. *Eur Neuropsychopharmacol*. (2015) 25:1136–46. doi: 10.1016/j.euroneuro.2015.04.012
32. Cornwell BR, Salvadore G, Furey M, Marquardt CA, Brutsche NE, Grillon C, et al. Synaptic potentiation is critical for rapid antidepressant response to ketamine in treatment-resistant major depression. *Biol Psychiatry*. (2012) 72:555–61. doi: 10.1016/j.biopsych.2012.03.029
33. Sanacora G, Smith MA, Pathak S, Su HL, Boeijinga PH, McCarthy DJ, et al. Lanicemine: a low-trapping NMDA channel blocker produces sustained antidepressant efficacy with minimal psychotomimetic adverse effects. *Mol Psychiatry*. (2014) 19:978–85. doi: 10.1038/mp.2013.130
34. Nugent AC, Ballard ED, Gould TD, Park LT, Moaddel R, Brutsche NE, et al. Ketamine has distinct electrophysiological and behavioral effects in depressed and healthy subjects. *Mol Psychiatry*. (2019) 24:1040–52. doi: 10.1038/s41380-018-0028-2
35. Nugent AC, Wills KE, Gilbert JR, Zarate CA. Synaptic potentiation and rapid antidepressant response to ketamine in treatment-resistant major depression: a replication study. *Psychiatry Res Neuroimaging*. (2019) 283:64–6. doi: 10.1016/j.pscychresns.2018.09.001
36. Dalgleish T, Watts FN. Biases of attention and memory in disorders of anxiety and depression. *Clin Psychol Rev*. (1990) 10:589–604. doi: 10.1016/0272-7358(90)90098-U
37. Mathews A, MacLeod C. Cognitive approaches to emotion and dmotional disorders. *Ann Rev Psychol*. (1994) 45:25–50. doi: 10.1146/annurev.ps.45.020194.000325
38. Gotlib IH, Krasnoperova E, Yue DN, Joormann J. Attentional biases for negative interpersonal stimuli in clinical depression. *J Abnorm Psychol*. (2004) 113:127–35. doi: 10.1037/0021-843X.113.1.121
39. Joormann J, Gotlib IH. Selective attention to emotional faces following recovery from depression. *J Abnorm Psychol*. (2007) 116:80–5. doi: 10.1037/0021-843X.116.1.80
40. Ma Y. Neuropsychological mechanism underlying antidepressant effect: a systematic meta-analysis. *Mol Psychiatry*. (2015) 20:311–9. doi: 10.1038/mp.2014.24
41. Peckham AD, McHugh RK, Otto MW. A meta-analysis of the magnitude of biased attention in depression. *Depress Anxiety*. (2010) 27:1135–42. doi: 10.1002/da.20755
42. Amico F, Carballedo A, Lisiecka D, Fagan AJ, Boyle G, Frodl T. Functional anomalies in healthy individuals with a first degree family history of major depressive disorder. *Biol Mood Anxiety Disord*. (2012) 2:1. doi: 10.1186/2045-5380-2-1
43. Reed JL, Nugent AC, Furey ML, Szczepanik JE, Evans JW, Zarate CA. Ketamine normalizes brain activity during emotionally valenced attentional processing in depression. *NeuroImage Clin*. (2018) 20:92–101. doi: 10.1016/j.nicl.2018.07.006
44. Hu B, Rao J, Li X, Cao T, Li J, Majoe D, et al. Emotion regulating attentional control abnormalities in major depressive disorder: an event-related potential study. *Sci Rep*. (2017) 7:13530. doi: 10.1038/s41598-017-13626-3
45. Ironside M, O'Shea J, Cowen PJ, Harmer CJ. Frontal cortex stimulation reduces vigilance to threat: implications for the treatment of depression and anxiety. *Biol Psychiatry*. (2016) 79:823–30. doi: 10.1016/j.biopsych.2015.06.012
46. Moran RJ, Symmonds M, Stephan KE, Friston KJ, Dolan RJ. An *in vivo* assay of synaptic function mediating human cognition. *Curr Biol*. (2011) 21:1320–5. doi: 10.1016/j.cub.2011.06.053
47. Gilbert JR, Zarate CA. Electrophysiological biomarkers of antidepressant response to ketamine in treatment-resistant depression: gamma power and long-term potentiation. *Pharmacol Biochem Behav*. (2020) 189:172856. doi: 10.1016/j.pbb.2020.172856
48. American Psychiatric Association. 4th ed. Washington, DC: American Psyciatric Association (1994).
49. Montgomery SA, Asberg M. A new depression scale designed to be sensitive to change. *Br J Psychiatry*. (1979) 134:382–9. doi: 10.1192/bjp.134.4.382

50. First MB, Spitzer RL, Gibbon M, Williams JB. *Structured Clinical Interview for DSM-IV-TR Axis I Disorders, Research Version, Patient Edition (SCID-I/P)*. New York: Biometrics Research, New York State Psychiatric Institute (2002).
51. Hong LE, Summerfelt A, Buchanan RW, O'Donnell P, Thaker GK, Weiler MA, et al. Gamma and delta neural oscillations and association with clinical symptoms under subanesthetic ketamine. *Neuropsychopharmacology*. (2010) 35:632–40. doi: 10.1038/npp.2009.168
52. Lazarewicz MT, Ehrlichman RS, Maxwell CR, Gandal MJ, Finkel LH, Siegel SJ. Ketamine modulates theta and gamma oscillations. *J Cogn Neurosci*. (2010) 22:1452–64. doi: 10.1162/jocn.2009.21305
53. David O, Kiebel SJ, Harrison LM, Mattout J, Kilner JM, Friston KJ. Dynamic causal modeling of evoked responses in EEG and MEG. *NeuroImage*. (2006) 30:1255–72. doi: 10.1016/j.neuroimage.2005.10.045
54. Symmonds M, Moran CH, Leite MI, Buckley C, Irani SR, Stephan KE, et al. Ion channels in EEG: isolating channel dysfunction in NMDA receptor antibody encephalitis. *Brain*. (2018) 141:1691–702. doi: 10.1093/brain/awy107
55. Moran RJ, Jones MW, Blockeel AJ, Adams RA, Stephan KE, Friston KJ. Losing control under ketamine: suppressed cortico-hippocampal drive following acute ketamine in rats. *Neuropsychopharmacology*. (2015) 40:268–77. doi: 10.1038/npp.2014.184
56. Gilbert JR, Yarrington JS, Wills KE, Nugent AC, Zarate CA Jr. Glutamatergic signaling drives ketamine-mediated response in depression: evidence from dynamic causal modeling. *Int J Neuropsychopharmacol*. (2018) 21:740–7. doi: 10.1093/ijnp/pyy041
57. Gilbert JR, Ballard ED, Galiano CS, Nugent AC, Zarate CA. Magnetoencephalographic correlates of suicidal ideation in major depression. *Biol Psychiatr*. (2020) 5:354–63. doi: 10.1016/j.bpsc.2019.11.011
58. Kveraga K, Boshyan J, Bar M. Magnocellular projections as the trigger of top-down facilitation in recognition. *J Neurosci*. (2007) 27:13232–40. doi: 10.1523/JNEUROSCI.3481-07.2007
59. Gilbert JR, Moran RJ. Inputs to prefrontal cortex support visual recognition in the aging brain. *Sci Rep*. (2016) 6:31943. doi: 10.1038/srep31943
60. Hochstein S, Ahissar M. View from the top: hierarchies and reverse hierarchies in the visual system. *Neuron*. (2002) 36:791–804. doi: 10.1016/S0896-6273(02)01091-7
61. Friston K, Mattout J, Trujillo-Barreto N, Ashburner J, Penny W. Variational free energy and the Laplace approximation. *Neuroimage*. (2007) 34:220–34. doi: 10.1016/j.neuroimage.2006.08.035
62. Friston KJ, Litvak V, Oswal A, Razi A, Stephan KE, van Wijk BCM, et al. Bayesian model reduction and empirical Bayes for group (DCM) studies. *Neuroimage*. (2016) 128:413–31. doi: 10.1016/j.neuroimage.2015.11.015
63. Drevets W, Videen T, Price J, Preskorn S, Carmichael S, Raichle M. A functional anatomical study of unipolar depression. *J Neurosci*. (1992) 12:3628–41. doi: 10.1523/JNEUROSCI.12-09-03628.1992
64. Shaw AD, Muthukumaraswamy SD, Saxena N, Sumner RL, Adams NE, Moran RJ, et al. Generative modelling of the thalamo-cortical circuit mechanisms underlying the neurophysiological effects of ketamine. *NeuroImage*. (2020) 221:117189. doi: 10.1016/j.neuroimage.2020.117189

Conflict of Interest: CZ is listed as a co-inventor on a patent for the use of ketamine in major depression and suicidal ideation; as a co-inventor on a patent for the use of (2R,6R) -hydroxynorketamine, (S)-dehydronorketamine, and other stereoisomeric dehydro and hydroxylated metabolites of (R,S)-ketamine metabolites in the treatment of depression and neuropathic pain; and as a co-inventor on a patent application for the use of (2R,6R)-hydroxynorketamine and (2S,6S)-hydroxynorketamine in the treatment of depression, anxiety, anhedonia, suicidal ideation, and post-traumatic stress disorders. He has assigned his patent rights to the U.S. government but will share a percentage of any royalties that may be received by the government.

The remaining authors declare that the research was conducted in the absence of any commercial or financial relationships that could be construed as a potential conflict of interest.

frontiers in Psychiatry

REVIEW
published: 10 August 2021
doi: 10.3389/fpsyt.2021.726365

D-Serine: A Cross Species Review of Safety

Amir Meftah[1,2], *Hiroshi Hasegawa*[3] *and Joshua T. Kantrowitz*[1,2,4]*

[1] College of Physicians and Surgeons, Columbia University, New York City, NY, United States, [2] New York State Psychiatric Institute, New York City, NY, United States, [3] Department of Pathophysiology, Tokyo University of Pharmacy and Life Sciences, Tokyo, Japan, [4] Nathan Kline Institute, Orangeburg, NY, United States

Background: D-Serine, a direct, full agonist at the D-serine/glycine modulatory site of the N-methyl-D-aspartate-type glutamate receptors (NMDAR), has been assessed as a treatment for multiple psychiatric and neurological conditions. Based on studies in rats, concerns of nephrotoxicity have limited D-serine research in humans, particularly using high doses. A review of D-serine's safety is timely and pertinent, as D-serine remains under active study for schizophrenia, both directly (R61 MH116093) and indirectly through D-amino acid oxidase (DAAO) inhibitors. The principal focus is on nephrotoxicity, but safety in other physiologic and pathophysiologic systems are also reviewed.

Methods: Using the search terms "D-serine," "D-serine and schizophrenia," "D-serine and safety," "D-serine and nephrotoxicity" in PubMed, we conducted a systematic review on D-serine safety. D-serine physiology, dose-response and efficacy in clinical studies and DAAO inhibitor safety is also discussed.

Results: When D-serine doses >500 mg/kg are used in rats, nephrotoxicity, manifesting as an acute tubular necrosis syndrome, seen within hours of administration is highly common, if not universal. In other species, however, D-serine induced nephrotoxicity has not been reported, even in other rodent species such as mice and rabbits. Even in rats, D-serine related toxicity is dose dependent and reversible; and does not appear to be present in rats at doses producing an acute Cmax of <2,000 nmol/mL. For comparison, the Cmax of D-serine 120 mg/kg, the highest dose tested in humans, is ∼500 nmol/mL in acute dosing. Across all published human studies, only one subject has been reported to have abnormal renal values related to D-serine treatment. This abnormality did not clearly map on to the acute tubular necrosis syndrome seen in rats, and fully resolved within a few days of stopping treatment. DAAO inhibitors may be nephroprotective. D-Serine may have a physiologic role in metabolic, extra-pyramidal, cardiac and other systems, but no other clinically significant safety concerns are revealed in the literature.

Conclusions: Even before considering human to rat differences in renal physiology, using current FDA guided monitoring paradigms, D-serine appears safe at currently studied maximal doses, with potential safety in combination with DAAO inhibitors.

Keywords: NMDA–N-methyl-D-aspartate, D-serine, schizophrenia, safety, kidney

OPEN ACCESS

Edited by:
Natasa Petronijevic, University of Belgrade, Serbia

Reviewed by:
Jumpei Sasabe, Keio University, Japan
Kenji Hashimoto, Chiba University, Japan

***Correspondence:**
Joshua T. Kantrowitz
jk3380@cumc.columbia.edu

Specialty section:
This article was submitted to Psychopharmacology, a section of the journal Frontiers in Psychiatry

Received: *16 June 2021*
Accepted: *13 July 2021*
Published: *10 August 2021*

Citation:
Meftah A, Hasegawa H and Kantrowitz JT (2021) D-Serine: A Cross Species Review of Safety. Front. Psychiatry 12:726365. doi: 10.3389/fpsyt.2021.726365

INTRODUCTION

Glutamate-targeted drugs remain a high priority for the treatment of schizophrenia (1, 2). While no compounds have successfully navigated the difficult process from Phase I to regulatory approval, recent meta-analyses support significant, moderate to large effect size improvements for both schizophrenia symptoms in general, along with specific improvements in negative symptoms, for pooled N-methyl-D-aspartate-type glutamate receptors (NMDAR) modulators adjunctive to antipsychotics compared to placebo (3). In addition to overall improvements in residual psychotic and negative symptoms, glutamatergic based medications have also targeted cognitive deficits (4, 5).

The vast majority of glutamate-based treatment trials have targeted the glycine modulatory site of the NMDAR with natural compounds such as D-serine, glycine, and sarcosine. Recently, the field has seen some successes and some failures with more traditional pharmaceutical glutamatergic treatment trials (5–8). In particular, dose finding, target engagement biomarker work has helped to guide the field (1, 9), allowing an assessment of the ideal doses of the correct compounds to use prior to larger Phase II studies.

The present report focuses on the safety of D-serine, one of the more thoroughly studied NMDAR modulators (3), with a specific focus on potential nephrotoxicity. A review of D-serine's safety is timely and pertinent, as D-serine remains under active study, both directly (10), and indirectly through D-amino acid oxidase (DAAO) inhibitors such as Luvadaxistat (NBI-1065844/TAK-831) and NaBen (sodium benzoate). In addition to a primary focus on D-serine and renal safety, specific topics covered include an overview of D-serine's physiology, efficacy and dose-response in treatment studies, physiology/pathophysiology in other systems and potential metabolic, extra-pyramidal, cardiac, and oncological adverse events and interaction with DAAO inhibitors.

METHODS

Using the search terms "D-serine," "D-serine and schizophrenia," "D-serine and safety," "D-serine and nephrotoxicity" in PubMed, we conducted a systematic review on D-serine safety. The reference lists of articles found were reviewed for additional sources.

OVERVIEW OF D-SERINE PHYSIOLOGY

Glutamate is the primary excitatory neurotransmitter in the brain, and the NMDAR is the primary glutamate receptor (11, 12). In addition to the primary binding site of glutamate, the NMDAR is modulated by multiple other binding sites. D-Serine is a naturally occurring amino acid that is present in high concentrations in the human brain (13, 14). D-Serine is an NMDAR modulator and a full agonist at the D-serine/glycine site of the NMDAR (15, 16). Binding by D-serine or glycine at this modulatory site is necessary for activation of the NMDAR (11).

D-Serine is the D-isomer of the more common amino acid L-serine. Along with D-aspartate and D-alanine, D-serine is one of the few D-amino acids present in high concentrations in the mammalian brain (or elsewhere in the human body), suggesting an important physiological role (17). The normal source for D-serine in brain appears to be conversion from L-serine, via serine racemase (18, 19). D-serine is converted to back to L-serine only to a limited degree, but in cortical areas with low DAAO, serine racemase appears to degrade D-serine via α/β-elimination of water (20). In general, D-serine is broken down through the action of DAAO (14). In rodents, DAAO is primarily expressed in the cerebellum (21), with only a limited expression in rodent forebrain (22), and thus appears to play a limited role in D-serine degradation in this area (23, 24). DAAO inhibition can modulate hippocampal function in rodents (25). In humans, DAAO is present in both cortical neurons and cerebellar glia (26).

Serine racemase is also present outside the brain (27), but pre-clinical studies suggest that it is less clearly involved in D-serine regulation in the periphery (28). By contrast, DAAO appears to be physiologically active in the periphery, with the largest expression in the cerebellum, small intestine, liver, and kidney (17, 29, 30). Thus, DAAO inhibitors appear to exert their putative therapeutic effects via reduced peripheral degradation of D-serine rather than by direct cortical action.

In humans, D-serine exhibits linear kinetics (31), with a TMax ∼1–2 h following administration (**Figure 1**, Left) and a $t^{½}$ of ∼3.3 h. The CMax of D-serine is 120.6 ± 34.6, 272.3 ± 62.0, and 530.3 ± 266.8 nmol/ml for the 30, 60, and 120 mg/kg doses, respectively (31). After 4 weeks of daily treatment, linear kinetics continued to be observed, although there may be some modest accumulations (**Figure 1**, Right).

D-Serine can cross the blood brain barrier, supporting the potential utility as a therapeutic agent (32, 33). Both D-serine and glycine have shown promise in clinical trials, although D-serine may be more pharmacologically potent than glycine (34–38) and is the main NMDAR regulator in cortex. Relevant to its potential as a cognitive enhancer (39), D-serine also has a specific role in long-term potentiation (LTP) and depression (LTD) (40–42), long-term plasticity (43, 44) and synaptogenesis (45). Studies suggest a basal deficit in D-serine in schizophrenia (31, 46), further supporting a role for D-serine as a treatment.

USE OF D-SERINE IN TREATMENT STUDIES: EFFICACY AND DOSE-DEPENDENT EFFECTS

A full listing of the 19 published human studies with D-serine is shown in **Table 1**. D-Serine has mainly been studied for schizophrenia and related psychotic disorders, but a role for use in tics disorder (61), movement disorders (58), alcohol dependence (64), dementia (65), post-traumatic syndrome disorder (56), and depression (66, 67) have also been proposed and studied.

D-Serine was originally reported to be beneficial in schizophrenia based upon studies conducted in Taiwan (52) and Israel (54). A recent meta-analysis of NMDAR modulators in

TABLE 1 | Renal safety of D-serine.

References	Active D-serine "n" & diagnosis	Dose	Renal Abnormalities
		High dose D-serine	
Kantrowitz et al. (47)	20 CHR (prodrome)	60 mg/kg/day for 16 weeks	None
Kantrowitz et al. (4)	21 schizophrenia (Sz)	60 mg/kg single dose × 1week	None
Kantrowitz et al. (48)	16 Sz	60 mg/kg/day for 6 weeks	None
Ermilov et al. (49)	10 Sz	3 g/day for 6 weeks (∼45 mg/kg)	None
Kantrowitz et al. (31)	47 Sz	4 week study 12 Sz at 30 mg/kg 19 at 60 mg/kg 16 at 120 mg/kg	1 subject showed 2+ proteinuria without glycosuria after 4 weeks of 120 mg/kg, without change in creatinine
Capitao et al. (50)	20 healthy controls	60 mg/kg single dose	None
Heresco-Levy et al. (51)	1 Sz with anti-NMDAR antibodies	4g for 6 weeks	None
		Low dose D-serine	
Tsai et al. (52)	14 Sz	30 mg/kg/day for 6 weeks	None
Tsai et al. (53)	10 Sz	30 mg/kg/day for 6 weeks	None
Heresco-Levy et al. (54)	19 Sz	30 mg/kg/day for 6 weeks	None
Lane et al. (55)	21 Sz	2 g/day for 6 weeks (∼30 mg/kg)	None
Heresco-Levy et al. (56)	21 PTSD	30 mg/kg/day for 6 weeks	None
Lane et al. (57)	20 Sz	2 g/day for 6 weeks (∼30 mg/kg)	None
Gelfin et al. (58)	8 Parkinson's disease	30 mg/kg/day for 6 weeks	None
D'souza et al. (59)	51 Sz	30 mg/kg/day for 12 weeks	None
Weiser et al. (60)	97 Sz	2 g/day for 16 weeks (∼30 mg/kg)	None
Lemmon et al. (61)	9 Tourette's	30 mg/kg/day for 6 weeks	None
Levin et al. (62)	35 healthy controls	2.1 g single dose (∼30 mg/kg)	None
Avellar et al. (63)	50 healthy older adults	30 mg/kg single dose	None
		CTP-692	
Unpublished	244 Sz	12 week study 81 Sz at 1 g 85 at 2 g 78 at 4 g	None

schizophrenia (3) has found specific improvement for D-serine adjunctive to antipsychotics for negative symptoms measured by both the Scale for the Assessment of Negative Symptoms (SANS) (68), with a standardized mean difference (SMD) = −0.56 and the Positive and Negative Symptom Scale (PANSS) negative symptom subscale (69), with a SMD of −0.49. The meta-analysis for D-serine for total PANSS symptoms was not significant (SMD = −0.3). Of note, while a positive trial of the closely related compound D-alanine (70) was included in the meta-analysis, it was not grouped with D-serine as we have done in the past (48). D-Serine's utility as a cognitive enhancer was not evaluated in this meta-analysis.

The majority of human D-serine studies have used a low (30 mg/kg, ∼2 g/day) dosage, with a significant, but small effect size improvement (SMD = −0.32) at this dose in meta-analyses (46). This provides proof of concept, but suggests 30 mg/kg may be inadequate to fully engage the NMDAR, as evidenced by larger multi-center studies of 30 mg/kg which failed to separate from placebo (59, 60).

Pre-clinical studies suggest the need for higher doses. As further discussed in the *Renal effects of* D*-serine* section, rats are especially, and possibly uniquely vulnerable to D-serine induced nephrotoxicity. Thus, pre-clinical behavioral studies need to be completed in mice. In mice, effective doses of D-serine have been

in the range of 600–1,000 mg/kg, roughly equivalent to human doses >30 mg/kg (60–120 mg/kg) (71). In other assay systems, numerical reversal of NMDAR antagonist induced (MK-801-induced) hyperactivity in mice was observed at a dose of 600 mg/kg, although significant reduction was not observed until 4,000 mg/kg (72).

Human studies have supported the safety and efficacy of higher dose D-serine, defined as ≥60 mg/kg, ≥4 g/day. An open label dose finding study compared cohorts of 30, 60, and 120 mg/kg/day, finding dose-dependent improvement (31). Significant improvement for total PANSS symptoms was seen at all doses, but specific improvement for both positive and negative symptoms individually was only seen in the 120 mg/kg/day cohort. Similarly, a dose-dependent effect for cognition was seen, finding significantly greater improvement at ≥60 mg/kg vs. Thirty milligram/kilogram dose for the Measurement and Treatment Research to Improve Cognition in Schizophrenia (MCCB) (73) composite ($p = 0.017$). A pharmacodynamic analysis supported a dose effect, finding that higher peak serum levels of D-serine predict greater MCCB scores and improvement on the PANSS in this study, consistent with studies suggesting that basal serum levels of D-serine are related to cognition (74, 75).

The initial double blind studies of high dose D-serine were conducted at a dose of 60 mg/kg, due to caution after a single subject with abnormal renal values at 120 mg/kg (31), as further discussed in the *Renal effects of D-serine* section. A double-blind high dose study in schizophrenia showed significant, large effect size improvements for both total (Cohen's $d = 0.8$) and negative symptoms ($d = 0.88$) (48). Additionally, a nonsignificant, moderate effect size improvement was seen for the MCCB composite ($d = 0.41$) and significant target engagement was seen using mismatch negativity. A high dose study in a clinically high risk (CHR) for schizophrenia group (47) also showed significant improvement in prodromal negative symptoms ($d = 0.68$). Meta-analysis including high dose studies demonstrate moderate to large effect sizes for negative symptoms (3, 48), improving on meta-analysis that only include low dose studies (46).

D-serine as an adjunct to cognitive remediation has been also been proposed (39, 76, 77). One trial used daily low dose D-serine without evidence of efficacy (59), but a trial of 60 mg/kg using an intermittent (once weekly) strategy has shown promising results (4). An ongoing double-blind dose finding study is assessing D-serine doses up to 120 mg/kg (10), using an intermittent dose strategy.

Further evidence for the necessity of testing higher doses of D-serine and related compounds come from the recent negative study of CTP-692 which is a deuterated form of D-serine that reportedly has both less potential renal toxicity and a longer $t^{1/2}$ (78). In this publicly reported, but not published study, fixed CTP-692 doses were used, and the highest tested dose was 4 g. Based on publicly available mean weight in kg per dose groups, the highest dose of CTP-692 tested were equivalent to ∼45 mg/kg on average (https://ir.concertpharma.com/news-releases/news-release-details/concert-pharmaceuticals-announces-results-ctp-692-phase-2-trial). Thus, even the highest tested doses of CTP-692 may have been too low, which may have contributed to the negative study.

RENAL EFFECTS OF D-SERINE

In addition to their importance in the brain, NMDAR are found throughout the body, including the kidney, where they play a diverse, if not fully elucidated role (79–81). D-Serine is also found in the kidney, with a potential physiological role (80).

The potential risk of D-serine induced nephrotoxicity has been described since the 1940's (82–84), primarily based on studies in rats, and classically leads to a reversible acute necrosis, termed acute tubular necrosis. Pathological changes are present within 1 to 2 h post D-serine administration, and are generally limited to necrotic changes of the straight segment of the proximal tubule (85–87), which is the primary site of D-serine reabsorption (88). The earliest changes are pronounced eosinophilia in the straight proximal tubules (87). Concurrently, acute increases in urine volume, glucosuria, proteinuria, and aminoaciduria, including D-serine are seen (85, 86), while sodium and potassium excretion remains stable. D-Serine excretion peaks within the first 8 h post dose (87). Other specific findings include granular (muddy) casts seen on urinalysis.

Despite these acute pathological changes, D-serine induced nephrotoxicity appears to be fully reversible (85), even in rats. Urine values of protein, glucose and amino acids begin to normalize 24–48 h after the last dose of D-serine and by 120 h post dose, largely return to normal (87). Pathological changes also completely resolve within this timeframe, with complete regrowth of new epithelium in tubules and renal tubular basophilia (87).

In addition to being reversible, D-serine induced nephrotoxicity has only been observed in rats. In other species, including other rodents, D-serine induced nephrotoxicity has not been reported. Tested species include guinea pigs, rabbits, and mice (84), along with dogs, hamsters, and gerbils (89). Most importantly for the treatment of psychiatric disease in humans, is the lack of evidence for D-serine induced nephrotoxicity in humans (**Table 1**). Even in rats, this heightened risk to D-serine does not appear to occur during "normal," physiological levels of D-serine.

The etiology for the isolated risk to rats as compared to other species is not completely clear, but appears to be due to both higher reabsorption of D-serine by rat kidneys compared to other species and differences in DAAO function. The presence of enhanced reabsorption is apparent from the low levels of D-serine in rat urine relative to that of other species, such humans and dogs, despite relatively similar serum levels (90). Moreover, nephrotoxicity during exogenous D-serine administration may be related to oxidative stress from the increased DAAO breakdown of D-serine (29, 91–93). DAAO is localized in pars recta of the kidney, where D-serine (94, 95) is primarily reabsorbed and the focal point of damage during D-serine nephrotoxicity. While levels of DAAO in rats do not appear to be quantitatively different than in other

species (96), rat DAAO may be less efficient, which may compound the risk of nephrotoxicity due to hyperfunction during periods of excess D-serine (97). Relatedly, reducing DAAO activity through DAAO knockouts or concurrent DAAO inhibitors may be nephroprotective to excess D-serine (see *DAAO clinical and safety* section). Finally, studies also suggest that rats may have a higher capacity of utilizing D-amino acids (29) and that NMDAR may be directly involved in producing nephrotoxicity (98).

By contrast to rats, in most other species, including humans, D-serine is not actively reabsorbed (90, 99, 100), as evidenced by relatively higher D-serine urine levels in humans compared to rats of D-serine under physiological conditions (90). In humans, D-serine does not accumulate in serum under physiologic conditions, other than in people (101, 102) or mice (103) with pre-existing renal impairment. Under these pathological conditions, D-serine may be a biomarker of renal disease or recovery in humans (104–107), rising or falling in proportion to creatinine. However, there does not appear to be a causal link between D-serine and renal impairment.

Even in rats, D-serine nephrotoxicity appears to be dose related. The initial rat toxicity studies used doses of 750–1,000 mg/kg (83, 85, 86), and in doses ≥500 mg/kg, nephrotoxicity after D-serine treatment appears to be very common, if not universal in rats. Similar to mice (71), however, the oral dose to serum concentration ratio does not appear to follow a 1:1 ratio in rats compared to humans, complicating direct translational studies.

Recently, the pharmacokinetics and toxicokinetics of D-serine in rats was systematically studied (108), potentially allowing for a more direct rat to human comparison. In this study, five intraperitoneal doses were tested, 0.6, 1.2, 1.8, 2.4, and 4.8 mmol/kg. Based on an assumption of linear pharmacokinetics and a comparison with human studies (31), the 1.8 mmol/kg rat dose is thought to be approximately equivalent to an oral human dose of 450 mg/kg, ∼3× the highest tested human dose. No nephrotoxicity was observed at either 6 or 24 h post dose at the 0.6 or 1.2 mmol/kg doses. Beginning at 1.8 mmol/kg, significant dose dependent elevations are seen for urine protein and glucose compared to the 0.6 mmol/kg dose at 6 h and for serum creatine from baseline at 24 h. Toxicity was also seen at higher doses (2.4 and 4.8 mmol/kg).

A Cmax of ∼2,000 nmol/mL was the dividing line between safety and nephrotoxicity in this study, which was achieved with the 450 mg/kg equivalent dose (1.8 mmol/kg) (see **Figure 1**). Additional support for a dose response for toxicity in rats was shown in a study in which doses ≤to 250 mg/kg were safe, while 500 mg/kg produced the expected nephrotoxicity (87). Other studies have reported toxicity at 400 mg/kg (92). For comparison, the single dose Cmax of 120 mg/kg, the highest dose tested in humans, was 530.3±266.8 nmol/mL in acute dosing (31). After 4 weeks of chronic dosing, there was some accumulation, but the Cmax remained well-below 2,000 nmol/mL (∼800 nmol/mL). We are aware of one study suggesting that extremely large doses of D-serine can induce nephrotoxicity in a cell culture of human renal tubular cells (109). However, this study used D-serine concentrations of 10 to 20 mM, which are 20 to 40 times greater than the Cmax of 120 mg/kg (0.5 mM or ∼500 μM).

Nineteen human trials have been published or publicly presented with D-serine or the closely related compound of CTP-692 (**Table 1**), including 490 subjects receiving D-serine with treatment durations ranging from single doses to 16 weeks of daily dosing and 244 patients on CTP-692. One hundred twenty-two subjects received high dose D-serine (>30 mg/kg), including 16 patients receiving 120 mg/kg for 4 weeks. Seventy-Eight subjects received high dose CTP-692, defined as 4 g per day. Across all studies, only one subject was reported to have abnormal renal values related to D-serine treatment (31). Overall, this 1 case represents 0.2% of all D-serine treated subjects, <1% of subjects treated with daily high dose D-serine and one of 16 (6.3%) of subjects treated with 120 mg/kg daily. Several mild out of range renal values were noted in the CHR study (47). No renal adverse effects were reported in the CTP-692 study.

The single abnormality at 120 mg/kg occurred in a subject after receiving 4 weeks of the 120 mg/kg dose. This abnormality was considered mild in that it involved only an increase in protein (2+ by dipstick) without granular casts or an accompanying increase in glycosuria, change in creatinine level or other clinical correlates of renal dysfunction, and fully resolved within a few days of stopping treatment. Thus, this abnormality does not clearly map on to the acute nephrotoxicity syndrome seen in rats. Under our current FDA approved safety monitoring criteria, fully described in the *Recommendations for monitoring during clinical D-serine studies* section, this abnormality would not have been considered a serious adverse event (SAE).

D-SERINE AND THE PANCREAS AND METABOLISM

Moving beyond the brain and the kidney, D-Serine may play a physiologic role in both appetite and insulin regulation in the pancreas, which is of potential clinical relevance since many antipsychotics are associated with clinically significant weight gain and metabolic disturbances (110, 111). D-Serine appears to be elevated in pre-clinical mice models of diabetes, but this seems to be an effect, and not a contributing cause of diabetes *in vivo* (112, 113). As recently reviewed (114, 115), functional NMDAR are found in pancreatic islets and β-cells, which regulate insulin release. The role of NMDAR in the pancreas is complex, with some studies suggesting that NMDAR antagonism would be therapeutic, and some suggesting the opposite. A similarly unclear role is found for D-serine itself, and D-serine has been studied both as a potential treatment for metabolic disorders and for adverse effects.

Part of the complexity and lack of clarity of the NMDAR and D-serine's role in glucose homeostasis stems from the varied dosages that were used in pre-clinical experiments. Under physiologic conditions, D-serine appears to activate pancreatic NMDAR to stimulate ß-cell and potentiate insulin release (116). At higher, non-physiologic doses, D-serine may lead to toxicity due to NMDAR internalization, reducing ß-cell activity, and reduced insulin release. Serine racemase is present and active in

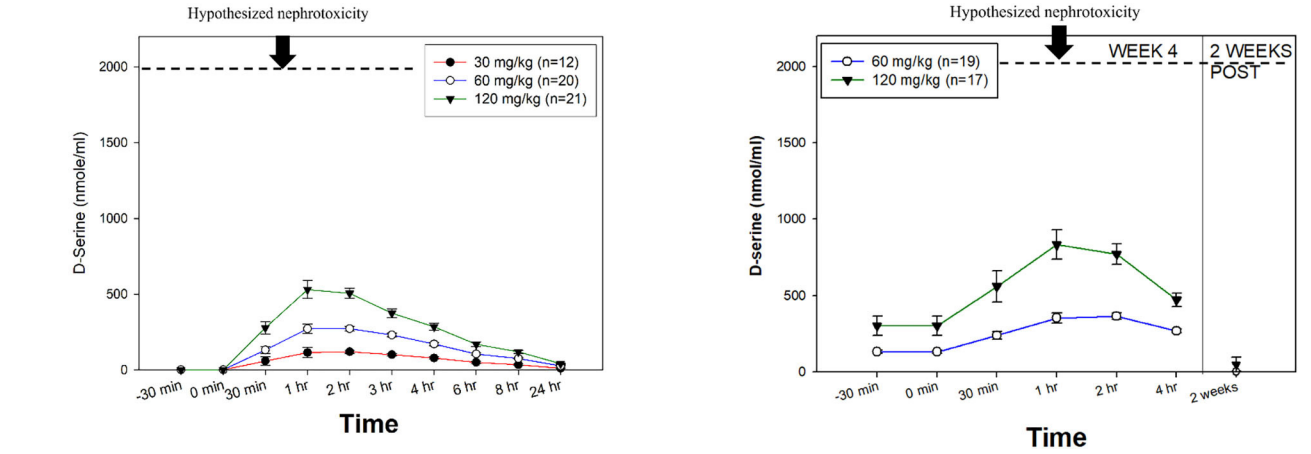

FIGURE 1 | D-serine Pharmacokinetics. **(Left)** 24-h pharmacokinetics of an acute dose of D-serine on day 1 of treatment. **(Right)** 4-h pharmacokinetics after 4 weeks of chronic dosing. In both figures, the hypothesized renal safety level is added based on experiments in rats. Modified from Kantrowitz et al. (31), Hasegawa et al. (108).

the pancreas (117), and helps regulate insulin secretion (118), further suggesting a role for D-serine. By contrast, a recent study (119) suggests that large doses chronic D-serine supplementation results in both reduced high fat diet intake and impaired insulin secretion in mice. In this study, mice received 10 g of D-serine/L of water, and assuming a 25 g mouse drinks 5 mL of water/day (120), the doses required to impair insulin secretion were large (∼2,000 mg/kg), and thus may be of questionable clinical relevance.

Other studies (121, 122) have also supported a dose dependent role for D-serine suppressing intake of high preference (high-fat) food, suggesting potential utility in modulating obesity. In these studies, an appetite suppressant effect was seen at D-serine >1.5 g/kg per day, but not at lower doses. The largest doses studied in humans are ∼10× smaller (120 mg/kg), limiting the translation of these findings to human studies.

Two recently published human studies assessing D-serine's role in monitoring diabetes have shown inconsistent results. Across one study with 96 women with gestational diabetes and 96 with normal glucose tolerance, serine was significantly higher in the gestational diabetes cohort (123). By contrast, in a separate study of 1,623 non-diabetic subjects (124), the opposite result was seen, as lower serine levels were predictive of impaired glucose tolerance. In both studies, we note that the term serine is used, and it is unclear if the measurements were of D-serine, L-serine or a combination. In published studies, no clinically relevant weight gain or metabolic alterations have been reported in clinical studies of D-serine (**Table 2**).

TABLE 2 | Adverse events reported in d-serine trials[a].

Adverse event	Total *n*	D-serine (%)	Placebo (%)	Risk ratio (95% CI); *p*-value
Abdominal discomfort	31	0	5.9	0.40 (0.02, 9.12); 0.57
Anxiety	84	4.9	9.3	0.52 (0.10, 2.70); 0.44
Constipation	115	7.3	0	3.93 (0.66, 23.25); 0.13
Depression	44	4.8	4.3	1.10 (0.07, 16.43); 0.95
Diarrhea	31	7.1	0	3.60 (0.16, 82.05); 0.42
Dizziness	192	15.8	26.5	0.61 (0.32, 1.18); 0.14
Dry mouth	149	5.4	0	9.12 (0.50, 166.46); 0.14
Fatigability	84	22.0	23.2	0.96 (0.19, 4.74); 0.96
Headache	149	17.6	38.7	0.45 (0.26, 0.80); 0.007
Nausea	31	14.3	0	6.00 (0.31, 115.56); 0.24
Palpitation	84	29.3	27.9	1.06 (0.45, 2.48); 0.89
Salivation	44	14.3	8.7	1.64 (0.30, 8.89); 0.56
Sexual dysfunction	26	7.7	0	3.00 (0.13, 67.51); 0.49
Sleep disturbance	115	21.8	20	1.07 (0.53, 2.18); 0.85
Weight gain	84	43.9	44.2	1.05 (0.69, 1.59); 0.81
Weight loss	84	7.3	4.7	1.36 (0.16, 11.68); 0.78

[a] *Modified from Goh (3).*

D-SERINE AND THE ENDOCRINE SYSTEM

Aside from the brain, the kidney and the pancreas, D-serine has been most thoroughly studied in endocrine systems. As recently reviewed (17), D-serine is detected *in vivo* in multiple endocrine glands, including the hypothalamus, pituitary, pineal, thyroid, adrenals, ovary, and testes. However, levels of D-serine in the endocrine organs are lower than those in the CNS, and the physiological role of D-serine in most endocrine organs is unclear.

A role for a regulation of sleep has been reported for both glycine and D-serine, following up on small clinical studies of glycine (125). In a pre-clinical study, improved sleep was seen with direct injection of either glycine or D-serine into the suprachiasmatic nucleus of the hypothalamus (126). D-Serine may also be involved in activating the NMDAR in

the corpus cavernosum, suggesting a possible role in treating impotence (127).

D-SERINE AND EXTRAPYRAMIDAL EFFECTS

Antipsychotics are associated with varying levels of extrapyramidal motor side-effects (EPS) (110), such as Parkinson's like motor disturbances, tremor and dystonia. While one of the clearest advantages of many second generation antipsychotics is a relatively reduced incidence of EPS and other movement disorders such as tardive dyskinesia (TD) (128), both remain a clinically significant issue for many schizophrenia patients.

Antipsychotics likely cause EPS via dopamine type 2 receptor blockade in the striatum. In a pre-clinical mouse study (129), both D-serine (300 mg/kg) and sodium benzoate (600 mg/kg) administered intraperitoneally attenuated haloperidol induced bradykinesia. D-serine showed a *U*-shaped curve for attenuation, as no effects were seen for 100 or 1,000 mg/kg doses. Our pre-clinical studies with mice (71), suggest a comparable mice dose of approximately 100 mg/kg for the 60 mg/kg clinical dose. In this study, D-cycloserine, which acts as an agonist at the D-serine/glycine site of the NMDAR, but a ketamine like antagonist at higher doses (130–132), also attenuated haloperidol induced bradykinesia at doses up to 30 mg/kg, which likely is in the NMDAR agonist range.

Two clinical studies with D-serine have suggested improvement in antipsychotic induced EPS and/or TD in schizophrenia patients (31, 54). One small study of 8 patients suggested efficacy of low dose D-serine for both the behavioral and motor symptoms of Parkinson's disease (58). A double blind study of high dose D-serine did not find a significant benefit for EPS (48).

Amyotrophic lateral sclerosis (ALS) is a fatal neurodegenerative disorder involving an extensive loss of motor neurons, and some familial and sporadic cases have been associated with D-serine metabolism. Specifically, mutations of DAAO have been reported (133), which are associated with pre-clinical and clinical increases of D-serine (30, 134). One recent study found elevated plasma levels of D-serine in ∼40% of ALS patients compared to healthy controls (135). Based on publicly presented, but unpublished observations in studies conducted to support our IND, there is no evidence of D-serine accumulation in motor neurons (71), and there has been no evidence of motor adverse events in human studies.

D-SERINE, THE LIVER AND THE GASTROINTESTINAL TRACT

D-Serine is cleared almost exclusively by the kidney, and is not metabolized by hepatic P450 enzymes. DAAO is present in the liver, and may contribute to D-serine degradation (136). The pre-clinical literature of D-serine's effects on the liver are sparse, but early experiments did not find evidence of a D-serine specific hepatoxic effect in rats using known nephrotoxic doses (1,000 mg/kg) (83). One study using extremely large doses of D-serine (20 mM) was hepatotoxic to *in vitro* rat liver cells and mitochondria, producing oxidative stress and swelling (137). In clinical studies, mild, asymptomatic transaminitis has been reported in two subjects receiving daily 120 mg/kg (31). Only one of the subjects had liver function tests (LFTs) $>2\times$ upper normal range. This mild transaminitis resolved completely after D-serine discontinuation for both patients, and may have been related to the recent administration of the hepatitis vaccine in the patient with the larger elevations, which in rare cases can give rise to elevated liver enzymes (http://vaers.hhs.gov).

In mice, D-serine has shown promise as a treatment and prophylaxis for inflammatory bowel disease (138), albeit at high doses, >1.5 g/kg per day. Finally, D-serine may be involved in lower esophageal sphincter contraction (139), with unclear clinical relevance. D-Serine has not been associated with elevated rates of gastrointestinal adverse events in clinical studies (**Table 2**).

D-SERINE AND THE CARDIOVASCULAR SYSTEM

As recently reviewed, NMDAR are also present in cardiac and vascular tissue (140), and activation of these peripheral NMDAR *in vitro* can lead to tachycardia and hypertension (141). While there is no known physiologic role for D-serine in the heart, D-serine could theoretically lead to increased cardiovascular tone by activating NMDAR. By contrast, the NMDAR antagonist ketamine, consistently produces tachycardia and hypertension in clinical studies (1). While direct application of ketamine on *in vitro* cardiac tissue induces bradycardia (142), the tachycardic/hypertensive effects of *in vivo* ketamine are mediated through brain, with evidence for both centrally mediated top-down control (143–145) and direct effects on the baroreflex in the nucleus tractus solitarii (NTS) in the brainstem (medulla) (146–149). No clinically relevant cardiovascular effects have been reported in clinical studies of D-serine.

D-SERINE AND CANCER

As recently reviewed (150), D-amino acids may be elevated in some cancers. D-Serine does not appear to be a causal factor in tumorigenesis, but there may be increased reuptake of D-serine by some cancer cells, particularly in high glucose environments (151). Alternatively, D-amino acids may be useful for the treatment of some cancers (152–154).

DAAO INHIBITOR CLINICAL STUDIES AND SAFETY

DAAO-inhibitors have been proposed as a treatment for schizophrenia, functioning in a similar way to a selective serotonin reuptake inhibitor (SSRI) by increasing D-serine levels indirectly. Several DAAO-inhibitors are in development, including luvadaxistat and sodium benzoate. Sodium benzoate

has shown efficacy in several, but not all published studies (155–158), and is being actively developed by SyneuRx International (NCT02261519). Luvadaxistat is under development by a partnership between Takeda and Neurocrine (159), and showed preliminary efficacy for cognitive outcomes in publicly presented, but unpublished results.

Although DAAO-inhibitors raise the levels of D-serine and increased DAAO activity may be contributory to nephrotoxicity in rats (91–93), pre-clinical studies suggest that DAAO-inhibitors may protect against D-serine induced nephrotoxicity (29, 160). In a study of rats without functional DAAO activity, D-serine 800 mg/kg did not cause renal damage (29). Furthermore, administration of D-propargylglycine, which is known to cause nephrotoxicity through DAAO (161), also did not cause renal damage in the DAAO knockout rats. By contrast, both D-serine and D-propargylglycine led to the expected nephrotoxicity in the control rats with normal DAAO.

Direct evidence that DAAO-inhibitors are nephroprotective has also been demonstrated in rats (160). In this study, rats were given D-serine 500 mg/kg 1 h after receiving one of 4 doses of sodium benzoate (125, 250, 500, or 750 mg/kg). A dose dependent nephroprotective effect was seen with pretreatment with sodium benzoate 500 mg/kg or greater. The protective effects were most apparent in the first urinalysis samples several hours after D-serine. Pathological samples after 24 h with and without sodium benzoate showed nephrotoxic changes, but sodium benzoate appeared to attenuate these changes as compared to the D-serine alone samples. There has been no reported renal toxicity reported in clinical studies of DAAO-inhibitors. Taken together, these studies support the safety of potential combined D-serine + DAAO-inhibitor studies, which have shown promise pre-clinically (162–164).

ADVERSE EVENTS IN CLINICAL STUDIES OF D-SERINE

In **Table 2**, we present a summary of adverse events in published trials of D-serine, modified from a similar table in a meta-analysis of NMDAR trials in schizophrenia (3). As in the meta-analysis, the present report uses the total of all subjects in which an adverse event is reported as the total potentially affected, rather than the total number in all studies. This allows for a more conservative estimate of the rates of an adverse event. The downside to the analysis is that adverse events were not systematically reported in most of these studies, and the overall n is small. Noting these caveats, in these studies, the only adverse event reported at a significantly different rate than placebo is headache, finding a significantly lower rate of headaches in the of D-serine group.

RECOMMENDATIONS FOR MONITORING DURING CLINICAL D-SERINE STUDIES

In our FDA-monitored studies, we monitor for safety as follows. Routine safety laboratory measures, including a chemistry with serum creatinine and LFTs, a complete blood count and a urinalysis with microscopics, are obtained at screening. Vitals and ECGs are also obtained. No subjects with baseline renal impairment, as evidenced by an estimated glomerular filtration rate (eGFR)<60 or clinically significant abnormal laboratories are enrolled.

During the study, potential nephrotoxicity is monitored through serum chemistry and urine microscopic examination looking for evidence of active sediment (e.g., casts), proteinuria or glycosuria, as per FDA guidance.

After randomization, we monitor as follows:

(a) Urinalysis with microscopics and chemistry biweekly for daily studies or after each dose for intermittent treatment.
(b) Immediately discontinue D-serine for unexplained serum creatinine increase >0.3 mg/dL over the pre-study value or for >1 granular or muddy casts. Treat as SAE possibly related to study medication. Repeat until clear × 2 to demonstrate reversibility.
(c) Hold D-serine for >1 hyaline casts, and repeat lab. Ask subject to eat more salt and drink more water. If absent on repeat, reinstate D-serine and treat as adverse event (AE). If present on repeat, continue to hold D-serine and repeat lab once again. If still present on second repeat, discontinue D-serine and treat as SAE possibly related to study medication. Repeat until clear × 2 to demonstrate reversibility.
(d) Hold D-serine for proteinuria >100 mg/dl or unexplained glucose >250 g/dl (both equivalent to 2+). If absent on repeat, resume D-serine and treat as AE. If still present on repeat, discontinue D-serine. Repeat until clear x 2 to demonstrate reversibility. This would be treated as SAE possibly related to study medication. Unexplained glycosuria is defined as increased urine glucose in absence of corresponding increase in serum glucose levels, in patients without glycosuria at baseline.
(e) Continue D-serine for proteinuria >30 but <100 mg/dl (1+), or unexplained glycosuria (>100 but < 250 g/dl) but repeat. If absent on repeat, continue D-serine and treat as AE. If still present on repeat, hold D-serine and repeat once more. If absent on repeat, resume D-serine and treat as AE. If still present on second repeat, discontinue D-serine and treat as SAE possibly related to study medication. Repeat until clear × 2 to demonstrate reversibility.
(f) For other kidney related measures (e.g., ketones, bilirubin, WBC, RBC, bacteria, crystals), repeat, but no need to discontinue even if present on repeat, since unlikely to be D-serine related. Manage in consultation with medical specialist.
(g) Contaminated samples (hemolyzed/non-clean catch/menstruation) will be repeated.

CONCLUSIONS

Schizophrenia remains a difficult to treat illness, with a large majority of patients not responding completely to FDA approved antipsychotics. D-Serine appears efficacious in schizophrenia, especially in high doses (≥60 mg/kg). Our literature review supports that D-serine is safe and well-tolerated in people without pre-existing renal dysfunction. While there is no evidence of

D-serine being nephrotoxic in humans, we require that people with pre-existing renal dysfunction (GFR<60) be excluded from clinical studies.

Thus far, 120 mg/kg is the highest D-serine dose tested in human studies, but animal studies suggest that even higher doses may be required for optimal target engagement. In this review, we have taken a conservative approach to interspecies dose equivalences, but note that standard mouse to human conversions of 12.3 to 1 have been proposed in the literature (165). Nevertheless, even before considering human to rodent differences in physiology, the literature supports that D-serine has potential safety at doses even higher than 120 mg/kg. Ongoing dose-response studies are assessing the safety and efficacy of doses up to 120 mg/kg, and future work is needed to explore the possibility of even higher doses or combined D-serine + DAAO-inhibitor studies.

AUTHOR CONTRIBUTIONS

JK and AM: substantial contributions to conception and design. JK, AM, and HH: drafting of the manuscript and critical revision of the manuscript for important intellectual content. All authors reviewed the final submission and gave final approval of the submitted version.

FUNDING

This work was supported by R61 MH116093 to JK.

REFERENCES

1. Kantrowitz JT, Grinband J, Goff DC, Lahti AC, Marder SR, Kegeles LS, et al. Proof of mechanism and target engagement of glutamatergic drugs for the treatment of schizophrenia: RCTs of pomaglumetad and TS-134 on ketamine-induced psychotic symptoms and pharmacoBOLD in healthy volunteers. *Neuropsychopharmacology.* (2020) 45:1842–50. doi: 10.1038/s41386-020-0706-z
2. Potkin SG, Kane JM, Correll CU, Lindenmayer JP, Agid O, Marder SR, et al. The neurobiology of treatment-resistant schizophrenia: paths to antipsychotic resistance and a roadmap for future research. *NPJ Schizophr.* (2020) 6:1. doi: 10.1038/s41537-019-0090-z
3. Goh KK, Wu TH, Chen CH, Lu ML. Efficacy of N-methyl-D-aspartate receptor modulator augmentation in schizophrenia: a meta-analysis of randomised, placebo-controlled trials. *J Psychopharmacol.* (2021) 35:236–52. doi: 10.1177/0269881120965937
4. Kantrowitz JT, Epstein ML, Beggel O, Rohrig S, Lehrfeld JM, Revheim N, et al. Neurophysiological mechanisms of cortical plasticity impairments in schizophrenia and modulation by the NMDA receptor agonist D-serine. *Brain.* (2016) 139:3281–95. doi: 10.1093/brain/aww262
5. Fleischhacker WW, Podhorna J, Groschl M, Hake S, Zhao Y, Huang S, et al. Efficacy and safety of the novel glycine transporter inhibitor BI 425809 once daily in patients with schizophrenia: a double-blind, randomised, placebo-controlled phase 2 study. *Lancet Psychiatry.* (2021) 8:191–201. doi: 10.1016/S2215-0366(20)30513-7
6. Bugarski-Kirola D, Iwata N, Sameljak S, Reid C, Blaettler T, Millar L, et al. Efficacy and safety of adjunctive bitopertin versus placebo in patients with suboptimally controlled symptoms of schizophrenia treated with antipsychotics: results from three phase 3, randomised, double-blind, parallel-group, placebo-controlled, multicentre studies in the SearchLyte clinical trial programme. *Lancet Psychiatry.* (2016) 3:1115–28. doi: 10.1016/S2215-0366(16)30344-3
7. Dunayevich E, Buchanan RW, Chen CY, Yang J, Nilsen J, Dietrich JM, et al. Efficacy and safety of the glycine transporter type-1 inhibitor AMG 747 for the treatment of negative symptoms associated with schizophrenia. *Schizophr Res.* (2017) 182:90–7. doi: 10.1016/j.schres.2016.10.027
8. Kantrowitz JT, Nolan KA, Epstein ML, Lehrfeld N, Shope C, Petkova E, et al. Neurophysiological effects of bitopertin in schizophrenia. *J Clin Psychopharmacol.* (2017) 37:447–51. doi: 10.1097/JCP.0000000000000722
9. Grabb MC, Cross AJ, Potter WZ, Mccracken JT. Derisking psychiatric drug development: the NIMH's fast fail program, a novel precompetitive model. *J Clin Psychopharmacol.* (2016) 36:419–21. doi: 10.1097/JCP.0000000000000536
10. De La Garrigue N, Glasser J, Sehatpour P, Iosifescu DV, Dias E, Carlson M, et al. Grant report on D-serine augmentation of neuroplasticity-based auditory learning in schizophrenia (dagger). *J Psychiatr Brain Sci.* (2020) 5:e200018. doi: 10.20900/jpbs.20200018
11. Kantrowitz JT, Javitt DC. Glutamatergic approaches to the conceptualization and treatment of schizophrenia. In: Javitt DC, Kantrowitz JT, editors. *Handbook of Neurochemistry and Molecular Neurobiology. 3rd edn.* New York, NY: Springer (2009). doi: 10.1007/978-0-387-30410-6_3
12. Kantrowitz JT, Javitt DC. N-methyl-d-aspartate (NMDA) receptor dysfunction or dysregulation: the final common pathway on the road to schizophrenia? *Brain Res Bull.* (2010) 83:108–21. doi: 10.1016/j.brainresbull.2010.04.006
13. Hashimoto A, Nishikawa T, Hayashi T, Fujii N, Harada K, Oka T, et al. The presence of free D-serine in rat brain. *FEBS Lett.* (1992) 296:33–6. doi: 10.1016/0014-5793(92)80397-Y
14. Schell MJ, Molliver ME, Snyder SH. D-serine, an endogenous synaptic modulator: localization to astrocytes and glutamate-stimulated release. *Proc Natl Acad Sci USA.* (1995) 92:3948–52. doi: 10.1073/pnas.92.9.3948
15. Balu DT, Li Y, Puhl MD, Benneyworth MA, Basu AC, Takagi S, et al. Multiple risk pathways for schizophrenia converge in serine racemase knockout mice, a mouse model of NMDA receptor hypofunction. *Proc Natl Acad Sci USA.* (2013) 110:E2400–9. doi: 10.1073/pnas.1304308110
16. Balu DT, Coyle JT. The NMDA receptor 'glycine modulatory site' in schizophrenia: D-serine, glycine, and beyond. *Curr Opin Pharmacol.* (2015) 20:109–15. doi: 10.1016/j.coph.2014.12.004
17. Chieffi Baccari G, Falvo S, Santillo A, Di Giacomo Russo F, Di Fiore MM. D-Amino acids in mammalian endocrine tissues. *Amino Acids.* (2020) 52:1263–73. doi: 10.1007/s00726-020-02892-7
18. Dunlop DS, Neidle A. The origin and turnover of D-serine in brain. *Biochem Biophys Res Commun.* (1997) 235:26–30. doi: 10.1006/bbrc.1997.6724
19. Wolosker H, Sheth KN, Takahashi M, Mothet JP, Brady RO Jr, Ferris CD, et al. Purification of serine racemase: biosynthesis of the neuromodulator D-serine. *Proc Natl Acad Sci USA.* (1999) 96:721–5. doi: 10.1073/pnas.96.2.721
20. Foltyn VN, Bendikov I, De Miranda J, Panizzutti R, Dumin E, Shleper M, et al. Serine racemase modulates intracellular D-serine levels through an alpha,beta-elimination activity. *J Biol Chem.* (2005) 280:1754–63. doi: 10.1074/jbc.M405726200
21. Horiike K, Tojo H, Arai R, Nozaki M, Maeda T. D-amino-acid oxidase is confined to the lower brain stem and cerebellum in rat brain: regional differentiation of astrocytes. *Brain Res.* (1994) 652:297–303. doi: 10.1016/0006-8993(94)90240-2
22. Moreno S, Nardacci R, Cimini A, Ceru MP. Immunocytochemical localization of D-amino acid oxidase in rat brain. *J Neurocytol.* (1999) 28:169–85. doi: 10.1023/A:1007064504007
23. Morikawa A, Hamase K, Inoue T, Konno R, Niwa A, Zaitsu K. Determination of free D-aspartic acid, D-serine and D-alanine in the brain of mutant mice lacking D-amino acid oxidase activity. *J Chromatogr B Biomed Sci Appl.* (2001) 757:119–25. doi: 10.1016/S0378-4347(01)00131-1
24. Miyoshi Y, Hamase K, Okamura T, Konno R, Kasai N, Tojo Y, et al. Simultaneous two-dimensional HPLC determination of free D-serine and D-alanine in the brain and periphery of mutant rats lacking D-amino-acid oxidase. *J Chromatogr B Analyt Technol*

Biomed Life Sci. (2011) 879:3184–9. doi: 10.1016/j.jchromb.2010.08.024
25. Strick CA, Li C, Scott L, Harvey B, Hajos M, Steyn SJ, et al. Modulation of NMDA receptor function by inhibition of D-amino acid oxidase in rodent brain. *Neuropharmacology.* (2011) 61:1001–15. doi: 10.1016/j.neuropharm.2011.06.029
26. Verrall L, Walker M, Rawlings N, Benzel I, Kew JN, Harrison PJ, et al. d-Amino acid oxidase and serine racemase in human brain: normal distribution and altered expression in schizophrenia. *Eur J Neurosci.* (2007) 26:1657–69. doi: 10.1111/j.1460-9568.2007.05769.x
27. Xia M, Liu Y, Figueroa DJ, Chiu CS, Wei N, Lawlor AM, et al. Characterization and localization of a human serine racemase. *Brain Res Mol Brain Res.* (2004) 125:96–104. doi: 10.1016/j.molbrainres.2004.03.007
28. Horio M, Kohno M, Fujita Y, Ishima T, Inoue R, Mori H, et al. Levels of D-serine in the brain and peripheral organs of serine racemase (Srr) knock-out mice. *Neurochem Int.* (2011) 59:853–9. doi: 10.1016/j.neuint.2011.08.017
29. Maekawa M, Okamura T, Kasai N, Hori Y, Summer KH, Konno R. D-amino-acid oxidase is involved in D-serine-induced nephrotoxicity. *Chem Res Toxicol.* (2005) 18:1678–82. doi: 10.1021/tx0500326
30. Sasabe J, Miyoshi Y, Suzuki M, Mita M, Konno R, Matsuoka M, et al. D-amino acid oxidase controls motoneuron degeneration through D-serine. *Proc Natl Acad Sci USA.* (2012) 109:627–32. doi: 10.1073/pnas.1114639109
31. Kantrowitz JT, Malhotra AK, Cornblatt B, Silipo G, Balla A, Suckow RF, et al. High dose D-serine in the treatment of schizophrenia. *Schizophr Res.* (2010) 121:125–30. doi: 10.1016/j.schres.2010.05.012
32. Takahashi K, Hayashi F, Nishikawa T. *In vivo* evidence for the link between L- and D-serine metabolism in rat cerebral cortex. *J Neurochem.* (1997) 69:1286–90. doi: 10.1046/j.1471-4159.1997.69031286.x
33. Pernot P, Maucler C, Tholance Y, Vasylieva N, Debilly G, Pollegioni L, et al. d-Serine diffusion through the blood-brain barrier: effect on D-serine compartmentalization and storage. *Neurochem Int.* (2012) 60:837–45. doi: 10.1016/j.neuint.2012.03.008
34. Matsui T, Sekiguchi M, Hashimoto A, Tomita U, Nishikawa T, Wada K. Functional comparison of D-serine and glycine in rodents: the effect on cloned NMDA receptors and the extracellular concentration. *J Neurochem.* (1995) 65:454–8. doi: 10.1046/j.1471-4159.1995.65010454.x
35. Priestley T, Laughton P, Myers J, Le Bourdelles B, Kerby J, Whiting PJ. Pharmacological properties of recombinant human N-methyl-D-aspartate receptors comprising NR1a/NR2A and NR1a/NR2B subunit assemblies expressed in permanently transfected mouse fibroblast cells. *Mol Pharmacol.* (1995) 48:841–8.
36. Berger AJ, Dieudonne S, Ascher P. Glycine uptake governs glycine site occupancy at NMDA receptors of excitatory synapses. *J Neurophysiol.* (1998) 80:3336–40. doi: 10.1152/jn.1998.80.6.3336
37. Mothet JP, Parent AT, Wolosker H, Brady RO Jr, Linden DJ. D-serine is an endogenous ligand for the glycine site of the N-methyl-D- aspartate receptor. *Proc Natl Acad Sci USA.* (2000) 97:4926–31. doi: 10.1073/pnas.97.9.4926
38. Otte DM, Barcena De Arellano ML, Bilkei-Gorzo A, Albayram O, Imbeault S, Jeung H, et al. Effects of chronic D-serine elevation on animal models of depression and anxiety-related behavior. *PLoS ONE.* (2013) 8:e67131. doi: 10.1371/journal.pone.0067131
39. Guercio GD, Panizzutti R. Potential and challenges for the clinical use of D-Serine as a cognitive enhancer. *Front Psychiatry.* (2018) 9:14. doi: 10.3389/fpsyt.2018.00014
40. Watanabe Y, Saito H, Abe K. Effects of glycine and structurally related amino acids on generation of long-term potentiation in rat hippocampal slices. *Eur J Pharmacol.* (1992) 223:179–84. doi: 10.1016/0014-2999(92)94837-L
41. Hunt DL, Castillo PE. Synaptic plasticity of NMDA receptors: mechanisms and functional implications. *Curr Opin Neurobiol.* (2012) 22:496–508. doi: 10.1016/j.conb.2012.01.007
42. Luscher C, Malenka RC. NMDA receptor-dependent long-term potentiation and long-term depression (LTP/LTD). *Cold Spring Harb Perspect Biol.* (2012) 4:a005710. doi: 10.1101/cshperspect.a005710
43. Van Horn MR, Sild M, Ruthazer ES. D-serine as a gliotransmitter and its roles in brain development and disease. *Front Cell Neurosci.* (2013) 7:39. doi: 10.3389/fncel.2013.00039
44. Ivanov AD, Mothet JP. The plastic D-serine signaling pathway: sliding from neurons to glia and vice-versa. *Neurosci Lett.* (2019) 689:21–5. doi: 10.1016/j.neulet.2018.05.039
45. Diniz LP, Almeida JC, Tortelli V, Vargas Lopes C, Setti-Perdigao P, Stipursky J, et al. Astrocyte-induced synaptogenesis is mediated by transforming growth factor beta signaling through modulation of D-serine levels in cerebral cortex neurons. *J Biol Chem.* (2012) 287:41432–45. doi: 10.1074/jbc.M112.380824
46. Cho SE, Na KS, Cho SJ, Kang SG. Low D-serine levels in schizophrenia: a systematic review and meta-analysis. *Neurosci Lett.* (2016) 634:42–51. doi: 10.1016/j.neulet.2016.10.006
47. Kantrowitz JT, Woods SW, Petkova E, Cornblatt B, Corcoran CM, Chen H, et al. D-serine for the treatment of negative symptoms in individuals at clinical high risk of schizophrenia: a pilot, double-blind, placebo-controlled, randomised parallel group mechanistic proof-of-concept trial. *Lancet Psychiatry.* (2015) 2:403–12. doi: 10.1016/S2215-0366(15)00098-X
48. Kantrowitz JT, Epstein ML, Lee M, Lehrfeld N, Nolan KA, Shope C, et al. Improvement in mismatch negativity generation during D-serine treatment in schizophrenia: correlation with symptoms. *Schizophr Res.* (2018) 191:70–9. doi: 10.1016/j.schres.2017.02.027
49. Ermilov M, Gelfin E, Levin R, Lichtenberg P, Hashimoto K, Javitt DC, et al. A pilot double-blind comparison of D-serine and high-dose olanzapine in treatment-resistant patients with schizophrenia. *Schizophr Res.* (2013) 150:604–5. doi: 10.1016/j.schres.2013.09.018
50. Capitao LP, Forsyth J, Thomaidou MA, Condon MD, Harmer CJ, Burnet PW. A single administration of 'microbial' D-alanine to healthy volunteers augments reaction to negative emotions: a comparison with D-serine. *J Psychopharmacol.* (2020) 34:557–66. doi: 10.1177/0269881120908904
51. Heresco-Levy U, Durrant AR, Ermilov M, Javitt DC, Miya K, Mori H. Clinical and electrophysiological effects of D-serine in a schizophrenia patient positive for anti-N-methyl-D-aspartate receptor antibodies. *Biol Psychiatry.* (2015) 77:e27–9. doi: 10.1016/j.biopsych.2014.08.023
52. Tsai G, Yang P, Chung LC, Lange N, Coyle JT. D-serine added to antipsychotics for the treatment of schizophrenia. *Biol Psychiatry.* (1998) 44:1081–9. doi: 10.1016/S0006-3223(98)00279-0
53. Tsai GE, Yang P, Chung LC, Tsai IC, Tsai CW, Coyle JT. D-serine added to clozapine for the treatment of schizophrenia. *Am J Psychiatry.* (1999) 156:1822–5.
54. Heresco-Levy U, Javitt DC, Ebstein R, Vass A, Lichtenberg P, Bar G, et al. D-serine efficacy as add-on pharmacotherapy to risperidone and olanzapine for treatment-refractory schizophrenia. *Biol Psychiatry.* (2005) 57:577–85. doi: 10.1016/j.biopsych.2004.12.037
55. Lane HY, Chang YC, Liu YC, Chiu CC, Tsai GE. Sarcosine or D-serine add-on treatment for acute exacerbation of schizophrenia: a randomized, double-blind, placebo-controlled study. *Arch Gen Psychiatry.* (2005) 62:1196–204. doi: 10.1001/archpsyc.62.11.1196
56. Heresco-Levy U, Vass A, Bloch B, Wolosker H, Dumin E, Balan L, et al. Pilot controlled trial of D-serine for the treatment of post-traumatic stress disorder. *Int J Neuropsychopharmacol.* (2009) 12:1275–82. doi: 10.1017/S1461145709000339
57. Lane HY, Lin CH, Huang YJ, Liao CH, Chang YC, Tsai GE. A randomized, double-blind, placebo-controlled comparison study of sarcosine (N-methylglycine) and D-serine add-on treatment for schizophrenia. *Int J Neuropsychopharmacol.* (2010) 13:451–60. doi: 10.1017/S1461145709990939
58. Gelfin E, Kaufman Y, Korn-Lubetzki I, Bloch B, Kremer I, Javitt DC, et al. D-serine adjuvant treatment alleviates behavioural and motor symptoms in Parkinson's disease. *Int J Neuropsychopharmacol.* (2012) 15:543–9. doi: 10.1017/S1461145711001015
59. D'souza DC, Radhakrishnan R, Perry E, Bhakta S, Singh NM, Yadav R, et al. Feasibility, safety, and efficacy of the combination of D-serine and computerized cognitive retraining in schizophrenia: an international collaborative pilot study. *Neuropsychopharmacology.* (2013) 38:492–503. doi: 10.1038/npp.2012.208
60. Weiser M, Heresco-Levy U, Davidson M, Javitt DC, Werbeloff N, Gershon AA, et al. A multicenter, add-on randomized controlled trial of low-dose D-serine for negative and cognitive symptoms of schizophrenia. *J Clin Psychiatry.* (2012) 73:e728–34. doi: 10.4088/JCP.11m07031

61. Lemmon ME, Grados M, Kline T, Thompson CB, Ali SF, Singer HS. Efficacy of glutamate modulators in tic suppression: a double-blind, randomized control trial of D-serine and riluzole in tourette syndrome. *Pediatr Neurol.* (2015) 52:629–34. doi: 10.1016/j.pediatrneurol.2015.02.002
62. Levin R, Dor-Abarbanel AE, Edelman S, Durrant AR, Hashimoto K, Javitt DC, et al. Behavioral and cognitive effects of the N-methyl-D-aspartate receptor co-agonist D-serine in healthy humans: initial findings. *J Psychiatr Res.* (2015) 61:188–95. doi: 10.1016/j.jpsychires.2014.12.007
63. Avellar M, Scoriels L, Madeira C, Vargas-Lopes C, Marques P, Dantas C, et al. The effect of D-serine administration on cognition and mood in older adults. *Oncotarget.* (2016) 7:11881–8. doi: 10.18632/oncotarget.7691
64. Wegner SA, Hu B, De Oliveira Sergio T, Darevsky D, Kwok CC, Lei K, et al. A novel NMDA receptor-based intervention to suppress compulsion-like alcohol drinking. *Neuropharmacology.* (2019) 157:107681. doi: 10.1016/j.neuropharm.2019.107681
65. Madeira C, Lourenco MV, Vargas-Lopes C, Suemoto CK, Brandão CO, Reis T, et al. D-serine levels in Alzheimer's disease: implications for novel biomarker development. *Transl Psychiatry.* (2015) 5:e561. doi: 10.1038/tp.2015.52
66. Malkesman O, Austin DR, Tragon T, Wang G, Rompala G, Hamidi AB, et al. Acute D-serine treatment produces antidepressant-like effects in rodents. *Int J Neuropsychopharmacol.* (2012) 15:1135–48. doi: 10.1017/S1461145711001386
67. Wei IH, Chen KT, Tsai MH, Wu CH, Lane HY, Huang CC. Acute amino acid D-serine administration, similar to ketamine, produces antidepressant-like effects through identical mechanisms. *J Agric Food Chem.* (2017) 65:10792–803. doi: 10.1021/acs.jafc.7b04217
68. Andreasen NC. *The Scale for the Assessment of Negative Symptoms (SANS).* Iowa City, IA: The University of Iowa (1984).
69. Kay SR, Fiszbein A, Opler LA. The positive and negative syndrome scale (PANSS) for schizophrenia. *Schizophr Bull.* (1987) 13:261–76. doi: 10.1093/schbul/13.2.261
70. Tsai GE, Yang P, Chang YC, Chong MY. D-alanine added to antipsychotics for the treatment of schizophrenia. *Biol Psychiatry.* (2006) 59:230–4. doi: 10.1016/j.biopsych.2005.06.032
71. Javitt DC, Malhotra AK, Woods SW, Kantrowitz JT, Cornblatt BA, Mathalon DH. Dose-finding PK/PD study of D-serine in schizophrenia: effects on symptoms and neurocognition. *Neuropharmacology.* (2008) 33.
72. Nilsson M, Carlsson A, Carlsson ML. Glycine and D-serine decrease MK-801-induced hyperactivity in mice. *J Neural Transm.* (1997) 104:1195–205. doi: 10.1007/BF01294720
73. Nuechterlein KH, Green MF, Kern RS, Baade LE, Barch DM, Cohen JD, et al. The MATRICS consensus cognitive battery, part 1: test selection, reliability, and validity. *Am J Psychiatry.* (2008) 165:203–13. doi: 10.1176/appi.ajp.2007.07010042
74. Panizzutti R, Fisher M, Garrett C, Man WH, Sena W, Madeira C, et al. Association between increased serum D-serine and cognitive gains induced by intensive cognitive training in schizophrenia. *Schizophr Res.* (2019) 207:63–9. doi: 10.1016/j.schres.2018.04.011
75. Hons J, Zirko R, Vasatova M, Doubek P, Klimova B, Masopust J, et al. Impairment of executive functions associated with lower D-serine serum levels in patients with schizophrenia. *Front Psychiatry.* (2021) 12:514579. doi: 10.3389/fpsyt.2021.514579
76. Kantrowitz JT, Swerdlow NR, Dunn W, Vinogradov S. Auditory system target engagement during plasticity-based interventions in schizophrenia: a focus on modulation of n-methyl-d-aspartate-type glutamate receptor function. *Biol Psychiatry Cogn Neurosci Neuroimaging.* (2018) 3:581–90. doi: 10.1016/j.bpsc.2018.02.002
77. Kantrowitz JT. N-methyl-d-aspartate-type glutamate receptor modulators and related medications for the enhancement of auditory system plasticity in schizophrenia. *Schizophr Res.* (2019) 207:70–9. doi: 10.1016/j.schres.2018.02.003
78. Brummel C, Vedananda S, Doller D, Wong D, Gallegos R, Liu J, et al. CTP-692: selective deuterium modification of D-serine markedly decreases renal toxicity in preclinical testing. In*: ACT 39th Annual Meeting.* West Palm Beach, FL (2018).
79. Deng A, Thomson SC. Renal NMDA receptors independently stimulate proximal reabsorption and glomerular filtration. *Am J Physiol Renal Physiol.* (2009) 296:F976–82. doi: 10.1152/ajprenal.90391.2008
80. Anderson M, Suh JM, Kim EY, Dryer SE. Functional NMDA receptors with atypical properties are expressed in podocytes. *Am J Physiol Cell Physiol.* (2011) 300:C22–32. doi: 10.1152/ajpcell.00268.2010
81. Dryer SE. Glutamate receptors in the kidney. *Nephrol Dial Transplant.* (2015) 30:1630–8. doi: 10.1093/ndt/gfv028
82. Fishman WH, Artom C. Serine injury. *J Biol Chem.* (1942) 145:345–6. doi: 10.1016/S0021-9258(18)45040-5
83. Morehead R, Fishman W, Artom C. Renal injury in the rat following the administration of serine by stomach tube. *Am J Pathology.* (1945) 21:803–15.
84. Morehead R, Poe W, Williams J, Lazenby M. The influence of age and species on the nephrotoxic action of DL-serine. *Am J Pathology.* (1946) 21:803–15.
85. Ganote CE, Peterson DR, Carone FA. The nature of D-serine–induced nephrotoxicity. *Am J Pathol.* (1974) 77:269–82.
86. Carone FA, Ganote CE. D-serine nephrotoxicity. The nature of proteinuria, glucosuria, and aminoaciduria in acute tubular necrosis. *Arch Pathol.* (1975) 99:658–62.
87. Williams RE, Jacobsen M, Lock EA. 1H NMR pattern recognition and 31P NMR studies with d-Serine in rat urine and kidney, time- and dose-related metabolic effects. *Chem Res Toxicol.* (2003) 16:1207–16. doi: 10.1021/tx030019q
88. Silbernagl S, Volker K, Dantzler WH. D-Serine is reabsorbed in rat renal pars recta. *Am J Physiol.* (1999) 276:F857–63. doi: 10.1152/ajprenal.1999.276.6.F857
89. Kaltenbach JP, Ganote CE, Carone FA. Renal tubular necrosis induced by compounds structurally related to D-serine. *Exp Mol Pathol.* (1979) 30:209–14. doi: 10.1016/0014-4800(79)90054-6
90. Huang Y, Nishikawa T, Satoh K, Iwata T, Fukushima T, Santa T, et al. Urinary excretion of D-serine in human: comparison of different ages and species. *Biol Pharm Bull.* (1998) 21:156–62. doi: 10.1248/bpb.21.156
91. Krug AW, Volker K, Dantzler WH, Silbernagl S. Why is D-serine nephrotoxic and alpha-aminoisobutyric acid protective? *Am J Physiol Renal Physiol.* (2007) 293:F382–90. doi: 10.1152/ajprenal.00441.2006
92. Orozco-Ibarra M, Medina-Campos ON, Sanchez-Gonzalez DJ, Martinez-Martinez CM, Floriano-Sanchez E, Santamaria A, et al. Evaluation of oxidative stress in D-serine induced nephrotoxicity. *Toxicology.* (2007) 229:123–35. doi: 10.1016/j.tox.2006.10.008
93. Soto A, Delraso NJ, Schlager JJ, Chan VT. D-Serine exposure resulted in gene expression changes indicative of activation of fibrogenic pathways and down-regulation of energy metabolism and oxidative stress response. *Toxicology.* (2008) 243:177–92. doi: 10.1016/j.tox.2007.10.009
94. Usuda N, Yokota S, Hashimoto T, Nagata T. Immunocytochemical localization of D-amino acid oxidase in the central clear matrix of rat kidney peroxisomes. *J Histochem Cytochem.* (1986) 34:1709–18. doi: 10.1177/34.12.2878022
95. Perotti ME, Gavazzi E, Trussardo L, Malgaretti N, Curti B. Immunoelectron microscopic localization of D-amino acid oxidase in rat kidney and liver. *Histochem J.* (1987) 19:157–69. doi: 10.1007/BF01695140
96. Konno R, Uchiyama S, Yasumura Y. Intraspecies and interspecies variations in the substrate specificity of D-amino acid oxidase. *Comp Biochem Physiol B.* (1982) 71:735–8. doi: 10.1016/0305-0491(82)90490-4
97. Frattini LF, Piubelli L, Sacchi S, Molla G, Pollegioni L. Is rat an appropriate animal model to study the involvement of D-serine catabolism in schizophrenia? Insights from characterization of D-amino acid oxidase. *FEBS J.* (2011) 278:4362–73. doi: 10.1111/j.1742-4658.2011.08354.x
98. Tseng YS, Liao CH, Wu WB, Ma MC. N-methyl-d-aspartate receptor hyperfunction contributes to D-serine-mediated renal insufficiency. *Am J Physiol Renal Physiol.* (2021) 320:F799–813. doi: 10.1152/ajprenal.00461.2020
99. Kragh-Hansen U, Sheikh MI. Serine uptake by luminal and basolateral membrane vesicles from rabbit kidney. *J Physiol.* (1984) 354:55–67. doi: 10.1113/jphysiol.1984.sp015361
100. Kimura T, Hesaka A, Isaka Y. D-Amino acids and kidney diseases. *Clin Exp Nephrol.* (2020) 24:404–10. doi: 10.1007/s10157-020-01862-3

101. Iwakawa H, Makabe S, Ito T, Yoshimura T, Watanabe H. Urinary D-serine level as a predictive biomarker for deterioration of renal function in patients with atherosclerotic risk factors. *Biomarkers.* (2019) 24:159–65. doi: 10.1080/1354750X.2018.1528632
102. Suzuki M, Gonda Y, Yamada M, Vandebroek AA, Mita M, Hamase K, et al. Serum D-serine accumulation after proximal renal tubular damage involves neutral amino acid transporter Asc-1. *Sci Rep.* (2019) 9:16705. doi: 10.1038/s41598-019-53302-2
103. Sasabe J, Suzuki M, Miyoshi Y, Tojo Y, Okamura C, Ito S, et al. Ischemic acute kidney injury perturbs homeostasis of serine enantiomers in the body fluid in mice: early detection of renal dysfunction using the ratio of serine enantiomers. *PLoS ONE.* (2014) 9:e86504. doi: 10.1371/journal.pone.0086504
104. Nagata Y, Akino T, Ohno K, Kataoka Y, Ueda T, Sakurai T, et al. Free D-amino acids in human plasma in relation to senescence and renal diseases. *Clin Sci.* (1987) 73:105–8. doi: 10.1042/cs0730105
105. Kimura T, Hamase K, Miyoshi Y, Yamamoto R, Yasuda K, Mita M, et al. Chiral amino acid metabolomics for novel biomarker screening in the prognosis of chronic kidney disease. *Sci Rep.* (2016) 6:26137. doi: 10.1038/srep26137
106. Hesaka A, Sakai S, Hamase K, Ikeda T, Matsui R, Mita M, et al. D-Serine reflects kidney function and diseases. *Sci Rep.* (2019) 9:5104. doi: 10.1038/s41598-019-41608-0
107. Hesaka A, Yasuda K, Sakai S, Yonishi H, Namba-Hamano T, Takahashi A, et al. Dynamics of D-serine reflected the recovery course of a patient with rapidly progressive glomerulonephritis. *CEN Case Rep.* (2019) 8:297–300. doi: 10.1007/s13730-019-00411-6
108. Hasegawa H, Masuda N, Natori H, Shinohara Y, Ichida K. Pharmacokinetics and toxicokinetics of D-serine in rats. *J Pharm Biomed Anal.* (2019) 162:264–71. doi: 10.1016/j.jpba.2018.09.026
109. Okada A, Nangaku M, Jao TM, Maekawa H, Ishimono Y, Kawakami T, et al. D-serine, a novel uremic toxin, induces senescence in human renal tubular cells via GCN2 activation. *Sci Rep.* (2017) 7:11168. doi: 10.1038/s41598-017-11049-8
110. Huhn M, Nikolakopoulou A, Schneider-Thoma J, Krause M, Samara M, Peter N, et al. Comparative efficacy and tolerability of 32 oral antipsychotics for the acute treatment of adults with multi-episode schizophrenia: a systematic review and network meta-analysis. *Lancet.* (2019) 394:939–51. doi: 10.1016/S0140-6736(19)31135-3
111. Meftah AM, Deckler E, Citrome L, Kantrowitz JT. New discoveries for an old drug: a review of recent olanzapine research. *Postgrad Med.* (2020) 132:80–90. doi: 10.1080/00325481.2019.1701823
112. Suzuki M, Sasabe J, Furuya S, Mita M, Hamase K, Aiso S. Type 1 diabetes mellitus in mice increases hippocampal D-serine in the acute phase after streptozotocin injection. *Brain Res.* (2012) 1466:167–76. doi: 10.1016/j.brainres.2012.05.042
113. Yang J, Song Y, Wang H, Liu C, Li Z, Liu Y, et al. Insulin treatment prevents the increase in D-serine in hippocampal CA1 area of diabetic rats. *Am J Alzheimers Dis Other Demen.* (2015) 30:201–8. doi: 10.1177/1533317514545379
114. Molnar E, Varadi A, Mcilhinney RA, Ashcroft SJ. Identification of functional ionotropic glutamate receptor proteins in pancreatic beta-cells and in islets of langerhans. *FEBS Lett.* (1995) 371:253–7. doi: 10.1016/0014-5793(95)00890-L
115. Marquard J, Otter S, Welters A, Stirban A, Fischer A, Eglinger J, et al. Characterization of pancreatic NMDA receptors as possible drug targets for diabetes treatment. *Nat Med.* (2015) 21:363–72. doi: 10.1038/nm.3822
116. Lockridge A, Gustafson E, Wong A, Miller RF, Alejandro EU. Acute D-serine Co-Agonism of beta-Cell NMDA receptors potentiates glucose-stimulated insulin secretion and excitatory beta-cell membrane activity. *Cells.* (2021) 10:93. doi: 10.3390/cells10010093
117. Lockridge AD, Baumann DC, Akhaphong B, Abrenica A, Miller RF, Alejandro EU. Serine racemase is expressed in islets and contributes to the regulation of glucose homeostasis. *Islets.* (2016) 8:195–206. doi: 10.1080/19382014.2016.1260797
118. Ndiaye FK, Ortalli A, Canouil M, Huyvaert M, Salazar-Cardozo C, Lecoeur C, et al. Expression and functional assessment of candidate type 2 diabetes susceptibility genes identify four new genes contributing to human insulin secretion. *Mol Metab.* (2017) 6:459–70. doi: 10.1016/j.molmet.2017.03.011
119. Suwandhi L, Hausmann S, Braun A, Gruber T, Heinzmann SS, Galvez EJC, et al. Chronic D-serine supplementation impairs insulin secretion. *Mol Metab.* (2018) 16:191–202. doi: 10.1016/j.molmet.2018.07.002
120. Yamauchi C, Fujita S, Obara T, Ueda T. Effects of room temperature on reproduction, body and organ weights, food and water intakes, and hematology in mice. *Jikken Dobutsu.* (1983) 32:1–11. doi: 10.1538/expanim1978.32.1_1
121. Sasaki T, Kinoshita Y, Matsui S, Kakuta S, Yokota-Hashimoto H, Kinoshita K, et al. N-methyl-d-aspartate receptor coagonist D-serine suppresses intake of high-preference food. *Am J Physiol Regul Integr Comp Physiol.* (2015) 309:R561–75. doi: 10.1152/ajpregu.00083.2015
122. Sasaki T, Matsui S, Kitamura T. Control of appetite and food preference by nmda receptor and its co-agonist D-serine. *Int J Mol Sci.* (2016) 17:1081. doi: 10.3390/ijms17071081
123. Bentley-Lewis R, Huynh J, Xiong G, Lee H, Wenger J, Clish C, et al. Metabolomic profiling in the prediction of gestational diabetes mellitus. *Diabetologia.* (2015) 58:1329–32. doi: 10.1007/s00125-015-3553-4
124. Cobb J, Eckhart A, Perichon R, Wulff J, Mitchell M, Adam KP, et al. A novel test for IGT utilizing metabolite markers of glucose tolerance. *J Diabetes Sci Technol.* (2015) 9:69–76. doi: 10.1177/1932296814553622
125. Inagawa K, Hiraoka T, Kohda T, Yamadera W, Takahashi M. Subjective effects of glycine ingestion before bedtime on sleep quality. *Sleep Biol Rhythms.* (2006) 4:75–7. doi: 10.1111/j.1479-8425.2006.00193.x
126. Kawai N, Sakai N, Okuro M, Karakawa S, Tsuneyoshi Y, Kawasaki N, et al. The sleep-promoting and hypothermic effects of glycine are mediated by NMDA receptors in the suprachiasmatic nucleus. *Neuropsychopharmacology.* (2015) 40:1405–16. doi: 10.1038/npp.2014.326
127. Ghasemi M, Rezania F, Lewin J, Moore KP, Mani AR. d-Serine modulates neurogenic relaxation in rat corpus cavernosum. *Biochem Pharmacol.* (2010) 79:1791–6. doi: 10.1016/j.bcp.2010.02.007
128. Kantrowitz JT. The potential role of lumateperone-something borrowed? Something new? *JAMA Psychiatry.* (2020) 77:343–4. doi: 10.1001/jamapsychiatry.2019.4265
129. Shimizu S, Sogabe S, Yanagisako R, Inada A, Yamanaka M, Iha HA, et al. Glycine-Binding site stimulants of NMDA receptors alleviate extrapyramidal motor disorders by activating the nigrostriatal dopaminergic pathway. *Int J Mol Sic.* (2017) 18:1416. doi: 10.3390/ijms18071416
130. Van Berckel BN, Lipsch C, Gispen-De Wied C, Wynne HJ, Blankenstein MA, Van Ree JM, et al. The partial NMDA agonist D-cycloserine stimulates LH secretion in healthy volunteers. *Psychopharmacology.* (1998) 138:190–7. doi: 10.1007/s002130050662
131. Kantrowitz JT, Milak MS, Mao X, Shungu DC, Mann JJ. d-Cycloserine, an NMDA glutamate receptor glycine site partial agonist, induces acute increases in brain glutamate plus glutamine and GABA comparable to ketamine. *Am J Psychiatry.* (2016) 173:1241–2. doi: 10.1176/appi.ajp.2016.16060735
132. Dong Z, Grunebaum MF, Lan MJ, Wagner V, Choo T-H, Milak MS, et al. Relationship of brain glutamate response to D-cycloserine and lurasidone to antidepressant response in bipolar depression: a pilot study. *Front Psychiatry.* (2021) 12:863. doi: 10.3389/fpsyt.2021.653026
133. Mitchell J, Paul P, Chen HJ, Morris A, Payling M, Falchi M, et al. Familial amyotrophic lateral sclerosis is associated with a mutation in D-amino acid oxidase. *Proc Natl Acad Sci USA.* (2010) 107:7556–61. doi: 10.1073/pnas.0914128107
134. Sasabe J, Chiba T, Yamada M, Okamoto K, Nishimoto I, Matsuoka M, et al. D-serine is a key determinant of glutamate toxicity in amyotrophic lateral sclerosis. *EMBO J.* (2007) 26:4149–59. doi: 10.1038/sj.emboj.7601840
135. Lee A, Arachchige BJ, Henderson R, Pow D, Reed S, Aylward J, et al. Elevated plasma levels of D-serine in some patients with amyotrophic lateral sclerosis. *Amyotroph Lateral Scler Frontotemporal Degener.* (2021) 22:206–10. doi: 10.1080/21678421.2020.1832120
136. Rais R, Thomas AG, Wozniak K, Wu Y, Jaaro-Peled H, Sawa A, et al. Pharmacokinetics of oral D-serine in D-amino acid oxidase knockout mice. *Drug Metab Dispos.* (2012) 40:2067–73. doi: 10.1124/dmd.112.046482
137. Gonzalez-Hernandez JC, Aguilera-Aguirre L, Perez-Vazquez V, Ramirez J, Clemente-Guerrero M, Cortes-Rojo C, et al. Effect of D-amino acids on

some mitochondrial functions in rat liver. *Amino Acids.* (2003) 24:163–9. doi: 10.1007/s00726-002-0317-5
138. Asakawa T, Onizawa M, Saito C, Hikichi R, Yamada D, Minamidate A, et al. Oral administration of D-serine prevents the onset and progression of colitis in mice. *J Gastroenterol.* (2021). doi: 10.1007/s00535-021-01792-1. [Epub ahead of print].
139. Ghasemi-Kasman M, Dehpour AR, Mani AR. D-serine modulates non-adrenergic non-cholinergic contraction of lower esophageal sphincter in rats. *Eur J Pharmacol.* (2012) 696:155–60. doi: 10.1016/j.ejphar.2012.09.011
140. Mcgee MA, Abdel-Rahman AA. N-Methyl-D-Aspartate receptor signaling and function in cardiovascular tissues. *J Cardiovasc Pharmacol.* (2016) 68:97–105. doi: 10.1097/FJC.0000000000000398
141. Mcgee MA, Abdel-Rahman AA. Enhanced vascular neuronal nitric-oxide synthase-derived nitric-oxide production underlies the pressor response caused by peripheral N-methyl-D-aspartate receptor activation in conscious rats. *J Pharmacol Exp Ther.* (2012) 342:461–71. doi: 10.1124/jpet.112.194464
142. Aya AG, Robert E, Bruelle P, Lefrant JY, Juan JM, Peray P, et al. Effects of ketamine on ventricular conduction, refractoriness, and wavelength: potential antiarrhythmic effects: a high-resolution epicardial mapping in rabbit hearts. *Anesthesiology.* (1997) 87:1417–27. doi: 10.1097/00000542-199712000-00021
143. Camargo LH, Alves FH, Biojone C, Correa FM, Resstel LB, Crestani CC. Involvement of N-methyl-D-aspartate glutamate receptor and nitric oxide in cardiovascular responses to dynamic exercise in rats. *Eur J Pharmacol.* (2013) 713:16–24. doi: 10.1016/j.ejphar.2013.04.046
144. Ferreira-Junior NC, Lagatta DC, Resstel LBM. Glutamatergic, GABAergic, and endocannabinoid neurotransmissions within the dorsal hippocampus modulate the cardiac baroreflex function in rats. *Pflugers Arch.* (2018) 470:395–411. doi: 10.1007/s00424-017-2083-y
145. Gillies MJ, Huang Y, Hyam JA, Aziz TZ, Green AL. Direct neurophysiological evidence for a role of the human anterior cingulate cortex in central command. *Auton Neurosci.* (2018) 216:51–8. doi: 10.1016/j.autneu.2018.09.004
146. Slogoff S, Allen GW. The role of baroreceptors in the cardiovascular response to ketamine. *Anesth Analg.* (1974) 53:704–7. doi: 10.1213/00000539-197409000-00015
147. Hoka S, Takeshita A, Sasaki T, Yoshitake J. Preservation of baroreflex control of vascular resistance under ketamine anesthesia in rats. *J Anesth.* (1988) 2:207–12. doi: 10.1007/s0054080020207
148. Ogawa A, Uemura M, Kataoka Y, Ol K, Inokuchi T. Effects of ketamine on cardiovascular responses mediated by N-methyl-D-aspartate receptor in the rat nucleus tractus solitarius. *Anesthesiology.* (1993) 78:163–7. doi: 10.1097/00000542-199301000-00022
149. Jin YH, Bailey TW, Doyle MW, Li BY, Chang KS, Schild JH, et al. Ketamine differentially blocks sensory afferent synaptic transmission in medial nucleus tractus solitarius (mNTS). *Anesthesiology.* (2003) 98:121–32. doi: 10.1097/00000542-200301000-00021
150. Bastings J, Van Eijk HM, Olde Damink SW, Rensen SS. D-amino acids in health and disease: a focus on cancer. *Nutrients.* (2019) 11:2205. doi: 10.3390/nu11092205
151. Du S, Wang Y, Alatrash N, Weatherly CA, Roy D, Macdonnell FM, et al. Altered profiles and metabolism of l- and d-amino acids in cultured human breast cancer cells vs. non-tumorigenic human breast epithelial cells. *J Pharm Biomed Anal.* (2019) 164:421–9. doi: 10.1016/j.jpba.2018.10.047
152. Piossek C, Thierauch KH, Schneider-Mergener J, Volkmer-Engert R, Bachmann MF, Korff T, et al. Potent inhibition of angiogenesis by D,L-peptides derived from vascular endothelial growth factor receptor 2. *Thromb Haemost.* (2003) 90:501–10. doi: 10.1160/TH03-02-0106
153. Gonzalez-Hernandez JA, Pita-Alcorta C, Padron A, Finale A, Galan L, Martinez E, et al. Basic visual dysfunction allows classification of patients with schizophrenia with exceptional accuracy. *Schizophr Res.* (2014) 159:226–33. doi: 10.1016/j.schres.2014.07.052
154. Pallerla S, Naik H, Singh S, Gauthier T, Sable R, Jois SD. Design of cyclic and d-amino acids containing peptidomimetics for inhibition of protein-protein interactions of HER2-HER3. *J Pept Sci.* (2018) 24:e3066. doi: 10.1002/psc.3066
155. Lane HY, Lin CH, Green MF, Hellemann G, Huang CC, Chen PW, et al. Add-on treatment of benzoate for schizophrenia: a randomized, double-blind, placebo-controlled trial of D-amino acid oxidase inhibitor. *JAMA Psychiatry.* (2013) 70:1267–75. doi: 10.1001/jamapsychiatry.2013.2159
156. Lin CH, Lin CH, Chang YC, Huang YJ, Chen PW, Yang HT, et al. Sodium benzoate, a d-amino acid oxidase inhibitor, added to clozapine for the treatment of schizophrenia: a randomized, double-blind, placebo-controlled trial. *Biol Psychiatry.* (2017) 84:422–32. doi: 10.1016/j.biopsych.2017.12.006
157. Lin CY, Liang SY, Chang YC, Ting SY, Kao CL, Wu YH, et al. Adjunctive sarcosine plus benzoate improved cognitive function in chronic schizophrenia patients with constant clinical symptoms: a randomised, double-blind, placebo-controlled trial. *World J Biol Psychiatry.* (2017) 18:357–68. doi: 10.3109/15622975.2015.1117654
158. Ryan A, Baker A, Dark F, Foley S, Gordon A, Hatherill S, et al. The efficacy of sodium benzoate as an adjunctive treatment in early psychosis - CADENCE-BZ: study protocol for a randomized controlled trial. *Trials.* (2017) 18:165. doi: 10.1186/s13063-017-1908-5
159. Yoneyama T, Sato S, Sykes A, Fradley R, Stafford S, Bechar S, et al. Mechanistic multilayer quantitative model for nonlinear pharmacokinetics, target occupancy and pharmacodynamics (PK/TO/PD) Relationship of d-amino acid oxidase inhibitor, TAK-831 in mice. *Pharm Res.* (2020) 37:164. doi: 10.1007/s11095-020-02893-x
160. Williams RE, Lock EA. Sodium benzoate attenuates D-serine induced nephrotoxicity in the rat. *Toxicology.* (2005) 207:35–48. doi: 10.1016/j.tox.2004.08.008
161. Konno R, Ikeda M, Yamaguchi K, Ueda Y, Niwa A. Nephrotoxicity of D-properglyglycine in mice. *Arch Toxicol.* (2000) 74:473–9. doi: 10.1007/s002040000156
162. Ferraris D, Duvall B, Ko YS, Thomas AG, Rojas C, Majer P, et al. Synthesis and biological evaluation of D-amino acid oxidase inhibitors. *J Med Chem.* (2008) 51:3357–9. doi: 10.1021/jm800200u
163. Hashimoto K, Fujita Y, Horio M, Kunitachi S, Iyo M, Ferraris D, et al. Co-Administration of a d-amino acid oxidase inhibitor potentiates the efficacy of D-serine in attenuating prepulse inhibition deficits after administration of dizocilpine. *Biol Psychiatry.* (2009) 65:1103–6. doi: 10.1016/j.biopsych.2009.01.002
164. Ferraris DV, Tsukamoto T. Recent advances in the discovery of D-amino acid oxidase inhibitors and their therapeutic utility in schizophrenia. *Curr Pharm Des.* (2011) 17:103–11. doi: 10.2174/138161211795049633
165. Nair AB, Jacob S. A simple practice guide for dose conversion between animals and human. *J Basic Clin Pharm.* (2016) 7:27–31. doi: 10.4103/0976-0105.177703

Conflict of Interest: The authors declare that the research was conducted in the absence of any commercial or financial relationships that could be construed as a potential conflict of interest.

Publisher's Note: All claims expressed in this article are solely those of the authors and do not necessarily represent those of their affiliated organizations, or those of the publisher, the editors and the reviewers. Any product that may be evaluated in this article, or claim that may be made by its manufacturer, is not guaranteed or endorsed by the publisher.

frontiers in Psychiatry

ORIGINAL RESEARCH
published: 31 August 2021
doi: 10.3389/fpsyt.2021.709559

Saracatinib Fails to Reduce Alcohol-Seeking and Consumption in Mice and Human Participants

Summer L. Thompson[1], Carol A. Gianessi[1,2], Stephanie S. O'Malley[1], Dana A. Cavallo[1], Julia M. Shi[3], Jeanette M. Tetrault[3], Kelly S. DeMartini[1], Ralitza Gueorguieva[4], Brian Pittman[1], John H. Krystal[1,5], Jane R. Taylor[1,5,6†] and Suchitra Krishnan-Sarin[1*†]*

[1] Department of Psychiatry, Yale University School of Medicine, New Haven, CT, United States, [2] Interdepartmental Neuroscience Program, Yale University Graduate School of Arts and Sciences, New Haven, CT, United States, [3] Program in Addiction Medicine, Department of Internal Medicine, Yale University School of Medicine, New Haven, CT, United States, [4] Department of Biostatistics, Yale University School of Public Health, New Haven, CT, United States, [5] Department of Neuroscience, Yale University School of Medicine, New Haven, CT, United States, [6] Department of Psychology, Yale University, New Haven, CT, United States

OPEN ACCESS

Edited by:
Nevena V. Radonjic, Upstate Medical University, United States

Reviewed by:
Anh Dzung Le, Centre for Addiction and Mental Health (CAMH), Canada
John J. Woodward, Medical University of South Carolina, United States
Nathan James Marchant, VU University Medical Center, Netherlands
Jonathan Covault, University of Connecticut Health Center, United States

***Correspondence:**
Summer L. Thompson
summer.thompson@yale.edu
Suchitra Krishnan-Sarin
suchitra.krishnan-sarin@yale.edu

† These authors share senior authorship

Specialty section:
This article was submitted to Psychopharmacology, a section of the journal Frontiers in Psychiatry

Received: 14 May 2021
Accepted: 03 August 2021
Published: 31 August 2021

Citation:
Thompson SL, Gianessi CA, O'Malley SS, Cavallo DA, Shi JM, Tetrault JM, DeMartini KS, Gueorguieva R, Pittman B, Krystal JH, Taylor JR and Krishnan-Sarin S (2021) Saracatinib Fails to Reduce Alcohol-Seeking and Consumption in Mice and Human Participants. Front. Psychiatry 12:709559. doi: 10.3389/fpsyt.2021.709559

More effective treatments to reduce pathological alcohol drinking are needed. The glutamatergic system and the NMDA receptor (NMDAR), in particular, are implicated in behavioral and molecular consequences of chronic alcohol use, making the NMDAR a promising target for novel pharmacotherapeutics. Ethanol exposure upregulates Fyn, a protein tyrosine kinase that indirectly modulates NMDAR signaling by phosphorylating the NR2B subunit. The Src/Fyn kinase inhibitor saracatinib (AZD0530) reduces ethanol self-administration and enhances extinction of goal-directed ethanol-seeking in mice. However, less is known regarding how saracatinib affects habitual ethanol-seeking. Moreover, no prior studies have assessed the effects of Src/Fyn kinase inhibitors on alcohol-seeking or consumption in human participants. Here, we tested the effects of saracatinib on alcohol consumption and craving/seeking in two species, including the first trial of an Src/Fyn kinase inhibitor to reduce drinking in humans. Eighteen male C57BL/6NCrl mice underwent operant conditioning on a variable interval schedule to induce habitual responding for 10% ethanol/0.1% saccharin. Next, mice received 5 mg/kg saracatinib or vehicle 2 h or 30 min prior to contingency degradation to measure habitual responding. In the human study, 50 non-treatment seeking human participants who drank heavily and met DSM-IV criteria for alcohol abuse or dependence were randomized to receive 125 mg/day saracatinib ($n = 33$) or placebo ($n = 17$). Alcohol Drinking Paradigms (ADP) were completed in a controlled research setting: before and after 7–8 days of treatment. Each ADP involved consumption of a priming drink of alcohol (0.03 mg%) followed by *ad libitum* access (3 h) to 12 additional drinks (0.015 g%); the number of drinks consumed and craving (Alcohol Urge Questionnaire) were recorded. In mice, saracatinib did not affect habitual ethanol seeking or consumption at either time point. In human participants, no significant effects of saracatinib on alcohol craving or consumption were identified. These results in mice and humans suggest that Fyn kinase inhibition using saracatinib, at the doses tested here, may not reduce alcohol consumption or craving/seeking among those habitually consuming alcohol,

in contrast to reports of positive effects of saracatinib in individuals that seek ethanol in a goal-directed manner. Nevertheless, future studies should confirm these negative findings using additional doses and schedules of saracatinib administration.

Keywords: saracatinib, AZD0530, Fyn kinase, alcohol use disorders, alcohol habit, NMDA receptor, glutamate, AM404

INTRODUCTION

Alcohol is a leading public health problem, presenting the largest risk factor for premature death for young to middle aged adults worldwide (1). Alcohol use disorder (AUD) is the most prevalent substance use disorder other than tobacco use disorder, yet currently available treatments are rarely used (1, 2). Three pharmacotherapies for AUD have U.S. Food and Drug Administration approval: disulfiram, naltrexone (oral and long-acting injectable), and acamprosate (2). However, these agents have issues of modest efficacy, adherence, and possible restricted effect to subpopulations (3, 4), which highlights the need for novel AUD treatment options.

The glutamatergic system is heavily implicated in the pathophysiology of AUD, providing potential targets for novel therapeutics (5, 6). Indeed, pharmacological manipulation of AMPA, kainate, mGlu, and NMDA glutamate receptors (NMDAR) can alter alcohol consumption, seeking, withdrawal or reinstatement (5, 7–14). The NMDAR is one of the highest affinity targets of ethanol in the brain (15), and chronic ethanol exposure is associated with altered NMDAR signaling (16–18). NMDARs play a role in various consequences of chronic alcohol use (19): NMDAR antagonists can reduce ethanol tolerance, craving/seeking, and consumption (20–24). For example, the uncompetitive NMDAR antagonist memantine reduces cue- and alcohol-induced craving in humans (7, 25) and we have also observed that a low dose of memantine combined with a standard dose of the opioid antagonist naltrexone was well-tolerated and resulted in reduced alcohol drinking and craving within a sample of individuals with a positive family history of AUD (21). Our earlier work has also observed that only lower doses of memantine reduce alcohol craving, whereas higher doses increase alcohol consumption, especially in individuals with high levels of baseline impulsivity (26). NMDAR antagonists can have undesirable cognitive and psychotomimetic effects (27, 28). Together, this evidence suggests that NMDARs may be a promising target for amelioration of the hyper-glutamatergic state in AUD, but that direct antagonism may present challenges and more nuanced approaches that target this system may be needed (5, 21).

Fyn is an Src family protein tyrosine kinase that indirectly upregulates NMDAR activity by phosphorylating the NR2B subunit, a component of the NMDAR that is particularly implicated in the molecular and behavioral adaptations to chronic ethanol exposure (29–31). Mounting evidence implicates Fyn in alcohol use behaviors in human participants and rodents. Multiple studies have identified polymorphisms in the Fyn gene associated with increased risk for AUD (32–34). Rodent studies revealed that ethanol activates Fyn in the dorsomedial striatum (DMS) (35–38). The DMS is a key brain region for goal-directed action, which refers to behaviors that are sensitive to changes in action-outcome contingencies (39). Furthermore, ethanol-induced long-term facilitation in the DMS is Fyn-dependent (36, 37). Importantly, pharmacological inhibition of Fyn using the Src/Fyn kinase inhibitor saracatinib (AZD0530) was reported to reduce ethanol-seeking and enhance extinction of ethanol-seeking in mice with goal-directed responding for ethanol (35) and reduce ethanol consumption in ethanol-naïve mice (40), suggesting that saracatinib may be a viable treatment option for goal-directed drinking.

Habits, in contrast to goal-directed behaviors, are insensitive to changes in action-outcome contingencies or devaluation of previously desirable outcomes and reflect a shift from recruitment of DMS to dorsolateral striatum (DLS) (39, 41–43). Ethanol cues can disrupt otherwise goal-directed food-seeking, and chronic ethanol exposure facilitates the development of food habits (41, 44). Ethanol-seeking transitions from goal-directed to habitual more readily than food-seeking (45–48). Indeed, overreliance on habits is thought to contribute to compulsive drug-seeking including in AUD (45, 49, 50), and has been observed in individuals with AUD (51). However, no studies have examined the efficacy of saracatinib for reducing ethanol-seeking and consumption in habitual alcohol consumers. Here, we performed two parallel studies in mice and human participants to assess the ability of saracatinib to reduce alcohol consumption and seeking/craving in habitual ethanol-seeking mice and participants who were heavy drinkers with an AUD.

MATERIALS AND METHODS

Mouse Study

Mice

Eighteen adult male C57BL/6NCrl mice (Charles River Laboratories, Wilmington, MA) were used for the mouse experiment. Mice were delivered at 8–9 weeks old and allowed to acclimate to the vivarium for 7 days before initiating food restriction to 85–90% of free-feeding body weight. Mice had *ad libitum* access to water in the home cage but were provided with their daily food 15 min prior to initiating operant sessions without water access to induce thirst. Mice were pre-exposed to 10% ethanol, 0.1% saccharin solution in the home cage for 1 h, 2 days in a row prior to initiating operant training with 10% ethanol, 0.1% saccharin as the reinforcer (10 μl per reward). All procedures were approved by the Yale University Institutional Animal Care and Use Committee and in accordance with the National Institutes of Health *Guide for the Care and Use of Laboratory Animals of the Institute of Animal Resources*.

Mouse Drugs

Saracatinib, also known as AZD0530, was obtained from AstraZeneca, Boston, MA. Saracatinib was dissolved in saline and administered at a dose of 5 mg/kg. This dose was based on preliminary studies showing that this dose reduces NR2B phosphorylation in the DMS (data not shown) and to match levels of saracatinib in cerebrospinal fluid with that expected for the human study (52), which was performed simultaneously. AM404 (R&D Systems, Minneapolis, MN) is an endocannabinoid transport inhibitor that we have previously shown to reduce habitual responding for ethanol (53): it was used as a positive control for testing the malleability of habitual ethanol-seeking. AM404 was dissolved in 5% DMSO, 15% Tween 80 in sterile physiological saline and administered at a dose of 10 mg/kg body weight. Drugs were administered via intraperitoneal injection (i.p.) at 10 ml/kg body weight.

Mouse Behavioral Paradigm

Apparatus and Training

Mice were trained and tested in standard mouse operant conditioning chambers in sound attenuation cabinets (Med Associates, St. Albans, VT). Chambers were equipped with three nose port apertures and a magazine with photobeam sensors to record entries and lights to indicate active ports. Ethanol reinforcers (10% ethanol v/v, 0.1% saccharin) were delivered into the magazine using a dipper arm holding a 10 μl cup that was submerged in a reservoir of the reinforcer solution and would then raise the cup through a hole into the magazine to deliver the reinforcer, which was provided for 10s before retraction of the arm back into the reservoir. Mice were trained daily in the same operant chamber throughout the experiment.

Mice first learned to associate the magazine with reinforcer delivery in two 40-min magazine training sessions. Each session began with a reinforcer delivered into the magazine 60 s into the session. This reinforcer remained available (i.e., dipper arm raised with cup accessible inside the magazine) until the mouse entered the magazine, and then for the subsequent 10 s before the dipper arm was retracted. Following this non-contingent delivery, reinforcers were delivered on a fixed interval-60 s schedule throughout the session, meaning that following a minimum of 60 s, the next magazine entry elicited a reinforcer delivery.

Next mice were trained to perform the operant response on a fixed ratio-1 (FR-1) schedule. One nose port was designated the "active" port for that mouse (left or right), counterbalanced between animals but consistent between sessions. The active port was indicated by illumination of the port. Sessions began with a single non-contingent reinforcer. Just like magazine training, reinforcers remained available until the animal entered the magazine, after which the dipper was available for 10 s before retraction. Following this free reinforcer, entries into the active nose port resulted in delivery of a single reinforcer. FR-1 sessions lasted 45 min or until the mouse earned 60 reinforcers, whichever occurred first. Mice completed FR-1 training upon reaching a criterion of 13 reinforcers within a single session.

Following FR-1 training, mice earned ethanol reinforcers on a variable interval (VI) schedule that we have previously shown to promote habitual responding for ethanol (53). The same active nose port assigned during FR-1 training remained the active port for each mouse during VI sessions, as indicated by illumination of the active port throughout the session. Intervals were selected pseudo-randomly from an exponential array that averaged to the schedule duration, after which the first active nose port response resulted in a reinforcer, as previously (53). Unlike during magazine and FR-1 training, these reinforcers remained available for the subsequent 10 s following the active nose port response, regardless of whether the mouse had yet entered the magazine. Sessions lasted 45 min. Mice were trained on a VI-30 schedule for 3 days, followed by VI-60 for ∼24 days.

Contingency Degradation

Contingency degradation sessions delivered ethanol reinforcers non-contingently at the same rate that mice earned rewards in the previous VI session. Active nose port entries had no programmed responses. Reinforcer delivery occurred at equal intervals that were individually tailored to the prior day reinforcement rate of that mouse, meaning each mouse received the same number of reinforcers as in the prior day VI session. Sessions lasted 45 min. Mice underwent multiple contingency degradation sessions to test effects of pharmacological agents. Initial testing occurred following a minimum of 20–25 days of VI-60 training. Between contingency degradation tests, mice underwent additional VI-60 training days to stabilize responding. Response rates, magazine entries, and incentivized entries (i.e., magazine entries while reinforcer is available) were measured and compared between the contingency degradation test and the preceding day's VI-60 session, which was used as a baseline. The amount of ethanol consumed relative to body weight was estimated based on the number of reinforcers earned. However, consumption could not be directly confirmed due to the design of the reinforcer delivery apparatus, which resubmerged the dipper cup into the reservoir after each reinforcer to refill the cup for the subsequent reinforcer.

Pharmacological Testing

For each contingency degradation test, the vehicle solution for the pharmacological agent was administered prior to the baseline VI-60 session. The day after completing the baseline session, mice received pharmacological challenge and underwent contingency degradation testing. First, all animals ($n = 18$) received AM404 or vehicle 30 min prior to the contingency degradation test session in a within-subject, counterbalanced manner. This test served to: (1) provide confirmation that the group exhibited habitual responding for ethanol (i.e., lack of decrease in responses during contingency degradation under vehicle conditions) and (2) provide a positive control testing whether the habitual responding was sensitive to goal-directed-promoting agents, as we have previously shown that AM404 reduces habitual responding for ethanol (53). AM404 was tested within-subject based on our previous experience with this drug not showing cross-over effects (53, 54). Following stabilization of responding on the VI-60 schedule following these contingency degradation tests, saracatinib was tested in a between-subject cross-over design, in which half the animals received saracatinib for the 2-h pretreatment condition

(n = 8/drug), which occurred first for all animals, whereas the other half received saracatinib for the 30-min pretreatment condition (n = 8/drug), which occurred second for all animals. One animal was excluded in each drug group in each time point due to computer error for a final n = 8/group. The 2-h pretreatment schedule was selected based on our preliminary studies showing reduced free-access ethanol consumption in the home cage at this time point (data not shown) and the 30-min pretreatment schedule was designed to match the effective time point for AM404 (53). Overall, animals received one administration of AM404 vehicle and AM404 prior to any saracatinib administration, and then all mice received one dose of saracatinib, at either a 2-h or 30-min pretreatment time point.

Statistical Analyses

Data were analyzed using SPSS 26 (IBM, Armonk, NY) and graphed using Prism 8 (Graphpad, San Diego, CA). Outcome measures included active responses, total magazine entries, and incentivized entries, which were assessed using generalized estimating equations with a Poisson distribution with Wald's chi square test statistics. Significant interactions were resolved by making pairwise comparisons of the estimated marginal means corrected for multiple comparisons using Sidak's method. Alpha was set to a threshold of 0.05.

Human Clinical Trial

Human Participants

Participants (n = 50 randomized to treatment; n = 33 saracatinib, n = 17 placebo) were non-treatment seeking, heavy drinkers that met the DSM-IV criteria for alcohol abuse or dependence (**Table 1**; **Supplementary Figure 1**). Additional inclusion criteria were: between 21 and 50 years of age, body mass index between 19 and 30, capable of reading English at the 6th grade level or above, average weekly alcohol consumption of 25–70 standard drinks for men and 20–65 for women with no more than 3 days of abstinence per week during the month prior to the intake [Timeline Follow-Back method; TFLB; (55)]. Exclusion criteria included medical contraindications to drinking alcohol or use of saracatinib, abuse or dependence on substances other than alcohol or nicotine, severe psychiatric disability, significant alcohol withdrawal at any intake appointment [Clinical Institute Withdrawal Assessment for Alcohol Scale score > 8 (56)], current use of psychoactive drugs or CYP3A4 inhibitors or warfarin, those who were not on stable use of prescribed antidepressants/anxiolytics, those who reported disliking spirits or were seeking treatment for their drinking, and those who were pregnant or nursing.

Study Medications

Participants were randomized on a 2:1 ratio (active vs. placebo) to receive saracatinib (125 mg/day, oral) or matching placebo for seven to 8 days to achieve steady state drug levels following exposure to 4–5 half-lives of the drug ($t_{1/2}$ = 40 h). The Yale New Haven Investigational Pharmacy randomized the participants and dispensed the study medications; all research staff and the participants were blind to treatment assignment. The dose was selected based on previous studies demonstrating safety and tolerability of 125 mg/day saracatinib in human participants (57) and evidence that this dose reached comparable levels in cerebrospinal fluid to that of 5 mg/kg in mice, a dose that has been shown to produce neural changes (52).

Study Design

This study was a randomized, double-blind, placebo-controlled trial that was approved by the Yale Human Investigations Committee, registered in ClinicalTrials.gov (NCT02955186), and followed the National Advisory Council for Alcohol Abuse and Alcoholism guidelines (58). Alcohol drinking behaviors were assessed using an established alcohol drinking paradigm (ADP) conducted in a private room at the Hospital Research Unit (HRU) of Yale New Haven Hospital (YNHH). The ADP involved consumption of a priming drinking of alcohol followed by choice *ad libitum* consumption of up to 12 drinks over three 1-h self-administration periods, as done previously (21). Participants completed a baseline ADP and were then randomized to receive saracatinib (125 mg/day) or placebo for a 7–8 day period (**Supplementary Figure 2**); participants were contacted daily either in person or virtually to observe medication administration and check for adverse events. At the end of this period, they completed the second, on-treatment ADP.

The YNHH Investigational Pharmacy calculated and delivered alcohol doses of each participant's preferred alcohol to the HRU; the doses were designed to raise blood alcohol levels to 0.03 g/dl for priming drink and 0.015 g/dl for all other drinks based on a formula that takes into account the sex, weight, and age of the participant (59). Each alcohol dose was mixed with the participant's preferred non-caffeinated, non-carbonated mixer in a 1:3 ratio. Each participant's preferred alcohol and mixer were determined at an earlier appointment.

Following completion of each ADP, participants spent the night at the HRU and were discharged the next morning. They also received a 1-week follow-up appointment to assess for adverse events and drinking, and a motivational intervention to discuss their alcohol use and encourage readiness to change. Participants were paid to participate and could earn up to $1,142 for completing all portions of the study.

Measures

Alcohol Craving

Craving was measured 30 min prior to the priming dose (baseline), and then 10, 20, 30, 40, and 50 min during the priming dose period and every half hour during each *ad libitum* period (i.e., 90, 120, 150, 180, 220, and 240 min) using the 8-item Alcohol Urge Questionnaire (AUQ) (60). Separate area under the curve (AUC) estimates for each phase were calculated using the trapezoidal rule based on the time points specified above.

TABLE 1 | Participant demographics and drinking histories.

	All Participants ($n = 50$)	Placebo ($n = 17$)	Saracatinib ($n = 33$)	*P*
Demographics				
Male, *n* (%)	25 (50%)	9 (53%)	16 (48%)	0.77
Current smokers, *n* (%)	19 (39%)	7 (44%)	12 (36%)	0.62
White, *n* (%)	31 (62%)	10 (59%)	21 (64%)	0.74
Family Hx positive, *n* (%)	20 (40%)	7 (41%)	13 (39%)	0.90
Age, mean (SD)	29 (7.8)	30 (7.9)	29 (7.8)	0.49
Drinking based on 30-day timeline followback interview				
Total # drinks, mean (SD)	171 (68)	175 (62)	169 (73)	0.75
Drinks/drinking day, mean (SD)	7.8 (2.8)	7.3 (1.8)	8.1 (3.2)	0.36
% drinking days, mean (SD)	74 (17)	79 (17)	71 (17)	0.10
Alcohol dependence score	10.7 (5.3)	9.9 (5.3)	11.2 (5.4)	0.43

N = 50 total; n = 17 placebo and n = 33 saracatinib. There were no differences between the groups for demographics or drinking measured in the Timeline Followback interview. Hx, history; SD, standard deviation.

Standard Drinks Consumed

Total number of standard drinks consumed during the 3-h self-administration period.

Alcohol-Induced Stimulation/Sedation

Determined at 10, 20, and 50 min during the priming dose period and then every hour at the end of each of the three *ad libitum* periods with the brief Biphasic Alcohol Effects Scale [BAES; (61)].

Adverse Events

Measured daily during the study medication period using the SAFTEE (62).

Statistical Analyses

Baseline demographics and drinking characteristics were compared among medication conditions using *t*-tests and chi-square tests as appropriate. Data were checked for normality and transformations applied as necessary. The two primary outcomes of interest were: craving (AUQ) and total drinks consumed during the *ad libitum* periods, each tested on an intent-to-treat (ITT) basis at the $\alpha = 0.05$ threshold. Subjective craving (AUQ) was quantified by calculating an area under the curve (AUC) for each phase (priming dose, *ad libitum*) within each ADP using the trapezoidal rule, and analyzed using linear mixed models with medication (placebo, saracatinib) included as a between-subjects factor and session (baseline, on-Tx) included as a within-subjects factor. The medication by time interaction was modeled and participant was the clustering factor. Total drinks consumed was analyzed using an identical linear mixed model as described for craving. Potential confounding factors (sex, family history, age, and baseline drinking variables) were tested by including them in each model but were not significant and dropped for parsimony. Similar models were used to assess BAES outcomes. For all models, the best-fitting variance-covariance structure was based on the Schwarz-Bayesian Criterion (BIC) (63). Least-square means were estimated and plotted to determine the nature of significant effects. All analyses were performed using SAS, version 9.4 (Cary, NC).

RESULTS

No Effect of 5 mg/kg Saracatinib on Habitual Responding for Ethanol in Mice

By the end of VI training, mice earned 1.04 ± 0.03 (standard error of the mean) g/kg ethanol within the final session. Although consumption could not be directly confirmed due to the refilling of the dipper cup for each reinforcer delivery, all mice entered the magazine while the dipper cup was available (i.e., incentivized entries) at least as many times as reinforcers earned, and the number of incentivized entries was significantly greater than the number of reinforcers earned [$\chi^2_{(1)} = 7.15$, $p < 0.01$], suggesting knowledge of the action-outcome contingency and the opportunity to consume the ethanol reinforcers.

Following training, AM404 was administered during contingency degradation to evaluate whether animals exhibited habitual responding for ethanol, and whether responding and ethanol consumption were sensitive to drug challenge with a known enhancer of goal-directed response patterns. As expected, AM404 reduced the number of active responses during the contingency degradation whereas vehicle administration did not affect responding (**Supplementary Figure 3**). These results suggest that the mice were sufficiently trained to respond habitually for ethanol, and that AM404 successfully reduced habitual responding for ethanol, consistent with our previous work (53).

Next, we sought to determine whether saracatinib could also reduce habitual responding for ethanol. A dose of 5 mg/kg saracatinib was administered 2 h prior to the contingency degradation test and did not significantly reduce habitual responding for ethanol (**Figure 1A**). An increase in responding was observed across groups during contingency degradation relative to baseline [$\chi^2_{(1)} = 37.01$, $p < 0.0001$]. Likewise, magazine entries were increased across groups during contingency degradation [$\chi^2_{(1)} = 46.22$, $p < 0.0001$; **Figure 1B**]. Finally, no effects of session or drug were identified for incentivized magazine entries (**Figure 1C**), a measure of ethanol-seeking behavior (53). Consistent with the amount of ethanol delivered

during VI training, mice received an average of 1.17 ± 0.03 (standard error of the mean) g/kg ethanol during testing, wherein an identical number of reinforcers were delivered during the baseline VI-60 and contingency degradation sessions. Overall, saracatinib did not alter habitual responding for ethanol or ethanol consumption when administered 2 h prior to contingency degradation testing.

Next, we sought to determine whether the lack of effect of saracatinib identified at the 2-h time point was due to a suboptimal time point. We assessed whether a 30-min pretreatment time point, the time point used for the positive control compound AM404, would reveal effects of saracatinib on habitual ethanol responding. Consistent with the 2-h pretreatment, mice increased active responding during contingency degradation across drug groups [$\chi^2_{(1)} = 4.45$, $p < 0.05$], but no effects of saracatinib were identified (**Figure 1D**). Magazine entries increased during contingency degradation across drug groups [$\chi^2_{(1)} = 6.33$, $p < 0.05$; **Figure 1E**]. No effects of saracatinib or session type were identified for incentivized magazine entries (**Figure 1F**). Consistent with prior testing phases, mice received an average of 1.11 ± 0.03 (standard error of the mean) g/kg ethanol. Overall, saracatinib did not affect habitual responding for ethanol when administered 30 min prior to contingency degradation testing.

No Effect of 125 mg/day Saracatinib on Alcohol Craving, Alcohol-Induced Stimulation/Sedation, or Alcohol Consumption in Human Participants

The final sample of randomized participants (**Table 1**) included 25 men and 25 women, with an average age of 29.0 [standard deviation (SD) = 7.8], a diverse racial distribution (31 White, 17 Black, 2 other), and 19 individuals who currently smoked tobacco (39%), with mean scores of 12.1 (SD = 5.6) on the Alcohol Dependence Scale (64). During the 30 days prior to the baseline ADP, participants consumed, on average 171 (SD = 68) drinks, 7.8 drinks per drinking occasion (SD = 2.8) and drank 3 out of every 4 days (74%, SD = 17%). No differences in demographic variables were observed between the saracatinib and placebo groups. See **Supplementary Figure 2** for CONSORT diagram.

Saracatinib was well-tolerated and we did not observe any serious adverse events. The most common adverse events reported included nausea (saracatinib: $n = 5$, 15%; placebo: $n = 1$, 6%) and headache (saracatinib: $n = 5$, 15%; placebo: $n = 1$, 6%). As shown in **Supplementary Table 1**, participants who received saracatinib also reported other gastrointestinal symptoms such as abdominal discomfort and diarrhea ($n = 3$, 9%), as well as cold symptoms ($n = 6$, 18%), nasal congestion ($n = 4$, 12%) and joint pain ($n = 3$, 9%). No one dropped out of the study due to adverse events. For detailed information on adverse events see **Supplementary Tables 1**, **2**.

Estimated least-square means and standard errors depicting the effects of saracatinib on craving for alcohol are shown in **Figures 2A,B**. Reductions in craving from baseline were observed across the placebo and saracatinib treatments during both the priming dose phase [**Figure 2A**; $F_{(1,39)} = 11.8$, $p = 0.0014$] and the *ad libitum* drinking phase [**Figure 2B**; $F_{(1,39)} = 10.1$, $p = 0.003$]. However, the observed patterns of reductions in craving were similar among medications during the priming dose [$F_{(1,39)} = 0.01$, $p = 0.91$] and *ad libitum* drinking [$F_{(1,39)} = 0.21$, $p = 0.65$] phases of the paradigm. Craving was not associated with any of the considered baseline covariates.

Similar to measures of craving, total drinks consumed (**Figure 2C**) showed an overall 25% reduction from the baseline ADP (8.5 ± 0.51 (standard error of the mean) to the on-treatment ADP session (6.4 ± 0.73) [$F_{(1,39)} = 10.9$, $p = 0.002$], but the reductions did not differ by medication [medication by session: $F_{(1,39)} = 0.10$, $p = 0.75$].

We did not observe significant effects of saracatinib on alcohol-induced stimulation or sedation measured using the BAES (data not shown).

DISCUSSION

In the present animal and human studies, we assessed the possibility of a role for Fyn in habitual alcohol-seeking and drinking in both mice and humans using the Fyn kinase inhibitor saracatinib. Overall, we did not identify effects of saracatinib in either mice or humans, suggesting that saracatinib, at the doses tested, may not be an effective treatment for reducing alcohol-seeking or consumption in individuals who habitually consume alcohol.

In mice, we used our established, extended instrumental training paradigm to induce habitual responding for ethanol and assessed the effects of acute administration of saracatinib on ethanol habit. We first demonstrated that this habitual responding for ethanol was sensitive to pharmacological manipulation by administering a positive control compound, AM404, an endocannabinoid transport inhibitor that we have previously shown to reduce habitual responding for ethanol (53). AM404 successfully reduced habitual ethanol-seeking, indicating that the habitual ethanol-seeking was receptive to pharmacological manipulation. However, 5 mg/kg saracatinib failed to alter habitual responding for ethanol in mice. This lack of effect was not likely to be due to time of saracatinib administration, as neither 2-h, nor 30-min pretreatment was sufficient to alter habitual ethanol-seeking in these mice. These time points encompass the 1-h pretreatment employed in a study that showed saracatinib-induced reduction in ethanol self-administration in mice reported to have goal-directed responding for ethanol (35). Furthermore, saracatinib is long-lasting in the mouse brain, with a half-life of approximately 16 h (52). Moreover, Fyn activity is upregulated in as little as 15 min (37) and for as long as 16 h (36) following ethanol exposure in rodents. Overall, these findings suggest that acute administration of 5 mg/kg saracatinib does not modulate ethanol habit in mice.

In the human clinical trial, we assessed alcohol craving and consumption in non-treatment seeking participants with heavy drinking habits using our established ADP paradigm before and after saracatinib administration. No effects of 7–8 days of oral 125 mg saracatinib were identified for craving in either the priming or *ad libitum* consumption phases. Furthermore, no

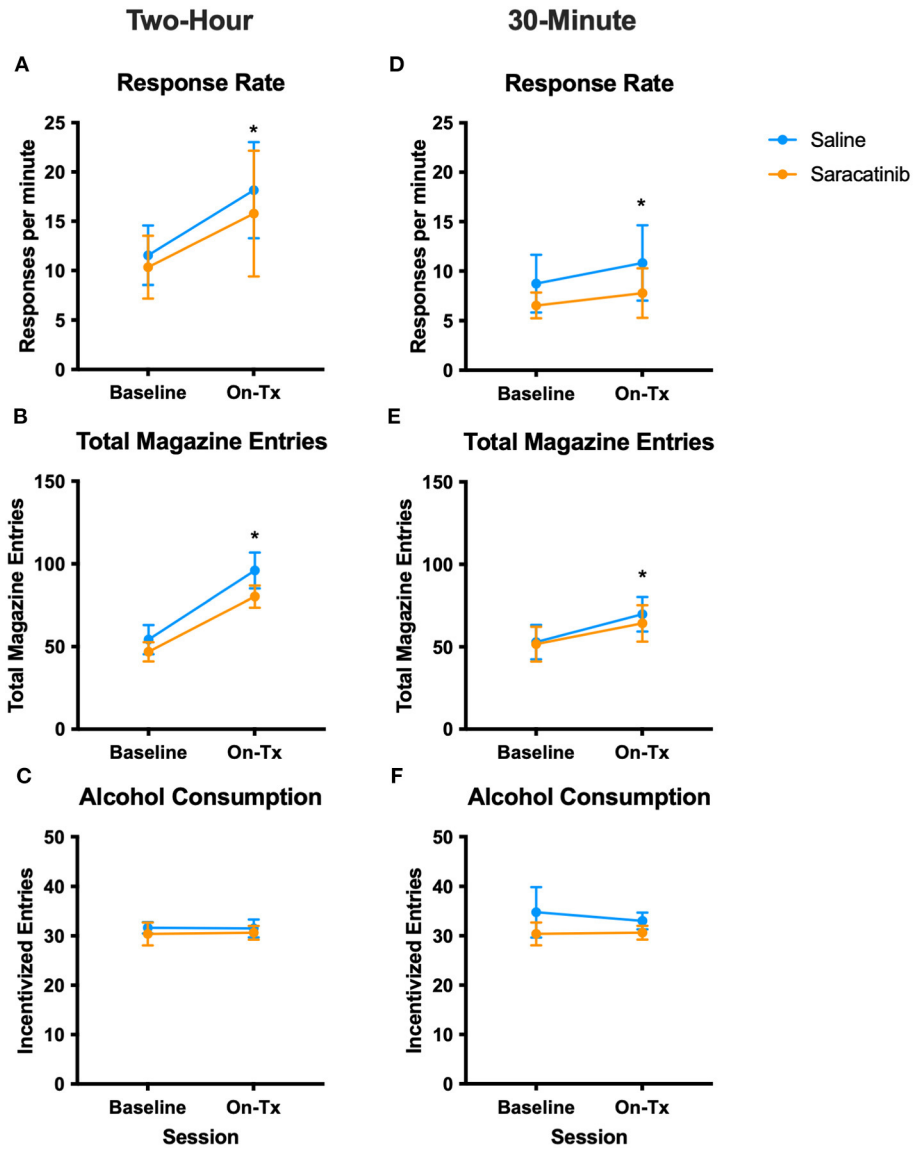

FIGURE 1 | 5 mg/kg saracatinib did not affect habitual ethanol-seeking or consumption in mice at either time point. Mice received an i.p. injection of saline 2 h **(A–C)** or 30 min **(D–F)** prior to the VI-60 session preceding contingency degradation ("Baseline"). The following day, mice received an i.p. injection of saline (control condition) or saracatinib 2 h **(A–C)** or 30 min **(D–F)** prior to the contingency degradation session ("On-Tx"). **(A–C)** Response rate, total magazine entries, and incentivized magazine entries for the 2-h time point, respectively. **(D–F)** Response rate, total magazine entries, and incentivized magazine entries for the 30-min time point. Two-hour time point: $n = 8$/drug. Thirty-minute time point: $n = 8$/drug. *$p < 0.05$ vs. baseline day across groups (main effect of session). Tx, treatment; i.p., intraperitoneal.

effects of saracatinib were observed for the number of drinks consumed. Of note, we observed a reduction in drinking and craving in the placebo group and in the saracatinib group. While it is possible that the decrease in the placebo group could have masked any effects of saracatinib, we have demonstrated drug-placebo differences in other studies using this ADP paradigm (21). Together, these results suggest that short-term saracatinib treatment at a dose of 125 mg/day may not reduce alcohol craving or consumption in people with heavy drinking habits.

The doses used in these studies were selected based on several factors: to match cerebrospinal fluid levels of saracatinib between the two species (52), verified behavioral effects and peripheral markers of reduced Src family activity (52, 57), and to mitigate risk of off-target pharmacological effects and side effects (57, 65). It is possible that alternative doses of saracatinib would yield different results in both species. Of note, the rate of adverse events observed, including neuropsychiatric adverse events, with the 125 mg/day saracatinib dose in human participants was low compared to what is commonly seen with glutamatergic agents (21). In contrast, larger clinical trials in older clinical populations with Alzheimer's disease (66) have identified higher rates of adverse effects within the range of the dose used in

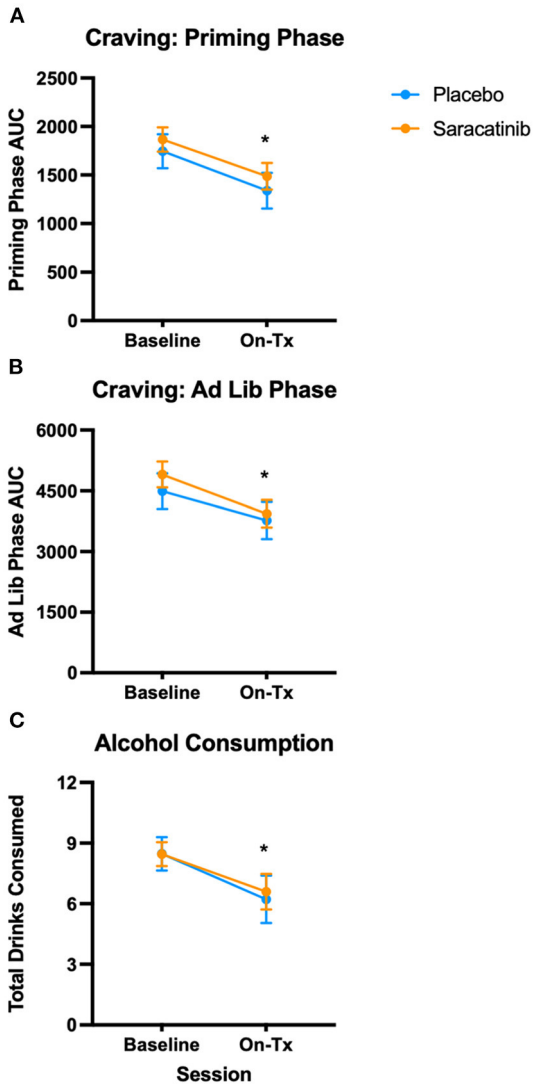

FIGURE 2 | 125 mg/day saracatinib did not affect alcohol craving or consumption in human participants. Participants underwent two ADPs: One prior to initiating treatment ("Baseline") and a second one following 7–8 days of 125 mg/day oral saracatinib treatment ("On-Tx"). **(A)** AUC for craving during the priming phase of the ADP session. **(B)** AUC for craving during the *ad libitum* phase. **(C)** Total drinks consumed. $N = 15$ placebo; $n = 26$ saracatinib. $^*p < 0.05$ vs. baseline ADP across groups (main effect of session). ADP, alcohol drinking paradigm; AUC, area under the curve; Tx, treatment.

our study. So, our observed lack of adverse events and efficacy may be related to the population studied, which may potentially tolerate, and require, higher doses to reverse alcohol-induced glutamatergic changes due to heavy drinking habits. For example, in mice, studies that used a dose of 10 mg/kg have reported saracatinib-mediated reductions in ethanol self-administration (35). However, in our preliminary work (data not shown) 5 mg/kg of saracatinib was sufficient to reduce phosphorylated NR2B in DMS, and several studies have used this dose to successfully ameliorate behavioral deficits or neurodegeneration in Alzheimer's models, albeit administered per oral and on a chronic treatment regimen (52, 67, 68). Nonetheless, future studies should perform a dose-response curve for effects of saracatinib on habitual responding for alcohol in mice to elucidate the present negative findings. Overall, further work to examine the dose-dependent effects of saracatinib on alcohol drinking behaviors is needed.

Another possibility for the lack of treatment effects is the time course of the treatment regimen. While positive effects of saracatinib on ethanol-seeking and consumption have been reported after acute administration in mice (35, 40), other behavioral effects of saracatinib, at the 5 mg/kg dose used in the present study, required longer time frames. For example, rescue of cognitive function in an Alzheimer's mouse model required 3–5 weeks of 5 mg/kg saracatinib administration for effects to emerge (52). Likewise, it is possible that a more extended treatment regimen in the clinical trial would have yielded positive results. Indeed, maximal plasma levels are augmented at steady state relative to acute administration at the 125 mg/day dose, with participants reaching steady state within 10–17 days (65), whereas the present study provided saracatinib for 7–8 days. However, a clinical trial that assessed the efficacy of saracatinib in Alzheimer's disease did not observe significant effects at this dose after a year of treatment, despite positive effects within shorter timeframes in mouse models (52, 66). Regardless, it is possible that extended treatment regimens may be needed when considering the use of this agent to treat alcohol drinking, which may yield different findings.

Alternatively, Fyn may have brain region- and function-specific roles that explain the present results. Fyn-dependent long term facilitation of NMDAR-mediated excitatory postsynaptic currents in response to ethanol are observed in the DMS, but not DLS (36, 37). The same study found that the Src family protein tyrosine kinase inhibitor PP2, which inhibits Fyn, reduced ethanol self-administration in rats when infused into the DMS, but not DLS. Furthermore, it was recently reported that stimulation of D1 neurons in the DMS, but not DLS upregulated phosphorylation of Fyn and its substrate NR2B (40), together suggesting that Fyn may play less of a role in the DLS. These findings align with the possibility that Fyn may mediate goal-directed, but not habitual, ethanol-seeking and consumption behaviors; the DMS is classically implicated in goal-directed action, whereas there is a lateral shift in activity over time as an action becomes more habitual, including ethanol-seeking (39, 41, 42). This possibility is supported by the current literature regarding effects of saracatinib on ethanol-seeking and consumption. One study reported a reduction in instrumental responding for ethanol in confirmed goal-directed mice after acute administration of saracatinib (35). Another study from the same group reported reductions in *ad libitum* ethanol consumption in ethanol-naïve mice (40). However, we did not test effects of saracatinib on goal-directed drinking in the present study, and thus cannot confirm this selectivity from the present results alone. To our knowledge, the current studies are the first to directly assess the effects of saracatinib in confirmed habitual ethanol consuming

individuals, who likely have greater DLS control of ethanol-seeking (41, 69).

While a strength of these parallel studies is the use of equivalent doses of saracatinib in chronically alcohol consuming individuals, there are disparities between the designs of the mouse and human studies that limit the comparability. Saracatinib was administered acutely in the mouse study, whereas the human participants received 7–8 days of saracatinib. In addition, only male subjects were used in the mouse study. Furthermore, the mice were not tested on measures of ethanol dependence, and blood ethanol concentrations were not measured, which precludes classification of these mice as heavy drinkers or as ethanol-dependent. However, prior studies have reported binge-level blood ethanol concentrations in mice consuming similar quantities of ethanol during self-administration. For example, one study reported an average blood ethanol concentration of 93 mg/dl after consuming 1.3 g/kg ethanol within a 60-min session, which may be comparable to the present study in which mice received approximately 1.1 g/kg ethanol within a 45-min session (70). In addition, in our other studies using this self-administration paradigm we have observed heightened withdrawal-induced aggression between male cage mates (data not shown), which suggests that this experimental setup may be capable of inducing ethanol dependence. Nonetheless, these features must be quantified in future studies for confirmation.

Another key difference between these studies was the direct assessment of habitual behavior in the mice, which was not tested in the clinical study. Previous studies have shown that alcohol-dependent individuals exhibit a shift toward more habitual, less goal-directed behavior in an outcome devaluation test (51). Furthermore, another study found that habitual, but not reward-driven alcohol use was associated with severity of alcohol dependence (71), and another found that abstinent participants with high alcohol expectancies and impaired goal-directed control were more susceptible to subsequent relapse (72). Together, these findings suggest that habitual behavior is associated with alcohol dependence and may be relevant for treatment outcomes. Yet, we cannot draw conclusions regarding the effects of saracatinib on habitual behavior *per se* in the clinical study presented here. There is little work in the literature regarding back-translatability of effective treatments for alcohol use disorder in habit paradigms. One study assessed the effects of naltrexone on ethanol self-administration in rats using reinforcement schedules that promote goal-directed (FR-5) vs. habitual (VI-30) responding. They found that naltrexone reduced responding in both schedules, although they did not test effects of naltrexone on habit itself, such as in a contingency degradation or outcome devaluation session (73). More work is needed in this area to determine the translational potential of ethanol habit in rodents as a screen for novel therapeutics.

Overall, we did not identify effects of saracatinib on alcohol-seeking/craving or consumption in habitual mice or heavy drinking human participants. These results suggest that Fyn kinase inhibition may not be effective at reducing these aspects of alcohol use at the doses and treatment regimens employed in the current study. Future studies should consider the use of higher doses of saracatinib and alternative treatment regimens to confirm and expand upon these findings.

DATA AVAILABILITY STATEMENT

The raw data supporting the conclusions of this article will be made available by the authors, without undue reservation.

ETHICS STATEMENT

The studies involving human participants were reviewed and approved by Yale Human Investigations Committee. The patients/participants provided their written informed consent to participate in this study. The animal study was reviewed and approved by Yale University Institutional Animal Care and Use Committee.

AUTHOR CONTRIBUTIONS

SK-S, JRT, JK, and SO'M: conceptualization. ST, CG, SO'M, DC, JS, JMT, KD, RG, BP, and SK-S: investigation and analyses. ST: writing original draft. ST, CG, SO'M, DC, JS, JMT, KD, RG, BP, JK, JRT, and SK-S: writing and editing. All authors contributed to the article and approved the submitted version.

FUNDING

Research reported in this publication was supported by the National Institute on Alcohol Abuse and Alcoholism of the National Institutes of Health under Award Number P50AA012870. Additional support was provided from the Charles B. G. Murphy Fund and the State of Connecticut Department of Mental Health and Addiction Services. ST was supported by T32 MH014276. Medications were provided by Astra Zeneca. CG was supported by T32 AA007573-22.

SUPPLEMENTARY MATERIAL

The Supplementary Material for this article can be found online at: https://www.frontiersin.org/articles/10.3389/fpsyt.2021.709559/full#supplementary-material

REFERENCES

1. GBD 2016 Alcohol and Drug Use Collaborators. The global burden of disease attributable to alcohol and drug use in 195 countries and territories, 1990-2016: a systematic analysis for the Global Burden of Disease Study 2016. *Lancet Psychiatry.* (2018) 5:987–1012. doi: 10.1016/S2215-0366(18)30337-7
2. Krishnan-Sarin S, O'Malley S, Krystal JH. Treatment implications: using neuroscience to guide the development of new

pharmacotherapies for alcoholism. *Alcohol Res Health.* (2008) 31:400–7.
3. Krishnan-Sarin S, Krystal JH, Shi J, Pittman B, O'Malley SS. Family history of alcoholism influences naltrexone-induced reduction in alcohol drinking. *Biol Psychiatry.* (2007) 62:694–7. doi: 10.1016/j.biopsych.2006.11.018
4. Snyder JL, Bowers TG. The efficacy of acamprosate and naltrexone in the treatment of alcohol dependence: a relative benefits analysis of randomized controlled trials. *Am J Drug Alcohol Abuse.* (2008) 34:449–61. doi: 10.1080/00952990802082198
5. Holmes A, Spanagel R, Krystal JH. Glutamatergic targets for new alcohol medications. *Psychopharmacology.* (2013) 229:539–54. doi: 10.1007/s00213-013-3226-2
6. Olive MF. Metabotropic glutamate receptor ligands as potential therapeutics for addiction. *Curr Drug Abuse Rev.* (2009) 2:83–98. doi: 10.2174/1874473710902010083
7. Krupitsky EM, Neznanova O, Masalov D, Burakov AM, Didenko T, Romanova T, et al. Effect of memantine on cue-induced alcohol craving in recovering alcohol-dependent patients. *Am J Psychiatry.* (2007) 164:519–23. doi: 10.1176/ajp.2007.164.3.519
8. Cagetti E, Baicy KJ, Olsen RW. Topiramate attenuates withdrawal signs after chronic intermittent ethanol in rats. *Neuroreport.* (2004) 15:207–10. doi: 10.1097/00001756-200401190-00040
9. Breslin FJ, Johnson BA, Lynch WJ. Effect of topiramate treatment on ethanol consumption in rats. *Psychopharmacology.* (2009) 207:529. doi: 10.1007/s00213-009-1683-4
10. Johnson KA, Lovinger DM. Allosteric modulation of metabotropic glutamate receptors in alcohol use disorder: insights from preclinical investigations. *Adv Pharmacol.* (2020) 88:193–232. doi: 10.1016/bs.apha.2020.02.002
11. Bauer MR, Garcy DP, Boehm SL. Systemic administration of the AMPA receptor antagonist, NBQX, reduces alcohol drinking in male C57BL/6J, but not female C57BL/6J or high-alcohol-preferring, mice. *Alcohol Clin Exp Res.* (2020) 44:2316–25. doi: 10.1111/acer.14461
12. Williams KL, Harding KM. Repeated alcohol extinction sessions in conjunction with MK-801, but not yohimbine or propranolol, reduces subsequent alcohol cue-induced responding in rats. *Pharmacol Biochem Behav.* (2014) 116:16–24. doi: 10.1016/j.pbb.2013.11.020
13. Huang G, Thompson SL, Taylor JR. MPEP lowers binge drinking in male and female C57BL/6 mice: relationship with mGlu5/Homer2/Erk2 signaling. *Alcohol Clin Exp Res.* (2021) 45:732–42. doi: 10.1111/acer.14576
14. Sidhpura N, Weiss F, Martin-Fardon R. Effects of the mGlu2/3 agonist LY379268 and the mGlu5 antagonist MTEP on ethanol seeking and reinforcement are differentially altered in rats with a history of ethanol dependence. *Biol Psychiatry.* (2010) 67:804–11. doi: 10.1016/j.biopsych.2010.01.005
15. Grant KA, Lovinger DM. Cellular and behavioral neurobiology of alcohol: receptor-mediated neuronal processes. *Clin Neurosci.* (1995) 3:155–64.
16. Clapp P, Gibson ES, Dell'Acqua ML, Hoffman PL. Phosphorylation regulates removal of synaptic N-methyl-d-aspartate receptors after withdrawal from chronic ethanol exposure. *J Pharmacol Exp Ther.* (2010) 332:720–9. doi: 10.1124/jpet.109.158741
17. Krystal JH, Petrakis IL, Limoncelli D, Webb E, Gueorgueva R, D'Souza DC, et al. Altered NMDA glutamate receptor antagonist response in recovering ethanol-dependent patients. *Neuropsychopharmacology.* (2003) 28:2020–8. doi: 10.1038/sj.npp.1300252
18. Acosta G, Hasenkamp W, Daunais JB, Friedman DP, Grant KA, Hemby SE. Ethanol self-administration modulation of NMDA receptor subunit and related synaptic protein mRNA expression in prefrontal cortical fields in cynomolgus monkeys. *Brain Res.* (2010) 1318:144–54. doi: 10.1016/j.brainres.2009.12.050
19. Krystal JH, Petrakis IL, Mason G, Trevisan L, D'Souza DC. N-methyl-D-aspartate glutamate receptors and alcoholism: reward, dependence, treatment, and vulnerability. *Pharmacol Ther.* (2003) 99:79–94. doi: 10.1016/S0163-7258(03)00054-8
20. Hölter SM, Danysz W, Spanagel R. Novel uncompetitive N-methyl-d-aspartate (NMDA)-receptor antagonist MRZ 2/579 suppresses ethanol intake in long-term ethanol-experienced rats and generalizes to ethanol cue in drug discrimination procedure. *J Pharmacol Exp Ther.* (2000) 292:545—52.
21. Krishnan-Sarin S, O'Malley SS, Franco N, Cavallo DA, Tetrault JM, Shi J, et al. Influence of combined treatment with naltrexone and memantine on alcohol drinking behaviors: a phase II randomized crossover trial. *Neuropsychopharmacology.* (2020) 45:319–26. doi: 10.1038/s41386-019-0536-z
22. Khanna JM, Shah G, Weiner J, Wu PH, Kalant H. Effect of NMDA receptor antagonists on rapid tolerance to ethanol. *Eur J Pharmacol.* (1993) 230:23–31. doi: 10.1016/0014-2999(93)90405-7
23. Rassnick S, Pulvirenti L, Koob GF. Oral ethanol self-administration in rats is reduced by the administration of dopamine and glutamate receptor antagonists into the nucleus accumbens. *Psychopharmacology.* (1992) 109:92–8. doi: 10.1007/BF02245485
24. Palachick B, Chen Y-C, Enoch AJ, Karlsson R-M, Mishina M, Holmes A. Role of major NMDA or AMPA receptor subunits in MK-801 potentiation of ethanol intoxication. *Alcohol Clin Exp Res.* (2008) 32:1479–92. doi: 10.1111/j.1530-0277.2008.00715.x
25. Arias AJ, Feinn R, Covault J, Kranzler HR. Memantine for alcohol dependence: an open-label pilot study. *Addict Disord Treat.* (2007) 6:77–83. doi: 10.1097/01.adt.0000210724.41187.4a
26. Krishnan-Sarin S, O'Malley SS, Franco N, Cavallo DA, Morean M, Shi J, et al. N-methyl-D-aspartate receptor antagonism has differential effects on alcohol craving and drinking in heavy drinkers. *Alcohol Clin Exp Res.* (2015) 39:300–7. doi: 10.1111/acer.12619
27. Zhou D, Lv D, Wang Z, Zhang Y, Chen Z, Wang C. GLYX-13 ameliorates schizophrenia-like phenotype induced by MK-801 in mice: role of hippocampal NR2B and DISC1. *Front Mol Neurosci.* (2018) 11:121. doi: 10.3389/fnmol.2018.00121
28. Krystal JH, Karper LP, Seibyl JP, Freeman GK, Delaney R, Bremner JD, et al. Subanesthetic effects of the noncompetitive NMDA antagonist, ketamine, in humans. Psychotomimetic, perceptual, cognitive, and neuroendocrine responses. *Arch Gen Psychiatry.* (1994) 51:199–214. doi: 10.1001/archpsyc.1994.03950030035004
29. Naassila M, Pierrefiche O. GluN2B subunit of the NMDA receptor: the keystone of the effects of alcohol during neurodevelopment. *Neurochem Res.* (2019) 44:78–88. doi: 10.1007/s11064-017-2462-y
30. Salter MW, Kalia LV. Src kinases: a hub for NMDA receptor regulation. *Nat Rev Neurosci.* (2004) 5:317–28. doi: 10.1038/nrn1368
31. Morisot N, Ron D. Alcohol-dependent molecular adaptations of the NMDA receptor system. *Genes Brain Behav.* (2017) 16:139–48. doi: 10.1111/gbb.12363
32. Ishiguro H, Saito T, Shibuya H, Toru M, Arinami T. Mutation and association analysis of the Fyn kinase gene with alcoholism and schizophrenia. *Am J Med Genet.* (2000) 96:716–20. doi: 10.1002/1096-8628(20001204)96:6<716::AID-AJMG3>3.0.CO;2-N
33. Pastor IJ, Laso FJ, Inés S, Marcos M, González-Sarmiento R. Genetic association between−93A/G polymorphism in the Fyn kinase gene and alcohol dependence in Spanish men. *Eur Psychiatry.* (2009) 24:191–4. doi: 10.1016/j.eurpsy.2008.08.007
34. Schumann G, Rujescu D, Kissling C, Soyka M, Dahmen N, Preuss UW, et al. Analysis of genetic variations of protein tyrosine kinase fyn and their association with alcohol dependence in two independent cohorts. *Biol Psychiatry.* (2003) 54:1422–6. doi: 10.1016/S0006-3223(03)00635-8
35. Morisot N, Berger AL, Phamluong K, Cross A, Ron D. The Fyn kinase inhibitor, AZD0530, suppresses mouse alcohol self-administration and seeking. *Addict Biol.* (2019) 24:1227–34. doi: 10.1111/adb.12699
36. Wang J, Lanfranco MF, Gibb SL, Yowell QV, Carnicella S, Ron D. Long-lasting adaptations of the NR2B-containing NMDA receptors in the dorsomedial striatum play a crucial role in alcohol consumption and relapse. *J Neurosci.* (2010) 30:10187–98. doi: 10.1523/JNEUROSCI.2268-10.2010
37. Wang J, Carnicella S, Phamluong K, Jeanblanc J, Ronesi JA, Chaudhri N, et al. Ethanol induces long-term facilitation of NR2B-NMDA receptor activity in the dorsal striatum: implications for alcohol drinking behavior. *J Neurosci.* (2007) 27:3593–602. doi: 10.1523/JNEUROSCI.4749-06.2007
38. Darcq E, Hamida SB, Wu S, Phamluong K, Kharazia V, Xu J, et al. Inhibition of striatal-enriched tyrosine phosphatase 61 in the dorsomedial striatum is sufficient to increased ethanol consumption. *J Neurochem.* (2014) 129:1024–34. doi: 10.1111/jnc.12701
39. Yin HH, Knowlton BJ. The role of the basal ganglia in habit formation. *Nat Rev Neurosci.* (2006) 7:464–76. doi: 10.1038/nrn1919

40. Ehinger Y, Morisot N, Phamluong K, Sakhai SA, Soneja D, Adrover MF, et al. cAMP-Fyn signaling in the dorsomedial striatum direct pathway drives excessive alcohol use. *Neuropsychopharmacology*. (2021) 46:334–42. doi: 10.1038/s41386-020-0712-1
41. Corbit LH, Nie H, Janak PH. Habitual alcohol seeking: time course and the contribution of subregions of the dorsal striatum. *Biol Psychiatry*. (2012) 72:389–95. doi: 10.1016/j.biopsych.2012.02.024
42. Quinn JJ, Pittenger C, Lee AS, Pierson JL, Taylor JR. Striatum-dependent habits are insensitive to both increases and decreases in reinforcer value in mice. *Eur J Neurosci.* (2013) 37:1012–21. doi: 10.1111/ejn.12106
43. Tricomi E, Balleine BW, O'Doherty JP. A specific role for posterior dorsolateral striatum in human habit learning. *Eur J Neurosci.* (2009) 29:2225–32. doi: 10.1111/j.1460-9568.2009.06796.x
44. Ostlund SB, Maidment NT, Balleine BW. Alcohol-paired contextual cues produce an immediate and selective loss of goal-directed action in rats. *Front Integr Neurosci.* (2010) 4:19. doi: 10.3389/fnint.2010.00019
45. Barker JM, Taylor JR. Habitual alcohol seeking: modeling the transition from casual drinking to addiction. *Neurosci Biobehav Rev*. (2014) 47:281–94. doi: 10.1016/j.neubiorev.2014.08.012
46. Dickinson A, Wood N, Smith JW. Alcohol seeking by rats: action or habit? *Q J Exp Psychol B.* (2002) 55:331–48. doi: 10.1080/0272499024400016
47. Mangieri RA, Cofresí RU, Gonzales RA. Ethanol exposure interacts with training conditions to influence behavioral adaptation to a negative instrumental contingency. *Front Behav Neurosci.* (2014) 8:220. doi: 10.3389/fnbeh.2014.00220
48. Mangieri RA, Cofresí RU, Gonzales RA. Ethanol seeking by long evans rats is not always a goal-directed behavior. *PLoS ONE.* (2012) 7:e42886. doi: 10.1371/journal.pone.0042886
49. Lüscher C, Robbins TW, Everitt BJ. The transition to compulsion in addiction. *Nat Rev Neurosci.* (2020) 21:247–63. doi: 10.1038/s41583-020-0289-z
50. Corbit LH, Janak PH. Habitual alcohol seeking: neural bases and possible relations to alcohol use disorders. *Alcohol Clin Exp Res.* (2016) 40:1380–9. doi: 10.1111/acer.13094
51. Sjoerds Z, de Wit S, van den Brink W, Robbins TW, Beekman ATF, Penninx BWJH, et al. Behavioral and neuroimaging evidence for overreliance on habit learning in alcohol-dependent patients. *Transl Psychiatry*. (2013) 3:e337. doi: 10.1038/tp.2013.107
52. Kaufman AC, Salazar SV, Haas LT, Yang J, Kostylev MA, Jeng AT, et al. Fyn inhibition rescues established memory and synapse loss in Alzheimer mice. *Ann Neurol.* (2015) 77:953–71. doi: 10.1002/ana.24394
53. Gianessi CA, Groman SM, Thompson SL, Jiang M, van der Stelt M, Taylor JR. Endocannabinoid contributions to alcohol habits and motivation: relevance to treatment. *Addict Biol.* (2020) 25:e12768. doi: 10.1111/adb.12768
54. Gianessi CA, Groman SM, Taylor JR. Bi-directional modulation of food habit expression by the endocannabinoid system. *Eur J Neurosci.* (2019) 49:1610–22. doi: 10.1111/ejn.14330
55. Sobell LC, Sobell MB. Timeline follow-back: A technique for assessing self-reported alcohol consumption. In: Litten RZ, Allen JP, editors. *Measuring Alcohol Consumption: Psychosocial and Biochemical Methods*. Totowa, NJ: Humana Press (1992). p. 41–72.
56. Sullivan JT, Sykora K, Schneiderman J, Naranjo CA, Sellers EM. Assessment of alcohol withdrawal: the revised clinical institute withdrawal assessment for alcohol scale (CIWA-Ar). *Addiction.* (1989) 84:1353–7. doi: 10.1111/j.1360-0443.1989.tb00737.x
57. Nygaard HB, Wagner AF, Bowen GS, Good SP, MacAvoy MG, Strittmatter KA, et al. A phase Ib multiple ascending dose study of the safety, tolerability, and central nervous system availability of AZD0530 (saracatinib) in Alzheimer's disease. *Alzheimers Res Ther.* (2015) 7:35. doi: 10.1186/s13195-015-0119-0
58. NACAA. *Administering Alcohol in Human Studies | National Institute on Alcohol Abuse and Alcoholism (NIAAA)*. (2006). Available online at: https://www.niaaa.nih.gov/research/guidelines-and-resources/administering-alcohol-human-studies (accessed April 3, 2021).
59. Watson PE. Total body water and blood alcohol levels: Updating the fundamentals. In: Crow K, Batt R, editors. *Human Metabolism of Alcohol (Vol. 1): Pharmacokinetics, Medicolegal Aspects, and General Interest*. Boca Raton, FL: CRC Press. p. 41–58.
60. Bohn MJ, Krahn DD, Staehler BA. Development and initial validation of a measure of drinking urges in abstinent alcoholics. *Alcohol Clin Exp Res.* (1995) 19:600–6. doi: 10.1111/j.1530-0277.1995.tb01554.x
61. Rueger SY, King AC. Validation of the brief biphasic alcohol effects scale (B-BAES). *Alcohol Clin Exp Res.* (2013) 37:470–6. doi: 10.1111/j.1530-0277.2012.01941.x
62. Levine J, Schooler NR. SAFTEE: a technique for the systematic assessment of side effects in clinical trials. *Psychopharmacol Bull.* (1986) 22:343–81.
63. Schwarz G. Estimating the dimension of a model. *Ann Stat.* (1978) 6:461–4. doi: 10.1214/aos/1176344136
64. Ross HE, Gavin DR, Skinner HA. Diagnostic validity of the MAST and the alcohol dependence scale in the assessment of DSM-III alcohol disorders. *J Stud Alcohol.* (1990) 51:506–13. doi: 10.15288/jsa.1990.51.506
65. Baselga J, Cervantes A, Martinelli E, Chirivella I, Hoekman K, Hurwitz HI, et al. Phase I safety, pharmacokinetics, and inhibition of Src activity study of saracatinib in patients with solid tumors. *Clin Cancer Res.* (2010) 16:4876–83. doi: 10.1158/1078-0432.CCR-10-0748
66. van Dyck CH, Nygaard HB, Chen K, Donohue MC, Raman R, Rissman RA, et al. Effect of AZD0530 on cerebral metabolic decline in Alzheimer disease: a randomized clinical trial. *JAMA Neurol.* (2019) 76:1219–29. doi: 10.1001/jamaneurol.2019.2050
67. Toyonaga T, Smith LM, Finnema SJ, Gallezot J-D, Naganawa M, Bini J, et al. *In vivo* synaptic density imaging with 11C-UCB-J detects treatment effects of saracatinib in a mouse model of Alzheimer disease. *J Nucl Med.* (2019) 60:1780–6. doi: 10.2967/jnumed.118.223867
68. Smith LM, Zhu R, Strittmatter SM. Disease-modifying benefit of Fyn blockade persists after washout in mouse Alzheimer's model. *Neuropharmacology.* (2018) 130:54–61. doi: 10.1016/j.neuropharm.2017.11.042
69. Corbit LH, Nie H, Janak PH. Habitual responding for alcohol depends upon both AMPA and D2 receptor signaling in the dorsolateral striatum. *Front Behav Neurosci.* (2014) 8:301. doi: 10.3389/fnbeh.2014.00301
70. Faccidomo S, Besheer J, Stanford PC, Hodge CW. Increased operant responding for ethanol in male C57BL/6J mice: specific regulation by the ERK1/2, but not JNK, MAP kinase pathway. *Psychopharmacology.* (2009) 204:135–47. doi: 10.1007/s00213-008-1444-9
71. Piquet-Pessôa M, Chamberlain SR, Lee RSC, Ferreira GM, Cruz MS, Ribeiro AP, et al. A study on the correlates of habit-, reward-, and fear-related motivations to use alcohol in alcohol use disorder. *CNS Spectr.* (2019) 24:597–604. doi: 10.1017/S1092852918001554
72. Sebold M, Nebe S, Garbusow M, Guggenmos M, Schad DJ, Beck A, et al. When habits are dangerous: alcohol expectancies and habitual decision making predict relapse in alcohol dependence. *Biol Psychiatry*. (2017) 82:847–56. doi: 10.1016/j.biopsych.2017.04.019
73. Hay RA, Jennings JH, Zitzman DL, Hodge CW, Robinson DL. Specific and nonspecific effects of naltrexone on goal-directed and habitual models of alcohol seeking and drinking. *Alcohol Clin Exp Res.* (2013) 37:1100–10. doi: 10.1111/acer.12081

Author Disclaimer: The content is solely the responsibility of the authors and does not necessarily represent the official views of the National Institutes of Health, the Department of Mental Health and Addiction Services, or the state of Connecticut.

Conflict of Interest: SO'M is a member of the American Society of Clinical Psychopharmacology's (ASCP's) Alcohol Clinical Trials Initiative, supported by Alkermes, Amygdala, Arbor Pharma, Dicerna, Ethypharm, Indivior, Lundbeck, Mitsubishi Tanabe, Otsuka; Consultant/advisory board member, Alkermes, Amygdala, Dicerna, Opiant; Medication supplies, Astra Zeneca, Novartis; DSMB member, Indiana University, Emmes Corporation. SK-S, PhD has received medication supplies from Astra Zeneca, Novartis. JK has been a consultant (<$10,000/year) for the following: Aptinyx, Inc., Atai Life Sciences, AstraZeneca Pharmaceuticals, Biogen, Idec, MA, Biomedisyn Corporation, Bionomics, Limited (Australia), Boehringer Ingelheim International, Cadent Therapeutics, Inc., Clexio Bioscience, Ltd., COMPASS Pathways, Limited, United Kingdom, Concert Pharmaceuticals, Inc., Epiodyne, Inc., EpiVario, Inc., Greenwich Biosciences, Inc., Heptares Therapeutics, Limited (UK), Janssen Research & Development, Jazz Pharmaceuticals, Inc., Otsuka America Pharmaceutical, Inc., Perception

Neuroscience, Holdings, Inc., Spring Care, Inc., Sunovion Pharmaceuticals, Inc., Takeda Industries, and Taisho Pharmaceutical Co., Ltd. JK serves on the scientific advisory board for: Biohaven Pharmaceuticals, BioXcel Therapeutics, Inc. (Clinical Advisory Board), Cadent Therapeutics, Inc. (Clinical Advisory Board), Cerevel Therapeutics, LLC, EpiVario, Inc., Eisai, Inc., Jazz Pharmaceuticals, Inc., Lohocla Research Corporation, Novartis Pharmaceuticals Corporation, PsychoGenics, Inc., RBNC Therapeutics, Inc., Tempero Bio, Inc., Terran Biosciences, Inc. JK holds stock in: Biohaven Pharmaceuticals, Sage Pharmaceuticals, Spring Care, Inc. JK has stock options in: Biohaven Pharmaceuticals Medical Sciences, EpiVario, Inc., RBNC Therapeutics, Inc., Terran Biosciences, Inc., Tempero Bio, Inc. JK has received income (>$10,000) from their position as Editor - Biological Psychiatry. JK holds the following patents and inventions: 1. Seibyl JP, Krystal JH, Charney DS. Dopamine and noradrenergic reuptake inhibitors in treatment of schizophrenia. US Patent #:5,447,948.September 5, 1995. 2. Vladimir, Coric, Krystal, John H, Sanacora, Gerard – Glutamate Modulating Agents in the Treatment of Mental Disorders. US Patent No. 8,778,979 B2 Patent Issue Date: July 15, 2014. US Patent Application No. 15/695,164: Filing Date: 09/05/2017. 3. Charney D, Krystal JH, Manji H, Matthew S, Zarate C., - Intranasal Administration of Ketamine to Treat Depression United States Patent Number: 9592207, Issue date: 3/14/2017. Licensed to Janssen Research & Development. 4. Zarate, C, Charney, DS, Manji, HK, Mathew, Sanjay J, Krystal, JH, Yale University "Methods for Treating Suicidal Ideation," Patent Application No. 15/379,013 filed on December 14, 2016 by Yale University Office of Cooperative Research. 5. Arias A, Petrakis I, Krystal JH. – Composition and methods to treat addiction. Provisional Use Patent Application no.61/973/961. April 2, 2014. Filed by Yale University Office of Cooperative Research. 6. Chekroud, A., Gueorguieva, R., & Krystal, JH. "Treatment Selection for Major Depressive Disorder" (filing date 3rd June 2016, USPTO docket number Y0087.70116US00). Provisional patent submission by Yale University. 7. Gihyun, Yoon, Petrakis I, Krystal JH – Compounds, Compositions and Methods for Treating or Preventing Depression and Other Diseases. U. S. Provisional Patent Application No. 62/444,552, filed on January10, 2017 by Yale University Office of Cooperative Research OCR 7088 US01. 8. Abdallah, C, Krystal, JH, Duman, R, Sanacora, G. Combination Therapy for Treating or Preventing Depression or Other Mood Diseases. U.S. Provisional Patent Application No. 62/719,935 filed on August 20, 2018 by Yale University Office of Cooperative Research OCR 7451 US01. 9. John Krystal, Godfrey Pearlson, Stephanie O'Malley, Marc Potenza, Fabrizio Gasparini, Baltazar Gomez-Mancilla, Vincent Malaterre. Mavoglurant in treating gambling and gaming disorders. U.S. Provisional Patent Application No. 63/125,181filed on December 14, 2020 by Yale University Office of Cooperative Research OCR 8065 US00. JK received the drug, Saracatinib from AstraZeneca Pharmaceuticals for research related to NIAAA grant "Center for Translational Neuroscience of Alcoholism" (CTNA-4). JK received the drug, Mavoglurant, from Novartis for research related to NIAAA grant "Center for Translational Neuroscience of Alcoholism" (CTNA-4). RG discloses the following interests unrelated to this work: royalties from book "Statistical Methods in Psychiatry and Related Fields" published by CRC Press, honorarium as a member of the Working Group for PTSD Adaptive Platform Trial of Cohen Veterans Bioscience and a United States patent application 20200143922 by Yale University: Chekroud, A., Krystal, J., Gueorguieva, R. and Chandra, A. "Methods and Apparatus for Predicting Depression Treatment Outcomes."

The remaining authors declare that the research was conducted in the absence of any commercial or financial relationships that could be construed as a potential conflict of interest.

Publisher's Note: All claims expressed in this article are solely those of the authors and do not necessarily represent those of their affiliated organizations, or those of the publisher, the editors and the reviewers. Any product that may be evaluated in this article, or claim that may be made by its manufacturer, is not guaranteed or endorsed by the publisher.

frontiers in Psychiatry

ORIGINAL RESEARCH
published: 17 September 2021
doi: 10.3389/fpsyt.2021.734984

Time of Day-Dependent Alterations in Hippocampal Kynurenic Acid, Glutamate, and GABA in Adult Rats Exposed to Elevated Kynurenic Acid During Neurodevelopment

Courtney J. Wright[1†], Katherine M. Rentschler[1†], Nathan T. J. Wagner[1], Ashley M. Lewis[1], Sarah Beggiato[2] and Ana Pocivavsek[1]*

[1] Department of Pharmacology, Physiology, and Neuroscience, University of South Carolina School of Medicine, Columbia, SC, United States, [2] Department of Medical, Oral and Biotechnological Sciences, University of Chieti-Pescara, Chieti, Italy

OPEN ACCESS

Edited by:
Natasa Petronijevic,
University of Belgrade, Serbia

Reviewed by:
Lihle Qulu,
Stellenbosch University, South Africa
Jorge M. Campusano,
Pontificia Universidad Católica de Chile, Chile

***Correspondence:**
Ana Pocivavsek
ana.pocivavsek@uscmed.sc.edu

[†] These authors have contributed equally to this work and share first authorship

Specialty section:
This article was submitted to Molecular Psychiatry, a section of the journal Frontiers in Psychiatry

Received: 01 July 2021
Accepted: 23 August 2021
Published: 17 September 2021

Citation:
Wright CJ, Rentschler KM, Wagner NTJ, Lewis AM, Beggiato S and Pocivavsek A (2021) Time of Day-Dependent Alterations in Hippocampal Kynurenic Acid, Glutamate, and GABA in Adult Rats Exposed to Elevated Kynurenic Acid During Neurodevelopment. Front. Psychiatry 12:734984. doi: 10.3389/fpsyt.2021.734984

Hypofunction of glutamatergic signaling is causally linked to neurodevelopmental disorders, including psychotic disorders like schizophrenia and bipolar disorder. Kynurenic acid (KYNA) has been found to be elevated in postmortem brain tissue and cerebrospinal fluid of patients with psychotic illnesses and may be involved in the hypoglutamatergia and cognitive dysfunction experienced by these patients. As insults during the prenatal period are hypothesized to be linked to the pathophysiology of psychotic disorders, we presently utilized the embryonic kynurenine (EKyn) paradigm to induce a prenatal hit. Pregnant Wistar dams were fed chow laced with kynurenine to stimulate fetal brain KYNA elevation from embryonic day 15 to embryonic day 22. Control dams (ECon) were fed unlaced chow. Plasma and hippocampal tissue from young adult (postnatal day 56) ECon and EKyn male and female offspring were collected at the beginning of the light (Zeitgeber time, ZT 0) and dark (ZT 12) phases to assess kynurenine pathway metabolites. Hippocampal tissue was also collected at ZT 6 and ZT 18. In separate animals, *in vivo* microdialysis was conducted in the dorsal hippocampus to assess extracellular KYNA, glutamate, and γ-aminobutyric acid (GABA). Biochemical analyses revealed no changes in peripheral metabolites, yet hippocampal tissue KYNA levels were significantly impacted by EKyn treatment, and increased in male EKyn offspring at ZT 6. Interestingly, extracellular hippocampal KYNA levels were only elevated in male EKyn offspring during the light phase. Decreases in extracellular glutamate levels were found in the dorsal hippocampus of EKyn male and female offspring, while decreased GABA levels were present only in males during the dark phase. The current findings suggest that the EKyn paradigm may be a useful tool for investigation of sex- and time-dependent changes in hippocampal neuromodulation elicited by prenatal KYNA elevation, which may influence behavioral phenotypes and have translational relevance to psychotic disorders.

Keywords: kynurenine, NMDA receptor, schizophrenia, psychotic disorders, prenatal

INTRODUCTION

Disruptions in neurotransmission are associated with the pathology of psychotic disorders such as schizophrenia (SZ) and bipolar disorder (BD). In particular, dysregulated modulation of the excitatory neurotransmitter glutamate and the inhibitory small molecule γ-aminobutyric acid (GABA) has been implicated in the etiology of cognitive, negative, and positive symptoms in individuals with severe psychiatric illness (1–4). Hypofunction of the cortical ionotropic glutamate receptor N-methyl-d-aspartate (NMDA) is thought to contribute to dysregulated tonic GABAergic inhibition, alterations in cortical glutamate levels, and the pathophysiological manifestation of cognitive and negative symptoms in individuals with SZ (2).

Abnormally high levels of the endogenous neuromodulator and tryptophan metabolite kynurenic acid (KYNA) (**Figure 1A**) are found in the brain and cerebrospinal fluid of individuals with SZ and BD (5–10). KYNA is of particular interest as it competitively antagonizes NMDA receptors at the glycine site, and inhibits α7 nicotinic acetylcholine (α7nACh) receptors, thereby directly influencing neurotransmission (11–14). Elevated KYNA is hypothesized to be causally related to neurocognitive impairments in patients with psychotic disorders (15). Preclinical studies in animal models postulate that increased KYNA impairs learning and memory, especially in brain regions like the prefrontal cortex and hippocampus, whereas KYNA reductions may feasibly improve learning and memory (16–22).

SZ and BD are classified as neurodevelopmental disorders, and perinatal insults, such as stress or infection, associated with these diseases can result in the activation of the kynurenine pathway (KP) and increase levels of KYNA. Further, the prenatal period has been found critical for elevations in KYNA to cause long term biochemical changes and cognitive dysfunction in adult rats (23–26). Hence, to further investigate the neurodevelopmental impacts of KYNA elevation, we utilize the embryonic kynurenine (EKyn) paradigm in rats, wherein pregnant Wistar dams are fed 100 mg of kynurenine-laced chow daily from embryonic day (ED) 15 to ED 22 (25, 27) (**Figure 1B**). This time course corresponds to the second trimester in human pregnancy, when the developing fetus is most vulnerable to exposure from infection or injury, thereby providing a translational model for *in utero* insults that instigate neurodevelopmental abnormalities (28–30). Substantial evidence also suggests that rodents subjected to elevated KYNA during this critical prenatal window will exhibit long-lasting deficits in adulthood (25, 31–35).

We recently determined conspicuous sex and time of day dependent changes in sleep, home cage activity, and arousal in young adult EKyn offspring (27). In a behavioral context, sleep and arousal states depend on hippocampal neuromodulation to regulate memory consolidation, retrieval, and locomotor activity (36, 37). Thus, our present aim was to investigate underlying abnormalities in levels of excitatory neurotransmitter glutamate and inhibitory neurotransmitter GABA, in relation to KYNA, in the hippocampus of young adult EKyn offspring. We hypothesized sex- and time-dependent changes in hippocampal GABAergic and glutamatergic neurotransmission in adulthood as a result of prenatal KYNA elevation. Of translational relevance, kynurenine pathway metabolites are modulated in a circadian-dependent manner in humans, with excreted metabolite levels peaking mid-morning after tryptophan administration (38). Therefore, we also evaluated KP metabolites in the plasma of young adult EKyn rats. Importantly we determined that while central levels of KYNA and neurotransmitters change in time of day and sex-dependent manners in our EKyn paradigm, plasma metabolites do not serve as predictors for changes in the brain. Interestingly, while KYNA levels were elevated in EKyn males, extracellular glutamate levels were attenuated in both EKyn males and females, yet GABA attenuation was only evident in EKyn males. Our study highlights sex differences in response to prenatal KYNA elevation and its impact on hippocampal neuromodulation of GABA and glutamate through altered cerebral KP metabolism.

Abbreviations: SZ, schizophrenia; BD, bipolar disorder; KYNA, kynurenic acid; EKyn, embryonic kynurenine treatment; ECon, embryonic control treatment; ZT, zeitgeber time; KP, kynurenine pathway; KYNA, kynurenic acid; NMDA, pertaining to the N-methyl-D-aspartate glutamate receptor; GABA, γ-aminobutyric acid; α7nACh, pertaining to the alpha 7 nicotinic acetylcholine receptor; ED, embryonic day; PD, postnatal day; AP, anterior-posterior; LM, lateral-medial; DV, dorsal-ventral; HPLC, high-performance liquid chromatography; UHPLC, ultra high-performance liquid chromatography; KAT II, kynurenine amino transferase II; REM, rapid eye movement.

METHODS

Animals

Pregnant, adult Wistar rats (ED 2) were obtained from Charles River Laboratories, acclimated to our animal facility, and fed laced diet (details below) beginning on ED 15. All animals were kept on a 12/12 h light-dark cycle, where Zeitgeber time (ZT) 0 corresponded to lights on and ZT 12 corresponded to lights off. The animal facility at the University of South Carolina School of Medicine is accredited by the American Association for the Accreditation of Laboratory Animal Care. All protocols were approved by the University of South Carolina Institutional Animal Care and Use Committees and were in accordance with the National Institutes of Health *Guide for the Care and Use of Laboratory Animals* (39).

EKyn Treatment

Beginning on ED 15, pregnant dams are fed a wet mash of ground control chow (ECon) or a mash of chow laced with 100 mg of kynurenine (EKyn) daily until ED 22, as previously described (25). Upon birth, dams received normal rodent chow pellets *ad libitum*. On postnatal day (PD) 21, offspring were weaned and pair-housed by sex. The offspring were weighed at PD 25, PD 35, PD 47, and PD 56, but otherwise remained experimentally undisturbed until they reached young adulthood at PD 56 (**Figure 1B**). A maximum of two rats per sex from a single prenatal litter were used within each experimental cohort to obtain a minimum $n = 4$ litters per experiment.

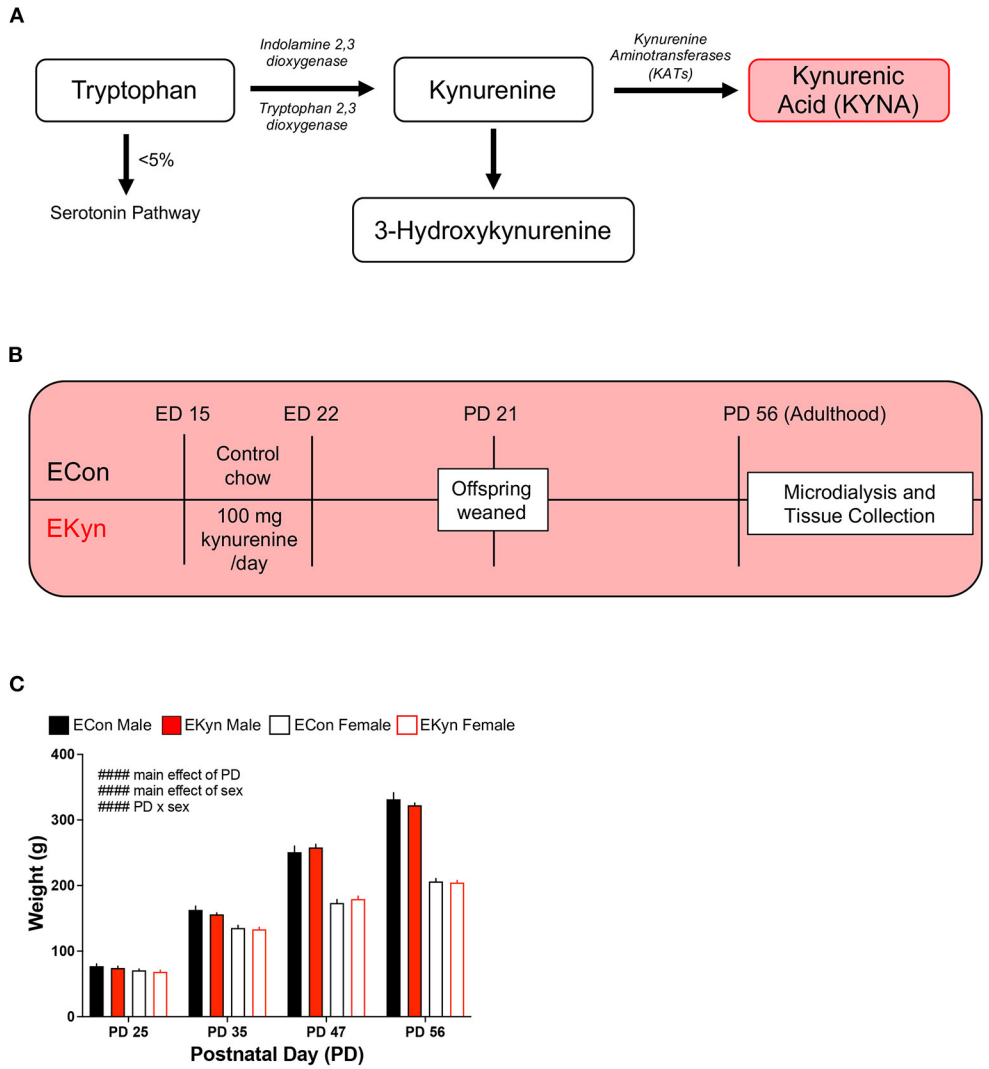

FIGURE 1 | Schematic showing the kynurenine pathway, experimental paradigm, and rat body weight across age. **(A)** A simplified schematic of the kynurenine pathway of tryptophan degradation, wherein kynurenic acid (KYNA) is synthesized from kynurenine via kynurenine aminotransferases (KATs). **(B)** EKyn experimental paradigm: pregnant rat dams are fed normal rodent chow (ECon) or rodent chow laced with 100 mg of kynurenine (EKyn) daily from embryonic day (ED) 15 to ED 22. Male and female offspring are weaned at postnatal day (PD) 21 and used in experiments at PD 56, when they reach adulthood. **(C)** Body weight of ECon and EKyn offspring at PD 25, PD 35, PD 47, and PD 56. Data are mean ± SEM. Repeated measures 3-way ANOVA effects (#### $P < 0.0001$) followed by Bonferroni's *post-hoc* test. $n = 4$–8 litters per group.

Chemicals

L-Kynurenine sulfate salt ("kynurenine," purity: 99.4%) was obtained from Sai Advantium (Hyderabad, India). All other chemicals were obtained from various suppliers but were of the highest commercially available purity.

Tissue Collection

Cohorts of offspring were euthanized via CO_2 asphyxiation at ZT 0, ZT 6, ZT 12, or ZT 18 to collect tissue. Whole trunk blood was collected into tubes containing K_3-EDTA (0.15%) and centrifuged at 300 × g for 10 min to separate plasma. Brains were promptly removed, and the hippocampus was dissected. All samples were snap frozen on dry ice and stored at −80°C until biochemical analyses.

Microdialysis

Surgery

Under isoflurane anesthesia (2–5%), animals were placed on a stereotaxic frame (Stoelting Co., Wood Dale, IL, USA). Carprofen was used as an analgesic and given at a dose of 5 mg/kg (subcutaneous) at the beginning of surgery. A guide cannula (1.0 mm outer diameter; SciPro Inc., Sanborn, NY, USA) was positioned over the dorsal hippocampus (AP: −3.4, LM: ± 2.3, DV: −1.5 from bregma after coordinates) and anchored in place using two surgical screws inserted into 0.5 mm burr

holes and acrylic dental cement. After 24–48 h of post-operative recovery, microdialysis experiments were initiated in freely moving animals.

Extracellular Fluid Collection by *in vivo* Microdialysis

Special attention was given to time of day of microdialysis experiments and experimental efforts were made to collect microdialysate for up to 24 h. To control for the contribution of the experimental start time, cohorts of animals were initiated with microdialysis perfusion at ZT 3, ZT 6, ZT 9, or ZT 22.5. On the day of microdialysis, a probe (2 mm PES membrane/14 mm shaft, 6 kD; SciPro Inc.) was inserted through the guide cannula in freely moving animals and a microperfusion pump (Harvard Apparatus, Holliston, MA, USA) set to a flow rate of 2.5 μL/min perfused Ringer solution (147 mM NaCl, 4 mM KCl, 1.4 mM $CaCl_2$) through the probe inlet. After 30 min, the flow was reduced to 1.0 μL/min for the duration of the experiment. Collection of dialysate samples began 2 h after the onset of perfusion for KYNA analysis. Glutamate and GABA were analyzed in dialysate samples collected at 4 h after the onset of perfusion, to achieve stable neurotransmitter levels (40). Extracellular KYNA, glutamate, and GABA were analyzed from the same hour fractions and analysis of data was divided by light phase fractions (ZT 0 – ZT 12) and dark phase fractions (ZT 12 – ZT 24). Samples were stored at −80°C until biochemical analyses.

At the end of the experiment, the probe was removed, and each animal was anesthetized using isoflurane, decapitated via guillotine, and the brain was carefully removed and dropped in a 10% formalin solution. Brains were moved step-wise to 20% sucrose before processing with 25–30 μm thick coronal cryostat section that were stained in neutral red to check proper microdialysis cannula placement (**Supplementary Figure 1**).

Biochemical Analysis

Plasma and Brain (Tryptophan, Kynurenine, KYNA)

On the day of biochemical analyses, plasma samples were thawed, diluted (1:1000 for tryptophan, 1:10 for kynurenine and KYNA), acidified with 6% perchloric acid, and centrifuged at 12,000 × g for 10 min. The hippocampus was weighed, diluted 1:5 (w/v) with ultrapure water, and homogenized with a sonicator. Protein was evaluated in the stock homogenate using the previously published Lowry method (41). A portion of the remaining hippocampal homogenate was further diluted with ultrapure water to a final concentration of 1:10, acidified using 25% perchloric acid, and centrifuged at 12,000 × g for 10 min.

Acidified plasma samples were evaluated for tryptophan, kynurenine, and KYNA and hippocampal samples were evaluated for KYNA by high-performance liquid chromatography (HPLC) analysis as previously described (26). Briefly, 20 μL of supernatant was injected into a ReproSil-Pur C18 column (4 × 150 mm; Dr. Maisch Gmbh, Ammerbuch, Germany) using a mobile phase of 50 mM sodium acetate, pH adjusted to 6.2 with glacial acetic acid, and 5% acetonitrile at a flow rate of 0.5 mL/min. A post column addition of 500 mM zinc acetate at a flow rate of 0.1 mL/min was used to fluorometrically detect tryptophan [excitation (ex): 285, emission (em): 365, retention time (rt): 11 min], kynurenine (ex: 365, em: 480, rt: 6 min), and KYNA (ex: 344, em: 398, rt: 11 min) in the eluate (Alliance, 2,475 fluorescence detector; Waters, Bedford, MA, USA). Data was analyzed using Empower 3 software (Waters).

Microdialysate (KYNA)

Extracellular KYNA was assessed by diluting the microdialysate sample 1:2 in ultrapure water and subjecting to fluorometric HPLC, as described above. Microdialysis data were not corrected for recovery from dialysis probe.

Microdialysate (Glutamate/GABA)

Extracellular glutamate and GABA from microdialysis samples were assessed using electrochemical ultra-high-performance liquid chromatography (UHPLC) ALEXYS analyzer with a Decade Elite detector (Antec Scientific, Zoeterwoude, Netherlands). Briefly, 9 μL of undiluted microdialysate was injected into a HSS T3 column (1.0 × 50 mm; Waters) using a step gradient elution comprised of the first mobile phase (base solution: 50 mM phosphoric acid, 50 mM citric acid, and 0.1 mM EDTA at a pH of 3.5) and 2% acetonitrile followed by the second mobile phase made from base solution and 50% acetonitrile. Each mobile phase is delivered at a flow rate of 200 μL/min. An in-needle derivatization added 5 μL of *o*-phthaldialdehyde reagent before eluting through the column. A VT03 microflow cell with a 0.7 mm glassy carbon working electrode was used for electrochemical detection (42). Data was acquired using Clarity 8 software (DataApex, Prague, Czech Republic). Microdialysis data were not corrected for recovery from dialysis probe.

Statistical Analysis

All statistical analyses were performed using Prism 9.0 (GraphPad Software, San Diego, CA, USA), and all results and samples sizes are shown in statistical tables (**Supplementary Materials**). Weight data were averaged across litters and assessed by 3-way repeated measures ANOVA with EKyn treatment, age, and sex as between-subject factors. Separate analyses by sex were performed by 2-way repeated measures ANOVA with EKyn treatment and age as between-subject factors. From weight data, Bonferroni's *post hoc* test was used for multiple comparisons. Plasma and brain metabolite data were averaged across litters and assessed by 3-way ANOVA with EKyn treatment, sex, and ZT as between-subject factors. Separate analyses by sex were performed by 2-way ANOVA with EKyn treatment and ZT as between-subject factors. Microdialysis data were averaged across litter depending on the start time of the experiment, with groups divided by early-light (ZT 3), mid-light (ZT 6), late-light (ZT 9), and late-dark (ZT 22.5). Samples below the limit of detection for individual analytes were not included in those respective analyses. Microdialysis data were analyzed separately by phase by 3-way ANOVA with EKyn treatment, sex, and ZT as between-subject factors. Separate analysis by sex was performed in each phase by 2-way ANOVA with EKyn treatment and ZT as between-subject factors. Analyses were followed up by appropriate 2-way interactions. Uncorrected Fisher's LSD was used for multiple comparisons in analysis of biochemical data. Statistical significance was defined as $P < 0.05$.

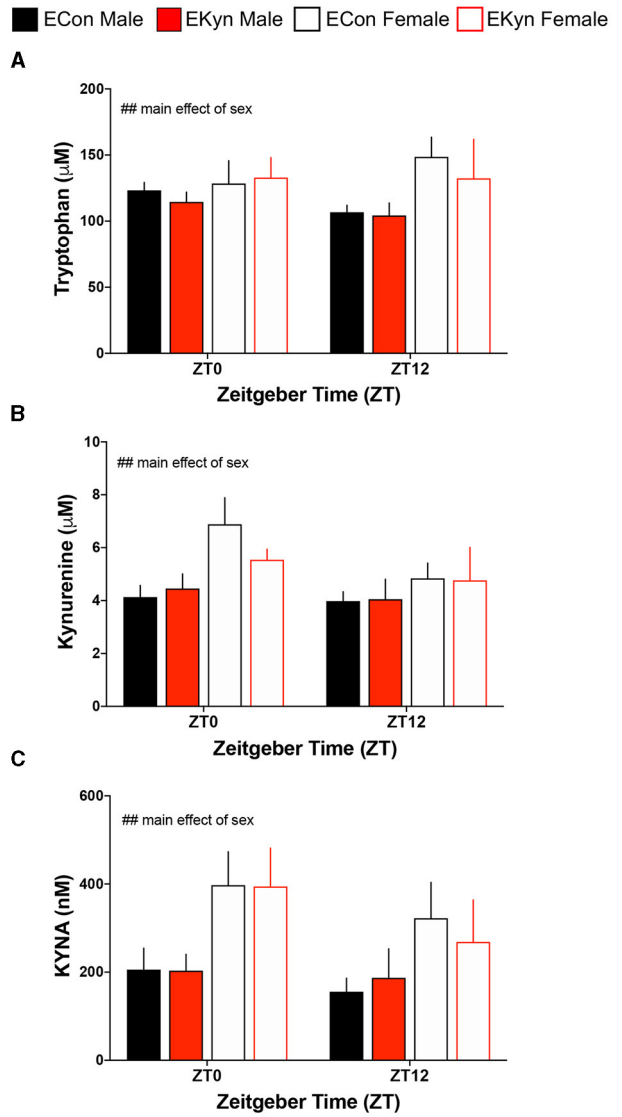

FIGURE 2 | Prenatal KYNA elevation elicits no changes in peripheral kynurenine pathway metabolism in young adult male EKyn. **(A)** Plasma tryptophan. **(B)** Plasma kynurenine. **(C)** Plasma KYNA. All data are mean ± SEM. Three-way ANOVA analyses effects: ## $P < 0.01$. $n = 3$–9 litters per group.

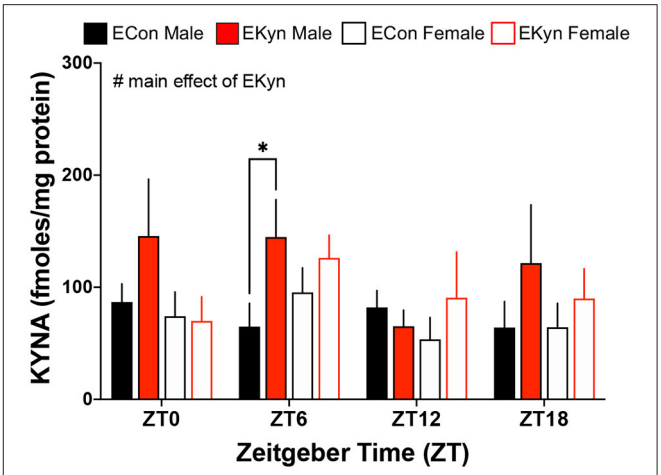

FIGURE 3 | Prenatal KYNA increases hippocampal KYNA in young adult male EKyn offspring. Hippocampal KYNA. All data are mean ± SEM. Three-way ANOVA analyses effects: # $P < 0.05$. 2-way ANOVA analyses by sex followed by Fisher's LSD *post-hoc* test: *$P < 0.05$. $n = 4$–12 litters per group.

RESULTS

Sex, but Not Prenatal KYNA Elevation, Influences the Weight of EKyn and ECon Offspring

To determine if elevated prenatal KYNA exposure impacts the body weight of offspring during adolescence and young adulthood, we weighed EKyn and ECon offspring at PD 25, PD 35, PD 47, and PD 56. We determined main effects of postnatal day ($F_{3,48} = 795.8$, $P < 0.0001$) and sex ($F_{1,48} = 1906$, $P < 0.0001$) and a significant postnatal day x sex interaction ($F_{3,48} = 474.7$, $P < 0.0001$) (**Figure 1C**). The body weight of males was consistently greater than females from PD 35, and this difference steadily increased across postnatal development. Of importance, body weight was not impacted by prenatal KYNA elevation in male or female offspring, complementing what has been previously described only in males (34).

Hippocampal KYNA Levels, but Not Peripheral KP Metabolites, Are Elevated in Young Adult EKyn Offspring

To evaluate circadian dynamics of KP metabolism, we first measured peripheral and hippocampal KP metabolites at specific time points during the light and dark phases. Plasma tryptophan (**Figure 2A**), kynurenine (**Figure 2B**), and KYNA (**Figure 2C**) were not impacted by EKyn treatment at the beginning of the light phase, ZT 0, or at the beginning of the dark phase, ZT 12. Peripheral metabolites tryptophan ($F_{1,40} = 7.658$, $P = 0.0085$), kynurenine ($F_{1,41} = 7.640$, $P = 0.0085$), and KYNA ($F_{1,41} = 11.53$, $P = 0.0015$) were significantly impacted by sex, as we determined that females had elevated metabolites compared to males. Hippocampal KYNA was significantly impacted by EKyn treatment ($F_{1,107} = 4.879$, $P = 0.0293$), with increased KYNA in hippocampal tissue in EKyn across the light phase, and *post-hoc* in EKyn males at ZT6 compared to ECon ($P = 0.0500$; **Figure 3**).

Prenatal KYNA Elevation Elicits an Increase in Extracellular KYNA Levels During the Light Phase in the Dorsal Hippocampus of Young Adult EKyn Males

To more precisely investigate circadian-dependent alterations in KYNA levels, we analyzed extracellular KYNA in the dorsal hippocampus of EKyn and ECon young adult offspring. During the light phase, extracellular KYNA was impacted by a main effect of EKyn treatment ($F_{1,207} = 10.62$, $P = 0.0013$ and a sex x EKyn treatment interaction ($F_{1,207} = 10.01$, $P = 0.0018$) (**Figure 4A**).

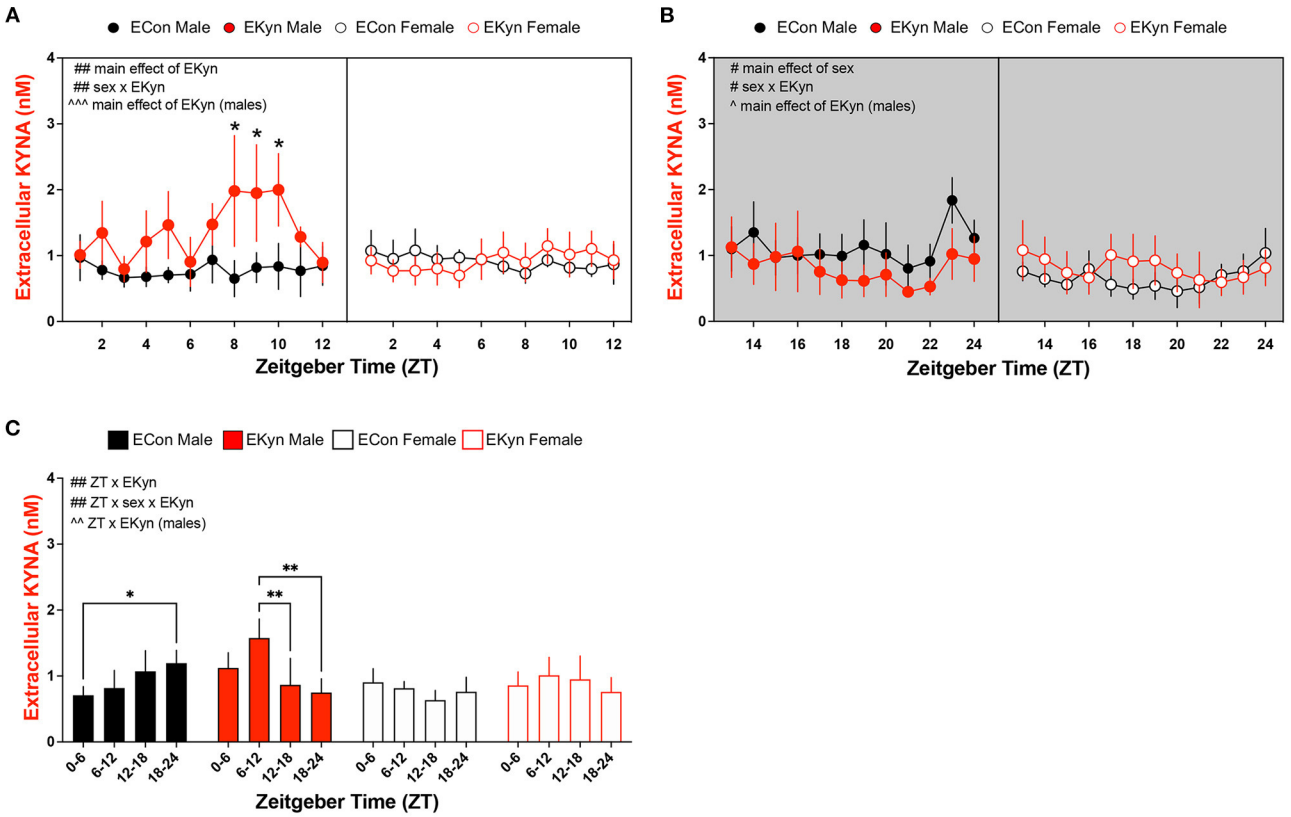

FIGURE 4 | Extracellular KYNA in the hippocampus is increased during the light phase and decreased during the dark phase in EKyn male offspring. Microdialysis in the dorsal hippocampus was conducted in young adult offspring, with special attention given to the time of day. Data are represented by phase, wherein light phase denotes ZT 0–12 and dark phase denotes ZT 12–24. **(A)** Light phase. **(B)** Dark phase. **(C)** Analysis of 6-h bins across light and dark phase. Data are mean ± SEM. 3-way ANOVA analyses effects: # $P < 0.05$, ## $P < 0.01$. 2-way ANOVA analyses by sex effects: ^$P < 0.05$, ^^$P < 0.01$, ^^^$P < 0.001$. Fishers LSD *post-hoc* test: *$P < 0.05$, **$P < 0.01$. $n = 4$–8 litters per group.

In males, extracellular KYNA was significantly influenced by EKyn treatment ($F_{1,87} = 13.39$, $P = 0.0004$), and EKyn males experienced elevated extracellular KYNA in the latter half of the light phase (ZT 8, $P = 0.0282$; ZT 9, $P = 0.0312$; ZT 10, $P = 0.0367$). Extracellular KYNA in female EKyn offspring, however, remained unchanged compared to female ECon offspring in the light phase. Within the dark phase, extracellular KYNA was significantly impacted by a main effect of sex ($F_{1,160} = 6.635$, $P = 0.0109$) and a sex x EKyn treatment interaction ($F_{1,160} = 6.744$, $P = 0.0103$) (**Figure 4B**). In males, extracellular KYNA was reduced in the EKyn group ($F_{1,68} = 4.556$, $P = 0.0364$), but not altered in EKyn females compared to controls. We also analyzed averaged 6-h bins of microdialysis data to evaluate the contribution of early light phase (ZT 0–6), late light phase (ZT 6–12), early dark phase (ZT 12–18) or late dark phase (ZT 18–24) on extracellular KYNA levels. We determined that extracellular KYNA was impacted by a significant ZT x EKyn treatment interaction ($F_{3,46} = 6.364$, $P = 0.0011$) and a three-way ZT x sex x EKyn treatment interaction ($F_{3,46} = 5.242$, $P = 0.0034$) (**Figure 4C**). When analyses were separated by sex, we determined in males that extracellular KYNA was impacted by a ZT x EKyn treatment interaction ($F_{3,19} = 5.279$, $P = 0.0081$). In ECon males, extracellular KYNA was elevated at the end of the dark phase when compared to the light phase (ZT 18–24 vs. ZT 0–6, $P = 0.0440$), while in EKyn males extracellular KYNA was reduced across the entire dark phase when compared to the light phase (ZT 12–18 vs. ZT 6–12, $P = 0.0091$; ZT 18–24 vs. ZT 6–12, $P = 0.0038$). In females, extracellular KYNA was not influenced by EKyn treatment or time of day.

Reduced Extracellular Glutamate in Young Adult EKyn Offspring

To test the hypothesis that elevated KYNA influences neurotransmitter levels, we evaluated levels of extracellular glutamate and GABA in EKyn and ECon offspring in the dorsal hippocampus. EKyn treatment significantly influenced extracellular glutamate during the light phase ($F_{1,311} = 6.984$, $P = 0.0086$) (**Figure 5A**). EKyn males, in particular, had reduced extracellular glutamate during the light phase when compared to controls ($F_{1,113} = 8.616$, $P = 0.0040$), but this reduction was not present in EKyn females. In the dark phase, extracellular

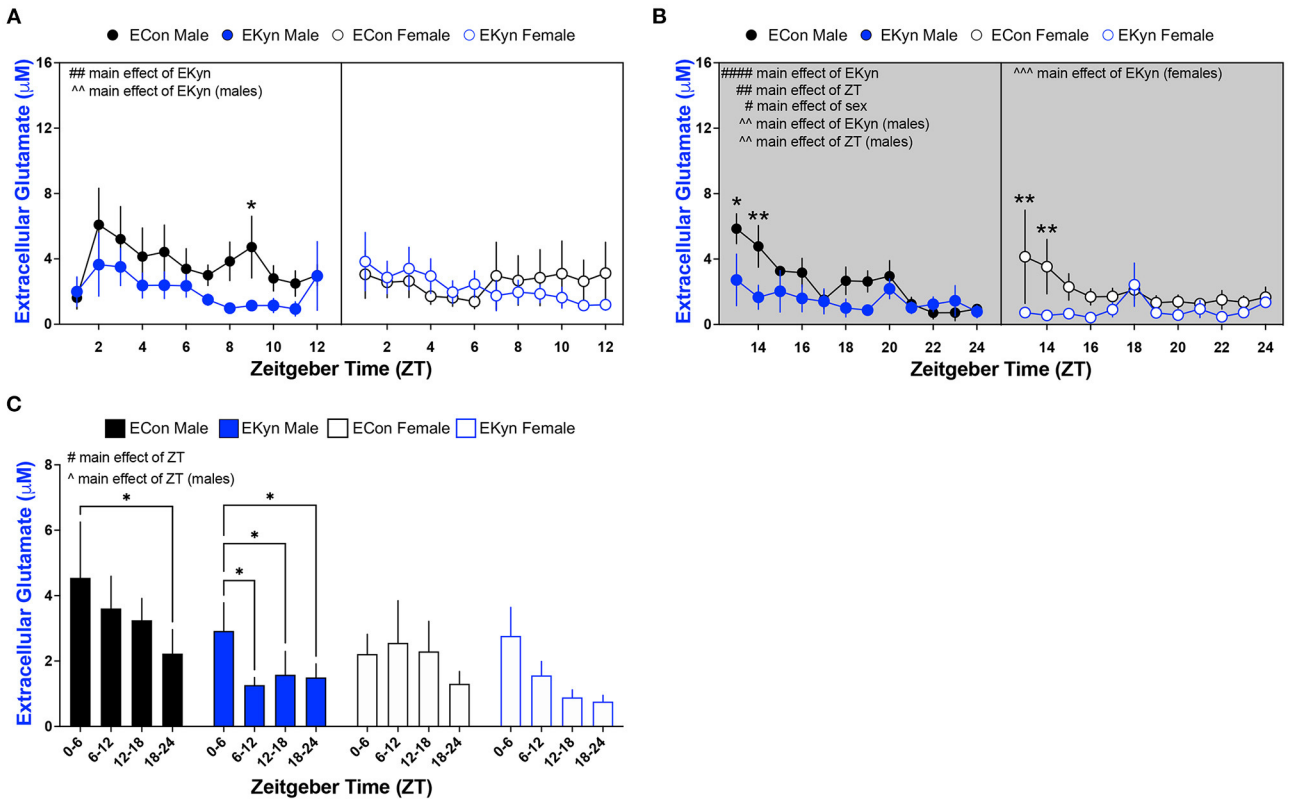

FIGURE 5 | Light phase- and sex-dependent alterations in extracellular glutamate in the hippocampus of young adult offspring exposed to elevated prenatal KYNA. Microdialysis in the dorsal hippocampus was conducted in young adult offspring, with special attention given to the time of day. Data are represented by phase, wherein light phase denotes ZT 0–12 and dark phase denotes ZT 12–24. **(A)** Light phase. **(B)** Dark phase. **(C)** Analysis of 6 - h bins across light and dark phase. Data are mean ± SEM. 3-way ANOVA analyses effects: # $P < 0.05$, ## $P < 0.05$, #### $P < 0.0001$. 2-way ANOVA analyses by sex effects: ^$P < 0.05$, ^^$P < 0.01$. ^^^$P < 0.001$. Fishers LSD *post-hoc* test: *$P < 0.05$, **$P < 0.01$. n = 5–12 litters per group.

glutamate was significantly impacted by main effects of ZT ($F_{11,179} = 2.941$, $P = 0.0013$), EKyn treatment ($F_{1,179} = 22.40$, $P < 0.0001$), and sex ($F_{1,179} = 6.416$, $P = 0.0122$) (**Figure 5B**). Glutamate was reduced by the end of the dark phase in male and female ECon and EKyn offspring, and lower in females than in males. Further, we determined that EKyn treatment resulted in reduced extracellular glutamate in both male ($F_{1,71} = 9{,}772$, $P = 0.0026$) and female ($F_{1,108} = 13.77$, $P = 0.0003$) offspring compared to counterpart ECon in the dark phase. The time of day, ZT, impacted extracellular glutamate levels in EKyn males during the dark phase ($F_{11,71} = 2.917$, $P = 0.0032$). When we evaluated averaged 6-h bins, we determined that the time of day significantly influenced extracellular glutamate ($F_{3,68} = 4.034$, $P = 0.0106$) (**Figure 5C**). EKyn males sustained reduced glutamate after ZT 6 (ZT 6–12 vs. ZT 0–6, $P = 0.0303$; ZT 12–18 vs. ZT 0–6, $P = 0.0318$; ZT 18–24 vs. ZT 0–6, $P = 0.0258$) and EKyn females after ZT 12 (ZT 12–18 vs. ZT 0–6, $P = 0.0422$; ZT 18–24 vs. ZT 0–6, $P = 0.0460$) when compared to the first 6 h of the light phase.

Prenatal KYNA Elevation Elicits Sex-Dependent Changes in Extracellular GABA in Young Adult Offspring

Lastly, we determined conspicuous disturbances in extracellular GABA in the hippocampus of young adult EKyn offspring. In the light phase, extracellular GABA was influenced by a main effect of sex ($F_{1,256} = 32.54$, $P < 0.0001$), but not time of day or EKyn treatment (**Figure 6A**). However, in the dark phase, we determined significant main effects of EKyn treatment ($F_{11,166} = 7.170$, $P = 0.0082$) and sex ($F_{1,166} = 4.213$, $P = 0.0417$), and a significant sex x EKyn treatment interaction ($F_{1,166} = 9.017$, $P = 0.0031$) (**Figure 6B**). Male EKyn offspring had reduced extracellular GABA when compared to controls ($F_{1,76} = 23.00$, $P < 0.0001$) in the dark phase. When 6-h bins were evaluated, we determined that extracellular GABA levels were significantly impacted by sex ($F_{1,31} = 6.548$, $P = 0.0156$), such that extracellular GABA was reduced in females compared to males (**Figure 6C**).

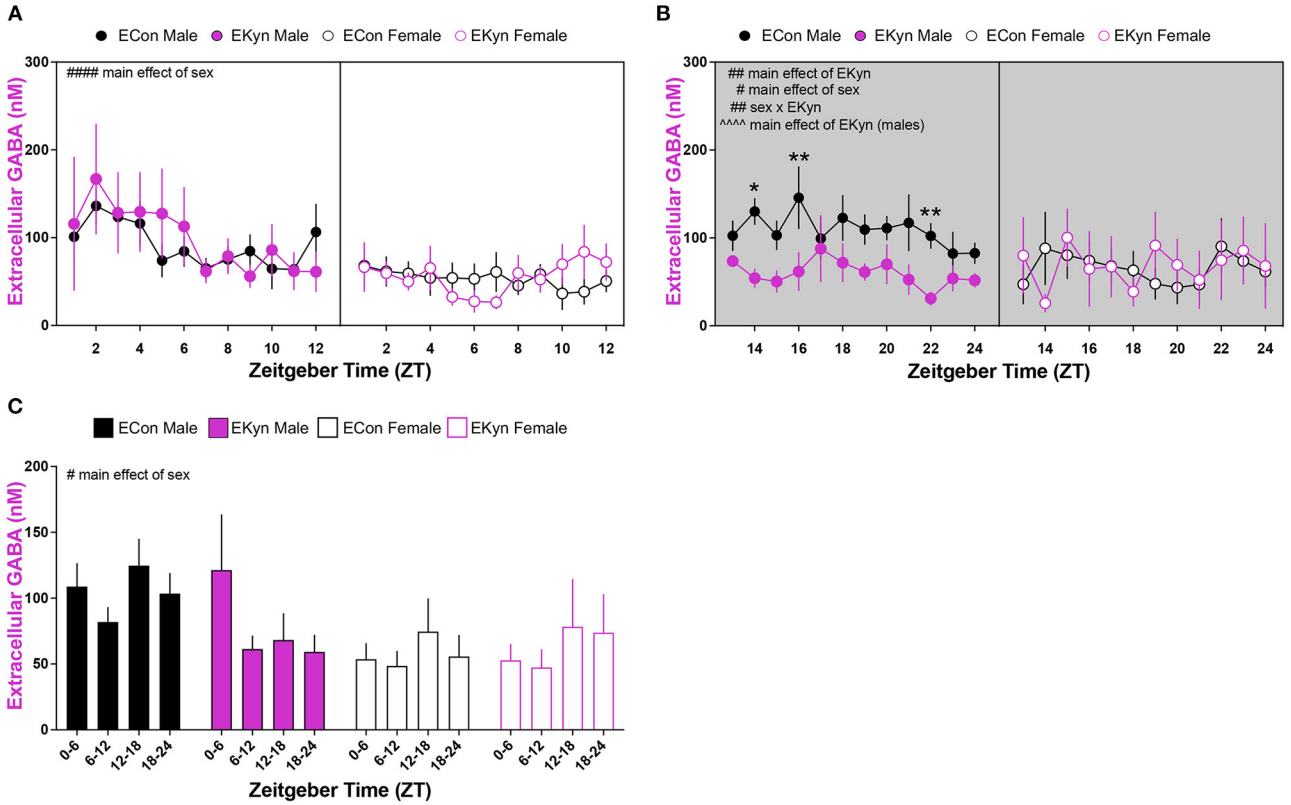

FIGURE 6 | Reduced extracellular GABA levels in the hippocampus during the dark phase in young adult male EKyn. Microdialysis in the dorsal hippocampus was conducted in young adult offspring, with special attention given to the time of day. Data are represented by phase, wherein light phase denotes ZT 0–12 and dark phase denotes ZT 12–24. **(A)** Light phase. **(B)** Dark phase. **(C)** Analysis of 6-hour bins across light and dark phase. Data are mean ± SEM. 3-way ANOVA analyses effects: # $P < 0.05$, ## $P < 0.01$, #### $P < 0.0001$. 2-way ANOVA analyses by sex effects: ^^^^$P < 0.0001$. Uncorrected Fishers LSD *post-hoc* test: *$P < 0.05$, **$P < 0.01$. $n = 4$–11 litters per group.

DISCUSSION

We presently confirmed that prenatal KYNA elevation results in elevated tissue KYNA levels and extracellular KYNA levels in the hippocampus of young adult male EKyn offspring (21, 25, 26). Of interest, our current focus extensively evaluated the contribution of the time of day of experimentation, while also expanding our understanding of biochemical dynamics in both sexes of EKyn offspring. Our results reinforce previous findings that the long term consequences of prenatal KYNA elevation manifest in the attenuation of glutamate levels in the rat hippocampus (21) and complement our recent characterization of sex-dependent diurnal changes in sleep and arousal behaviors in EKyn offspring (27). As no differences in weight were observed between EKyn and control offspring, we presently provide critical evidence, in both sexes, that the reported long-term manifestation of prenatal KYNA elevation are not attributed to body weight differences.

Consistent with our previous evaluation of KP metabolites in the plasma of EKyn offspring (26, 27), plasma tryptophan, kynurenine, and KYNA remained unchanged between experimental groups at ZT 0 and ZT 12. Within the brain however, KYNA levels in dissected hippocampal tissue were significantly elevated in male EKyn offspring during the middle of the light phase (ZT 6), supporting our findings from previous studies evaluating brain tissue KYNA content in EKyn compared to ECon offspring (25–27, 33). We presently selected the time points that correspond to transitions between the light and dark phases for rodents, as we previously studied time points that corresponded to the middle of the light and dark phases for rodents (27). As such, we determined that female offspring had conspicuously higher tryptophan, kynurenine, and KYNA levels in the plasma compared to males. However, levels of KP metabolites in the periphery did not serve as strong predictors for the observed changes in brain KYNA, though perhaps limited by time intervals of plasma sampling in our animals. As brain KP metabolism is uniquely regulated (43), peripheral KP metabolism in clinical studies especially may limit the understanding of changes in the central nervous system (5, 7, 15, 44).

Notably, KYNA in the hippocampus, both tissue content and extracellular levels, were elevated in male EKyn offspring during the light phase, followed by a sustained decrease in levels during the dark phase. KYNA elevation during the light phase corresponds to evolutionarily conserved circadian

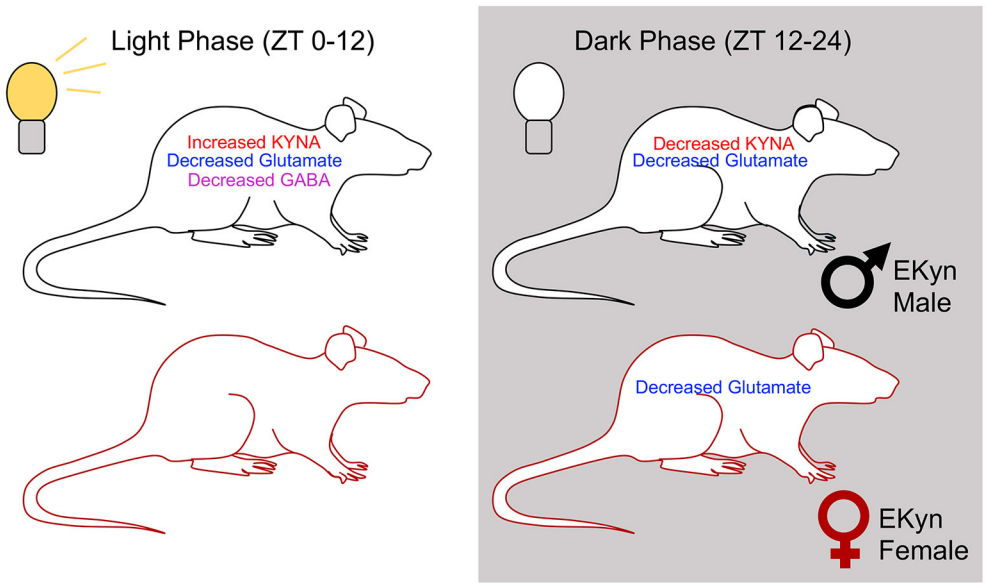

FIGURE 7 | Summary figure representing overall trends in extracellular concentrations of KYNA, glutamate, and GABA in EKyn males and females across the two light phases.

rhythmicity of tryptophan catabolism in rodents and humans (38, 45). This diurnal pattern of KYNA modulation in EKyn male offspring corresponds with concurrent glutamate attenuation across the light and first 4 h of the dark phase yet sustained normal levels of the neurotransmitter during the latter half of the dark phase. Most notably, when extracellular hippocampal KYNA levels decrease from ZT 18 to ZT 24 in EKyn males, extracellular glutamate stabilizes to levels comparable to ECon males, suggesting that KYNA levels are influencing extracellular glutamate fluctuations. This notion is supported by evidence that acute elevations of KYNA, in a dose-dependent manner, result in locally reduced glutamate levels in several brain regions, including the hippocampus (18, 46), and further reinforced by restoration of glutamate levels when KYNA levels are modulated via kynurenine amino transferase II (KAT II) inhibition or the α7nACh positive allosteric modulator, galantamine (18, 19, 47, 48). Pharmacological intervention with galantamine or a KAT II inhibitor has also been shown to restore cognitive flexibility and glutamate levels in offspring exposed to elevated KYNA during neurodevelopment, further supporting the notion that these neurochemical alterations are related to the neuromodulatory properties of KYNA (19, 21).

In adult female EKyn offspring, extracellular KYNA was not elevated extracellularly. However, glutamate levels were found to be reduced during the first 6 h of the dark phase compared to counterpart controls. It is important to note that the exact relationship between KYNA and its impact on extracellular neurotransmitters in females specifically remains understudied, as most acute, dose-response pharmacological studies have been conducted only in male rodents (18, 40, 46, 49, 50). Attenuated glutamate levels in EKyn offspring could be related to changes in local synaptic connections and dendritic morphology in adult animals exposed to high levels of KYNA during neurodevelopment (23, 24, 33, 34). Conspicuously, the alterations in glutamate presently characterized may shed insight on our recent determination of altered arousal patterns in female EKyn offspring, specifically reduced home cage activity and prolonged bouts of wakefulness during the dark phase (27). Aside from glutamate levels, future studies will be critical to determine if EKyn offspring suffer from an overall reduction of neurotransmission which may thereby influence the array of neurocognitive impairments determined in these animals (21, 25, 26, 34, 35).

In parallel to the observed diurnal fluctuations in glutamate, we determined a phase-dependent decrease in hippocampal GABA levels in EKyn male offspring compared to controls. These results are consistent with previous findings where acute local KYNA elevation dose-dependently decreases extracellular GABA levels in the brain (40). Yet curiously, in our EKyn paradigm, GABA levels are reduced in male offspring transiently, in a phase-dependent manner, after the late light phase elevation in KYNA levels. The temporal delay and alteration in extracellular GABA in the absence of elevated KYNA levels could potentially be explained by a transient disinhibition of α7nACh receptor activation on GABAergic interneurons from the stratum radiatum, which could create a $GABA_A$ receptor-mediated negative feedback loop (51). Relating these present findings to the sleep and behavioral changes reported in male EKyn offspring, we speculate that reduced extracellular hippocampal GABA concentrations toward the end of the dark phase could be related to aberrant rapid eye movement (REM) sleep and contextual memory impairment observed in male EKyn offspring. REM sleep is tightly regulated by afferent medial septal GABAergic projections to the hippocampus, and when

silenced, block the consolidation of contextual memory during REM sleep (37, 52). Interestingly, female EKyn offspring do not exhibit reduced GABA levels compared to their male EKyn counterparts, which may also be related to sex-specific changes in behavior and arousal previously reported (26, 27). However, sparse information exists on neurochemical profiles of female rats from studies using neurodevelopmental manipulations. Thereby, we presently provide novel information regarding hippocampal KYNA, GABA, and glutamate levels, while considering sex as a biological variable (See **Figure 7**).

As individuals with SZ and BD have elevated levels of KYNA in the brain (5, 11, 15), the enhanced KYNA found in the brain of adult EKyn rats presents critical translational value to investigate the longstanding ability of KYNA to influence multiple neuromodulatory systems implicated in the pathology of psychotic disorders. As described presently, several impairments observed in adult EKyn rats resemble hallmark neurochemical and behavioral deficits found in individuals with psychotic disorders including SZ and BD (53–57). EKyn rats exhibit neurochemical changes in hippocampal glutamate levels, analogous to reduced temporal lobe glutamate levels reported clinically (53, 55, 56). In patients with psychotic disorders, glutamatergic and GABAergic deficits have been linked to impairments in working and association memory, as well as increased risk for presentation of negative symptoms (58, 59).

Our findings also parallel neurochemical alterations observed in other prenatal insult paradigms that attempt to capture pathophysiological alterations common to psychotic disorders (30, 60–63). The contribution of each individual prenatal litter is an important consideration in studies like ours, and albeit a small sample size compared to clinical investigations, our results provide novel mechanistic insights regarding the neurodevelopmental implications for elevated KYNA and its impact on hippocampal excitatory and inhibitory neuromodulation. A misbalance of gating through excitation and inhibition is postulated to form the basis for cognitive and behavioral disturbances (64). Imbalances observed in GABA and glutamate levels may also be applicable to neurodevelopmental disorders such as autism spectrum disorders, where reduced GABA and glutamate levels are found in specific frontal, thalamic, and striatal brain regions (65, 66). Ultimately, the deficits in glutamatergic and GABAergic neuromodulation in relation to KYNA elevation in EKyn young adult offspring bridge our understanding between KYNA and neuromodulatory deficits which may contribute to the observed impairments in cognition, sleep, and arousal (21, 26, 27). In conclusion, sex-specific neurochemical changes observed in this study highlight the importance of evaluating sex as a biological variable when considering therapeutics strategies, including inhibition of KAT II to inhibit KYNA synthesis (48, 67, 68), and improve behavioral dysfunction and clinical outcomes for individuals suffering from psychiatric disorders.

DATA AVAILABILITY STATEMENT

The raw data supporting the conclusions of this article will be made available by the authors, without undue reservation.

ETHICS STATEMENT

The animal study was reviewed and approved by Institutional Animal Care and Use Committees and were in accordance with the National Institutes of Health Guide for the Care and Use of Laboratory Animals at the University of South Carolina.

AUTHOR CONTRIBUTIONS

CW: conducted research, formal analysis, writing – original draft, writing – review & editing, visualization, and project administration. KR: conducted research, methodology, formal analysis, writing – original draft, writing – review & editing, and visualization. NW and AL: conducted research and writing – review & editing. SB: conceptualization, methodology, and writing – review & editing. AP: conceptualization, methodology, formal analysis, writing – original draft, writing – review & editing, visualization, supervision, project administration, and funding acquisition. All authors contributed to the article and approved the submitted version.

FUNDING

This work was funded by the National Institutes of Health Grant Nos. NIH R01 NS102209, P50 MH103222, and support from the University of South Carolina (Magellan Scholar) and the University of South Carolina Honors College (Science Undergraduate Research Fellowships).

ACKNOWLEDGMENTS

The authors would like to acknowledge Hayley Nicholson for her excellent assistance with histological analysis.

SUPPLEMENTARY MATERIAL

The Supplementary Material for this article can be found online at: https://www.frontiersin.org/articles/10.3389/fpsyt.2021.734984/full#supplementary-material

REFERENCES

1. Bowers MB Jr, Heninger GR, Sternberg D, Meltzer HY. Clinical processes and central dopaminergic activity in psychotic disorders. *Commun Psychopharmacol.* (1980) 4:177–83.
2. Tsapakis EM, Travis MJ. Glutamate and psychiatric disorders. *Adv Psychiatr Treatment.* (2002) 8:189–97. doi: 10.1192/apt.8.3.189
3. Wang J, Tang Y, Zhang T, Cui H, Xu L, Zeng B, et al. Reduced gamma-Aminobutyric acid and glutamate+glutamine levels in drug-naive patients

with first-episode schizophrenia but not in those at ultrahigh risk. *Neural Plast.* (2016) 2016:3915703. doi: 10.1155/2016/3915703
4. Wenneberg C, Glenthoj BY, Glenthoj LB, Fagerlund B, Krakauer K, Kristensen TD, et al. Baseline measures of cerebral glutamate and GABA levels in individuals at ultrahigh risk for psychosis: implications for clinical outcome after 12 months. *Eur Psychiatry.* (2020) 63:e83. doi: 10.1192/j.eurpsy.2020.77
5. Erhardt S, Blennow K, Nordin C, Skogh E, Lindstrom LH, Engberg G. Kynurenic acid levels are elevated in the cerebrospinal fluid of patients with schizophrenia. *Neurosci Lett.* (2001) 313:96–98. doi: 10.1016/S0304-3940(01)02242-X
6. Schwarcz R, Rassoulpour A, Wu HQ, Medoff D, Tamminga CA, Roberts RC. Increased cortical kynurenate content in schizophrenia. *Biol Psychiatry.* (2001) 50:521–30. doi: 10.1016/S0006-3223(01)01078-2
7. Nilsson LK, Linderholm KR, Engberg G, Paulson L, Blennow K, Lindstrom LH, et al. Elevated levels of kynurenic acid in the cerebrospinal fluid of male patients with schizophrenia. *Schizophr Res.* (2005) 80:315–22. doi: 10.1016/j.schres.2005.07.013
8. Miller CL, Llenos IC, Dulay JR, Weis S. Upregulation of the initiating step of the kynurenine pathway in postmortem anterior cingulate cortex from individuals with schizophrenia and bipolar disorder. *Brain Res.* (2006) 1073–1074:25–37. doi: 10.1016/j.brainres.2005.12.056
9. Sathyasaikumar KV, Stachowski EK Wonodi I, Roberts RC, Rassoulpour A, Mcmahon RP, et al. Impaired kynurenine pathway metabolism in the prefrontal cortex of individuals with schizophrenia. *Schizophr Bull.* (2011) 37:1147–56. doi: 10.1093/schbul/sbq112
10. Linderholm KR, Skogh E, Olsson SK, Dahl ML, Holtze M, Engberg G, et al. Increased levels of kynurenine and kynurenic acid in the CSF of patients with schizophrenia. *Schizophr Bull.* (2012) 38:426–32. doi: 10.1093/schbul/sbq086
11. Hilmas C, Pereira EF, Alkondon M, Rassoulpour A, Schwarcz R, Albuquerque EX. The brain metabolite kynurenic acid inhibits alpha7 nicotinic receptor activity and increases non-alpha7 nicotinic receptor expression: physiopathological implications. *J Neurosci.* (2001) 21:7463–73. doi: 10.1523/JNEUROSCI.21-19-07463.2001
12. Schwarcz R, Bruno JP, Muchowski PJ, Wu HQ. Kynurenines in the mammalian brain: when physiology meets pathology. *Nat Rev Neurosci.* (2012) 13:465–77. doi: 10.1038/nrn3257
13. Flores-Barrera E, Thomases DR, Cass DK, Bhandari A, Schwarcz R, Bruno JP, et al. Preferential disruption of prefrontal GABAergic function by nanomolar concentrations of the alpha7nACh negative modulator kynurenic acid. *J Neurosci.* (2017) 37:7921–9. doi: 10.1523/JNEUROSCI.0932-17.2017
14. Nakazawa K, Sapkota K. The origin of NMDA receptor hypofunction in schizophrenia. *Pharmacol Ther.* (2020) 205:107426. doi: 10.1016/j.pharmthera.2019.107426
15. Sellgren CM, Kegel ME, Bergen SE, Ekman CJ, Olsson S, Larsson M, et al. A genome-wide association study of kynurenic acid in cerebrospinal fluid: implications for psychosis and cognitive impairment in bipolar disorder. *Mol Psychiatry.* (2016) 21:1342–50. doi: 10.1038/mp.2015.186
16. Chess AC, Simoni MK, Alling TE, Bucci DJ. Elevations of endogenous kynurenic acid produce spatial working memory deficits. *Schizophrenia bulletin.* (2007) 33:797–804. doi: 10.1093/schbul/sbl033
17. Chess AC, Landers AM, Bucci DJ. L-kynurenine treatment alters contextual fear conditioning and context discrimination but not cue-specific fear conditioning. *Behav Brain Res.* (2009) 201:325–31. doi: 10.1016/j.bbr.2009.03.013
18. Pocivavsek A, Wu HQ, Potter MC, Elmer GI, Pellicciari R, Schwarcz R. Fluctuations in endogenous kynurenic acid control hippocampal glutamate and memory. *Neuropsychopharmacology.* (2011) 36:2357–67. doi: 10.1038/npp.2011.127
19. Alexander KS, Wu HQ, Schwarcz R, Bruno JP. Acute elevations of brain kynurenic acid impair cognitive flexibility: normalization by the alpha7 positive modulator galantamine. *Psychopharmacology.* (2012) 220:627–37. doi: 10.1007/s00213-011-2539-2
20. Liu XC, Holtze M, Powell SB, Terrando N, Larsson MK, Persson A, et al. Behavioral disturbances in adult mice following neonatal virus infection or kynurenine treatment–role of brain kynurenic acid. *Brain Behav Immun.* (2014) 36:80–9. doi: 10.1016/j.bbi.2013.10.010
21. Pocivavsek A, Elmer GI, Schwarcz R. Inhibition of kynurenine aminotransferase II attenuates hippocampus-dependent memory deficit in adult rats treated prenatally with kynurenine. *Hippocampus.* (2019) 29:73–7. doi: 10.1002/hipo.23040
22. Phenis D, Vunck SA, Valentini V, Arias H, Schwarcz R, Bruno JP. Activation of alpha7 nicotinic and NMDA receptors is necessary for performance in a working memory task. *Psychopharmacology.* (2020) 237:1723–35. doi: 10.1007/s00213-020-05495-y
23. Khalil OS, Pisar M, Forrest CM, Vincenten MC, Darlington LG, Stone TW. Prenatal inhibition of the kynurenine pathway leads to structural changes in the hippocampus of adult rat offspring. *Eur J Neurosci.* (2014) 39:1558–71. doi: 10.1111/ejn.12535
24. Pisar M, Forrest CM, Khalil OS, Mcnair K, Vincenten MC, Qasem S, et al. Modified neocortical and cerebellar protein expression and morphology in adult rats following prenatal inhibition of the kynurenine pathway. *Brain Res.* (2014) 1576:1–7. doi: 10.1016/j.brainres.2014.06.016
25. Pocivavsek A, Thomas MA, Elmer GI, Bruno JP, Schwarcz R. Continuous kynurenine administration during the prenatal period, but not during adolescence, causes learning and memory deficits in adult rats. *Psychopharmacology.* (2014) 231:2799–809. doi: 10.1007/s00213-014-3452-2
26. Buck SA, Baratta AM, Pocivavsek A. Exposure to elevated embryonic kynurenine in rats: sex-dependent learning and memory impairments in adult offspring. *Neurobiol Learn Mem.* (2020) 174:107282. doi: 10.1016/j.nlm.2020.107282
27. Rentschler KM, Baratta AM, Ditty AL, Wagner NTJ, Wright CJ, Milosavljevic S, et al. Prenatal kynurenine elevation elicits sex-dependent changes in sleep and arousal during adulthood: implications for psychotic disorders. *Schizophr Bull.* (2021) 47:1320–30. doi: 10.1093/schbul/sbab029
28. Rice D, Barone Jr S. Critical periods of vulnerability for the developing nervous system: evidence from humans and animal models. *Env Health Pers.* (2000) 108(Suppl. 3):511–33. doi: 10.1289/ehp.00108s3511
29. Clancy B, Darlington RB, Finlay BL. Translating developmental time across mammalian species. *Neuroscience.* (2001) 105:7–17. doi: 10.1016/S0306-4522(01)00171-3
30. Bagasrawala I, Zecevic N, Radonjic NV. N-Methyl D-Aspartate receptor antagonist kynurenic acid affects human cortical development. *Front Neurosci.* (2016) 10:435. doi: 10.3389/fnins.2016.00435
31. Forrest CM, Khalil OS, Pisar M, Darlington LG, Stone TW. Prenatal inhibition of the tryptophan-kynurenine pathway alters synaptic plasticity and protein expression in the rat hippocampus. *Brain Res.* (2013) 1504:1–15. doi: 10.1016/j.brainres.2013.01.031
32. Forrest CM, Khalil OS, Pisar M, Mcnair K, Kornisiuk E, Snitcofsky M, et al. Changes in synaptic transmission and protein expression in the brains of adult offspring after prenatal inhibition of the kynurenine pathway. *Neuroscience.* (2013) 254:241–59. doi: 10.1016/j.neuroscience.2013.09.034
33. Pershing ML, Bortz DM, Pocivavsek A, Fredericks PJ, Jorgensen CV, Vunck SA, et al. Elevated levels of kynurenic acid during gestation produce neurochemical, morphological, and cognitive deficits in adulthood: implications for schizophrenia. *Neuropharmacology.* (2015) 90:33–41. doi: 10.1016/j.neuropharm.2014.10.017
34. Pershing ML, Phenis D, Valentini V, Pocivavsek A, Lindquist DH, Schwarcz R, et al. Prenatal kynurenine exposure in rats: age-dependent changes in NMDA receptor expression and conditioned fear responding. *Psychopharmacology.* (2016) 233:3725–35. doi: 10.1007/s00213-016-4404-9
35. Hahn B, Reneski CH, Pocivavsek A, Schwarcz R. Prenatal kynurenine treatment in rats causes schizophrenia-like broad monitoring deficits in adulthood. *Psychopharmacology.* (2018) 235:651–61. doi: 10.1007/s00213-017-4780-9
36. Schomburg EW, Fernandez-Ruiz A, Mizuseki K, Berenyi A, Anastassiou CA, Koch C, et al. Theta phase segregation of input-specific gamma patterns in entorhinal-hippocampal networks. *Neuron.* (2014) 84:470–85. doi: 10.1016/j.neuron.2014.08.051
37. Sans-Dublanc A, Razzauti A, Desikan S, Pascual M, Monyer H, Sindreu C. Septal GABAergic inputs to CA1 govern contextual memory retrieval. *Sci Adv.* (2020) 6:eaba5003. doi: 10.1126/sciadv.aba5003
38. Rapoport MI, Beisel WR. Circadian periodicity of tryptophan metabolism. *J Clin Invest.* (1968) 47:934–9. doi: 10.1172/JCI105785
39. Council NR. *Guide for the Care and Use of Laboratory Animals.* 8th ed. Washington, DC: The National Academies Press (2011).

40. Beggiato S, Tanganelli S, Fuxe K, Antonelli T, Schwarcz R, Ferraro L. Endogenous kynurenic acid regulates extracellular GABA levels in the rat prefrontal cortex. *Neuropharmacology.* (2014) 82:11–8. doi: 10.1016/j.neuropharm.2014.02.019
41. Lowry OH, Rosebrough NJ, Farr AL, Randall RJ. Protein measurement with the folin phenol reagent. *J Biol Chem.* (1951) 193:265–75. doi: 10.1016/S0021-9258(19)52451-6
42. Reinhoud NJ, Brouwer HJ, Van Heerwaarden LM, Korte-Bouws GA. Analysis of glutamate, GABA. Noradrenaline, dopamine, serotonin, and metabolites using microbore UHPLC with electrochemical detection. *ACS Chem Neurosci.* (2013) 4:888–94. doi: 10.1021/cn400044s
43. Gramsbergen JB, Hodgkins PS, Rassoulpour A, Turski WA, Guidetti P, Schwarcz R. Brain-specific modulation of kynurenic acid synthesis in the rat. *J Neurochem.* (1997) 69:290–8. doi: 10.1046/j.1471-4159.1997.69010290.x
44. Sellgren CM, Gracias J, Jungholm O, Perlis RH, Engberg G, Schwieler L, et al. Peripheral and central levels of kynurenic acid in bipolar disorder subjects and healthy controls. *Transl Psychiatry.* (2019) 9:37. doi: 10.1038/s41398-019-0378-9
45. Rapoport MI, Feigin RD, Bruton J, Beisel WR. Circadian rhythm for tryptophan pyrrolase activity and its circulating substrate. *Science.* (1966) 153:1642–4. doi: 10.1126/science.153.3744.1642
46. Wu HQ, Pereira EF, Bruno JP, Pellicciari R, Albuquerque EX, Schwarcz R. The astrocyte-derived alpha7 nicotinic receptor antagonist kynurenic acid controls extracellular glutamate levels in the prefrontal cortex. *J Mol Neurosci.* (2010) 40:204–10. doi: 10.1007/s12031-009-9235-2
47. Koshy Cherian A, Gritton H, Johnson DE, Young D, Kozak R, Sarter M. A systemically-available kynurenine aminotransferase II (KAT II) inhibitor restores nicotine-evoked glutamatergic activity in the cortex of rats. *Neuropharmacology.* (2014) 82:41–8. doi: 10.1016/j.neuropharm.2014.03.004
48. Bortz DM, Wu HQ, Schwarcz R, Bruno JP. Oral administration of a specific kynurenic acid synthesis (KAT II) inhibitor attenuates evoked glutamate release in rat prefrontal cortex. *Neuropharmacology.* (2017) 121:69–78. doi: 10.1016/j.neuropharm.2017.04.023
49. Pellicciari R, Natalini B, Costantino G, Mahmoud MR, Mattoli L, Sadeghpour BM, et al. Modulation of the kynurenine pathway in search for new neuroprotective agents. Synthesis and preliminary evaluation of (m-nitrobenzoyl)alanine, a potent inhibitor of kynurenine-3-hydroxylase. *J Med Chem.* (1994) 37:647–55. doi: 10.1021/jm00031a015
50. Carpenedo R, Pittaluga A, Cozzi A, Attucci S, Galli A, Raiteri M, et al. Presynaptic kynurenate-sensitive receptors inhibit glutamate release. *Eur J Neurosci.* (2001) 13:2141–7. doi: 10.1046/j.0953-816x.2001.01592.x
51. Wanaverbecq N, Semyanov A, Pavlov I, Walker MC, Kullmann DM. Cholinergic axons modulate GABAergic signaling among hippocampal interneurons via postsynaptic alpha 7 nicotinic receptors. *J Neurosci.* (2007) 27:5683–93. doi: 10.1523/JNEUROSCI.1732-07.2007
52. Bandarabadi M, Boyce R, Gutierrez Herrera C, Bassetti CL, Williams S, Schindler K, et al. Dynamic modulation of theta-gamma coupling during rapid eye movement sleep. *Sleep.* (2019) 42:zsz182. doi: 10.1093/sleep/zsz182
53. Tamminga CA, Stan AD, Wagner AD. The hippocampal formation in schizophrenia. *Am J Psychiatry.* (2010) 167:1178–93. doi: 10.1176/appi.ajp.2010.09081187
54. Tamminga CA, Thomas BP, Chin R, Mihalakos P, Youens K, Wagner AD, et al. Hippocampal novelty activations in schizophrenia: disease and medication effects. *Schizophr Res.* (2012) 138:157–63. doi: 10.1016/j.schres.2012.03.019
55. Stan AD, Ghose S, Zhao C, Hulsey K, Mihalakos P, Yanagi M, et al. Magnetic resonance spectroscopy and tissue protein concentrations together suggest lower glutamate signaling in dentate gyrus in schizophrenia. *Mol Psychiatry.* (2015) 20:433–9. doi: 10.1038/mp.2014.54
56. Merritt K, Egerton A, Kempton MJ, Taylor MJ, Mcguire PK. Nature of glutamate alterations in schizophrenia: a meta-analysis of proton magnetic resonance spectroscopy studies. *JAMA Psychiatry.* (2016) 73:665–74. doi: 10.1001/jamapsychiatry.2016.0442
57. Wijtenburg SA, Wright SN, Korenic SA, Gaston FE, Ndubuizu N, Chiappelli J, et al. Altered glutamate and regional cerebral blood flow levels in schizophrenia: a (1)H-MRS and pCASL study. *Neuropsychopharmacology.* (2017) 42:562–71. doi: 10.1038/npp.2016.172
58. Bora E, Yucel M, Pantelis C. Cognitive impairment in schizophrenia and affective psychoses: implications for DSM-V criteria and beyond. *Schizophr Bull.* (2010) 36:36–42. doi: 10.1093/schbul/sbp094
59. Rowland LM, Edden RA, Kontson K, Zhu H, Barker PB, Hong LE. GABA predicts inhibition of frequency-specific oscillations in schizophrenia. *J Neuropsychiatry Clin Neurosci.* (2013) 25:83–7. doi: 10.1176/appi.neuropsych.11120368
60. Osborne AL, Solowij N, Babic I, Huang XF, Weston-Green K. Improved social interaction, recognition and working memory with cannabidiol treatment in a prenatal infection (poly I:C) rat model. *Neuropsychopharmacology.* (2017) 42:1447–57. doi: 10.1038/npp.2017.40
61. Osborne AL, Solowij N, Babic I, Lum JS, Huang XF, Newell KA, et al. Cannabidiol improves behavioural and neurochemical deficits in adult female offspring of the maternal immune activation (poly I:C) model of neurodevelopmental disorders. *Brain Behav Immun.* (2019) 81:574–87. doi: 10.1016/j.bbi.2019.07.018
62. Beggiato S, Ieraci A, Tomasini MC, Schwarcz R, Ferraro L. Prenatal THC exposure raises kynurenic acid levels in the prefrontal cortex of adult rats. *Prog Neuropsychopharmacol Biol Psychiatry.* (2020) 100:109883. doi: 10.1016/j.pnpbp.2020.109883
63. Percelay S, Billard JM, Freret T, Andrieux A, Boulouard M, Bouet V. Functional dysregulations in CA1 hippocampal networks of a 3-hit mouse model of schizophrenia. *Int J Mol Sci.* (2021) 22:2644. doi: 10.3390/ijms22052644
64. Vogels TP, Abbott LF. Gating multiple signals through detailed balance of excitation and inhibition in spiking networks. *Nat Neurosci.* (2009) 12:483–91. doi: 10.1038/nn.2276
65. Harada M, Taki MM, Nose A, Kubo H, Mori K, Nishitani H, et al. Non-invasive evaluation of the GABAergic/glutamatergic system in autistic patients observed by MEGA-editing proton MR spectroscopy using a clinical 3 tesla instrument. *J Autism Dev Disord.* (2011) 41:447–54. doi: 10.1007/s10803-010-1065-0
66. Horder J, Petrinovic MM, Mendez MA, Bruns A, Takumi T, Spooren W, et al. Glutamate and GABA in autism spectrum disorder-a translational magnetic resonance spectroscopy study in man and rodent models. *Transl Psychiatry.* (2018) 8:106. doi: 10.1038/s41398-018-0155-1
67. Kozak R, Campbell BM, Strick CA, Horner W, Hoffmann WE, Kiss T, et al. Reduction of brain kynurenic acid improves cognitive function. *J Neurosci.* (2014) 34:10592–602. doi: 10.1523/JNEUROSCI.1107-14.2014
68. Blanco Ayala TB, Ramirez Ortega DR, Ovalle Rodriguez PO, Pineda B, Perez De La Cruz GP, Gonzalez Esquivel DG, et al. Subchronic N-acetylcysteine treatment decreases brain kynurenic acid levels and improves cognitive performance in mice. *Antioxidants.* (2021) 10:147. doi: 10.3390/antiox10020147

Conflict of Interest: The authors declare that the research was conducted in the absence of any commercial or financial relationships that could be construed as a potential conflict of interest.

frontiers in Psychiatry

REVIEW
published: 01 October 2021
doi: 10.3389/fpsyt.2021.742058

Directly and Indirectly Targeting the Glycine Modulatory Site to Modulate NMDA Receptor Function to Address Unmet Medical Needs of Patients With Schizophrenia

Ju-Chun Pei[1†], *Da-Zhong Luo*[1†], *Shiang-Shin Gau*[1], *Chia-Yuan Chang*[1,2] *and Wen-Sung Lai*[1,2,3*]

[1] Department of Psychology, National Taiwan University, Taipei, Taiwan, [2] Neurobiology and Cognitive Science Center, National Taiwan University, Taipei, Taiwan, [3] Graduate Institute of Brain and Mind Sciences, National Taiwan University, Taipei, Taiwan

OPEN ACCESS

Edited by:
Hsien-Yuan Lane,
China Medical University, Taiwan

Reviewed by:
Qiang Zhou,
Peking University, China
Loredano Pollegioni,
University of Insubria, Italy
Artur Palasz,
Medical University of Silesia, Poland

***Correspondence:**
Wen-Sung Lai
wslai@ntu.edu.tw

[†] These authors have contributed equally to this work

Specialty section:
This article was submitted to Psychopharmacology, a section of the journal Frontiers in Psychiatry

Received: 15 July 2021
Accepted: 02 September 2021
Published: 01 October 2021

Citation:
Pei J-C, Luo D-Z, Gau S-S, Chang C-Y and Lai W-S (2021) Directly and Indirectly Targeting the Glycine Modulatory Site to Modulate NMDA Receptor Function to Address Unmet Medical Needs of Patients With Schizophrenia. Front. Psychiatry 12:742058. doi: 10.3389/fpsyt.2021.742058

Schizophrenia is a severe mental illness that affects ∼1% of the world's population. It is clinically characterized by positive, negative, and cognitive symptoms. Currently available antipsychotic medications are relatively ineffective in improving negative and cognitive deficits, which are related to a patient's functional outcomes and quality of life. Negative symptoms and cognitive deficits are unmet by the antipsychotic medications developed to date. In recent decades, compelling animal and clinical studies have supported the NMDA receptor (NMDAR) hypofunction hypothesis of schizophrenia and have suggested some promising therapeutic agents. Notably, several NMDAR-enhancing agents, especially those that function through the glycine modulatory site (GMS) of NMDAR, cause significant reduction in psychotic and cognitive symptoms in patients with schizophrenia. Given that the NMDAR-mediated signaling pathway has been implicated in cognitive/social functions and that GMS is a potential therapeutic target for enhancing the activation of NMDARs, there is great interest in investigating the effects of direct and indirect GMS modulators and their therapeutic potential. In this review, we focus on describing preclinical and clinical studies of direct and indirect GMS modulators in the treatment of schizophrenia, including glycine, D-cycloserine, D-serine, glycine transporter 1 (GlyT1) inhibitors, and D-amino acid oxidase (DAO or DAAO) inhibitors. We highlight some of the most promising recently developed pharmacological compounds designed to either directly or indirectly target GMS and thus augment NMDAR function to treat the cognitive and negative symptoms of schizophrenia. Overall, the current findings suggest that indirectly targeting of GMS appears to be more beneficial and leads to less adverse effects than direct targeting of GMS to modulate NMDAR functions. Indirect

GMS modulators, especially GlyT1 inhibitors and DAO inhibitors, open new avenues for the treatment of unmet medical needs for patients with schizophrenia.

Keywords: schizophrenia, unmet medical need, negative symptoms, cognitive impairments, glycine modulatory site (GMS), d-serine, glycine transporter 1 (GlyT1) inhibitor, D-amino acid oxidase (DAO) inhibitor

INTRODUCTION TO SCHIZOPHRENIA AND UNMET MEDICAL NEEDS IN PATIENT WITH SCHIZOPHRENIA

Schizophrenia is a devastating mental illness, and the lifetime prevalence of schizophrenia is ∼1%. Globally, there were 1.13 million schizophrenia cases and 12.66 million DALYs (disability-adjusted life years) due to schizophrenia in 2017 (1). The global burden of schizophrenia remains large and continues to increase, increasing the burden on health-care systems worldwide. This debilitating brain disorder typically emerges in late adolescence and early adulthood and is characterized by three main symptoms: positive symptoms, negative symptoms, and cognitive deficits (2, 3). Positive symptoms include delusions, hallucinations, and disorganized thoughts and speech typically regarded as manifestations of psychosis. Negative symptoms include reduced affect display, alogia, anhedonia, asociality, avolition, lack of emotional response, and motivation. Cognitive deficits include dysfunctions in working memory, attention, processing speed, visual and verbal learning with substantial deficits in reasoning, planning, abstract thinking, and problem solving. Cognitive impairments and negative symptoms, as the core features of schizophrenia, are enduring and correlate with the degree of disability (4, 5).

Currently, antipsychotic medications are mainstays in the treatment of schizophrenia and a range of other psychotic disorders. Positive symptoms of schizophrenia often respond well to antipsychotic drugs. In contrast, the available antipsychotic medications, which mainly affect the dopamine and serotonin receptor systems, are relatively ineffective in improving negative and cognitive deficits. Negative symptoms of schizophrenia tend to linger or worsen over time and are accompanied by impaired cognitive function in patients with schizophrenia (6). The improvement of cognitive dysfunction is a better predictor of patient quality of life (7, 8). Since existing pharmacological and biological therapeutic modalities fail to improve cognitive symptoms, various cognitive remediation strategies have been adopted (9). In addition, the cognitive deficits in adolescents at risk for schizophrenia and in patients after their first episode of schizophrenia suggest that schizophrenia-related cognitive dysfunction is not the result of chronic illness (10). The US National Institute of Mental Health (NIMH) thus developed the Measurement and Treatment Research to Improve Cognition in Schizophrenia (MATRICS), which significantly raised awareness of the cognitive dysfunction in schizophrenia (11). In addition to the reliance on the dopamine receptor D2 (DRD2) as a conventional therapeutic target (12), a focus on the different symptom domains of schizophrenia may lead to the identification of different endophenotypic markers that can promote the development of novel therapeutics useful for rational cellular and molecular targets.

THE ROLES OF GLUTAMATERGIC TRANSMISSION AND NMDAR (N-METHYL-D-ASPARTATE RECEPTOR) HYPOFUNCTION IN THE PATHOPHYSIOLOGY OF SCHIZOPHRENIA

Similar to those of many other psychiatric disorders, the etiology and pathophysiology of schizophrenia remain unclear. Accumulating evidence from human genetic studies and association studies has revealed several schizophrenia susceptibility loci and genes. A genome-wide association study (GWAS) revealed notable associations relevant to the major hypotheses of the etiology and treatment of schizophrenia, including *DRD2* (the main target of many effective antipsychotics) and multiple genes [e.g., *metabotropic glutamate receptor 3 (GRM3*), *glutamate ionotropic receptor NMDA type subunit 2A (GRIN2A*), *serine racemase (SR)*, and *glutamate receptor, ionotropic, AMPA receptor 1 (GRIA1)*] involved in glutamatergic neurotransmission and synaptic plasticity (13). In contrast to the conventional view of dopamine involvement in schizophrenia (i.e., the dopamine hypothesis of schizophrenia), glutamatergic neurotransmission has been gradually attracting attention in the investigation of the pathophysiology and treatment of schizophrenia in recent decades (14–16).

In the central nervous system (CNS), glutamate is the main excitatory neurotransmitter and activates metabotropic and ionotropic glutamate receptors. NMDARs are ionotropic glutamate-gated cation channels with high calcium permeability that play vital roles in synaptic transmission, neuroplasticity, and cognitive functions. Heterotetrameric NMDARs are widely distributed throughout most of the brain and are composed of two obligatory GluN1 (NR1) subunits with either two GluN2 (NR2) subunits or a combination of GluN2 (NR2) and GluN3 (NR3) subunits. As illustrated in the top left panel of **Figure 1**, activation of NMDARs requires not only the binding of glutamate on the GluN2 subunit but also the binding of the coagonist glycine or D-serine at the glycine modulatory site (GMS, also referred to as the glycine-B site or the strychnine-insensitive glycine site) on the GluN1 subunit (17). Intriguingly, although the endogenous high-potency coagonists glycine and D-serine are present in the extracellular space (18), the GMSs on NMDARs are not saturated *in vivo* (19). D-serine appears to be the dominant endogenous coagonist for NMDARs and a modulator for NMDAR-related neurotoxicity, even though

the levels of glycine are 10-fold higher than those of D-serine (20–22). The activation of NMDARs produces prolonged increases in intracellular calcium concentration and thus triggers downstream signaling cascades involved in the regulation of many physiological and pathophysiological processes (23).

NMDAR has been proposed to be an important and potential therapeutic target for many CNS and psychiatric disorders (24). There is increasing evidence acquired through different approaches supports the supposition that NMDAR hypofunction plays a role in schizophrenia. In addition to the abovementioned large-scale GWAS, copy number variant studies have also led to the identification of rare genetic variants in NMDAR-related genes and components related to the postsynaptic density associated with increased risk for schizophrenia (25, 26). Postmortem brain studies have also indicated decreased expression of the NR1 subunit (mRNA and protein) and NR2C subunit (mRNA) in the postmortem dorsolateral prefrontal cortex in schizophrenic patients (27) and reductions in D-serine and serine racemase (SR) levels in patients with schizophrenia (28). A meta-analysis study further indicated significant decreases in the expression of NR1 mRNA and protein in the prefrontal cortex of schizophrenic patients (29). In addition to these genetic and postmortem studies, aberrant NMDAR function has been identified via the use of psychotomimetic agents. Pharmacological studies have revealed that the use of NMDAR antagonists (e.g., phencyclidine (PCP) and ketamine) causes not only positive symptoms of schizophrenia but also negative symptoms and cognitive deficits in healthy humans (30–32). Subanesthetic doses of ketamine not only induce psychotomimetic effects but also increase amphetamine-induced dopamine release in the striatum, which has been observed in schizophrenic patients (33). In addition, positron emission tomography (PET) imaging data have indicated links between glutamatergic system dysfunction and schizophrenia (34). NMDAR hypofunction in parvalbumin (PV) interneurons has also been proposed as a pathological mechanism of schizophrenia (35). Proton magnetic resonance spectroscopy (MRS) studies have revealed increased glutamine levels in the medial prefrontal cortex, anterior cingulate cortex, and thalamus in drug-naïve patients with first-episode psychosis (36, 37), suggesting dysregulation of glutamate neurotransmission (38). Moreover, reduced activation of the prefrontal cortices (i.e., hypofrontality) has been considered to underlie negative symptoms and cognitive deficits in schizophrenia (39–41). Notably, it has been proposed that antipsychotic medications may reduce NMDARs activity and produce dysfunctions in the corticolimbothalamic circuit and hypofrontality in patients with schizophrenia (42). Accordingly, these studies indicate the involvement of NMDARs in the pathophysiology of schizophrenia and provide new potential targets for the treatment of schizophrenia.

Given the importance of glutamate in the NMDAR hypofunction hypothesis for schizophrenia and NMDAR-mediated neurotransmission, one possible strategy to boost NMDAR functions involves either directly or indirectly enhancing glutamate levels in synapses, as illustrated in the bottom left and top right portions of **Figure 1**. However, excessive glutamate induces high levels of calcium influx, which has been shown to lead to excitotoxicity and neuronal injury in cellular and animal models (43, 44). In addition, indirect enhancement of glutamate via DL-TBOA, a glutamate transporter 1 (GLT1) inhibitor, resulted in attenuated baroreflex control of sympathetic nerve activity and heart rate (45). Apparently, from a safety perspective, neither direct nor indirect enhancement of synaptic glutamate levels is a reasonable therapeutic approach in the regulation of NMDAR functions. Alternatively, agents that act at the GMSs of NMDARs have been proposed to be promising treatments to moderate severe negative symptoms and cognitive impairments.

DIRECTLY TARGETING THE GMS ON NMDARs

A unique characteristic of NMDAR is that the GMS must be occupied by glycine and/or D-serine for glutamate to induce channel opening. GMS was first reported by Johnson and Ascher to facilitate the activation of NMDARs in cultured mouse brain neurons (18). It was later demonstrated that glycine is necessary to activate NMDARs (46). Mice carrying targeted point mutations in the GMS of the NMDAR NR1 subunit gene (*Grin1*) exhibited marked NMDAR hypofunctions and deficits in long-term potentiation and spatial learning (47, 48), as well as impaired social ability and spatial recognition (49). Accumulating evidence has indicated that binding to the GMS can enhance the affinity and efficacy of glutamate neurotransmission (50), and the administration of GMS agonists (e.g., glycine) can benefit schizophrenic patients by regulating NMDAR-mediated neurotransmission (19). The disturbance of GMS modulators found in schizophrenia patients has been identified as a contributor to NMDAR hypofunction. Previous studies have revealed reduced D-serine and SR in schizophrenia (28). In addition, the levels of kynurenic acid, the only known competitively endogenous antagonist of the GMS in NMDAR, are elevated in the postmortem brain tissue (51) and in the cerebrospinal fluid (CSF) of living schizophrenic patients (52), suggesting that GMS occupancy might be shifted toward antagonism in this disorder. Accordingly, modulation of NMDAR through the GMS has been proposed as a possible therapeutic target for the treatment of negative and cognitive symptoms in schizophrenia (53, 54).

Indeed, several agonists have been designed to either directly or indirectly target GMS due to its great potential for the treatment of negative and positive symptoms in schizophrenia. For example, 3-(4,6-dichloro-2-carboxyindol-3-yl) propionic acid, an indole-2-carboxylic acid derivative, has been found to have $>$ 2,100-fold greater affinity for the GMS than glycine (55), and 3-hydroxy-imidazolidin-4-one derivatives are partial agonists of the GMS (56). Additional computational methods that can be used to identify potential agonists have been used (57). In addition to agonists of the GMS, GMS-specific antagonists, such as 7-chlorkynurenic or L-701,324, have been developed for research purposes (58, 59). Although numerous potential agonists and antagonists have been developed or identified,

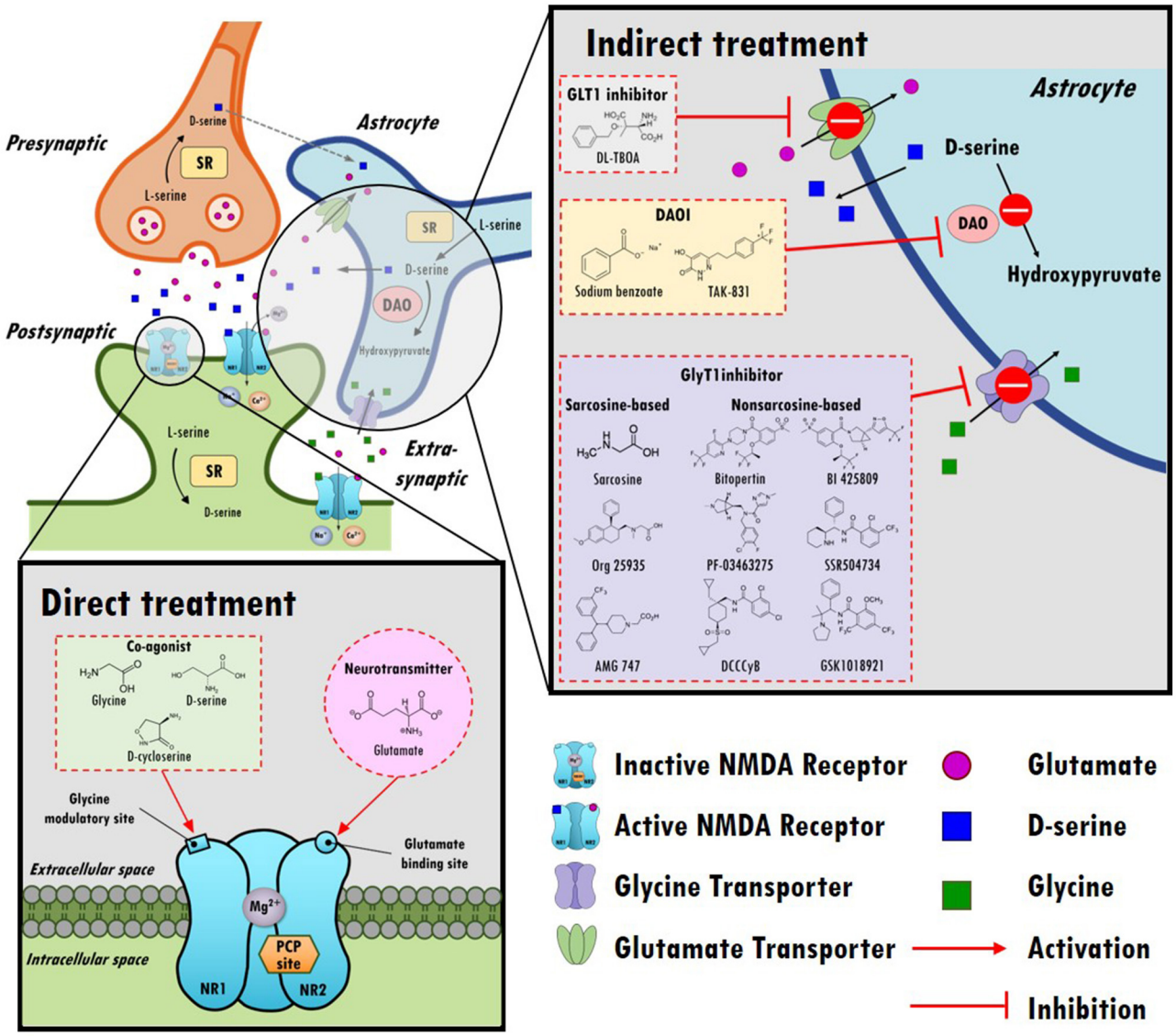

FIGURE 1 | An overview of the hypothesis of N-methyl-D-aspartate receptor (NMDAR) hypofunction in schizophrenia and the direct/indirect treatments in the regulation of NMDAR functioning. Top left panel: A model of glutamatergic trisynapses: pre-synapses, post-synapses, and astrocytes. Activation of NMDAR requires not only the binding of glutamate to the GluN2 (NR2) subunit but also the binding of the coagonist glycine or D-serine at the glycine modulatory site (GMS) of the GluN1 (NR1) subunit. In response to NMDAR activation, the intracellular calcium concentration increases and thereby triggers downstream signaling cascades. After activation, glutamate and glycine are taken up by astrocytes through the glutamate transporter (GLT1) and glycine transporter (GlyT1), respectively. D-serine, another coagonist of GMS, is predominantly produced in neurons, is synthesized from L-serine by serine racemase (SR) and is shuttled to astrocytes, where it is stored and released. NMDARs are critical for synaptic plasticity, cortical maturation, and learning and memory processes. The hypofunction of ionotropic glutamate NMDARs has been proposed to be a model of schizophrenia in humans, and NMDAR hypofunction plays a key role in the pathophysiology of schizophrenia. Bottom left panel: Enhancing NMDAR functions through direct treatments. Glutamate, glycine, D-cycloserine, and D-serine compounds directly target postsynaptic NMDAR and activate NMDAR functioning. Top right panel: Boosting NMDAR functions via indirect treatments (e.g., GLT1 inhibitors, DAO inhibitors, and GlyT1 inhibitors). GLT1 inhibitors block the reuptake of glutamate and increase the synaptic levels of glutamate. D-serine is metabolized into hydroxypyruvate by D-amino acid oxidase (DAO) in astrocytes. DAO inhibitors block the metabolism of D-serine, which prolongs the synaptic concentration of D-serine. GlyT1 inhibitors block the reuptake of glycine and increase synaptic levels of glycine.

only a few of the candidates are suitable for advancement from preclinical studies to clinical trials. To date, most clinical studies have focused mainly on targeting the GMS using single amino acids as agonists of GMS, including glycine, D-cycloserine, and D-serine, as indicated in the bottom left panel of **Figure 1**.

Direct Modulation of NMDAR Functions by Glycine

Glycine is the simplest amino acid and acts as a neurotransmitter in the CNS. In addition to glycinergic terminals, glycine may be simultaneously released into the synaptic cleft with GABA (60). Extracellular glycine is immediately recycled through glycine transporters, including glycine transporter 1 (GlyT1) in glial cells or glutamatergic neurons, and glycine transporter 2 (GlyT2) in presynaptic neurons (61). Intracellular glycine is then metabolized into L-serine by serine hydroxymethyltransferase in glial cells or catabolized into carbon dioxide and ammonium by the glycine cleavage system in neurons (62). Glycine causes inhibitory and excitatory neural transmission via strychnine-sensitive glycine receptors and NMDA receptors, respectively. Glycine receptors are mainly located in the brainstem and spinal cord. In contrast, NMDARs are present in high density within the cerebral cortices and hippocampus and are thought to be involved in the pathophysiology of schizophrenia (24, 63).

Numerous investigations support decreased glutamatergic signaling and NMDAR hypofunction as pathogenic mechanisms of schizophrenia. Interestingly, it has been reported that glycine is upregulated in patients with schizophrenia. Findings on schizophrenic patients obtained postmortem have revealed increased binding activity of radiolabeled [3H]glycine in the brain, especially in the parietal cortex and occipital cortex (64). Rats treated with a glycine-rich diet for a long period also exhibit schizophrenia-like abnormalities, including altered sensory gating function, enlarged cerebral ventricles, and diminished hippocampal dimensions (65). Similarly, high serum glycine levels have been reported in patients with chronic schizophrenia, and these levels have been associated with impaired sensorimotor gating function in pre-pulse inhibition (66). These findings imply that glycine levels might compensate for alterations in glutamate-NMDAR transmission in patients with chronic schizophrenia. For example, a postmortem study indicated a striking decrease in tyrosine phosphorylation of the GluN2 subunit in the dorsolateral prefrontal cortex of schizophrenic patients, but the postsynaptic density of NMDAR complexes in these patients was, in fact, increased (67). Inconsistently, lower plasma glycine levels have reported in schizophrenic patients compared to healthy controls and have been correlated with negative symptoms of schizophrenia (68). To further elucidate the glycine levels in the brains of schizophrenia patients, it is necessary to measure glycine levels in serum and CSF in a large sample size.

Despite the controversial findings regarding glycine levels in patients with schizophrenia, glycine-induced augmentation of NMDAR-mediated neurotransmission has been considered a potentially safe, and feasible approach for ameliorating negative symptoms of schizophrenia. Glycine appears to be safe, even at dosages of as high as 5 g/kg per day in rats (69) and 0.8 g/kg body weight per day in schizophrenic patients (70). In addition to its high biocompatibility and low toxicity, the effect of glycine on the amelioration of schizophrenia-related symptoms has been demonstrated in animal models of schizophrenia. Subchronic administration of glycine at doses relevant to its clinical effects (71) significantly prevents PCP-induced abnormalities in auditory mismatch negativity (MMN, a neurophysiological characteristic of schizophrenia) (72). Glycine also significantly reduced novelty- and methamphetamine-induced locomotor activity in neonatal ventral hippocampal damaged rats compared with sham rats (73). In addition, microinjection of 1 μmol of glycine into the mouse prefrontal cortex alleviated PCP-induced behavioral deficits in latent learning (74), suggesting the involvement of glycine in the regulation of frontocortical NMDARs and cognitive functions. Glycinamide, a prodrug of glycine, can be converted to glycine in CNS by hydrolysis and it prevented MK-801 (dizocilpine, a non-competitive antagonist of NMDAR)-induced deficits in a novel object recognition task in rabbits (75, 76). Despite contrasting neurochemical profiles, a recent study further proved that partial glycine site agonists and glycine reuptake inhibitors display comparable precognitive effects in rats and therefore have potential relevance as treatments of cognitive impairments in schizophrenia (77).

The effects of glycine on the treatment of schizophrenic symptoms in clinical studies are summarized in **Table 1**. Briefly, in the late 1980s, a series of open-label clinical studies failed to demonstrate the therapeutic potential of glycine in the amelioration of negative symptoms of schizophrenia (78–80). Milacemide, an acylated prodrug of glycine, did not alleviate schizophrenic symptoms, and psychotic symptoms were worsened (91, 92). Later, glycine was demonstrated to improve negative symptoms at 0.4 g/kg/day (81). Consistently, recent clinical studies have also indicated that a high dose of glycine is associated with improvement in clinical rating scales of schizophrenia, especially scales of negative symptoms (70, 71, 82, 83, 86, 89, 90). However, inconsistent results have been reported and indicate that glycine administered with clozapine had no effect on patients with schizophrenia (84, 85, 87). In a 16-week randomized double-blind, double-dummy, and parallel-group clinical trial conducted at four sites in the United States and one site in Israel, no significant differences were found between the total average scores on the Scale for the Assessment of Negative Symptoms (SANS) of patients treated with glycine or placebo, and no change in the average cognitive scores was apparent (88). The lack of consistency across trials could be due to small sample sizes, different doses of glycine, different trial durations, and different clinical ratings. Notably, glycine is an inhibitory neurotransmitter in glycinergic neurons, and it has been reported to have poor CNS penetration (i.e., rate of permeation across the blood-brain barrier) (93). Therefore, higher doses of glycine might be required for treatment purpose in patients. Unfortunately, systemic administration of high-does glycine is problematic and is not well-tolerated. The administration of high-dose glycine can result in some unwanted adverse effects, such as nausea (71, 83, 87) and sensorimotor gating deficits (94). Thus, these studies suggest that glycine is not a generally effective therapeutic option for treating negative symptoms or cognitive impairments. It seems wise to explore other drug candidates targeting GMS in the glutamatergic system.

TABLE 1 | Summary of effects of glycine on the treatment of schizophrenic symptoms in clinical studies.

Compound	Type	Study site	Patient	Usage	Subject number (placebo vs. experiment)	Dosage	Trial duration (weeks)	Clinical outcomes	Clinical ratings	References
Glycine	OL	US	SZ	Add on	11 (no placebo)	5–25 (g/day)	32–36	–	Neuroleptics intake	(78)
	OL	US	SZ	Add on	6 (no placebo)	10.8 (g/day)	0.6–8	–	BPRS, SANS, CGI, SAS, AIMS	(79)
	OL	US	SZ	Add on	6 (no placebo)	15 (g/day)	6	–	BPRS	(80)
	DB + additional OL	US	SZ	Add on	7 vs. 7	2–30 (g/day)	8 DB + 8 OL	+ (Negative symptoms)	PANSS, ESRS, AIMS	(81)
	OL	US	SZ	Add on	5 (no placebo)	0.14–0.8 (g/kg/day)	8	+ (Negative symptoms)	PANSS, SANS, ESRS, AIMS	(82)
	DB (Crossover)	Israel	TRS SZ	Add on	11 vs. 11	0.8 (g/kg/day)	6	+ (Negative, depressive, cognitive symptoms)	PANSS, SAS, AIMS	(70)
	DB (Crossover)	Israel	TRS SZ	Add on	22 vs. 22	0.8 (g/kg/day)	6	+ (Negative, depressive, cognitive symptoms)	BPRS, PANSS, SAS, AIMS	(83)
	DB (Parallel)	US	TRS SZ	Add on (Clozapine)	10 vs. 9	30 (g/day)	12	–	BPRS, SANS, SAS, SAFTEE	(84)
	DB (Parallel)	US	SZ	Add on (Clozapine)	13 vs. 14	60 (g/day)	2 SB + 8 DB	–	BPRS, PNASS, SANS, HDRS, SAS, GAS	(85)
	DB (Crossover)	US	SZ	Add on	6 vs. 6	0.2–0.8 (g/kg/day)	6	+ (Negative symptoms)	PANSS, BARS, SAS, AIMS	(86)
	DB (Crossover)	Israel	SZ	Add on (Olanzapine & risperidone)	17 vs. 17 (Olanzapine: 12; Risperidone: 5)	0.06–0.8 (g/kg/day)	6	+ (Negative, cognitive, positive symptoms, excitement, depression)	BPRS, PANSS, SAS, AIMS	(71)
	DB (Crossover)	Canada	TRS SZ	Add on (Clozapine)	12 vs. 12	60 (g/day)	28	–	BPRS, PANSS, GAF, ESRS	(87)
	DB (Parallel) (NCT00222235)	US & Israel	SZ or SZA	Add on (Without clozapine)	45 (55) vs. 42 (54)	15–60 (g/day)	16	–	BPRS, SANS, CGI, SAS, AIMS	(88)
	DB (Parallel)	Australia	SZ or SZA	Add on	21 vs. 22 (SZ:17; SZA:5)	0.2–0.6 (g/kg/day)	6	+ (Acute: duration MMN; chronic:PANSS scores)	PANSS, CDRS, WSAS, ERP (MMN)	(89)
	DB (Crossover)	US	SZ (9p24.1 CNV)	Add on	2 vs. 2	6–48 (g/day)	6	+ (Clinical symptoms)	BPRS, PANSS, CGI, Motor abnormalities	(90)
	OL				2 (no placebo)	5.4–86.5 (g/day)	47	+ (Clinical symptoms)		

+, Positive clinical results; –, Negative clinical results; AIMS, Abnormal Involuntary Movements Scale; BPRS, Brief Psychiatric Rating Scale; CDRS, Calgary Depression Rating Scale; CGI, Clinical Global Impression; DB, double-blind; ERP, Event Related Potential; ESRS, Extrapyramidal Symptom Rating Scale; GAF, Global Assessment of Functioning Scale; GAS, Global Assessment Scale; HDRS, Hamilton Depression Rating Scale; MMN, Mismatch negativity; OL, open-label; PANSS, Positive and Negative Syndrome Scale; SAFTEE, Systematic Assessment for Treatment Emergent Event; SANS, Scale for the Assessment of Negative Symptoms; SAS, Simpson Angus Scale for Assessment of Extrapyramidal Side Effects; SZ, schizophrenia; SZA, schizoaffective disorder; TRS: treatment-resistant; WSAS: Work and Social Adjustment Scale.

Direct Modulation of NMDAR Functions by D-Cycloserine

D-cycloserine is a well-known antibiotic metabolite produced by *Streptomyces orchidaceus* and *Streptomyces garyphalus* that has therapeutic effects on tuberculosis. D-cycloserine has also been found to act as a partial agonist targeting the GMS of NMDAR (95), and its binding affinity is 100-fold less than that of glycine (96). Similar to glycine, D-cycloserine has been reported to improve cognitive functions through modulation of NMDAR function in animal studies. For example, both systemic administration and intra-amygdala infusions of D-cycloserine facilitated conditioned fear extinction and improved memory consolidation in rats (97, 98). Single administration of D-cycloserine also significantly improved visual recognition memory in rhesus monkeys (99). However, inconsistently, some studies reported that D-cycloserine had no effect on neural activity in a mouse model of schizophrenia (100), MK-801-induced sensorimotor gating dysfunction in mice (101), or acquisition of memory performance in MK-801-treated rats in the radial arm maze and the water maze (102).

Similarly, inconsistent findings have also been reported in clinical studies. Effects of D-cycloserine on the treatment of schizophrenic symptoms in clinical studies are summarized in **Table 2**. Briefly, some studies indicated that D-cycloserine at a dosage of 50 or 100 mg/day had therapeutic effects in the treatment of negative symptoms and/or cognitive deficits (90, 103, 106, 108, 111, 112, 115–119). In contrast, others reported that D-cycloserine had no effect on patients with schizophrenia (88, 104, 107, 113, 114). There are several possible explanations for the contradictory findings in clinical studies. First, D-cycloserine has a very narrow therapeutic window. The administration of D-cycloserine >100 mg/day has been reported to result in the deterioration of clinical outcomes in patients with schizophrenia (96, 103, 110). It has been shown that D-cycloserine has neurotoxic side effects, including hyperexcitability, depression, anxiety, memory deficits, and even seizures (121). Second, D-cycloserine administered with clozapine can result in drug-drug interactions, which might lead to the exacerbation of symptoms in patients (105, 109). Third, the treatment effect of D-cycloserine might be influenced by heterogeneity caused by differences in onset age and white matter integrity (120). In addition, a study revealed that patients receiving D-cycloserine demonstrated a significant increase in temporal lobe activation, suggesting that the addition of D-cycloserine to conventional neuroleptics may improve negative symptoms through enhanced temporal lobe function (115). Finally, a meta-analysis indicated that full agonists (such as glycine and D-serine) appear to be more effective than partial agonists (such as D-cycloserine) (122, 123). Thus, the therapeutic potential of D-cycloserine appears to be limited and not particularly effective.

Direct Modulation of NMDAR Functions by D-Serine

D-serine is enriched in the forebrain and is an endogenous ligand of the GMS on NMDAR (124). Emerging evidence suggests the potential role of D-serine in the regulation of NMDAR functions for the treatment of schizophrenia. For the GluN1/N2 subunits of NMDAR, the binding affinity of D-serine is three-fold more potent than that of glycine (125). D-serine is mainly expressed by glutamatergic neurons, even though there has been considerable controversy regarding the concentration and function of D-serine in glial cells and neurons (126). D-serine is predominantly produced in neurons by the stereoconversion of L-serine (provided by astrocytes) via the PLP-dependent enzyme serine racemase (SR) and is then shuttled to astrocytes, where it is stored and released. Studies using more-selective antibodies have demonstrated that SR and D-serine are prominently expressed in forebrain glutamatergic neurons (127–130). In addition, the distribution of D-serine residues in the brain is similar to that of NMDARs (131). Intriguingly, it has been reported that the deletion of neuronal SR resulted in impaired NMDAR functions and synaptic plasticity, whereas deletion of astrocytic SR had no effect (132). Notably, D-serine is the primary coagonist of synaptic NMDARs, whereas glycine is the primary coagonist of extrasynaptic NMDARs (22). In general, D-serine is an allosteric modulator of brain NMDARs and is predominantly released from glutamatergic neurons.

Emerging evidence suggests that D-serine is involved in the pathophysiology of schizophrenia and is a potential therapeutic agent and/or biomarker for schizophrenia. Indeed, decreased levels of D-serine in serum and CSF have been found in patients with schizophrenia compared to those in healthy controls (133). A CSF and postmortem brain study also revealed a 25% decreases in D-serine levels and the D/L-serine ratio in the CSF of schizophrenia patients, suggesting that reduced brain SR and elevated D-amino acid oxidase (DAO) protein levels may contribute to the lower D-serine levels observed in the CSF of schizophrenic patients (28). A recent study further indicated that poor executive function performance is associated with a lower D-serine/total serine ratio in schizophrenic patients (134). Moreover, accumulating evidence has indicated that alteration of D-serine is associated with neuroplasticity and cognitive deficits in schizophrenia. For example, supplementation with D-serine prevented the onset of cognitive deficits in adult offspring after maternal immune activation in pregnant mice (135), suggesting that early intervention with D-serine may prevent the occurrence of psychosis in high-risk subjects. Decreasing synaptic D-serine by enhancing Na^+-independent alanine–serine–cysteine transporter-1 abolished long-term potentiation (LTP) and reduced synaptic NMDAR responses by 60–70% (136). Taking advantage of SR-null mice, a series of studies confirmed that D-serine is required for NMDAR responses, NMDAR-dependent LTP, dendritic spine formation, cognitive functions, and social memory (137–141). However, D-serine is metabolized rapidly by DAO, reducing its bioavailability and requiring the administration of high doses, which may lead to peripheral neuropathies, creating a potential problem for the use of D-serine in treating schizophrenia-related symptoms (142, 143). D-serine levels in blood and urine are sensitive to the presence of kidney dysfunction of different origins. There are also concerns that high concentrations of D-serine augment kidney dysfunction and cause potential nephrotoxicity, which has been reported in rats that have developed acute tubular necrosis

TABLE 2 | Major findings in clinical trials examining effects of D-cycloserine on the treatment of schizophrenic symptoms.

Compound	Type	Study site	Patient	Usage	Subject number (placebo vs. experiment)	Dosage	Trial duration (weeks)	Clinical outcomes	Clinical ratings	References
D-cycloserine	OL	Italy	SZ	Add on	7 (No placebo)	250 (mg/day)	6	– (Worsen symptoms)	BPRS, SANS, CGI	(96)
	SB & RB (Dose finding)	US	SZ	Add on	9	5, 15, 50, 250 (mg/day)	10 (2 wks/dose)	+ (50 mg/day: negative, cognitive symptoms)	BPRS, SANS, GAS, SIRP, AIMS	(103)
	DB (Parallel)	US	SZ	Add on (Molindone)	4 vs. 3 vs. 6 (Placebo vs. 10 vs. 30)	10, 30 (mg/day)	4	–	BPRS, SANS, CGI	(104)
	SB & RB (Dose finding)	US	SZ	Add on (Clozapine)	10	5, 15, 50, 250 (mg/day)	10 (2 wks/dose)	– (Worsen symptoms)	BPRS, SANS, SIRP	(105)
	SB (Dose finding)	Netherlands	SZ (Drug-free)	Alone	13	15, 25, 50, 100, 250 (mg/day)	24 days (4 days/dose)	+ (100 mg/day: negative symptoms)	PANSS, CGI, ESRS	(106)
	DB (Crossover)	Israel	TRS SZ	Add on	8 vs. 9	50 (mg/day)	6	-	PANSS, HDRS, SAS, AIMS	(107)
	DB (Parallel)	US	SZ	Add on	23 (24) vs. 23 (23)	50 (mg/day)	8	+ (Nnegative symptoms)	PANSS, SANS, HDRS, GAS, SIRP, AIMS, Stroop Test, Miller-Selfridge Test, Verbal fluency, Digit span, Finger tapping	(108)
	DB (Crossover)	US	SZ	Add on (Clozapine)	11 vs. 11	50 (mg/day)	6	– (Worsen negative symptoms)	PANSS, SANS, HDRS, GAS, SAS, AIMS, BARS	(109)
	DB (Parallel)	Netherlands	SZ	Add on (Without antidepressants)	13:13	100 (mg/day)	8	– (Worsen symptoms)	PANSS, CGI, ESRS	(110)
	SB & RB (Dose finding)	US	SZ	Add on (Risperidone)	10	5, 15, 50, 250 (mg/day)	10 (2 wks/dose)	+ (50 mg/day: negative symptoms)	BPRS, SANS, HDRS, GAS, SAS, AIMS, Word list generation, Digit span, Finger tapping, Stroop test,	(111)
	DB (Crossover)	Israel	TRS SZ	Add on	16 vs. 16	50 (mg/day)	6	+ (Negative symptoms)	PANSS,HDRS, SAS, AIMS	(112)
	DB (Parallel)	US	SZ	Add on	12 vs. 10	50 (mg/day)	4	–	BPRS, SANS, ATRS, SAS, CPT, Sternberg paradigm	(113)
	DB (Parallel)	US	SZ	Add on	12 (28) vs. 14 (27)	50 (mg/day)	24	–	PANSS, SANS, HDRS, QOL, GAS, CVLT, WAIS III, ANART, Stroop Test, Finger tapping, WCST, SAS, AIMS	(114)
	DB (Parallel)	US	SZ	Add on	6 vs. 6	50 (mg/day)	8	+ (Improved negative symptoms associated with temporal lobe activation)	PANSS, SANS, SAS, AIMS, fMRI,	(115)
	DB (Parallel)	US & Israel	SZ or SZA	Add on (Without cloazpine)	45 (55) vs. 46 (56)	25–50 (mg/day)	16	–	BPRS, SANS, CGI, SAS, AIMS	(88)
	DB (Parallel)	US	SZ	Add on (Without cloazpine)	16 (19) vs. 16 (19)	50 (mg/day)	8	+ (Negative symptmos, logical memory)	PANSS, SANS, CGI, SAFTEE, WMS-III, HVLT, WCST, TMT, Phonemic fluency, Category fluency, Letter-number sequencing, Grooved pegboard	(116)

(Continued)

TABLE 2 | Continued

Compound	Type	Study site	Patient	Usage	Subject number (placebo vs. experiment)	Dosage	Trial duration (weeks)	Clinical outcomes	Clinical ratings	References
	DB (Crossover) (NCT00742079)	US	SZ or SZA	Add on (Combined with CBT)	9 (10) vs. 11 (11) (PCB-first vs. DCS-first)	50 (mg/day)	1	+ (DCB-first: delusional severity, distress, belief conviction)	PSYRATS, SAPS, ABA, Bead Task	(117)
	DB (Parallel) (NCT00963924)	US	SZ or SZA	Add on	15 (18) vs. 17 (18)	50 (mg/day)	8	+ (Cognitive, negative symptoms)	PANSS, SANS, MATRICS, CDSS, QOL, GAS, SAFTEE, Auditory discrimination task	(118)
	DB (Parallel)	US	SZ	Add on	21 vs. 24	100 (mg/once)	1 day	+ (Neural response, working memory)	BPRS, WASI, EEG, N-back task, IIT, WPT	(119)
	DB (Crossover) (UMIN000000468)	Japan	SZ	Add on	19 (22) vs. 17 (19) (PCB-first vs. DCS-first)	50 (mg/day)	6	–	PANSS, SANS, BACS, JCDSS, GAF, EQS, DIEPSS, AIMS, MR-DTI	(120)
	DB (Crossover)	US	SZ (9p24.1 CNV)	Add on	2 vs. 2	50 (mg/day)	6	+ (Clinical symptoms)	BPRS, PANSS, CGI, Motor abnormalities	(90)

+, Positive clinical results; –, Negative clinical results; ABA, Alternative Beliefs Assessment; AIMS, Abnormal Involuntary Movements Scale; ANART, Adult North American Reading Test; ATRS, Abrams and Taylor Rating Scale; BACS, Brief Assessment of Cognition in Schizophrenia; BARS, Barnes Akathisia Rating Scale; BPRS, Brief Psychiatric Rating Scale; CDSS, Calgary Depression Scale of Schizophrenia; CGI, Clinical Global Impression; CPT, Continuous Performance Test; CVLT, California Verbal Learning Test; DB, double-blind; DCS, D-cycloserine; DIEPSS, Drug Induced Extrapyramidal Symptoms Scale; DTI, Diffusion Tensor Imaging; EEG, electroencephalogram; EQS, Emotional Intelligence Scale; ESRS, Extrapyramidal Symptom Rating Scale; fMRI, functional Magnetic Resonance Imaging; GAF, Global Assessment of Functioning Scale; GAS, Global Assessment Scale; HDRS, Hamilton Depression Rating Scale; HVLT, Hopkins Verbal Learning Test; IIT, Information Integration Task; JCDSS, Japanese version of Calgary Depression Scale of Schizophrenia; MATRICS, Measurement and Treatment Research to Improve Cognition in Schizophrenia; OL, open-label; PANSS, Positive and Negative Syndrome Scale; PSYRATS, Psychotic Symptom Rating Scales; QOL, Quality of Life; RB, rater-blind; SAFTEE, Systematic Assessment for Treatment Emergent Event; SANS, Scale for the Assessment of Negative Symptoms; SAPS, Assessment of Positive Symptoms; SAS, Simpson Angus Scale for Assessment of Extrapyramidal Side Effects; SB, single-blind; SIRP, Sternherg's Item Recognition Paradigm; SZ, schizophrenia; SZA, schizoaffective disorder; TMT, Trail Making Test; TRS, treatment-resistant; WAIS-III, Wechsler Adult Intelligence Scale-III; WASI, Weschler Abbreviated Scale of Intelligence; WCST, Wisconsin Card Sorting Test; WPT, Weather Prediction Task.

associated with higher doses of D-serine (144, 145). Nevertheless, serum D/L-serine levels might provide a measurable biological marker for schizophrenia, and D-serine may be effective for the treatment of negative symptoms and cognitive dysfunction in schizoprhenia. The study of D-serine requires accurate methodologies and specific controls, and a specific guideline for accurate measurement and detection methods has been described previously (146).

Along the same lines, D-serine has been employed alone or as an add-on treatment to standard antipsychotics for improving positive, negative, and cognitive symptoms of schizophrenia in numerous clinical studies (147–159). Effects of D-serine on the treatment of schizophrenic symptoms in clinical studies are summarized in **Table 3**. Briefly, some clinical studies have demonstrated positive outcomes for D-serine (147, 149–151), and repeated D-serine administrations have been shown to improve MMN and cortical plasticity in patients with schizophrenia (156, 157). However, other studies have revealed negative results (148, 152–155). A meta-analysis indicated that the effect size of D-serine on the treatment of negative symptoms (SMD = −0.319) and positive symptoms (SMD = −0.211) appeared to be small (160). In particular, in the first randomized double-blind placebo-controlled study with 60 mg/kg D-serine in schizophrenia, D-serine led to significant improvement in MMN frequency generation and clinical symptoms (157), which is consistent with another meta-analyses showing significant effects of D-serine on schizophrenia. This study also implied that a minimum daily dose of 3.6 g D-serine is needed to improve negative symptoms. However, high concentrations of D-serine can lead to peripheral neuropathies, such as oxidative damage (161), neurotoxicity (162), and renal toxicity (150, 163). In summary, these studies indicate that the therapeutic benefit of D-serine may be limited due to its adverse effects.

INDIRECTLY TARGETING THE GMS ON NMDARs

As described previously, activation of NMDARs requires the binding of a coagonist, D-serine or glycine, at the GMS of NMDARs. To date, the GMS on NMDAR is one of the most promising therapeutic targets for contributing to the medical needs of patients with schizophrenia. However, the beneficial effect of directly targeting the GMS with D-serine is limited because of the requirements for a high dose, narrow therapeutic window and poor CNS penetration rate, concomitant side effects and potential drug-drug interactions. Alternatively, as illustrated in the right panel of **Figure 1**, indirectly targeting the GMS of NMDARs via enhancement of synaptic glycine/D-serine levels from in astrocytes provides a new approach to modulate NMDAR functions and to help meet the needs of patients in schizophrenia (164).

Indirect Modulation of NMDAR Functions by Targeting Astrocytic GlyT1

A glycine reuptake inhibitor inhibits the reuptake of synaptic glycine by blocking astrocytic glycine transporters and increasing the availability of glycine at the synaptic cleft. Glycine transporter type 1 (GlyT1) is expressed at glutamatergic synapses throughout mammalian brain regions and primarily regulates the synaptic concentrations of glycine (165). GlyT1 is highly colocalized with NMDARs on glial cells and neurons in the cortex, hippocampus, septum and thalamus (166). GlyT1 effectively regulates synaptic glycine reuptake and governs GMS occupancy at NMDARs in excitatory synapses (19). Thus, selective inhibition of astrocytic GlyT1 is a promising new therapeutic target for indirectly enhancing synaptic glycine concentrations and facilitating NMDAR function.

Accumulating evidence from preclinical studies indicates that inhibition of GlyT1 enhances NMDAR functions in animals. Initial studies have revealed that glycyldodecylamide, a non-selective glycine transport antagonist, reverses PCP-induced behavioral deficits (167, 168). Subsequently, a series of studies consistently demonstrated that administration of N[3-(40-fluorophenyl)-3-(40-phenylphenoxy)propyl]-sarcosine (NFPS, also known as Alx5470), a GlyT1 inhibitor, enhanced LTP and behavioral performances in associative learning, spatial and object memory, and social memory (140, 141, 169–171). In agreement with the results obtained with NFPS, a series of studies also indicated that sarcosine, another GlyT1 inhibitor, has promising therapeutic potential in ameliorating behavioral impairments and cognitive deficits in both pharmacological and genetic mouse models of schizophrenia (139, 172, 173). Furthermore, sarcosine has been proven to effectively regulate the surface trafficking of NMDARs, NMDAR-evoked electrophysiological activity, brain glycine levels and MK-801-induced abnormalities in the brain, which might contribute to the therapeutic effect for the treatment of schizophrenia (139). Intriguingly, it has been proven that sarcosine also binds to the GMS of NMDARs and enhances NMDAR functions through more than one mechanism (139, 174). In addition, other GlyT1 inhibitors, such as SSR504734 and ORG 24598, have also displayed similar beneficial effects in sensorimotor gating, learning and memory functions, and schizophrenia-like behaviors (175–178). Furthermore, selective genetic disruption of GlyT1 resulted in enhancement of NMDAR functions, spatial retention memory, selective attention, and procognitive and antipsychotic phenotypic profiles, suggesting that inhibition of GlyT1 might have both cognitive-enhancing and antipsychotic effects (179–181). These studies indicate that GlyT1 is an attractive and promising drug target for the treatment of schizophrenia-related behaviors and cognitive deficits, even though the high binding affinity of the GlyT1 inhibitor can cause unpredictable toxicity leading to a coma-like state, compulsive walking or respiratory distress (15, 182).

With the aim of treating unmet medical needs in schizophrenia, a number of pharmaceutical industries have developed selective GlyT1 inhibitors as novel therapeutic drugs for schizophrenia. Numerous clinical studies have been carried out to evaluate the effects of special GlyT1 inhibitors on the treatment of schizophrenic symptoms. Based on the chemical structures of GlyT1 inhibitors, these clinical studies can be divided into two major structural classes: sarcosine-based and non-sarcosine-based inhibitors, and the summaries of these studies are shown in **Tables 4**, **5**, respectively.

TABLE 3 | Summary of clinical outcomes and benefits related to D-serine in patients with schizophrenia.

Compound	Type	Study site	Patient	Usage	Subject number (placebo vs. experiment)	Dosage	Trial duration (weeks)	Clinical outcomes	Clinical ratings	References
D-serine	DB (Parallel)	Taiwan	SZ	Add on	15 vs. 14	30 (mg/kg/day)	6	+ (Positive, negative, cognitive symptoms)	PANSS, SANS, CGI, HDRS, SAS, AIMS, BARS, UKU	(149)
	DB (Parallel)	Taiwan	SZ	Add on (Clozapine)	10 vs. 10	30 (mg/kg/day)	6	–	PANSS, SANS, CGI, HDRS, SAS, AIMS, BARS, UKU	(152)
	DB (Crossover)	Israel	TRS SZ	Add on (Olanzapine & risperidone)	38 vs. 37 (Risperidone: 21; Olanzapine: 18)	20–30 (mg/kg/day)	6	+ (Negative, positive, cognitive, depression symptoms)	BPRS, PANSS, SANS, SAS, AIMS,	(147)
	DB (Parallel)	Taiwan	SZ (Acute exacerbation)	Add on (Risperidone)	20 (23) vs. 19 (21)	2 (g/day)	6	–	PANSS, SANS, SAS, AIMS, BARS, UKU	(149)
	DB (Parallel) (NCT00491569)	Taiwan	SZ	Add on	16 (20) vs. 16 (20)	2 (g/day)	6	–	PANSS, SANS, GAF,QOL, SAS, AIMS, BARS, UKU	(153)
	OL (NCT00322023)	US	SZ or SZA	Add on (Without cloazpine)	12 vs. 19 vs. 16 (30 vs. 60 vs. 120; no placebo)	30, 60, 120 (mg/kg/day)	4	+ (PANSS, MATRICS, neuropsychological measures)	PANSS, SANS, CGI, CDSS MATRICS, SAS, AIMS, BARS	(150)
	DB (Parallel) (NCT00138775)	Israel	SZ or SZA	Add on	69 (98) vs. 73 (97)	2 (g/day)	16	–	PANSS, SANS, CGI, SAS, AIMS, UKU	(154)
	DB (Parallel)	Israel	TRS SZ	Alone	5 (10) vs. 3 (8) (D-serine vs. Olanzapine)	1.5–3 (g/day)	10	Treatment effect: Olanzapine > D-serine	PANSS, SAS, AIMS, UKU	(158)
	DB (Parallel)	US & India	SZ or SZA	Add on	23 (26) vs. 25 (27) vs. 22 (27) vs. 21 (24) (control vs. D-serine vs. CRT vs. D-serine + CRT)	30 (mg/kg/day)	12	–	PANSS, CDS, QOL, CPT, WAIS-III, HVLT-R, TOL, WCST, SAS, AIMS, BARS, UKU,	(155)
	OL	Israel	TRS SZ	Add on	17 (no placebo)	1.5–4 (g/day)	6	+ (Extreme delta brush electrographic pattern)	MRI, continuous EEG	(159)
	DB (Parallel) (NCT00826202)	US	SZ Prodrome	Add on	20 (24) vs. 15 (20)	60 (mg/kg/day)	16	+ (Negative symptoms)	SOPS, MATRICS, PSQI, SAS, AIMS, SAFTEE	(151)
	DB (Crossover) (NCT01474395)	US	SZ or SZA	Add on	13 (one placebo session + two D-serine sessions)	60 (mg/kg/day)	2–3	+ (Auditory plasticity, θ-frequency response, MMN generation)	Auditory emotion paradigm, ERP(MMN)	(156)
	OL (NCT02156908)				3 vs. 5					
	DB (Crossover) (NCT00817336)	US	SZ or SZA	Add on	16 vs. 16	60 (mg/kg/day)	6	+ (MMN frequency, generation, clinical symptoms)	PANSS, MCCB, ERP (MMN)	(157)
	OL (NCT00322023)		SZ or SZA		5 vs. 8 vs. 6 (30 vs. 60 vs. 120; no placebo)	30, 60, 120 (mg/kg/day)	4	+ (MMN frequency)		

+, Positive clinical results; –, Negative clinical results; AIMS, Abnormal Involuntary Movements Scale; ANSS, Positive and Negative Syndrome Scale; BARS, Barnes Akathisia Rating Scale; BPRS, Brief Psychiatric Rating Scale; CDS, Calgary Depression Scale; CDSS, Calgary Depression Scale of Schizophrenia; CGI, Clinical Global Impression; CPT, Continuous Performance Test; DB, double-blind; EEG, Electroencephalogram; ERP, Event Related Potential; GAF, Global Assessment of Functioning Scale; HDRS, Hamilton Depression Rating Scale; HVLT-R, Hopkins Verbal Learning Test-Revised; MATRICS, Measurement and Treatment Research to Improve Cognition in Schizophrenia; MCCB, MATRICS consensus cognitive battery; MMN, Mismatch negativity; MRI, Magnetic Resonance Imaging; OL, open-label; PSQI, Pittsburgh Sleep Quality Index; QOL, Quality of Life; SAFTEE, Systematic Assessment for Treatment Emergent Event; SAS, Simpson Angus Scale for Assessment of Extrapyramidal Side Effects; SANS, Scale for the Assessment of Negative Symptoms; SOPS, Scale of Prodromal Symptoms; SZ, schizophrenia; SZA, schizoaffective disorder; TOL, Tower of London Test; TRS, treatment-resistant; UKU, Udvalg for Kliniske Undersogelser Side Effects Rating Scale; WAIS-III, Wechsler Adult Intelligence Scale-III; WCST, Wisconsin Card Sorting Test.

TABLE 4 | Summary of clinical trials evaluating effects of sarcosine-based GlyT1 inhibitors on the treatment of schizophrenic symptoms.

Compound	Type	Study site	Patient	Usage	Subject number (placebo vs. experiment)	Dosage	Trial duration (weeks)	Clinical outcomes	Clinical ratings	References
Org 25935	DB (Parallel) (NCT00725075)	Worldwide (GINAT trial)	SZ (Negative symptom)	Add on	62 (70) vs. 62 (71) vs. 67 (73) (Placebo vs. low-dose vs. high-dose)	4–8 & 12-16 (mg, BID)	12	–	PANSS, SANS, GAF, CDSS, NES, Cognitive battery, ESRS	(183)
AMG 747	DB (Parallel) (NCT01568216 & NCT01568229)	Worldwide	SZ	Add on	76 (90) vs. 54 (60) vs. 51 (60) vs. 51 (60) (placebo vs. 5 vs. 15 vs. 40)	5, 15, 40 (mg/day)	12	Terminated (Adverse event)	PANSS, NSA-16, CGI, MCCB, PSP, Q-LES-Q-18, SDS	(184)
Sarcosine	DB (Parallel)	Taiwan	SZ	Add on	21 vs. 17	2 (g/day)	6	+ (Positive, negative, cognitive, gnenral symptoms)	BPRS, PANSS, SANS, HDRS, SAS, AIMS, BARS, UKU	(185)
	DB (Parallel)	Taiwan	SZ (Acute exacerbation)	Add on (Risperidone)	20 (23) vs. 18 (21)	2 (g/day)	6	+ (Positive, negative symptoms)	PANSS, SANS, SAS, AIMS, BARS, UKU	(148)
	DB (Parallel)	Taiwan	TRS SZ	Add on (Clozapine)	10:10	2 (g/day)	6	–	PANSS, SAS, AIMS, BARS, UKU	(186)
	DB (Parallel) (NCT00328276)	Taiwan	SZ (Drug-free) (Acute exacerbation)	Alone	6 (9) vs. 10 (11) (1 vs. 2; no placebo)	1, 2 (g/day)	6	–	PANSS, SANS, QOL, SAS, AIMS, BARS, UKU	(187)
	DB (Parallel) (NCT00491569)	Taiwan	SZ	Add on	16 (20) vs. 19 (20)	2 (g/day)	6	+ (Positive, negative symptoms)	PANSS, SANS, GAF, QOL, SAS, AIMS, BARS, UKU	(153)
	OL (Case report)	Poland	SZ	Add on (Quetiapine and citalopram)	1	1, 2 (g/day)	4 (2 g/day: 2 + 1 g/day: 2)	+ (2 g: negative symptom but cause hypomania)	PANSS, HDRS	(188)
	OL (Case report)	Poland	SZ (Negative/ cognitive symptoms)	Add on (Olanzapine and venlafaxine)	1	2 (g/day)	12 (24)	Terminated (Cause hypomania)	PANSS, HDRS	(189)
	DB (Parallel) (NCT01503359)	Poland (PULSAR)	SZ (Negative symptom)	Add on	25 vs. 25	2 (g/day)	24	– (Negative, general symptoms) (Decreased in hippocampal Glx/Cr, Glx/Cho)	PANSS, 1H-MRS	(190)
			Paranoid SZ	Add on	29 vs. 30	2 (g/day)	24	No changes of cardiometabolic & body composition parameters	PNASS, BIA, Cardiometabolic characteristics	(191)
			SZ (Negative symptom)	Add on	25 vs. 25	2 (g/day)	24	+ (Negative symptom) (Increased in DLPFC NAA/Cho, mI/Cho, mI/Cr)	PANSS, 1H-MRS	(192)
			SZ (Negative symptom)	Add on	25 vs. 25	2 (g/day)	24	+ (Negative symptom) (Decreased in WM Glx/Cr. Glx/Cho)	PANSS, 1H-MRS	(193)
			Paranoid SZ	Add on	30 vs. 28	2 (g/day)	24	+ (Negative, total symptoms) (MMP-9 no changed)	PANSS, CDSS, BIA serum MMP-9 measure	(194)

(Continued)

TABLE 4 | Continued

Compound	Type	Study site	Patient	Usage	Subject number (placebo vs. experiment)	Dosage	Trial duration (weeks)	Clinical outcomes	Clinical ratings	References
			Paranoid SZ	Add on	30 vs. 27	2 (g/day)	24	+ (Negative, total symptoms) (BDNF no changed)	PANSS, CDSS, BIA Serum BDNF measure	(195)
			SZ (Negative symptom)	Add on	29 vs. 27	2 (g/day)	24	+ (Negative, total symptoms) (IL-6 no changed)	PANSS, CDSS, BIA Serum IL-6 measure	(196)
			Paranoid SZ	Add on	29 vs. 27	2 (g/day)	24	+ (Negative, total symptoms) (TNFα no changed)	PANSS, CDSS, BIA Serum TNFα measure	(197)
	OL	Israel	SZ or SZA	Add on	5 vs. 5	2 (g/day)	1	No result (Sample size too small)	PANSS, CGI, MCCB, CDSS, SAS, AIMS	(198)
					17 vs. 17	4 (g/day)		+ (Positive, general symptoms)		
	DB (Parallel)	Taiwan	SZ	Add on	16 (21) vs. 16 (21) (Placebo vs. sarcosine)	2 (g/day)	12	–	PANSS, CGI, GAF, MCCB, SAS, AIMS, BARS, UKU	(199)

+, Positive clinical results; –, Negative clinical results; 1H-MRS, Proton magnetic resonance spectroscopy; AIMS, Abnormal Involuntary Movements Scale; BARS, Barnes Akathisia Rating Scale; BDNF, Brain-derived neurotrophic factor; BIA, Bioelectrical Impedance Analysis; BPRS, Brief Psychiatric Rating Scale; CDSS, Calgary Depression Scale of Schizophrenia; CGI, Clinical Global Impression; Cho, Choline; Cr, Creatine; DB, double-blind; ESRS, Extrapyramidal Symptom Rating Scale; GAF, Global Assessment of Function; Glx, Complex of glutamate, glutamine and GABA; HDRS, Hamilton Depression Rating Scale; IL-6, Interleukin-6; MCCB, MATRICS consensus cognitive battery; mI, Myo-inositol; MMP-9, Matrix metallopeptidase-9; NAA, N-acetylaspartate; NES, Neurological Evaluation Scale; NSA-16, Negative Symptom Assessment-16; OL, open-label; PANSS, Positive and Negative Syndrome Scale; PSP, Personal and Social Performance Scale; Q-LES-Q-18, Quality of Life Enjoyment and Satisfaction Questionnaire; QOL, Quality of Life; SANS, Scale for the Assessment of Negative Symptoms; SAS, Simpson Angus Scale for Assessment of Extrapyramidal Side Effects; SDS, Sheehan Disability Scale; SZ, schizophrenia; SZA, schizoaffective disorder; TNFα, Tumor necrosis factor α; UKU, Udvalg for Kliniske Undersogelser Side Effects Rating Scale; WM, White matter.

Sarcosine-Based GlyT1 Inhibitors

In the early period of drug discovery, several high-affinity GlyT1 inhibitors derived from sarcosine derivatives [e.g., NFPS (141, 169, 177) and Org 24598 (178)] were produced but caused unexpected toxicity and side effects (15, 178). Only two sarcosine-based GlyT1 inhibitors, AMG 747 (184) and Org 25935 (also known as SCH 900435 or MK-8435) (183), were advanced into clinical trials. Both AMG 747 and Org 25935 trials ended due to unspecified safety events and failure to benefit schizophrenia, respectively (182). Researchers have focused on the low-affinity GlyT1 inhibitor sarcosine as an adjunctive medication to conventional antipsychotics. Off-label use of sarcosine in clinical studies has been demonstrated to improve positive symptoms, negative symptoms, and quality of life with minimal side effects in patients with schizophrenia (148, 153, 185, 198). Moreover, findings from previous clinical trials and moderator analyses further indicated that sarcosine is more efficacious than D-serine in general psychopathology for chronically ill stable schizophrenic patients as well as for schizophrenic patients with acutely exacerbated symptoms of schizophrenia (123, 148, 153). Along the same lines, a series of studies from the Polish Sarcosine Study in Schizophrenia (PULSAR) project illustrated that schizophrenic patients treated with sarcosine for 6 months displayed significant improvements in negative symptoms, general psychopathology and changes in glutamatergic transmission in the brain (190, 192, 193). However, no significant differences in cardiometabolic systems, body composition or neurochemical levels (e.g., BDNF, IL-6 and TNF-α) were found in PULSAR studies (191, 194–197). Double-blind clinical studies revealed no beneficial effect of adjunctive sarcosine in drug-free schizophrenia patients or patients treated with clozapine (186, 187, 199). In terms of the side effects and safety profile of sarcosine, the overall results have been satisfactory in most clinical studies; however, sarcosine administered with glutamatergic and serotoninergic agents may have had a synergistic effect that exacerbated schizophrenic symptoms and hypomania in two case reports (188, 189).

Non-sarcosine-based GlyT1 Inhibitors

In addition to sarcosine-based inhibitors, non-sarcosine-derived GlyT1 inhibitors are potential alternatives for indirectly modulating the GMS on NMDARs. Compared to sarcosine-based GlyT1 inhibitors, non-sarcosine-based compounds are associated with faster off-rates and less toxic side effects (182). The earliest non-sarcosine-based GlyT1 inhibitors, including SSR504734 (216), SSR103800 (217), GSK1018921 (218), and DCCCyB (219), were developed and have been entered into phase I clinical trials. However, the trials with all these compounds were halted or discontinued for undisclosed reasons (182, 200, 220). In addition, PF-3463275, another non-sarcosine-based GlyT1 inhibitor developed by Pfizer (221), was entered into clinical trials and provided positive results for the enhancement of cognitive remediation in schizophrenia (201). However, the first phase II clinical trial (203) on the use of PF-3463275 as an add-on therapy for the treatment of negative symptoms was terminated because of unspecified scientific reasons and safety concerns. The second phase II clinical trial

TABLE 5 | Major findings in clinical trials examining effects of non-sarcosine-non-sarcosine-based glycine transporter 1 (GlyT1) inhibitors in patients with schizophrenia.

Compound	Type	Study site	Patient	Usage	Subject number (placebo vs. experiment)	Dosage	Trial duration (weeks)	Clinical outcomes	Clinical ratings	References
SSR504734	Phase I		SZ		Undisclosed details			Terminated		(182)
SSR103800	Phase I		SZ		Undisclosed details			Terminated		(182)
GSK1018921	DB (Parallel) (NCT00929370)		SZ		Undisclosed details		4	Terminated	PANSS, CGI, VAS, SAS, AIMS, BARS	(200)
DCCCyB	Phase I		SZ		Undisclosed details			Terminated		(182)
PF-03463275	DB (Crossover) (NCT01911676)	US	SZ	Add on (Risperidone, aripiprazole)	9 (12) (Risperidone: 5 (6), aripiprazole: 4 (6))	10, 20, 40 (mg, BID)	1	+ (40 mg: enhanced neuroplasticity)	PET, EEG (LTP)	(201)
				Add on	10 (11)	60 (mg, BID)	1	–		(202)
	DB (Parallel) (NCT00977522)	US	SZ (Negative Symptom)	Add on	207 (Total)	30 (mg, BID)	12	Teminated	PANSS, SANS, CGI, GAS, MCCB, SQLS, C-SSRS, ESRS	(203)
Bitopertin	DB (Parallel) (NCT01192867)	Worldwide (FlashLyte)	SZ (Negative Symptom)	Add on	594 (total)	10, 20 (mg/day)	24	–	PANSS, CGI, PSP	(204)
	DB (Parallel)	Worldwide (CandleLyte)	SZ (Acute exacerbation)	Alone	58 (80) vs. 56 (80) vs. 60 (77) (Placebo vs. 10 vs. 30)	10, 30 (mg/day)	4	–	PANSS, CGI, C-SSRS, SCID-CT, ESRS, NOSIE, ESRS	(205)
	DB (Parallel) (NCT01192906)	Worldwide (DayLyte)	SZ (Negative Symptom)	Add on	605 (Total)	5, 10 (mg/day)	24	–	PANSS, PSP	(206)
	DB (Parallel) (NCT00616798)	Worldwide	SZ (Negative/ disorganized thought)	Add on	61 (81) vs. 60 (82) vs. 57 (81) vs. 53 (79) (Placebo vs. 10 vs. 30 vs. 60)	10, 30, 60 (mg/day)	8	+ (Negative symptoms)	PANSS, CGI, PSP, SQLS, HRQoL, SAS, AIMS, BARS	(207)
										(208)
								– (Quality of life)		(209)
	DB (Parallel) (JapicCTI-111627)	Japan	SZ (Negative Symptom)	Add on	9 (15) vs. 57 (73) vs. 48 (73) (No placebo)	5, 10, 20 (mg/day)	52	+ (Negative & sub-optimally controlled symptoms) (20 mg: adverse events)	PANSS, CGI, PSP, C-SSRS, ESRS	(210)
	DB (Parallel) (NCT01235520)	Worldwide (TwiLyte)	SZ	Add on	186 (196) vs. 188 (198) vs. 186 (194) (Placebo vs. 10 vs. 20)	10, 20 (mg/day)	12	–	PANSS, CGI, PSP, C-SSRS, ESRS	(211)
	DB (Parallel) (NCT01235585)	Worldwide (MoonLyte)			186 (193) vs. 187 (195) vs. 191 (200) (Placebo vs. 5 vs. 10)	5, 10 (mg/day)		–		
	DB (Parallel) (NCT01235559)	Worldwide (NightLyte)			189 (199) vs. 190 (198) vs. 190 (199) (Placebo vs. 10 vs. 20)	10, 20 (mg/day)		+ (10 mg: positvie symptoms)		
	DB (Parallel) (NCT01192880)	Worldwide (SunLyte)	SZ (Negative Sympt)	Add on	625 (630)	10, 20 (mg/day)	24	– (Small Effect size)	PANSS, NSA-16, CGI, PSP, C-SSRS, ESRS	(212)

(Continued)

TABLE 5 | Continued

Compound	Type	Study site	Patient	Usage	Subject number (placebo vs. experiment)	Dosage	Trial duration (weeks)	Clinical outcomes	Clinical ratings	References
	DB (Parallel) (NCT01192906)	Worldwide (DayLyte)			203 (209) vs. 205 (211) vs. 197 (201) (Placebol vs. 5 vs. 10)	5, 10 (mg/day)		–		
	DB (Parallel) (NCT01192867)	Worldwide (FlashLyte)			197 (210) vs. 200 (208) vs. 197 (208) (Placebo vs. 10 vs. 20)	10, 20 (mg/day)		–		
	DB (Parallel) (NCT01116830)	US	SZ or SZA	Add on	12 vs. 17	10 (mg/day)	6	–	PANSS, MCCB, ERP (MMN)	(213)
	OL (NCT01116830)	US	SZ or SZA	Add on	12 vs. 17	10 (mg/day)	6	–	PANSS, MCCB, ERP (MMN)	(157)
BI 425809	DB (Parallel) (NCT03859973)	Worldwide	SZ	Add on (without clozapine)	200 (Total)	10 (mg/day)	12	Recruiting	PANSS, CGI, MCCB, SCoRS, BET, VRFCAT, PRECIS	(214)
	DB (Parallel) (NCT02832037)	Worldwide	SZ	Add on	160 (170) vs. 77 (85) vs. 79 (84) vs. 81 (85) vs. 83 (85) (Placebo vs. 2 vs. 5 vs. 10 vs. 25)	2, 5, 10, 25 (mg/day)	12	+ (Cognitive symptoms)	PANSS, MCCB, PSP, SCoRS, C-SSRS	(215)

+, Positive clinical results; –, Negative clinical results; AIMS, Abnormal Involuntary Movements Scale; BARS, Barnes Akathisia Rating Scale; BET, Balloon Effort Task; CGI, Clinical Global Impression; C-SSRS, Columbia-Suicide Severity Rating Scale; DB, double-blind; EEG, Electroencephalogram; ERP, Event Related Potential; ESRS, Extrapyramidal Symptom Rating Scale; GAS, Global Assessment Scale; HRQoL, Health-Related Quality of Life; LTP, Long-term potentiation; MCCB, MATRICS consensus cognitive battery; MMN, Mismatch negativity; NOSIE, Nurses' Observation Scale for Inpatient Evaluation; NSA-16, Negative Symptom Assessment-16; OL, open-label; PANSS, Positive and Negative Syndrome Scale; PRECIS, Patient Reported Experience of Cognitive Impairment in Schizophrenia; PSP, Personal and Social Performance Scale; SANS, Scale for the Assessment of Negative Symptoms; SAS, Simpson Angus Scale for Assessment of Extrapyramidal Side Effects; SCID-CT, Structured Clinical Interview for DSM-IV–Clinical Trials version; SCoRS, Schizophrenia Cognition Rating Scale; SQLS, Schizophrenia Quality of Life Scale; SZ, schizophrenia; SZA, schizoaffective disorder; VAS, Visual Assessment Scale; VRFCAT, Virtual Reality Functional Capacity Assessment Tool.

(202) was initiated in 2013, and although it has remained active, to the best of our knowledge, there has been no recruitment efforts to date.

In addition to the abovementioned non-sarcosine-based GlyT1 inhibitors, bitopertin (also known as RG1678 or RO4917838) is an oral, non-competitive GlyT1 inhibitor that was originally developed by Roche as a potential drug candidate for the treatment of negative symptoms of schizophrenia. Preclinical studies revealed that bitopertin modulated schizophrenia-like behaviors in several naïve and pharmacologically challenged animal models (222, 223). The most promising finding of bitopertin was the result of an 8-week randomized, double-blind, proof-of-concept phase II study, in which bitopertin was proven to be safe, with the results showing an inverted U-shaped dose–response efficacy against the predominant negative symptoms of stable schizophrenia patients (207, 208), but no similar effect was observed in the quality of life of these patients (209). Subsequently, in a phase II/III clinical trial, bitopertin monotherapy improved only the positive subscale score of the PANSS (Positive and Negative Syndrome Scale) with respect to acute exacerbation of schizophrenia (205). In a randomized double-blind phase III study following one-year as an adjunctive treatment, bitopertin was found to be generally safe and well-tolerated for the treatment of Japanese patients with schizophrenia, and all three bitopertin-treated groups showed improvements in all the efficacy endpoints for both "negative symptoms" and "suboptimally controlled symptoms" throughout the duration of the study (210). Except for this study, unfortunately, the superior efficacy over placebo of adjunctive bitopertin at any of the doses tested in patients with persistent predominant negative symptoms of schizophrenia could not be proven in several randomized, double-blind, placebo-controlled phase III trials (204, 206, 211, 212). Furthermore, bitopertin did not significantly affect any symptoms, NMDAR-related biomarkers, or MMN frequency at the doses tested in double-blind clinical trials with patients with schizophrenia (157, 213). Accordingly, the negative results and small improvements associated with bitopertin suggest that adjunctive bitopertin treatment might only offer a modest benefit and that bitopertin might not be a broadly effective or optimal therapeutic candidate for the treatment of schizophrenia. Further study will be needed to elucidate the effect of bitopertin in animal models and clinical trials.

Furthermore, BI 425809 was recently developed by Boehringer Ingelheim as a novel, investigational GlyT1 inhibitor to improve cognitive function and memory in patients with schizophrenia and Alzheimer's disease (224–226). A recent randomized double-blind, placebo-controlled phase II study revealed that BI 425809 improved cognitive functions after 12 weeks in patients with schizophrenia (215), suggesting that BI 425809 can provide an effective treatment for cognitive impairment associated with schizophrenia. Currently, another phase II trial of BI 425809 combined with computerized cognitive training for schizophrenic patients is in progress (214, 227). Further large-scale phase III clinical trials will be necessary to replicate these encouraging findings and to confirm the therapeutic potential of BI 425809 for the treatment of cognitive deficits in schizophrenia.

In summary, both sarcosine-based and non-sarcosine-based GlyT1 inhibitors are generally well-tolerated and exhibit a satisfactory safety profile. GlyT1 inhibitors also exert more-promising therapeutic potential than agonists directly targeting the GMS in the improvement of schizophrenic symptoms. However, in consideration of the etiology and pathophysiology of schizophrenia, no evidence has supported a proposal that GlyT1 is overexpressed in the brains of schizophrenic patients. In contrast, a series of negative findings of association studies have revealed that neither glycine transmission nor GlyT1 is implicated in the pathogenesis of schizophrenia (228–230). As described previously, although concentrations of glycine are 10-fold higher than D-serine, D-serine is considered the dominant endogenous coagonist of NMDARs and a modulator of NMDAR-related neurotoxicity (20, 21). Thus, targeting GlyT1 might not be an optimal strategy for modulation of NMDAR functions. Furthermore, functional distinctions between synaptic and extrasynaptic NMDARs in brain physiology, in which synaptic and extrasynaptic NMDARs are gated by D-serine and glycine, respectively, have been reported (22, 231). D-serine and glycine differentially impact NMDAR membrane diffusion and neuroplasticity (21, 22). Given that glycine, but not D-serine, preferentially gates NMDARs located at extrasynaptic sites and that synaptic, but not extrasynaptic, NMDARs are essential for LTP induction, it is plausible that the efficacy and therapeutic effect of GlyT1 inhibitors might be relatively less effective than those of D-serine. Thus, as an alternative to GlyT1 inhibitors, one of the promising approaches for the development of novel therapeutic compounds to treat schizophrenia is based on increased synaptic D-serine levels realized through the indirect modulation of astrocytic D-serine synthesis.

Indirect Modulation of NMDAR Functions by Targeting DAO

DAO (or DAAO) encodes D-amino acid oxidase which has a flavin adenine dinucleotide (FAD) as the prosthetic group, and DAO catalyzes the oxidative deamination of a wide range of D-amino acids, including D-serine (232–234). The human *DAO* gene is located on chromosome 12q24, and DAO is mainly expressed in the liver, kidney and CNS (235). DAO is abundant in both neurons and glial cells in the cerebral cortex, hippocampus and cerebellum and contributes to normal neuronal functioning (236, 237). DAO has been of interest in psychiatry because its major substrate in the brain is D-serine, which modulates NMDAR functions and contributes to NMDAR hypofunction in schizophrenia. D-serine is synthesized from L-serine by SR and is metabolized by DAO and SR through an α, β-elimination reaction. Among DAO substrates in the brain, D-serine is clearly the most abundant. DAO is believed to play a crucial role in the regulation of cellular D-serine concentrations and release (143). In particular, the three-dimensional structure of human DAO is a stable homodimer and it is highly conserved compared to the microorganism sources (238, 239). Human DAO possesses a low FAD binding function and mainly presents in an inactive apoprotein form (238, 240) because of its specific structure. DAO also exhibits a low substrate affinity and catalytic efficiency for

D-serine (234, 241). The inactive apoprotein form of human DAO prevents excessive degradation of D-serine in the brain. The active holeenzyme of human DAO is reconstituted by binding of active-site ligands, such as FAD and the substrate stabilizes flavin binding, and thus pushing the acquisition of catalytic competence (238, 242). Intriguingly, it has been reported that DAO inhibitor (e.g., benzoate) increases the holoenzyme reconstitution of human DAO and stabilizes the flavoprotein (243). In addition, human DAO is mainly colocalized with pyramidal neurons in the prefrontal cortex and hippocampus (236). Enhanced DAO activity is considered a potential cause of reduced D-serine and subsequent impairment to NMDAR functioning in schizophrenia (123, 244).

The glutamate hypothesis of schizophrenia suggests that increased DAO activity leads to decreased D-serine levels, which may subsequently lead to NMDAR hypofunction. Supporting evidence from association studies, DAO expression in schizophrenic patients and behavioral outcomes observed in rodent models have suggested potential therapeutic benefits of DAO inhibitors (DAOIs). Accumulating evidence from genetic studies has indicated that *DAO* and *G72* are putative genes related to schizophrenia (235, 245, 246). Schizophrenic patients with genetic variation in *DAO* and *G72* genes also display negative valence and cognitive deficits (247–250). In complementary findings, a recent GWAS revealed that of 108 schizophrenia-associated loci, none were within the *DAO* or *G72* gene regions (13). Although reports on the association of *DAO* and *G72* with schizophrenia are ambiguous, these genes remain candidates in schizophrenia because of their roles in glutamatergic signaling, which has been associated with schizophrenia in multiple lines of research (157, 166, 246). Both *G72* mRNA and G72 protein (as known as pLG72) are detected in higher levels in brain and blood of schizophrenia patients (251, 252). Intriguingly, DAO-pLG72 complex was reported to modulate intracellular D-serine concentration in human (233, 238), which suggests a novel avenue to design molecules to regulate human DAO activity and thus NMDAR function for future research. In the same vein, the expression and activity of DAO are significantly increased in patients with schizophrenia (28, 236, 244, 253). Intriguingly, it has been reported that chlorpromazine (i.e., a first-generation antipsychotic) and risperidone (i.e., a second-generation antipsychotic) are potentially active substances that inhibit DAO function (254, 255). In addition, inactivation of DAO in rodents produces behavioral and biochemical effects, suggesting potential therapeutic benefits (143). Indeed, increasing levels of D-serine have been observed in rodents after the administration of DAOIs (256–258). Consistently, PCP- or MK-801-induced pre-pulse inhibition deficits and cognitive deficits relevant to schizophrenia were ameliorated after treatment with DAOIs (256, 259, 260). DAOIs increase the levels of D-alanine, which might also be beneficial for increasing NMDAR function (260). Moreover, ddY/DAO(–) mice, which lack active DAO due to a point mutation, exhibited increased cerebellar NMDAR functions (261), enhanced hippocampal LTP, and improved spatial learning in a water maze (262). Other animal studies have indicated that DAO is involved in the mechanism of D-serine nephrotoxicity (263), which is attenuated by DAOIs (264). D-serine combined with DAOI or DAOI alone might be beneficial for enhancing NMDAR functions in schizophrenia.

In agreement with the abovementioned studies, DAOIs are among the most attractive therapeutic targets for improving cognition and reducing negative symptoms in schizophrenia discovered in recent decades. Basically, DAOIs can be divided into two categories: cofactor-competitive and substrate-competitive inhibitors (238, 240, 241, 265–267). Chlorpromazine, the first antipsychotic medication, is a traditional dopamine D2 receptor antagonist but it has been reported that chlorpromazine is also a FAD-competitive DAO inhibitor (243, 255). Compared to the cofactor-competitive inhibitor of DAO, substrate-competitive DAOIs (such as CBIO and benzoate) are frequently used as scaffolds for developing novel drugs. In the late 2000s, a series of structurally similar molecules (such as ASO57278 (256), Merck compound (257), Pfizer compounds (258), and CBIO (268), displayed a potent inhibition of DAO *in vitro* but had limited elevation of D-serine *in vivo*. Especially, it has been reported that acute and chronic administrations of ASO57278 produced inverted U-shaped dose-response curves to reverse PCP-induced PPI deficits (256). And co-administration of CBIO with D-serine also significantly increased D-serine level and attenuated MK-801 induced PPI deficit (259). Thus, these studies imply that DAOIs have beneficial effects in treatment of schizophrenia.

To date, there are at least two potential DAOIs that have been advanced into clinical evaluation, including sodium benzoate and TAK-831. Effects of these two DAOIs on the treatment of schizophrenic symptoms in clinical studies are summarized in **Table 6**. Sodium benzoate is known as a preservative that is widely used as a food pickling agent. Sodium benzoate is a prototype competitive inhibitor of DAO, and preclinical studies have indicated that it attenuates PCP-induced pre-pulse inhibition deficits as well as D-serine-induced nephrotoxicity (264, 277). The first randomized, double-blind, placebo-controlled trial with chronic schizophrenia patients reported that add-on sodium benzoate relieved positive, negative, and cognitive symptoms as well as improved quality of life (269). Sodium benzoate also showed efficacy and safety for schizophrenic patients who had a poor response to clozapine (270). Moreover, adjunctive sodium benzoate plus sarcosine, but not sarcosine alone, improved the cognitive and global functioning of chronic schizophrenia patients (199). However, a randomized clinical study in Australia indicated that adjunctive use of sodium benzoate had no effect on individuals with early psychosis (271, 272). Two adaptive clinical phase II studies performed to evaluate the safety and efficacy of sodium benzoate in adolescent schizophrenia patients (273) and treatment-resistant schizophrenia patients (274) are currently recruiting. One probable drawback for the development of sodium benzoate as a drug candidate is that it lacks patentability due to its simple chemical structure. More evidence on the therapeutic effect of sodium benzoate, especially in larger-scale clinical trials in schizophernia, is required to prove its effectiveness and applicability. In addition, another highly selective and potent DAOI from Takeda known as TAK-831

TABLE 6 | Potential clinical efficacy and benefits related to D-amino acid oxidase inhibitors (DAOIs) on the treatment of schizophrenic symptoms.

Compound	Type	Study site	Patient	Usage	Subject number (placebo vs. experiment)	Dosage	Trial duration (weeks)	Clinical outcomes	Clinical ratings	References
Sodium benzoate	DB (Parallel) (NCT00960219)	Taiwan	SZ	Add on	23 (27) vs. 24 (25)	1 (g/day)	6	+ (Positive, negative, general symptoms)	PANSS, SANS, CGI, GAF, MCCB, HDRS, QOLS, SAS, AIMS, BARS, UKU	(269)
	DB (Parallel)	Taiwan	SZ	Add on	16 (21) vs. 17 (21) (Placebo vs. sarcosine + Bezoate)	Sarcosine: 2 (g/day) Benzoate: 1 (g/day)	12	+ (Cognitive symptom)	PANSS, CGI, GAF, MCCB, SAS, AIMS, BARS, UKU	(199)
	DB (Parallel) (NCT01390376)	Taiwan	TRS SZ	Add on (Clozapine)	20 vs. 20 vs. 20 (Placebo vs. 1 vs. 2)	1, 2 (g/day)	6	+ (Positive, negative symptoms)	PANSS, SANS, GAF, MCCB, HDRS, QOLS, SAS, AIMS, BARS, UKU	(270)
	DB (Parallel) (ACTRN12615000187549)	Australia	Early psychosis (SZ, SCHF, delusion, bipolar)	Add on	160 (Total)	1 (g/day)	12	Protocol	PANSS, CGI, GAF, HDRS, AQOL, PAQ, PGI	(271)
					40 (50) vs. 39 (50)			–		(272)
	DB (Parallel) (NCT01908192)	US & Taiwan	SZ (Adolescent)	Add on	126 (Total)	1 (g/day)	6	Recruiting	PANSS, SANS, CGI, CGAS, CDRS-R	(273)
	DB (Parallel) (NCT03094429)	US	TRS SZ	Add on (Clozapine)	287 (Total)	1, 2 (g/day)	8	Recruiting	PANSS, CGI, HDRS, PSP, SQLS, C-SSRS, SAS, AIMS, BARS, C-SSRS	(274)
TAK-831	DB (Crossover) (NCT03359785)	US	SZ	Add on	31 (32) (Total)	50, 500 (mg/day)	8 days	Complete	BACS, EBC, ASSR, ERP (MMN)	(275)
	DB (Parallel) (NCT03382639)	Worldwide	SZ	Add on	307 (315) (Total)	50, 125, 500 (mg/day)	12	Complete	PANSS, BNSS, BACS, CGI, SCoRS	(276)

+, Positive clinical results; –, Negative clinical results; AIMS, Abnormal Involuntary Movements Scale; AQOL, Assessment of Quality of Life; ASSR, Auditory Steady State Response; BACS, Brief Assessment of Cognition in Schizophrenia; BARS, Barnes Akathisia Rating Scale; BNSS, Brief Negative Symptom Scale; CDRS-R, Children's Depression Rating Scale-Revised; CGAS, Children's Global Assessment Scale; CGI, Clinical Global Impression; C-SSRS, Columbia-Suicide Severity Rating Scale; DB, double-blind; EBC, Eye Blink Conditioning; ERP, Event Related Potential; GAF, Global Assessment of Function; HDRS, Hamilton Depression Rating Scale; MCCB, MATRICS consensus cognitive battery; MMN, Mismatch negativity; PANSS, Positive and Negative Syndrome Scale; PAQ, Physical Activity Questionnaire; PGI, Patient Global Impression; PSP, Personal and Social Performance scale; QOLS, Quality of Life Scale; SANS, Scale for the Assessment of Negative Symptoms; SAS, Simpson Angus Scale for Assessment of Extrapyramidal Side Effects; SCoRS, Schizophrenia Cognition Rating Scale; SQLS, Schizophrenia Quality of Life Scale; SZ, schizophrenia; SCHF, Schizophreniform disorder; TRS, treatment-resistant; UKU, Udvalg for Kliniske Undersogelser Side Effects Rating Scale.

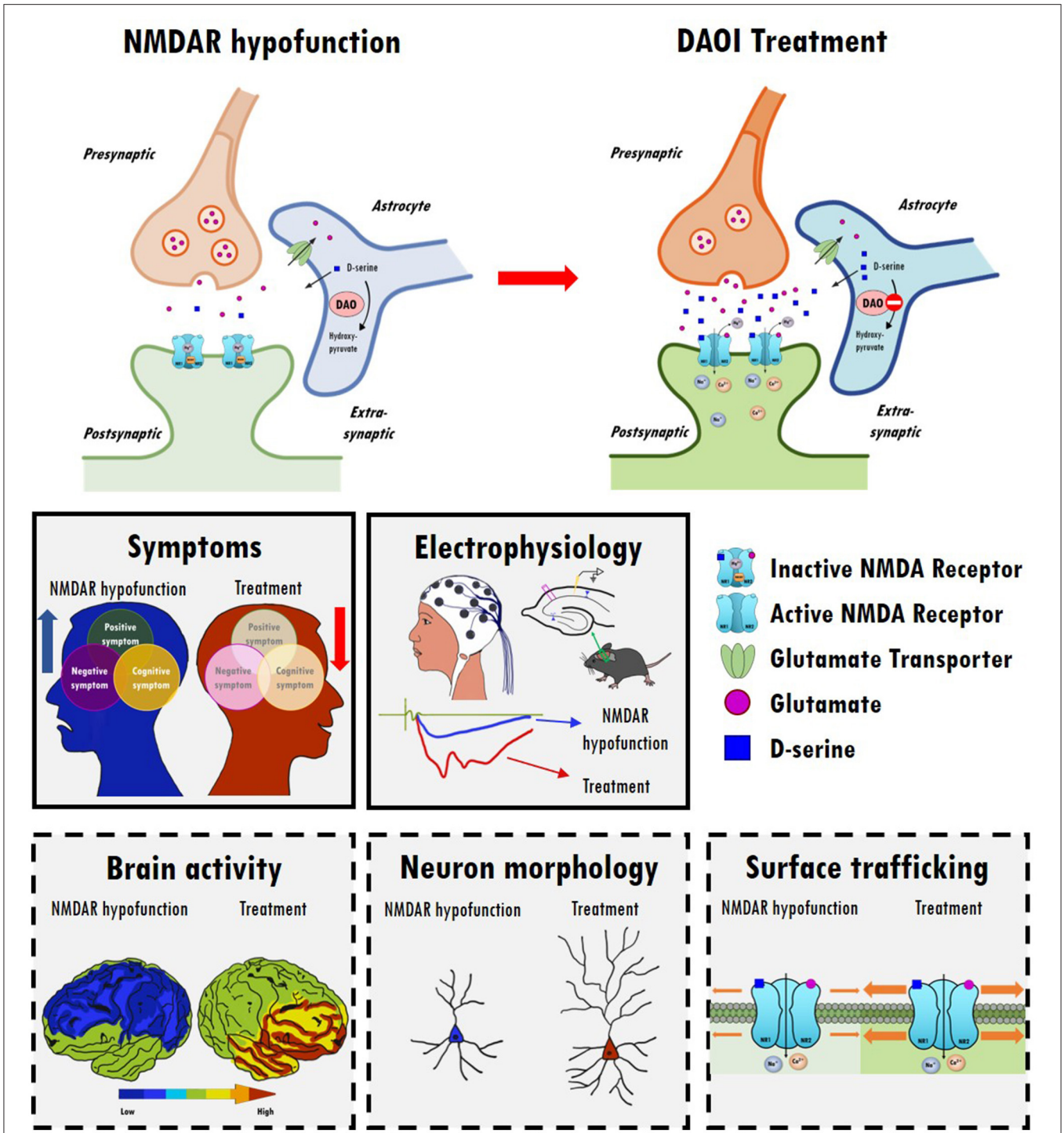

FIGURE 2 | The therapeutic effects and possible underlying mechanisms of D-amino acid oxidase inhibitors (DAOIs) in the treatment of schizophrenia. Top panel: Indirect modulation of NMDAR functions by DAOIs restores NMDAR hypofunction. Inhibition of DAO results in increased synaptic levels of D-serine. Middle panels: DAOIs significantly alleviate positive, negative, and cognitive symptoms in patients with schizophrenia and moderate schizophrenia-like behavioral deficits in animal models. DAOIs enhance NMDAR functions and hippocampal LTP in animal studies. Bottom panels: Possible mechanism of action of DAOIs. The effects of DAOIs on brain activity, neuromorphology, and cell surface trafficking of NMDARs, which contribute to the amelioration of NMDAR hypofunction and restoration of mental functions, are worthy of further investigation.

is currently being evaluated for schizophrenia in a phase II clinical trial (275, 276, 278). A series of studies of TAK831, including those directed to pharmacokinetics, target occupancy, and D-serine concentrations in the brain, have detected and

analyzed a non-linear quantitative multilayer mechanistic model for multilayer biomarker-assisted clinical development with multiple CNS indications (279). Investigations to discover the characteristics and potential development of TAK-831 are needed to determine its efficacy and tolerability in the management of different domains of schizophrenia. In addition to sodium benzoate and TAK-831, there are additional unpublished data on DAOIs for which patent applications have been filed and which have been claimed to have specific therapeutic utility in the treatment of schizophrenia and other neuropsychiatric disorders (280). It is worth further investigating the safety and therapeutic potential of these novel DAOIs for the treatment of unmet medical needs of patients with in schizophrenia in future studies.

CONCLUSION

Data from clinical, genetic, postmortem, and animal studies strongly implicate NMDARs as central hubs for many pathophysiological processes in the brains of schizophrenic patients. Notably, several NMDAR-enhancing agents, particularly those directed to the GMS of NMDARs, result in the significant alleviation of schizophrenia-like behavioral deficits and cognitive dysfunctions in animal models as well as in patients with schizophrenia. There is great interest in identifying potential drug candidates targeting the GMS of NMDARs and to evaluate their therapeutic effectiveness in attenuating the negative and cognitive symptoms of schizophrenia with minimal adverse effects. Modulation of NMDAR functions through the GMS has been proposed as a possible therapeutic approach to drug development, and either direct or indirect activation of GMS results in differential benefits and adverse effects in the treatment of schizophrenia. A summary of the relevant animal study data, as well as those from clinical trials, examining the therapeutic effects and experimental outcomes of direct and indirect GMS modulators is provided in this article. Overall, current findings suggest that indirectly targeting GMS appears to be more beneficial and results in fewer adverse effects than directly targeting GMS to modulate NMDAR functions. In particular, compared with GlyT1 inhibitors, one of the promising approaches to the development of novel therapeutic compounds for treating schizophrenia is to indirectly increase synaptic D-serine levels by targeting DAO. As illustrated in **Figure 2**, inhibition of DAO via DAOIs not only results in increased synaptic D-serine levels but also the regulation of NMDAR-evoked electrophysiological activity, which contributes to the amelioration of NMDAR hypofunction and restoration of mental functions. There is great interest in further investigating the effects of DAOIs on brain activity, neuromorphology, and cell surface trafficking of NMDARs, which contribute to the amelioration of NMDAR hypofunction and untreated symptoms of schizophrenia. Thus, GMS modulators, especially GlyT1 inhibitors and DAOIs, may open new avenues to the treatment of unmet medical needs in patients with schizophrenia, which is worthy of further investigation. For the development of new antipsychotic drugs, the establishment of safety profiles of these potential compounds will be beneficial and informative, possibly leading to the elucidation of their precise mechanisms of action and the evaluation of their therapeutic effects in both animal models and clinical studies. Notably, however, this review presents an oversimplified summary of the treatment alternatives for an extremely complex psychiatric disorder. Indeed, human diseases are far more complex and only some aspects of human diseases can be partially modeled in animal models. Clinical trials are essential and irreplaceable in drug development. In complementary to human studies, preclinical animal studies are highly valuable and indispensable to the understanding of the underlying mechanism and for the development of new drugs. And we simply focus on discussing the importance of NMDAR functions on excitatory rather than inhibitory neurons in this review article. The role of inhibitory neurons and the impact of NMDAR hypofunction on GABAergic neurons in the pathophysiology of schizophrenia are worth further investigating (281, 282). Because the etiology of schizophrenia remains unclear, disturbances to the GABAergic, cholinergic, and dopaminergic neurotransmitter systems (283, 284), as well as disruptions to astrocyte function (164), are also worthy of further investigation.

AUTHOR CONTRIBUTIONS

J-CP and D-ZL are the key persons to wrote and prepare this review article. S-SG collected data and prepared tables. C-YC wrote some paragraphs of this article. W-SL organized, wrote, and modified the whole article. All authors contributed to the article and approved the submitted version.

FUNDING

This research was supported by Grant Nos. 109-2918-I-002-008, 109-2926-I-002-509, 109-2410-H-002-087-MY3, and 110-2410-H-002-235-MY3 from the Ministry of Science and Technology in Taiwan to W-SL and by grant support from National Taiwan University and National Taiwan University Hospital.

ACKNOWLEDGMENTS

We thank all members of the Laboratory of Integrated Neuroscience and Ethology (LINE) in the Department of Psychology, National Taiwan University, for their assistance and comments.

REFERENCES

1. He H, Liu Q, Li N, Guo L, Gao F, Bai L, et al. Trends in the incidence and DALYs of schizophrenia at the global, regional and national levels: results from the global burden of disease study 2017. *Epidemiol Psychiatr Sci.* (2020) 29:e91. doi: 10.1017/S2045796019000891
2. Lewis DA, Sweet RA. Schizophrenia from a neural circuitry perspective: advancing toward rational pharmacological therapies. *J Clin Invest.* (2009) 119:706–16. doi: 10.1172/JCI37335
3. Powell CM, Miyakawa T. Schizophrenia-relevant behavioral testing in rodent models: a uniquely human disorder? *Biol Psychiatry.* (2006) 59:1198–207. doi: 10.1016/j.biopsych.2006.05.008

4. McCleery A, Green MF, Hellemann GS, Baade LE, Gold JM, Keefe RS, et al. Latent structure of cognition in schizophrenia: a confirmatory factor analysis of the MATRICS consensus cognitive battery (MCCB). *Psychol Med.* (2015) 45:2657–66. doi: 10.1017/S0033291715000641
5. Strauss GP, Horan WP, Kirkpatrick B, Fischer BA, Keller WR, Miski P, et al. Deconstructing negative symptoms of schizophrenia: avolition-apathy and diminished expression clusters predict clinical presentation and functional outcome. *J Psychiatr Res.* (2013) 47:783–90. doi: 10.1016/j.jpsychires.2013.01.015
6. Elert E. Aetiology: searching for schizophrenia's roots. *Nature.* (2014) 508:S2–3. doi: 10.1038/508S2a
7. Bowie CR, Harvey PD. Cognitive deficits and functional outcome in schizophrenia. *Neuropsychiatr Dis Treat.* (2006) 2:531–6. doi: 10.2147/nedt.2006.2.4.531
8. Correll CU, Schooler NR. Negative symptoms in schizophrenia: a review and clinical guide for recognition, assessment, and treatment. *Neuropsychiatr Dis Treat.* (2020) 16:519–34. doi: 10.2147/NDT.S225643
9. Tripathi A, Kar SK, Shukla R. Cognitive deficits in schizophrenia: understanding the biological correlates and remediation strategies. *Clin Psychopharmacol Neurosci.* (2018) 16:7–17. doi: 10.9758/cpn.2018.16.1.7
10. Mohamed S, Paulsen JS, O'Leary D, Arndt S, Andreasen N. Generalized cognitive deficits in schizophrenia: a study of first-episode patients. *Arch Gen Psychiatry.* (1999) 56:749–54. doi: 10.1001/archpsyc.56.8.749
11. Marder SR. The NIMH-MATRICS project for developing cognition-enhancing agents for schizophrenia. *Dialogues Clin Neurosci.* (2006) 8:109–13. doi: 10.31887/DCNS.2006.8.1/smarder
12. Lally J, MacCabe JH. Antipsychotic medication in schizophrenia: a review. *Br Med Bull.* (2015) 114:169–79. doi: 10.1093/bmb/ldv017
13. Schizophrenia Working Group of the Psychiatric Genomics C. Biological insights from 108 schizophrenia-associated genetic loci. *Nature.* (2014) 511:421–7. doi: 10.1038/nature13595
14. Egerton A, Stone JM. The glutamate hypothesis of schizophrenia: neuroimaging and drug development. *Curr Pharm Biotechnol.* (2012) 13:1500–12. doi: 10.2174/138920112800784961
15. Moghaddam B, Javitt D. From revolution to evolution: the glutamate hypothesis of schizophrenia and its implication for treatment. *Neuropsychopharmacology.* (2012) 37:4–15. doi: 10.1038/npp.2011.181
16. Uno Y, Coyle JT. Glutamate hypothesis in schizophrenia. *Psychiatry Clin Neurosci.* (2019) 73:204–15. doi: 10.1111/pcn.12823
17. Parsons CG, Danysz W, Quack G. Glutamate in CNS disorders as a target for drug development: an update. *Drug News Perspect.* (1998) 11:523–69. doi: 10.1358/dnp.1998.11.9.863689
18. Johnson JW, Ascher P. Glycine potentiates the NMDA response in cultured mouse brain neurons. *Nature.* (1987) 325:529–31. doi: 10.1038/325529a0
19. Bergeron R, Meyer TM, Coyle JT, Greene RW. Modulation of N-methyl-D-aspartate receptor function by glycine transport. *Proc Natl Acad Sci USA.* (1998) 95:15730–4. doi: 10.1073/pnas.95.26.15730
20. Shleper M, Kartvelishvily E, Wolosker H. D-serine is the dominant endogenous coagonist for NMDA receptor neurotoxicity in organotypic hippocampal slices. *J Neurosci.* (2005) 25:9413–7. doi: 10.1523/JNEUROSCI.3190-05.2005
21. Wolosker H, Balu DT. D-Serine as the gatekeeper of NMDA receptor activity: implications for the pharmacologic management of anxiety disorders. *Transl Psychiatry.* (2020) 10:184. doi: 10.1038/s41398-020-00870-x
22. Papouin T, Ladepeche L, Ruel J, Sacchi S, Labasque M, Hanini M, et al. Synaptic and extrasynaptic NMDA receptors are gated by different endogenous coagonists. *Cell.* (2012) 150:633–46. doi: 10.1016/j.cell.2012.06.029
23. Cull-Candy S, Brickley S, Farrant M. NMDA receptor subunits: diversity, development and disease. *Curr Opin Neurobiol.* (2001) 11:327–35. doi: 10.1016/S0959-4388(00)00215-4
24. Balu DT. The NMDA receptor and schizophrenia: from pathophysiology to treatment. *Adv Pharmacol.* (2016) 76:351–82. doi: 10.1016/bs.apha.2016.01.006
25. Fromer M, Pocklington AJ, Kavanagh DH, Williams HJ, Dwyer S, Gormley P, et al. De novo mutations in schizophrenia implicate synaptic networks. *Nature.* (2014) 506:179–84. doi: 10.1038/nature12929
26. Kirov G, Pocklington AJ, Holmans P, Ivanov D, Ikeda M, Ruderfer D, et al. De novo CNV analysis implicates specific abnormalities of postsynaptic signalling complexes in the pathogenesis of schizophrenia. *Mol Psychiatry.* (2012) 17:142–53. doi: 10.1038/mp.2011.154
27. Weickert CS, Fung SJ, Catts VS, Schofield PR, Allen KM, Moore LT, et al. Molecular evidence of N-methyl-D-aspartate receptor hypofunction in schizophrenia. *Mol Psychiatry.* (2013) 18:1185–92. doi: 10.1038/mp.2012.137
28. Bendikov I, Nadri C, Amar S, Panizzutti R, De Miranda J, Wolosker H, et al. A CSF and postmortem brain study of D-serine metabolic parameters in schizophrenia. *Schizophr Res.* (2007) 90:41–51. doi: 10.1016/j.schres.2006.10.010
29. Catts VS, Lai YL, Weickert CS, Weickert TW, Catts SV. A quantitative review of the postmortem evidence for decreased cortical N-methyl-D-aspartate receptor expression levels in schizophrenia: how can we link molecular abnormalities to mismatch negativity deficits? *Biol Psychol.* (2016) 116:57–67. doi: 10.1016/j.biopsycho.2015.10.013
30. Javitt DC, Zukin SR. Recent advances in the phencyclidine model of schizophrenia. *Am J Psychiatry.* (1991) 148:1301–8. doi: 10.1176/ajp.148.10.1301
31. Krystal JH, Abi-Saab W, Perry E, D'Souza DC, Liu N, Gueorguieva R, et al. Preliminary evidence of attenuation of the disruptive effects of the NMDA glutamate receptor antagonist, ketamine, on working memory by pretreatment with the group II metabotropic glutamate receptor agonist, LY354740, in healthy human subjects. *Psychopharmacology.* (2005) 179:303–9. doi: 10.1007/s00213-004-1982-8
32. Krystal JH, Karper LP, Seibyl JP, Freeman GK, Delaney R, Bremner JD, et al. Subanesthetic effects of the noncompetitive NMDA antagonist, ketamine, in humans. Psychotomimetic, perceptual, cognitive, and neuroendocrine responses. *Arch Gen Psychiatry.* (1994) 51:199–214. doi: 10.1001/archpsyc.1994.03950030035004
33. Kegeles LS, Abi-Dargham A, Zea-Ponce Y, Rodenhiser-Hill J, Mann JJ, Van Heertum RL, et al. Modulation of amphetamine-induced striatal dopamine release by ketamine in humans: implications for schizophrenia. *Biol Psychiatry.* (2000) 48:627–40. doi: 10.1016/S0006-3223(00)00976-8
34. Bressan RA, Pilowsky LS. Imaging the glutamatergic system *in vivo*–relevance to schizophrenia. *Eur J Nucl Med.* (2000) 27:1723–31. doi: 10.1007/s002590000372
35. Gonzalez-Burgos G, Lewis DA. NMDA receptor hypofunction, parvalbumin-positive neurons, and cortical gamma oscillations in schizophrenia. *Schizophr Bull.* (2012) 38:950–7. doi: 10.1093/schbul/sbs010
36. Bartha R, Williamson PC, Drost DJ, Malla A, Carr TJ, Cortese L, et al. Measurement of glutamate and glutamine in the medial prefrontal cortex of never-treated schizophrenic patients and healthy controls by proton magnetic resonance spectroscopy. *Arch Gen Psychiatry.* (1997) 54:959–65. doi: 10.1001/archpsyc.1997.01830220085012
37. Theberge J, Bartha R, Drost DJ, Menon RS, Malla A, Takhar J, et al. Glutamate and glutamine measured with 4.0 T proton MRS in never-treated patients with schizophrenia and healthy volunteers. *Am J Psychiatry.* (2002) 159:1944–6. doi: 10.1176/appi.ajp.159.11.1944
38. Olney JW, Newcomer JW, Farber NB. NMDA receptor hypofunction model of schizophrenia. *J Psychiatr Res.* (1999) 33:523–33. doi: 10.1016/S0022-3956(99)00029-1
39. Gao WJ, Yang SS, Mack NR, Chamberlin LA. Aberrant maturation and connectivity of prefrontal cortex in schizophrenia-contribution of NMDA receptor development and hypofunction. *Mol Psychiatry.* (2021). doi: 10.1038/s41380-021-01196-w
40. Wolkin A, Sanfilipo M, Wolf AP, Angrist B, Brodie JD, Rotrosen J. Negative symptoms and hypofrontality in chronic schizophrenia. *Arch Gen Psychiatry.* (1992) 49:959–65. doi: 10.1001/archpsyc.1992.01820120047007
41. Carter CS, Perlstein W, Ganguli R, Brar J, Mintun M, Cohen JD. Functional hypofrontality and working memory dysfunction in schizophrenia. *Am J Psychiatry.* (1998) 155:1285–7. doi: 10.1176/ajp.155.9.1285
42. Krzystanek M, Palasz A. NMDA receptor model of antipsychotic drug-induced hypofrontality. *Int J Mol Sci.* (2019) 20:1442. doi: 10.3390/ijms20061442
43. Muir KW. Glutamate-based therapeutic approaches: clinical trials with NMDA antagonists. *Curr Opin Pharmacol.* (2006) 6:53–60. doi: 10.1016/j.coph.2005.12.002

44. Rothman SM, Olney JW. Glutamate and the pathophysiology of hypoxic–ischemic brain damage. *Ann Neurol.* (1986) 19:105–11. doi: 10.1002/ana.410190202
45. Yamamoto K, Mifflin S. Inhibition of glial glutamate transporter GLT1 in the nucleus of the solitary tract attenuates baroreflex control of sympathetic nerve activity and heart rate. *Physiol Rep.* (2018) 6:e13877. doi: 10.14814/phy2.13877
46. Kleckner NW, Dingledine R. Requirement for glycine in activation of NMDA-receptors expressed in xenopus oocytes. *Science.* (1988) 241:835–7. doi: 10.1126/science.2841759
47. Ballard TM, Pauly-Evers M, Higgins GA, Ouagazzal AM, Mutel V, Borroni E, et al. Severe impairment of NMDA receptor function in mice carrying targeted point mutations in the glycine binding site results in drug-resistant nonhabituating hyperactivity. *J Neurosci.* (2002) 22:6713–23. doi: 10.1523/JNEUROSCI.22-15-06713.2002
48. Kew JN, Koester A, Moreau JL, Jenck F, Ouagazzal AM, Mutel V, et al. Functional consequences of reduction in NMDA receptor glycine affinity in mice carrying targeted point mutations in the glycine binding site. *J Neurosci.* (2000) 20:4037–49. doi: 10.1523/JNEUROSCI.20-11-04037.2000
49. Labrie V, Lipina T, Roder JC. Mice with reduced NMDA receptor glycine affinity model some of the negative and cognitive symptoms of schizophrenia. *Psychopharmacology.* (2008) 200:217–30. doi: 10.1007/s00213-008-1196-6
50. Fadda E, Danysz W, Wroblewski JT, Costa E. Glycine and D-serine increase the affinity of N-methyl-D-aspartate sensitive glutamate binding sites in rat brain synaptic membranes. *Neuropharmacology.* (1988) 27:1183–5. doi: 10.1016/0028-3908(88)90015-9
51. Schwarcz R, Bruno JP, Muchowski PJ, Wu HQ. Kynurenines in the mammalian brain: when physiology meets pathology. *Nat Rev Neurosci.* (2012) 13:465–77. doi: 10.1038/nrn3257
52. Erhardt S, Blennow K, Nordin C, Skogh E, Lindstrom LH, Engberg G. Kynurenic acid levels are elevated in the cerebrospinal fluid of patients with schizophrenia. *Neurosci Lett.* (2001) 313:96–8. doi: 10.1016/S0304-3940(01)02242-X
53. Javitt DC, Spencer KM, Thaker GK, Winterer G, Hajos M. Neurophysiological biomarkers for drug development in schizophrenia. *Nat Rev Drug Discov.* (2008) 7:68–83. doi: 10.1038/nrd2463
54. Lin CH, Huang CL, Chang YC, Chen PW, Lin CY, Tsai GE, et al. Clinical symptoms, mainly negative symptoms, mediate the influence of neurocognition and social cognition on functional outcome of schizophrenia. *Schizophr Res.* (2013) 146:231–7. doi: 10.1016/j.schres.2013.02.009
55. Salituro FG, Harrison BL, Baron BM, Nyce PL, Stewart KT, McDonald IA. 3-(2-carboxyindol-3-yl)propionic acid derivatives: antagonists of the strychnine-insensitive glycine receptor associated with the N-methyl-D-aspartate receptor complex. *J Med Chem.* (1990) 33:2944–6. doi: 10.1021/jm00173a003
56. Cordi A, Lacoste JM, Audinot V, Millan M. Design, synthesis and structure-activity relationships of novel strychnine-insensitive glycine receptor ligands. *Bioorg Med Chem Lett.* (1999) 9:1409–14. doi: 10.1016/S0960-894X(99)00194-8
57. Krueger BA, Weil T, Schneider G. Comparative virtual screening and novelty detection for NMDA-GlycineB antagonists. *J Comput Aided Mol Des.* (2009) 23:869–81. doi: 10.1007/s10822-009-9304-1
58. Bristow LJ, Flatman KL, Hutson PH, Kulagowski JJ, Leeson PD, Young L, et al. The atypical neuroleptic profile of the glycine/N-methyl-D-aspartate receptor antagonist, L-701,324, in rodents. *J Pharmacol Exp Ther.* (1996) 277:578–85.
59. Witkin JM, Brave S, French D, Geter-Douglass B. Discriminative stimulus effects of R-(+)-3-amino-1-hydroxypyrrolid-2-one, [(+)-HA-966], a partial agonist of the strychnine-insensitive modulatory site of the N-methyl-D-aspartate receptor. *J Pharmacol Exp Ther.* (1995) 275:1267–73.
60. Jonas P, Bischofberger J, Sandkühler J. Corelease of two fast neurotransmitters at a central synapse. *Science.* (1998) 281:419–24. doi: 10.1126/science.281.5375.419
61. Zafra F, Giménez C. Glycine transporters and synaptic function. *IUBMB Life.* (2008) 60:810–7. doi: 10.1002/iub.128
62. Murtas G, Marcone GL, Sacchi S, Pollegioni L. L-serine synthesis via the phosphorylated pathway in humans. *Cell Mol Life Sci.* (2020) 77:5131–48. doi: 10.1007/s00018-020-03574-z
63. Béchade C, Sur C, Triller A. The inhibitory neuronal glycine receptor. *Bioessays.* (1994) 16:735–44. doi: 10.1002/bies.950161008
64. Ishimaru M, Kurumaji A, Toru M. Increases in strychnine-insensitive glycine binding sites in cerebral cortex of chronic schizophrenics: evidence for glutamate hypothesis. *Biol Psychiatry.* (1994) 35:84–95. doi: 10.1016/0006-3223(94)91197-5
65. Waziri R, Baruah S. A hyperglycinergic rat model for the pathogenesis of schizophrenia: preliminary findings. *Schizophr Res.* (1999) 37:205–15. doi: 10.1016/S0920-9964(98)00169-8
66. Heresco-Levy U, Bar G, Levin R, Ermilov M, Ebstein RP, Javitt DC. High glycine levels are associated with prepulse inhibition deficits in chronic schizophrenia patients. *Schizophr Res.* (2007) 91:14–21. doi: 10.1016/j.schres.2006.12.003
67. Banerjee A, Wang HY, Borgmann-Winter KE, MacDonald ML, Kaprielian H, Stucky A, et al. Src kinase as a mediator of convergent molecular abnormalities leading to NMDAR hypoactivity in schizophrenia. *Mol Psychiatry.* (2015) 20:1091–100. doi: 10.1038/mp.2014.115
68. Neeman G, Blanaru M, Bloch B, Kremer I, Ermilov M, Javitt DC, et al. Relation of plasma glycine, serine, and homocysteine levels to schizophrenia symptoms and medication type. *Am J Psychiatry.* (2005) 162:1738–40. doi: 10.1176/appi.ajp.162.9.1738
69. Shoham S, Javitt DC, Heresco-Levy U. Chronic high-dose glycine nutrition: effects on rat brain cell morphology. *Biol Psychiatry.* (2001) 49:876–85. doi: 10.1016/S0006-3223(00)01046-5
70. Heresco-Levy U, Javitt DC, Ermilov M, Mordel C, Horowitz A, Kelly D. Double-blind, placebo-controlled, crossover trial of glycine adjuvant therapy for treatment-resistant schizophrenia. *Br J Psychiatry.* (1996) 169:610–7. doi: 10.1192/bjp.169.5.610
71. Heresco-Levy U, Ermilov M, Lichtenberg P, Bar G, Javitt DC. High-dose glycine added to olanzapine and risperidone for the treatment of schizophrenia. *Biol Psychiatry.* (2004) 55:165–71. doi: 10.1016/S0006-3223(03)00707-8
72. Um SM, Ha S, Lee H, Kim J, Kim K, Shin W, et al. NGL-2 deletion leads to autistic-like behaviors responsive to NMDAR modulation. *Cell Rep.* (2018) 23:3839–51. doi: 10.1016/j.celrep.2018.05.087
73. Kato K, Shishido T, Ono M, Shishido K, Kobayashi M, Niwa S. Glycine reduces novelty- and methamphetamine-induced locomotor activity in neonatal ventral hippocampal damaged rats. *Neuropsychopharmacology.* (2001) 24:330–2. doi: 10.1016/S0893-133X(00)00213-X
74. Mouri A, Noda Y, Noda A, Nakamura T, Tokura T, Yura Y, et al. Involvement of a dysfunctional dopamine-D1/N-methyl-d-aspartate-NR1 and Ca2+/calmodulin-dependent protein kinase II pathway in the impairment of latent learning in a model of schizophrenia induced by phencyclidine. *Mol Pharmacol.* (2007) 71:1598–609. doi: 10.1124/mol.106.032961
75. Hoffman KL, Basurto E. Clozapine and glycinamide prevent MK-801-induced deficits in the novel object recognition (NOR) test in the domestic rabbit (*Oryctolagus cuniculus*). *Behav Brain Res.* (2014) 271:203–11. doi: 10.1016/j.bbr.2014.06.012
76. Alonso ER, Kolesniková L, Białkowska-Jaworska E, Kisiel Z, León I, Guillemin JC, et al. Glycinamide, a glycine precursor, caught in the gas phase: a laser-ablation jet-cooled rotational study. *Astrophys J.* (2018) 861:70. doi: 10.3847/1538-4357/aac6e9
77. Fone KCF, Watson DJG, Billiras RI, Sicard DI, Dekeyne A, Rivet JM, et al. Comparative pro-cognitive and neurochemical profiles of glycine modulatory site agonists and glycine reuptake inhibitors in the rat: potential relevance to cognitive dysfunction and its management. *Mol Neurobiol.* (2020) 57:2144–66. doi: 10.1007/s12035-020-01875-9
78. Waziri R. Glycine therapy of schizophrenia. *Biol Psychiatry.* (1988) 23:210–1. doi: 10.1016/0006-3223(88)90093-5
79. Rosse RB, Theut SK, Banay-Schwartz M, Leighton M, Scarcella E, Cohen CG, et al. Glycine adjuvant therapy to conventional neuroleptic treatment in schizophrenia: an open-label, pilot study. *Clin Neuropharmacol.* (1989) 12:416–24. doi: 10.1097/00002826-198910000-00006

80. Costa J, Khaled E, Sramek J, Bunney W, Jr., Potkin SG. An open trial of glycine as an adjunct to neuroleptics in chronic treatment-refractory schizophrenics. *J Clin Psychopharmacol.* (1990) 10:71–2. doi: 10.1097/00004714-199002000-00027
81. Javitt DC, Zylberman I, Zukin SR, Heresco-Levy U, Lindenmayer JP. Amelioration of negative symptoms in schizophrenia by glycine. *Am J Psychiatry.* (1994) 151:1234–6. doi: 10.1176/ajp.151.8.1234
82. Leiderman E, Zylberman I, Zukin SR, Cooper TB, Javitt DC. Preliminary investigation of high-dose oral glycine on serum levels and negative symptoms in schizophrenia: an open-label trial. *Biol Psychiatry.* (1996) 39:213–5. doi: 10.1016/0006-3223(95)00585-4
83. Heresco-Levy U, Javitt DC, Ermilov M, Mordel C, Silipo G, Lichtenstein M. Efficacy of high-dose glycine in the treatment of enduring negative symptoms of schizophrenia. *Arch Gen Psychiatry.* (1999) 56:29–36. doi: 10.1001/archpsyc.56.1.29
84. Potkin SG, Jin Y, Bunney BG, Costa J, Gulasekaram B. Effect of clozapine and adjunctive high-dose glycine in treatment-resistant schizophrenia. *Am J Psychiatry.* (1999) 156:145–7. doi: 10.1176/ajp.156.1.145
85. Evins AE, Fitzgerald SM, Wine L, Rosselli R, Goff DC. Placebo-controlled trial of glycine added to clozapine in schizophrenia. *Am J Psychiatry.* (2000) 157:826–8. doi: 10.1176/appi.ajp.157.5.826
86. Javitt DC, Silipo G, Cienfuegos A, Shelley AM, Bark N, Park M, et al. Adjunctive high-dose glycine in the treatment of schizophrenia. *Int J Neuropsychopharmacol.* (2001) 4:385–91. doi: 10.1017/S1461145701002590
87. Diaz P, Bhaskara S, Dursun SM, Deakin B. Double-blind, placebo-controlled, crossover trial of clozapine plus glycine in refractory schizophrenia negative results. *J Clin Psychopharmacol.* (2005) 25:277–8. doi: 10.1097/01.jcp.0000165740.22377.6d
88. Buchanan RW, Javitt DC, Marder SR, Schooler NR, Gold JM, McMahon RP, et al. The cognitive and negative symptoms in schizophrenia trial (CONSIST): the efficacy of glutamatergic agents for negative symptoms and cognitive impairments. *Am J Psychiatry.* (2007) 164:1593–602. doi: 10.1176/appi.ajp.2007.06081358
89. Greenwood LM, Leung S, Michie PT, Green A, Nathan PJ, Fitzgerald P, et al. The effects of glycine on auditory mismatch negativity in schizophrenia. *Schizophr Res.* (2018) 191:61–9. doi: 10.1016/j.schres.2017.05.031
90. Bodkin JA, Coleman MJ, Godfrey LJ, Carvalho CMB, Morgan CJ, Suckow RF, et al. Targeted treatment of individuals with psychosis carrying a copy number variant containing a genomic triplication of the glycine decarboxylase gene. *Biol Psychiatry.* (2019) 86:523–35. doi: 10.1016/j.biopsych.2019.04.031
91. Rosse RB, Schwartz BL, Leighton MP, Davis RE, Deutsch SI. An open-label trial of milacemide in schizophrenia: an NMDA intervention strategy. *Clin Neuropharmacol.* (1990) 13:348–54. doi: 10.1097/00002826-199008000-00010
92. Rosse RB, Schwartz BL, Davis RE, Deutsch SI. An NMDA intervention strategy in schizophrenia with "low-dose" milacemide. *Clin Neuropharmacol.* (1991) 14:268–72. doi: 10.1097/00002826-199106000-00012
93. Toth E, Lajtha A. Elevation of cerebral levels of nonessential amino acids *in vivo* by administration of large doses. *Neurochem Res.* (1981) 6:1309–17. doi: 10.1007/BF00964352
94. O'Neill BV, Croft RJ, Mann C, Dang O, Leung S, Galloway MP, et al. High-dose glycine impairs the prepulse inhibition measure of sensorimotor gating in humans. *J Psychopharmacol.* (2011) 25:1632–8. doi: 10.1177/0269881110372546
95. Thomas JW, Hood WF, Monahan JB, Contreras PC, O'Donohue TL. Glycine modulation of the phencyclidine binding site in mammalian brain. *Brain Res.* (1988) 442:396–8. doi: 10.1016/0006-8993(88)91533-8
96. Cascella NG, Macciardi F, Cavallini C, Smeraldi E. d-cycloserine adjuvant therapy to conventional neuroleptic treatment in schizophrenia: an open-label study. *J Neural Transm Gen Sect.* (1994) 95:105–11. doi: 10.1007/BF01276429
97. Walker DL, Ressler KJ, Lu KT, Davis M. Facilitation of conditioned fear extinction by systemic administration or intra-amygdala infusions of D-cycloserine as assessed with fear-potentiated startle in rats. *J Neurosci.* (2002) 22:2343–51. doi: 10.1523/JNEUROSCI.22-06-02343.2002
98. Ledgerwood L, Richardson R, Cranney J. Effects of D-cycloserine on extinction of conditioned freezing. *Behav Neurosci.* (2003) 117:341–9. doi: 10.1037/0735-7044.117.2.341
99. Matsuoka N, Aigner TG. D-cycloserine, a partial agonist at the glycine site coupled to N-methyl-D-aspartate receptors, improves visual recognition memory in rhesus monkeys. *J Pharmacol Exp Ther.* (1996) 278:891–7. doi: 10.1016/S0021-5198(19)36628-4
100. Yao L, Wang Z, Deng D, Yan R, Ju J, Zhou Q. The impact of D-cycloserine and sarcosine on *in vivo* frontal neural activity in a schizophrenia-like model. *BMC Psychiatry.* (2019) 19:314. doi: 10.1186/s12888-019-2306-1
101. Kanahara N, Shimizu E, Ohgake S, Fujita Y, Kohno M, Hashimoto T, et al. Glycine and D-serine, but not D-cycloserine, attenuate prepulse inhibition deficits induced by NMDA receptor antagonist MK-801. *Psychopharmacology.* (2008) 198:363–74. doi: 10.1007/s00213-008-1151-6
102. Pitkänen M, Sirviö J, MacDonald E, Niemi S, Ekonsalo T, Riekkinen P. The effects of D-cycloserine and MK-801 on the performance of rats in two spatial learning and memory tasks. *Eur Neuropsychopharmacol.* (1995) 5:457–63. doi: 10.1016/0924-977X(95)80004-L
103. Goff DC, Tsai G, Manoach DS, Coyle JT. Dose-finding trial of D-cycloserine added to neuroleptics for negative symptoms in schizophrenia. *Am J Psychiatry.* (1995) 152:1213–5. doi: 10.1176/ajp.152.8.1213
104. Rosse RB, Fay-McCarthy M, Kendrick K, Davis RE, Deutsch SI. D-cycloserine adjuvant therapy to molindone in the treatment of schizophrenia. *Clin Neuropharmacol.* (1996) 19:444–50. doi: 10.1097/00002826-199619050-00008
105. Goff DC, Tsai G, Manoach DS, Flood J, Darby DG, Coyle JT. D-cycloserine added to clozapine for patients with schizophrenia. *Am J Psychiatry.* (1996) 153:1628–30. doi: 10.1176/ajp.153.12.1628
106. van Berckel BN, Hijman R, van der Linden JA, Westenberg HG, van Ree JM, Kahn RS. Efficacy and tolerance of D-cycloserine in drug-free schizophrenic patients. *Biol Psychiatry.* (1996) 40:1298–300. doi: 10.1016/S0006-3223(96)00311-3
107. Heresco-Levy U, Javitt DC, Ermilov M, Silipo G, Shimoni J. Double-blind, placebo-controlled, crossover trial of D-cycloserine adjuvant therapy for treatment-resistant schizophrenia. *Int J Neuropsychopharmacol.* (1998) 1:131–5. doi: 10.1017/S1461145798001242
108. Goff DC, Tsai G, Levitt J, Amico E, Manoach D, Schoenfeld DA, et al. A placebo-controlled trial of D-cycloserine added to conventional neuroleptics in patients with schizophrenia. *Arch Gen Psychiatry.* (1999) 56:21–7. doi: 10.1001/archpsyc.56.1.21
109. Goff DC, Henderson DC, Evins AE, Amico E. A placebo-controlled crossover trial of D-cycloserine added to clozapine in patients with schizophrenia. *Biol Psychiatry.* (1999) 45:512–4. doi: 10.1016/S0006-3223(98)00367-9
110. van Berckel BN, Evenblij CN, van Loon BJ, Maas MF, van der Geld MA, Wynne HJ, et al. D-cycloserine increases positive symptoms in chronic schizophrenic patients when administered in addition to antipsychotics: a double-blind, parallel, placebo-controlled study. *Neuropsychopharmacology.* (1999) 21:203–10. doi: 10.1016/S0893-133X(99)00014-7
111. Evins AE, Amico E, Posever TA, Toker R, Goff DC. D-Cycloserine added to risperidone in patients with primary negative symptoms of schizophrenia. *Schizophr Res.* (2002) 56:19–23. doi: 10.1016/S0920-9964(01)00220-1
112. Heresco-Levy U, Ermilov M, Shimoni J, Shapira B, Silipo G, Javitt DC. Placebo-controlled trial of D-cycloserine added to conventional neuroleptics, olanzapine, or risperidone in schizophrenia. *Am J Psychiatry.* (2002) 159:480–2. doi: 10.1176/appi.ajp.159.3.480
113. Duncan EJ, Szilagyi S, Schwartz MP, Bugarski-Kirola D, Kunzova A, Negi S, et al. Effects of D-cycloserine on negative symptoms in schizophrenia. *Schizophr Res.* (2004) 71:239–48. doi: 10.1016/j.schres.2004.03.013
114. Goff DC, Herz L, Posever T, Shih V, Tsai G, Henderson DC, et al. A six-month, placebo-controlled trial of D-cycloserine co-administered with conventional antipsychotics in schizophrenia patients. *Psychopharmacology.* (2005) 179:144–50. doi: 10.1007/s00213-004-2032-2
115. Yurgelun-Todd DA, Coyle JT, Gruber SA, Renshaw PF, Silveri MM, Amico E, et al. Functional magnetic resonance imaging studies of schizophrenic patients during word production: effects of D-cycloserine. *Psychiatry Res.* (2005) 138:23–31. doi: 10.1016/j.pscychresns.2004.11.006

116. Goff DC, Cather C, Gottlieb JD, Evins AE, Walsh J, Raeke L, et al. Once-weekly D-cycloserine effects on negative symptoms and cognition in schizophrenia: an exploratory study. *Schizophr Res.* (2008) 106:320–7. doi: 10.1016/j.schres.2008.08.012
117. Gottlieb JD, Cather C, Shanahan M, Creedon T, Macklin EA, Goff DC. D-cycloserine facilitation of cognitive behavioral therapy for delusions in schizophrenia. *Schizophr Res.* (2011) 131:69–74. doi: 10.1016/j.schres.2011.05.029
118. Cain CK, McCue M, Bello I, Creedon T, Tang DI, Laska E, et al. d-Cycloserine augmentation of cognitive remediation in schizophrenia. *Schizophr Res.* (2014) 153:177–83. doi: 10.1016/j.schres.2014.01.016
119. Forsyth JK, Bachman P, Mathalon DH, Roach BJ, Ye E, Asarnow RF. Effects of augmenting N-Methyl-D-Aspartate receptor signaling on working memory and experience-dependent plasticity in schizophrenia: an exploratory study using acute d-cycloserine. *Schizophr Bull.* (2017) 43:1123–33. doi: 10.1093/schbul/sbw193
120. Takiguchi K, Uezato A, Itasaka M, Atsuta H, Narushima K, Yamamoto N, et al. Association of schizophrenia onset age and white matter integrity with treatment effect of D-cycloserine: a randomized placebo-controlled double-blind crossover study. *BMC Psychiatry.* (2017) 17:249. doi: 10.1186/s12888-017-1410-3
121. Zareifopoulos N, Panayiotakopoulos G. Neuropsychiatric effects of antimicrobial agents. *Clin Drug Investig.* (2017) 37:423–37. doi: 10.1007/s40261-017-0498-z
122. Heresco-Levy U, Javitt DC. Comparative effects of glycine and d-cycloserine on persistent negative symptoms in schizophrenia: a retrospective analysis. *Schizophr Res.* (2004) 66:89–96. doi: 10.1016/S0920-9964(03)00129-4
123. Tsai GE, Lin PY. Strategies to enhance N-methyl-D-aspartate receptor-mediated neurotransmission in schizophrenia, a critical review and meta-analysis. *Curr Pharm Des.* (2010) 16:522–37. doi: 10.2174/138161210790361452
124. Schell MJ, Molliver ME, Snyder SH. D-serine, an endogenous synaptic modulator: localization to astrocytes and glutamate-stimulated release. *Proc Natl Acad Sci USA.* (1995) 92:3948–52. doi: 10.1073/pnas.92.9.3948
125. Mothet JP, Le Bail M, Billard JM. Time and space profiling of NMDA receptor co-agonist functions. *J Neurochem.* (2015) 135:210–25. doi: 10.1111/jnc.13204
126. Papouin T, Henneberger C, Rusakov DA, Oliet SHR. Astroglial versus neuronal d-serine: fact checking. *Trends Neurosci.* (2017) 40:517–20. doi: 10.1016/j.tins.2017.05.007
127. Kartvelishvily E, Shleper M, Balan L, Dumin E, Wolosker H. Neuron-derived D-serine release provides a novel means to activate N-methyl-D-aspartate receptors. *J Biol Chem.* (2006) 281:14151–62. doi: 10.1074/jbc.M512927200
128. Miya K, Inoue R, Takata Y, Abe M, Natsume R, Sakimura K, et al. Serine racemase is predominantly localized in neurons in mouse brain. *J Comp Neurol.* (2008) 510:641–54. doi: 10.1002/cne.21822
129. Wolosker H. Serine racemase and the serine shuttle between neurons and astrocytes. *Biochim Biophys Acta.* (2011) 1814:1558–66. doi: 10.1016/j.bbapap.2011.01.001
130. Wolosker H, Balu DT, Coyle JT. The rise and fall of the d-serine-mediated gliotransmission hypothesis. *Trends Neurosci.* (2016) 39:712–21. doi: 10.1016/j.tins.2016.09.007
131. Schell MJ, Brady RO, Jr., Molliver ME, Snyder SH. D-serine as a neuromodulator: regional and developmental localizations in rat brain glia resemble NMDA receptors. *J Neurosci.* (1997) 17:1604–15. doi: 10.1523/JNEUROSCI.17-05-01604.1997
132. Benneyworth MA, Li Y, Basu AC, Bolshakov VY, Coyle JT. Cell selective conditional null mutations of serine racemase demonstrate a predominate localization in cortical glutamatergic neurons. *Cell Mol Neurobiol.* (2012) 32:613–24. doi: 10.1007/s10571-012-9808-4
133. Hashimoto K, Fukushima T, Shimizu E, Komatsu N, Watanabe H, Shinoda N, et al. Decreased serum levels of D-serine in patients with schizophrenia: evidence in support of the N-methyl-D-aspartate receptor hypofunction hypothesis of schizophrenia. *Arch Gen Psychiatry.* (2003) 60:572–6. doi: 10.1001/archpsyc.60.6.572
134. Hons J, Zirko R, Vasatova M, Doubek P, Klimova B, Masopust J, et al. Impairment of executive functions associated with lower d-serine serum levels in patients with schizophrenia. *Front Psychiatry.* (2021) 12:514579. doi: 10.3389/fpsyt.2021.514579
135. Fujita Y, Ishima T, Hashimoto K. Supplementation with D-serine prevents the onset of cognitive deficits in adult offspring after maternal immune activation. *Sci Rep.* (2016) 6:37261. doi: 10.1038/srep37261
136. Rosenberg D, Artoul S, Segal AC, Kolodney G, Radzishevsky I, Dikopoltsev E, et al. Neuronal D-serine and glycine release via the Asc-1 transporter regulates NMDA receptor-dependent synaptic activity. *J Neurosci.* (2013) 33:3533–44. doi: 10.1523/JNEUROSCI.3836-12.2013
137. Basu AC, Tsai GE, Ma CL, Ehmsen JT, Mustafa AK, Han L, et al. Targeted disruption of serine racemase affects glutamatergic neurotransmission and behavior. *Mol Psychiatry.* (2009) 14:719–27. doi: 10.1038/mp.2008.130
138. Balu DT, Li Y, Puhl MD, Benneyworth MA, Basu AC, Takagi S, et al. Multiple risk pathways for schizophrenia converge in serine racemase knockout mice, a mouse model of NMDA receptor hypofunction. *Proc Natl Acad Sci USA.* (2013) 110:E2400–9. doi: 10.1073/pnas.1304308110
139. Pei JC, Hung WL, Lin BX, Shih MH, Lu LY, Luo DZ, et al. Therapeutic potential and underlying mechanism of sarcosine (N-methylglycine) in N-methyl-D-aspartate (NMDA) receptor hypofunction models of schizophrenia. *J Psychopharmacol.* (2019) 33:1288–302. doi: 10.1177/0269881119856558
140. Shimazaki T, Kaku A, Chaki S. D-Serine and a glycine transporter-1 inhibitor enhance social memory in rats. *Psychopharmacology.* (2010) 209:263–70. doi: 10.1007/s00213-010-1794-y
141. Karasawa J, Hashimoto K, Chaki S. D-Serine and a glycine transporter inhibitor improve MK-801-induced cognitive deficits in a novel object recognition test in rats. *Behav Brain Res.* (2008) 186:78–83. doi: 10.1016/j.bbr.2007.07.033
142. MacKay MB, Kravtsenyuk M, Thomas R, Mitchell ND, Dursun SM, Baker GB. D-Serine: potential therapeutic agent and/or biomarker in schizophrenia and depression? *Front Psychiatry.* (2019) 10:25. doi: 10.3389/fpsyt.2019.00025
143. Verrall L, Burnet PW, Betts JF, Harrison PJ. The neurobiology of D-amino acid oxidase and its involvement in schizophrenia. *Mol Psychiatry.* (2010) 15:122–37. doi: 10.1038/mp.2009.99
144. Carone FA, Ganote CE. D-serine nephrotoxicity. The nature of proteinuria, glucosuria, and aminoaciduria in acute tubular necrosis. *Arch Pathol.* (1975) 99:658–62.
145. Suzuki M, Gonda Y, Yamada M, Vandebroek AA, Mita M, Hamase K, et al. Serum D-serine accumulation after proximal renal tubular damage involves neutral amino acid transporter Asc-1. *Sci Rep.* (2019) 9:16705. doi: 10.1038/s41598-019-53302-2
146. Mothet JP, Billard JM, Pollegioni L, Coyle JT, Sweedler JV. Investigating brain d-serine: advocacy for good practices. *Acta Physiol.* (2019) 226:e13257. doi: 10.1111/apha.13257
147. Heresco-Levy U, Javitt DC, Ebstein R, Vass A, Lichtenberg P, Bar G, et al. D-serine efficacy as add-on pharmacotherapy to risperidone and olanzapine for treatment-refractory schizophrenia. *Biol Psychiatry.* (2005) 57:577–85. doi: 10.1016/j.biopsych.2004.12.037
148. Lane HY, Chang YC, Liu YC, Chiu CC, Tsai GE. Sarcosine or D-serine add-on treatment for acute exacerbation of schizophrenia: a randomized, double-blind, placebo-controlled study. *Arch Gen Psychiatry.* (2005) 62:1196–204. doi: 10.1001/archpsyc.62.11.1196
149. Tsai G, Yang P, Chung LC, Lange N, Coyle JT. D-serine added to antipsychotics for the treatment of schizophrenia. *Biol Psychiatry.* (1998) 44:1081–9. doi: 10.1016/S0006-3223(98)00279-0
150. Kantrowitz JT, Malhotra AK, Cornblatt B, Silipo G, Balla A, Suckow RF, et al. High dose D-serine in the treatment of schizophrenia. *Schizophr Res.* (2010) 121:125–30. doi: 10.1016/j.schres.2010.05.012
151. Kantrowitz JT, Woods SW, Petkova E, Cornblatt B, Corcoran CM, Chen H, et al. D-serine for the treatment of negative symptoms in individuals at clinical high risk of schizophrenia: a pilot, double-blind, placebo-controlled, randomised parallel group mechanistic proof-of-concept trial. *The Lancet Psychiatry.* (2015) 2:403–12. doi: 10.1016/S2215-0366(15)00098-X
152. Tsai GE, Yang P, Chung LC, Tsai IC, Tsai CW, Coyle JT. D-serine added to clozapine for the treatment of schizophrenia. *Am J Psychiatry.* (1999) 156:1822–5.

153. Lane HY, Lin CH, Huang YJ, Liao CH, Chang YC, Tsai GE. A randomized, double-blind, placebo-controlled comparison study of sarcosine (N-methylglycine) and D-serine add-on treatment for schizophrenia. *Int J Neuropsychopharmacol.* (2010) 13:451–60. doi: 10.1017/S1461145709990939
154. Weiser M, Heresco-Levy U, Davidson M, Javitt DC, Werbeloff N, Gershon AA, et al. A multicenter, add-on randomized controlled trial of low-dose d-serine for negative and cognitive symptoms of schizophrenia. *J Clin Psychiatry.* (2012) 73:e728–34. doi: 10.4088/JCP.11m07031
155. D'Souza DC, Radhakrishnan R, Perry E, Bhakta S, Singh NM, Yadav R, et al. Feasibility, safety, and efficacy of the combination of D-serine and computerized cognitive retraining in schizophrenia: an international collaborative pilot study. *Neuropsychopharmacology.* (2013) 38:492–503. doi: 10.1038/npp.2012.208
156. Kantrowitz JT, Epstein ML, Beggel O, Rohrig S, Lehrfeld JM, Revheim N, et al. Neurophysiological mechanisms of cortical plasticity impairments in schizophrenia and modulation by the NMDA receptor agonist D-serine. *Brain.* (2016) 139 (Pt. 12):3281–95. doi: 10.1093/brain/aww262
157. Kantrowitz JT, Epstein ML, Lee M, Lehrfeld N, Nolan KA, Shope C, et al. Improvement in mismatch negativity generation during d-serine treatment in schizophrenia: correlation with symptoms. *Schizophr Res.* (2018) 191:70–9. doi: 10.1016/j.schres.2017.02.027
158. Ermilov M, Gelfin E, Levin R, Lichtenberg P, Hashimoto K, Javitt DC, et al. A pilot double-blind comparison of d-serine and high-dose olanzapine in treatment-resistant patients with schizophrenia. *Schizophr Res.* (2013) 150:604–5. doi: 10.1016/j.schres.2013.09.018
159. Heresco-Levy U, Durrant AR, Ermilov M, Javitt DC, Miya K, Mori H. Clinical and electrophysiological effects of D-serine in a schizophrenia patient positive for anti-N-methyl-D-aspartate receptor antibodies. *Biol Psychiatry.* (2015) 77:e27–9. doi: 10.1016/j.biopsych.2014.08.023
160. Cho SE, Na KS, Cho SJ, Kang SG. Low d-serine levels in schizophrenia: a systematic review and meta-analysis. *Neurosci Lett.* (2016) 634:42–51. doi: 10.1016/j.neulet.2016.10.006
161. da Silva Lde B, Leipnitz G, Seminotti B, Fernandes CG, Beskow AP, Amaral AU, et al. D-serine induces lipid and protein oxidative damage and decreases glutathione levels in brain cortex of rats. *Brain Res.* (2009) 1256:34–42. doi: 10.1016/j.brainres.2008.12.036
162. Katsuki H, Nonaka M, Shirakawa H, Kume T, Akaike A. Endogenous D-serine is involved in induction of neuronal death by N-methyl-D-aspartate and simulated ischemia in rat cerebrocortical slices. *J Pharmacol Exp Ther.* (2004) 311:836–44. doi: 10.1124/jpet.104.070912
163. Ganote CE, Peterson DR, Carone FA. The nature of D-serine–induced nephrotoxicity. *Am J Pathol.* (1974) 77:269–82.
164. Chang CY, Luo DZ, Pei JC, Kuo MC, Hsieh YC, Lai WS. Not just a bystander: the emerging role of astrocytes and research tools in studying cognitive dysfunctions in schizophrenia. *Int J Mol Sci.* (2021) 22:5343. doi: 10.3390/ijms22105343
165. Zafra F, Gomeza J, Olivares L, Aragon C, Gimenez C. Regional distribution and developmental variation of the glycine transporters GLYT1 and GLYT2 in the rat CNS. *Eur J Neurosci.* (1995) 7:1342–52. doi: 10.1111/j.1460-9568.1995.tb01125.x
166. Balu DT, Coyle JT. The NMDA receptor 'glycine modulatory site' in schizophrenia: D-serine, glycine, and beyond. *Curr Opin Pharmacol.* (2015) 20:109–15. doi: 10.1016/j.coph.2014.12.004
167. Javitt DC, Frusciante M. Glycyldodecylamide, a phencyclidine behavioral antagonist, blocks cortical glycine uptake: implications for schizophrenia and substance abuse. *Psychopharmacology.* (1997) 129:96–8. doi: 10.1007/s002130050168
168. Javitt DC, Sershen H, Hashim A, Lajtha A. Reversal of phencyclidine-induced hyperactivity by glycine and the glycine uptake inhibitor glycyldodecylamide. *Neuropsychopharmacology.* (1997) 17:202–4. doi: 10.1016/S0893-133X(97)00047-X
169. Hashimoto K, Fujita Y, Ishima T, Chaki S, Iyo M. Phencyclidine-induced cognitive deficits in mice are improved by subsequent subchronic administration of the glycine transporter-1 inhibitor NFPS and D-serine. *Eur Neuropsychopharmacol.* (2008) 18:414–21. doi: 10.1016/j.euroneuro.2007.07.009
170. Mao SC, Lin HC, Gean PW. Augmentation of fear extinction by infusion of glycine transporter blockers into the amygdala. *Mol Pharmacol.* (2009) 76:369–78. doi: 10.1124/mol.108.053728
171. Manahan-Vaughan D, Wildforster V, Thomsen C. Rescue of hippocampal LTP and learning deficits in a rat model of psychosis by inhibition of glycine transporter-1 (GlyT1). *Eur J Neurosci.* (2008) 28:1342–50. doi: 10.1111/j.1460-9568.2008.06433.x
172. Chen HH, Stoker A, Markou A. The glutamatergic compounds sarcosine and N-acetylcysteine ameliorate prepulse inhibition deficits in metabotropic glutamate 5 receptor knockout mice. *Psychopharmacology.* (2010) 209:343–50. doi: 10.1007/s00213-010-1802-2
173. Kopec K, Flood DG, Gasior M, McKenna BA, Zuvich E, Schreiber J, et al. Glycine transporter (GlyT1) inhibitors with reduced residence time increase prepulse inhibition without inducing hyperlocomotion in DBA/2 mice. *Biochem Pharmacol.* (2010) 80:1407–17. doi: 10.1016/j.bcp.2010.07.004
174. Zhang HX, Hyrc K, Thio LL. The glycine transport inhibitor sarcosine is an NMDA receptor co-agonist that differs from glycine. *J Physiol.* (2009) 587 (Pt. 13):3207–20. doi: 10.1113/jphysiol.2009.168757
175. Nishikawa H, Inoue T, Izumi T, Nakagawa S, Koyama T. SSR504734, a glycine transporter-1 inhibitor, attenuates acquisition and expression of contextual conditioned fear in rats. *Behav Pharmacol.* (2010) 21:576–9. doi: 10.1097/FBP.0b013e32833d419d
176. Singer P, Feldon J, Yee BK. The glycine transporter 1 inhibitor SSR504734 enhances working memory performance in a continuous delayed alternation task in C57BL/6 mice. *Psychopharmacology.* (2009) 202:371–84. doi: 10.1007/s00213-008-1286-5
177. Lipina T, Labrie V, Weiner I, Roder J. Modulators of the glycine site on NMDA receptors, D-serine and ALX 5407, display similar beneficial effects to clozapine in mouse models of schizophrenia. *Psychopharmacology.* (2005) 179:54–67. doi: 10.1007/s00213-005-2210-x
178. Le Pen G, Kew J, Alberati D, Borroni E, Heitz MP, Moreau JL. Prepulse inhibition deficits of the startle reflex in neonatal ventral hippocampal-lesioned rats: reversal by glycine and a glycine transporter inhibitor. *Biol Psychiatry.* (2003) 54:1162–70. doi: 10.1016/S0006-3223(03)00374-3
179. Tsai G, Ralph-Williams RJ, Martina M, Bergeron R, Berger-Sweeney J, Dunham KS, et al. Gene knockout of glycine transporter 1: characterization of the behavioral phenotype. *Proc Natl Acad Sci USA.* (2004) 101:8485–90. doi: 10.1073/pnas.0402662101
180. Gabernet L, Pauly-Evers M, Schwerdel C, Lentz M, Bluethmann H, Vogt K, et al. Enhancement of the NMDA receptor function by reduction of glycine transporter-1 expression. *Neurosci Lett.* (2005) 373:79–84. doi: 10.1016/j.neulet.2004.09.064
181. Yee BK, Balic E, Singer P, Schwerdel C, Grampp T, Gabernet L, et al. Disruption of glycine transporter 1 restricted to forebrain neurons is associated with a procognitive and antipsychotic phenotypic profile. *J Neurosci.* (2006) 26:3169–81. doi: 10.1523/JNEUROSCI.5120-05.2006
182. Cioffi CL. Glycine transporter-1 inhibitors: a patent review (2011-2016). *Expert Opin Ther Pat.* (2018) 28:197–210. doi: 10.1080/13543776.2018.1429408
183. Schoemaker JH, Jansen WT, Schipper J, Szegedi A. The selective glycine uptake inhibitor org 25935 as an adjunctive treatment to atypical antipsychotics in predominant persistent negative symptoms of schizophrenia: results from the GIANT trial. *J Clin Psychopharmacol.* (2014) 34:190–8. doi: 10.1097/JCP.0000000000000073
184. Dunayevich E, Buchanan RW, Chen CY, Yang J, Nilsen J, Dietrich JM, et al. Efficacy and safety of the glycine transporter type-1 inhibitor AMG 747 for the treatment of negative symptoms associated with schizophrenia. *Schizophr Res.* (2017) 182:90–7. doi: 10.1016/j.schres.2016.10.027
185. Tsai G, Lane HY, Yang P, Chong MY, Lange N. Glycine transporter I inhibitor, N-methylglycine (sarcosine), added to antipsychotics for the treatment of schizophrenia. *Biol Psychiatry.* (2004) 55:452–6. doi: 10.1016/j.biopsych.2003.09.012
186. Lane HY, Huang CL, Wu PL, Liu YC, Chang YC, Lin PY, et al. Glycine transporter I inhibitor, N-methylglycine (sarcosine), added to clozapine for the treatment of schizophrenia. *Biol Psychiatry.* (2006) 60:645–9. doi: 10.1016/j.biopsych.2006.04.005
187. Lane HY, Liu YC, Huang CL, Chang YC, Liau CH, Perng CH, et al. Sarcosine (N-methylglycine) treatment for acute schizophrenia:

a randomized, double-blind study. *Biol Psychiatry.* (2008) 63:9–12. doi: 10.1016/j.biopsych.2007.04.038
188. Strzelecki D, Szyburska J, Rabe-Jablonska J. Two grams of sarcosine in schizophrenia - is it too much? A potential role of glutamate-serotonin interaction. *Neuropsychiatr Dis Treat.* (2014) 10:263–6. doi: 10.2147/NDT.S54024
189. Strzelecki D, Szyburska J, Kotlicka-Antczak M, Kaluzynska O. Hypomania after augmenting venlafaxine and olanzapine with sarcosine in a patient with schizophrenia: a case study. *Neuropsychiatr Dis Treat.* (2015) 11:533–6. doi: 10.2147/NDT.S75734
190. Strzelecki D, Podgorski M, Kaluzynska O, Gawlik-Kotelnicka O, Stefanczyk L, Kotlicka-Antczak M, et al. Supplementation of antipsychotic treatment with sarcosine - GlyT1 inhibitor - causes changes of glutamatergic (1)NMR spectroscopy parameters in the left hippocampus in patients with stable schizophrenia. *Neurosci Lett.* (2015) 606:7–12. doi: 10.1016/j.neulet.2015.08.039
191. Strzelecki D, Kaluzynska O, Szyburska J, Wlazlo A, Wysokinski A. No changes of cardiometabolic and body composition parameters after 6-month add-on treatment with sarcosine in patients with schizophrenia. *Psychiatry Res.* (2015) 230:200–4. doi: 10.1016/j.psychres.2015.08.040
192. Strzelecki D, Podgorski M, Kaluzynska O, Stefanczyk L, Kotlicka-Antczak M, Gmitrowicz A, et al. Adding sarcosine to antipsychotic treatment in patients with stable schizophrenia changes the concentrations of neuronal and glial metabolites in the left dorsolateral prefrontal cortex. *Int J Mol Sci.* (2015) 16:24475–89. doi: 10.3390/ijms161024475
193. Strzelecki D, Podgorski M, Kaluzynska O, Gawlik-Kotelnicka O, Stefanczyk L, Kotlicka-Antczak M, et al. Supplementation of antipsychotic treatment with the amino acid sarcosine influences proton magnetic resonance spectroscopy parameters in left frontal white matter in patients with schizophrenia. *Nutrients.* (2015) 7:8767–82. doi: 10.3390/nu7105427
194. Strzelecki D, Kaluzynska O, Szyburska J, Wysokinski A. MMP-9 serum levels in schizophrenic patients during treatment augmentation with sarcosine (results of the PULSAR study). *Int J Mol Sci.* (2016) 17:1075. doi: 10.3390/ijms17071075
195. Strzelecki D, Kaluzynska O, Wysokinski A. BDNF serum levels in schizophrenic patients during treatment augmentation with sarcosine (results of the PULSAR study). *Psychiatry Res.* (2016) 242:54–60. doi: 10.1016/j.psychres.2016.05.019
196. Strzelecki D, Urban-Kowalczyk M, Wysokinski A. Serum levels of interleukin 6 in schizophrenic patients during treatment augmentation with sarcosine (results of the PULSAR study). *Hum Psychopharmacol.* (2018) 33:e2652. doi: 10.1002/hup.2652
197. Strzelecki D, Urban-Kowalczyk M, Wysokinski A. Serum levels of TNF-alpha in patients with chronic schizophrenia during treatment augmentation with sarcosine (results of the PULSAR study). *Psychiatry Res.* (2018) 268:447–53. doi: 10.1016/j.psychres.2018.08.002
198. Amiaz R, Kent I, Rubinstein K, Sela BA, Javitt D, Weiser M. Safety, tolerability and pharmacokinetics of open label sarcosine added on to anti-psychotic treatment in schizophrenia - preliminary study. *Isr J Psychiatry Relat Sci.* (2015) 52:12–5.
199. Lin CY, Liang SY, Chang YC, Ting SY, Kao CL, Wu YH, et al. Adjunctive sarcosine plus benzoate improved cognitive function in chronic schizophrenia patients with constant clinical symptoms: a randomised, double-blind, placebo-controlled trial. *World J Biol Psychiatry.* (2017) 18:357–68. doi: 10.3109/15622975.2015.1117654
200. GlaxoSmithKline. *A Repeat Dose Study With GSK1018921 to Assess Safety, Tolerability, Pharmacokinetics, Pharmacodynamics in Healthy Volunteers and Patients With Schizophrenia and to Evaluate Its Effect on PK of Midazolam (GT1110791) U.S.: clinicaltrials.gov*. (2009). Available online at: https://clinicaltrials.gov/ct2/show/NCT00929370
201. D'Souza DC, Carson RE, Driesen N, Johannesen J, Ranganathan M, Krystal JH, et al. Dose-Related target occupancy and effects on circuitry, behavior, and neuroplasticity of the glycine transporter-1 inhibitor pf-03463275 in healthy and schizophrenia subjects. *Biol Psychiatry.* (2018) 84:413–21. doi: 10.1016/j.biopsych.2017.12.019
202. Yale University. *Translational Neuroscience Optimization of GlyT1 Inhibitor (NCATS) U.S.: ClinicalTrials.gov*. (2013). Available online at: https://clinicaltrials.gov/ct2/show/NCT01911676 (accessed January 7, 2021).
203. Pfizer. *A Study of PF-03463275 as Add-On Therapy in Outpatients With Persistent Negative Symptoms of Schizophrenia U.S.: ClinicalTrials.gov*. (2009). Available online at: https://clinicaltrials.gov/ct2/show/NCT00977522 (accessed February 7, 2012).
204. Blaettler T, Bugarski-Kirola D, Fleischhacker WW, Bressan R, Arango C, Abi-Saab D, et al. Efficacy and safety of adjunctive bitopertin (10 and 20mg) versus placebo in subjects with persistent predominant negative symptoms of schizophrenia treated with antipsychotics — results from the phase III FlashLyte study. *Schizophr Res.* (2014) 158:e2–3. doi: 10.1016/j.schres.2014.07.036
205. Bugarski-Kirola D, Wang A, Abi-Saab D, Blattler T. A phase II/III trial of bitopertin monotherapy compared with placebo in patients with an acute exacerbation of schizophrenia - results from the CandleLyte study. *Eur Neuropsychopharmacol.* (2014) 24:1024–36. doi: 10.1016/j.euroneuro.2014.03.007
206. Arango C, Nasrallah H, Lawrie S, Lohmann TO, Zhu JL, Garibaldi G, et al. Efficacy and safety of adjunctive bitopertin (5 and 10mg) versus placebo in subjects with persistent predominant negative symptoms of schizophrenia treated with antipsychotics — results from the phase III DayLyte study. *Schizophr Res.* (2014) 158:e1. doi: 10.1016/j.schres.2014.07.038
207. Umbricht D, Alberati D, Martin-Facklam M, Borroni E, Youssef EA, Ostland M, et al. Effect of bitopertin, a glycine reuptake inhibitor, on negative symptoms of schizophrenia: a randomized, double-blind, proof-of-concept study. *JAMA Psychiatry.* (2014) 71:637–46. doi: 10.1001/jamapsychiatry.2014.163
208. Edgar CJ, Blaettler T, Bugarski-Kirola D, Le Scouiller S, Garibaldi GM, Marder SR. Reliability, validity and ability to detect change of the PANSS negative symptom factor score in outpatients with schizophrenia on select antipsychotics and with prominent negative or disorganized thought symptoms. *Psychiatry Res.* (2014) 218:219–24. doi: 10.1016/j.psychres.2014.04.009
209. Rofail D, Regnault A, le Scouiller S, Berardo CG, Umbricht D, Fitzpatrick R. Health-related quality of life in patients with prominent negative symptoms: results from a multicenter randomized phase II trial on bitopertin. *Qual Life Res.* (2016) 25:201–11. doi: 10.1007/s11136-015-1057-9
210. Hirayasu Y, Sato S, Takahashi H, Iida S, Shuto N, Yoshida S, et al. A double-blind randomized study assessing safety and efficacy following one-year adjunctive treatment with bitopertin, a glycine reuptake inhibitor, in Japanese patients with schizophrenia. *BMC Psychiatry.* (2016) 16:66. doi: 10.1186/s12888-016-0778-9
211. Bugarski-Kirola D, Iwata N, Sameljak S, Reid C, Blaettler T, Millar L, et al. Efficacy and safety of adjunctive bitopertin versus placebo in patients with suboptimally controlled symptoms of schizophrenia treated with antipsychotics: results from three phase 3, randomised, double-blind, parallel-group, placebo-controlled, multicentre studies in the SearchLyte clinical trial programme. *Lancet Psychiatry.* (2016) 3:1115–28. doi: 10.1016/S2215-0366(16)30344-3
212. Bugarski-Kirola D, Blaettler T, Arango C, Fleischhacker WW, Garibaldi G, Wang A, et al. Bitopertin in negative symptoms of schizophrenia-results from the phase III FlashLyte and DayLyte studies. *Biol Psychiatry.* (2017) 82:8–16. doi: 10.1016/j.biopsych.2016.11.014
213. Kantrowitz JT, Nolan KA, Epstein ML, Lehrfeld N, Shope C, Petkova E, et al. Neurophysiological effects of bitopertin in schizophrenia. *J Clin Psychopharmacol.* (2017) 37:447–51. doi: 10.1097/JCP.0000000000000722
214. Harvey PD, Bowie CR, McDonald S, Podhorna J. Evaluation of the efficacy of BI 425809 pharmacotherapy in patients with schizophrenia receiving computerized cognitive training: methodology for a double-blind, randomized, parallel-group trial. *Clin Drug Investig.* (2020) 40:377–85. doi: 10.1007/s40261-020-00893-8
215. Fleischhacker WW, Podhorna J, Gröschl M, Hake S, Zhao Y, Huang S, et al. Efficacy and safety of the novel glycine transporter inhibitor BI 425809 once daily in patients with schizophrenia: a double-blind, randomised, placebo-controlled phase 2 study. *The Lancet Psychiatry.* (2021) 8:191–201. doi: 10.1016/S2215-0366(20)30513-7
216. Depoortere R, Dargazanli G, Estenne-Bouhtou G, Coste A, Lanneau C, Desvignes C, et al. Neurochemical, electrophysiological and pharmacological profiles of the selective inhibitor of the glycine transporter-1 SSR504734,

a potential new type of antipsychotic. *Neuropsychopharmacology.* (2005) 30:1963–85. doi: 10.1038/sj.npp.1300772
217. Boulay D, Pichat P, Dargazanli G, Estenne-Bouhtou G, Terranova JP, Rogacki N, et al. Characterization of SSR103800, a selective inhibitor of the glycine transporter-1 in models predictive of therapeutic activity in schizophrenia. *Pharmacol Biochem Behav.* (2008) 91:47–58. doi: 10.1016/j.pbb.2008.06.009
218. Ouellet D, Sutherland S, Wang T, Griffini P, Murthy V. First-time-in-human study with GSK1018921, a selective GlyT1 inhibitor: relationship between exposure and dizziness. *Clin Pharmacol Ther.* (2011) 90:597–604. doi: 10.1038/clpt.2011.154
219. Blackaby WP, Lewis RT, Thomson JL, Jennings AS, Goodacre SC, Street LJ, et al. Identification of an orally bioavailable, potent, and selective inhibitor of GlyT1. *ACS Med Chem Lett.* (2010) 1:350–4. doi: 10.1021/ml1001085
220. Singer P, Dubroqua S, Yee BK. Inhibition of glycine transporter 1: the yellow brick road to new schizophrenia therapy? *Curr Pharm Des.* (2015) 21:3771–87. doi: 10.2174/1381612821666150724100952
221. Lowe JA, 3rd, Hou X, Schmidt C, David Tingley F, 3rd, McHardy S, Kalman M, et al. The discovery of a structurally novel class of inhibitors of the type 1 glycine transporter. *Bioorg Med Chem Lett.* (2009) 19:2974–6. doi: 10.1016/j.bmcl.2009.04.035
222. Alberati D, Moreau JL, Lengyel J, Hauser N, Mory R, Borroni E, et al. Glycine reuptake inhibitor RG1678: a pharmacologic characterization of an investigational agent for the treatment of schizophrenia. *Neuropharmacology.* (2012) 62:1152–61. doi: 10.1016/j.neuropharm.2011.11.008
223. Eddins D, Hamill TG, Puri V, Cannon CE, Vivian JA, Sanabria-Bohorquez SM, et al. The relationship between glycine transporter 1 occupancy and the effects of the glycine transporter 1 inhibitor RG1678 or ORG25935 on object retrieval performance in scopolamine impaired rhesus monkey. *Psychopharmacology.* (2014) 231:511–9. doi: 10.1007/s00213-013-3260-0
224. Rosenbrock H, Desch M, Kleiner O, Dorner-Ciossek C, Schmid B, Keller S, et al. Evaluation of pharmacokinetics and pharmacodynamics of BI 425809, a novel GlyT1 inhibitor: translational studies. *Clin Transl Sci.* (2018) 11:616–23. doi: 10.1111/cts.12578
225. Moschetti V, Schlecker C, Wind S, Goetz S, Schmitt H, Schultz A, et al. Multiple rising doses of oral BI 425809, a GlyT1 inhibitor, in young and elderly healthy volunteers: a randomised, double-blind, phase i study investigating safety and pharmacokinetics. *Clin Drug Investig.* (2018) 38:737–50. doi: 10.1007/s40261-018-0660-2
226. Moschetti V, Desch M, Goetz S, Liesenfeld KH, Rosenbrock H, Kammerer KP, et al. Safety, tolerability and pharmacokinetics of oral BI 425809, a glycine transporter 1 inhibitor, in healthy male volunteers: a partially randomised, single-blind, placebo-controlled, first-in-human study. *Eur J Drug Metab Pharmacokinet.* (2018) 43:239–49. doi: 10.1007/s13318-017-0440-z
227. Boehringer Ingelheim. *This Study Tests Whether BI 425809 Together With Brain Training Using a Computer Improves Mental Functioning in Patients With Schizophrenia U.S.: Clinicaltrials.gov*. (2019). Available online at: https://clinicaltrials.gov/ct2/show/NCT03859973 (accessed June 29, 2021).
228. Feng J, Craddock N, Jones IR, Cook EH, Jr., Goldman D, et al. Systematic screening for mutations in the glycine receptor alpha2 subunit gene (GLRA2) in patients with schizophrenia and other psychiatric diseases. *Psychiatr Genet.* (2001) 11:45–8. doi: 10.1097/00041444-200103000-00009
229. Tsai SJ, Cheng CY, Hong CJ, Liao DL, Hou SJ, et al. Association study of polymorphisms in glycine transporter with schizophrenia. *J Neural Transm (Vienna).* (2006) 113:1545–9. doi: 10.1007/s00702-006-0438-1
230. Merk W, Kucia K, Medrala T, Kowalczyk M, Owczarek A, Kowalski J. Association study of the excitatory amino acid transporter 2 (EAAT2) and glycine transporter 1 (GlyT1) gene polymorphism with schizophrenia in a polish population. *Neuropsychiatr Dis Treat.* (2019) 15:989–1000. doi: 10.2147/NDT.S194924
231. Li Y, Sacchi S, Pollegioni L, Basu AC, Coyle JT, Bolshakov VY. Identity of endogenous NMDAR glycine site agonist in amygdala is determined by synaptic activity level. *Nat Commun.* (2013) 4:1760. doi: 10.1038/ncomms2779
232. Sacchi S, Cappelletti P, Murtas G. Biochemical properties of human D-amino acid oxidase variants and their potential significance in pathologies. *Front Mol Biosci.* (2018) 5:55. doi: 10.3389/fmolb.2018.00055
233. Sacchi S, Bernasconi M, Martineau M, Mothet JP, Ruzzene M, Pilone MS, et al. pLG72 modulates intracellular D-serine levels through its interaction with D-amino acid oxidase: effect on schizophrenia susceptibility. *J Biol Chem.* (2008) 283:22244–56. doi: 10.1074/jbc.M709153200
234. Murtas G, Sacchi S, Valentino M, Pollegioni L. Biochemical properties of human d-amino acid oxidase. *Front Mol Biosci.* (2017) 4:88. doi: 10.3389/fmolb.2017.00088
235. Chumakov I, Blumenfeld M, Guerassimenko O, Cavarec L, Palicio M, Abderrahim H, et al. Genetic and physiological data implicating the new human gene G72 and the gene for D-amino acid oxidase in schizophrenia. *Proc Natl Acad Sci USA.* (2002) 99:13675–80. doi: 10.1073/pnas.182412499
236. Verrall L, Walker M, Rawlings N, Benzel I, Kew JN, Harrison PJ, et al. d-Amino acid oxidase and serine racemase in human brain: normal distribution and altered expression in schizophrenia. *Eur J Neurosci.* (2007) 26:1657–69. doi: 10.1111/j.1460-9568.2007.05769.x
237. Moreno S, Nardacci R, Cimini A, Ceru MP. Immunocytochemical localization of D-amino acid oxidase in rat brain. *J Neurocytol.* (1999) 28:169–85. doi: 10.1023/A:1007064504007
238. Pollegioni L, Piubelli L, Molla G, Rosini E. D-Amino acid oxidase-pLG72 interaction and D-serine modulation. *Front Mol Biosci.* (2018) 5:3. doi: 10.3389/fmolb.2018.00003
239. Kawazoe T, Tsuge H, Pilone MS, Fukui K. Crystal structure of human D-amino acid oxidase: context-dependent variability of the backbone conformation of the VAAGL hydrophobic stretch located at the si-face of the flavin ring. *Protein Sci.* (2006) 15:2708–17. doi: 10.1110/ps.062421606
240. Molla G. Competitive inhibitors unveil structure/function relationships in human D-amino acid oxidase. *Front Mol Biosci.* (2017) 4:80. doi: 10.3389/fmolb.2017.00080
241. Molla G, Sacchi S, Bernasconi M, Pilone MS, Fukui K, Polegioni L. Characterization of human D-amino acid oxidase. *FEBS Lett.* (2006) 580:2358–64. doi: 10.1016/j.febslet.2006.03.045
242. Caldinelli L, Molla G, Sacchi S, Pilone MS, Pollegioni L. Relevance of weak flavin binding in human D-amino acid oxidase. *Protein Sci.* (2009) 18:801–10. doi: 10.1002/pro.86
243. Caldinelli L, Molla G, Bracci L, Lelli B, Pileri S, Cappelletti P, et al. Effect of ligand binding on human D-amino acid oxidase: implications for the development of new drugs for schizophrenia treatment. *Protein Sci.* (2010) 19:1500–12. doi: 10.1002/pro.429
244. Burnet PW, Eastwood SL, Bristow GC, Godlewska BR, Sikka P, Walker M, et al. D-amino acid oxidase activity and expression are increased in schizophrenia. *Mol Psychiatry.* (2008) 13:658–60. doi: 10.1038/mp.2008.47
245. Allen NC, Bagade S, McQueen MB, Ioannidis JP, Kavvoura FK, Khoury MJ, et al. Systematic meta-analyses and field synopsis of genetic association studies in schizophrenia: the SzGene database. *Nat Genet.* (2008) 40:827–34. doi: 10.1038/ng.171
246. Jagannath V, Gerstenberg M, Correll CU, Walitza S, Grunblatt E. A systematic meta-analysis of the association of Neuregulin 1 (NRG1), D-amino acid oxidase (DAO), and DAO activator (DAOA)/G72 polymorphisms with schizophrenia. *J Neural Transm.* (2018) 125:89–102. doi: 10.1007/s00702-017-1782-z
247. Jagannath V, Theodoridou A, Gerstenberg M, Franscini M, Heekeren K, Correll CU, et al. Prediction analysis for transition to schizophrenia in individuals at clinical high risk for psychosis: the relationship of DAO, DAOA, and NRG1 variants with negative symptoms and cognitive deficits. *Front Psychiatry.* (2017) 8:292. doi: 10.3389/fpsyt.2017.00292
248. Hall J, Whalley HC, Moorhead TW, Baig BJ, McIntosh AM, Job DE, et al. Genetic variation in the DAOA (G72) gene modulates hippocampal function in subjects at high risk of schizophrenia. *Biol Psychiatry.* (2008) 64:428–33. doi: 10.1016/j.biopsych.2008.03.009
249. Jansen A, Krach S, Krug A, Markov V, Eggermann T, Zerres K, et al. A putative high risk diplotype of the G72 gene is in healthy individuals

associated with better performance in working memory functions and altered brain activity in the medial temporal lobe. *Neuroimage.* (2009) 45:1002–8. doi: 10.1016/j.neuroimage.2008.12.054

250. Opgen-Rhein C, Lencz T, Burdick KE, Neuhaus AH, DeRosse P, Goldberg TE, et al. Genetic variation in the DAOA gene complex: impact on susceptibility for schizophrenia and on cognitive performance. *Schizophr Res.* (2008) 103:169–77. doi: 10.1016/j.schres.2008.04.020
251. Korostishevsky M, Kaganovich M, Cholostoy A, Ashkenazi M, Ratner Y, Dahary D, et al. Is the G72/G30 locus associated with schizophrenia? Single nucleotide polymorphisms, haplotypes, and gene expression analysis. *Biol Psychiatry.* (2004) 56:169–76. doi: 10.1016/j.biopsych.2004.04.006
252. Lin CH, Chang HT, Chen YJ, Lin CH, Huang CH, Tun R, et al. Distinctively higher plasma G72 protein levels in patients with schizophrenia than in healthy individuals. *Mol Psychiatry.* (2014) 19:636–7. doi: 10.1038/mp.2013.80
253. Madeira C, Freitas ME, Vargas-Lopes C, Wolosker H, Panizzutti R. Increased brain D-amino acid oxidase (DAAO) activity in schizophrenia. *Schizophr Res.* (2008) 101:76–83. doi: 10.1016/j.schres.2008.02.002
254. Abou El-Magd RM, Park HK, Kawazoe T, Iwana S, Ono K, Chung SP, et al. The effect of risperidone on D-amino acid oxidase activity as a hypothesis for a novel mechanism of action in the treatment of schizophrenia. *J Psychopharmacol.* (2010) 24:1055–67. doi: 10.1177/0269881109102644
255. Iwana S, Kawazoe T, Park HK, Tsuchiya K, Ono K, Yorita K, et al. Chlorpromazine oligomer is a potentially active substance that inhibits human D-amino acid oxidase, product of a susceptibility gene for schizophrenia. *J Enzyme Inhib Med Chem.* (2008) 23:901–11. doi: 10.1080/14756360701745478
256. Adage T, Trillat AC, Quattropani A, Perrin D, Cavarec L, Shaw J, et al. *In vitro* and *in vivo* pharmacological profile of AS057278, a selective d-amino acid oxidase inhibitor with potential anti-psychotic properties. *Eur Neuropsychopharmacol.* (2008) 18:200–14. doi: 10.1016/j.euroneuro.2007.06.006
257. Duplantier AJ, Becker SL, Bohanon MJ, Borzilleri KA, Chrunyk BA, Downs JT, et al. Discovery, SAR, and pharmacokinetics of a novel 3-hydroxyquinolin-2(1H)-one series of potent D-amino acid oxidase (DAAO) inhibitors. *J Med Chem.* (2009) 52:3576–85. doi: 10.1021/jm900128w
258. Smith SM, Uslaner JM, Yao L, Mullins CM, Surles NO, Huszar SL, et al. The behavioral and neurochemical effects of a novel D-amino acid oxidase inhibitor compound 8 [4H-thieno [3,2-b]pyrrole-5-carboxylic acid] and D-serine. *J Pharmacol Exp Ther.* (2009) 328:921–30. doi: 10.1124/jpet.108.147884
259. Hashimoto K, Fujita Y, Horio M, Kunitachi S, Iyo M, Ferraris D, et al. Co-administration of a D-amino acid oxidase inhibitor potentiates the efficacy of D-serine in attenuating prepulse inhibition deficits after administration of dizocilpine. *Biol Psychiatry.* (2009) 65:1103–6. doi: 10.1016/j.biopsych.2009.01.002
260. Horio M, Fujita Y, Ishima T, Iyo M, Ferraris D, Tsukamoto T, et al. Effects of D-Amino acid oxidase inhibitor on the extracellular d-alanine levels and the efficacy of D-alanine on dizocilpine-induced prepulse inhibition deficits in mice. *Open Clin Chem J.* (2009) 2:16–21. doi: 10.2174/1874241600902010016
261. Almond SL, Fradley RL, Armstrong EJ, Heavens RB, Rutter AR, Newman RJ, et al. Behavioral and biochemical characterization of a mutant mouse strain lacking D-amino acid oxidase activity and its implications for schizophrenia. *Mol Cell Neurosci.* (2006) 32:324–34. doi: 10.1016/j.mcn.2006.05.003
262. Maekawa M, Watanabe M, Yamaguchi S, Konno R, Hori Y. Spatial learning and long-term potentiation of mutant mice lacking D-amino-acid oxidase. *Neurosci Res.* (2005) 53:34–8. doi: 10.1016/j.neures.2005.05.008
263. Maekawa M, Okamura T, Kasai N, Hori Y, Summer KH, Konno R. D-amino-acid oxidase is involved in D-serine-induced nephrotoxicity. *Chem Res Toxicol.* (2005) 18:1678–82. doi: 10.1021/tx0500326
264. Williams RE, Lock EA. Sodium benzoate attenuates D-serine induced nephrotoxicity in the rat. *Toxicology.* (2005) 207:35–48. doi: 10.1016/j.tox.2004.08.008
265. Sacchi S, Caldinelli L, Cappelletti P, Pollegioni L, Molla G. Structure-function relationships in human D-amino acid oxidase. *Amino Acids.* (2012) 43:1833–50. doi: 10.1007/s00726-012-1345-4
266. Hopkins SC, Heffernan ML, Saraswat LD, Bowen CA, Melnick L, Hardy LW, et al. Structural, kinetic, and pharmacodynamic mechanisms of D-amino acid oxidase inhibition by small molecules. *J Med Chem.* (2013) 56:3710–24. doi: 10.1021/jm4002583
267. Terry-Lorenzo RT, Chun LE, Brown SP, Heffernan ML, Fang QK, Orsini MA, et al. Novel human D-amino acid oxidase inhibitors stabilize an active-site lid-open conformation. *Biosci Rep.* (2014) 34:e00133. doi: 10.1042/BSR20140071
268. Ferraris D, Duvall B, Ko YS, Thomas AG, Rojas C, Majer P, et al. Synthesis and biological evaluation of D-amino acid oxidase inhibitors. *J Med Chem.* (2008) 51:3357–9. doi: 10.1021/jm800200u
269. Lane HY, Lin CH, Green MF, Hellemann G, Huang CC, Chen PW, et al. Add-on treatment of benzoate for schizophrenia: a randomized, double-blind, placebo-controlled trial of D-amino acid oxidase inhibitor. *JAMA Psychiatry.* (2013) 70:1267–75. doi: 10.1001/jamapsychiatry.2013.2159
270. Lin CH, Lin CH, Chang YC, Huang YJ, Chen PW, Yang HT, et al. Sodium benzoate, a D-amino acid oxidase inhibitor, added to clozapine for the treatment of schizophrenia: a randomized, double-blind, placebo-controlled trial. *Biol Psychiatry.* (2018) 84:422–32. doi: 10.1016/j.biopsych.2017.12.006
271. Ryan A, Baker A, Dark F, Foley S, Gordon A, Hatherill S, et al. The efficacy of sodium benzoate as an adjunctive treatment in early psychosis - CADENCE-BZ: study protocol for a randomized controlled trial. *Trials.* (2017) 18:165. doi: 10.1186/s13063-017-1908-5
272. Scott JG, Baker A, Lim CCW, Foley S, Dark F, Gordon A, et al. Effect of sodium benzoate vs placebo among individuals with early psychosis: a randomized clinical trial. *JAMA Netw Open.* (2020) 3:e2024335. doi: 10.1001/jamanetworkopen.2020.24335
273. SyneuRx International (Taiwan) Corp. *Adaptive Phase II Study to Evaluate the Safety & Efficacy of NaBen®*. U.S: ClinicalTrials.gov (2013). Available online at: https://www.clinicaltrials.gov/ct2/show/NCT01908192 (accessed April 7, 2020).
274. SyneuRx International (Taiwan) Corp. *An Adaptive Phase II/III, Two-Part, Double-Blind, Randomized, Placebo-controlled, Dose-Finding, Multi-center Study of the Safety and Efficacy of NaBen®, as an Add-on Therapy With Clozapine, for Residual Symptoms of Refractory Schizophrenia in Adults U.S.: Clinicaltrials.gov*. (2017). Available online at: https://www.clinicaltrials.gov/ct2/show/NCT03094429 (accessed April 7, 2020).
275. Neurocrine Biosciences. *A Study to Evaluate Efficacy, Tolerability, Pharmacodynamic and Pharmacokinetics of Multiple Oral Doses of TAK-831 in Adults With Schizophrenia U.S.: ClinicalTrials.gov*. (2017). Available online at: https://www.clinicaltrials.gov/ct2/show/NCT03359785
276. Neurocrine Biosciences. *A Study to Evaluate Efficacy, Safety, Tolerability, and Pharmacokinetics of 3 Dose Levels of TAK-831 in Adjunctive Treatment of Adult Participants With Negative Symptoms of Schizophrenia U.S.: clinicaltrials.gov*. (2017). Available online at: https://www.clinicaltrials.gov/ct2/show/NCT03382639
277. Matsuura A, Fujita Y, Iyo M, Hashimoto K. Effects of sodium benzoate on pre-pulse inhibition deficits and hyperlocomotion in mice after administration of phencyclidine. *Acta Neuropsychiatr.* (2015) 27:159–67. doi: 10.1017/neu.2015.1
278. Krogmann A, Peters L, von Hardenberg L, Bodeker K, Nohles VB, Correll CU. Keeping up with the therapeutic advances in schizophrenia: a review of novel and emerging pharmacological entities. *CNS Spectr.* (2019) 24:38–69. doi: 10.1017/S109285291900124X
279. Yoneyama T, Sato S, Sykes A, Fradley R, Stafford S, Bechar S, et al. Mechanistic multilayer quantitative model for nonlinear pharmacokinetics, target occupancy and pharmacodynamics (PK/TO/PD) relationship of d-amino acid oxidase inhibitor, TAK-831 in mice. *Pharm Res.* (2020) 37:164. doi: 10.1007/s11095-020-02893-x
280. Tseng YFJ, Liu YL, Sun CM, Hwu HG, Liu CM, Lai WS. *Use of Known Compounds as D-Amino Acid Oxidase Inhibitors U.S.* (2014). Available online at: https://patents.google.com/patent/US9868975B2/en
281. Cohen SM, Tsien RW, Goff DC, Halassa MM. The impact of NMDA receptor hypofunction on GABAergic neurons in the pathophysiology of schizophrenia. *Schizophr Res.* (2015) 167:98–107. doi: 10.1016/j.schres.2014.12.026
282. Nakazawa K, Zsiros V, Jiang Z, Nakao K, Kolata S, Zhang S, et al. GABAergic interneuron origin of schizophrenia pathophysiology. *Neuropharmacology.* (2012) 62:1574–83. doi: 10.1016/j.neuropharm.2011.01.022

283. Coyle JT, Balu D, Benneyworth M, Basu A, Roseman A. Beyond the dopamine receptor: novel therapeutic targets for treating schizophrenia. *Dialogues Clin Neurosci.* (2010) 12:359–82. doi: 10.31887/DCNS.2010.12.3/jcoyle
284. Lisman JE, Coyle JT, Green RW, Javitt DC, Benes FM, Heckers S, et al. Circuit-based framework for understanding neurotransmitter and risk gene interactions in schizophrenia. *Trends Neurosci.* (2008) 31:234–42. doi: 10.1016/j.tins.2008.02.005

Conflict of Interest: The authors declare that the research was conducted in the absence of any commercial or financial relationships that could be construed as a potential conflict of interest.

Publisher's Note: All claims expressed in this article are solely those of the authors and do not necessarily represent those of their affiliated organizations, or those of the publisher, the editors and the reviewers. Any product that may be evaluated in this article, or claim that may be made by its manufacturer, is not guaranteed or endorsed by the publisher.

frontiers in Psychiatry

REVIEW
published: 11 October 2021
doi: 10.3389/fpsyt.2021.754032

An Overview of the Involvement of D-Serine in Cognitive Impairment in Normal Aging and Dementia

Magdalena Orzylowski[1,2], *Esther Fujiwara*[2,3], *Darrell D. Mousseau*[4] *and Glen B. Baker*[2,3]*

[1] Villa Caritas Geriatric Psychiatry Hospital, Edmonton, AB, Canada, [2] Department of Psychiatry, University of Alberta, Edmonton, AB, Canada, [3] Neuroscience and Mental Health Institute, University of Alberta, Edmonton, AB, Canada, [4] Department of Psychiatry, University of Saskatchewan, Saskatoon, SK, Canada

Dementia, of which Alzheimer's disease (AD) is the most common form, is characterized by progressive cognitive deterioration, including profound memory loss, which affects functioning in many aspects of life. Although cognitive deterioration is relatively common in aging and aging is a risk factor for AD, the condition is not necessarily a part of the aging process. The N-methyl-D-aspartate glutamate receptor (NMDAR) and its co-agonist D-serine are currently of great interest as potential important contributors to cognitive function in normal aging and dementia. D-Serine is necessary for activation of the NMDAR and in maintenance of long-term potentiation (LTP) and is involved in brain development, neuronal connectivity, synaptic plasticity and regulation of learning and memory. In this paper, we review evidence, from both preclinical and human studies, on the involvement of D-serine (and the enzymes involved in its metabolism) in regulation of cognition. Potential mechanisms of action of D-serine are discussed in the context of normal aging and in dementia, as is the potential for using D-serine as a potential biomarker and/or therapeutic agent in dementia. Although there is some controversy in the literature, it has been proposed that in normal aging there is decreased expression of serine racemase and decreased levels of D-serine and down-regulation of NMDARs, resulting in impaired synaptic plasticity and deficits in learning and memory. In contrast, in AD there appears to be activation of serine racemase, increased levels of D-serine and overstimulation of NMDARs, resulting in cytotoxicity, synaptic deficits, and dementia.

Keywords: D-serine, glutamate, NMDA receptor, dementia, Alzheimer's disease, long-term potentiation, aging, cognition

OPEN ACCESS

Edited by:
Hsien-Yuan Lane,
China Medical University, Taiwan

Reviewed by:
Mahesh Shivarama Shetty,
The University of Iowa, United States
Joshua T. Kantrowitz,
Columbia University, United States
Hisashi Mori,
University of Toyama, Japan

***Correspondence:**
Glen B. Baker
glen.baker@ualberta.ca

Specialty section:
This article was submitted to Molecular Psychiatry, a section of the journal Frontiers in Psychiatry

Received: *06 August 2021*
Accepted: *02 September 2021*
Published: *11 October 2021*

Citation:
Orzylowski M, Fujiwara E, Mousseau DD and Baker GB (2021) An Overview of the Involvement of D-Serine in Cognitive Impairment in Normal Aging and Dementia. Front. Psychiatry 12:754032. doi: 10.3389/fpsyt.2021.754032

INTRODUCTION

Dementia, and its most common form, Alzheimer's disease (AD), is a complex and progressive neurological disorder characterized by many neuropsychiatric symptoms, e.g. aggression, anxiety, depression and sleep disorder, and the better known symptoms associated with progressive memory loss and cognitive impairment, all of which can significantly alter the quality of life of those afflicted with this disorder (1, 2). Age is a major risk factor for dementia, and 1.5% of the population will be affected directly by dementia by the age of 65 and >20% of the population by the age of 85 (3). Neurocognitive disorders such as AD are expected to steadily increase in prevalence and incidence as the population ages. It is estimated that the global number of individuals suffering from dementia will reach 65 million by 2030 and 113 million by 2050 (2, 4). The impact of the high prevalence of

dementia in the elderly is noteworthy, as seen in the substantial direct healthcare costs as well as in the devastating social costs for individuals and their families and caregivers (2). Yet, despite the growing importance of understanding dementia, we are still in search of effective methods for its diagnosis and treatment.

In this review, we provide a summary of the potential role of the amino acid D-serine, a potent co-agonist at the N-methyl-D-aspartate glutamate receptor (NMDAR), in normal and pathological aging, with a focus on neurocognition. A brief discussion on the diagnostic and therapeutic potential of D-serine is also included. The evidence suggests that this is a promising avenue of research into the pathophysiology of neurocognition and its potential treatment in dementing illnesses. Literature searches were performed in PubMed and Web of Science for the period January 1970 to May 2021, and the key search terms used were "D-serine and dementia", "D-serine and Alzheimer's disease", "D-serine and mild cognitive impairment", "D-serine and LTP", as well as "D-serine and NMDA receptors". Only papers in English were used in preparation of the review, and some of the review papers found were searched for additional relevant references. Each reference used was screened by at least two of the authors.

PHYSIOLOGY OF NORMAL AGING

Aging is a normal dynamic process, characterized by the development of a mild inflammatory environment and a progressive deterioration of certain physiological functions, including in the central nervous system (CNS) (5, 6). Although cognitive decline is relatively common in old age, the relationship between aging and degenerative dementias such as AD remains unclear. Whereas aging is a risk factor for AD, it is not inevitable that AD be part of the aging process. While obvious and oftentimes widespread structural changes can be seen within the CNS with dementia pathophysiology, normal aging is not associated with a significant loss of neurons (7); rather, brain alterations in normal aging are much more subtle, involving changes in connectivity and altered functions at the cellular and molecular level (8). Several cognitive domains are affected in normal aging and dementia, including learning and memory (particularly for newly acquired information), processing speed, working memory, and executive function (9, 10). An intriguing feature of aging is the variation of degree of cognitive impairment between individuals, from a mild deficit to a severe dementia, as in the case of AD (11, 12).

The decline in learning and memory performance during non-pathological aging appears to be primarily the result of alterations in neuronal network plasticity within the hippocampus (12). Memory formation is viewed as being closely dependent on the capacity of the brain to regulate long-lasting changes in neuronal communication *via* synapses, and appears to be proportional to the strength of those communications (13, 14). The first convincing support for neuronal plasticity changes underlying changes in cognition came in the 1970s when long-term potentiation (LTP), a mechanism now known to underpin synaptic strengthening critical for learning and memory, was characterized in the hippocampus (15). It was later shown that LTP was regulated in large part by NMDAR signaling (16–18).

Dynamic synapses facilitate remodeling of neuronal circuits, and changes in the functional properties of these networks could play a critical role in the induction of age-related memory decline (19). However, the mechanisms governing dynamic synapses in the brain are still not well understood (20, 21). The hippocampus is the area most frequently implicated in memory decline and this structure seems to be particularly vulnerable to aging (22–24). Interestingly, the circuits that are vulnerable to aging are composed to a large extent of glutamatergic neurons (25).

Proper brain functioning requires healthy neurons and neuronal connections, which in turn require properly functioning neurotransmitters and enzymes that supply these dendritic and neuronal connections. It has been shown repeatedly that deficits in glutamatergic transmission mediated by the NMDAR are related to cognitive impairment in both laboratory animals and humans. Administration of an NMDAR antagonist in rhesus monkeys impairs recognition memory (26), which represents cognitive impairment (27). Similarly, specific ablation of *GRINs* (Glutamate Ionotropic Receptor NMDA Type 1-3), i.e., the genes that encode for subunits of the NMDAR heterotetrameric complex, in the hippocampus or pharmacological blockade of NMDAR function can lead to brain atrophy, impaired neuroplasticity, reduced LTP and deficits in learning and contextual memory (18, 28, 29). In contrast, increasing NMDAR function by over-expression or reduced degradation in the hippocampus can enhance LTP and learning (30, 31).

Particular attention has been paid to learning and memory, and to whether activation of NMDARs could be altered in the course of aging. Various studies in wild-type rodents have revealed that aging is associated with reductions in the magnitude of LTP in the hippocampus and have implicated alterations in NMDAR signaling and a decline in the activation of NMDARs associated with a decrease in levels of D-serine, a co-agonist at the NMDA receptor. Therefore, age-related decreases in D-serine could be contributing to the cognitive decline (10). Since activation of the NMDAR co-agonist-binding site by D-serine and glycine is mandatory for the induction of synaptic plasticity, the LTP rescue observed in aged animals after supplementation with the co-agonist D-serine also suggests that the mechanisms managed by endogenous D-serine are altered with age (11).

D-SERINE PHYSIOLOGY, METABOLISM AND ROLE IN AGING

Memory formation relies on the capacity of neuronal networks to manage long-term changes in synaptic communication. This property is driven, at least in part, by NMDARs (32). The NMDAR is a tetrameric ion channel that may be composed of many configurations of three subunits, i.e., GluN1, GluN2, and less commonly, GluN3 (33–35). To be activated, the NMDAR requires simultaneous binding of the agonist glutamate to the GluN2 subunit and a co-agonist to GluN1 (34–37). This binding is crucial for NMDAR activation and originally it

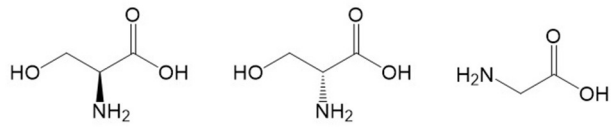

FIGURE 1 | Chemical structures of L-serine (left), D-serine (center) and glycine (right). Structures were located with Google and drawn with ChemDraw.

was thought that the major co-agonist was glycine (10, 36, 37); however, later studies found that D-serine is more potent than glycine at binding to the co-agonist site on the GluN1 subunit of the NMDAR and stimulating the receptor in forebrain regions, including hippocampus (38). D-Serine has a regional distribution in the brain more similar to that of NMDARs than does glycine (39–41) and it has been reported that D-serine acts primarily at synaptic NMDARs whereas glycine acts primarily at extrasynaptic NMDARs (38). Interestingly, glycine is similar structurally to D-serine (**Figure 1**) and it is formed by conversion of L-serine catalyzed by the enzyme serine hydroxymethyltransferase.

Balanced NMDAR activity is required for optimal brain function. Hypo- or hyper-function of NMDAR-mediated neurotransmission can result in cognitive dysfunction or neurotoxicity, respectively. Depletion of D-serine diminishes NMDAR activity, LTP, and synaptic plasticity (33). NMDAR-mediated neurotransmission and its modulation by D-serine play a critical role in memory formation, learning, and neuronal plasticity (34, 42–44). In CNS development, D-serine shapes synaptogenesis and neuronal circuitry through activation of NMDARs and it is also a key player in astrocyte-mediated LTP associated with hippocampal plasticity (20).

The reports by Hashimoto et al. were the first to demonstrate high concentrations of D-serine in the rodent brain and in the human brain (45, 46). It was only later discovered that D-serine is enriched in brain regions containing high concentrations of NMDARs, such as the cerebral cortex, hippocampus, and amygdala (41). The source of D-amino acids in mammals was historically attributed to diet or intestinal bacteria (47) until the racemization of L-serine by serine racemase was identified as the endogenous source of D-serine (48) (see **Figure 1** for structures of L- and D-serine). Serine racemase was first described to be exclusively present in astrocytes (49–51), but subsequent work has shown that serine racemase is also present in neurons (52). Thus, D-serine may be a glial transmitter as well as a neurotransmitter, and this has been a matter of considerable controversy [for discussions of this matter see: (52–54)]. Wolosker et al. (52) proposed that L-serine is synthesized in astrocytes and then shuttled to neurons where it is converted to D-serine. For a detailed description of D-serine circuits and the "serine shuttle", see Wolosker and Balu (55).

Serine racemase is expressed by many CNS cells, including pyramidal neurons in the cerebral cortex and the CA1 region of the hippocampus (41, 56), regions that also have high levels of D-serine (57). Wong et al. (58) have shown an age-dependent dendritic and postsynaptic localization of serine racemase in CA1 pyramidal neurons of the mouse. These same researchers, in studies using serine racemase knockout (KO) mice, showed a cell-autonomous role for this enzyme in regulating synaptic NMDAR function at Schaffer collateral (CA3)-CA1 synapses and found that single-neuron genetic deletion of serine racemase eliminated LTP at the age of 1 month and that this loss of LTP could be rescued by administering D-serine (58). The enzyme responsible for the catabolism (breakdown) of D-serine is D-amino acid oxidase (DAAO); this enzyme is most abundant in cerebellum and brain stem, areas with low levels of D-serine (59).

D-Serine levels vary across different CNS areas. The level of D-serine is in the order of 200–300 pmoles per milligram of tissue in the hippocampus and frontal cortex in mice, 20-fold higher than in the pancreas, lung, or testis and almost 50-fold higher than in muscle (60). Within the brain, highest levels of D-serine are in the cortex and hippocampus, and there are much lower levels in the cerebellum and brain stem, likely reflecting the regional variation in expression of serine racemase and DAAO (review: 61).

D-Serine, through its regulatory effect on glutamatergic transmission, participates in multiple processes, including synaptic plasticity (61, 62), cell migration and synaptogenesis (41, 63), and in homeostatic functions, as a mediator of hypercapnia-induced respiratory response (64). The production of D-serine and its tightly regulated release, mainly through calcium-dependent exocytosis (65), keep its concentration within a narrow range. Any deviation from this range may lead to pathology, with abnormally increased levels of D-serine associated with NMDAR-mediated neurotoxicity (66–68) and abnormally decreased levels of D-serine associated with impairments in functional plasticity and with memory deficits (11). The complexity of its actions and its modulatory effects are not well understood; indeed, Coyle et al. (69) referred to D-serine as a "shape-shifting NMDAR co-agonist" and provided a possible explanation for these dueling effects of D-serine on driving neuronal plasticity or neurodegeneration based on the localization of the activated NMDARs involved. It is known that synaptic NMDARs prompt trophic effects while extra-synaptic NMDARs on the dendrites or soma drive excitotoxicity (38, 70, 71). Coyle et al. (69) propose that D-serine synthesized by serine racemase binds preferentially to synaptic NMDARs and facilitates glutamatergic neurotransmission, while proliferation of inflammatory A1 astrocytes results in a new source of D-serine that is released into the extracellular space to activate extra-synaptic NMDARs.

D-Serine levels in the CNS change during development and aging. In early developmental stages, a transient increase in D-serine production matches a transient increase of NMDAR activity (72). The early postnatal period with high D-serine levels in glia coincides with a period of intense plasticity, synaptogenesis and maturation in the CNS, suggesting the existence of distinct functional roles for D-serine throughout development (72). Healthy newborn children have elevated CSF D-serine levels that are rapidly reduced during the first year of life and reach 15% of the initial concentration at 3 years of age (73).

In the hippocampus of normal aged rats, both D-serine (but not glycine) and serine racemase levels are decreased relative

to younger rats (74, 75). In contrast, these reductions in D-serine and serum racemase are not observed in the LOU/c/jall rat strain regardless of age (5, 76). The LOU/c/jall strain of rat (derived from the Wistar strain) is a model of healthy aging (with resistance to obesity and lower oxidative metabolic rates than the routinely used other inbred strains of rats) (76). Interestingly, the possibility that D-serine-related pathways could be targeted by the age-related accumulation of reactive oxygen species (ROS) has been suggested (5), and LOU/c/jall rats do not develop oxidative stress (5, 76).

D-SERINE, NMDARs AND COGNITIVE IMPAIRMENT IN AD/DEMENTIA

Animal Studies

Characterizing the processes associated with hippocampal dysfunction has been an area of focus in research on AD, where β-amyloid (Aβ) deposits, intracellular neurofibrillary tangles, abnormal tau protein phosphorylation and synaptic loss are typical pathological features (77–79). The pathological changes that are detected in the brains of patients with AD, such as the presence of amyloid plaques and neurofibrillary tangles, are now known to appear several years before the development of clinical symptoms. As such, current research is focusing more on early detection and treatment in these earlier stages in the hope of delaying the onset or slowing the progression of AD.

Although NMDAR function is vital for memory and cognitive function, its role in the pathophysiology of AD is still not completely understood. NMDAR over-activation can lead to cell death mediated by calcium overload. The associated excitotoxicity is one of the accepted neurochemical models of AD in rodents and may be involved with the pathophysiology associated with Aβ, a hallmark of the pathogenesis of AD (80–82). Interestingly, different forms of Aβ aggregates increase glutamate release from neurons and astrocytes (2, 83) and Aβ can increase NMDAR activity and induce inward Ca^{2+} current and neurotoxicity; this NMDAR activation may stimulate Aβ production and Aβ-associated synaptic loss (2). Aβ deposition appears to play an important role in the pathophysiology of AD, and the mechanism underlying glutamate excitotoxicity in AD may be related to Aβ deposition (84, 85). Aβ aggregation interferes with NMDAR-mediated neurotransmission, suppressing NMDAR-dependent synaptic function and LTP, which may lead to cognitive impairment (86–89). Furthermore, Aβ can lead to intracellular trapping of NMDARs, decreasing LTP; this effect can be rescued by a Reelin- and Src kinase-dependent tyrosine phosphorylation in the GluN2 subunit of the NMDARs, restoring normal synaptic plasticity (90). In addition to Aβ, apolipoprotein E4 (APOE4), a protein isoform that has lower Aβ-binding capacity than APOE2 and APOE3, and is a genetic risk factor for AD (91), reduces NMDAR function and synaptic plasticity by impairing APOE receptor recycling (92).

Aβ peptides have also been shown to stimulate the synthesis and release of D-serine (93) in preclinical models (80). The excessive D-serine release from neurons and glia leads to synaptic loss and stimulation of extra-synaptic NMDAR currents (94, 95). Excessive levels of D-serine create a dramatic overload of Ca^{2+} (96), and degradation of D-serine by DAAO or D-serine deaminase protects against cell death (97). Dysfunctional D-serine metabolism may be a downstream outcome of Aβ toxicity, and excess D-serine release may contribute to neuronal death in AD through excitotoxicity. However, whether levels of free D-serine are elevated in the brains of AD is still a matter of debate as levels vary depending on brain region and stages of pathology (10).

Ongoing interest in amyloid precursor protein (APP), the precursor of the Aβ peptide in AD, has been refueled by evidence indicating its multifaceted complex role in synaptic (patho)physiology and development (98). Animal studies have shown that a lack of APP impairs the structural plasticity of dendritic spines (important for cognition and memory) and that APP plays a key role in regulating D-serine homeostasis, which is an important factor in synaptic plasticity in the adult brain (98). These authors measured cortical extracellular and total D-serine concentrations in APP-KO mice and found an increase in concentrations of total D-serine, but a concurrent decrease in concentrations of extracellular D-serine. Treatment with exogenous D-serine not only restored the extracellular D-serine levels and synaptic plasticity, but also normalized the concentrations of total D-serine and rescued the cognitive deficit observed in the APP-KO mice. These results suggest that the maintenance of D-serine homeostasis requires APP and demonstrate D-serine's essential role in adaptive remodeling in the adult brain (98).

Microglia are the main immune effector cells of the brain and the main source of inflammatory cytokines and reactive oxygen species (ROS) in the CNS (5). Alterations in the activation and regulation of microglia can promote a chronic inflammatory condition in the CNS in normal and pathological aging (5), an inflammatory environment termed immunosenescence. This process induces changes in gene expression related to the immune response and inflammation, causing increased susceptibility to inflammatory responses to stressors, which could facilitate the onset of neurodegeneration (5, 6, 99–102). Activation of microglial cells, as part of a chronic inflammatory response, is a prominent component of AD that drives neurotoxicity through the release of excitotoxins including glutamate, and increased activity of Aβ, which not only promotes glutamate release from microglia, but also stimulates expression of serine racemase and D-serine release from these glial cells (2, 93, 103). Aβ also promotes serine racemase activity through increases in intracellular levels of calcium, upregulating the activity of the enzyme. How much of the changes in D-serine levels during aging are determined by microglial cell actions is unclear. However, it is speculated that age-dependent changes in microglia regulation result in neuroinflammation and increased oxidative stress (104), in turn eventually activating production of D-serine by glia and neurons in AD (5).

The functioning of neuronal networks within the CNS requires high levels of oxygen, and the CNS is particularly sensitive to oxidative stress (105). Studies have found that antioxidant levels in the brain are low compared to other

TABLE 1 | Abnormal D-serine function in normal aging and Alzheimer's disease.

	Serine racemase expression	D-serine levels	NMDARs	Cognitive changes
Normal Aging	⇩	⇩	Down-regulation, leading to reduced LTP and impaired synaptic plasticity	Variable learning and memory deficits
AD	⇧	⇧	Over-stimulation, interactions with activated microglia and Aβ, increased release of glutamate, excitotoxicity	Dementia

⇩ *= decrease;* ⇧ *= increase; AD, Alzheimer's disease; NMDARs, N-methyl-D-aspartate receptors; LTP, long-term potentiation; Aβ, β-amyloid. [adapted from Billard (11)].*

organs (106). Changes in redox regulation in the CNS may be accompanied by neuronal dysfunction, particularly alterations of synaptic plasticity (107, 108). Assuming synaptic plasticity is an essential neuronal mechanism for learning and memory (13, 14), it may be a preferred target by which oxidative stress could alter memory functions. DAAO plays a key role in the process of oxidative stress and results in formation of ROS; through this effect and its regulatory function on NMDARs by reducing levels of D-serine, DAAO may play an important role in the process of aging and age-related cognitive decline (109). Nagy et al. (110) studied the effects of the DAAO inhibitor CPD30 on passive avoidance learning and neuronal firing activity in rats and concluded that inhibition of DAAO is an effective strategy for cognitive enhancement; CPD30 increased hippocampal firing and reversed MK-801-induced memory impairment in the passive avoidance test.

Human Studies

The preclinical studies mentioned above have suggested that while normal aging may result in decreases in D-serine synthesis and levels, NMDAR activity, the magnitude of LTP and synaptic plasticity (all of which may be reversed by administration of D-serine), pathological aging may involve activation of serine racemase, increased levels of D-serine, NMDAR hyperstimulation and excitotoxicity, resulting in dementia (**Table 1**).

Madeira et al. (16) conducted a comprehensive combined clinical-preclinical study on D-serine in AD. D-Serine levels were measured in post-mortem hippocampal and cortical samples from non-demented individuals and AD patients. D-Serine was also measured in hippocampus from wild type rats and mice after intracerebroventricular injections of Aβ and in the APP/PS-1 transgenic mouse model of AD. In addition, D-serine levels in CSF of people with probable AD were also measured and compared to those of patients with normal pressure hydrocephalus or major depression, and to healthy controls. D-Serine levels were higher in the post-mortem hippocampus and parietal cortex samples of AD patients than in healthy controls. The researchers also found higher levels of D-serine and serine racemase in all the rodent models compared to controls. Furthermore, D-serine levels were higher in the CSF of probable AD patients compared to the non-demented control groups; mean D-serine levels in the probable AD group were five-fold higher than in healthy controls, and approximately two-fold higher than in the depression or hydrocephalus groups. These researchers concluded that D-serine levels in brain and CSF are increased in AD and that D-serine might be a candidate for early AD diagnosis (16). In contrast, three earlier studies using post-mortem prefrontal, parietal, frontal or temporal cortical tissue failed to detect altered D-serine levels between AD and controls (111–113). All of the post-mortem studies had small sample sizes and a wide range of participant ages and postmortem collection times. One study (16) had equal numbers of males and females, one (113) had all male participants and the other two studies (111, 112) did not indicate the male/female ratio.

POTENTIAL ROLE OF D-SERINE IN DIAGNOSIS OF AD

Significant efforts are being made to identify diagnostic markers and modifiable risk factors for AD, specifically any factor that influences the earliest stages of the disease process, when intervention might still provide therapeutic benefit. In this context, CSF levels of Aβ, total tau protein and hyperphosphorylated tau (p-tau) have now been included in diagnostic guidelines (114). Such CSF biomarkers have been advocated for research purposes, but sensitivity and specificity issues have generally raised concerns about their widespread clinical use (15). Madeira et al. (16) proposed that combining CSF D-serine levels with the Aβ/tau index could markedly increase the sensitivity and specificity of diagnosis of probable AD. However, Biemans et al. (115) and Nuzzo et al. (116) did not find a difference in CSF D-serine levels between AD patients and elderly controls.

Lin et al. (109) found increased levels of DAAO in the serum of patients with mild cognitive impairment (MCI) and AD and observed that the severity of cognitive deficits correlated positively with DAAO blood levels, suggesting that this enzyme catabolizing D-serine may also serve as a biomarker for MCI/AD. These researchers found that DAAO levels were significantly lower in healthy controls than in the patients, and moreover, lower in patients with amnestic MCI than in those with moderate to severe AD (109). In the same study, D-serine levels in serum were reported to be higher in AD patients than in the healthy controls. The clinical benefit of DAAO inhibition in AD may be mediated in part by an antioxidant effect since D-serine degradation by DAAO generates hydrogen peroxide, a precursor to many ROS (10, 109). In a later study of D-serine levels in 144 patients with varying degrees of cognitive impairment, Lin et al. (117) concluded that higher D-serine levels predict worse cognitive function, particularly with regard to word recall, orientation, comprehension, and word-finding.

In a recent metabolomics study in a cohort of women aged 65–80 years old, Kimura et al. (118) reported a higher D-proline/(D-proline+L-proline) ratio in women with MCI compared to matched controls, and found this biomarker's accuracy was improved by further adding the D-serine/(D-serine+L-serine) ratio. Piubelli et al. (119) measured serum levels of D- and L-serine in AD patients with either a score of 1 (mild dementia) or 2 (moderate dementia) in the Clinical Dementia Rating Scale, and found that D-serine levels and the D-serine/total serine ratio increased significantly with disease progression. These researchers suggested using the combination of the above ratio with other blood-based biomarkers presently under development and reviewed by Hampel et al. (120).

The role of D-serine in AD is complex and the literature is often ambiguous. It has been suggested that some of the differences between findings in laboratory animals and human AD patients could be due to the fact that current animal models do not mimic the slow progression and the changes in Aβ and tau protein that occur in AD in humans (11). It has also been proposed that studies on D-serine and AD should be done at various stages of AD since at early stages with low levels of Aβ oligomers there is also decreased synthesis of L-serine and, hence, decreased D-serine levels and weaker NMDAR activation. However, at later stages when there is increased soluble Aβ, glia start to express more serine racemase and release large amounts of D-serine, resulting in NMDAR over-activation and resultant excitotoxicity, neurodegeneration and marked memory deficits (117). There is also some speculation that D-serine increases observed in AD patients may be part of a protective mechanism to counter Aβ signaling and prevent AD pathology (10).

TREATMENT POTENTIAL OF D-SERINE

As mentioned above, there is a loss of production of D-serine and a decline in NMDAR activation and a corresponding reduction of LTP magnitude in the normal aging process, which can be reversed in animal models by administration of D-serine (11). These findings imply that increasing D-serine levels in cases of initial cognitive decline or in early stages of AD may be therapeutically useful (10).

Findings that the co-agonist modulatory site was not saturated *in vivo* prompted investigators to consider whether exogenous D-serine could act as a cognitive enhancer (10). Although the focus of the present review is on dementia, it should be mentioned that much of the research on the effects of D-serine in cognition in humans has been done on schizophrenia (57, 121–130), reporting either cognitive benefits (121, 122, 125, 126, 130) or no effects on cognition (123, 128, 129). It is difficult to compare the studies since they were performed at several doses, the patients were taking antipsychotics (which presents a possible confound), and a variety of tests were conducted to measure cognition. Most of the studies were carried out using a daily dose of 30 mg/kg, but Kantrowitz et al. (126, 130) also used higher doses (60 and 120 mg/kg) and reported improvements in cognition.

D-Serine administration can improve cognition in aged rodents and correct age-related decline in synaptic plasticity (10). In mouse models, the learning deficits caused by NMDAR hypofunction can be rescued by administration of D-serine (131). Although conflicting results have been reported, D-cycloserine (**Figure 2**; a cyclized form of D-serine that is hydrolyzed to give D-serine and hydroxylamine) has been reported to improve memory functions in animal studies and in dementia patients (132, 133). Lin and Lane (133) speculated that D-cycloserine may have different effects on mood and learning depending on the stage of dementia involved. D-Serine given intraperitoneally to rats can increase NMDAR activation in the hippocampus and improve social memory in rats and recognition and working memory in mice (10). The potency of exogenous D-serine to enhance NMDAR activation appears significantly higher in hippocampal slices from aged rats when compared to effects in younger adult rats (134). Nikseresht et al. (135), using a rat model of AD (intracerebroventricular injection of Aβ), reported a synergistic memory-enhancing effect of D-serine and the mitochondrial calcium uniporter blocker RU360. The findings in this report suggested that the coadministration of these drugs ameliorated memory impairment, probably in part through an increase in hippocampal levels of cyclic AMP response element binding protein (CREB) and brain-derived neurotrophic factor (BDNF).

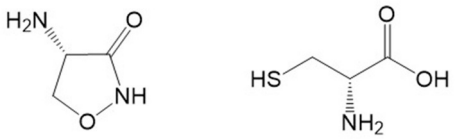

FIGURE 2 | Chemical structures of D-cycloserine (left) and D-cysteine (right). Structures were located with Google and drawn with ChemDraw.

In a randomized controlled clinical trial (RCT) by Avellar et al. (9), 50 healthy elderly human adults received a single dose of D-serine or placebo, and the effects of D-serine administration on cognitive test performance and a mood scale were measured. In addition, blood samples were analyzed for levels of D-serine, L-serine, glutamate and glutamine. D-Serine levels measured while the participants were on placebo were inversely associated with aging. D-Serine administration improved performance in the Groton Maze Learning Test of spatial memory, learning and problem solving. Individuals who achieved higher increases in plasma D-serine levels after administration improved more in test performance. D-Serine administration was not associated with any significant changes in other cognitive domains, such as verbal working memory, visual attention or cognitive flexibility. There were also no changes observed in mood (9). In a similar study, but in young healthy adults, Levin et al. (136) demonstrated that D-serine administration improved attention, verbal learning and memory as well as subjective feelings of sadness and anxiety.

These above studies suggest an important role for D-serine in brain networks underlying memory impairment and provide useful information in the search for new therapeutic strategies for the treatment of memory deficits. However, an important question is whether the improvements seen so far with the

addition of D-serine in animal models and healthy human controls will have real-life effects in AD (11).

OTHER TREATMENT APPROACHES RELATED TO D-SERINE

In the aging brain, ROS accumulation may trigger age-related reduction of cognitive function through oxidative stress. Consequently, ROS accumulation could be viewed as a major process acting on the D-serine-related pathway in the aging hippocampus, especially considering that serine racemase activity is particularly sensitive to oxidative stress (105). Long-term dietary supplementation with L-N-acetylcysteine (L-NAC, a precursor to the antioxidant glutathione) prevented oxidative damage in the hippocampus and restored D-serine-dependent NMDAR activation and LTP induction in aged rats (20). These data provide evidence that maintaining elevated D-serine levels in the aging hippocampus through the control of the redox state is able to prevent the cellular injury underlying cognitive aging, specifically in the CA1 hippocampal area (11).

An increase in D-serine availability in the brain could be achieved by reducing its degradation by DAAO. Treatment of rats with a DAAO inhibitor has been reported to increase levels of D-serine in the cerebral cortex and midbrain (137). Although DAAO KO mice have been reported to have markedly increased levels of D-serine in cerebellum and brain stem but little or no change in D-serine levels in cortex or hippocampus (138, 139), support for a physiological role for DAAO in modulating cognition comes from the enhanced learning abilities reported for DAAO KO mice (57, 140). The DAAO inhibitor sodium benzoate, which also modulates the immune system and is an antioxidant, has been shown to improve cognition, global functioning and positive and negative symptoms of schizophrenia (141). Modi et al. (142), using an animal model of AD, reported that sodium benzoate reduced oxidative stress and protected memory and learning. In addition, in RCTs of 6 weeks daily treatment with sodium benzoate, Lin and colleagues reported that cognitive scores were improved in early stage dementia patients and in women, but not men, with later phase dementia (143).

The D-amino acid D-cysteine, which is derived from the gut, and is structurally related to D-serine (it is also referred to as thioserine; **Figure 2**) also exerts neuroprotection, but it does so *via* a DAAO-dependent conversion to H_2S (144). Interestingly DAAO has greater affinity for D-cysteine even though D-serine is found in far greater concentrations in the brain (145). It is all the more interesting that D-cysteine has been shown to be a potent inhibitor of serine racemase (146), thereby making it a potential treatment for pathologies where D-serine might exert deleterious effects, such as in AD.

LIMITATIONS IN THE USE OF D-SERINE AS A BIOMARKER AND TREATMENT

The fact that body fluid levels of D-serine have been reported to be altered in other psychiatric and neurological disorders, such as depression, anxiety, schizophrenia, bipolar disorder and hydrocephalus (16, 61, 147, 148) suggests that D-serine would not be a specific biomarker for AD. There are also potential challenges for the clinical use of D-serine, including the possibility of nephrotoxicity (149, 150). However, this nephrotoxicity may only be a problem with rats since it has not been reported in other species, including rodents such as mice and rabbits (151, 152). Even in rats, the nephrotoxicity is reversible and appears to occur only at high doses (152). In a comprehensive review of safety of D-serine across species, Meftah et al. (152) listed the studies on humans with D-serine that have been published and reported that only one subject in one study showed renal abnormalities. These researchers concluded that D-serine is safe and well tolerated in humans even at the highest dose (120 mg/kg) tested to date, but that people with pre-existing renal dysfunction should be excluded from clinical studies. Co-administration of a DAAO inhibitor with D-serine may be a strategy to prevent nephrotoxicity since lower doses of D-serine could be used and hence formation of peripheral metabolites of D-serine reduced (153). In mice, treatment with a DAAO inhibitor has been reported to render a low dose of D-serine effective in treating pre-pulse inhibition deficits caused by the NMDAR antagonist dizocilpine, compared to the same dose of D-serine alone (154).

Poor oral bioavailability can also limit the effects of D-serine on cognition. Accordingly, D-serine had better effects on cognition when administered as an adjunct to patients with schizophrenia when higher doses such as 60 mg/kg/day or higher were used (review: 61). In general, poor oral D-serine bioavailability may account for mixed results in clinical trials, and alternative treatment paradigms may need to be considered, including larger doses of D-serine or a combination of D-serine and sodium benzoate (thus using lower doses of both drugs while retaining high efficacy). Because D-serine and sodium benzoate have different pharmacokinetic and pharmacodynamic profiles, it is possible that D-serine may be especially useful for treating depression because of its acute and chronic antidepressant effects, whereas sodium benzoate may be a safer approach in older adults with impaired renal function (10).

CHALLENGES AND POSSIBLE FUTURE DIRECTIONS IN RESEARCH ON D-SERINE AND COGNITION

Considerable evidence in the literature supports the involvement of D-serine in reduction of cognitive deficits, but there are some contradictory findings that indicate that further research is warranted. For example, Capitao et al. (155), in a study of a single dose (60 mg/kg) in human volunteers, found that D-alanine modulated emotional processing while D-serine did not. Some researchers have questioned the physiological role of DAAO in controlling D-serine availability because this enzyme is expressed at low levels in forebrain areas relevant to cognition such as the hippocampus and cortex, and D-serine levels have been reported to be elevated markedly in the cerebellum and brain stem but not in cortex or hippocampus

of DAAO KO mice (138, 139). However, other researchers have found that systemic administration of a DAAO inhibitor to rats increases levels of D-serine in the cortex (137). Labrie et al. (140) reported that DAAO KO mice had a marked increase in levels of D-serine in the cerebellum, but also had a relatively small, but significant, increase in D-serine levels in the hippocampus and showed enhanced extinction and reversal learning.

Although it has been proposed that CSF and/or serum levels of D-serine could be novel biomarkers for AD (16, 119, 156), other researchers have reported that D-serine levels in these body fluids are unaltered in AD (115, 116). It has also been reported that perinatal epigenetic mechanisms play a role in the regulation of levels of D-serine in the brain (157), and future studies in AD should include epigenetic investigations on expression of serine racemase and DAAO genes. Dysregulation of aerobic glycolysis in the brain is often observed early in the course of AD, and Le Douce et al. (158) have shown that the astrocytic biosynthetic pathway for L-serine (the precursor for D-serine), which branches from glycolysis, is impaired in young AD mice and in AD patients. These researchers found that dietary supplementation with L-serine prevented the synaptic and behavioral deficits in AD mice, which suggests that oral L-serine could be a therapy for AD.

RELEVANCE OF D-SERINE TO COMORBID DEPRESSION, ANXIETY AND OTHER BEHAVIORAL CHANGES IN DEMENTIA

The focus of this review has been on the involvement of D-serine in cognitive deficits, but dementia is complex and often there is a high degree of comorbidity with depression, anxiety, aggression, and/or sleep disorders. There is now an extensive body of literature indicating involvement of D-serine in each of these disorders. It may seem contradictory for D-serine to have antidepressant effects considering the known antidepressant effects of the NMDAR antagonist ketamine (159), but several preclinical and clinical studies report antidepressant actions of D-serine [reviews: (61, 160, 161)]. It has been proposed that the antidepressant actions of ketamine and D-serine may be due to common effects on α-amino-3-hydroxy-5-methyl-4-isoxazole propionic acid (AMPA) glutamate receptors and similar differential actions on synaptic *vs.* extra-synaptic NMDARs (160). Wolosker and Balu (55) have provided a comprehensive review of mainly preclinical studies suggesting a role of D-serine in fear conditioning and anxiety disorders. As an abnormal social behavior, aggression (often studied in mice as social interaction deficits with intruder strains of mice) has been observed in rodents to show an association with NMDAR function (162–165). Both D-cycloserine and D-serine have been reported to improve impaired social interaction skills, for example in inbred Balb/c mice used as models for autism (164–167). Nagai et al. (168) reported that mice treated neonatally with polyI:C (elicits viral-like immune responses) had emotional and cognitive deficits which could be ameliorated in adulthood by treatment with D-serine. With regard to sleep disorders, studies in mammals and Drosophila flies have shown that NMDARs and D-serine participate in sleep regulation (169–171). Drosophila has been used as a model for genetic studies of sleep for several years (172). In a detailed study of sleep in this model, Dai et al. (173) showed that sleep is regulated by D-serine through NMDAR1 and that intestinal expression of serine racemase is important for this sleep regulation.

Longitudinal studies, both preclinical and clinical, involving larger samples sizes will be needed in future research on D-serine, and such investigations should include both males and females, along with assessments of the comorbid disorders mentioned above.

SUMMARY

In normal aging there is development of a mild inflammatory environment and progressive deterioration of several physiological functions, including cognition involving learning and memory performance. With aging, the degree of cognitive impairment can vary markedly among individuals. Memory formation depends on the capacity of the brain to regulate long-lasting changes in neuronal communication *via* synapses, and these changes in neuronal plasticity are dependent on LTP, which is regulated in large part by NMDARs. Functioning of NMDARs is in turn dependent on co-agonists, the most important of which appears to be D-serine. Numerous animal studies have shown that even with normal aging there is a reduction in the magnitude of LTP in the hippocampus accompanied by a decline in NMDAR action and a decrease in production and levels of D-serine. It has also been demonstrated in animal models that administration of D-serine can rescue the reduced NMDAR function and loss of LTP observed in aging.

Preclinical studies suggest that D-serine may be useful in treating cognitive impairment, but while abnormally decreased levels of D-serine are associated with impairments in functional plasticity, abnormally increased levels of D-serine can be associated with NMDAR-mediated excitotoxicity such as occurs in later-stage AD. Activation of microglia is part of a chronic inflammatory response in AD that increases release of glutamate and D-serine from glia and neurons, and Aβ also stimulates expression of serine racemase in microglia. It has been suggested that with cognitive deficits associated with normal aging and in early AD, there may be decreased expression of serine racemase, decreased levels of D-serine, NMDAR down-regulation and impaired synaptic plasticity, while in advanced AD serine racemase activation and D-serine levels are increased and NMDARs are overstimulated, resulting in excitotoxicity and dementia.

D-Serine and DAAO have been proposed as possible biomarkers in the diagnosis of AD, although there have been conflicting results reported and differences found in animal models and humans. Current animal models do not mimic the slow progression and the changes in Aβ and tau protein

that occur in humans; it has also been proposed that future studies on D-serine in humans should be done at several stages of AD. Research to date suggests that earlier stages of AD would benefit from D-serine supplementation, whereas D-serine supplementation should be avoided in later stages of AD. DAAO inhibitors may also be useful for increasing brain D-serine levels and enhancing learning.

Although we understand a great deal about the roles of D-serine in brain function, about changes in its brain levels with normal and pathological aging, and about its potential role as a cognitive enhancer from experimental and preclinical studies, much still remains to be learned about its potentially targetable role in development, treatment and possibly even prevention of dementia in a clinical setting.

AUTHOR CONTRIBUTIONS

MO and GB conducted the initial literature search. Each reference was screened by at least two of the authors. MO prepared the initial draft of the manuscript and all authors then contributed to editing. All authors have agreed to submission of this version of the manuscript.

FUNDING

DM acknowledges financial support from the Office of Research, College of Medicine, University of Saskatchewan as well as from a philanthropic Saskatchewan family. DM also acknowledges the *Saskatchewan Research Chair in Alzheimer disease and related dementias* funded jointly by the Alzheimer Society of Saskatchewan and the Saskatchewan Health Research Foundation. GB has a TRIP Research Allowance (TRP-GB) from the Faculty of Medicine & Dentistry at the University of Alberta. EF acknowledges funding from CIHR (FRN 201803).

ACKNOWLEDGMENTS

The authors are grateful to Ms. Tricia Kent for technical support.

REFERENCES

1. World Health Organization. Dementia. *Fact sheet No 362. (2015)* Available online at: www.who.int/mediacentre/factsheets/fs362/en/ (accessed September 12, 2020).
2. Huang Y, Lin C, Lane H, Tsai G. NMDA neurotransmission dysfunction in behavioral and psychological symptoms of Alzheimers disease. *Curr Neuropharmacol.* (2012) 10:272–85. doi: 10.2174/157015912803217288
3. Ritchie K, Kildea D. Is senile dementia "age related" or "ageing related"? Evidence from meta-analysis of dementia prevalence in the oldest old. *Lancet.* (1995) 346:9314. doi: 10.1016/S0140-6736(95)91556-7
4. Brodaty H, Breteler MM, Dekosky ST, Dorenlot P, Fratiglioni L, Hock C, et al. The world of dementia beyond 2020. *J Am Geriatr Soc.* (2011) 59:9237. doi: 10.1111/j.1532-5415.2011.03365.x
5. Beltran-Castillo S, Eugenin J, von Bernhardi R. Impact of aging in microglia-mediated D-serine balance in the central nervous system. *Mediat of Inflamm.* (2018) 721973. doi: 10.1155/2018/7219732
6. von Bernhardi R, Eugenin-von Bernhardi L, Eugenin J. Microglial cell dysregulation in brain aging and neurodegeneration. *Front Aging Neurosci.* (2015) *7*:124. doi: 10.3389/fnagi.2015.00124
7. Burke SN, Barnes CA. Senescent synapses and hippocampal circuit dynamics. *Trends Neurosci.* (2010) 33:153–61. doi: 10.1016/j.tins.2009.12.003
8. Driscoll DA, Hamilton H, Petropoulos RA, Yeo WM, Brooks RN, Baumgartner RJ et al. The aging hippocampus: cognitive, biochemical and structural findings. *Cerebral Cortex.* (2003) 13:1344–51. doi: 10.1093/cercor/bhg081
9. Avellar M, Scoriels L, Madeira C, Vargas-Lopes C, Marques P, Dantas C, et al. The effect of D-serine administration on cognition and mood in older adults. *Oncotarget J.* (2016) 7: 11881-8. doi: 10.18632/oncotarget.7691
10. Guercio G, Panizzutti R. Potential and challenges for the clinical use of D-serine as a cognitive enhancer. *Front Psychiat.* (2018) 9:14. doi: 10.3389/fpsyt.2018.00014
11. Billard JM. D-serine signalling as a prominent determinant of neuronal-glial dialogue in the healthy and diseased brain. *J Cell Mol Med.* (2008) 12:1872–84. doi: 10.1111/j.1582-4934.2008.00315.x
12. Dreary IJ, Corley J, Gow AJ, Harris SE, Houlihan LM, Marioni RE, et al. Age-associated cognitive decline. *Br Med Bull.* (2009) 92:135–52. doi: 10.1093/bmb/ldp033
13. Lisman JE, McIntyre CC. Synaptic plasticity: a molecular memory switch. *Curr Biol. (2001) 11:* R788-91. doi: 10.1016/S0960-9822(01)00472-9
14. Martin SJ, Grimwood PD, Morris RG. Synaptic plasticity and memory: an evaluation of the hypothesis. *Ann Rev Neurosci.* (2000) 23:649–711. doi: 10.1146/annurev.neuro.23.1.649
15. Bliss TV, Gardner-Medwin AR. Long-lasting potentiation of synaptic transmission in the dentate area of the unanaestetized rabbit following stimulation of the perforant path. *J Physiol.* (1973) 232: 357–74. doi: 10.1113/jphysiol.1973.sp010274
16. Madeira C, Lourenco MV, Vargas-Lopes C, Suemoto CK, Brandao CO, Reis T, et al. D-serine levels in Alzheimers disease: implications for novel biomarker development. *Transl Psychiatry.* (2015) 5: e561. doi: 10.1038/tp.2015.52
17. Manabe T, Aiba A, Yamada A, Ichise T, Sakagami H, Kondo H, et al. Regulation of long-term potentiation by H-Ras through NMDA receptor phosphorylation. *J Neurosci.* (2000) 20:2504–11. doi: 10.1523/JNEUROSCI.20-07-02504.2000
18. Zhao MG, Toyoda H, Lee YS, Wu LJ, Ko SW, Zhang XH, et al. Roles of NMDA NR2B subtype receptor in prefrontal long-term potentiation and contextual fear memory. *Neuron.* (2005) 47:859–72. doi: 10.1016/j.neuron.2005.08.014
19. Rosenzweig ES, Barnes CA. Impact of aging on hippocampal function: plasticity, network dynamics, and cognition. *Progr Neurobiol.* (2003) 69:143–79. doi: 10.1016/S0301-0082(02)00126-0
20. Haxaire C, Turpin R, Potier B, Kervern M, Sinet PM, Barbanel G, et al. Reversal of age-related oxidative stress prevents hippocampal synaptic plasticity deficits by protecting D-serine dependent NMDA receptor activation. *Aging Cell.* (2012) 11:336–44. doi: 10.1111/j.1474-9726.2012.00792.x
21. Mateos-Aparicio P, Rodriguez-Moreno A. The impact of studying brain plasticity. *Front Cell Neurosci.* (2019) 13:66. doi: 10.3389/fncel.2019.00066
22. Landfield PW, Cadwallader-Neal L. Long-term treatment with calcitriol (1,25(OH)2 vit D3) retards a biomarker of hippocampal aging in rats. *Neurobiol Aging.* (1998) 19:469–77. doi: 10.1016/S0197-4580(98)00079-7
23. Foster TC, Norris CM. Age-associated changes in Ca(2+)-dependent processes: relation to hippocampal synaptic plasticity. *Hippocampus.* (1997) 7:60–12. doi: 10.1002/(SICI)1098-1063(1997)7:6<602::AID-HIPO3>3.0.CO;2-G
24. Gallagher M, Rapp PR. The use of animal models to study the effects of aging on cognition. *Ann Rev Psychol.* (1997) 48:339–70. doi: 10.1146/annurev.psych.48.1.339
25. Morrison JH, Baxter MG. The ageing cortical synapse: hallmarks and implications for cognitive decline. *Nat Rev Neurosci.* (2012) 13:240–50. doi: 10.1038/nrn3200

26. Taffe MA, Weed MR, Gutierrez T, Davis SA. Gold, LH. Differential muscarinic and NMDA contributions to visuo-spatial paired-associate learning in rhesus monkeys. *Psychopharmacol (Berl).* (2002) 160:253–62. doi: 10.1007/s00213-001-0954-5
27. Algarabel S, Fuentes M, Escudero J, Pitarque A, Peset V, Mazon J-F, et al. Recognition memory deficits in mild cognitive impairment. *Aging Neuropsychol Cogn*. (2012) 19:608–19. doi: 10.1080/13825585.2011.640657
28. Nakazawa T, Komai S, Watabe AM, Kiyama Y., Fukaya M., Arima-Yoshida F, et al. NR2B tyrosine phosphorylation modulates fear learning as well as amygdaloid synaptic plasticity. *EMBO J*. (2006) 25:2867–77. doi: 10.1038/sj.emboj.7601156
29. Gardoni F, Mauceri D, Malinverno M, Polli F, Costa C, Tozzi A et al. Decreased NR2B subunit synaptic levels cause impaired long-term potentiation but not long-term depression. *J Neurosci*. (2009) 29:669–77. doi: 10.1523/JNEUROSCI.3921-08.2009
30. Tang YP, Shimizu E, Dube GR, Rampon C, Kerchner GA, Zhuo M, et al. Genetic enhancement of learning and memory in mice. *Nature*. (1999) 401:63–9. doi: 10.1038/43432
31. Hawasli AH, Benavides DR, Nguyen C, Kansy JW, Hayashi K, Chambon P, et al. Cyclin-dependent kinase 5 governs learning and synaptic plasticity via control of NMDAR degradation. *Nat Neurosci*. (2007) 10:880–6. doi: 10.1038/nn1914
32. Traynelis SF, Wollmuth LP, McBain CJ, Menniti FS, Vance KM, Ogden KK, et al. Glutamate receptor ion channels: structure, regulation, and function. *Pharmacol Rev*. (2010) 62:405–96. doi: 10.1124/pr.109.002451
33. Clayton DA, Mesches MH, Alvarez A, Bickford PC, Browning MD. A hippocampal NR2B deficit can mimic age-related changes in long-term potentiation and spatial learning in the Fischer-344 rat. *J Neurosci*. (2002) 22:3628–37. doi: 10.1523/JNEUROSCI.22-09-03628.2002
34. Vyklicky V, Korinek M, Smejkalova T, Balik A, Krausova B, Kaniakova M, et al. Structure, function and pharmacology of NMDA receptor channels. *Physiol Res*. (2014) 63:S191–203. doi: 10.33549/physiolres.932678
35. Paoletti, P. Molecular basis of NMDA receptor functional diversity. *Eur J Neurosci*. (2011) 33:1351–65. doi: 10.1111/j.1460-9568.2011.07628.x
36. Johnson JW, Ascher P. Glycine potentiates the NMDA response in cultured mouse brain neurons. *Nature*. (1987) 325:529–31. doi: 10.1038/325529a0
37. Kleckner NW, Dingledine R. Requirement for glycine in activation of NMDA receptors expressed in Xenopus oocytes. *Science.* (1988) 241:835–7. doi: 10.1126/science.2841759
38. Papouin T, Ladpeche L, Ruel J, Sacchi S, Labasque M, Hanini M, et al. Synaptic and extrasynaptic NMDA receptors are gated by different endogenous coagonists. *Cell.* (2012) 150:633–46. doi: 10.1016/j.cell.2012.06.029
39. Shleper M, Kartvelishvily E, Wolosker H. D-serine is the dominant endogenous coagonist for NMDA receptor neurotoxicity in organotypic hippocampal slices. *J Neurosci.* (2005) 25:9413–7. doi: 10.1523/JNEUROSCI.3190-05.2005
40. Matsui T, Sekiguchi M, Hashimoto A, Tomita U, Nishikawa T, Wada K. Functional comparison of D-serine and glycine in rodents: the effect on cloned NMDA receptors and the extracellular concentration. *J Neurochem*. (1995) 65:454–8. doi: 10.1046/j.1471-4159.1995.65010454.x
41. Schell MJ, Brady RO, Molliver ME, Snyder SH. D-serine as a neuromodulator: regional and developmental localizations in rat brain glia resemble NMDA receptors. *J Neurosci*. (1997) 17:1604–15. doi: 10.1523/JNEUROSCI.17-05-01604.1997
42. Martineau M, Baux G, Mothet JP. D-serine signalling in the brain: friend and foe. *Trends Neurosci*. (2006) 29: 481–91. doi: 10.1016/j.tins.2006.06.008
43. Wolosker H. D-serine regulation of NMDA receptor activity. *Sciences STKE*. (2006) 2006:pe41. doi: 10.1126/stke.3562006pe41
44. Wolosker H. The neurobiology of D-serine signaling. *Adv Pharmacol.* (2018) 82:325–48. doi: 10.1016/bs.apha.2017.08.010
45. Hashimoto A, Nishikawa T, Oka T, Takahashi K, Hayashi T. Determination of free amino acid enantiomers in rat brain and serum by high-performance liquid chromatography after derivatization with N-tert-butyloxycarbonyl-L-cysteine and ophthaldialdehyde. *J Chromatogr.* (1992) 582:41–8. doi: 10.1016/0378-4347(92)80300-F
46. Hashimoto A, Kumashiro S, Nishikawa T, Oka T, Takahashi K, Miko T, et al. Embryonic development and postnatal changes in free D-aspartate and D-serine in the human prefrontal cortex. *J Neurochem*. (1993) 61:348–51. doi: 10.1111/j.1471-4159.1993.tb03575.x
47. Corrigan JJ. D-amino acids in animals. *Science*. (1969) 164:142. doi: 10.1126/science.164.3876.142
48. Wolosker H, Blackshaw S, Snyder SH. Serine racemase: a glial enzyme synthesizing D-serine to regulate glutamate-N-methyl-D-aspartate neurotransmission. *Proc Natl Acad Sci USA*. (1999) 96:13409–14. doi: 10.1073/pnas.96.23.13409
49. Henneberger C, Papouin T, Oliet SHR, Rusakov DA. Long-term potentiation depends on release of D-serine from astrocytes. *Nature*. (2010) 463:232–6. doi: 10.1038/nature08673
50. Panatier A, Theodosis DT, Mothet JP, Touquet B, Pollegioni L, Poulain DA, et al. Glia-derived D-serine controls NMDA receptor activity and synaptic memory. *Cell*. (2006) 125:775–84. doi: 10.1016/j.cell.2006.02.051
51. Wolosker H, Sheth KN, Takahashi M, Mothet JP, Brady RO, Ferris CD, et al. Purification of serine racemase: biosynthesis of the neuromodulator D-serine. *Proc Natl Acad Sci USA*. (1999) 96:721–5. doi: 10.1073/pnas.96.2.721
52. Wolosker H, Balu DT, Coyle JT. The rise and fall of the D-serine-mediated gliotransmission hypothesis. *Trends Neurosci.* (2016) 39:712–21. doi: 10.1016/j.tins.2016.09.007
53. Papouin T, Henneberger C, Rusakov DA, Oliet SHR. Astroglial versus neuronal D-serine: fact checking. *Trends Neurosci*. (2017) 40:517–520. doi: 10.1016/j.tins.2017.05.007
54. Van Horn MR, Sild M, Ruthazer ES. D-serine as a gliotransmitter and its roles in brain development and disease. *Front Cell Neurosci*. (2013) 7:39. doi: 10.3389/fncel.2013.00039
55. Wolosker H, Balu DT. D-serine as the gatekeeper of NMDA receptor activity: implications for the pharmacologic management of anxiety disorders. *Transl Psychiatry*. (2020) 9;10:184. doi: 10.1038/s41398-020-00870-x
56. Perez EJ, Tapanes SA, Loris ZB, Balu DT, Sick TJ, Coyle JT, et al. Enhanced astrocytic d-serine underlies synaptic damage after traumatic brain injury. *J Clin Invest*. (2017) 127:3114–25. doi: 10.1172/JCI92300
57. Labrie V, Wong AH, Roder JC. Contributions of the D-serine pathway to schizophrenia. *Neuropsychopharmacology*. (2012) 62:1484–503. doi: 10.1016/j.neuropharm.2011.01.030
58. Wong JM, Folorunso OO, Barragan EV, Berciu C, Harvey TL, Coyle JT, et al. Postsynaptic serine racemase regulates NMDA receptor function. *J Neurosci.* (2020) 40:9564–75. doi: 10.1523/JNEUROSCI.1525-20.2020
59. Verrall L, Burnet PW, Betts JF, Harrison PJ. The neurobiology of D-amino acid oxidase and its involvement in schizophrenia. *Mol Psychiatry*. (2010) 15:122–37. doi: 10.1038/mp.2009.99
60. Horio M, Kohno M, Fujita Y, Ishima T, Inoue R, Mori H, et al. Levels of D-serine in the brain and peripheral organs of serine racemase (Srr) knock-out mice. *Neurochem Int*. (2011) 59:853–59. doi: 10.1016/j.neuint.2011.08.017
61. Mac Kay MB, Kravtsenyuk M, Thomas R, Mitchell N, Dursun SM, Baker GB. D-Serine: Potential therapeutic agent and/or biomarker in schizophrenia and depression? *Front Psychiatry*. (2019) 10:25. doi: 10.3389/fpsyt.2019.00025
62. Junjaud G, Rouaud E, Turpin F, Mothet JP, Billard JM. Age-related effects of the neuromodulator D-serine on neurotransmission and synaptic potentiation in the CA1 hippocampal area of the rat. *J Neurochem*. (2006) 98:1159–66. doi: 10.1111/j.1471-4159.2006.03944.x
63. Diniz LP, Almeida JC, Tortelli V, Vargas Lopes C, Setti- Perdigao P, Stipursky J, et al. Astrocyte-induced synaptogenesis is mediated by transforming growth factor β signaling through modulation of D-serine levels in cerebral cortex neurons. *J Biol Chem*. (2012) 287:41432–45. doi: 10.1074/jbc.M112.380824
64. Beltran-Castillo S, Olivares MJ, Contreras RA, Zuniga G, Llona I, von Bernhardi R, et al. D-serine released by astrocytes in brainstem regulates breathing response to CO_2 levels. *Nat Communic*. (2017) 8:838. doi: 10.1038/s41467-017-00960-3
65. Martineau M, Parpura V, Mothet JP. Cell-type specific mechanisms of D-serine uptake and release in the brain. *Front Synaptic Neurosci.* (2014) 6:12. doi: 10.3389/fnsyn.2014.00012
66. Wolosker H, Dumin E, Balan L, Foltyn VN. D-amino acids in the brain: D-serine neurotransmission and neurodegeneration. *FEBS J*. (2008) 275:3514–26. doi: 10.1111/j.1742-4658.2008.06515.x
67. Steinmetz RD, Fava E, Nicotera P, Steinhilber D. A simple cell line based *in vitro* test system for N-methyl-D-aspartate (NMDA) receptor

ligands. *J Neurosci Methods*. (2002) 113:99–110. doi: 10.1016/S0165-0270(01)00482-4
68. Katsuki H, Watanabe Y, Fujimoto S, Kume T, Akaike A. Contribution of endogenous glycine and d-serine to excitotoxic and ischemic cell death in rat cerebrocortical slice cultures. *Life Sci*. (2007) 81:740–9. doi: 10.1016/j.lfs.2007.07.001
69. Coyle JT, Balu D, Wolosker H. D-serine, the shape-shifting NMDA receptor co-agonist. *Neurochem Res*. (2020) 45:1344–53. doi: 10.1007/s11064-020-03014-1
70. Hardingham GE, Bading H. Synaptic versus extrasynaptic NMDA receptor signalling: implications for neurodegenerative disorders. *Nat Rev Neurosci*. (2010) 11:682–96. doi: 10.1038/nrn2911
71. Parsons MP, Raymond LA. Extra-synaptic NMDA receptor involvement in central nervous system disorders. *Neuron*. (2014) 82:279–93. doi: 10.1016/j.neuron.2014.03.030
72. Ewald RC, Cline HT. "NMDA receptors and brain development". In: Van Dongen AM, editor. *Biology of the NMDA Receptor*. Boca Raton, FL: CRC Press/Taylor & Francis (2009).
73. Fuchs SA, Dorland L, de Sain-van der Velden MG, Hendriks M, Klomp LWJ, Berger R, et al. D-serine in the developing human central nervous system. *Ann Neurol*. (2006) 60:476–80. doi: 10.1002/ana.20977
74. Potier B, Turpin FR, Sinet PM, Rouaud E, Mothet JP, Videau C, et al. Contribution of the D-serine dependent pathway to the cellular mechanisms underlying cognitive aging. *Front Aging Neurosci*. (2010) *2*:1. doi: 10.3389/neuro.24.001.2010
75. Billard J-M. D-Serine in the aging hippocampus. *J Pharmaceut Biomed Anal*. (2015) 116:18–24. doi: 10.1016/j.jpba.2015.02.013
76. Alliot J, Boghossian S, Jourdan D, Veyrat-Durebex C, Pickering G, Meynial-Denis D, et al. The LOU/c/jall rat as an animal model of healthy aging? *J Gerontol A Biol Sci Med Sci*. (2002) 57:B312–20. doi: 10.1093/gerona/57.8.B312
77. Crook TH, Larrabee GJ, Youngjohn JR. Diagnosis and assessment of age-associated memory impairment. *Clin Neuropsychopharmacol*. (1990) 13:S81–91. doi: 10.1097/00002826-199013003-00009
78. Sobow T, Flirski M, Liberski PP. Amyloid-beta and tau proteins as biochemical markers of Alzheimer's disease. *Acta Neurobiol Express*. (2004) 64:53–70. doi: 10.2174/1567205052772704
79. Furcila D, Dominguez-Alvaro M, De Felipe J, Alonso-Nanclares L. Subregional density of neurons, neurofibrillary tangles and amyloid plaques in the hippocampus of patients with Alzheimer's disease. *Front Neuroanat*. (2019) 13:99. doi: 10.3389/fnana.2019.00099
80. Chen QS, Wei WZ, Shimahara T, Xie CW. Alzheimer amyloid beta-peptide inhibits the late phase of long-term potentiation through calcineurin-dependent mechanisms in the hippocampal dentate gyrus. *Neurobiol Learn Mem*. (2002) 77:354–71. doi: 10.1006/nlme.2001.4034
81. Glenner GG., Wong CW, Quaranta V, Eanes ED. The amyloid deposits in Alzheimers disease: their nature and pathogenesis. *App Pathol*. (1984) 2:357–69.
82. Holtzman DM, Morris JC, Goate AM. Alzheimer's Disease: The challenge of the second century. *Sci Transl Med*. (2011) 3:77sr1. doi: 10.1126/scitranslmed.3002369
83. Revett TJ, Baker GB, Jhamandas J, Kar S. Glutamate system, amyloid β peptides and tau protein: functional interrelationships and relevance to Alzheimer disease pathology. *J Psychiatry Neurosci*. (2013) 38:6–23. doi: 10.1503/jpn.110190
84. Hoey SE, Williams RJ, Perkinton MS. Synaptic NMDA receptor activation stimulates alpha-secretase amyloid precursor protein processing and inhibits amyloid-beta production. *J Neurosci*. (2009) 29:4442–60. doi: 10.1523/JNEUROSCI.6017-08.2009
85. Marcello E, Gardoni F, Mauceri D, Romorini S, Jeromin A, Epis R, et al. Synapse-associated protein-97 mediates alpha-secretase ADAM10 trafficking and promotes its activity. *J Neurosci*. (2007) 27:1682–91. doi: 10.1523/JNEUROSCI.3439-06.2007
86. Shankar GM, Bloodgood BL, Townsend M, Walsh DM, Selkoe DJ, Sabatini BL. Natural oligomers of the Alzheimer amyloid-beta protein induce reversible synapse loss by modulating an NMDA-type glutamate receptor-dependent signaling pathway. *J Neurosci*. (2007) 27:2866–75. doi: 10.1523/JNEUROSCI.4970-06.2007
87. Yamin G. NMDA receptor-dependent signaling pathways that underlie amyloid beta-protein disruption of LTP in the hippocampus. *J Neurosci Res*. (2009) 87:1729–36. doi: 10.1002/jnr.21998
88. Cisse M, Halabisky B, Harris J, Devidze N, Dubal DB, Binggui S, et al. Reversing EphB2 depletion rescues cognitive functions in Alzheimer model. *Nature*. (2011) 469:47–52. doi: 10.1038/nature09635
89. Kamenetz F, Tomita T, Hsieh H, Seabrook G, Borchelt D, Iwatsubo T, et al. APP processing and synaptic function. *Neuron*. (2003) 37:925–37. doi: 10.1016/S0896-6273(03)00124-7
90. Durakoglugil MS, Chen Y, White CL, Kavalali ET, Herz J. Reelin signaling antagonizes beta-amyloid at the synapse. *Proc Natl Acad Sci USA*. (2009) 106:15938–43. doi: 10.1073/pnas.0908176106
91. Poirier J, Davignon J, Bouthillier D, Kogan S, Bertrand P, Gauthier S, et al. Apolipoprotein E polymorphism and Alzheimers disease. *Lancet*. (1993) 342:697-9. doi: 10.1016/0140-6736(93)91705-Q
92. Chen Y, Durakoglugil MS, Xian X, Herz J. ApoE4 reduces glutamate receptor function and synaptic plasticity by selectively impairing ApoE receptor recycling. *Proc Natl Acad Sci USA*. (2010) 107:12011–16. doi: 10.1073/pnas.0914984107
93. Wu SZ, Bodles AM, Porter MM, Griffin WS, Basile AS, Barger SW. Induction of serine racemase expression and D-serine release from microglia by amyloid β-peptide. *J Neuroinflamm*. (2004) 1:2. doi: 10.1186/1742-2094-1-2
94. Talantova M, Sanz-Blasco S, Zhang X, Xia P, Akhtar MW, Okamoto S, et al. Aβ induces astrocytic glutamate release, extrasynaptic NMDA receptor activation, and synaptic loss. *Proc Natl Acad Sci USA*. (2013) 110:E2518–27. doi: 10.1073/pnas.1306832110
95. Rush T, Buisson A. Reciprocal disruption of neuronal signaling and Aβ production mediated by extrasynaptic NMDA receptors: a downward spiral. *Cell Tissue Res*. (2014) 356:279–86. doi: 10.1007/s00441-013-1789-1
96. Daniels BA, Baldridge WH. D-Serine enhancement of NMDA receptor-mediated calcium increases in rat retinal ganglion cells. *J Neurochem*. (2010) 112:1180–9. doi: 10.1111/j.1471-4159.2009.06532.x
97. Katsuki H, Nonaka M, Shirakawa H, Kume T, Akaike A. Endogenous D-serine is involved in induction of neuronal death by N-methyl-D-aspartate and simulated ischemia in rat cerebrocortical slices. *J Pharmacol Exp Ther*. (2004) 311:836–44. doi: 10.1124/jpet.104.070912
98. Zou C, Crux S, Marinesco S, Montagna E, Sgobio C, Shi Y, et al. Amyloid precursor protein maintains constitutive and adaptive plasticity of dendritic spines in adult brain by regulating D-serine homeostasis. *EMBO J*. (2016) 35:2213–22. doi: 10.15252/embj.201694085
99. Block ML, Zecca L, Hong JS. Microglia-mediated neurotoxicity: uncovering the molecular mechanisms. *Nat Rev Neurosci*. (2007) 8:57–69. doi: 10.1038/nrn2038
100. Magalhaes JP, Curado J, Church GM. Meta-analysis of age-related gene expression profiles identifies common signatures of aging. *Bioinformatics*. (2009) 25:875–81. doi: 10.1093/bioinformatics/btp073
101. Gao HM, Hong JS. Why neurodegenerative diseases are progressive: uncontrolled inflammation drives disease progression. *Trends Immunol*. (2008) 29:357–365. doi: 10.1016/j.it.2008.05.002
102. Lee CK, Weindruch R, Prolla TA. Gene-expression profile of the ageing brain in mice. *Nature Gen*. (2000) 25:294–7. doi: 10.1038/77046
103. Wu S, Barger S. Induction of serine racemase by inflammatory stimuli is dependent on AP-1. *Ann New York Acad Sci*. (2004) 1035:133–46. doi: 10.1196/annals.1332.009
104. Ye SM, Johnson RW. Increased interleukin-6 expression by microglia from brain of aged mice. *J Neuroimmun*. (1999) 93:139–48. doi: 10.1016/S0165-5728(98)00217-3
105. Droge W, Schipper HM. Oxidative stress and aberrant signaling in aging and cognitive decline. *Aging Cell*. (2007) 6:361–70. doi: 10.1111/j.1474-9726.2007.00294.x
106. Halliwell B. Reactive oxygen species and the central nervous system. *J Neurochem*. (1992) 59:1609–23. doi: 10.1111/j.1471-4159.1992.tb10990.x
107. Bernard CL, Hirsch JC, Khazipov R, Ben-Ari Y, Gozlan H. Redox modulation of synaptic responses and plasticity in rat CA1 hippocampal neurons. *Exp Brain Res*. (1997) 113:343–52. doi: 10.1007/BF02450332
108. Kamsler A, Segal M. Control of neuronal plasticity by reactive oxygen species. *Antiox Redox Signal*. (2007) 9:165–7. doi: 10.1089/ars.2007.9.165

109. Lin C-H, Yang H-T, Chiu C-C, Lane H-Y. Blood levels of D-amino acid oxidase vs. D-amino acids in reflecting cognitive aging. *Sci Rep.* (2017) 7:14849. doi: 10.1038/s41598-017-13951-7
110. Nagy LV, Bali ZK, Kapus G, Pelsoczi P, Farkas B, Lendvai B, et al. Converging evidence on D-amino acid oxidase-dependent enhancement of hippocampal firing activity and passive avoidance learning in rats. *Int J Neuropsychopharmacol.* (2021) 24:434–45. doi: 10.1093/ijnp/pyaa095
111. Chouinard ML, Gaitan D, Wood PL. Presence of the N-methyl-D-aspartate-associated glycine receptor agonist, D-serine, in human temporal cortex: comparison of normal, Parkinson, and Alzheimer tissues. *J Neurochem.* (1993) 61:1561–4. doi: 10.1111/j.1471-4159.1993.tb13657.x
112. Kumashiro S, Hashimoto A, Nishikawa T. Free D-serine in post-mortem brains and spinal cords of individuals with and without neuropsychiatric diseases. *Brain Res.* (1995) 681:117–25. doi: 10.1016/0006-8993(95)00307-C
113. Nagata Y, Borghi M, Fisher GH, D'Aniello A. Free D-serine concentration in normal and Alzheimer human brain. *Brain Res Bull.* (1995) 38:181–3. doi: 10.1016/0361-9230(95)00087-U
114. McKhann GM, Knopman DS, Chertkow H, Hyman BT, Jack CR, Kawas CH, et al. The diagnosis of dementia due to Alzheimer's disease: Recommendations from the National Institute on Aging-Alzheimer's Association workgroups on diagnostic guidelines for Alzheimer's disease. *Alzheimers Dement.* (2011) 7:263–9. doi: 10.1016/j.jalz.2011.03.005
115. Biemans EALM, Verhoeven-Duif NM, Gerrits J, Claassen JAHR, Kuiperij HB, Verbeek MM, et al. CSF d-serine concentrations are similar in Alzheimer's disease, other dementias, and elderly controls. *Neurobiol Aging.* (2016) 42:213–6. doi: 10.1016/j.neurobiolaging.2016.03.017
116. Nuzzo T, Miroballo M, Casamassa A, Mancini A, Gaetani L, Nistico R, et al. Cerebrospinal fluid and serum D-serine concentrations are unaltered across the whole clinical spectrum of Alzheimer's disease. *Biochim Biophys Acta Proteins Proteom.* (2020) 1868:140537. doi: 10.1016/j.bbapap.2020.140537
117. Lin CH. Yang, Y-T, Lane H-Y. D-glutamate, D-serine, and D-alanine differ in their roles in cognitive decline in patients with Alzheimer's disease or mild cognitive impairment. *Pharmcol, Biochem Behav.* (2019) 185:172760. doi: 10.1016/j.pbb.2019.172760
118. Kimura R, Tsujimara H, Tsuchiya M, Soga S, Ota N, Tanaka A, et al. Development of a cognitive function marker based on D-amino acid proportions using new chiral tandem LC-MS/MS systems. *Sci Rep*. (2020) 10:804. doi: 10.1038/s41598-020-57878-y
119. Piubelli L, Pollegioni L, Rabattoni V, Mauri M, Princiotta Cariddi L, Versino M, et al. Serum D-serine levels are altered in early phases of Alzheimer's disease: toward a precocious biomarker. *Transl Psychiatry.* (2021) 11:77. doi: 10.1038/s41398-021-01202-3
120. Hampel H, O'Bryant SE, Molinuevo JL, Zetterberg H, Masters CL, Lista S, et al. Blood-based biomarkers for Alzheimer's disease: mapping the road to the clinic. *Nat Rev Neurol.* (2018) 14:639–65. doi: 10.1038/s41582-018-0079-7
121. Tsai G, Yang P, Chung L-C, Lange N, Coyle JT. D-Serine added to antipsychotics for the treatment of schizophrenia. *Biol Psychiatry.* (1998) 44:1081–9. doi: 10.1016/S0006-3223(98)00279-0
122. Heresco-Levy U, Javitt DC, Ebstein R, Vass A, Lichtenberg P, Bar G, et al. D-Serine efficacy as add-on pharmacotherapy to risperidone and olanzapine for treatment-refractory schizophrenia. *Biol Psychiatry.* (2005) 57:577–85. doi: 10.1016/j.biopsych.2004.12.037
123. Lane H-Y, Lin C-H, Huang Y-J, Liao C-H, Chang Y-C, Tsai GE, et al. A randomized, double-blind, placebo-controlled comparison study of sarcosine (N-methylglycine) and D-serine add-on treatment for schizophrenia. *Int J Neuropsychopharmacol.* (2010) 13:451–60. doi: 10.1017/S1461145709990939
124. D'Souza DC, Radhakrishnan R, Perry E, Bhakta S, Singh NM, Yaadav R, et al. Feasibility, safety, and efficacy of the combination of D-serine and computerized cognitive retraining in schizophrenia: An international collaborative pilot study. *Neuropsychopharmacology*. (2013) 38:492–503. doi: 10.1038/npp.2012.208
125. Kantrowitz JT, Epstein ML, Beggel O, Rohrig S, Lehrfeld JM, Revheim N, et al. Neuropysiological mechanisms of cortical plasticity impairments in schizophrenia and modulation by the NMDA receptor agonist D-serine. *Brain.* (2016) 139:3281–95. doi: 10.1093/brain/aww262
126. Kantrowitz, JT, Epstein ML, Lee M, Lehrfeld N, Nolan KA, Shope C, et al. Improvement in mismatch negativity generation during D-serine treatment in schizophrenia: Correlation with symptoms. *Schizophrenia Res.* (2018) 191:70–79. doi: 10.1016/j.schres.2017.02.027
127. Alzheimer's Drug Discovery Foundation. *D-Serine. Cognitive Vitality.org.* (2017) p. 1–9.
128. Tsai GE, Yang P, Chung LC, Tsai IC, Tsai CW, Coyle JT. D-Serine added to clozapine for the treatment of schizophrenia. *Am J Psychiatry*. (1999). 156:1822–25.
129. Weiser M, Heresco-Levy U, Davidson M, Javitt DC, Werbeloff N, Gershon AA, et al. A multi-center, add-on randomized, controlled trial of low-dose D-serine for negative and cognitive symptoms of schizophrenia. *J Clin Psychiatry.* (2012) 73:e728–34. doi: 10.4088/JCP.11m07031
130. Kantrowitz JT, Malhotra AK, Cornblatt B, Silipo G, Balla A, Suckow RF, et al. High-dose D-serine in the treatment of schizophrenia. *Schizophrenia Res.* (2010) 121:125–30. doi: 10.1016/j.schres.2010.05.012
131. Ploux E, Freret T, Billard JM. D-serine in physiological and pathological brain aging. *Biochim Biophys Acta Proteins Proteom.* (2020) 1869:140542. doi: 10.1016/j.bbapap.2020.140542
132. Flood JF, Morley JE, Lanthorn TH. Effect on memory processing by D-cycloserine, an agonist of the NMDA/glycine receptor. *Eur J Pharmacol.* (1992) 221:249–54. doi: 10.1016/0014-2999(92)90709-D
133. Lin CH, Lane HY. The role of N-methyl-D-aspartate receptor neurotransmission and precision medicine in behavioral and psychological symptoms of dementia. *Front Pharmacol.* (2019) 10:540. doi: 10.3389/fphar.2019.00540
134. Mothet JP, Rouaud E, Sinet PM, Potier B, Jouvenceau A, Dutar P, et al. A critical role for the glial-derived neuromodulator D-serine in the age-related deficits of cellular mechanisms of learning and memory. *Aging Cell.* (2006) 5:267–74. doi: 10.1111/j.1474-9726.2006.00216.x
135. Nikseresht Z, Ahangar N, Badrikoohi M, Babaei P. Synergistic enhancing-memory effect of D-serine and RU360, a mitochondrial calcium uniporter blocker in rat model of Alzheimer's disease. *Behav Brain Res.* (2021) 409:113307. doi: 10.1016/j.bbr.2021.113307
136. Levin R, Dor-Abarbanel AE, Edelman S, Durrant AR, Hashimoto K, Javitt DC, et al. Behavioral and cognitive effects of the N-methyl-d-aspartate receptor co-agonist d-serine in healthy humans: Initial findings. *J Psychiatric Res.* (2015) 61:188–95. doi: 10.1016/j.jpsychires.2014.12.007
137. Adage T, Trillat AC, Quattropani A, Perrin D, Cavarec L, Shaw J. *In vitro* and *in vivo* pharmacological profile of AS057278, a selective d-amino acid oxidase inhibitor with potential anti-psychotic properties. *Eur Neuropsychopharmacol.* (2008) 18:200–14. doi: 10.1016/j.euroneuro.2007.06.006
138. Hashimoto A. Nishikawa T, Konno R, Niwa, A, Yasamura Y, Oka T, et al. Free D-serine, D-aspartate and D-alanine in central nervous system and serum in mutant mice lacking D-amino acid oxidase. *Neurosci Lett.* (1993) 152:33–6. doi: 10.1016/0304-3940(93)90476-2
139. Morikawa A, Hamase K, Inoue T, Konno R, Niwa A, Zaitsu K. Determination of free D-aspartic acid, D-serine and D-alanine in the brain of mutant mice lacking D-amino acid oxidase activity. *J Chromatogr B Biomed Sci Appl.* (2001) 757:119–25. doi: 10.1016/S0378-4347(01)00131-1
140. Labrie V, Duffy S, Wang W, Barger SW, Baker GB, Order JC. Genetic inactivation of D-amino acid oxidase enhances extinction and reversal learning in rats. *Learning Memory.* (2009) 16:28–37. doi: 10.1101/lm.1112209
141. Lane HY, Lin CH, Green MF, Hellemann G, Huang CC, Chen PW, et al. Add-on treatment of benzoate for schizophrenia: a randomized, double-blind, placebo-controlled trial of D-amino acid oxidase inhibitor. *JAMA Psychiatry.* (2013) 70:1267–75. doi: 10.1001/jamapsychiatry.2013.2159
142. Modi KK, Roy A, Brahmachari S, Rangasamy SB, Pahan K. Cinnamon and its metabolite sodium benzoate attenuate the activation of p21rac and protect memory and learning in an animal model of Alzheimer's disease. *PLoS ONE.* (2015) 10:e0130398. doi: 10.1371/journal.pone.0130398
143. Lin C-H, Chen P-K, Wang S-H, Lane H-Y. Effect of sodium benzoate on cognitive function among patients with behavioral and psychological symptoms of dementia. *JAMA Network Open.* (2021) 4:e216156. doi: 10.1001/jamanetworkopen.2021.6156
144. Chen W-L, Niu Y-Y, Jiang W-Z, Tang H-L, Zhang C, Xia Q, et al. Neuroprotective effects of hydrogen sulfide and the underlying signaling

pathways. *Rev Neurosci.* (2015) 26:129–42. doi: 10.1515/revneuro-2014-0051
145. Murtas G, Sacchi S, Valentino M, Pollegioni L. Biochemical properties of human D-amino acid oxidase. *Front Mol Biosci.* (2017) 4:88. doi: 10.3389/fmolb.2017.00088
146. Panizzutti R, De Miranda J, Ribeiro CS, Engelender S, Wolosker H, et al. A new strategy to decrease N-methyl-D-aspartate (NMDA) receptor coactivation: Inhibiiton of D-serine synthesis by converting serine racemase into an eliminase. *Proc Natl Acad Sci USA*. (2001) 98:5295–99. doi: 10.1073/pnas.091002298
147. Palsson E, Jakobsson J, Sodersten K, Fujita Y, Sellgren C, Ekman C-J, et al. Markers of glutamate signaling in cerebrospinal fluid and serum from patients with bipolar disorder and healthy controls. *Eur Neuropsychopharmacol.* (2015) 25:133–40. doi: 10.1016/j.euroneuro.2014.11.001
148. Cho, S-E, Na K-S, Cho S-J, Kang SG. Low D-serine levels in schizophrenia: A systematic review and meta-analysis. *Neurosci Lett*. (2016) 634:42–51. doi: 10.1016/j.neulet.2016.10.006
149. Ganote CE, Peterson DR, Carone FA. The nature of D-serine-induced nephrotoxicity. *Am J Pathol*. (1974) 77:269–82.
150. Maekawa M, Okamura T, Kasai N, Hori Y, Summer KH, Konno R. D-amino-acid oxidase is involved in D-serine-induced nephrotoxicity. *Chem Res Toxicol.* (2005) 18:1678–82. doi: 10.1021/tx0500326
151. Labrie V, Roder J. The involvement of the NMDA receptor D-serine/glycine site in the pathophysiology and treatment of schizophrenia. *Neurosi Biobehav Rev*. (2010) 34:351–72. doi: 10.1016/j.neubiorev.2009.08.002
152. Meftah A, Hasegawa H, Kantrowitz J. D-Serine: A cross species review of safety. *Front Psychiatry*. (2021) 12:726365. doi: 10.3389/fpsyt.2021.726365
153. Williams RE, Lock EA. Sodium benzoate attenuates D-serine induced nephrotoxicity in the rat. *Toxicology*. (2005) 207:35–48. doi: 10.1016/j.tox.2004.08.008
154. Hashimoto K, Fujita Y, Horio M, Kunitachi S, Iyo M, Ferraris D, et al. Co-administration of a D-amino acid oxidase inhibitor potentiates the efficacy of D-serine in attenuating prepulse inhibition deficits after administration of dizocilpine. *Biol Psychiat*. (2009) 65:1103–6. doi: 10.1016/j.biopsych.2009.01.002
155. Capitao LP, Forsyth J, Thomaidou MA, Condon MD, Harmer CJ, Burnet PWJ, et al. single administration of 'microbial' D-alanine to healthy volunteers augments reaction to negative emotions: A comparison with D-serine. *J Psychopharmacol.* (2020) 5:557–66. doi: 10.1177/0269881120908904
156. Chang C-H, Kuo H-L, Ma W-F, Tsai H-C. Cerebrospinal fluid and serum D-serine levels in patients with Alzheimer's disease: A systematic review and meta-analysis. *J Clin Med.* (2020) 9:3840. doi: 10.3390/jcm9123840
157. Cuomo M, Keller S, Punzo D, Nuzzo T, Affinito O, Coretti L, et al. Selective demethylation of two CpG sites causes postnatal activation of the Dao gene and consequent removal of D-serine within the mouse cerebellum. *Clin Epigenetics.* (2019) 11:49. doi: 10.1186/s13148-019-0732-z
158. Le Douce J, Maugard M, Veran J, Matos M, Jego P, Vigneron PA, et al. Impairment of glycolysis-derived L-Serine production in astrocytes contributes to cognitive deficits in Alzheimers Disease. *Cell Metab.* (2020) 31:503–17. doi: 10.1016/j.cmet.2020.02.004
159. Zarate CA Jr, Niciu MJ. Ketamine for depression: evidence, challenges and promise. *World Psychiatry.* (2015) 14:348–50. doi: 10.1002/wps.20269
160. Durrant AR, Heresco-Levy U. D-Serine in neuropsychiatric disorders: New advances. *Adv Psychiatry*. (2014) 2014:859735. doi: 10.1155/2014/859735
161. Chen Z, Tang Z, Zou K, Huang Z, Liu L, Yang Y-J, et al. D-serine has antidepressant effects in mice through suppression of the BDNF signaling pathway and regulation of synaptic plasticity in the nucleus accumbens. *Authorea*. (2021). doi: 10.22541/au.161684855.51774092/v1
162. Zoicas I, Kornhuber J. The role of the N-methyl-D-aspartate receptors in social behavior in rodents. *Int J Mol Sci*. (2019). 20:5599. doi: 10.3390/ijms20225599
163. McAllister KH. D-cycloserine enhances social behaviour in individually-housed mice in the resident-intruder test. *Psychoapharmacology*. (1994) 116:317–25. doi: 10.1007/BF02245335
164. Deutsch SI, Burket JA, Jacome LF, Cannon WR, Herndon AL. d-Cycloserine improves the impaired sociability of of the Balb/c mouse. *Brain Res Bull.* (2011) 84:8–11. doi: 10.1016/j.brainresbull.2010.10.006
165. Jacome LF, Burket JA, Herndon AL, Deutsch SI. D-Cycloserine enhances social exploration in the Balb/c mouse. *Brain Res Bull.* (2011) 85:141–4. doi: 10.1016/j.brainresbull.2011.03.004
166. Deutsch SI, Pepe GJ, Burket JA, Winebarger EE, Herndon AL, Benson AD. d-Cycloserine improves sociability and spontaneouns sterotypic behaviors in 4-week old mice. *Brain Res.* (2012) 1439:96–107. doi: 10.1016/j.brainres.2011.12.040
167. Benson AD, Burket JA, Deutsch SI. Balc/c mice treated with d-cycloserine arouse increased social interest in conspecifics. *Brain Res Bull.* (2013) 99:95–9. doi: 10.1016/j.brainresbull.2013.10.006
168. Nagai T, Yu J, Kitahara Y, Nabeshima T, Yamada K. D-Serine ameliorates neonatal polyI:C treatment-induced emotional and cognitive impairments in adult mice. *J Pharmacol Sci.* (2012) 120:213. doi: 10.1254/jphs.12142FP
169. Tomita J, Ueno T, Mitsuyoshi M, Kume S, Kume K. The NMDA receptor promotes sleep in the fruit fly, *Drosophila melanogaster. PloS ONE.* (2015) 10:e0128101. doi: 10.1371/journal.pone.0128101
170. Liu S, Liu Q, Tabuchi M, Wu MN. Sleep drive is encoded by neural plastic changes in a dedicated circuit. *Cell.* (2016) 165:1347–60. doi: 10.1016/j.cell.2016.04.013
171. Papouin T, Dunphy JM, Tolman M, Dineley KT, Haydon PG. Septal cholinergic neuromodulation tunes the astrocyte-dependent gating of hippocampal NMDA receptors to wakefulness. *Neuron.* (2017) 94:840–54. doi: 10.1016/j.neuron.2017.04.021
172. Cirelli, C. The genetic and molecular regulation of sleep: from fruit flies to humans. *Nat Rev Neurosci*. (2009) 10:549–60. doi: 10.1038/nrn2683
173. Dai X, Zhou E, Yang W, Zhang Z, Zhang W, Rao Y. D-Serine made by serine racemase in *Drosophila* instestine plays a physiological role in sleep. *Nature Commun*. (2019) 10:1986. doi: 10.1038/s41467-019-09544-9

Conflict of Interest: GB is an advisor to NeuraWell Therapeutics. The company had no involvement with this review.

The remaining authors declare that the research was conducted in the absence of any commercial or financial relationships that could be construed as a potential conflict of interest.

Publisher's Note: All claims expressed in this article are solely those of the authors and do not necessarily represent those of their affiliated organizations, or those of the publisher, the editors and the reviewers. Any product that may be evaluated in this article, or claim that may be made by its manufacturer, is not guaranteed or endorsed by the publisher.

frontiers in Psychiatry

ORIGINAL RESEARCH
published: 25 November 2021
doi: 10.3389/fpsyt.2021.750106

Cre-Activation in ErbB4-Positive Neurons of Floxed *Grin1*/NMDA Receptor Mice Is Not Associated With Major Behavioral Impairment

Anne S. Mallien[1], *Natascha Pfeiffer*[1], *Miriam A. Vogt*[2], *Sabine Chourbaji*[2], *Rolf Sprengel*[3,4†], *Peter Gass*[1*†] *and Dragos Inta*[1,5†]

[1] *Department of Psychiatry and Psychotherapy, Medical Faculty Mannheim, RG Animal Models in Psychiatry, Central Institute of Mental Health, Heidelberg University, Mannheim, Germany,* [2] *Interfaculty Biomedical Research Facility (IBF), Heidelberg University, Heidelberg, Germany,* [3] *Research Group of the Max Planck Institute for Medical Research at the Institute for Anatomy and Cell Biology, Heidelberg University, Heidelberg, Germany,* [4] *Interdisciplinary Center for Neurosciences (IZN), Heidelberg University, Heidelberg, Germany,* [5] *Department of Psychiatry (UPK), University of Basel, Basel, Switzerland*

OPEN ACCESS

Edited by:
Nevena V. Radonjic, Upstate Medical University, United States

Reviewed by:
Guillermo Gonzalez-Burgos, University of Pittsburgh, United States
Rose Chesworth, Western Sydney University, Australia

***Correspondence:**
Peter Gass
Peter.Gass@zi-mannheim.de

†These authors have contributed equally to this work

Specialty section:
This article was submitted to Molecular Psychiatry, a section of the journal Frontiers in Psychiatry

Received: *30 July 2021*
Accepted: *27 October 2021*
Published: *25 November 2021*

Citation:
Mallien AS, Pfeiffer N, Vogt MA, Chourbaji S, Sprengel R, Gass P and Inta D (2021) Cre-Activation in ErbB4-Positive Neurons of Floxed Grin1/NMDA Receptor Mice Is Not Associated With Major Behavioral Impairment. Front. Psychiatry 12:750106. doi: 10.3389/fpsyt.2021.750106

Extensive evidence suggests a dysfunction of the glutamate NMDA receptor (NMDAR) in schizophrenia, a severe psychiatric disorder with putative early neurodevelopmental origins, but clinical onset mainly during late adolescence. On the other hand, pharmacological models using NMDAR antagonists and the clinical manifestation of anti-NMDAR encephalitis indicate that NMDAR blockade/hypofunction can trigger psychosis also at adult stages, without any early developmental dysfunction. Previous genetic models of NMDAR hypofunction restricted to parvalbumin-positive interneurons indicate the necessity of an early postnatal impairment to trigger schizophrenia-like abnormalities, whereas the cellular substrates of NMDAR-mediated psychosis at adolescent/adult stages are unknown. Neuregulin 1 (NRG1) and its receptor ErbB4 represent schizophrenia-associated susceptibility factors that closely interact with NMDAR. To determine the neuronal populations implicated in "late" NMDAR-driven psychosis, we analyzed the effect of the inducible ablation of NMDARs in *ErbB4*-expressing cells in mice during late adolescence using a pharmacogenetic approach. Interestingly, the tamoxifen-inducible NMDAR deletion during this late developmental stage did not induce behavioral alterations resembling depression, schizophrenia or anxiety. Our data indicate that post-adolescent NMDAR deletion, even in a wider cell population than parvalbumin-positive interneurons, is also not sufficient to generate behavioral abnormalities resembling psychiatric disorders. Other neuronal substrates that have to be revealed by future studies, may underlie post-adolescent NMDAR-driven psychosis.

Keywords: glutamate, neurodevelopment, pharmacogenetic, neuregulin-1, schizophrenia, NMDA receptor, post-adolescent

INTRODUCTION

Despite intense research, the molecular and cellular mechanisms of psychotic disorders, like schizophrenia and anti-NMDA receptor (NMDAR) encephalitis that emerge often during post-adolescence/young adulthood, are only partly understood. Glutamate is the main excitatory neurotransmitter in the mammalian brain. NMDAR represent one of the ligand-gated non-selective ionotropic glutamate receptors, which are widely present throughout the brain, in high density within the hippocampus and the cerebral cortex (1). NMDAR are preferentially expressed in excitatory neurons that represent about 70% of the neurons containing NMDAR (1). Nevertheless, GABAergic interneurons express as well NMDAR, numerous onto parvalbumin (PV)-positive interneurons that show a particularly strong glutamatergic input (2). Extensive evidence implicates dysfunction of the glutamate NMDAR in the emergence of psychotic symptoms (3). The glutamate hypothesis of schizophrenia is the most influential alternative explanatory model of schizophrenia, postulating hypofunction of NMDAR as pathophysiological mechanism (4). It emerged from observations that NMDAR antagonists (phencyclidine/PCP, ketamine, MK-801) mimic better than any other psychotomimetic drug the whole spectrum of psychotic symptoms, i.e., not only positive, but also negative symptoms and cognitive deficits (5). Several studies reported NMDAR abnormalities in schizophrenia, showing reduced NMDAR expression in post-mortem brain tissue in schizophrenia (6, 7), diminished expression of NMDAR/associated proteins in induced pluripotent stem cell-derived (iPSC) neurons in schizophrenia (8), and increased cerebrospinal fluid and post-stress levels of kynurenic acid, an endogenous NMDAR antagonist in schizophrenia (9). In addition, proteins structurally and functionally closely linked to NMDAR, like NRG1 display strong positive genetic association with schizophrenia (10), whereas abnormal cortical oscillations triggered by NMDAR dysfunction (11) represent an electrophysiological endophenotype of schizophrenia (12). Moreover, subjects suffering from anti-NMDAR encephalitis show an initial psychotic phase often indistinguishable from schizophrenia; therefore, an estimated 77% of cases with anti-NMDAR encephalitis is initially misdiagnosed as schizophrenia (13). Patients with anti-NMDAR encephalitis produce anti-GluN1 autoantibodies that reduce surface NMDAR clusters and protein in a titer-dependent fashion in rodents and humans *in vitro* and *in vivo* (14). Interestingly, the clinical manifestation of anti-NMDAR encephalitis shows age-dependent variations: autistic-like features during childhood (15), psychosis during young adulthood and less severe symptoms with predominant cognitive deficits in older patients (16). Moreover, the susceptibility to the psychotomimetic effects of NMDAR antagonists is minimal or absent in children and becomes maximal in early adulthood (17). In fact, the NMDR hypofunction hypothesis of schizophrenia is relying on initial clinical observations in adults. Although some rodent studies report protracted schizophrenia-like abnormalities following perinatal treatment with NMDAR antagonists (18), it appears clear that NMDAR hypofunction at young adult stages, without any previous developmental impairment, can induce as well abnormalities resembling psychosis. Animal models represent a useful experimental tool to clarify the role of abnormal NMDAR in psychosis-like abnormalities. Mice with reduced NMDAR expression (GluN1/*Grin1* knockdown, KD) that express 5–10% of the normal NMDAR levels, are viable and display schizophrenia-like abnormalities (19). However, this global NMDAR KD model does not allow the identification of the neuronal populations implicated in psychosis. Meanwhile conditional genetic models provide insights into these cell-specific mechanisms. Numerous data suggest that GABAergic interneurons play a central role in schizophrenia showing abnormal distribution and loss of subpopulations of GABAergic interneurons (20). Most studies focus on NMDAR hypofunction in fast-spiking PV-positive GABAergic interneurons that play a key role in generating cortical oscillatory activity (21). Abnormal synchronization of gamma-band activity may underlie cognitive deficits in schizophrenia (22).

However, mice with conditional ablation of NMDAR in PV-positive interneurons show largely normal behaviors (no hyperlocomotion and sensorimotor gating deficits as correlates of positive symptoms of schizophrenia), except for selective cognitive impairments (23, 24). Cre-driven recombination in these mice was detected in the somatosensory cortex and hippocampus at postnatal day 13 (P13) with about 80% recombination at 29 days (P29) (24). On contrary, mice with conditional ablation of NMDAR under the control of the Ppp1r2 (protein phosphatase 1, regulatory subunit 2) gene promoter, targeting mostly (about 75%), but not exclusively PV-positive interneurons, displayed schizophrenia-like abnormalities (25). Interestingly, these abnormalities were observed only in the mouse line in which Cre-driven recombination started at early postnatal stages, with NMDR expression absent in 40–50% of cortical and hippocampal interneurons in P28 mutant mice, but not in mice were recombination started at young adult stages (P56) (25). Therefore, NMDAR deficiency in PV-positive interneurons appears not sufficient to induce all psychosis-like features and if yes, only when occurring already at early postnatal stages and most likely, also in other neurons. However, the cellular substrates of NMDAR-driven psychosis at post-adolescent/young adult stages remain unknown, these results suggesting that a different neuronal population, larger than PV-positive interneurons may be implicated. In sum, there is a discrepancy between the currently available genetic models of NMDAR dysfunction, showing psychosis-like changes only when deleted at early postnatal stages, and pharmacological/clinical data, indicating that NMDAR blockade also/rather at later/even adult stages can induce psychosis. We hypothesized that if NMDAR deletion in PV-positive is insufficient to trigger psychosis-like changes during adulthood, extension to the larger population of ErbB4-positive cells may lead to such phenotype.

The schizophrenia-associated susceptibility factors that interact closely with NMDARs like neuregulin 1 (NRG1) and its receptor ErbB4, both main genetic risk factors associated with

schizophrenia (26). Altered NRG1/ErbB4 signaling has been shown to contribute to NMDAR hypofunction in patients with schizophrenia (27) and mice with NRG1 deletion have 16% fewer functional NMDAR than wild-type mice, whereas if a similar change occurs also in ErbB4 KO mice was not determined (26). The expression pattern of ErbB4 is highly conserved during evolution from rodents to humans (28). ErbB4 mRNA is widely expressed throughout the adult brain, however, it is restricted in cortical regions to PV-positive interneurons (28). Considerable expression occurs in the subventricular zone (SVZ) and along the rostral migratory stream, as well as in other interneuronal clusters generated in the SVZ and potentially implicated in the pathophysiology of schizophrenia, forming the Islands of Calleja (ICj) (29, 30). Moreover, in the midbrain, ErbB4 mRNA expression is prominent in dopaminergic neurons in the substantia nigra pars compacta and adjacent ventral tegmental area (29). Further forebrain areas with ErbB4 expression are the septum, bed nucleus of stria terminalis, medial preoptic nucleus, suprachiasmatic nucleus, nucleus of the lateral olfactory tract, subthalamic nucleus, zona incerta, hypothalamus, pre- and supramammillary nuclei, the central gray, anterior pretectal nucleus and superior colliculus (29). In contrast, expression is minimal or absent in most areas of the thalamus, excepting the reticular nucleus and habenula (29).

We sought in the present study to delineate the specific contribution of NMDA receptors located on ErbB4-expressing neurons in the post-adolescent brain to abnormalities relevant for neuropsychiatric disorders by avoiding deleterious effects on early cortical circuitry by ablation of the obligatory GluN1 (formerly NR1) subunit of the NMDAR. The aim of our study is to identify the cellular substrates of psychosis induced by NMDAR hypofunction at post-adolescent stages, and not of schizophrenia in general (as a disease with most likely early neurodevelopmental impairment). We do not aim to find the cause of schizophrenia, but to determine if restricted ablation of NMDAR in a relevant cell population is associated with psychosis-like changes.

We employed the Cre/loxP recombination system and tamoxifen-controlled gene manipulation (31) for time- and cell type specific depletion of NMDARs during late adolescence in ErbB4-expressing neurons. Due to fast genetic inactivation of the functional *Grin1* mRNA expression within two weeks, the NMDAR signaling can be affected specifically in mature mice, avoiding any interference with earlier developmental brain circuitry formation. For the Tamoxifen-induced genetic NMDAR ablation we selected in mice the "late" developmental stage that corresponds to transition from adolescence to adulthood, which is the most frequent time of onset of both schizophrenia and anti-NMDAR encephalitis.

MATERIALS AND METHODS

Mouse Lines Used in This Study

Mouse lines used in this study are available from the mouse repositories of the Jackson laboratories or the EMMA infrafrontier (*B6.129-Grin1*^{tm2Rsp}/kctt, EM:09220; B6. *Cg*$^{Erbb4tm1.1(cre/ERT2)Aibs/J}$, Stock: 012360; B6.Cg-*Gt(ROSA)26Sor*$^{tm14(CAG-tdTomato)Hze}$ Stock 007914).

Generation of *Grin1*$^{\Delta Erb}$ Mice and Induction of Cre-Mediated Recombination

To achieve NMDAR ablation specifically in most interneurons, we crossed the well-established *Grin1*$^{f/f}$ line (32–34) with the tamoxifen inducible *ErbB4-CreERT2*-driver line (35). Mice harboring one copy of the *ErbB4-CreERT2 gene* and two copies of the *Grin1*^{2lox} (*Grin1*$^{f/f}$) allele were used as cell-specific knockouts (herein called *Grin1*$^{f/f}$ / *ErbB4-CreERT2*). Littermates without the *ErbB4-CreERT2* gene and only haploid or diploid the floxed *Grin1* allele (*Grin1*$^{f/+}$ or *Grin1*$^{f/lf}$) were used as controls (called hereafter *Grin1*^{2lox} or controls). We proved, the tamoxifen-induced interneuronal Cre activity by using tdTomato Cre reporter mice B6.Cg-*Gt(ROSA)26Sor*$^{tm14(CAG-tdTomato)Hze}$, also known A14 (35). Mice were genotyped according to the public available resources of the mouse repositories: *A14*: (https://www.jax.org/Protocol?stockNumber=007914&protocolID=29436), *ErbB4-CreERT2*: (https://www.jax.org/Protocol?stockNumber=012360&protocolID=28814), and *Grin1*: for Grin1 genotyping the forward primer NR1.2: CTC AAG TGA GTC TGC CCC ATG CTG A and the reverse primer NR1.3as: CAC AGG GGA GGC AAC ACT GTG GAC F were used to amplify a 369 bp gene fragment for the *Grin1-2lox* allele and a 315 bp fragment for the wild type allele. Alternatively, the genotyping PCR of the EMMA mouse repository can be employed: https://www.infrafrontier.eu/sites/infrafrontier.eu/files/upload/public/pdf/genotype_protocols/EM09220_geno.pdf. The mice were bred and maintained group housed in the IBF Heidelberg. There were brought to the animal facility at the Central Institute of Mental Health Mannheim at the age of 10–14 weeks. To induce the Cre-mediated recombination at post-adolescence stages both *Grin1*$^{f/f}$*/ErbB4-CreERT2* mice and control littermates were injected intraperitoneally twice a day with 100 µl (i.e., 1 mg) tamoxifen (T5648, Sigma-Aldrich) dissolved in 20 mg/ml peanut old, Sigma-Aldrich) for 5 days (36, 37) at the age of 7–8 weeks. After recovery the 10–14 days old mice were transferred to the behavioral facility (at the Central Institute of Mental Health in Mannheim) the mouse cohorts were subjected to the behavioral test battery for the next 2–3 weeks.

Histological Analysis

Mice were anesthetized with isofluran (Baxter Healthcare Corporation) and perfused intracardiac with PBS and 4% paraformaldehyde (PFA, Merck) in PBS prior to decapitation (38). Brains were removed and fixed in ice-cold 4% PFA for 12 h, embedded in 2.5% agarose (Invitrogen) in PBS. After 12 h coronal vibratome sections (50 µm, Leica Vibratome VT100) were taken and transferred to a 24 ml well plate and in PBS. Slices were then briefly (1–5 min) counterstained in with DAPI (4′,6-diamidino-2-phenylindole, Thermo Fisher), 300 nM in PBS. Slices were washed 3–5 times with PBS. After final wash in PBS slices were mounted on glass slides (Menzel-Gläser), air dried for 10 min and embedded in aqua polymount (Polyscience).

Overview images were acquired with an Axioimager/ Axiovision (Zeiss) and high-resolution images with the SP8 confocal microscope (Leica). Images were processed by Adobe Illustrator CS5 (Adobe).

Behavioral Experiments

At the Central Institute of Mental Health Mannheim the animals were single-housed in Macrolon type II cages (26.8 × 21.5 × 14.1 cm) on a 12 h reversed dark-light cycle (lights on at 7 pm) and supplied with bedding (aspen wood ABEDD LTE E-002, ssniff-Spezialdiäten, Soest, Germany), nesting material (cotton square Zoonlab, Castrop-Rauxel) and water and food (LASQCdiet Rod16, Altromin, Lage) *ad libitum*. We assessed body weight once a week during cage changes under red light.

We assessed nesting behavior, locomotion and exploration (barrier test, open field and novel object test), anxiety (elevated o-maze, dark-light test), prepulse inhibition, cognition (radial arm maze, puzzle box, novel object recognition test) and stress coping (forced swim test). The behavioral observation started one week after the arrival with the observation of nesting in the home cage. Experiments were performed during the dark phase, at least 1 h after the light change, except for the nest test due to special demands. The mice were acclimatized to the testing room for at least 30 min, except for the FST, when acclimatization was limited to 6–10 min. Experimental equipment was cleaned after each trial with 70% ethanol. The testing order was of the mice was randomized for each behavioral test using randomizer.org. The experimenters were unaware of the genotype throughout the experimentation.

Nesting Test

Nest building was evaluated according to a rating scale on shape and cohesion of the nest as previously described (39). The mice were placed in a new home cage with cotton nestled 1 h before the onset of the dark phase and the score was determined 5 and 24 h later.

Barrier Test

The barrier test was performed as we described earlier (40). In brief, the mouse was introduced into the rear end of a clean Type III cage (42.5 x 27.6 x 15.3 cm) with reduced amount of bedding material. A transparent barrier (2 cm) separated the cage into two equal compartments. The setup was illuminated with 25 lux. The latency to cross the barrier, the number of crosses and the rearing were monitored.

Open Field and Novel Object Test

Locomotion was detected in a white open field (50 x 50 x 50 cm) illuminated by 25 lux, recorded by a video camera and analyzed by the imaging processing software Ethovision XT (Noldus Information Technology). Assessed parameters were total distance moved, center time (10 cm distance to the walls), movement and velocity (41). For the open field test the mouse was introduced to the center of the field for 10 min. In the subsequent novel object test, a water-filled 50 ml Falcon tube was introduced upside down in the center of the field. Latency and number of approaches to this novel object were counted manually for another 10 min.

Elevated o-Maze Test

To evaluate the approach-avoidance conflict in both mouse lines, the mice were introduced into the closed section of an o-shaped gray plastic runway (outer diameter 46 cm, width 6 cm, 50 cm of the ground). Two walled (height, 10 cm) sections of gray polyvinyl that were placed opposite to each other. The other sections were open. The floor was covered by grip tape to prevent falling. The latency to exit into the open arm, the time on the open arm and the number of crosses between the closed sections were monitored for 5 min.

Dark-Light Test

In another test for approach-avoidance conflict the mice were placed into the dark chamber (20 x 15 cm, black acryl with a black lid) of a 2-chamber box for 5 min. The latency to the first exit, the time spent in the light compartment and the number of exits into the chamber (30 x 15 cm, white acryl) illuminated with 600 lux was detected.

Acoustic Startle Response and Pre-pulse Inhibition

The mouse was introduced into a startle chamber (SR-LAB; San Diego Instruments) as previously described (37). Briefly, in the chamber a loudspeaker produced continuous background noise of 60 dB of sound pressure level (SPL) and the acoustic startle pulses (white noise, 115 dB SPL, 40 ms). After the acclimatization of 5 min, 5 initial startle stimuli were presented, followed by pseudorandomized presentation of pulse alone, control stimulus, pulse with prepulse (72 or 76 or 80 or 84 db, 100 ms before pulse) with 10 presentations of each trial type. The intertrial stimulus was randomized between 10 and 20 s. PPI was calculated as the percent decrease of the ASR magnitude in trials when the startle stimulus was preceded by a prepulse [100 x (mean ASR amplitude on pulse alone trials—mean ASR amplitude on prepulse-pulse trials)/mean ASR amplitude on pulse alone trials].

Radial Arm Maze

This learning task was performed as previously described (37). Briefly, the mouse was introduced into the center of a maze consisting of a central platform (20 cm in diameter) connected to eight arms (50 cm long, 8 cm wide), elevated 50 cm and covered with Plexiglas tunnels to permit visual orientation by extra-maze cues. The mouse was free to explore all arms and eat the bait (one millet seed) out of the food cups at the end of the arm for max. 10 min per day on 10 consecutive days. Otherwise, the session ended after the mouse ate all baits. Assessed movement parameters were distance moved, immobility, movement, time to complete and velocity, parameters on choices and errors were aborted trials, number of choices, correct choices, errors, procedural errors and working memory errors and angel choices. Working memory errors occurred when a mouse revisited an arm repetitively. The classification of working memory errors was based on the disparity to previous entries of the identical arm, ranging from 0 (re-entry) to max. 8 (more than eight entries in between were cumulated). Mice were tested for 10 day, with one

run per day. The results of two consecutive days were given as one trial.

Puzzle Box Test

We assessed puzzle solving and memory as previously described in the puzzle box test (42). Briefly, the mouse was introduced into a brightly lit white chamber (58 × 28 cm, 600 lux) from where it could escape into a black goal zone (15 × 28 cm, covered with lid). The passage into the goal box was modified with increasing difficulty in the total trials on three consecutive days: run 1) open door over the underpass location; run 2–4, open underpath; run 5–7, underpath was filled with sawdust (bedding closed tunnel), and runs 8 and 9, underpath was blocked by a cardboard plug (blocked channel). A trial started by placing the mouse in the start zone and ended when all four paws of the mouse entered the goal zone or after a total time of 5 min. The performance of mice in the puzzle box was assessed by measuring the latency to enter the goal zone.

Novel Object Recognition

The novel object recognition was performed in the same setup as the open field test in a modified protocol (43). On a first day, the mouse was habituated to the arena for 10 min. On day two, the habituation of 10 min was repeated and followed by an exposure to two identical objects [either a transparent plastic cube (8 cm) standing on its tip filled with black paper in a frame made of coated clay or a glass candy jar filled with turquoise stones and a silver plastic lid (8 cm)] 2 h later for 7 min with at least 15 s of exploration to be included. Two hours later, the mouse was introduced again and was free to explore one familiar and one novel object for 5 min. Between the trials the mice were brought to their home cage. We assessed the time spent and the number of approaches exploring the objects.

Forced Swim Test

Mice were placed for 6 min into a glass cylinder (height 23 cm; diameter 13 cm) filled with water (21 °C) to a height of 12 cm. The latency to immobility and percentage of time spent immobile were determined by the image-processing system EthoVision XT, Noldus Information Technology (44, 45). This test was conducted twice, with a 24 h inter-trial interval.

Statistical Analyses

Statistical analyses were performed using SPSS Statistics version 24 (IBM, Armonk, NY). Differences were considered to be significant at a $P < 0.05$. The data were analyzed through two-way ANOVA with treatment and sex as factors or, when appropriate, by using repeated-measures ANOVA. Whenever no sex differences were observed, we merged the data of the groups ($n = 14$). No animals were excluded from the study. The sample size for all experiments was $n = 7$ per sex and genotype. The experimental unit was the single animal.

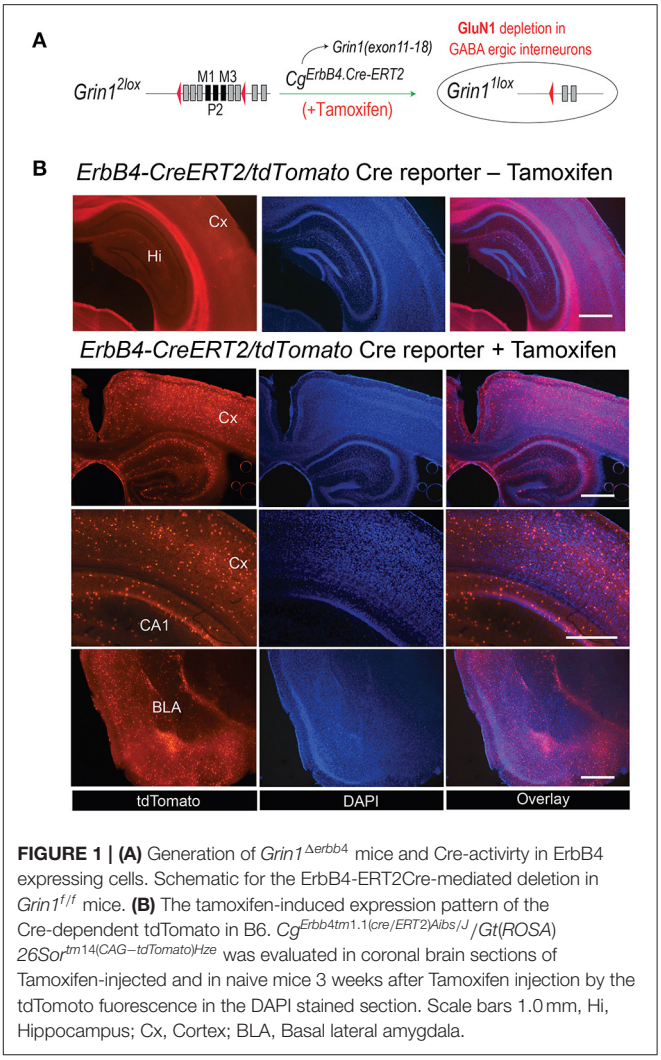

FIGURE 1 | (A) Generation of *Grin1*$^{\Delta erbb4}$ mice and Cre-activirty in ErbB4 expressing cells. Schematic for the ErbB4-ERT2Cre-mediated deletion in *Grin1*$^{f/f}$ mice. **(B)** The tamoxifen-induced expression pattern of the Cre-dependent tdTomato in B6. *Cg*$^{ErbB4tm1.1(cre/ERT2)Aibs/J}$/*Gt(ROSA)26Sor*$^{tm14(CAG-tdTomato)Hze}$ was evaluated in coronal brain sections of Tamoxifen-injected and in naive mice 3 weeks after Tamoxifen injection by the tdTomoto fuorescence in the DAPI stained section. Scale bars 1.0 mm, Hi, Hippocampus; Cx, Cortex; BLA, Basal lateral amygdala.

RESULTS

Strategy for the ErbB4-CreERT2-Mediated GluN1 Expression

For our experimental approach of NMDAR deletion specifically in ErbB4 expressing neurons approach we selected the *Cg*$^{ErbB4tm1.1(cre/ERT2)Aibs/J}$ for the tamoxifen-induced Cre expression (**Figure 1A**). In several previous studies this line was used reliably to study the *erbB4* gene expression in the mouse brain (46–48). Similarly, our gene-targeted floxed *Grin1* mice encoding the *Grin1*$^{f/f}$ targeted allele was shown in our previous studies to be highly accessible for Cre-mediated inactivation (32) and for inducible inactivation later in development (33) or for PV knockout in PV-positive interneurons (49). For the demonstration of the cell type specific gene inactivation we employed the Cre-inducible tdTomato indicator mouse (Cg-*Gt(ROSA)26Sor*$^{tm14(CAG-tdTomato)Hze}$) as this mouse line was used routinely to monitor the Cre activity in neuronal cell population e.g., (50). Thus coronal sections of our *Cg*$^{ErbB4tm1.1(cre/ERT2)Aibs/J}$ Cg-*Gt(ROSA)26Sor*$^{tm14(CAG-tdTomato)Hze}$ mice confirmed the

Tamoxifen induced Cre expression in a subpopulation of neurons that was published before and that demonstrated the *erbB4* expression in a subpopulation of brain cells (**Figure 1B**, **Supplementary Figure 1**) which were previously described as interneurons and some glia cells (50) providing indirect evidence for Tamoxifen induced the deletions of NMDAR in those cells in our *Grin1*^{ff}*/ErbB4-CreERT2* mice, similar to previous studies (23–25).

Deletion of GluN1 in ErbB4-Expressing Cells During Adolescence Did Not Alter Basic Behavior

Behavioral testing of the animals was performed according to the time line given in **Figure 2**. We detected no differences in body weight (**Figure 3A**) due to genotype, but a time*genotype interaction $F(8,192) = 2.384$, $p = 0.018$, showing that *Grin1*^{ff}*/ErbB4-CreERT2* increased faster in body weight than the controls. In addition, we found the typical body weight gain over time $F(8,192) = 136.919$, $p < 0.001$ and sex differences $F(1,24) = 74.860$, $p < 0.001$, as well as time*sex interactions $F(8,192) = 9.895$, $p < 0.001$ as the weight of the males increased quicker than the weight of the females. Nesting behavior also revealed a sex effect in the 5 h time window [5h: $F(1,24) = 10.347$, $p = 0.004$; 24 h: $F(1,24) = 4.595$, $p = 0.042$], but neither genotype effects nor interactions (**Figure 3B**). Locomotion and exploration were not affected by the genetic manipulation either, neither in the barrier test (genotype: number of rearings: $F(1,27) = 0.062$, $p = 0.806$; latency to cross: $F(1,27)=0.247$, $p = 0.623$; number of crosses $F(1,27) = 0.098$, $p = 0.757$) (**Figures 3C–E**) or the open field novel object test (genotype: open field (OF) distance moved: $F(1,26) = 0.163$, $p = 0.690$; novel object distance moved: $F(1,26) = 2.502$, $p = 0.126$; OF center time: $F(1,26) = 0.394$, $p = 0.536$; NO center time: $F(1,26) = 2.394$, $p = 0.134$; NO approaches: $F(1,26) = 0.699$, $p = 0.411$), (**Figure 3F**). Neither did we find sex specific differences or interactions in the Test (**Figures 3C–F**).

Affective and Sensory-Gating Behavior Was Not Affected by the Genetic Manipulation

Anxiety-like behavior was similar in the dark-light test and the elevated o-maze (**Figures 4A,B**) for genotype and sex (genotype: time in lit compartment: $F(1,26) = 0.141$, $p = 0.710$; time on open arm: $F(1,26) = 0.048$, $p = 0.829$). Immobility, a coping behavior in the forced swim test, which is often associated with despair behavior and hence used as a marker for depressive-like behavior, was also not influenced by sex or genotype (genotype: immobility day 1: $F(1,26) = 0.170$, $p = 0.684$; immobility day 2: $F(1,26) = 0.101$, $p = 0.753$; **Figure 4C**). The acoustic startle response as well as the prepulse inhibition also displayed no differences between the factors (genotype: acoustic startle response: $F(1,26) = 0.397$, $p = 0.534$; intensity: $F(3,78) = 100.971$, $p < 0.001$; genotype: $F(1,261 = 0.669$, $p = 0.208$); **Figures 4D,E**). We found an intensity*genotype interaction $F(3,78) = 2.689$, $p = 0.052$, which indicates a tendency to lower responsivity to the different noise intensities in *Grin1*^{ff}*/ErbB4-CreERT2* mice.

Learning and Memory Was Not Affected by the ErbB4-CreERT2-Induced NMDAR Knockout

Since in the novel object recognition was normal *Grin1*^{ff}*/ErbB4-CreERT2* mice (**Supplementary Table S1**) we analyzed the learning behavior in our mutant mice in more detail, in order to detect shuttle differences in complex attentional tasks: the puzzle box and in the radial maze (**Figure 5**). In our analysis we found that in learning in all tasks of the puzzle box of *ErbB4-CreERT2*-mice was comparable to control littermates (**Figure 5A**). Moreover, when the conflict solution (puzzle), the short term (STM) or long term (LTM memory was analyzed we could not find a statistical difference between genotypes [genotype: puzzle: $F(1,26) = 0.540$, $p = 0.469$; STM: $F(1,26) = 0.675$, $p = 0.390$; LTM: $F(1,26) = 0.241$, $p = 0.628$; **Figure 5B**]. Similarly, in the spatial radial maze (RAM) we detected no increased working memory errors in *Grin1*^{ff}*/ErbB4-CreERT2* mice compared to controls during the acquisition of the task [genotype: $F(1,26) = 0.517$, $p = 0.478$; **Figure 5C**] indicating that the *Grin1*^{ff}*/ErbB4-CreERT2* are not impaired in responses to natural stimuli.

DISCUSSION

Here we report that ablation of GluN1-containing NMDAR in ErbB4 expressing cells in adults mice does not significantly affect cognition and does not induce the typical behavioral correlates of schizophrenia, depression and anxiety. To our knowledge, our study provides the first characterization of a genetic model of inducible genetic ablation of NMDAR during late adolescence in neurons expressing the NRG1 receptor ErbB4, with relevance for psychiatric disorders, considering that NRG1 and ErbB4 are main candidate risk genes gene for schizophrenia (26).

The present results appear at a first glance surprising since mutant mice heterozygous for either NRG1 or ErbB4 show a behavioral phenotype that resembles alterations seen in schizophrenia and, furthermore, NRG1 hypomorphs, expressing 50% of the normal levels of NRG1, have 16% fewer functional NMDARs than wild-type mice (26). However, as mentioned by these authors, such results have to be interpreted with caution so that they do not necessarily mean that the principal pathogenic alteration in schizophrenia lies in the glutamate system (26). One important aspect that needs to be taken into consideration refers to the fact that NMDAR expression is affected already in early brain development in the NRG1 hypomorph mice, whereas they are ablated only postnatally in our inducible pharmacogenetic model. As mentioned previously, only early postnatal, but not early adult ablation of NMDAR in (mainly, but not exclusive) PV-positive interneurons triggers psychosis-like changes (25), causing an excitation-inhibition E/I imbalance which emerges after adolescence concomitantly with significant dendritic retraction and dendritic spine re-localization in pyramidal neurons (51). One possible explanation could be that NMDA currents gradually decrease and even became undetectable during cortical development, with most (74%) of the parvalbumin-positive interneurons exhibiting no NMDA

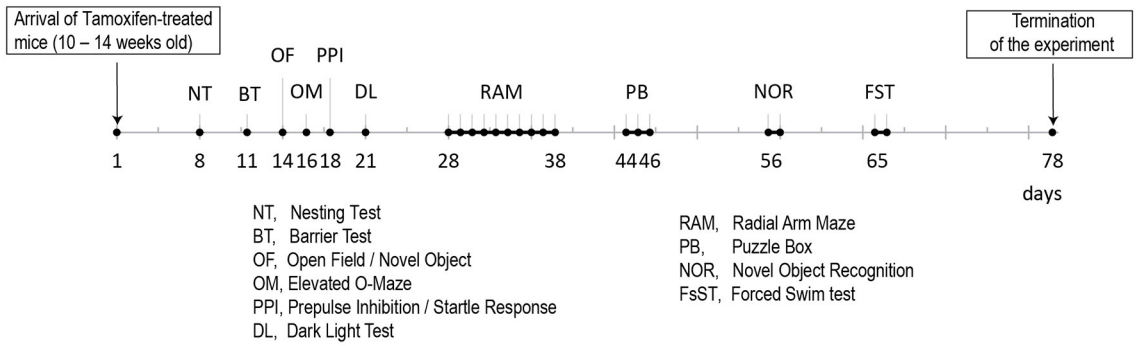

FIGURE 2 | Time line for the behavioral analyses of the two Tamoxifen treated cohorts (B6. *Cg*$^{Erbb4tm1.1(cre/ERT2)Aibs/J}$*/Gt(ROSA)26Sor*$^{tm14(CAG-tdTomato)Hze}$ and control littermates).

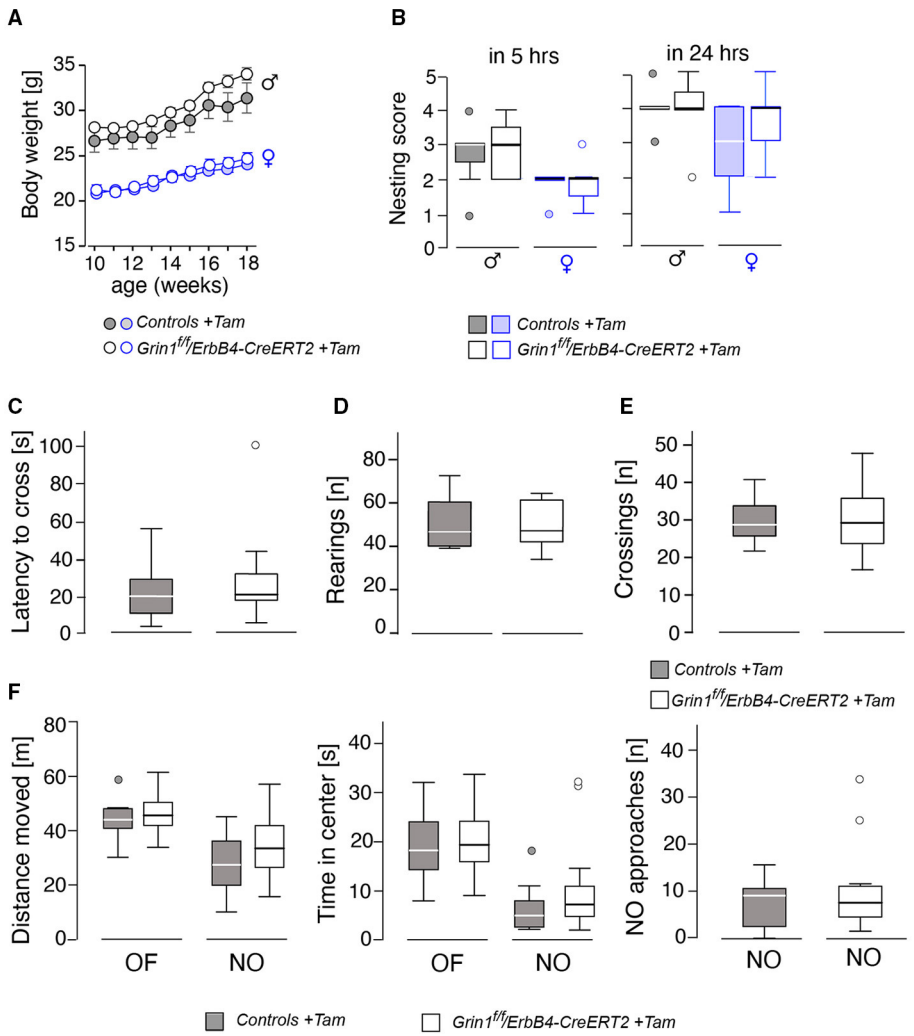

FIGURE 3 | Assessment of basic physiological and locomotor parameters in male and female mice revealed no significant effects on the genotype. **(A)** Body weight, **(B)** nest building score after 5 and 24 h, **(C)** results of the barrier test in latency to cross the barrier, **(D)** number of rearings, **(E)** number of crossings over the barrier. In **(F)** the results of the open field (OF) and novel object (NO) test on gives the (left) the distance moved, (middle) time spent in center and (right) the approaches toward the novel object. Group size $n = 14$. Data is represented as means + SEM.

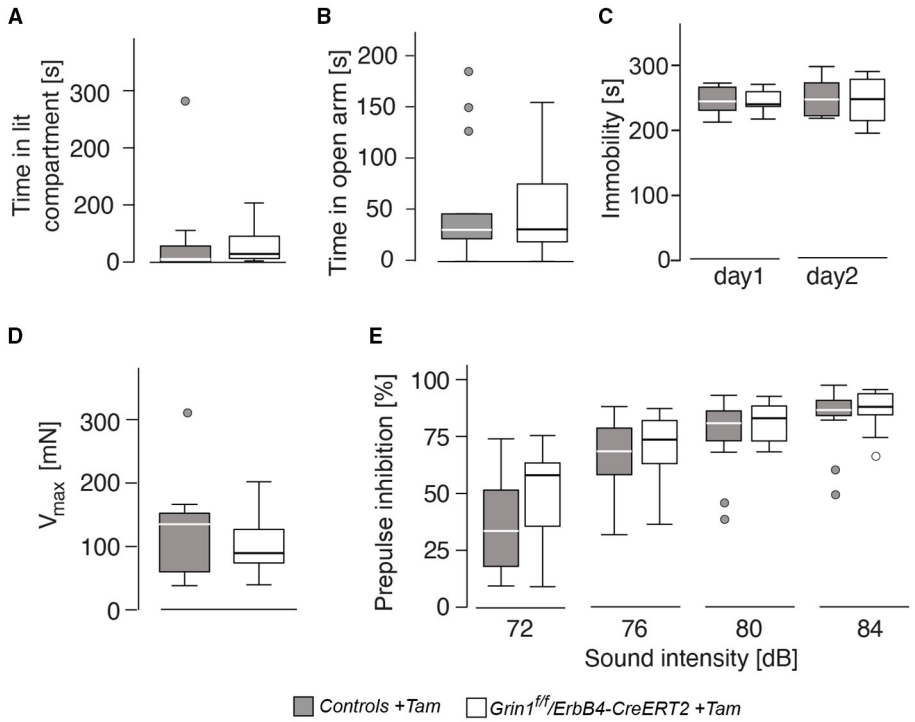

FIGURE 4 | The genetic manipulation did not lead to alteration in affective behavior and prepulse-inhibition of the acoustic startle response. **(A)** Time spent in the illuminated part of the dark-light box, **(B)** time spent on the open arm of the elevated o-maze, **(C)** immobility in the forced swim test, **(D)** acoustic startle response and **(E)** prepulse inhibition of the startle response. Group size $n = 7$. Data is represented as means + SEM.

current in adults, in contrast to other interneuronal populations, where they remain stable (52). Therefore, an early postnatal ablation of NMDARs appears crucial in inducing protracted neuroplastic impairment that underlies schizophrenia-associated abnormalities. We cannot exclude that ablation of NMDAR in ErbB4-positive cells induced at earlier time-points than in the present investigation may trigger schizophrenia-like abnormalities. Future studies should determine and compare such stage-dependent effects of cell type-restricted NMDAR genetic manipulation.

Our data indicate that post-adolescent deletion of NMDAR even extended to a much larger neuronal population than PV-positive interneurons is insufficient to trigger behavioral changes associated with psychosis. The identification of the neural substrate of these alterations is not yet finalized, other brain regions such as thalamic neurons (53) or other interneuronal subpopulations, such as those expressing somatostatin (54), are as well valid candidates. Another possibility is that NMDAR deficiency in PV and possibly ErbB4 neurons may be a risk factor for developing schizophrenia, but is not sufficient on its own: environmental risk factors or other supplementary triggers may be needed to lead to clinical manifestation (50). In line with this view is as well the finding that global pharmacological blockade of NMDAR with MK-801 induces catatonia-like changes, as a feature both of a severe schizophrenia and anti-NMDAR encephalitis, in $Grin1^{\Delta PV}$ mice (34).

Limitations of the Study

Finally, we wish to mention that the validation of the current inducible pharmacogenetic model is limited by various factors. Providing experimental evidence for the quantitative removal of NMDAR from cells expressing the *erbB4* gene in animal models with cell type specific deletions using the *erbB4-CreERT2* knockin line is a big experimental challenge. In previous mice with interneuron-restricted NMDAR depletion (*Grin1* cKOs), the authors used single cell electrophysiology to demonstrate the loss of NMDAR currents, which complemented the demonstration that the CRE expression was restricted to interneurons using Cre-indicator mice (23). In our conditional NMDAR knock out mouse model inducible deletion was started not early postnatally as in that model, but at post-adolescent stages, requiring functional analysis at later, adult time points. However, preparing consistently healthy acute brain slices from mature animals for patch clamping experiments is challenging, due to extensive myelination, reduced tissue viability and increased vulnerability to damage etc., the vast majority of brain electrophysiologists working with brain slices from juvenile animals. Therefore, a reliable electrophysiological single call analysis is very difficult to be performed due to the technical limitations of single cell patch analysis of adult mice. Hence we relied–as all of previous studies, on the Cre-dependent tdTomato expression pattern induced in our mice, which was used before for efficient Cre-dependent removal of the NMDAR. For our studies, we have specifically

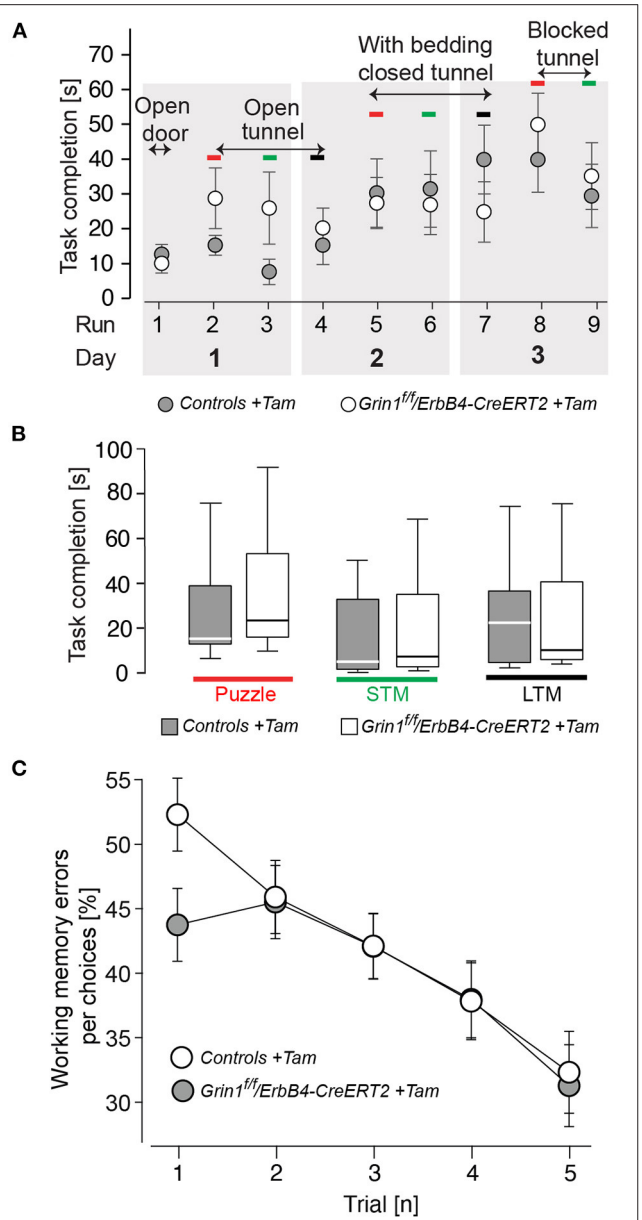

FIGURE 5 | Mutant mice showed no impairments in learning and puzzle solving. **(A)** Time to complete the puzzle per trial due to condition. **(B)** Puzzle, analysis of the recognition of a novel task; STM, short-term memory (repetitive task on the same day); LTM, long-term memory (repetitive task of the last day). **(C)** Working memory errors in the radial maze in 5 consecutive trials (1 tial = 2 runs). Controls are shown in black, *Grin1*$^{\Delta ErbB4f/f//ErbB4-CreERT2}$ in white. Group size $n = 14$. Data is represented as means + SEM.

imported the Erbb4tm1.1(cre/ERT2)Aibs/J mouse line from Jackson Labs to Heidelberg and used it in our experiments. We selected this line because it has already been successfully used in multiple studies. Thus, the functional tamoxifen-induced Cre recombinase activity in Rosa Cre-Indicator A14 mice was reproducible and also clearly detected in erbB4-positive cells (35, 50, 55). In addition, we used our floxed GluN1 mice, which we used successfully in three manuscripts (32–34), indicating that the Cre-mediated inactivation of our floxed *Grin1*^{f} allele is efficient.

In this context, it is important to mention that the detection of successful conditional Cre-induced gene ablation of highly expressed CNS specific genes, such as *Grin1* in a small population of widely scattered cells in the CNS, such as here the ErbB4-positive neurons, is experimentally challenging. Belforte et al. has succeeded in using double *in situ* hybridization to detect the loss of NMDAR in most GAD67-positive interneurons in S1 somatosensory cortex (25), although NMDARs are tightly distributed in the CNS (32, 56). For the electrophysiological NMDAR analysis in the GAD67-positive cells he adopted a method that was initially developed to determine the expression profile in single 5HT3A1 expressing cells in the mouse brain. In this method, the 5HT3A neurons were tagged by the a fluorescent protein (FP). By Laser Capture Microscopy (LCM) the RNA of the FP positive cells was isolated and the mRNA was amplified by single cell RT-PCR. In this example, the gene expression profiles of EGFP-tagged 5HT3A expressing neurons was determined (57). To date several publicly available "Fluorescent Cre-activity indicator mouse lines" (see Jackson labs, and the A14 line used in this study) are available. Their usage have greatly facilitated the specialized task of detecting Cre expressing single cells in brain slices. By using one of those CRE-FP transgenes Belforte et al., was able to detect the loss of NMDAR currents in CRE-FP expressing GAD67 interneurons of young mice (25) and Lin et al., succeeded in determining the electrophysiological profile of vGat deficient ErbB4 cells (58). Thus, the implementation of combined CRE-FP in in the same cell opened the possibility of optimal, reliable electrophysiological analysis of gene defects in sparse neuronal subpopulations. A lot of patience and breeding effort is required here to cross three different mouse lines. However, this cellular electrophysiological analysis appears to be largely limited to brain slices from young mice. Thus, Belforte et al. also show E-phys patching of Cre-FP-expressing GAD67 cells only in young mice but not in old mice from an independent cohort of a second NMDAR-KO mouse line (25). For adult mice LCM the RNA of single cells is still an option.

In conclusion, our results showing that restricted post-adolescent deletion of NMDAR from a relatively large neuronal population of ErbB4-positive neurons does not affect behavior is once again emphasizing the role of neurodevelopmental impairment in the emergence of several psychiatric disorders. Inducible genetic models represent useful tools toward identifying the neuronal populations implicated in NMDAR-driven psychosis at specific developmental stages, including adulthood.

DATA AVAILABILITY STATEMENT

The original contributions presented in the study are included in the article/**Supplementary Material**, further inquiries can be directed to the corresponding author.

ETHICS STATEMENT

All experimental procedures were approved by the Animal Welfare Committee (Regierungspräsidium Karlsruhe) and carried out according to the European Communities Council Directive 63/2010/EU (license number: 35-9185-81-G-3-17).

AUTHOR CONTRIBUTIONS

AM, PG, and DI designed the study, analyzed the results, and wrote the manuscript. MV, SC, and RS generated, bred, and analyzed the transgenic animal lines. NP and AM performed the behavioral analyses. All authors contributed to the article and approved the submitted version.

FUNDING

The present work was supported by grants from the Deutsche Forschungsgemeinschaft (DFG) IN 168/3-1, the Ingeborg Ständer Foundation, the ERA-NET NEURON program, the Bundesministerium für Bildung und Forschung (BMBF) under the frame of Neuron Cofund (ERA-NET NEURON NMDAR-PSY) and the Swiss National Foundation (SNF) 186346 to DI.

ACKNOWLEDGMENTS

We acknowledge financial support by DFG within the funding program Open Access Publishing, by the Baden-Württemberg Ministry of Science, Research and the Arts and by the Ruprecht-Karls-Universität Heidelberg.

SUPPLEMENTARY MATERIAL

The Supplementary Material for this article can be found online at: https://www.frontiersin.org/articles/10.3389/fpsyt.2021.750106/full#supplementary-material

REFERENCES

1. Conti F, Minelli A, DeBiasi S, Melone M. Neuronal and glial localization of NMDA receptors in the cerebral cortex. *Mol Neurobiol.* (1997) 14:1–18. doi: 10.1007/BF02740618
2. Freund TF. Interneuron Diversity series: Rhythm and mood in perisomatic inhibition. *Trends Neurosci.* (2003) 26:489–95. doi: 10.1016/S0166-2236(03)00227-3
3. Inta D, Monyer H, Sprengel R, Meyer-Lindenberg A, Gass P. Mice with genetically altered glutamate receptors as models of schizophrenia: a comprehensive review. *Neurosci Biobehav Rev.* (2010) 34:285–94. doi: 10.1016/j.neubiorev.2009.07.010
4. Coyle JT. Glutamate and schizophrenia: beyond the dopamine hypothesis. *Cell Mol Neurobiol.* (2006) 26:365–84. doi: 10.1007/s10571-006-9062-8
5. Lahti AC, Koffel B, LaPorte D, Tamminga CA. Subanesthetic doses of ketamine stimulate psychosis in schizophrenia. *Neuropsychopharmacology.* (1995) 13:9–19. doi: 10.1016/0893-133X(94)00131-I
6. Kristiansen LV, Beneyto M, Haroutunian V, Meador-Woodruff JH. Changes in NMDA receptor subunits and interacting PSD proteins in dorsolateral prefrontal and anterior cingulate cortex indicate abnormal regional expression in schizophrenia. *Mol Psychiatry.* (2006) 11:737–47, 705. doi: 10.1038/sj.mp.4001844
7. Weickert CS, Fung SJ, Catts VS, Schofield PR, Allen KM, Moore LT, et al. Molecular evidence of N-methyl-D-aspartate receptor hypofunction in schizophrenia. *Mol Psychiatry.* (2013) 18:1185–92. doi: 10.1038/mp.2012.137
8. Brennand K, Savas JN, Kim Y, Tran N, Simone A, Hashimoto-Torii K, et al. Phenotypic differences in hiPSC NPCs derived from patients with schizophrenia. *Mol Psychiatry.* (2015) 20:361–8. doi: 10.1038/mp.2014.22
9. Chiappelli J, Pocivavsek A, Nugent KL, Notarangelo FM, Kochunov P, Rowland LM, et al. Stress-induced increase in kynurenic acid as a potential biomarker for patients with schizophrenia and distress intolerance. *JAMA Psychiatry.* (2014) 71:761–8. doi: 10.1001/jamapsychiatry.2014.243
10. Li D, Collier DA, He L. Meta-analysis shows strong positive association of the neuregulin 1 (NRG1) gene with schizophrenia. *Hum Mol Genet.* (2006) 15:1995–2002. doi: 10.1093/hmg/ddl122
11. Rotaru DC, Lewis DA, Gonzalez-Burgos G. The role of glutamatergic inputs onto parvalbumin-positive interneurons: relevance for schizophrenia. *Rev Neurosci.* (2012) 23:97–109. doi: 10.1515/revneuro-2011-0059
12. Rosen AM, Spellman T, Gordon JA. Electrophysiological endophenotypes in rodent models of schizophrenia and psychosis. *Biol Psychiatry.* (2015) 77:1041–9. doi: 10.1016/j.biopsych.2015.03.021
13. Dalmau J, Gleichman AJ, Hughes EG, Rossi JE, Peng X, Lai M, et al. Anti-NMDA-receptor encephalitis: case series and analysis of the effects of antibodies. *Lancet Neurol.* (2008) 7:1091–8. doi: 10.1016/S1474-4422(08)70224-2
14. Hughes EG, Peng X, Gleichman AJ, Lai M, Zhou L, Tsou R, et al. Cellular and synaptic mechanisms of anti-NMDA receptor encephalitis. *J Neurosci.* (2010) 30:5866–75. doi: 10.1523/JNEUROSCI.0167-10.2010
15. Creten C, van der Zwaan S, Blankespoor RJ, Maatkamp A, Nicolai J, van Os J, et al. Late onset autism and anti-NMDA-receptor encephalitis. *Lancet.* (2011) 378:98. doi: 10.1016/S0140-6736(11)60548-5
16. Titulaer MJ, McCracken L, Gabilondo I, Iizuka T, Kawachi I, Bataller L, et al. Late-onset anti-NMDA receptor encephalitis. *Neurology.* (2013) 81:1058–63. doi: 10.1212/WNL.0b013e3182a4a49c
17. Farber NB, Wozniak DF, Price MT, Labruyere J, Huss J, St Peter H, et al. Age-specific neurotoxicity in the rat associated with NMDA receptor blockade: potential relevance to schizophrenia? *Biol Psychiatry.* (1995) 38:788–96. doi: 10.1016/0006-3223(95)00046-1
18. Uehara T, Sumiyoshi T, Seo T, Itoh H, Matsuoka T, Suzuki M, et al. Long-term effects of neonatal MK-801 treatment on prepulse inhibition in young adult rats. *Psychopharmacology (Berl).* (2009) 206:623–30. doi: 10.1007/s00213-009-1527-2
19. Mohn AR, Gainetdinov RR, Caron MG, Koller BH. Mice with reduced NMDA receptor expression display behaviors related to schizophrenia. *Cell.* (1999) 98:427–36. doi: 10.1016/S0092-8674(00)81972-8
20. Hashimoto T, Bazmi HH, Mirnics K, Wu Q, Sampson AR, Lewis DA. Conserved regional patterns of GABA-related transcript expression in the neocortex of subjects with schizophrenia. *Am J Psychiatry.* (2008) 165:479–89. doi: 10.1176/appi.ajp.2007.07081223
21. Sohal VS, Zhang F, Yizhar O, Deisseroth K. Parvalbumin neurons and gamma rhythms enhance cortical circuit performance. *Nature.* (2009) 459:698–702. doi: 10.1038/nature07991
22. Uhlhaas PJ, Singer W. Abnormal neural oscillations and synchrony in schizophrenia. *Nat Rev Neurosci.* (2010) 11:100–13. doi: 10.1038/nrn2774
23. Korotkova T, Fuchs EC, Ponomarenko A, von Engelhardt J, Monyer H, NMDA. receptor ablation on parvalbumin-positive interneurons impairs hippocampal synchrony, spatial representations, and working memory. *Neuron.* (2010) 68:557–69. doi: 10.1016/j.neuron.2010.09.017
24. Carlén M, Meletis K, Siegle JH, Cardin JA, Futai K, Vierling-Claassen D, et al. A critical role for NMDA receptors in parvalbumin interneurons for gamma rhythm induction and behavior. *Mol Psychiatry.* (2012) 17:537–48. doi: 10.1038/mp.2011.31
25. Belforte JE, Zsiros V, Sklar ER, Jiang Z, Yu G, Li Y, et al. Postnatal NMDA receptor ablation in corticolimbic interneurons confers schizophrenia-like phenotypes. *Nat Neurosci.* (2010) 13:76–83. doi: 10.1038/nn.2447

26. Stefansson H, Sigurdsson E, Steinthorsdottir V, Bjornsdottir S, Sigmundsson T, Ghosh S, et al. Neuregulin 1 and susceptibility to schizophrenia. *Am J Hum Genet.* (2002) 71:877–92. doi: 10.1086/342734
27. Hahn CG, Wang HY, Cho DS, Talbot K, Gur RE, Berrettini WH, et al. Altered neuregulin 1-erbB4 signaling contributes to NMDA receptor hypofunction in schizophrenia. *Nat Med.* (2006) 12:824–8. doi: 10.1038/nm1418
28. Neddens J, Buonanno A. Expression of the neuregulin receptor ErbB4 in the brain of the rhesus monkey (Macaca mulatta). *PLoS ONE.* (2011) 6:e27337. doi: 10.1371/journal.pone.0027337
29. Steiner H, Blum M, Kitai ST, Fedi P. Differential expression of ErbB3 and ErbB4 neuregulin receptors in dopamine neurons and forebrain areas of the adult rat. *Exp Neurol.* (1999) 159:494–503. doi: 10.1006/exnr.1999.7163
30. Inta D, Meyer-Lindenberg A, Gass P. Alterations in postnatal neurogenesis and dopamine dysregulation in schizophrenia: a hypothesis. *Schizophr Bull.* (2011) 37:674–80. doi: 10.1093/schbul/sbq134
31. Erdmann G, Schütz G, Berger S. Inducible gene inactivation in neurons of the adult mouse forebrain. *BMC Neurosci.* (2007) 8:63. doi: 10.1186/1471-2202-8-63
32. Niewoehner B, Single FN, Hvalby Ø, Jensen V. Meyer zum Alten Borgloh S, Seeburg PH, et al. Impaired spatial working memory but spared spatial reference memory following functional loss of NMDA receptors in the dentate gyrus. *Eur J Neurosci.* (2007) 25:837–46. doi: 10.1111/j.1460-9568.2007.05312.x
33. Bannerman DM, Bus T, Taylor A, Sanderson DJ, Schwarz I, Jensen V, et al. Dissecting spatial knowledge from spatial choice by hippocampal NMDA receptor deletion. *Nat Neurosci.* (2012) 15:1153–9. doi: 10.1038/nn.3166
34. Bygrave AM, Masiulis S, Nicholson E, Berkemann M, Barkus C, Sprengel R, et al. Knockout of NMDA-receptors from parvalbumin interneurons sensitizes to schizophrenia-related deficits induced by MK-801. *Transl Psychiatry.* (2016) 6:e778. doi: 10.1038/tp.2016.44
35. Madisen L, Zwingman TA, Sunkin SM, Oh SW, Zariwala HA, Gu H, et al. A robust and high-throughput Cre reporting and characterization system for the whole mouse brain. *Nat Neurosci.* (2010) 13:133–40. doi: 10.1038/nn.2467
36. Vogt MA, Chourbaji S, Brandwein C, Dormann C, Sprengel R, Gass P. Suitability of tamoxifen-induced mutagenesis for behavioral phenotyping. *Exp Neurol.* (2008) 211:25–33. doi: 10.1016/j.expneurol.2007.12.012
37. Inta D, Vogt MA, Elkin H, Weber T, Lima-Ojeda JM, Schneider M, et al. Phenotype of mice with inducible ablation of GluA1 AMPA receptors during late adolescence: relevance for mental disorders. *Hippocampus.* (2014) 24:424–35. doi: 10.1002/hipo.22236
38. Gass P, Prior P, Kiessling M. Correlation between seizure intensity and stress protein expression after limbic epilepsy in the rat brain. *Neuroscience.* (1995) 65:27–36. doi: 10.1016/0306-4522(95)92049-P
39. Chourbaji S, Brandwein C, Vogt MA, Dormann C, Hellweg R, Gass P. Nature vs. nurture: can enrichment rescue the behavioural phenotype of BDNF heterozygous mice? *Behav Brain Res.* (2008) 192:254–8. doi: 10.1016/j.bbr.2008.04.015
40. Mallien AS, Häger C, Palme R, Talbot SR, Vogt MA, Pfeiffer N, et al. Systematic analysis of severity in a widely used cognitive depression model for mice. *Lab Anim.* (2020) 54:40–9. doi: 10.1177/0023677219874831
41. Zueger M, Urani A, Chourbaji S, Zacher C, Roche M, Harkin A, et al. Olfactory bulbectomy in mice induces alterations in exploratory behavior. *Neurosci Lett.* (2005) 374:142–6. doi: 10.1016/j.neulet.2004.10.040
42. Ben Abdallah NM, Fuss J, Trusel M, Galsworthy MJ, Bobsin K, Colacicco G, et al. The puzzle box as a simple and efficient behavioral test for exploring impairments of general cognition and executive functions in mouse models of schizophrenia. *Exp Neurol.* (2011) 227:42–52. doi: 10.1016/j.expneurol.2010.09.008
43. Mutlu O, Ulak G, Belzung C. Effects of nitric oxide synthase inhibitors 1-(2-trifluoromethylphenyl)–imidazole (TRIM) and 7-nitroindazole (7-NI) on learning and memory in mice. *Fundam Clin Pharmacol.* (2011) 25:368–77. doi: 10.1111/j.1472-8206.2010.00851.x
44. Kronenberg G, Balkaya M, Prinz V, Gertz K, Ji S, Kirste I, et al. Exofocal dopaminergic degeneration as antidepressant target in mouse model of poststroke depression. *Biol Psychiatry.* (2012) 72:273–81. doi: 10.1016/j.biopsych.2012.02.026
45. Lima-Ojeda JM, Vogt MA, Pfeiffer N, Dormann C, Köhr G, Sprengel R, et al. Pharmacological blockade of GluN2B-containing NMDA receptors induces antidepressant-like effects lacking psychotomimetic action and neurotoxicity in the perinatal and adult rodent brain. *Prog Neuropsychopharmacol Biol Psychiatry.* (2013) 45:28–33. doi: 10.1016/j.pnpbp.2013.04.017
46. Golub MS, Germann SL, Lloyd KC. Behavioral characteristics of a nervous system-specific erbB4 knock-out mouse. *Behav Brain Res.* (2004) 153:159–70. doi: 10.1016/j.bbr.2003.11.010
47. Shamir A, Kwon OB, Karavanova I, Vullhorst D, Leiva-Salcedo E, Janssen MJ, et al. The importance of the NRG-1/ErbB4 pathway for synaptic plasticity and behaviors associated with psychiatric disorders. *J Neurosci.* (2012) 32:2988–97. doi: 10.1523/JNEUROSCI.1899-11.2012
48. Chen YH, Lan YJ, Zhang SR Li WP, Luo ZY, Lin S, et al. ErbB4 signaling in the prelimbic cortex regulates fear expression. *Transl Psychiatry.* (2017) 7:e1168. doi: 10.1038/tp.2017.139
49. Bygrave AM, Kilonzo K, Kullmann DM, Bannerman DM, Kätzel D. Can N-Methyl-D-Aspartate Receptor Hypofunction in Schizophrenia Be Localized to an Individual Cell Type? *Front Psychiatry.* (2019) 10:835. doi: 10.3389/fpsyt.2019.00835
50. Bean JC, Lin TW, Sathyamurthy A, Liu F, Yin DM, Xiong WC, et al. Genetic labeling reveals novel cellular targets of schizophrenia susceptibility gene: distribution of GABA and non-GABA ErbB4-positive cells in adult mouse brain. *J Neurosci.* (2014) 34:13549–66. doi: 10.1523/JNEUROSCI.2021-14.2014
51. Pafundo DE, Pretell Annan CA, Fulginiti NM, Belforte JE. Early NMDA Receptor ablation in interneurons causes an activity-dependent e/i imbalance in vivo in prefrontal cortex pyramidal neurons of a mouse model useful for the study of schizophrenia. *Schizophr Bull.* (2021) 47:1300–9. doi: 10.1093/schbul/sbab030
52. Wang HX, Gao WJ. Cell type-specific development of NMDA receptors in the interneurons of rat prefrontal cortex. *Neuropsychopharmacology.* (2009) 34:2028–40. doi: 10.1038/npp.2009.20
53. Vukadinovic Z, NMDA. receptor hypofunction and the thalamus in schizophrenia. *Physiol Behav.* (2014) 131:156–9. doi: 10.1016/j.physbeh.2014.04.038
54. Alherz F, Alherz M, Almusawi H, NMDAR. hypofunction and somatostatin-expressing GABAergic interneurons and receptors: A newly identified correlation and its effects in schizophrenia. *Schizophr Res Cogn.* (2017) 8:1–6. doi: 10.1016/j.scog.2017.02.001
55. Harris JA, Hirokawa KE, Sorensen SA, Gu H, Mills M, Ng LL, et al. Anatomical characterization of Cre driver mice for neural circuit mapping and manipulation. *Front Neural Circuits.* (2014) 8:76. doi: 10.3389/fncir.2014.00076
56. Monyer H, Burnashev N, Laurie DJ, Sakmann B, Seeburg PH. Developmental and regional expression in the rat brain and functional properties of four NMDA receptors. *Neuron.* (1994) 12:529–40. doi: 10.1016/0896-6273(94)90210-0
57. Khodosevich K, Inta D, Seeburg PH, Monyer H. Gene expression analysis of in vivo fluorescent cells. *PLoS One.* (2007) 2:e1151. doi: 10.1371/journal.pone.0001151
58. Lin TW, Tan Z, Barik A, Yin DM, Brudvik E, Wang H, et al. Regulation of synapse development by Vgat deletion from ErbB4-positive interneurons. *J Neurosci.* (2018) 38:2533–50. doi: 10.1523/JNEUROSCI.0669-17.2018

Conflict of Interest: The authors declare that the research was conducted in the absence of any commercial or financial relationships that could be construed as a potential conflict of interest.

frontiers in Psychiatry

ORIGINAL RESEARCH
published: 27 January 2022
doi: 10.3389/fpsyt.2022.737295

Activity-State Dependent Reversal of Ketamine-Induced Resting State EEG Effects by Clozapine and Naltrexone in the Freely Moving Rat

Christien Bowman[1,2†], *Ulrike Richter*[3†], *Christopher R. Jones*[4†], *Claus Agerskov*[3†] *and Kjartan Frisch Herrik*[3*†]

[1] Faculty of Psychology and Neuroscience, Maastricht University, Maastricht, Netherlands, [2] Bio Imaging Laboratory, Faculty of Pharmaceutical, Biomedical and Veterinary Sciences, University of Antwerp, Antwerp, Belgium, [3] Department of Circuit Biology, Lundbeck, Copenhagen, Denmark, [4] Department of Pharmacokinetic and Pharmacodynamic Modeling and Simulation, Lundbeck, Copenhagen, Denmark

Ketamine is a non-competitive N-Methyl-D-aspartate receptor (NMDAR) antagonist used in the clinic to initiate and maintain anaesthesia; it induces dissociative states and has emerged as a breakthrough therapy for major depressive disorder. Using local field potential recordings in freely moving rats, we studied resting state EEG profiles induced by co-administering ketamine with either: clozapine, a highly efficacious antipsychotic; or naltrexone, an opioid receptor antagonist reported to block the acute antidepressant effects of ketamine. As human electroencephalography (EEG) is predominantly recorded in a passive state, head-mounted accelerometers were used with rats to determine active and passive states at a high temporal resolution to offer the highest translatability. In general, pharmacological effects for the three drugs were more pronounced in (or restricted to) the passive state. Specifically, during inactive periods clozapine induced increases in delta (0.1–4 Hz), gamma (30–60 Hz) and higher frequencies (>100 Hz). Importantly, it reversed the ketamine-induced reduction in low beta power (10–20 Hz) and potentiated ketamine-induced increases in gamma and high frequency oscillations (130–160 Hz). Naltrexone inhibited frequencies above 50 Hz and significantly reduced the ketamine-induced increase in high frequency oscillations. However, some frequency band changes, such as clozapine-induced decreases in delta power, were only seen in locomoting rats. These results emphasise the potential in differentiating between activity states to capture drug effects and translate to human resting state EEG. Furthermore, the differential reversal of ketamine-induced EEG effects by clozapine and naltrexone may have implications for the understanding of psychotomimetic as well as rapid antidepressant effects of ketamine.

Keywords: NMDAR (NMDA receptor), resting state EEG, translational biomarker, schizophrenia, antidepressant, naltrexone, clozapine, ketamine

OPEN ACCESS

Edited by:
Celia J. A. Morgan,
University of Exeter, United Kingdom

Reviewed by:
Debamitra Das,
Lieber Institute for Brain Development, United States
Tomas Palenicek,
National Institute of Mental Health, Czechia

***Correspondence:**
Kjartan Frisch Herrik
KFH@lundbeck.com

†ORCID:
Christien Bowman
orcid.org/0000-0001-7953-6585
Ulrike Richter
orcid.org/0000-0001-6100-7984
Christopher R. Jones
orcid.org/0000-0002-3338-7702
Claus Agerskov
orcid.org/0000-0003-2244-713X
Kjartan Frisch Herrik
orcid.org/0000-0002-1194-0394

Specialty section:
This article was submitted to Psychopharmacology, a section of the journal Frontiers in Psychiatry

Received: *06 July 2021*
Accepted: *06 January 2022*
Published: *27 January 2022*

Citation:
Bowman C, Richter U, Jones CR, Agerskov C and Herrik KF (2022) Activity-State Dependent Reversal of Ketamine-Induced Resting State EEG Effects by Clozapine and Naltrexone in the Freely Moving Rat. Front. Psychiatry 13:737295. doi: 10.3389/fpsyt.2022.737295

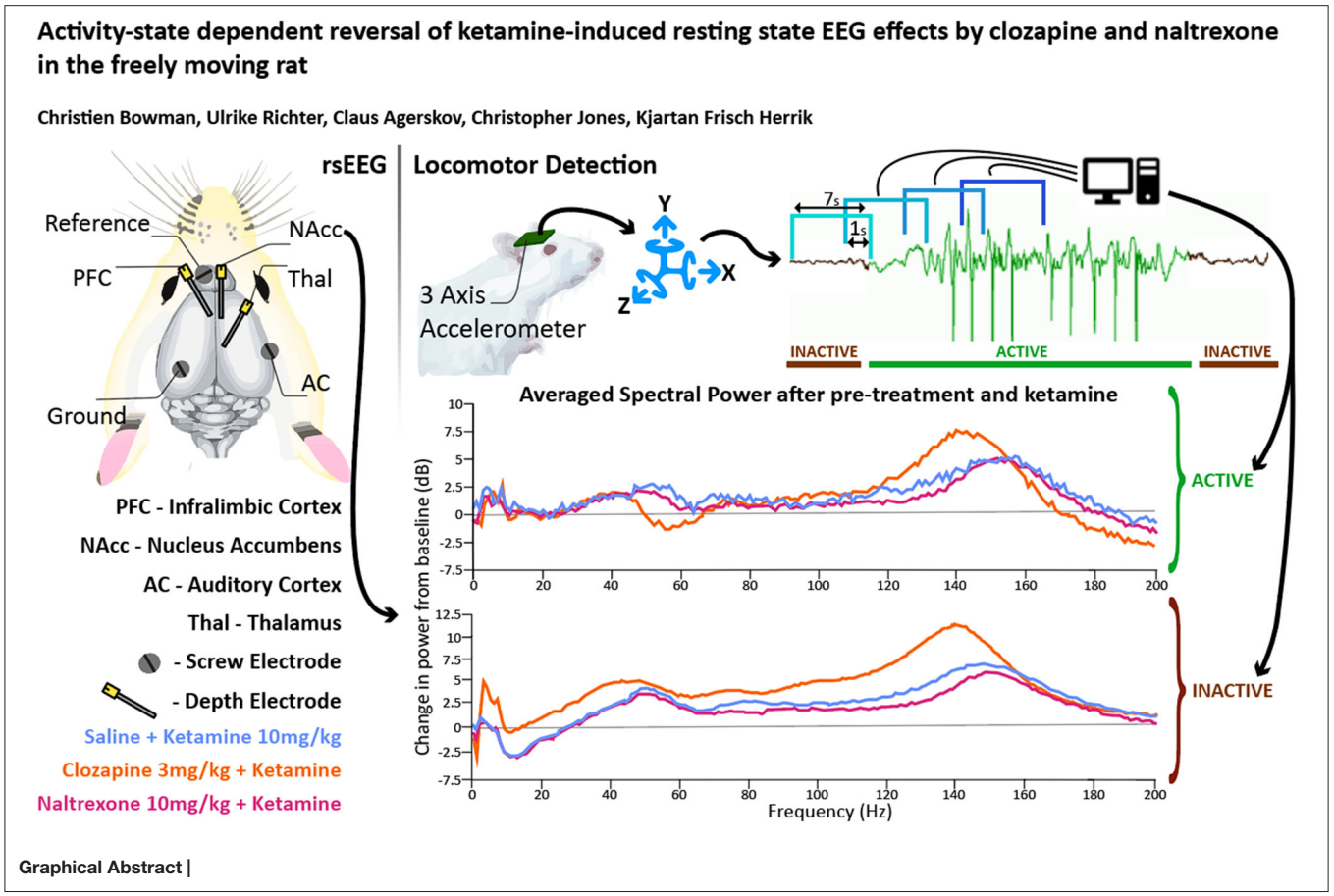

Graphical Abstract |

INTRODUCTION

Ketamine is a non-competitive N-Methyl-D-aspartate receptor (NMDAR) antagonist investigated for its psychotomimetic properties (1, 2) and has, among other NMDAR antagonists, been used to model positive, negative and cognitive symptoms of schizophrenia (SZ) (3, 4). More recently, ketamine has gained attention for its robust, long-lasting, rapid-acting antidepressant (RAAD) effects (5, 6). The mechanism of therapeutic effect remains un-elucidated and understanding RAAD pathways is complicated by ketamine's affinities to receptors in opioid, norepinephric, dopaminergic and serotonergic systems (1, 7, 8).

Concerns that ketamine RAAD effects are opioid dependent were raised (9–13) after publication of two human studies using naltrexone (opioid antagonist) and ketamine (14, 15). Williams' study reported that naltrexone pre-treatment completely prevented ketamine RAAD improvements but left dissociation intact. Yoon's study found the opposite, but differed substantially in methodology. Subsequent research in rodents both implicates and refutes opioid involvement in the RAAD effect of NMDAR antagonists (9, 16–18). Debate remains as to whether acute naltrexone administration prevents RAAD effects, but further research in human subjects is stymied by ethical concerns.

In vivo local field potentials (LFP), electrocorticography (ECoG) and electroencephalography (EEG) are regularly used in translational research of disorders and potential therapeutics including Major Depressive Disorder (19–23). Despite the potential utility of these techniques to clarify the ketamine-opioid debate, at the time of writing no LFP or EEG data of acute 'naltrexone plus ketamine' have been published.

LFP and ECoG paradigms are also translationally informative for schizophrenia (SZ) (20, 24, 25). Compared to healthy controls, unmedicated patients with SZ often present depressed activity between 7.5 and 20 Hz (26–31) and increases in higher bands > 30 Hz (24, 31–34). NMDAR antagonists including ketamine are used to model positive, negative and cognitive symptoms of this disorder (3, 4). After ketamine administration, rodents (35–40), healthy human volunteers (41–47) and unmedicated patients with SZ (48) all exhibit EEG disturbances similar to those seen in SZ patiesnts vs. healthy controls. In animal studies, where it is easier to record higher frequencies without interference from the skin and skull as in human s subjects, profound increases to high frequency oscillations (HFO [130–160 Hz]) are the most significant change reported

Abbreviations: AC, Auditory cortex; ECoG, Electrocorticography; EEG, Electroencephalography; FFT, Fast Fourier Transform; GABA - γ-aminobutyric acid; HFO, High frequency oscillations; LFP, Local field potential; PFC, Prefrontal cortex (human) / Infralimbic Cortex (rat); NAc, Nucleus accumbens; NMDAR, N-Methyl-D-aspartate receptor; RAAD, Rapid acting antidepressant; rsEEG, Resting state EEG; S.C, Subcutaneous; SZ, Schizophrenia; VEH, Vehicle.

(35–40, 49). In rodent studies in which locomotor states were tracked and separated with video tracking, ketamine-induced power spectra are distinctly different (50). The most clinically efficacious neuroleptic, clozapine, is effective in reducing positive and negative symptoms of SZ (51–53) and is known to modulate ketamine-induced spectral amplitudes (35, 36, 38, 40), however its efficacy at ameliorating induced power across different locomotor states is unknown.

Our research goals were to: apply an accelerometer-based behavioural detection method during LFP recordings to separate behavioural states and see if LFP profiles differed between them; identify if ketamine-induced LFP is modulated by naltrexone, a combination which is ethically problematic to study further in humans; and to investigate whether new LFP biomarkers of the most efficacious antipsychotic could be observed if recording data is behaviourally segregated; in particular the bands most disturbed by ketamine exposure: low Beta and HFO.

We characterised how LFP and ECoG spectra are modulated during ketamine exposure with and without pre-administration of naltrexone or clozapine. We recorded drug-induced LFP/ECoG in freely moving rats from four brain structures relevant to schizophrenia and major depressive disorder: LFPs from the thalamus (54–60), prefrontal cortex (PFC) (61–64), the nucleus accumbens (NAc) (65–69), and ECoG above the auditory cortex (AC) (70–76). To control for behavioural states, data from head-mounted accelerometers were utilised to algorithmically define if the animal was active or passive in each LFP/ECoG window. Additionally, to investigate whether neuroleptic effects on power spectra are occluded by behavioural artefacts, we employed the same paradigm with clozapine and ketamine. Freely moving rats were recorded during pre-treatment with either naltrexone or clozapine, ketamine challenge and pre-treatment with naltrexone or clozapine followed by ketamine challenge.

MATERIALS AND METHODS

Materials

Subjects

Male Wistar rats ($n = 115$, 270–300 g, Charles River, Germany), were housed in cages with sawdust bedding and environmental enrichment (plastic shelter, gnawing blocks and paper strips) with food and water ad-libitum. Temperature and humidity were controlled and a 12:12 h reversed cycle (lights off at 6:00 AM) was implemented. All experiments were time matched and began at 09:00, during the lights off cycle in order to capture naturalistic wake behaviour. During the "lights off" period, red light was used to facilitate handling of animals. Animal welfare and weight recording was carried out daily.

Experimental procedures, animal housing and care were carried out in accordance with the Danish legislation according to the European Union regulation (directive 2010/63 of 22 September 2010), granted by the Animal Welfare Committee, appointed by the Ministry of Environment and Food of Denmark.

Drugs

Naltrexone (Lundbeck, 12 mg/ml) was diluted in 0.9% saline solution and administered subcutaneously (SC) at 1, 3 and 10 mg/kg; clozapine (Novartis, 10 mg/ml) was diluted with 0.5% methylcellulose was administered SC at 0.3, 1, and 3 mg/kg; ketamine (Ketolar, 50 mg/ml, Sigma) was diluted with 0.9% saline and administered SC at 10 mg/kg; Vehicle (VEH) control was 0.9% saline solution.

Rat pharmacologically relevant doses and timing to peak effect of pre-treatment were estimated on the basis of a review of the literature (35, 77–84) in conjunction with application of the "Human Effective Dose conversion formula" (85) in reverse to existing human study data in which the combination of naltrexone plus ketamine have been evaluated (14, 86). Ketamine dose was determined through extensive in-house studies (unpublished) and literature (37, 87) which demonstrate profound modulation of LFPs at 10 mg/kg.

Electrodes and Accelerometer

Custom accelerometers were manufactured by Ellegaard Systems and cables by PlasticsOne. Summed accelerometer output [equal to sqrt ($X^2 + Y^2 + Z^2$)] was amplified (Precision Model 440; Brownlee, Palo Alto, CA, USA). Each of the 4 recording boxes with their own accelerometer and amplifier were calibrated to ensure equal output.

Depth electrodes (8IE3633SPCXE, E363-3-SPC, Elec.005-125MM SS, 25MM Length) and 6-way pedestals were purchased from PlasticsOne, manufactured by Bilaney Consultants GMBH.

Methods

Surgical Procedure

Animals were habituated to placebo rimadyl pellets (Rimadyl MDs, BioServ, Flemington USA) 5 days prior to surgery. On the day of surgery, rats were anaesthetised with 0.25–0.3 ml/100 g subcutaneous (S.C.) injection of 1:1 hypnorm/dormicum and mounted in a stereotaxic frame (David Kopf Instruments, Tujunga, CA, USA) with blunt ear bars. marcain (0.2 ml s.c.) was injected under the scalp, and gel (Neutral Opthta Eye Gel) put on the eyes.

Holes were drilled in the skull for three depth electrodes (**Figure 1A**) (E363-series; Invivo1/PlasticsOne, Roanoke, VA, USA) in the right infralimbic PFC (AP: +3.0 mm and ML:−0.7 mm from bregma, DV:−3.0 mm from the skull surface), Nucleus Accumbens shell (AP: +1.6 mm and ML: +1.0 mm from bregma and DV:−6.8 mm from the skull surface) and thalamus (AP:−2.8 mm and ML: +0.7 mm from bregma, DV:−4.4 mm from the skull surface) and three screw electrodes (E363-series, 15 mm, Invivo1/PlasticsOne, Roanoke, VA, USA) at vertex (AP:−5.0 mm and ML: +5.0 mm from bregma), auditory cortex (AP:−4.8 mm and ML:−6.4 mm from bregma) and a reference electrode (AP: +8.0 mm and ML: −2.0 mm from bregma). Ends of depth electrodes were cut before use to create an exposed tip. During the procedure, the rat's nails were trimmed to prevent grooming damage to surgical site.

Rats received 0.3 ml each of Norodyl and Noromox SC during the procedure, were placed under a warming lamp for 4 h and provided extra muesli. Rats were closely observed for 10–14-days

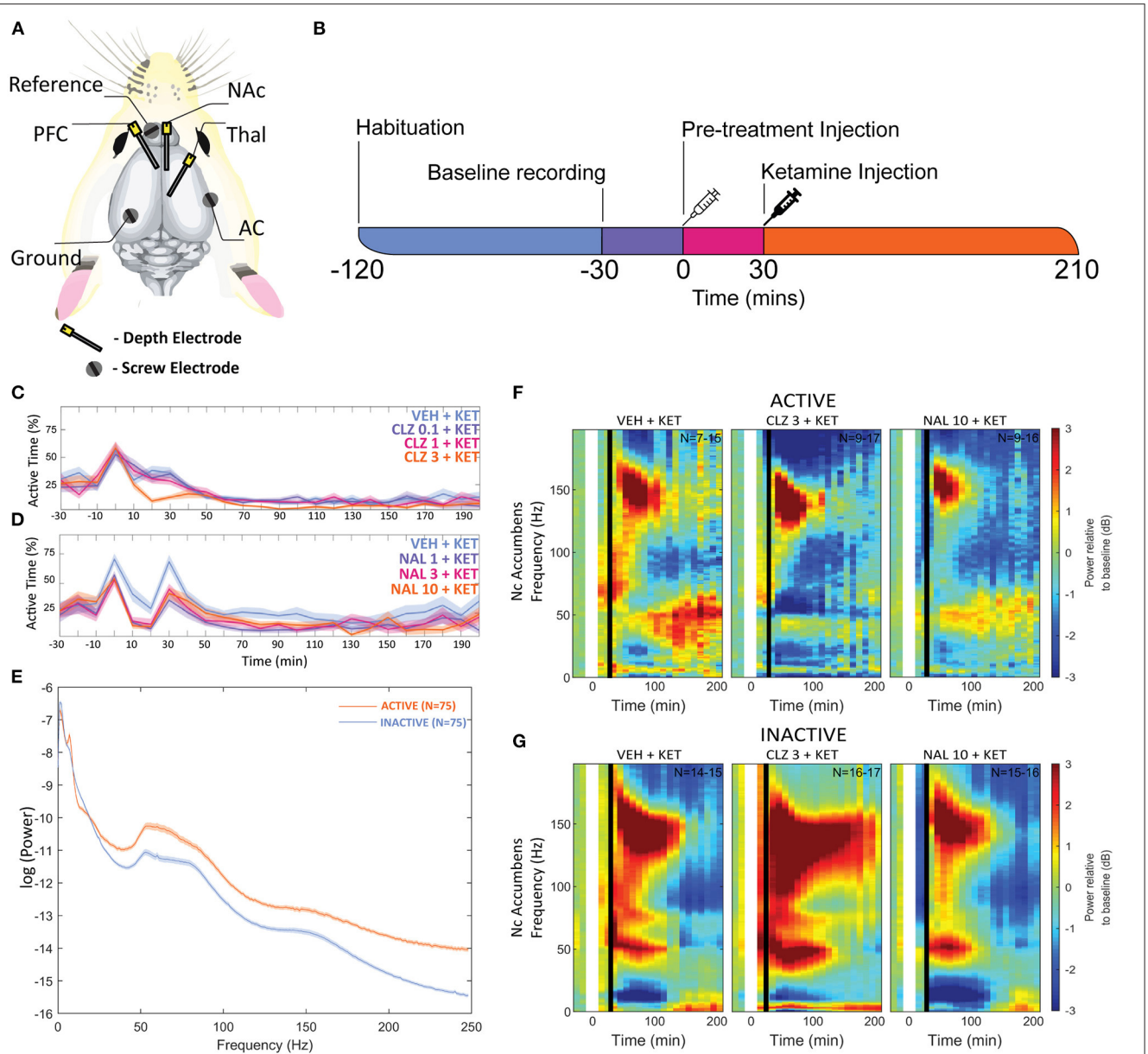

FIGURE 1 | (A) Overview of electrode placements. **(B)** Diagram of experimental procedures in one recording session. Plots depicting the mean proportion of time spent in Active state for Clozapine **(C)** and Naltrexone **(D)** groups. Pre-treatment doses given in mg/kg. **(E)** A plot of mean baseline power in the Active and Inactive state taken at the NAc between "-30" and "0" min between 0 and 250 Hz. **(F,G)** Heatmaps depicting grand mean LFP [0–200 Hz] for an exemplar brain region, the NAc, for animals given VEH+VEH, VEH+KET, NAL+KET, and CLZ+KET during Active **(F)** and Inactive **(G)** epochs. Pre-treatment doses given in mg/kg. The first (leftmost, evenly green) timebin at the start of each plot indicates the baseline recording, to which the rest of the session was normalised. The white vertical bar at time 0 represents pre-treatment injection, and the black bar at time 30 indicates KET injection. Colours indicate change (in dB, which is logarithmic) to baseline. Number of subjects is given as a range (lowest-highest *n* subjects included in a timebin) in the top right of each plot; group sizes were equal, however not all subjects were included in all timebins as inclusion was conditional on 1) histological validation of electrode placement and 2) sufficient time spent in the Active or Inactive state in any given timebin. Full heatmaps for other regions can be found in **Supplementary Information**. VEH, saline; KET, ketamine 10 mg/kg; CLZ, clozapine 3 mg/kg; NAL, naltrexone 10 mg/kg.

recovery, sutures removed after 7–10 days. No rats lost >10% pre surgery weight. Animals received rimadyl pellets twice a day for 5 days.

Up until surgery, rats were maintained a normal 12 hr light cycle (lights on at 0600) so that surgery could be performed in full light without disturbing the rat's circadian rhythm. After surgery, the light cycle was reversed (lights off 0600) and 21 days was allowed to elapse between experimental recording in order to allow rats to fully acclimatise.

Rats were anaesthetised with sevoflurane and 0.1 mV passed through the electrodes to create a lesion for histological validation of depth electrode placement. Rats were then decapitated, whole brains extracted, and the brains were placed in labelled, protective bags and frozen at −80°C until cryosectioning. On the day of placement validation, frozen brains were cut at the transverse fissure with a scalpel to remove the cerebellum and mounted with polyethylene glycol & alcohol (OCT Tissue Tek®, Sakure, The Netherlands) to a metal stand, placed in a cryostat (Leica CM3050 S) and 20 μm slices of the lesion sites were taken for examination with an optical microscope. Data from electrodes placed outside of NAc, PFC or thalamus was discarded.

Groups

The rats were split into three groups:

Group 1 ($n = 50$) received VEH + ketamine (10 mg/kg), clozapine (0.3, 1, and 3 mg/kg) + ketamine (10 mg/kg). Each rat was dosed twice (different treatments) following a pseudo-randomised schedule that balanced for drug doses and order with at least 7 days of washout in between to prevent cumulative tolerance.

Group 2 ($n = 50$) received VEH + VEH, VEH + ketamine (10 mg/kg), naltrexone (1, 3, and 10 mg/kg) + ketamine (10 mg/kg). Each rat was dosed twice (different treatments) following a pseudo-randomised schedule that balanced for drug doses and order with at least 7 days of washout in between to prevent cumulative tolerance.

Group 3 ($n = 15$) received clozapine (0.3, 1 mg/kg) or naltrexone (1, 3, 10 mg/kg) to quantify peak plasma and brain concentrations.

EEG Recording

To facilitate habituation, rats were handled and placed individually into their respective EEG monitoring cage (Acrylic, 30 x 45 x 55 cm) within an electrically shielded, sound-proof box (90 x 55 x 65 cm) for at least 8 h (in <2-h sessions) in the week preceding experimental recording. during habituation, animals were connected to the EEG recording wire with the equipment switched off. Strict sound discipline was observed within the lab, preparation of drugs was performed under conditions that minimised disturbance sound.

On the days of recording, rats were placed into the cage, attached to a 6-pin recording wire on a rotating swivel and allowed to habituate for 120 min. A plastic spring (2.5 cm long when compressed and 2.5 cm diameter) was affixed to the rotating swivel and the recording wire affixed to the spring to allow 5 cm between the base of the cage and the terminal end of the wire. This alleviated the weight stress on the animal, allowed for vertical flexibility and prevented excess wire impeding animal movement. After 90 min of habituation to the recording environment, EEG and accelerometer recording began to establish a 30-min baseline for each session (**Figure 1B**). After the 30-min baseline recording, animals received a pre-treatment bolus of VEH (saline 0.9%), naltrexone (1, 3 or 10 mg/kg) or clozapine (0.3, 1, or 3 mg/kg) via SC flank injection.

Thirty minutes after pre-treatment, the animals received SC ketamine challenge (10 mg/kg) or VEH. Thirty minutes was selected as the optimal time for pre-treatment(s) to become effective following review of the literature (35, 77–84) and extensive in-house studies (unpublished). Recording of ECoG, LFP, and accelerometers continued for an additional 180 min after which animals were returned to their home cage.

Analogue LFP/ECoG signals were amplified (Precision Model 440; Brownlee, Palo Alto, CA, USA) and converted to a digital signal (CED Power 1401, Power 1 (625 k Hz, 16 bit) and CED Expansion ADC16; CED, Cambridge, England) at a sampling rate of 1 k Hz. LFP/ECoG signals were band-pass filtered at 0.01–300 Hz. Spike2 was used to simultaneously record inputs from microelectrodes, cameras and accelerometers, this ensured synchronised timestamps across file types.

Behavioural State Classification

Animal behaviour was recorded in parallel with a video camera and an accelerometer (custom-made with ADXL335Z, Analogue Devices) during each recording session. The accelerometer was fixed inside the plastic docking connector at the terminal end of the recording tether which screws onto the thread of the rodent's electrode headstage. The recorded video was used to qualify whether the animal was active or inactive, the latter here being defined as a state with no visible body movement with the exception of occasional micromovements of the nose and head. The accelerometer signal was then reviewed in parallel with the video recording, and an *ad hoc* threshold for distinguishing activity from inactivity was determined. For further processing the signal was smoothed with a gaussian kernel and divided into 7-s segments bins with 1-s overlap. If the signal during a segment was above the threshold for at least 60% of the time the segment was determined to be from an active period, correspondingly if the signal was below the threshold for at least 60% of the time the segment was determined to be from an inactive period. Segments that fulfilled neither criteria were left unclassified.

Data Analysis

This study was intended to test whether the investigated drugs and behavioural states affect LFP and ECoG signals. This hypothesis was measured by consideration of EEG profiles across the following frequency bands: Delta (0.1–4 Hz), Theta (4–10 Hz), low Beta (10–20 Hz), high Beta (20–30 Hz), low Gamma (30–60 Hz), high Gamma (60–130 Hz), HFO (130–160 Hz), and Ultra High Frequency Oscillations UHFO (160–200 Hz) separated by behavioural state. To avoid power line interference, 2-Hz sections of frequency centred at 50, 100, and 150 Hz were excluded from analysis.

Analysis was carried out in MATLAB (MathWorks, Natick, MA). Signals were divided into consecutive 2-s segments with 1-s overlap. To minimise influence of artefacts, 2-s segments in which the signal exceeded ± 7 standard deviations (SD) from the mean were excluded from analysis. Furthermore, through comparison with the outcome of the behavioural state classification, each 2-s segment was assigned to either the active or inactive motor state or left unclassified. Next, a spectrogram with time and frequency resolution of 1 s and 0.5 Hz, respectively,

TABLE 1 | Tables of averaged power spectra between 40 and 70 min of experimentation for "Inactive" and "Active" epochs of animals given vehicle pre-treatment (at 0 min) + vehicle or ketamine (10 mg/kg at 30 min).

Region	Dose	Active								Inactive							
Ketamine 40–70 min																	
		0–4	4–10	10–20	20–30	30–60	60–130	130–160	160–200	0–4	4–10	10–20	20–30	30–60	60–130	130–160	160–200
NAc	V	0.43	0.90	0.21	0.30	0.31	0.75	−0.13	−0.13	0.20	−0.64	−0.43	0.19	0.60	1.12	1.03	1.10
	V+K	0.49	0.87	−0.59	−0.79	0.81	0.64	3.67	0.78	−0.38	−1.72	−3.67	−1.45	2.08	2.24	6.09	2.51

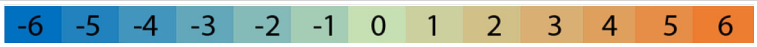

Values are given in normalised dB change from baseline of each session. dB is a logarithmic scale, meaning that "−3dB" = 50% of original value, whilst "3dB" = 200% of original value. Values significantly different vs. vehicle are coloured according to the valence of change from baseline. Full tables of p-values and non-segregated 'Any' spectra can be found in ***Supplementary Information****. Dose is given in mg/kg; V, Vehicle; K, ketamine 10 mg/kg.*

TABLE 2 | Table of averaged power spectra at 10–30 min.

Region	Dose	Active								Inactive							
Clozapine 10–30 min																	
		0–4	4–10	10–20	20–30	30–60	60–130	130–160	160–200	0–4	4–10	10–20	20–30	30–60	60–130	130–160	160–200
NAc	V+K	0.63	1.20	0.60	0.41	0.72	0.94	−0.07	−0.05	0.77	0.27	0.20	0.47	0.80	0.94	0.46	0.45
	0.3	0.14	1.39	0.98	0.43	0.17	0.71	−0.13	−0.54	1.28	0.11	−0.25	0.53	1.42	1.82	1.39	1.37
	1	−0.26	0.82	0.15	−0.09	0.33	0.58	0.05	−0.18	2.02	0.87	0.46	1.28	2.43	2.35	1.95	1.83
	3	−1.14	0.27	−0.47	−0.21	0.13	0.66	−0.11	−0.78	1.57	0.43	0.01	0.69	2.25	2.01	1.71	0.95

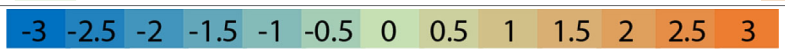

Pre-treatment with Clozapine was given at 0 mins. Separated by Active (left) and Inactive (right) epochs. Values are given in dB change from baseline. dB is a logarithmic scale, meaning that "−3dB" = 50% of original value, whilst "3dB" = 200% of original value. Values that are significantly different vs. vehicle + ketamine are coloured according to the valence of change from baseline. Full tables of p-values and non-segregated "Any" spectra can be found in ***Supplementary Information****. Dose is given in mg/kg; V, Vehicle; K, ketamine 10 mg/kg.*

was produced for each brain area by applying the Fast Fourier transform (FFT) to each 2-s segment. A spectrogram is a time series of power spectral densities and allows assessment of the spectral content of a signal over time, such as the presence of oscillatory activity in certain frequency bands.

When analysing the raw power, the logarithm was taken, otherwise each power spectral density was normalised to the baseline by dividing with the average power spectral density during the stable 30-min baseline period immediately prior to injection. The baseline-normalised spectral content was then converted to decibel (dB). Next, the power spectral densities were averaged over non-overlapping consecutive 10-min bins, positioned such that the time of injection is at 0 min, thereby producing spectrograms with 10-min time resolution. The steps of baseline normalisation and 10-min averaging were done both disregarding the behavioural state as well as only considering power spectral densities from segments classified as active or inactive, respectively. As a final step, grand averages were produced for each combination of brain area, behavioural state and treatment group.

Statistical analysis was conducted for averages over certain time intervals (10–30 min for pre-treatment, 40–70 min for ketamine challenge) and/or the already outlined frequency bands (see **Tables 1**–**3**). To investigate whether there were any significant treatment effects compared to the VEH + ketamine group, repeated measures analysis of variance (RM-ANOVA) was performed using MATLABs fitglme function with subsequent multiple comparison correction using Tukey's honest significant difference (HSD). $P < 0.05$ were considered significant. The fitted generalised linear mixed effects (GLME) model included an intercept and a factor for the treatment group, as well as a random-effects intercept for each animal to account for animal-specific variations. If applicable (i.e., when averaging only over a time interval or frequency band), the model also included a factor for the frequency/time bin and its interaction with the treatment group.

For each recording, the time the animal spent in the active and inactive behavioural state, respectively, was also calculated during non-overlapping 10-min bins, and grand averages were calculated for each treatment group. Statistical differences were assessed similar as for the spectral power in a certain frequency band, i.e., by using a GLME model with an intercept, a factor for the treatment group and the time interval and their interaction, and random-effects intercept for each animal, followed by Tukey's HSD. An animated visualization of the fundamental principles behind LFP recording, our recording procedure and some of the locomotor state differences is provided in the **Supplementary Material**.

Drug Exposure Determination

To determine if the selected doses of naltrexone, clozapine and ketamine resulted in translationally relevant concentrations

TABLE 3 | Table of averaged power spectra at 40–70 min.

Region	Dose	Active								Inactive							
Clozapine 40–70 min																	
		0–4	4–10	10–20	20–30	30–60	60–130	130–160	160–200	0–4	4–10	10–20	20–30	30–60	60–130	130–160	160–200
NAc	V+K	−0.23	1.21	−0.45	−0.51	0.54	1.16	3.05	0.60	0.02	−1.48	−2.37	−0.82	1.63	1.77	4.63	1.31
	0.3	−0.15	0.64	−1.28	−1.54	−0.49	0.31	4.47	−0.92	0.91	−0.29	−3.02	−0.42	2.92	3.33	7.37	1.90
	1	−0.77	0.66	−1.82	−1.66	−0.53	0.25	4.61	−0.56	1.34	0.63	−2.15	−0.16	2.73	3.25	7.76	2.11
	3	−1.33	0.34	−1.77	−1.44	−0.58	0.65	5.97	−1.79	0.75	0.56	−1.73	0.10	2.78	3.90	8.51	0.93

-6 -5 -4 -3 -2 -1 0 1 2 3 4 5 6

Baseline-normalised power (db)

Pre-treatment with Clozapine was given at 0 min, and ketamine at 30 min. Separated by Active (left) and Inactive (right) epochs. Values are given in dB change from baseline. dB is a logarithmic scale, meaning that "−3dB" = 50% of original value, whilst "3dB" = 200% of original value. Values that are significantly different vs. vehicle + ketamine are coloured according to the valence of change from baseline. Full tables of p-values and non-segregated "Any" spectra can be found in ***Supplementary Information****. Dose is given in mg/kg; V, Vehicle; K, ketamine 10 mg/kg.*

in the blood and brain of subjects, a drug exposure study was performed. Satellite animals ($n = 3$ per dose per drug) were treated by subcutaneous (SC) injection with Clozapine (0.3, 1, or 3 mg/kg) or Naltrexone (1, 3, or 10 mg/kg) then terminal venous blood and whole brain samples were taken at 1 h for exposure determination. In brief, plasma was isolated from whole blood and whole brains were isolated according to a previously described protocol (87). The brain tissue was prepared for extraction by dilution in buffer (1:5 w/v in deionised water) then homogenised by isothermal focused acoustic ultra-sonication using a Covaris instrument [Covaris E220x, 3.5 min at a bath temperature of 7°C with a peak power of 500 W and average power of 250 W (1,000 cycles per burst, duty cycle 50%)].

Total drug concentrations (Naltrexone or Clozapine) were determined in plasma and brain samples using high performance liquid chromatography coupled with tandem mass spectrometry (LC-MS/MS). The plasma (25 μL) and brain homogenate (25 μL) samples were precipitated with acetonitrile (4 volumes), centrifuged (3,500 g, 20 min, 5°C) and the supernatant (50 μL) diluted with water (3 volumes) before injection on the LC-MS/MS system. Drug concentrations were determined from calibration lines of known concentrations spiked into control plasma or brain homogenate and extracted under identical conditions. Bioanalysis was performed using a Waters Aquity UPLC coupled to a Waters XevoTQXS detector. A Waters Acquity UPLC HSS C18 SB, 1.7 μm, 30 × 2.1 mm column was used operating at 40°C. Mobile phase A consisted of 0.1% Formic Acid in water and mobile phase B of 0.1% Formic Acid in Acetonitrile. The LC flow rate was 0.6 mL/min. Analytes were separated on the LC column using a gradient. From 0 to 0.5 min the gradient was held at 2% mobile phase B. From 0.5 to 2 min B changed from 2 to 95% and was held at 95% until 2.5 min. Thereafter, between 2.5 and 2.7 min, B changed to 2% and was held at 2% from 2.7 to 4 min. Electrospray ionisation-MS (ESI-MS) was performed in positive MRM mode. For ketamine, clozapine, and naltrexone the parent:daughter $[M+H]^+$ ions: $327.09^+ \rightarrow 270.08^+$ and $342.17^+ \rightarrow 270.15^+$ were selectively monitored for quantification, respectively.

RESULTS

LFPs were similarly modulated by each drug combination across all recorded brain structures. Thus, in the interests of space and clarity, figures and tables in the manuscript are restricted to the Active and Inactive state in an exemplar region, the NAc, as this is where ketamine's effects are frequently the most profound in both our study and the wider literature (35, 36, 39, 66). The full figures and tables for each brain structure, activity state and un-separated LFP data may be found in the **Supplementary Information**.

Locomotor State Globally Alters Local Field Potentials

To control for animal behaviour during freely moving rsEEG, recorded epochs (2 s) were separated by locomotor activity level. This produced separate Active and Inactive baseline-corrected data for each 10-min timebin. Active or Inactive state was defined by a two-state classifier using data from a 3-axis, head-mounted accelerometer. Experimental animals were Inactive >50% in all conditions, and passivity increased towards the end of each recording session. Animals were transiently more active after injections at 0 and 30 min, however pre-treatment with Naltrexone (1, 3, and 10 mg/kg, dose dependent relationship) and clozapine (3 mg/kg) abolished this (**Figures 1C,D**). No hyperlocomotion was observed in any pre-treatment conditions after ketamine challenge (30 min).

Separating LFP by locomotor activity revealed activity-state-specific changes to spontaneous neural activity. Power in Active epochs was higher in all but Delta and low Beta bands (**Figure 1E**). In addition, a peak in baseline Theta amplitude is observed only in the Active state. Some compound induced changes were occluded entirely by analysing Active and Inactive LFP together (**Supplementary Figures 1**, **2** and **Supplementary Tables 1–9**). Pharmacologically-induced spectra were more pronounced during inactivity – mixed modelling of dB change from baseline found that Activity State significantly predicted magnitude of change from baseline ($F_{1,9} = 138.20$; $p <$

0.0001). Differences between Active and Inactive were confirmed with a *post hoc* investigation using Tukey's HSD ($p < 0.0001$).

Ketamine Suppresses Beta, Enhances HFO

After ketamine administration (30 min), rats pre-treated with saline displayed broad depression of frequencies below 30 Hz, barring Theta [4–10 Hz] in the Active PFC. These effects were more pronounced during Inactive epochs with few exceptions. Beta power [10–30 Hz] was suppressed by ketamine at all recording electrodes and across all activity states. Low beta [10–20 Hz] underwent the most profound depression in the Inactive thalamus and AC [4.39 and 4.99 dB decrease vs. baseline, respectively].

By contrast, ketamine induced increased power in frequencies 30–160 Hz. Inactive HFO [130–160 Hz] was subject to the most robust increase in oscillatory power, brain wide and across both motor states. Of note, the magnitude of HFO power during Inactive epochs [3.69–6.09 dB increase from baseline] did not overlap with the range during Active [1.22–3.67 dB increase from baseline]. In particular, the NAc (**Figures 1F,G**) and PFC recorded the most robust increases to spectral power.

Effect of Clozapine on Spontaneous Power Spectra

Pre-treatment

Clozapine pre-treatment elicited oscillatory activity throughout the recording regions during Inactive epochs. Interestingly, the mid-dose (1 mg/kg) induced Inactive LFP power across the broadest range of frequency bands and brain areas (**Figures 1F,G**, **Table 2** and **Supplementary Tables 2**, **3**). Clozapine dose dependently increased Delta [0-4 Hz] activity in the Inactive Thalamus, PFC, and most substantially in the AC ($p = 0.0006$; $p = 0.004$; $p = 0.0009$). During Inactivity, clozapine (1 and 3 mg/kg) substantially enhanced spectral power in frequency bands between 30 and 60 Hz and across all electrodes.

Clozapine's effects on Active spectra were primarily depressive. In the Active PFC and Thalamus, activity in several frequency bands (low and high beta [10–20 Hz; 20–30 Hz] and low *y* [30–60 Hz]) were depressed by clozapine (3 mg/kg). Suppression in Active epochs was eclipsed when analysing both motor states.

After Ketamine Challenge

Clozapine largely reversed ketamine's effects on lower bands, and enhanced effects >60 Hz. Ketamine induced depression of Theta [4–10 Hz] was completely ameliorated by clozapine in the Inactive state. In low beta [10–20 Hz], where ketamine induced suppression was more profound, clozapine partially returned LFP power towards baseline throughout the AC, PFC and Thalamus (3 mg/kg: $p = 0.0006$; $p = 0.0007$; $p = 0.0009$) (**Supplementary Tables 6**, **7**). In the AC for example, ketamine depressed low beta to 40.18% of baseline, and 3 mg/kg clozapine returned this to 84.14% of baseline. A similar relationship, though of a lower magnitude, was also displayed in neighbouring frequency band high beta [20–30 Hz]. Reversal of beta suppression was exclusively seen in the Inactive state. By contrast, Active beta depression at the PFC and NAc (**Table 3** and **Supplementary Tables 6**, **7**) was exacerbated by clozapine (3 mg/kg) ($p = 0.015$; $p = 0.005$).

Ketamine-induced power in higher frequencies was synergistically enhanced by clozapine. Robust, dose-dependent increases were seen to ketamine-induced *y* [60–130 Hz] and HFO [130–160 Hz] in the Inactive NAc [3.05dB to 3.90dB, $p = 0.00097$; 4.63–8.51 dB, $p = 0.00096$, respectively]. Clozapine (3 mg/kg) also dose dependently reversed ketamine-induced depression of low *y* in the Active PFC, returning it almost to baseline. Analysis of LFP without separating by locomotor state rendered this effect invisible (**Supplementary Table 3**).

Increasing doses of clozapine also modulated the peak frequency of ketamine-induced spectra in the NAc. Clozapine increased peak power, but downshifted HFO peak frequency [from 151 to 143 Hz] and low *y* [58 Hz to 51 Hz] (**Figure 2A**). Interestingly, clozapine dose and peak HFO exhibit a biphasic relationship – 1 mg/kg clozapine peak HFO was higher than either 0.3 or 3 mg/kg. The nadir of beta suppression was also downshifted by clozapine, from 18 to 15 Hz.

Effect of Naltrexone on Spontaneous LFP Spectra

Pre-treatment

Naltrexone (time 0) reduced oscillatory power globally in the acute pre-treatment phase (10–30 min) across a broad range of frequency bands (**Figures 1F,G**, **Table 4** and **Supplementary Tables 4**, **5**). Naltrexone decreased Inactive high beta [20–30 Hz] power and a biphasic relationship was seen between dose strength, with the mid dose (3 mg/kg) inducing the greatest depression [NAc, $p = 0.001$; PFC, $p = 0.006$; Thalamus, $p = 0.0008$]. Increasing doses of naltrexone depressed all frequency bands >30 Hz during Inactive epochs and across all electrodes. Active HFO power was also reduced below baseline at every electrode (10 mg/kg/Active; AC, $p = 0.0007$; NAc, $p = 0.0009$; PFC, $p = 0.04$; Thalamus, $p = 0.0009$).

After Ketamine Challenge

Naltrexone pre-treatment did not significantly alter ketamine-induced beta depression in the Inactive or Active state (**Table 5** and **Supplementary Tables 8**, **9**). Non-modulation of low beta [10–20 Hz] was consistent at all electrodes and states (10 mg/kg: Inactive: AC, $p = 0.99$/; NAc, $p = 0.99$; PFC, $p = 0.99$; Thalamus, $p = 0.39$; Inactive: AC, $p = 0.77$; NAc, $p = 0.19$; PFC, $p = 0.83$; Thalamus, $p = 0.74$). In bands *y* and above, naltrexone reduced ketamine-induced power in the Inactive PFC (10 mg/kg, low *y*, $p = 0.006$; high *y*, $p = 0.001$; HFO, $p = 0.0009$; UHFO, $p = 0.007$), though the resulting LFP power remained substantially higher than baseline. Similar, but less consistent suppression was observed at other electrodes, and during Active epochs (**Supplementary Tables 8**, **9**).

The width of peak HFO that ketamine affected was also modulated by naltrexone. Animals pre-treated with saline saw significant ketamine-induced power in a moderate band [135–167 Hz], 1 mg/kg naltrexone widened the band of affected frequencies by 43.8% [121–167 Hz] vs. saline, whilst 10 mg/kg naltrexone thinned affected HFO 84.4% [152–157 Hz] vs. saline (**Figure 2B**).

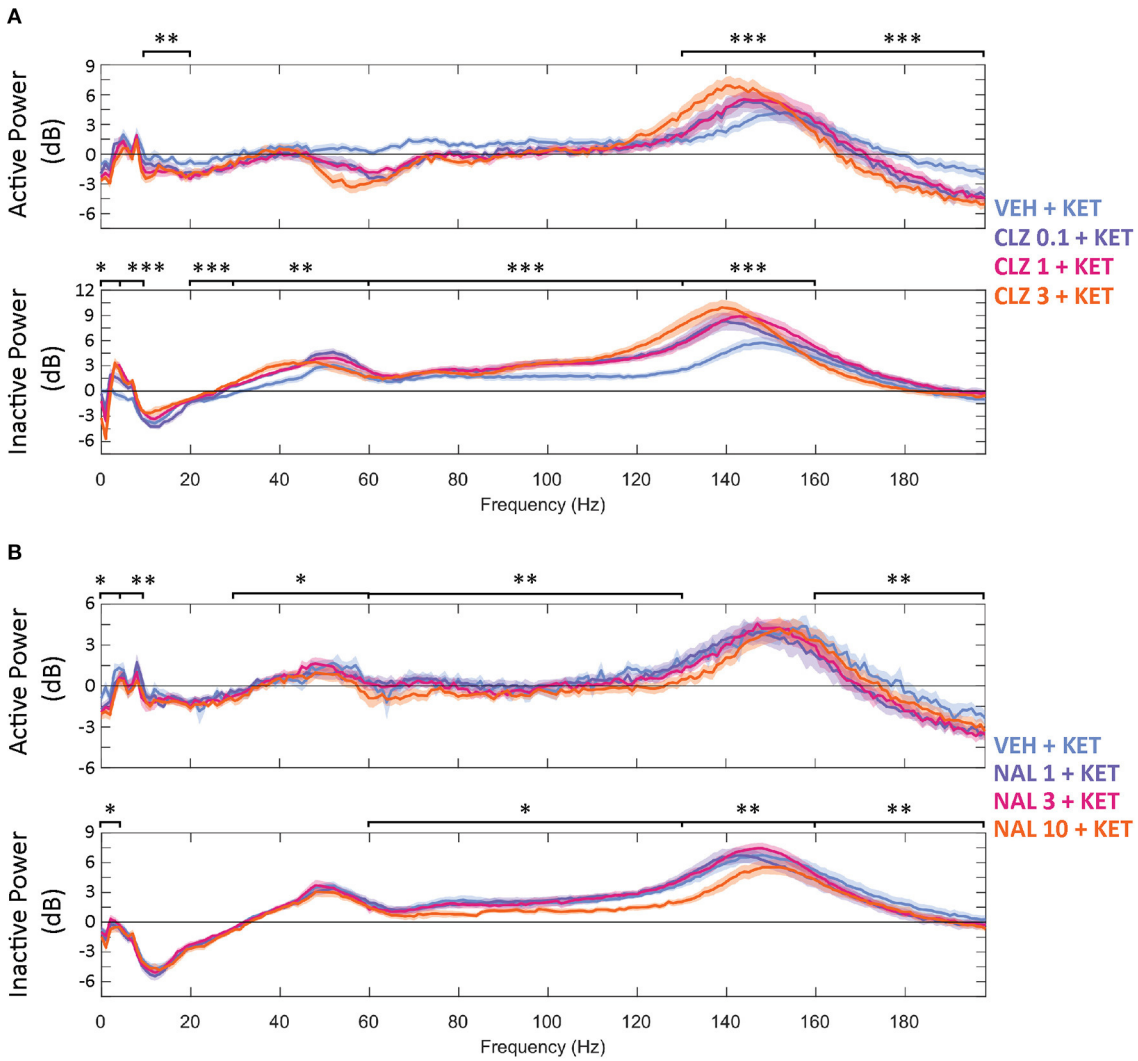

FIGURE 2 | Baseline-normalised, averaged spectra recorded at the NAc of CLZ **(A)** and NAL **(B)** groups between 40 and 70 min (10 min after KET and 40 min after pre-treatment). Displayed in dB change from baseline. Legends give pre-treatment doses in mg/kg. Significant differences of pre-treatment + KET spectra vs. VEH = KET are indicated by $*p < 0.05$/$**p < 0.01$/$***p < 0.001$. VEH, saline; KET, ketamine 10 mg/kg; CLZ, clozapine; NAL, naltrexone.

TABLE 4 | Table of averaged power spectra at 10–30 min.

Region	Dose	Active								Inactive							
Naltrexone 10–30 min																	
		0–4	4–10	10–20	20–30	30–60	60–130	130–160	160–200	0–4	4–10	10–20	20–30	30–60	60–130	130–160	160–200
NAc	V+K	0.45	0.58	0.25	−0.16	0.29	0.67	−0.21	−0.13	0.50	−0.06	−0.34	0.27	0.97	1.21	0.39	1.20
	0.3	0.08	0.52	0.35	0.63	0.88	0.67	−0.29	−0.49	−0.18	−1.17	−0.99	−0.37	0.27	0.51	0.39	−0.01
	1	−0.57	0.73	−0.13	0.14	0.53	0.17	−0.78	−0.89	−0.15	−1.11	−1.08	−0.37	0.24	−0.11	−0.18	−0.36
	3	−0.70	−0.03	−0.24	0.13	0.39	−0.89	−1.26	−1.15	−0.34	−0.63	−0.38	−0.06	0.13	−1.83	−2.01	−1.67

-3 -2.5 -2 -1.5 -1 -0.5 0 0.5 1 1.5 2 2.5 3

Baseline-normalised power (db)

Pre-treatment with Naltrexone was given at 0 min. Separated by Active (left) and Inactive (right) epochs. Values are given in dB change from baseline. dB is a logarithmic scale, meaning that "−3dB" = 50% of original value, whilst "3dB" = 200% of original value. Values that are significantly different vs. vehicle + ketamine are coloured according to the valence of change from baseline. Full tables of p-values and non-segregated "Any" spectra can be found in ***Supplementary Information****. Dose is given in mg/kg; V, Vehicle; K, ketamine 10 mg/kg.*

TABLE 5 | Table of averaged power spectra at 40–70 min.

Region	Dose	Active								Inactive							
Naltrexone 40–70 min																	
		0–4	4–10	10–20	20–30	30–60	60–130	130–160	160–200	0–4	4–10	10–20	20–30	30–60	60–130	130–160	160–200
NAc	V+K	0.45	0.58	0.25	−0.16	0.29	0.67	−0.21	−0.13	0.50	−0.06	−0.34	0.27	0.97	1.21	0.39	1.20
	0.3	0.08	0.52	0.35	0.63	0.88	0.67	−0.29	−0.49	−0.18	−1.17	−0.99	−0.37	0.27	0.51	0.39	−0.01
	1	−0.57	0.73	−0.13	0.14	0.53	0.17	−0.78	−0.89	−0.15	−1.11	−1.08	−0.37	0.24	−0.11	−0.18	−0.36
	3	−0.70	−0.03	−0.24	0.13	0.39	−0.89	−1.26	−1.15	−0.34	−0.63	−0.38	−0.06	0.13	−1.83	−2.01	−1.67

-6 -5 -4 -3 -2 -1 0 1 2 3 4 5 6

Baseline-normalised power (db)

Pre-treatment with Naltrexone was given at 0 min, and ketamine at 30 min. Separated by Active (left) and Inactive (right) epochs. Values are given in dB change from baseline. dB is a logarithmic scale, meaning that "−3dB" = 50% of original value, whilst "3dB" = 200% of original value. Values that are significantly different vs. vehicle + ketamine are coloured according to the valence of change from baseline. Full tables of p-values and non-segregated "Any" spectra can be found in ***Supplementary Information****. Dose is given in mg/kg; V, Vehicle; K, ketamine 10 mg/kg.*

TABLE 6 | Clozapine and Naltrexone concentrations measured in terminal plasma and brain homogenate samples 1 h after subcutaneous injection ($n = 3$ satellite animals).

Drug pre-treatment	Clinical dose (mg)	Back translated rat dose (mg/kg)	SC Dose (mg/kg)	Time point (h)	Total plasma concentration; Mean ± SD (ng/mL)	Total brain concentration; Mean ± SD (ng/mL)	Total brain: plasma concentration ratio (Kp); Mean ± SD
Clozapine	12.5	1.29	0.3	0.5	12.4 ± 1.7	268 ± 35	22 ± 1.3
			1	0.5	55 ± nv	1322 ± nv	13 ± nv
			3	0.5	112 ± 12	3055 ± 421	27 ± 1
Naltrexone	25–50	3.875	1	0.5	69 ± 5	305 ± 31	4.4 ± 0.2
			3	0.5	221 ± 33	883 ± 48	4.0 ± 0.5
			10	0.5	875 ± 125	2899 ± 227	3.4 ± 0.5

Quantification of Clozapine and Naltrexone Concentrations in Satellite Animals

Drug concentrations were determined in satellite animals ($n = 3$ per dose per drug) and are presented in **Table 6**. Both drugs distributed to the brain with total brain to plasma ratios ∼3.9 and 21, respectively. Ketamine exposures were not assessed in order to avoid animal handling causing interference during the pharmacodynamic measurement window. The ketamine SC dose was selected based on data from several rat cognitive pharmacology models (data not presented). The Cmax in these studies confirmed consistent plasma and brain ketamine exposures were achieved following 10 mg/kg SC administration (mean total plasma concentration at 0.5 h post dose = 951 ng/mL (range 670–1,311 ng/mL; $n = 5$ studies), brain: plasma total concentration ratio at 0.5 h post dose = 3.6).

DISCUSSION

The primary findings of this study are: (1) the effect on LFP/ECoG power of clozapine, ketamine and naltrexone depends on locomotor state; (2) ketamine-induced beta suppression in the Inactive state is reversed by the antipsychotic clozapine but is preserved during naltrexone co-administration; and (3) broadband ketamine induced enhancement of higher frequencies, especially HFO, is bolstered by clozapine but dampened by naltrexone.

Locomotor State Separation

The two-state classifier revealed locomotor-state specific effects on LFP amplitudes that otherwise would have been occluded, validating head mounted accelerometers as an alternative to video-tracking solutions. More sophisticated machine learning solutions utilising both LFP and accelerometers can detect up to 7 behaviours (88), but may not be suitable for every study i.e.,: when recording from different brain structures than the original study. Non-invasive head-mounted accelerometers are compatible with any freely moving recording paradigm (EEG, 2-photon calcium microscopy, etc.) and require 0.008% as much data storage when compared to video files from the same recording session. As substantial differences in spontaneous brain activity exist between locomotor states, seen previously (37) and in the present study, it is imperative that efficient and economical behavioural segregation of freely moving experimentation is implemented in future studies.

Separating locomotor states highlighted Active state spectra that were obscured when looking at non-classified LFP epochs summed together. The Active-state peak in baseline Theta has some precedent: Theta power is known to spike during exploratory behaviour in rodents (89, 90) and more recently was observed to increase in walking human subjects (91). During

pharmacological manipulations, Active spectra were generally outweighed due to 1) the inclination of rats in this study to remain passive >50% of the recording session in all groups and pharmacological conditions; and 2) pharmacologically induced changes to spontaneous Inactive power were of a substantially larger magnitude. As neuronal firing increases during movement in response to increased sensory input and processing (37, 92), we hypothesise that the smaller pharmacological deviations in Active vs. Inactive results from 1) circuits modulated by clozapine/ketamine/naltrexone are also engaged during locomotion, thus baseline Active LFPs are closer to physiological maximum and pharmacological enhancement above baseline is limited; or 2) distinct circuits of neurons engaged during Active behaviour generate spectral activity that outweighs LFPs generated by modulation of drug-susceptible circuits. In support of the former proposition, comparing raw baseline power showed that Active power was almost exclusively higher than Inactive (**Figure 1E**). Investigation of LFP properties of specific neural circuits exclusively during movement is required to elucidate the degree to which either hypothesis is responsible.

We did not observe significant ketamine-induced hyperlocomotion in any compound combination. This is concurrent with other observations in rats given 10 mg/kg ketamine (37, 39) but is contrary to other studies using 2.5–10 mg/kg (40, 93, 94). Habitation differences between studies reporting hyperlocomotion may explain this: rats habituated to the recording box for 90 min in this study before recording of EEG or locomotor activity began, vs. 60 min (94) and 30 min to room/0 min to arena (40, 93). We primarily suspect that this study's decision to employ a reversed light cycle may be responsible. This decision was made to allow rats to be recorded during their usual waking hours (as in human rsEEG) to capture the most translatable data. As animals in the present study had already been awake for several hours (experiments started at 0900, 3 h after "lights out") their level of wakefulness may have been higher than rats in other studies recorded during the light phase (when they are naturally inclined to sleep). Ketamine (2.5–10 mg/kg) delays onset of sleep (95) and this may be interpreted as induction of hyperactivity during the light phase.

Irrespective of hyperlocomotion, the importance of separating LFP data by activity state is clear from our report. Developing user friendly systems capable of automatically detecting three or more behaviours may improve the reliability of spectral activity studies even further. Controlling for motor activity is certain to be a building block in bridging the translation gap between pre-clinical and clinical research.

Beta Suppression and Psychotomimetic Features

Beta band suppression could indicate manifestation of psychomimetic properties of ketamine. We observed that beta amplitudes were depressed by ketamine during Inactive epochs, and that the antipsychotic clozapine dose dependently reversed this. Clinical findings are strikingly resemblant to our own: low beta is found to be depressed in unmedicated schizophrenic patients (26, 27, 30) as are EEG spectra between [7.5–12.5 Hz] (termed alpha in human EEG studies, overlapping with low beta [10–20 Hz]) (30). Both low beta disturbances and symptoms measured by the Positive and Negative Symptoms Scale (PANSS) are reduced by acute and chronic clozapine treatment (29). Moreover, suppression of low beta during ketamine exposure has been correlated with symptom severity as scored by the Clinician Administered Dissociative States Scale (CADSS) (43, 44) and other purpose-built self-report questionnaires (47) when administered to healthy subjects. Finally, in one study that failed to find significance between CADSS scores and ketamine induced low beta suppression, it was found that restoration of low beta by midazolam and improvement in dissociation scores in CADSS were causally linked (46). These results dovetail with the presence and absence of low beta suppression reported in our study; suppression occurs during psychotomimetic drug exposure, while clozapine ameliorates this. Importantly, these human EEG studies were performed in an "Inactive"-like state i.e.,: 10 min of eyes closed sitting still—and we only saw reversal of ketamine induced effects on beta in this state, which may explain why it has not received attention in preclinical studies until now.

Behavioural measures follow a similar pattern. Positive, negative and cognitive symptoms were inhibited by administering clozapine to human patients with SZ (53, 96–99), even when given ketamine (48). Ketamine-induced cognitive deficits are also prevented in mice by clozapine administration (100). Naltrexone did not change the dissociative aspects of acute ketamine exposure in Williams (2019) study, and the same combination of compounds produced no changes in beta in this study. The results of this study contribute more evidence towards an association between beta depression at rest and dissociative symptoms. Reversal of beta suppression may prove to be a useful preclinical biomarker for assessing neuroleptics.

Higher Frequencies

Clozapine and Ketamine Enhances HFO Power Through Asynchrony

In agreement with previous locomotor-state-separated EEG analyses (37), power in frequencies above 30 Hz were broadly enhanced by ketamine, particularly in the Inactive state. Drug effects in the gamma band largely resemble those in HFO albeit with a lower magnitude, therefore as in other NMDAR antagonist LFP studies (35, 36, 38, 39, 49) we focus the discussion on effects in the HFO band. Ketamine induced-HFO were further strengthened by clozapine across both locomotor states. Increased HFO power can represent asynchronous activity in several distinct local neuronal populations, and/or circuit(s) that have become dysregulated (101, 102). Such asynchrony was indicated by the broader peak of spectral power/greater spectral entropy observed with increasing doses of clozapine in the present study (101, 103). Whilst it could be hypothesised that circuit desynchronisation occurs from clozapine (104) and ketamine (2) possessing opposing affinities for NMDAR on GABAergic interneurons, it has been demonstrated that the firing rate of local GABAergic interneurons in the rat thalamus and PFC are not significantly altered by ketamine (87). Ketamine potentially drives HFO through increased

firing of excitatory pyramidal neurons (105–107). According to the "direct" hypothesis, ketamine-induced, NMDAR-dependent plasticity-related protein synthesis seen in pyramidal neurons (108, 109) is responsible for increased excitatory drive (107, 110).

Clozapine has affinities for several receptors that could recruit additional neuronal populations, generating more power yet less synchrony in the HFO band compared to ketamine alone. Agonism at NMDAR on local GABAergic interneurons, known generators of fast rhythmic activity in their own right (106), is one example. Clozapine additionally increases the firing of dopaminergic neurons in the ventral tegmental area by 100% (111), which innervates two structures this study observed broadband HFO increases within: the PFC (112) and NAc (113). However, single unit electrophysiology studies are necessary to characterise the precise neuronal sub-populations that are recruited during acute ketamine and clozapine exposure vs. ketamine alone.

Naltrexone Modulates Ketamine Induced Excitatory Disinhibition

Our findings indicate a clear difference in LFPs between ketamine, and ketamine plus naltrexone; a combination that is suspected to block RAAD effects (11, 14). While ketamine's RAAD effects are suspected to be driven through transient excitation of pyramidal neurons and synaptogenesis in key brain structures such as the PFC (114–119), the precise mechanistic pathway(s) through which improvement manifests is not yet fully elucidated. In addition, mechanisms have been identified through which opioid blockade could prevent RAAD (120) including BDNF upregulation and synaptogenesis (121), which is blocked by naltrexone (122); and acute agonism at mu-opioid receptors situated on neurons in the lateral habenula, dorsal raphe nucleus and ventral tegmental area. Inhibition of these neurons, *via* ketamine's antagonism at NMDAR and agonism at mu-opioid receptors, triggers downstream disinhibition of serotonergic and dopaminergic neurons in the PFC and NAc (120, 123–127). In this proposed circuit, as increasing doses of naltrexone block mu-opioid receptor agonism by ketamine, less excitatory disinhibition manifests in the PFC and NAc. Accordingly, we report a dose-dependent decrease of ketamine-induced HFO in these locations. If future studies confirm that naltrexone blocks ketamine's RAAD properties, increased HFO in the PFC and NAc should prove to be valuable biomarkers for antidepressant drug research.

Whilst naltrexone and clozapine had opposite effects in this band, it is important to be cautious drawing direct comparisons between the two until more acute studies have been conducted. One important limitation of this study is the exclusion of behavioural outcome measures for depressive and psychotomimetic symptoms. Thus, we can only say that in drug combinations that block RAAD effects in humans, we see suppression of ketamine induced HFO. Investigation in human subjects and in pre-clinical depression models to characterise the relationship between HFO amplitudes and RAAD effects is recommended.

CONCLUDING REMARKS

This is the first study to investigate differences in locomotor state ketamine LFP induced by the neuroleptic clozapine and the opioid antagonist naltrexone. Our results reveal distinct profiles of LFP activity across locomotor states and demonstrate the pressing need to separate these for accurate analysis in future studies. Separating out Activity states stands to make translational research more directly comparable to human data. We also show powerful modulation of ketamine LFPs by clozapine and naltrexone. Potent reversal of beta suppression by clozapine exclusively during the Inactive state hints at its potential value as a biomarker for neuroleptic efficacy. We also establish here for the first time that HFO is materially different between ketamine with/without naltrexone pre-treatment, and the relationship we document here aligns with the proposed outcomes of a previously proposed pathway through which ketamine's RAAD effects are impacted by opioid blockade. Our findings in both beta and HFO bands appear to support literature describing opioid involvement in ketamine's therapeutic mechanism. Future acute studies in humans with these compounds will help tease out the intricate dance between LFP and subjective, symptomatic changes. Both HFO and beta may prove to be invaluable biomarkers in the hunt for more efficacious antidepressant and neuroleptic medications with milder side effects.

DATA AVAILABILITY STATEMENT

The raw data supporting the conclusions of this article will be made available by the authors, without undue reservation.

ETHICS STATEMENT

The animal study was reviewed and approved by Experimental Procedures, Animal Housing and Care were carried out in accordance with the Danish legislation according to the European Union Regulation (directive 2010/63 of 22 September 2010), granted by the Welfare Committee, appointed by the Ministry of Environment and Food of Denmark.

AUTHOR CONTRIBUTIONS

CB: study design, writing, pilot data collection, graphical abstract, figure production, and data analysis. UR: data analysis, figure production, and writing. CA: data analysis and review. CJ: exposure study and writing. KH: study design, writing, direction, and review. All authors contributed to the article and approved the submitted version.

FUNDING

Facilities and funding was provided by Lundbeck (Denmark). Additional funding was given in the form of an Erasmus+ grant for international research *via* Maastricht University. Sponsors did not influence study design.

ACKNOWLEDGMENTS

Unreserved gratitude is expressed to Kasper Larsen who performed all recordings and surgeries, Trine Nielsen and Camilla Stampe Nielsen for histological support and verification of electrode placements, Dat Chau Lee for technical design and support, Johan Juhl Weisser and Heidi Toft for bioanalysis support, Wim Riedel and Rudy Schreiber for supervision of the Master's thesis during which this study was designed and trialled, and the entire animal welfare team at Lundbeck, without whom this would not have been possible.

SUPPLEMENTARY MATERIAL

The Supplementary Material for this article can be found online at: https://www.frontiersin.org/articles/10.3389/fpsyt.2022.737295/full#supplementary-material

REFERENCES

1. Roth BL, Gibbons S, Arunotayanun W, Huang XP, Setola V, Treble R, et al. The ketamine analogue methoxetamine and 3- and 4-methoxy analogues of phencyclidine are high affinity and selective ligands for the glutamate NMDA receptor. *PLoS ONE.* (2013) 8:59334. doi: 10.1371/journal.pone.0059334
2. Zorumski CF, Izumi Y, Mennerick S. Ketamine: NMDA receptors and beyond. *J Neurosci.* (2016) 36:11158–64. doi: 10.1523/JNEUROSCI.1547-16.2016
3. Frohlich J, Van Horn JD. Reviewing the ketamine model for schizophrenia. *J Psychopharmacol.* (2014) 28:287–302. doi: 10.1177/0269881113512909
4. Grent-'t-Jong T, Rivolta D, Gross J, Gajwani R, Lawrie SM, Schwannauer M, et al. Acute ketamine dysregulates task-related gamma-band oscillations in thalamo-cortical circuits in schizophrenia. *Brain.* (2018) 141:2511–26. doi: 10.1093/brain/awy175
5. Anacker C. New insight into the mechanisms of fast-acting antidepressants: what we learn from scopolamine. *Biol Psychiatry.* (2018) 83:e5–7. doi: 10.1016/j.biopsych.2017.11.001
6. Tuck AN, Ghazali DH. Ketamine as a rapid-acting antidepressant: promising clinical and basic research. *Am J Psychiatry Resid J.* (2017) 12:3–5. doi: 10.1176/appi.ajp-rj.2017.120302
7. Kubota T, Anzawa N, Hirota K, Yoshida H, Kushikata T, Matsuki A. Effects of ketamine and pentobarbital on noradrenaline release from the medial prefrontal cortex in rats. *Can J Anaesth.* (1999) 46:388–92. doi: 10.1007/BF03013235
8. Sleigh J, Harvey M, Voss L, Denny B. Ketamine - more mechanisms of action than just NMDA blockade. *Trends Anaesthesia Critical Care.* (2014) 4:76–81. doi: 10.1016/j.tacc.2014.03.002
9. Zhang K, Hashimoto K. Lack of opioid system in the antidepressant actions of ketamine. *Biol Psychiatry.* (2019) 45:e25–7. doi: 10.1016/j.biopsych.2018.11.006
10. Amiaz R. Attenuation of antidepressant effects of ketamine by opioid receptor antagonism: Is it a ketamine-specific effect? *Am J Psychiatry.* (2019) 176:250–1. doi: 10.1176/appi.ajp.2018.18111231
11. Heifets BD, Williams NR, Bentzley BS, Schatzberg AF. Rigorous trial design is essential to understand the role of opioid receptors in ketamine's antidepressant effect. *JAMA Psychiatry.* (2019) 76:657–8. doi: 10.1001/jamapsychiatry.2019.0766
12. Krystal JH, Yoon G, Petrakis IL. Rigorous trial design is essential to understand the role of opioid receptors in ketamine's antidepressant effect - Reply. *JAMA Psychiatry.* (2019) 76:658–9. doi: 10.1001/jamapsychiatry.2019.0763
13. Sanacora G. Caution against overinterpreting opiate receptor stimulation as mediating antidepressant effects of ketamine. *Am J Psychiatry.* (2019) 176:249. doi: 10.1176/appi.ajp.2018.18091061
14. Williams NR, Heifets BD, Bentzley BS, Sudheimer KD, Williams NR. Attenuation of antidepressant and antisuicidal effects of ketamine by opioid receptor antagonism. *Mol Psychiatry.* (2019) 24:1779–86. doi: 10.1038/s41380-019-0503-4
15. Yoon G, Petrakis IL, Krystal JH. Association of combined naltrexone and ketamine with depressive symptoms in a case series of patients with depression and alcohol use disorder. *JAMA Psychiatry.* (2019) 76:337–8. doi: 10.1001/jamapsychiatry.2018.3990
16. Klein ME, Chandra J, Sheriff S, Malinow R. Opioid system is necessary but not sufficient for antidepressive actions of ketamine in rodents. *Proc Natl Acad Sci USA.* (2020) 117:2656–62. doi: 10.1073/pnas.1916570117
17. Hashimotoa K. Are NMDA and opioid receptors involved in the antidepressant actions of ketamine?. *Proc Natl Acad Sci USA.* (2020) 117:11200–1. doi: 10.1073/pnas.2001264117
18. Ostadhadi S, Norouzi-Javidan A, Chamanara M, Akbarian R, Imran-Khan M, Ghasemi M, et al. Involvement of NMDA receptors in the antidepressant-like effect of tramadol in the mouse forced swimming test. *Brain Res Bull.* (2017) 134:136–41. doi: 10.1016/j.brainresbull.2017.07.016
19. Fitzgerald PJ, Watson BO. *In vivo* electrophysiological recordings of the effects of antidepressant drugs. *Experi Brain Res.* (2019) 237:593–614. doi: 10.1007/s00221-019-05556-5
20. Drinkenburg WHIM, Ruigt GSF, Ahnaou A. Pharmaco-EEG studies in animals: an overview of contemporary translational applications. *Neuropsychobiology.* (2016) 72:151–64. doi: 10.1159/000442210
21. Hunter AM, Cook IA, Leuchter AF. Does prior antidepressant treatment of major depression impact brain function during current treatment? *Eur Neuropsychopharmacol.* (2012) 22:711–20. doi: 10.1016/j.euroneuro.2012.02.005
22. Iosifescu DV. Electroencephalography-derived biomarkers of antidepressant response. *Harvard Rev Psychiatry.* (2011) 119:144–54. doi: 10.3109/10673229.2011.586549
23. Kemp AH, Griffiths K, Felmingham KL, Shankman SA, Drinkenburg W, Arns M, et al. Disorder specificity despite comorbidity: Resting EEG alpha asymmetry in major depressive disorder and post-traumatic stress disorder. *Biol Psychol.* (2010) 85:350–4. doi: 10.1016/j.biopsycho.2010.08.001
24. Uhlhaas PJ, Singer W. Abnormal neural oscillations and synchrony in schizophrenia. *Nat Rev Neurosci.* (2010) 11:100–13. doi: 10.1038/nrn2774
25. Hunt MJ, Kopell NJ, Traub RD, Whittington MA. Aberrant network activity in schizophrenia. *Trends Neurosci.* (2017) 40:371–82. doi: 10.1016/j.tins.2017.04.003
26. Giannitrapani D, Kayton L. Schizophrenia and EEG spectral analysis. *Electroencephalogr Clin Neurophysiol.* (1974) 36:377–86. doi: 10.1016/0013-4694(74)90187-4
27. Itil TM, Saletu B, Coffin C, Klingenberg H. Quantitative EEG changes during thiothixene treatment of chronic schizophrenics. *Clin Electroencephalogr.* (1972) 3:109–17. doi: 10.1177/155005947200300206
28. Itil TM, Saletu B, Davis S. EEG findings in chronic schizophrenics based on digital computer period analysis and analog power spectra. *Biol Psychiatry.* (1972) 5:1–13.
29. Knott V, Labelle A, Jones B, Mahoney C. Quantitative EEG in schizophrenia and in response to acute and chronic clozapine treatment. *Schizophr Res.* (2001) 50:41–53. doi: 10.1016/S0920-9964(00)00165-1
30. Newson JJ, Thiagarajan TC. EEG frequency bands in psychiatric disorders: a review of resting state studies. *Front Human Neurosci.* (2019) 12:521. doi: 10.3389/fnhum.2018.00521
31. Yeragani VK, Cashmere D, Miewald J, Tancer M, Keshavan MS. Decreased coherence in higher frequency ranges (beta and gamma) between central and frontal EEG in patients with schizophrenia: A preliminary report. *Psychiatry Res.* (2006) 141:53–60. doi: 10.1016/j.psychres.2005.07.016
32. Andreou C, Nolte G, Leicht G, Polomac N, Hanganu-Opatz IL, Lambert M, et al. Increased resting-state gamma-band connectivity in first-episode schizophrenia. *Schizophr Bull.* (2015) 41:930–9. doi: 10.1093/schbul/sbu121

33. Di Lorenzo G, Daverio A, Ferrentino F, Santarnecchi E, Ciabattini F, Monaco L, et al. Altered resting-state EEG source functional connectivity in schizophrenia: The effect of illness duration. *Front Hum Neurosci.* (2015) 9:234. doi: 10.3389/fnhum.2015.00234
34. Jonak K, Krukow P, Jonak KE, Grochowski C, Karakuła-Juchnowicz H. Quantitative and qualitative comparison of EEG-based neural network organization in two schizophrenia groups differing in the duration of illness and disease burden: graph analysis with application of the minimum spanning tree. *Clin EEG Neurosci.* (2019) 50:231–41. doi: 10.1177/1550059418807372
35. Olszewski M, Piasecka J, Goda SA, Kasicki S, Hunt MJ. Antipsychotic compounds differentially modulate high-frequency oscillations in the rat nucleus accumbens: A comparison of first- and second-generation drugs. *Int J Neuropsychopharmacol.* (2013) 16:1009–20. doi: 10.1017/S1461145712001034
36. Goda SA, Olszewski M, Piasecka J, Rejniak K, Whittington MA, Kasicki S, et al. Aberrant high frequency oscillations recorded in the rat nucleus accumbens in the methylazoxymethanol acetate neurodevelopmental model of schizophrenia. *Prog Neuro-Psychopharmacol Biol Psychiatry.* (2015) 61:44–51. doi: 10.1016/j.pnpbp.2015.03.016
37. Hansen IH, Agerskov C, Arvastson L, Bastlund JF, Sørensen HBD, Herrik KF. Pharmaco-electroencephalographic responses in the rat differ between active and inactive locomotor states. *Eur J Neurosci.* (2019) 50:1948–71. doi: 10.1111/ejn.14373
38. Hunt MJ, Olszewski M, Piasecka J, Whittington MA, Kasicki S. Effects of NMDA receptor antagonists and antipsychotics on high frequency oscillations recorded in the nucleus accumbens of freely moving mice. *Psychopharmacology.* (2015) 232:4525–35. doi: 10.1007/s00213-015-4073-0
39. Hunt MJ, Raynaud B, Garcia R. Ketamine dose-dependently induces high-frequency oscillations in the nucleus accumbens in freely moving rats. *Biol Psychiatry.* (2006) 60:1206–14. doi: 10.1016/j.biopsych.2006.01.020
40. Jones NC, Reddy M, Anderson P, Salzberg MR, O'Brien TJ, Pinault D. Acute administration of typical and atypical antipsychotics reduces EEG gamma power, but only the preclinical compound LY379268 reduces the ketamine-induced rise in gamma power. *Int J Neuropsychopharmacol.* (2012) 15:657–68. doi: 10.1017/S1461145711000848
41. Knott V, McIntosh J, Millar A, Fisher D, Villeneuve C, Ilivitsky V, et al. Nicotine and smoker status moderate brain electric and mood activation induced by ketamine, an N-methyl-d-aspartate (NMDA) receptor antagonist. *Pharmacol Biochem Behav.* (2006) 85:228–42. doi: 10.1016/j.pbb.2006.08.005
42. Kocsis B, Brown RE, McCarley RW, Hajos M. Impact of ketamine on neuronal network dynamics: translational modeling of schizophrenia-relevant deficits. *CNS Neurosci Ther.* (2013) 19:437–47. doi: 10.1111/cns.12081
43. de la Salle S, Choueiry J, Shah D, Bowers H, McIntosh J, Ilivitsky V, et al. Effects of ketamine on resting-state EEG activity and their relationship to perceptual/dissociative symptoms in healthy humans. *Front Pharmacol.* (2016) 7:348. doi: 10.3389/fphar.2016.00348
44. de la Salle S, Choueiry J, Shah D, Bowers H, McIntosh J, Ilivitsky V, et al. Resting-state functional EEG connectivity in salience and default mode networks and their relationship to dissociative symptoms during NMDA receptor antagonism. *Pharmacol Biochem Behav.* (2021) 201:173092. doi: 10.1016/j.pbb.2020.173092
45. Curic S, Andreou C, Nolte G, Steinmann S, Thiebes S, Polomac N, et al. Ketamine alters functional gamma and theta resting-state connectivity in healthy humans: implications for schizophrenia treatment targeting the glutamate system. *Front Psychiatry.* (2021) 12:671007. doi: 10.3389/fpsyt.2021.671007
46. Chamadia S, Gitlin J, Mekonnen J, Ethridge BR, Ibala R, Colon KM, et al. Ketamine induces EEG oscillations that may aid anesthetic state but not dissociation monitoring. *Clin Neurophysiol.* (2021) 132:3010–8. doi: 10.1016/j.clinph.2021.08.021
47. Vlisides PE, Bel-Bahar T, Nelson A, Chilton K, Smith E, Janke E, et al. Subanaesthetic ketamine and altered states of consciousness in humans. *Br J Anaesth.* (2018) 121:249–59. doi: 10.1016/j.bja.2018.03.011
48. Malhotra AK, Adler CM, Kennison SD, Elman I, Pickar D, Breier A. Clozapine blunts N-methyl-D-aspartate antagonist-induced psychosis: A study with ketamine. *Biol Psychiatry.* (1997) 42:664–8. doi: 10.1016/S0006-3223(96)00546-X
49. Sredniawa W, Wróbel J, Kublik E, Wójcik DK, Whittington MA, Hunt MJ. Network and synaptic mechanisms underlying high frequency oscillations in the rat and cat olfactory bulb under ketamine-xylazine anesthesia. *Sci Rep.* (2021) 11:1–14. doi: 10.1038/s41598-021-85705-5
50. Hansen IH. *Investigation of Pharmacological Manipulationon Brain Connectivity in Rats and Humans for Improvement of Drug Development. DTU Health Technology.* (2019). Available online at: https://orbit.dtu.dk/en/publications/investigation-of-pharmacological-manipulationon-brain-connectivit (accessed March 23, 2021).
51. Nucifora FC, Mihaljevic M, Lee BJ, Sawa A. Clozapine as a model for antipsychotic development. *Neurotherapeutics.* (2017) 14:750–61. doi: 10.1007/s13311-017-0552-9
52. Leucht S, Cipriani A, Spineli L, Mavridis D, Örey D, Richter F, et al. Comparative efficacy and tolerability of 15 antipsychotic drugs in schizophrenia: A multiple-treatments meta-analysis. *Lancet.* (2013) 382:951–62. doi: 10.1016/S0140-6736(13)60733-3
53. Buchanan RW. Clozapine: efficacy and safety. *Schizophr Bull.* (1995) 21:579–91. doi: 10.1093/schbul/21.4.579
54. Abi-Dargham A. From "bedside" to "bench" and back: a translational approach to studying dopamine dysfunction in schizophrenia. *Neurosci Biobehav Rev.* (2020) 110:174–9. doi: 10.1016/j.neubiorev.2018.12.003
55. Liebe T, Li M, Colic L, Munk MHJ, Sweeney-Reed CM, Woelfer M, et al. Ketamine influences the locus coeruleus norepinephrine network, with a dependency on norepinephrine transporter genotype-a placebo controlled fMRI study. *NeuroImage Clin.* (2018) 20:715–23. doi: 10.1016/j.nicl.2018.09.001
56. Anticevic A, Cole MW, Repovš G, Savic A, Driesen NR, Yang G, et al. Connectivity, pharmacology, and computation: toward a mechanistic understanding of neural system dysfunction in schizophrenia. *Front psychiatry.* (2013) 4:169. doi: 10.3389/fpsyt.2013.00169
57. Barch DM. *Cerebellar-Thalamic Connectivity in Schizophrenia*. Oxford: Oxford University Press US (2014). doi: 10.1093/schbul/sbu076
58. Kulikova SP, Tolmacheva EA, Anderson P, Gaudias J, Adams BE, Zheng T, et al. Opposite effects of ketamine and deep brain stimulation on rat thalamocortical information processing. *Eur J Neurosci.* (2012) 36:3407–19. doi: 10.1111/j.1460-9568.2012.08263.x
59. Ferrarelli F, Tononi G. Reduced sleep spindle activity point to a TRN-MD thalamus-PFC circuit dysfunction in schizophrenia. *Schizophr Res.* (2017) 180:36–43. doi: 10.1016/j.schres.2016.05.023
60. Zhang F, Peng W, Sweeney JA, Jia Z, Gong Q. Brain structure alterations in depression: Psychoradiological evidence. *CNS Neurosci Ther.* (2018) 24:994–1003. doi: 10.1111/cns.12835
61. Guo W, Liu F, Chen J, Wu R, Li L, Zhang Z, et al. Hyperactivity of the default-mode network in first-episode, drug-naive schizophrenia at rest revealed by family-based case-control and traditional case-control designs. *Medicine.* (2017) 96:6223. doi: 10.1097/MD.0000000000006223
62. Sapkota K, Mao Z, Synowicki P, Lieber D, Liu M, Ikezu T, et al. GluN2D N-methyl-d-aspartate receptor subunit contribution to the stimulation of brain activity and gamma oscillations by ketamine: implications for schizophrenia. *J Pharmacol Exp Ther.* (2016) 356:702–11. doi: 10.1124/jpet.115.230391
63. Dawson N, McDonald M, Higham DJ, Morris BJ, Pratt JA. Subanesthetic ketamine treatment promotes abnormal interactions between neural subsystems and alters the properties of functional brain networks. *Neuropsychopharmacology.* (2014) 39:1786–98. doi: 10.1038/npp.2014.26
64. Young AMJ, Stubbendorff C, Valencia M, Gerdjikov T. Disruption of medial prefrontal synchrony in the subchronic phencyclidine model of schizophrenia in rats. *Neuroscience.* (2015) 287:157–63. doi: 10.1016/j.neuroscience.2014.12.014
65. Spiga S, Talani G, Mulas G, Licheri V, Fois GR, Muggironi G, et al. Hampered long-term depression and thin spine loss in the nucleus accumbens of ethanol-dependent rats. *Proc Natl Acad Sci USA.* (2014) 111:E3745–54. doi: 10.1073/pnas.1406768111
66. Matulewicz P, Kasicki S, Hunt MJ. The effect of dopamine receptor blockade in the rodent nucleus accumbens on local field potential oscillations and motor activity in response to ketamine. *Brain Res.* (2010) 1366:226–32. doi: 10.1016/j.brainres.2010.09.088

67. Garcia SV, Fort P. Nucleus Accumbens, a new sleep-regulating area through the integration of motivational stimuli. *Acta Pharmacol Sin.* (2018) 39:165–6. doi: 10.1038/aps.2017.168
68. McCollum LA, Walker CK, Roche JK, Roberts RC. Elevated excitatory input to the nucleus accumbens in schizophrenia: a postmortem ultrastructural study. *Schizophr Bull.* (2015) 41:1123–32. doi: 10.1093/schbul/sbv030
69. McCollum LA, Roberts RC. Uncovering the role of the nucleus accumbens in schizophrenia: a postmortem analysis of tyrosine hydroxylase and vesicular glutamate transporters. *Schizophr Res.* (2015) 169:369–73. doi: 10.1016/j.schres.2015.08.041
70. Konopaske GT, Coyle JT. Possible compensatory mechanisms for glutamatergic disconnection found in the auditory cortex in schizophrenia. *Biol Psychiatry.* (2015) 77:923. doi: 10.1016/j.biopsych.2015.03.031
71. Sweet RA, Henteleff RA, Zhang W, Sampson AR, Lewis DA. Reduced dendritic spine density in auditory cortex of subjects with schizophrenia. *Neuropsychopharmacology.* (2009) 34:374–89. doi: 10.1038/npp.2008.67
72. Mørch-Johnsen L, Nesvåg R, Jørgensen KN, Lange EH, Hartberg CB, Haukvik UK, et al. Auditory cortex characteristics in schizophrenia: associations with auditory hallucinations. *Schizophr Bull.* (2017) 43:75–83. doi: 10.1093/schbul/sbw130
73. Hirano S, Nakhnikian A, Hirano Y, Oribe N, Kanba S, Onitsuka T, et al. Phase-amplitude coupling of the electroencephalogram in the auditory cortex in schizophrenia. *Biol Psychiatry Cogn Neurosci Neuroimaging.* (2018) 3:69–76. doi: 10.1016/j.bpsc.2017.09.001
74. Shi W-X. The auditory cortex in schizophrenia. *Biol Psychiatry.* (2007) 61:829. doi: 10.1016/j.biopsych.2007.02.007
75. MacDonald ML, Garver M, Newman J, Sun Z, Kannarkat J, Salisbury R, et al. Synaptic proteome alterations in the primary auditory cortex of individuals with schizophrenia. *JAMA Psychiatry.* (2020) 77:86–95. doi: 10.1001/jamapsychiatry.2019.2974
76. Curtis MT, Coffman BA, Salisbury DF. Pitch and duration mismatch negativity are associated with distinct auditory cortex and inferior frontal cortex volumes in the first-episode schizophrenia spectrum. *Schizophr Bull Open.* (2021) 2:sgab005. doi: 10.1093/schizbullopen/sgab005
77. Bartus RT, Emerich DF, Hotz J, Blaustein M, Dean RL, Perdomo B, et al. Vivitrex®, an Injectable, extended-release formulation of naltrexone, provides pharmacokinetic and pharmacodynamic evidence of efficacy for i month in rats. *Neuropsychopharmacology.* (2003) 28:1973–82. doi: 10.1038/sj.npp.1300274
78. Ciano P, Foll B. Evaluating the impact of naltrexone on the rat gambling task to test its predictive validity for gambling disorder. *PLoS ONE.* (2016) 11:e0155604. doi: 10.1371/journal.pone.0155604
79. Nilforoushan D, Shirazi M, Dehpour A-R. The role of opioid systems on orthodontic tooth movement in cholestatic rats. *Angle Orthod.* (2002) 72:476–80. doi: 10.1043/0003-3219(2002)072<0476:TROOSO>2.0.CO;2
80. Sun L, Lau CE. Intravenous and oral clozapine pharmacokinetics, pharmacodynamics, and concentration-effect relations: acute tolerance. *Eur J Pharmacol.* (2000) 398:225–38. doi: 10.1016/S0014-2999(00)00277-6
81. Thomas SP, Nandhra HS, Singh SP. Pharmacologic treatment of first-episode schizophrenia: a review of the literature. *Prim Care Companion CNS Disord.* (2012) 14:1198. doi: 10.4088/PCC.11r01198
82. Olsen CK, Brennum LT, Kreilgaard M. Using pharmacokinetic-pharmacodynamic modelling as a tool for prediction of therapeutic effective plasma levels of antipsychotics. *Eur J Pharmacol.* (2008) 584:318–27. doi: 10.1016/j.ejphar.2008.02.005
83. Rame M, Caudal D, Schenker E, Svenningsson P, Spedding M, Jay TM, et al. Clozapine counteracts a ketamine-induced depression of hippocampal-prefrontal neuroplasticity and alters signaling pathway phosphorylation. *PLoS ONE.* (2017) 12:e0177036. doi: 10.1371/journal.pone.0177036
84. Lin YT, Chen CC, Huang CC, Nishimori K, Hsu K. Oxytocin stimulates hippocampal neurogenesis via oxytocin receptor expressed in CA3 pyramidal neurons. *Nat Commun.* (2017) 8:1–16. doi: 10.1038/s41467-017-00675-5
85. Nair AB, Jacob S. A simple practice guide for dose conversion between animals and human. *J Basic Clin Pharm.* (2016) 7:27. doi: 10.4103/0976-0105.177703
86. Krystal JH, Madonick S, Perry E, Gueorguieva R, Brush L, Wray Y, et al. Potentiation of low dose ketamine effects by naltrexone: potential implications for the pharmacotherapy of alcoholism. *Neuropsychopharmacology.* (2006) 31:1793–800. doi: 10.1038/sj.npp.1300994
87. Amat-Foraster M, Celada P, Richter U, Jensen AA, Plath N, Artigas F, et al. Modulation of thalamo-cortical activity by the NMDA receptor antagonists ketamine and phencyclidine in the awake freely-moving rat. *Neuropharmacology.* (2019) 158:107745. doi: 10.1016/j.neuropharm.2019.107745
88. Dhawale AK, Smith MA, Ölveczky BP. The role of variability in motor learning. *Annu Rev Neurosci.* (2017) 40:479–98. doi: 10.1146/annurev-neuro-072116-031548
89. Buzsaki G. *Rhythms of the Brain*. Oxford: Oxford University Press (2006).
90. Vanderwolf CH. Hippocampal electrical activity and voluntary movement in the rat. *Electroencephalogr Clin Neurophysiol.* (1969) 26:407–18. doi: 10.1016/0013-4694(69)90092-3
91. Aghajan ZM, Schuette P, Fields TA, Tran ME, Siddiqui SM, Hasulak NR, et al. Theta oscillations in the human medial temporal lobe during real-world ambulatory movement. *Curr Biol.* (2017) 27:3743–51. doi: 10.1016/j.cub.2017.10.062
92. Insel N, Barnes CA. Differential activation of fast-spiking and regular-firing neuron populations during movement and reward in the dorsal medial frontal cortex. *Cereb Cortex.* (2015) 5:2631–47. doi: 10.1093/cercor/bhu062
93. Hakami T, Jones NC, Tolmacheva EA, Gaudias J, Chaumont J, Salzberg M, et al. NMDA receptor hypofunction leads to generalized and persistent aberrant γ oscillations independent of hyperlocomotion and the state of consciousness. *PLoS ONE.* (2009) 4:e6755. doi: 10.1371/journal.pone.0006755
94. Usun Y, Eybrard S, Meyer F, Louilot A. Ketamine increases striatal dopamine release and hyperlocomotion in adult rats after postnatal functional blockade of the prefrontal cortex. *Behav Brain Res.* (2013) 256:229–37. doi: 10.1016/j.bbr.2013.08.017
95. Ahnaou A, Huysmans H, Biermans R, Manyakov N V, Drinkenburg W. Ketamine: differential neurophysiological dynamics in functional networks in the rat brain. *Transl Psychiatry.* (2017) 7:e1237. doi: 10.1038/tp.2017.198
96. Meltzer HY, McGurk SR. The effects of clozapine, risperidone, and olanzapine on cognitive function in schizophrenia. *Schizophr Bull.* (1999) 25:233–56. doi: 10.1093/oxfordjournals.schbul.a033376
97. Meltzer HY, Alphs L, Green AI, Altamura AC, Anand R, Bertoldi A, et al. Clozapine treatment for suicidality in schizophrenia: International Suicide Prevention Trial (InterSePT). *Arch Gen Psychiatry.* (2003) 60:82–91. doi: 10.1001/archpsyc.60.1.82
98. Meltzer HY, Okayli G. Reduction of suicidality during clozapine treatment of neuroleptic-resistant schizophrenia: impact on risk-benefit assessment. *Am J Psychiatry.* (1995) 152:183–90. doi: 10.1176/ajp.152.2.183
99. Ranjan R, Meltzer HY. Acute and long-term effectiveness of clozapine in treatment-resistant psychotic depression. *Biol Psychiatry.* (1996) 40:253–8. doi: 10.1016/0006-3223(95)00305-3
100. Szlachta M, Pabian P, Kuśmider M, Solich J, Kolasa M, Zurawek D, et al. Effect of clozapine on ketamine-induced deficits in attentional set shift task in mice. *Psychopharmacology.* (2017) 234:2103–12. doi: 10.1007/s00213-017-4613-x
101. Guyon N, Zacharias LR, de Oliveira EF, Kim H, Leite JP, Lopes-Aguiar C, et al. Network asynchrony underlying increased broadband gamma power. *J Neurosci.* (2021) 41:2944–63. doi: 10.1101/2020.08.26.265439
102. Uhlhaas PJ, Singer W. Oscillations and neuronal dynamics in schizophrenia: The search for basic symptoms and translational opportunities. *Biol Psychiatry.* (2015) 77:1001–9. doi: 10.1016/j.biopsych.2014.11.019
103. Valero M, Averkin RG, Fernandez-Lamo I, Aguilar J, Lopez-Pigozzi D, Brotons-Mas JR, et al. Mechanisms for selective single-cell reactivation during offline sharp-wave ripples and their distortion by fast ripples. *Neuron.* (2017) 94:1234–47.e7. doi: 10.1016/j.neuron.2017.05.032
104. Heresco-Levy U. Glutamatergic neurotransmission modulation and the mechanisms of antipsychotic atypicality. *Prog Neuro-Psychopharmacology Biol Psychiatry.* (2003) 27:1113–23. doi: 10.1016/j.pnpbp.2003.09.007
105. Seamans J. Losing inhibition with ketamine. *Nat Chem Biol.* (2008) 4:91–3. doi: 10.1038/nchembio0208-91

106. Homayoun H, Moghaddam B. NMDA receptor hypofunction produces opposite effects on prefrontal cortex interneurons and pyramidal neurons. *J Neurosci.* (2007) 27:11496–500. doi: 10.1523/JNEUROSCI.2213-07.2007
107. Miller OH, Yang L, Wang C-C, Hargroder EA, Zhang Y, Delpire E, et al. GluN2B-containing NMDA receptors regulate depression-like behavior and are critical for the rapid antidepressant actions of ketamine. *Elife.* (2014) 3:e03581. doi: 10.7554/eLife.03581
108. Wang C-C, Held RG, Chang S-C, Yang L, Delpire E, Ghosh A, et al. A critical role for GluN2B-containing NMDA receptors in cortical development and function. *Neuron.* (2011) 72:789–805. doi: 10.1016/j.neuron.2011.09.023
109. Wang C-C, Held RG, Hall BJ. SynGAP regulates protein synthesis and homeostatic synaptic plasticity in developing cortical networks. *PLoS ONE.* (2013) 8:e83941. doi: 10.1371/journal.pone.0083941
110. Miller OH, Moran JT, Hall BJ. Two cellular hypotheses explaining the initiation of ketamine's antidepressant actions: Direct inhibition and disinhibition. *Neuropharmacology.* (2016) 100:17–26. doi: 10.1016/j.neuropharm.2015.07.028
111. Chiodo LA, Bunney BS. Possible mechanisms by which repeated clozapine administration differentially affects the activity of two subpopulations of midbrain dopamine neurons. *J Neurosci.* (1985) 5:2539–44. doi: 10.1523/JNEUROSCI.05-09-02539.1985
112. Pierce RC, Kumaresan V. The mesolimbic dopamine system: The final common pathway for the reinforcing effect of drugs of abuse? *Neurosci Biobehav Rev.* (2006) 30:215–38. doi: 10.1016/j.neubiorev.2005.04.016
113. Ikemoto S. Brain reward circuitry beyond the mesolimbic dopamine system: A neurobiological theory. *Neurosci Biobehav Rev.* (2010) 35:129–50. doi: 10.1016/j.neubiorev.2010.02.001
114. Moghaddam B, Adams B, Verma A, Daly D. Activation of glutamatergic neurotransmission by ketamine: a novel step in the pathway from NMDA receptor blockade to dopaminergic and cognitive disruptions associated with the prefrontal cortex. *J Neurosci.* (1997) 17:2921–7. doi: 10.1523/JNEUROSCI.17-08-02921.1997
115. Autry AE, Adachi M, Nosyreva E, Na ES, Los MF, Cheng P, et al. NMDA receptor blockade at rest triggers rapid behavioural antidepressant responses. *Nature.* (2011) 475:91–5. doi: 10.1038/nature10130
116. Li N, Liu R-J, Dwyer JM, Banasr M, Lee B, Son H, et al. Glutamate N-methyl-D-aspartate receptor antagonists rapidly reverse behavioral and synaptic deficits caused by chronic stress exposure. *Biol Psychiatry.* (2011) 69:754–61. doi: 10.1016/j.biopsych.2010.12.015
117. Li N, Lee B, Liu R-J, Banasr M, Dwyer JM, Iwata M, et al. mTOR-dependent synapse formation underlies the rapid antidepressant effects of NMDA antagonists. *Science.* (2010) 329:959–64. doi: 10.1126/science.1190287
118. Gerhard DM, Pothula S, Liu R-J, Wu M, Li X-Y, Girgenti MJ, et al. GABA interneurons are the cellular trigger for ketamine's rapid antidepressant actions. *J Clin Invest.* (2020) 130:30808. doi: 10.1172/JCI130808
119. Gerhard DM, Wohleb ES, Duman RS. Emerging treatment mechanisms for depression: focus on glutamate and synaptic plasticity. *Drug Discov Today.* (2016) 21:454–64. doi: 10.1016/j.drudis.2016.01.016
120. Jelen LA, Young AH, Stone JM. Ketamine: A tale of two enantiomers. *J Psychopharmacol.* (2020) 35:109–23. doi: 10.1177/0269881120959644
121. Yang C, Shirayama Y, Zhang JC, Ren Q, Yao W, Ma M, et al. R-ketamine: a rapid-onset and sustained antidepressant without psychotomimetic side effects. *Transl Psychiatry.* (2015) 5:e632. doi: 10.1038/tp.2015.136
122. Zhang H, Torregrossa MM, Jutkiewicz EM, Shi YG, Rice KC, Woods JH, et al. Endogenous opioids upregulate brain-derived neurotrophic factor mRNA through δ- and μ-opioid receptors independent of antidepressant-like effects. *Eur J Neurosci.* (2006) 23:984–94. doi: 10.1111/j.1460-9568.2006.04621.x
123. Lutz P-E, Kieffer BL. Opioid receptors: distinct roles in mood disorders. *Trends Neurosci.* (2013) 36:195–206. doi: 10.1016/j.tins.2012.11.002
124. Fadda P, Scherma M, Fresu A, Collu M, Fratta W. Dopamine and serotonin release in dorsal striatum and nucleus accumbens is differentially modulated by morphine in DBA/2J and C57BL/6J mice. *Synapse.* (2005) 56:29–38. doi: 10.1002/syn.20122
125. Margolis EB, Fields HL. Mu opioid receptor actions in the lateral habenula. *PLoS ONE.* (2016) 11:e0159097. doi: 10.1371/journal.pone.0159097
126. Le Merrer J, Becker JAJ, Befort K, Kieffer BL. Reward processing by the opioid system in the brain. *Physiol Rev.* (2009) 89:1379–412. doi: 10.1152/physrev.00005.2009
127. Tao R, Auerbach SB. Opioid receptor subtypes differentially modulate serotonin efflux in the rat central nervous system. *J Pharmacol Exp Ther.* (2002) 303:549–56. doi: 10.1124/jpet.102.037861

Conflict of Interest: The authors declare that the research was conducted in the absence of any commercial or financial relationships that could be construed as a potential conflict of interest.

Advantages of publishing in Frontiers

OPEN ACCESS
Articles are free to read for greatest visibility and readership

FAST PUBLICATION
Around 90 days from submission to decision

HIGH QUALITY PEER-REVIEW
Rigorous, collaborative, and constructive peer-review

TRANSPARENT PEER-REVIEW
Editors and reviewers acknowledged by name on published articles

Frontiers
Avenue du Tribunal-Fédéral 34
1005 Lausanne | Switzerland

Visit us: www.frontiersin.org
Contact us: frontiersin.org/about/contact

REPRODUCIBILITY OF RESEARCH
Support open data and methods to enhance research reproducibility

DIGITAL PUBLISHING
Articles designed for optimal readership across devices

FOLLOW US
@frontiersin

IMPACT METRICS
Advanced article metrics track visibility across digital media

EXTENSIVE PROMOTION
Marketing and promotion of impactful research

LOOP RESEARCH NETWORK
Our network increases your article's readership